This is a digital copy of a book that was preserved for generations on library shelves before it was carefully scanned by Google as part of a project to make the world's books discoverable online.

It has survived long enough for the copyright to expire and the book to enter the public domain. A public domain book is one that was never subject to copyright or whose legal copyright term has expired. Whether a book is in the public domain may vary country to country. Public domain books are our gateways to the past, representing a wealth of history, culture and knowledge that's often difficult to discover.

Marks, notations and other marginalia present in the original volume will appear in this file - a reminder of this book's long journey from the publisher to a library and finally to you.

Usage guidelines

Google is proud to partner with libraries to digitize public domain materials and make them widely accessible. Public domain books belong to the public and we are merely their custodians. Nevertheless, this work is expensive, so in order to keep providing this resource, we have taken steps to prevent abuse by commercial parties, including placing technical restrictions on automated querying.

We also ask that you:

+ *Make non-commercial use of the files* We designed Google Book Search for use by individuals, and we request that you use these files for personal, non-commercial purposes.

+ *Refrain from automated querying* Do not send automated queries of any sort to Google's system: If you are conducting research on machine translation, optical character recognition or other areas where access to a large amount of text is helpful, please contact us. We encourage the use of public domain materials for these purposes and may be able to help.

+ *Maintain attribution* The Google "watermark" you see on each file is essential for informing people about this project and helping them find additional materials through Google Book Search. Please do not remove it.

+ *Keep it legal* Whatever your use, remember that you are responsible for ensuring that what you are doing is legal. Do not assume that just because we believe a book is in the public domain for users in the United States, that the work is also in the public domain for users in other countries. Whether a book is still in copyright varies from country to country, and we can't offer guidance on whether any specific use of any specific book is allowed. Please do not assume that a book's appearance in Google Book Search means it can be used in any manner anywhere in the world. Copyright infringement liability can be quite severe.

About Google Book Search

Google's mission is to organize the world's information and to make it universally accessible and useful. Google Book Search helps readers discover the world's books while helping authors and publishers reach new audiences. You can search through the full text of this book on the web at `http://books.google.com/`

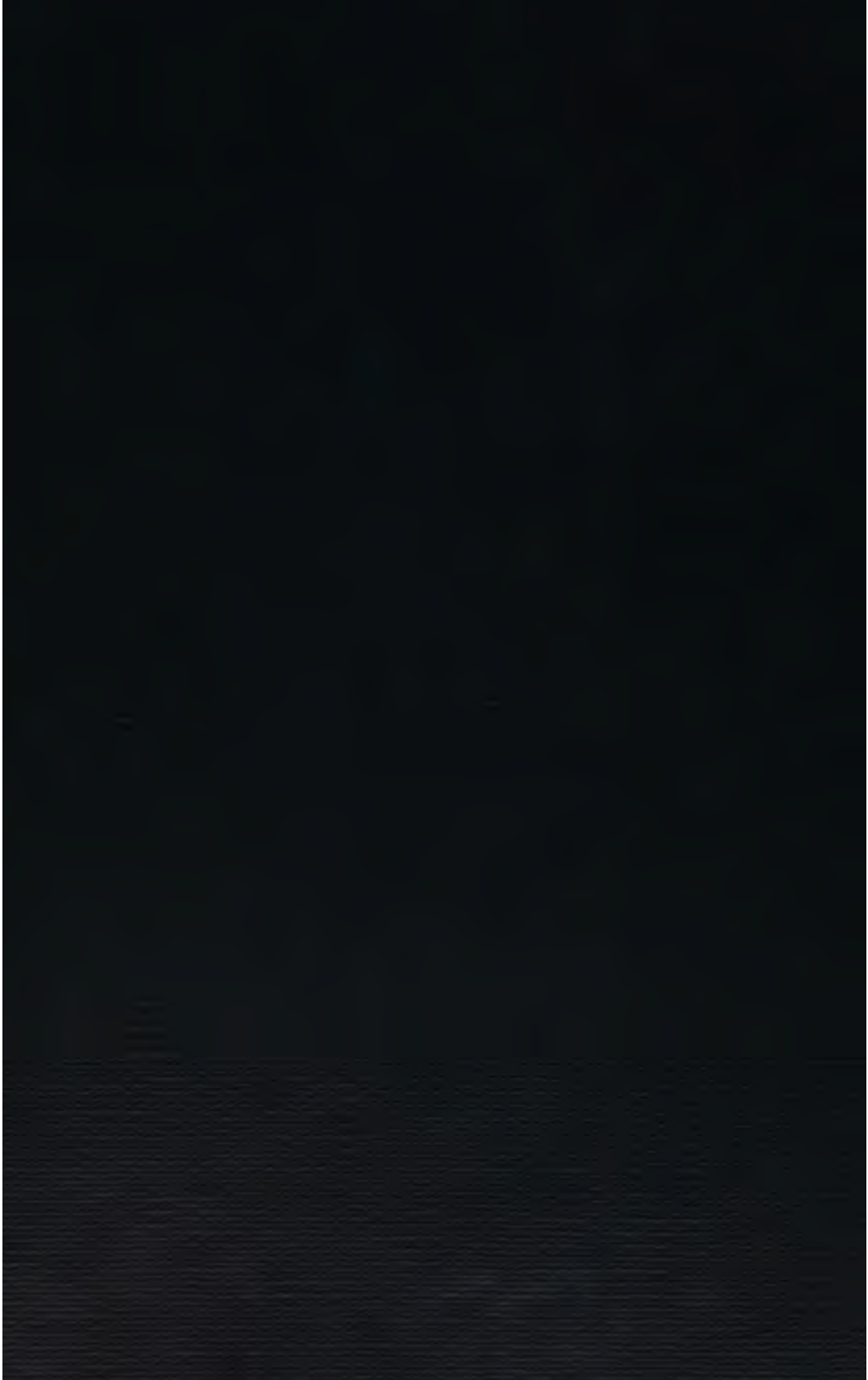

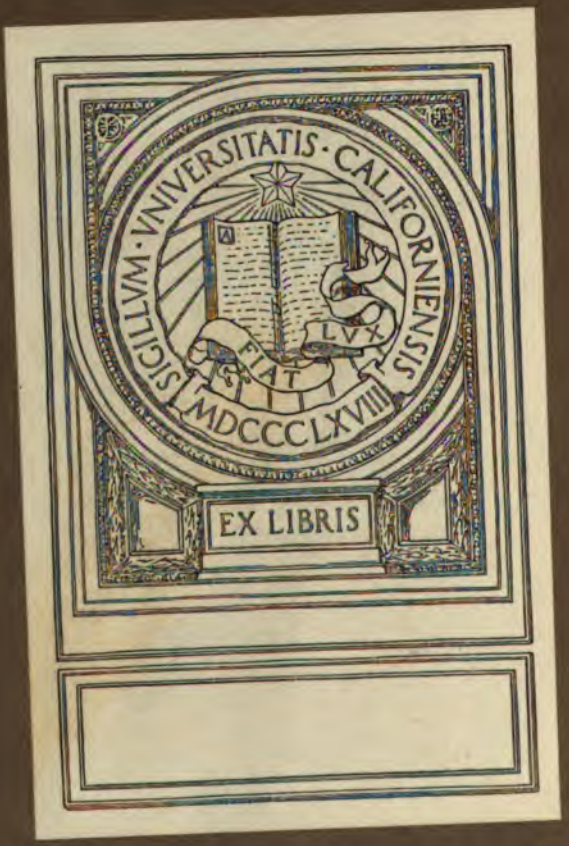
SIGILLVM · VNIVERSITATIS · CALIFORNIENSIS
LVX
FIAT
MDCCCLXVIII
EX LIBRIS

CENTRIFUGAL PUMPS

THEIR

DESIGN AND CONSTRUCTION

BY

LOUIS C. LOEWENSTEIN, E.E., PH.D.

AND

CLARENCE P. CRISSEY, M.E.

320 *ILLUSTRATIONS*
8 *FOLDING PLATES*

NEW YORK
D. VAN NOSTRAND COMPANY
23 MURRAY AND 27 WARREN STS.
1911

TJ915
L7

COPYRIGHT, 1911,
BY
D. VAN NOSTRAND COMPANY

Stanbope Press
F. H. GILSON COMPANY
BOSTON, U. S. A.

PREFACE.

THE rapid substitution of rotating for reciprocating machinery has been one of the most striking engineering developments of recent years. The marked success of the steam turbine no doubt stimulated the development and introduction of the high-pressure and high-speed centrifugal pump. Although centrifugal pumps have been used for many years they were as a rule employed only for very large capacities and low heads. During the last ten years, however, high-pressure and high-speed centrifugal pumps have come into general use and centrifugal pump design has passed through a surprising stage of development. It is a significant fact that almost all large manufacturers of pumping machinery are building centrifugal pumps, and that to-day centrifugal pumps compete with reciprocating piston pumps for all services. This is chiefly on account of their lower initial cost, smaller space requirements, greater adaptability, lower cost and ease of operation and their great advantage of being capable of direct connection to high-speed drivers.

An examination of centrifugal pump literature, published in the English language, yields little information of value to those interested in this subject. The initial development and introduction of high-pressure centrifugal pumps were due to the energy and enterprise of European engineers, as was the case in the development of the steam turbine. It is quite natural, therefore, that the best literature upon this subject is published abroad, although even there we find few complete and satisfactory works, the information as a rule being distributed in the technical magazines.

The success of European installations of high-pressure centrifugal pumps led quickly to the manufacture of such pumps in this country. Our manufacturers adopted the European designs and until a short time ago relied wholly upon the experiments and data furnished by the foreign builders. Experience and research have brought about, during the last few years, remarkable progress in the design of centrifugal pumps, both in this country and abroad. At the present time the most progressive American pump manufacturers are pro-

241323

ducing new designs based upon their own experience and data, and nearly all the larger pump builders are developing centrifugal pumps of high efficiency and great reliability. This concentrated study by a large number of able engineers is producing an immediate and rapid growth of the centrifugal pump industry.

The object of this book is to present to those interested in centrifugal pump manufacture and design and to technical students a clear presentation of the fundamental principles involved, a full explanation of the calculations necessary in securing the best efficiencies and performance, a proper understanding of the constructive details of the various types, the best methods of manufacture and a correct knowledge of the proper proportions of pump parts in order to secure safe and smooth operation. The authors have made use of material furnished from many sources. Much of the theoretical presentation was obtained from *Die Zentrifugalpumpen*, with the kind permission of the author, Mr. Fritz Neumann. Dr. H. Lorenz's recent publication *Neue Theorie und Berechnung der Kreiselräder* has also been quite helpful. The theory presented by Dr. Lorenz is based upon the calculation of the flow of fluids by means of three dimensional equations as compared to the prevalent practice of using two dimensional equations. A new and welcome point of view is secured by this theory, but as yet it has not been sufficiently developed to supplant the older and more generally accepted methods of calculation. The constructive details of the various types and makes of pumps were obtained in most part from manufacturers and the technical magazines. The methods of calculating the strength of impellers, casings and diaphragms, and the critical speeds of high-speed pumps have been used by the authors for a number of years and are partly their own work and partly based upon the results obtained and published by other investigators.

In conclusion the authors can but express a hope that the publication of this work, written during the spare time of a very active engineering life, may tend to make clear some of the technical and practical considerations necessary in the design and construction of centrifugal pumps, and so help to promote, in a slight degree, the application of scientific principles to some of the problems presented to engineers of to-day.

L. C. L.
C. P. C.

LYNN, MASS., *January*, 1911.

CONTENTS.

PAGE

PREFACE iii

CHAPTER I.

THEORY OF CENTRIFUGAL PUMPS.

1. THE CENTRIFUGAL PUMP 1
2. CLASSIFICATION OF CENTRIFUGAL PUMPS 4
3. DERIVATION OF THE FUNDAMENTAL EQUATION 7
4. FRICTION AND SHOCK LOSSES IN CENTRIFUGAL PUMPS 12
   (*a*) Losses in Entrance or Suction Pipe 12
   (*b*) Losses in Impeller 13
   (*c*) Losses in Guide Vanes 15
   (*d*) Losses in Guide Vane Casing 17
5. PRESSURE DIFFERENCE IN THE CLEARANCE SPACE AND CLEARANCE SPACE LOSSES 17
6. DIMENSIONS OF THE SUCTION PIPE 22
7. DETERMINATION OF THE EXIT DIMENSIONS FOR $\delta_c = 90°$ 24
8. INFLUENCE OF THE IMPELLER AND GUIDE VANE ANGLES UPON THE PERIPHERAL VELOCITY 28
9. INFLUENCE OF THE IMPELLER AND GUIDE VANE ANGLES UPON THE PRESSURE DIFFERENCE AND SHORT-CIRCUIT LOSS OF THE CLEARANCE SPACE 30
10. THE ANGLES β_a AND δ_a AND THE PERIPHERAL VELOCITY OF A CENTRIFUGAL PUMP WITHOUT PRESSURE DIFFERENCE IN THE CLEARANCE SPACE 35
11. DETERMINATION OF THE EXIT VALUES BY MEANS OF κ AND λ CURVES .. 37
12. GRAPHICAL DETERMINATION OF THE EXIT VELOCITY DIAGRAM 40
13. MATHEMATICAL AND GRAPHICAL DETERMINATION OF THE ENTRANCE VELOCITY DIAGRAM WHEN $\delta_e = 90°$ 42
14. THE ENTRANCE AND EXIT DIMENSIONS WHEN $\delta_e \gtrless 90°$ 44
15. THE ENTRANCE AND EXIT DIMENSIONS FOR EQUAL HEADS WITH VARYING QUANTITIES 51
16. CONSTRUCTION OF THE ENTRANCE AND EXIT VELOCITY DIAGRAMS AND DETERMINATION OF SUCTION PIPE VELOCITY FOR $\delta_c \lesseqgtr 90°$ 57
17. THE INVOLUTES FOR IMPELLER AND GUIDE VANES 60
   (*a*) General Consideration of the Use of the Involute 60
   (*b*) The Involutes at Impeller Entrance 63
   (*c*) The Involutes at Impeller Exit 66
   (*d*) The Involutes at Guide Vane Entrance 71
18. THE GUIDE VANE CASING 73
19. AXIAL THRUST 76
20. THE MULTI-STAGE CENTRIFUGAL PUMP 79
21. THE CENTRIFUGAL PUMP WITHOUT GUIDE VANES 82

CHAPTER II.

CONSUMPTION OF POWER AND EFFICIENCY.

PAGE
22. General Consideration of Consumption of Power and Efficiency 85
23. Efficiency when the Number of Revolutions is Varied 88
24. Decreasing Friction Head in Impeller by Decreasing the Number of Blades 93
25. Increase of Hydraulic Efficiency when $\delta_e = \beta_e$ and by Using Directing Vanes at Entrance to Impeller 95
26. Comparison of the Friction Heads of Centrifugal Pumps with Impeller Angles $\beta_a = 135°$, $\beta_a = 90°$, and $\beta_a = 45°$; and the Influence of Curvature of Blades upon Efficiency 98
27. The Efficiency as Determined by Experiment 106

CHAPTER III.

THE REGULATION AND CLASSIFICATION OF CENTRIFUGAL PUMPS.

28. Regulating the Quantity of Water by Throttling. Influence of the Quantity of Water upon Head and Losses due to Throttling 112
29. Adjustable Guide Vanes 119
30. Classification of Centrifugal Pumps 122

CHAPTER IV.

THE CALCULATION OF IMPELLER AND GUIDE VANES.

31. Impeller Channel Sections of the Ordinary Type 126
(*a*) Calculation of Two High-pressure Centrifugal Pumps 126
(*b*) Calculation and Blade Form of a Low-pressure Centrifugal Pump. 140
32. The Channel Cross Sections and Development of the Blade Ends upon the Surface of the Cone 144
(*a*) In General 144
(*b*) Description of the Channel Cross Sections, with the Calculation and Design of the Blades for Two Low-pressure Centrifugal Pumps 146
33. Pressure Distribution in a Centrifugal Pump in which Entrance to the Impeller is not Parallel to the Shaft 158

CHAPTER V.

DESIGN OF IMPORTANT PUMP PARTS.

34. Bearings 161
35. Packings 164
36. Impellers 167
37. Diaphragms, Casings, and Heads 184
38. Critical Speeds 191

CHAPTER VI.

TYPES OF CENTRIFUGAL PUMPS.

PAGE

39. Historical Review 223
40. Modern Centrifugal Pumps 225
41. Sulzer Pumps 229
42. Rateau Pumps of Sautter, Harle & Co. 246
43. Jaeger Pumps 257
44. Kugel-Gelpke Pumps of Escher, Wyss & Co. 271
45. Worthington Pumps 272
46. Pumps of the Armaturen und Maschinenfabrik A. G. 301
47. I. P. Morris Pumps 311
48. Skoda Pumps 321
49. Allis-Chalmers Pumps 325
50. Weise and Monski Pumps 328
51. Byron Jackson Pumps 330
52. Pumps of the John McDougall Caledonian Iron Works Company, Limited 335
53. Alberger Pumps 343
54. Mather & Platt Pumps 353
55. De Laval Pumps 371
56. R. D. Wood Pumps 381
57. Brodnitz & Seydel Pumps 384
58. Berliner Maschinenbau Pumps 388
59. Willans & Robinson Pumps 392
60. Dayton Pumps 393
61. Borsig Pumps 399
62. Buffalo Pumps 403
63. Gebauer Pumps 405
64. Allen Pumps 406
65. Novel and Miscellaneous Designs 413

CHAPTER VII.

TESTING OF CENTRIFUGAL PUMPS.

66. Methods of Testing Pumps 418
(*a*) The Venturi Water Meter 420
(*b*) The Weir Tank 421
(*c*) The Nozzle 421
(*d*) The Pitot Tube 422

CENTRIFUGAL PUMPS

I. THEORY OF CENTRIFUGAL PUMPS.

1. The Centrifugal Pump.

A CENTRIFUGAL pump is the reverse of a water turbine. In a turbine the kinetic energy of the water flowing through the wheel is changed into mechanical work, while in a centrifugal pump mechanical work is changed into kinetic energy of the water. A centrifugal pump usually consists of four main parts as shown in Fig. 1:

1. The pipe S, called the suction pipe when the pump is above the level of the supply water, and called the entrance pipe when the pump is below the level of the supply water.
2. The impeller L_a.
3. The guide vanes L_e, which are sometimes omitted.
4. The casing G.

The water flows through a centrifugal pump from part 1 to part 4, while in a water turbine it flows in the opposite direction.

As the name *centrifugal pump* indicates, centrifugal force plays an important part. The water particles enter the impeller (see Fig. 2) at a diameter D_e and leave at a greater diameter D_a. The impeller is rotated by a motor at an angular velocity ω; the water particles are thrown outward by centrifugal force and thus exert a pressure or possess kinetic energy which can be expressed by the equation

$$\frac{\left(\frac{D_a}{2}\right)^2 - \left(\frac{D_e}{2}\right)^2}{2g}\omega^2 = \frac{u_a^2 - u_e^2}{2g},$$

in which u_a and u_e represent the peripheral velocities at the diameters D_a and D_e respectively.

The water particles flowing through the suction or entrance pipe with a velocity w_s, enter the impeller at the mean diameter D_e with a relative velocity v_e and leave the impeller at the outer diameter D_a

UNIV. OF CALIFORNIA

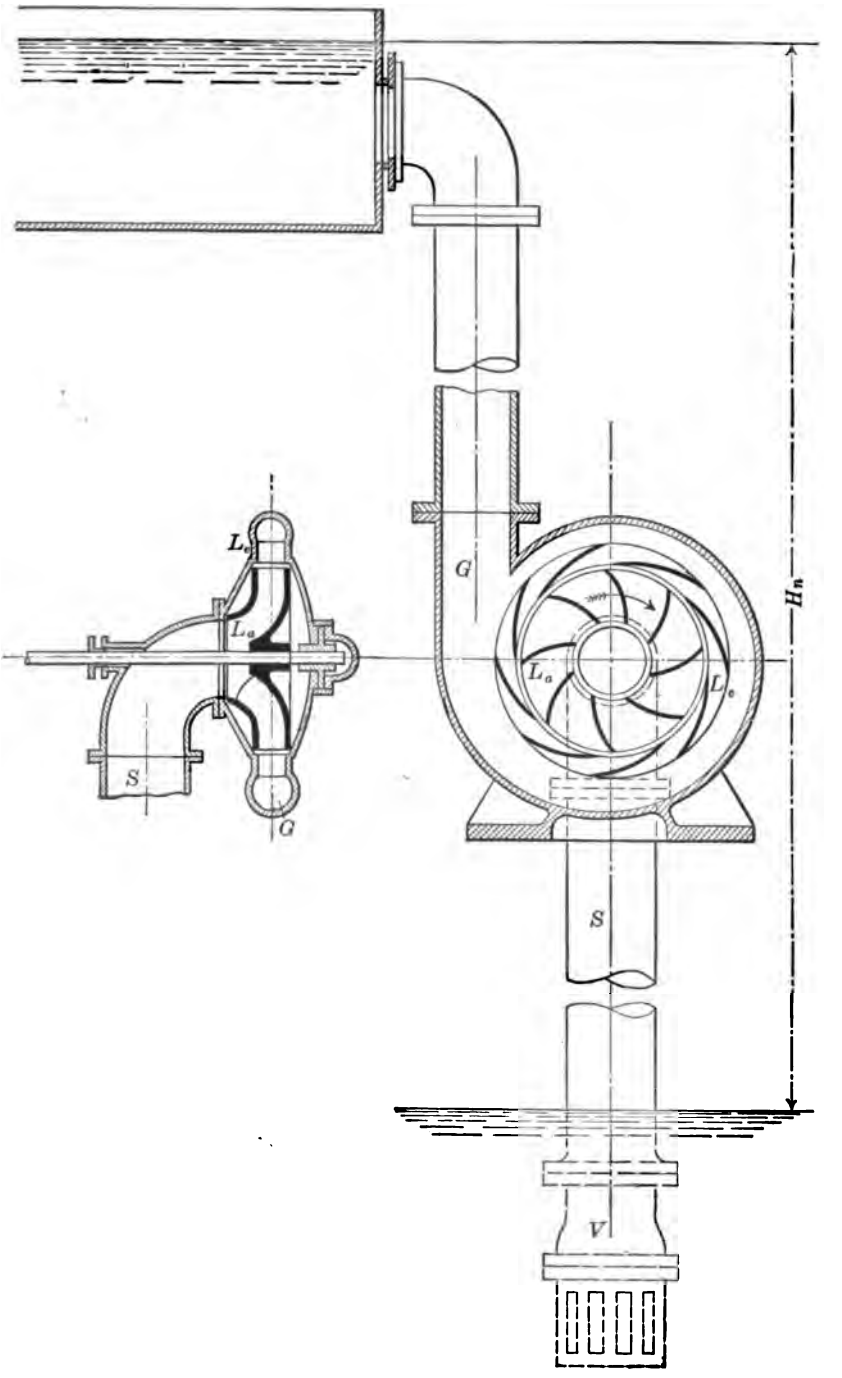

Fig. 1.

with a relative velocity v_a. In order to obtain discharge without shock, the resultant absolute exit velocity w_a of u_a and v_a must form a diagonal of a parallelogram whose sides are u_a and v_a. This parallelogram is called the exit velocity diagram. In this exit velocity diagram u_a and v_a form an angle β_a, which is called the exit angle of the impeller. The angle δ_a, formed by u_a and w_a, must be that of the guide vanes. The object of the guide vanes is to reduce gradually, with minimum shock losses, the absolute exit velocity w_a and thus transform as much as possible of the velocity head $\frac{w_a^2}{2g}$ into pressure.

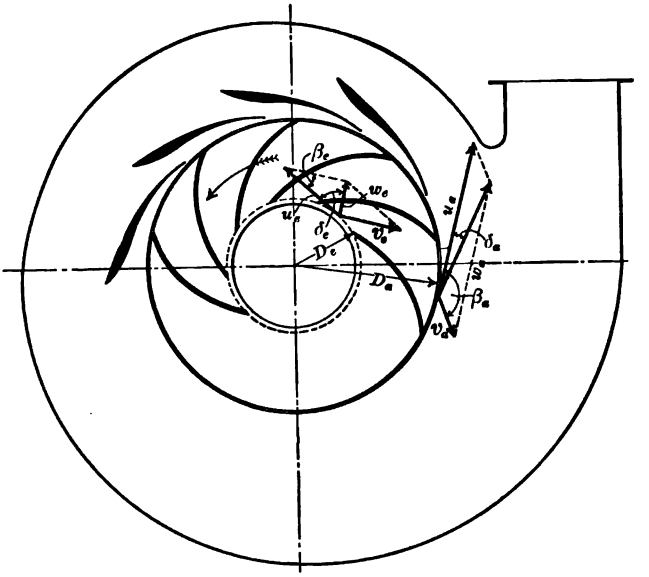

Fig. 2.

The entrance velocity diagram must be drawn in a manner similar to that of the exit velocity diagram in order to reduce shock losses at entrance to the impeller. The entrance velocity w_e must form a diagonal of a parallelogram whose sides are u_e and v_e. The entrance angle of the impeller will be designated by β_e and the angle between u_e and w_e by δ_e. The entrance and exit velocity diagrams are drawn in Fig. 2. These are similar to the velocity diagrams drawn for water turbines, but with directions reversed.

After the water flows from the guide vanes it is generally led by the casing to the pressure or discharge pipe. The velocity at which

the water leaves the casing will be designated by w_d. In the following determination of the efficiency of centrifugal pumps it must be remembered that only the path of the water from entrance to the suction pipe to exit from the guide vanes will be considered.

2. Classification of Centrifugal Pumps.

Centrifugal pumps are classified as high- or low-pressure pumps according to the magnitude of the pressure or water head delivered. The dividing line between these two types of pumps is taken, by most builders, to be about 30 to 50 feet head. The same rules are employed in calculating both types.

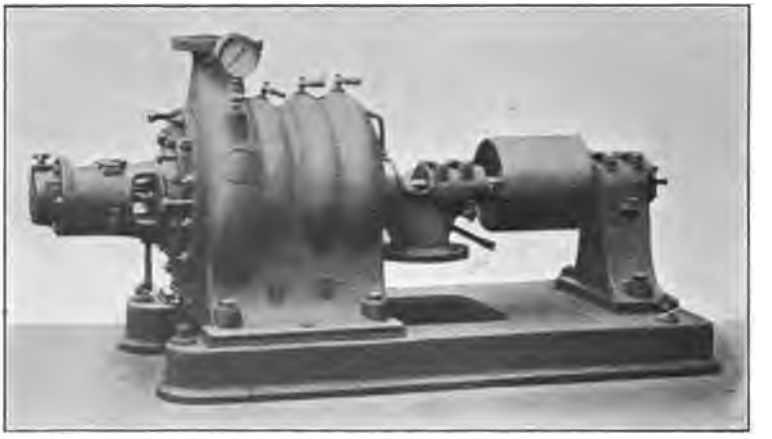

Fig. 3.

Centrifugal pumps are also classified as horizontal or vertical pumps, depending upon the position of the shaft. The choice of arrangement depends upon local conditions. Fig. 3 shows a horizontal shaft pump built by Sulzer Bros., of Winterthur, Switzerland, and Fig. 4 shows a vertical shaft Sulzer pump. Vertical pumps are chiefly used in mine shafts.

There are also the enclosed and open types of pumps, depending upon whether the guide vanes are or are not enclosed in a casing. Open-type pumps are only used for very small heads and, in general, where large volumes of water are required. They are constructed with vertical shafts (Fig. 5). Axial pumps, in which the water enters and leaves axially, were formerly used for this service, but

this method of construction has been entirely abandoned and therefore will not be considered. An enclosed-type pump has its guide vanes surrounded by either a spiral or a round casing as shown in Figs. 6 and 7.

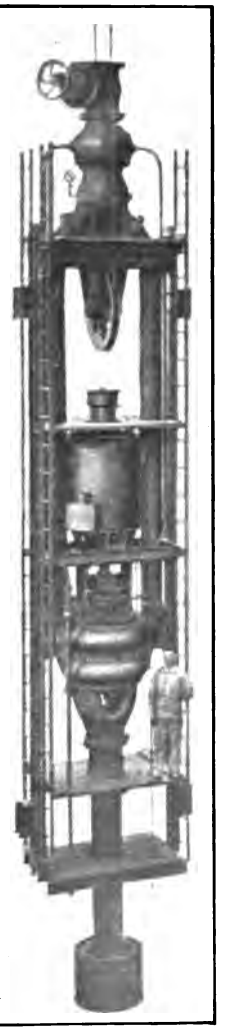

Fig. 4.

Distinction is also made between pumps with and without guide vanes. Pumps with guide vanes have a much higher efficiency than those without guide vanes, and the former should always be used when the least expenditure of power is a vital factor. It is astonishing that the importance of guide vanes was not recognized until high-pressure centrifugal pumps were built. It was found that the use of guide vanes with high-pressure pumps produced a higher efficiency, in spite of the fact that they worked under considerably less favorable conditions than when used in low-pressure pumps; and therefore guide vanes came into use also with low-pressure pumps. The increased cost of a pump with guide vanes is very quickly offset by its greater efficiency and hence smaller expenditure of power. For this reason pumps with guide vanes will be principally considered in this book.

The centrifugal pump has either an entrance or a suction pipe, depending upon the manner in which the water is led to it. Fig. 9 shows an arrangement with an entrance pipe, that is, water entering under its own head. This arrangement is often found with low-pressure pumps having very small heads. The pump in this case is placed below the level of the supply water and is therefore always ready for service. The inaccessibility of this type of pump is a decided disadvantage. In cleaning, a valve placed in the entrance pipe must be closed and the water in and about the pump removed.

In most cases a suction pipe is used, that is, the pump is installed above the supply level (Fig. 1). This has the advantage of ac-

cessibility, because the pump can be quickly drained without any great trouble. A disadvantage of the suction-pipe type is that in

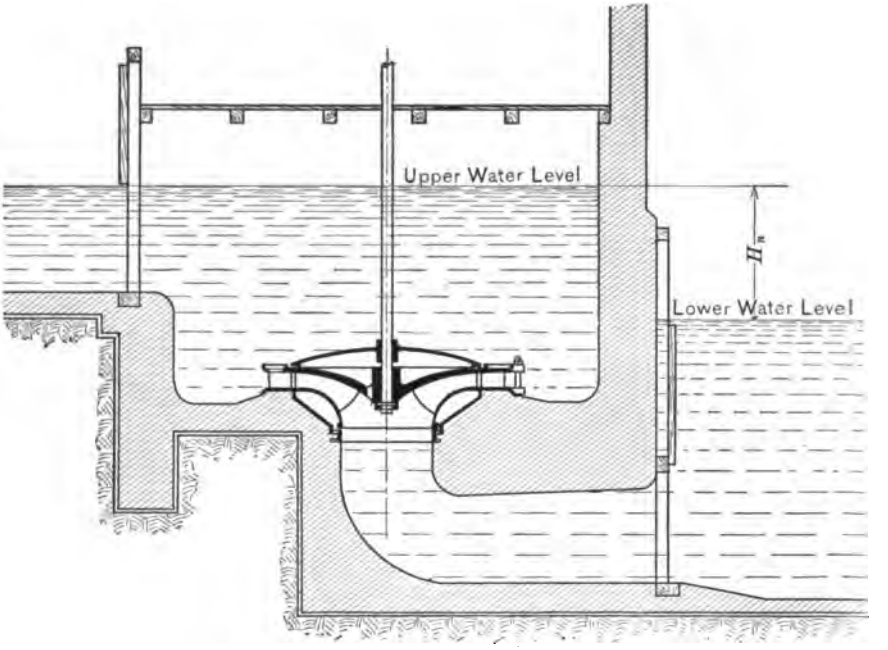

Fig. 5.

most cases the pump must be filled with water before it can be operated. Sometimes it is possible to lift the water to the impeller by speeding up the pump.

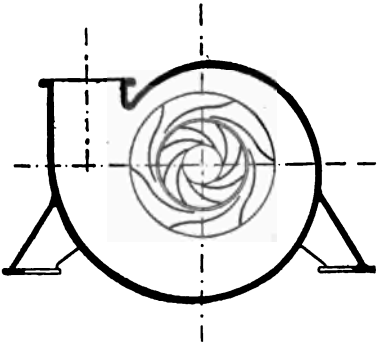

Fig. 6.

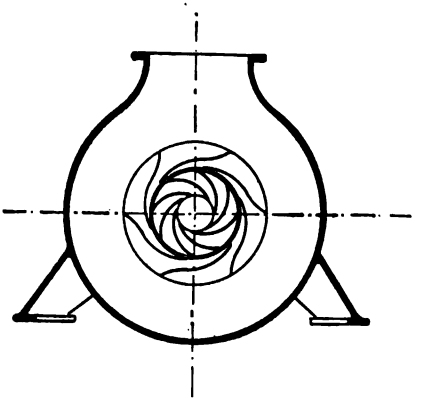

Fig. 7.

High-pressure pumps are built single- or multi-stage, depending upon the magnitude of the desired head. Single-stage pumps

have one impeller, while multi-stage pumps have two or more impellers arranged successively upon the same shaft. For instance, Fig. 8 shows a six-stage high-pressure Sulzer pump.

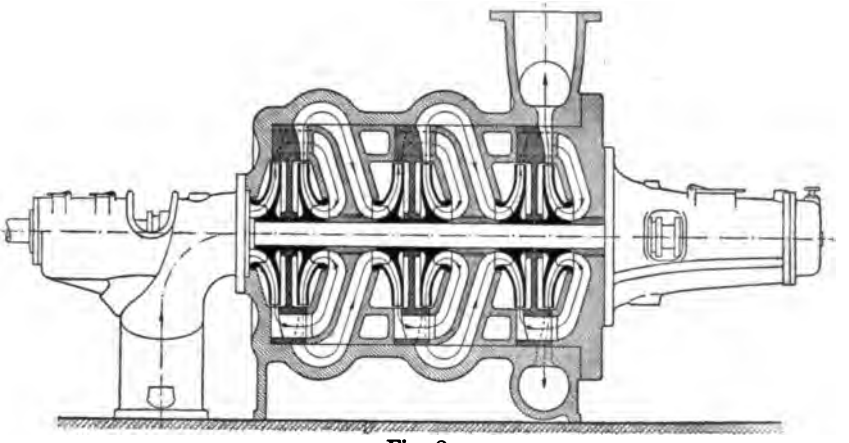

Fig. 8.

The construction of centrifugal pumps varies considerably. There are many different arrangements of both high- and low-pressure pumps, which will be treated later under the head of centrifugal pumps of various types.

3. Derivation of the Fundamental Equation.

Fig. 9 shows schematically an arrangement of a low-pressure centrifugal pump having a vertical shaft. In every part of the pump proper there exists a pressure above the atmosphere, due to its depth below the level of the supply water. Imagine small pipes connected to the inside of the pump at points s, e, a, l, and d. As these points all lie in a horizontal plane there exists at all points the same pressure head h_a when the pump is standing still.

When the pump is run at its normal speed the pressure at each of these points will vary, and the magnitude of the pressure head at these points will now be investigated.

The following derivation of the so-called "condition equation" is an old method used for determining the fundamental equation of water turbines. While this method is rather lengthy, it gives a clear conception of the pressure and velocity distribution in the interior of a centrifugal pump. The pump shown in Fig. 9 is placed below the level of the supply water in order that all the pressure heads

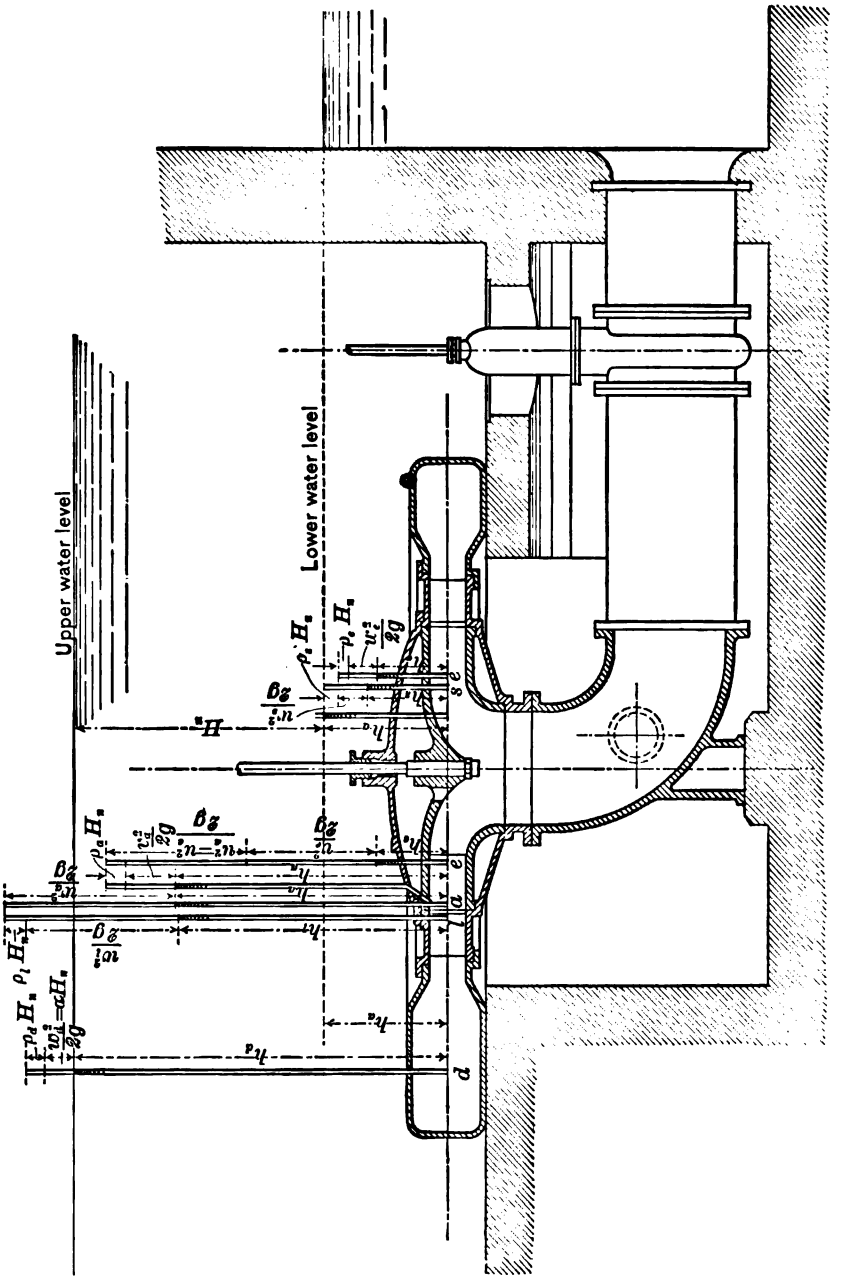

Fig. 9.

may be positive, that is, so that no suction exists. The following equations can of course be derived also for a pump placed above the level of the water.

When the pump is running there will be a pressure head h_s in the pipe at point s which will be less than the pressure head h_a existing at point s when the pump is at rest. It is less by an amount equal to a velocity head $\frac{w_s^2}{2g}$ plus a friction head $\rho_s H_n$. The friction head is dissipated in forcing the water through the entrance pipe up to the point s. The velocity in the entrance pipe or suction tube is designated by w_s, and the velocity head $\frac{w_s^2}{2g}$ represents the loss of pressure head necessary to obtain the velocity w_s in the pipe.

Let H_n be the effective pressure or desired head of the pump. The condition equation may now be expressed by

$$h_w = h_s + \frac{w_s^2}{2g} + \rho_s H_n \quad . \quad . \quad . \quad . \quad . \quad . \quad . \quad . \quad 1$$

The next point e is taken directly at the entrance to the impeller. At this point a pressure head h_e and a velocity head $\frac{w_e^2}{2g}$ exist, w_e being the absolute velocity of the water at this point. In the water flowing from point s to e shock losses occur at entrance to the channels of the impeller which can be expressed as a friction head $\rho_e H_n$, hence

$$h_s + \frac{w_s^2}{2g} = h_e + \frac{w_e^2}{2g} + \rho_e H_n \quad . \quad . \quad . \quad . \quad . \quad . \quad . \quad 2$$

If, at point e, the relative velocity v_e is considered instead of the absolute velocity w_e, then a relative velocity head $\frac{v_e^2}{2g}$ is obtained, while the pressure head h_e remains the same. It is of course understood that absolute velocity is the velocity of the water relative to some fixed or stationary point and that relative velocity is the velocity of the water relative to the rotating parts.

The water now passes through the impeller to point a, which is directly at the exit of the impeller. Through the action of centrifugal force the water, in flowing through the channels of the impeller, has its pressure increased by the value $\frac{u_a^2 - u_e^2}{2g}$. u_a and u_e are the peripheral velocities of the impeller at exit and entrance respectively. Due to friction of the water against the impeller walls and of the

individual water particles amongst themselves there is lost a friction head $\rho_a H_n$. At point a a pressure head h_a and a velocity head $\frac{v_a^2}{2g}$ exist, v_a being the relative exit velocity. The following equation may therefore be written:

$$h_e + \frac{v_e^2}{2g} + \frac{u_a^2 - u_e^2}{2g} = h_a + \frac{v_a^2}{2g} + \rho_a H_n \quad . \quad . \quad . \quad . \quad 3$$

At point l, which is directly at entrance to the guide vanes, there exists a pressure head h_l and also a velocity head $\frac{w_l^2}{2g}$. Due to shock losses at entrance to the guide vanes a friction head $\rho_l H_n$ is lost in passing from a to l. At point a the pressure head h_a and the velocity head $\frac{w_a^2}{2g}$ exist, w_a being the absolute exit velocity. Hence

$$h_a + \frac{w_a^2}{2g} = h_l + \frac{w_l^2}{2g} + \rho_l H_n \quad . \quad . \quad . \quad . \quad . \quad . \quad 4$$

In order to convert as much as possible of the velocity head $\frac{w_l^2}{2g}$ into pressure the velocity w_l should be gradually reduced in passing from point l through the guide vanes. Let w_d represent the velocity and $\frac{w_d^2}{2g}$ the velocity head at exit from the casing, and let $\rho_d H_n$ be the friction head expended in carrying the water through the guide passages and casing. Then

$$h_l + \frac{w_l^2}{2g} = h_d + \frac{w_d^2}{2g} + \rho_d H_n \quad . \quad . \quad . \quad . \quad . \quad . \quad 5$$

The first form of the so-called fundamental equation is obtained by adding equations 1 to 5, which gives equation 6. For convenience equations 1 to 5 are here restated:

1. $$h_w = h_e + \frac{w_e}{2g} + \rho_e H_n.$$

2. $$h_e + \frac{w_e^2}{2g} = h_e + \frac{w_e^2}{2g} + \rho_e H_n.$$

3. $$h_e + \frac{v_e^2}{2g} + \frac{u_a^2 - u_e^2}{2g} = h_a + \frac{v_a^2}{2g} + \rho_a H_n.$$

4. $$h_a + \frac{w_a^2}{2g} = h_l + \frac{w_l^2}{2g} + \rho_l H_n.$$

5. $$h_l + \frac{w_l^2}{2g} = h_d + \frac{w_d^2}{2g} + \rho_d H_n.$$

$$\frac{v_e^2 - w_e^2 - u_e^2 - v_a^2 + w_a^2 + u_a^2}{2g} = h_d - h_w + H_n(\rho_s + \rho_e + \rho_a + \rho_l + \rho_d) + \frac{w_d^2}{2g} \quad . \quad 6$$

From Fig. 9 it follows that

$$h_d - h_w = H_n \quad . \quad . \quad . \quad . \quad . \quad . \quad . \quad . \quad . \quad 7$$

As already explained, H_n is the desired head at exit from the casing. The friction head necessary to overcome the losses in the delivery pipe has not been considered, because these losses may vary between wide limits and are dependent upon the length and cross section of the pipe. The velocity head $\frac{w_d^2}{2g}$ at the exit of the pump is a certain fraction of the desired head H_n. This fraction can be represented by the coefficient α, so that

$$\frac{w_d^2}{2g} = \alpha H_n \quad . \quad . \quad . \quad . \quad . \quad . \quad . \quad . \quad . \quad 8$$

The coefficient α gives the magnitude of the exit losses, and varies with the desired pressure head when the velocity w_d is constant. This will be shown more clearly later.

In order to simplify equation 6 let

$$(\rho_s + \rho_e + \rho_a + \rho_l + \rho_d) = \rho \quad . \quad . \quad . \quad . \quad . \quad . \quad 9$$

Substituting equations 7, 8, and 9 in equation 6 the general form of the fundamental equation is obtained,

$$v_e^2 - w_e^2 - u_e^2 - v_a^2 + w_a^2 + u_a^2 = 2gH_n(1 + \rho + \alpha) \quad . \quad 10$$

Let

$$(1 + \rho + \alpha) = \eta \quad . \quad . \quad . \quad . \quad . \quad . \quad . \quad 11$$

In order to obtain the total head H_b, which is used in the calculation of centrifugal pumps and represents the theoretical head which the pump can deliver considering no losses whatever, the desired head H_n can be multiplied by the factor η. The hydraulic efficiency of the pump can be represented by $\epsilon = \frac{1}{\eta}$. Hence

$$\eta H_n = H_b \quad . \quad . \quad . \quad . \quad . \quad . \quad . \quad . \quad . \quad 12$$

From the entrance velocity diagram (Fig. 10)

$$v_e^2 = u_e^2 + w_e^2 - 2\,u_e w_e \cos \delta_e \quad . \quad . \quad . \quad . \quad . \quad 13$$

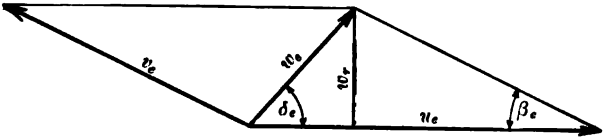

Fig. 10.

and from the exit velocity diagram (Fig. 11)

$$v_a^2 = u_a^2 + w_a^2 - 2\,u_a w_a \cos \delta_a \quad . \quad . \quad . \quad . \quad . \quad 14$$

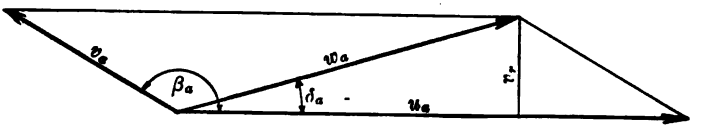

Fig. 11.

Substituting in equation 10 the values of v_e^2, v_a^2, and $(1 + \rho + \alpha)$ from equations 11, 12, and 13, the second form of the fundamental equation is derived, and is

$$u_a w_a \cos \delta_a - u_e w_e \cos \delta_e = \eta\, g H_n \quad . \quad . \quad . \quad . \quad . \quad 15$$

Before these equations are transformed and other equations determined for the calculation of the dimensions of pumps we shall investigate by what means high efficiencies may be obtained, that is, how to make η as small as possible. With a view of obtaining the highest total efficiency the various parts of centrifugal pumps will be studied in the following order: 1, the suction or entrance pipe; 2, the impeller; 3, the guide vanes; 4, the casing.

4. Friction and Shock Losses in Centrifugal Pumps.

(*a*). *Losses in Entrance or Suction Pipe.*

In equation 1 the friction head lost by the water in passing from the inlet of entrance or suction pipe to the inlet of the impeller is represented by $\rho_e H_n$. If the pump has a suction pipe this pipe will contain a non-return valve which closes automatically when the pump is stopped. This valve is installed to prevent the loss of suction head, which would occur if the water flowed back and out of the suction pipe. The resistance to the flow of water should be

brought to a minimum and therefore it is best to make the cross section of the pipe ample. The velocity of flow through the valve should not be greater than the mean suction pipe velocity. This can be accomplished by enlarging the suction pipe at the valve seat. The device for preventing return flow may be of light construction, because, due to the continuity of flow, it remains open when the pump is operating, and only closes every time the pump is brought to rest. It is therefore subject to hardly any wear.

The friction head $\rho_e H_n$ is also dependent upon the length and diameter of the suction pipe as well as upon the suction pipe velocity w_s. With high velocities it is desirable to enlarge the pipe conically downwards in order to decrease the friction losses and to keep the shock losses, which occur in the water at entrance to the suction pipe, as small as possible.

The suction pipe generally terminates at the casing around the center of the impeller through which the shaft is carried. A stuffing box must be used where the shaft passes through the casing. Great care must be exercised in its design in order to prevent on the one hand too great a friction load being placed upon the shaft when the stuffing gland is tightened and on the other hand to guard against air leakage into the casing.

(*b*). *Losses in Impeller.*

The friction head $\rho_e H_n$ is lost by the water at entrance to the impeller channel. On account of the thickness of the impeller blades a diminution of cross section occurs, causing the suction pipe velocity w_s to increase suddenly to a velocity w_e.

Fig. 12 shows the entrance to an impeller channel. The blade thickness is s_e, the channel height is a_e, and the pitch of blades at entrance is t_e'. The diminution of cross section due to the thickness of blades is proportional to the ratio $\frac{x}{t_e'}$; hence, as the velocities are inversely proportional to the cross section of flow, the absolute entrance velocity w_e will equal

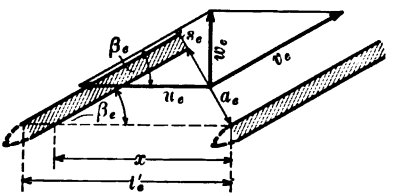

Fig. 12.

$$w_e = w_s \frac{t_e'}{x}.$$

From Fig. 12 it is seen that

$$\frac{t_e'}{x} = \frac{a_e + s_e}{a_e};$$

hence

$$w_e = w_e \frac{a_e + s_e}{a_e} \quad \ldots \ldots \ldots \quad 16$$

At entrance to the impeller the velocity w_e is suddenly increased to the velocity w_e, which naturally is accompanied by shock losses. In order to have the change of velocity occur gradually the blades are sharpened, and the length of this sharpening is generally equal to twice the blade thickness. It is advisable, in order to have $\frac{a_e + s_e}{a_e}$ as small as possible, to design the blades thin and to have as few blades as possible, thereby increasing a_e.

The friction losses occurring while the water flows through the impeller channels is expressed as $\rho_a H_n$. To make this a minimum the impeller should have as few channels as possible; and great care should be taken also to have very smooth castings on account of the narrow passages, which make machining almost impossible. This is especially true of high-pressure pumps. When the impellers are large, blades of sheet steel may be used which can be ground smooth before being set in the impeller. The friction losses are considerably reduced by such a construction.

The coefficient ρ_a is also dependent upon the design of the entire blade channel. Care should be taken that the relative entrance velocity v_e decreases gradually to that of the relative exit velocity v_a. In Fig. 13 the path ea represents the mean length of the channel. At e the velocity is v_e and at a it is v_a. If possible, the blades should be so constructed that the velocity of the water in passing from e to a decreases linearly, that is, equal amounts in equal distances and not as shown by the dotted line in the figure, where poor blade form has caused the velocity to increase again after it has started to decrease.

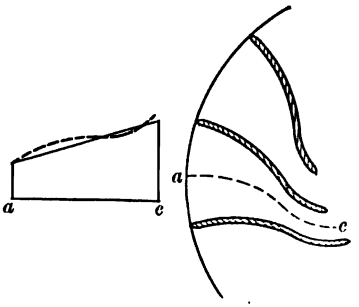

Fig. 13.

A part of the friction head $\rho_l H_n$ is lost at exit from the impeller by

the sudden increase of cross section. If a_a represents the height of the channel and s_a the thickness of blade at exit from the impeller, then the absolute exit velocity w_a will be decreased after leaving the impeller, by the value $\frac{a_a}{a_a + s_a}$. A smaller velocity w_a' therefore exists in the clearance space between the impeller and guide vanes and equals

$$w_a' = w_a \frac{a_a}{a_a + s_a} \quad . \quad . \quad . \quad . \quad . \quad . \quad . \quad . \quad 17$$

The blades should be sharpened, as at entrance, in order that the change of velocity from w_a to w_a' will not occur too suddenly.

(c). *Losses in Guide Vanes.*

Another portion of the friction head $\rho_l H_n$ is lost during the passage of the water through the clearance space and at entrance to the guide vanes. As the impeller blades are constantly moving past the guide vanes there is a constant change of the clear guide channel cross section. At a certain instant the rotating impeller is in the

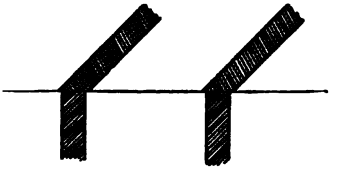

Fig. 14.

Fig. 15.

position shown by Fig. 14 with respect to the guide vanes and in which position no decrease of the guide channel area occurs. When the impeller reaches the position shown in Fig. 15 the guide channel area is decreased by the blades of the impeller. By sharpening the blade ends and having sufficient clearance space (Fig. 16) the shock losses can be diminished. The number of guide and of impeller blades should not be equal, in order to avoid periodic impulses or vibrations. These impulses are due to the fact that with an equal number of guide and impeller blades the clear cross sections of all guide channels are increasing or decreasing in unison.

In spite of all precautions, it is almost impossible to prevent the entrance of foreign matter into the pump. It is therefore advisable to avoid small clearance spaces, for there is danger that the foreign

matter may come between the guide and impeller blades. Such an occurrence may break the blade ends and finally destroy the pump, whereas sufficient clearance space might have saved it. As has been stated, shock losses occur at entrance to the guide vanes, due to the decrease of cross section, just as at the entrance to the impeller. Let w_l be the velocity at entrance to the guide channel, a_l the height of channel at the beginning of guide vanes, and s_l the

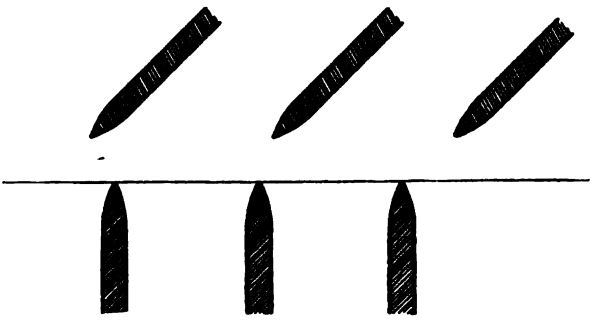

Fig. 16.

thickness of the vanes. No further proof is necessary to show that as before,

$$w_l = w_a' \frac{a_l + s_l}{a_l} \quad \ldots\ldots\ldots \quad 18$$

This shock loss may be minimized by making the guide vanes as thin as possible and sharpening them decidedly at the entrance as previously described for the impeller blades.

A part of the friction head $\rho_d H_n$ is lost by the water in flowing through the guide vanes. The object of the guide vanes is to change the absolute exit velocity w_a into a smaller velocity which should equal, if possible, the velocity of flow in the casing surrounding the guide vanes. In other words, by the aid of guide vanes as much as possible of the velocity head $\frac{w_a^2}{2g}$ should be changed into pressure. The diminution of velocity must occur gradually. The guide channels should be constructed with an easy divergence of cross section and be of sufficient length, and what was said regarding the impeller channels is also true of the guide channels (see Fig. 13). To decrease the friction coefficient the guide vanes must be made very smooth. Their proper shape will be taken up later.

If guide vanes are not used the friction and shock losses mentioned above do not exist, but greater losses take place, because the change from velocity w_a to w_d occurs in an open space and therefore suddenly. The velocity w_a in changing to the velocity w_d in the casing must also choose its own path. The decrease of velocity, hence the change into pressure, will not occur gradually as when guide vanes are used. Experiments prove that the shock losses thus occurring are larger than the losses in the guide vanes.

(*d*). *Losses in Guide Vane Casing.*

Generally the water on leaving the guide vanes is carried by the casing surrounding them to the outlet or pressure pipe. The second part of the friction head $\rho_d H_n$ is consumed by the water in passing through the guide vane casing. The magnitude of this loss is dependent upon the shape of the casing. The best form is the so-called spiral casing (Fig. 6). With guide vanes of correct form the water can enter the spiral casing at a proper velocity and direction of flow, thereby reducing the shock losses. When using the round casing (Fig. 7), which is a cheaper construction, care must be taken to have the casing of sufficient size, for in such a casing it is necessary that the water flowing from the guide vanes find its own direction of flow. This causes a loss due to eddy currents thus formed. A round casing placed eccentrically about the guide vanes is incorrect and must be avoided. In the narrow part intense shock and eddy current losses occur because a sudden division of the direction of flow towards either side is set up at this point.

5. Pressure Difference in the Clearance Space and Clearance Space Losses

Besides the losses due to shock and friction there is another loss which influences the efficiency more or less. It is the so-called clearance space loss. When the pump is operating there is, as has been shown, a pressure h_a at point a between the impeller and guide vanes and a pressure h_s at point s (Fig. 9). Generally the pressure h_a is greater than h_s. Their difference, H_{sp}, is called the pressure difference in the clearance space. Strictly, point a' instead of point a should be taken in the calculation for H_{sp}, so that the velocity w_a' as derived in equation 17 should be used instead of the velocity w_a.

The error made in considering $w_a = w_a'$ is, however, small, that is, the thickness of the blades is neglected. This assumption is made in order to keep the equations in as simple a form as possible. The pressure difference in the clearance space can therefore be expressed as

$$H_{sp} = h_a - h_s \quad \ldots\ldots\ldots \quad 19$$

From Fig. 9 it can be seen that

$$h_a = h_d + \alpha H_n + \rho_d H_n + \rho_l H_n - \frac{w_a^2}{2g} \quad \ldots\ldots \quad 20$$

Further,

$$h_s = h_w - \rho_s H_n - \frac{w_s^2}{2g} \quad \ldots\ldots\ldots \quad 21$$

The values of h_a and h_s substituted in equation 19 give

$$H_{sp} = h_d - h_w + H_n(\alpha + \rho_d + \rho_l + \rho_s) + \frac{w_s^2}{2g} - \frac{w_a^2}{2g} \quad \ldots \quad 22$$

Assume $$\frac{w_s^2}{2g} = (\rho_a + \rho_s) H_n,$$

which is approximately true. Considering equations 9 and 11 and substituting the value $H_n = h_d - h_w$ from equation 7, equation 22 becomes

$$H_{sp} = \eta H_n - \frac{w_a^2}{2g} \quad \ldots\ldots\ldots \quad 23$$

The water will flow through the clearance space between impeller rim and casing back to the suction pipe. Let ξ_a be the velocity coefficient and w_{sp} the velocity of the water in this clearance space. Then

$$w_{sp} = \xi_a \sqrt{2g\eta H_n - w_a^2} \quad \ldots\ldots\ldots \quad 24$$

If i is the amount of clearance between casing and rim of impeller, the clearance area f_a is approximately

$$f_a = D_a \pi i \quad \ldots\ldots\ldots \quad 25$$

The quantity of water passing through this space is $Q_{sp} = D_a \pi i w_{sp}$. The substitution of the value for w_{sp} from equation 24 in this equation gives

$$Q_{sp} = D_a \pi i \xi_a \sqrt{2\eta g H_n - w_a^2} \quad \ldots\ldots \quad 26$$

An axial thrust occurs because the pressure on the side of the impeller opposite the suction pipe is greater than that in the pipe. In order to neutralize this thrust, holes connecting the two spaces are often provided in the impeller. Such an arrangement, of course, sacrifices efficiency, for the quantity of short-circuited water flowing through the clearance space to the suction pipe is doubled or equals $2\,Q_{sp}$.

By the arrangement of suitable rims or rings the space through which leakage can occur is made as small as possible. This decreases the coefficient ξ_a. The design of such rims will now be discussed.

Many pumps are designed with a very close clearance between the rotating impeller and the suction pipe connection, so that the water after passing through a clearance space i_a at diameter D_a (Fig. 17) must also flow through a clearance space i_i at diameter D_i. This small clearance is obtained by suitable rims or rings cast on the impeller and suction pipe connection. In order to avoid axial thrust it is necessary to have a similar clearance between impeller and casing on the opposite side of the impeller at the same diameter D_i.

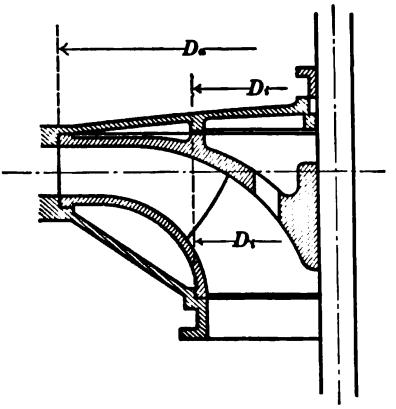

Fig. 17.

The quantity of water short-circuited is determined as follows:

Let f_a be the outer clearance area, f_i the inner clearance area, H_{spi} the pressure existing in the space between the rims at diameters D_a and D_i, w_{spa} the velocity of flow at D_a, w_{spi} the velocity of flow at D_i, and ξ_a, ξ_i the corresponding velocity coefficients. The following condition equation may now be written:

$$Q_{sp} = f_a w_{spa} = f_i w_{spi} \quad . \quad . \quad . \quad . \quad . \quad . \quad . \quad 27$$

Further,

$$w_{spa} = \xi_a \sqrt{2\,g\,(H_{spa} - H_{spi})} \quad . \quad . \quad . \quad . \quad . \quad 28$$

and

$$w_{spi} = \xi_i \sqrt{2\,g H_{spi}} \quad . \quad . \quad . \quad . \quad . \quad . \quad . \quad 29$$

The values of w_{spa} and w_{spi} placed in equation 27 give

$$H_{spi} = \frac{H_{spa}}{1 + \frac{\xi_i^2 f_i^2}{\xi_a^2 f_a^2}}.$$

Substitute for H_{spa} its value from equation 23, and as $\xi_a = \xi_i$ it follows that

$$H_{spi} = \frac{\eta H_n - \frac{w_a^2}{2g}}{1 + \left(\frac{f_i}{f_a}\right)^2} \quad \ldots\ldots\ldots \quad 30$$

This value for H_{spi} substituted in equation 29 gives the velocity of flow existing in the inner clearance space and is

$$w_{spi} = \xi_i \sqrt{\frac{2\eta g H_n - w_a^2}{1 + \left(\frac{f_i}{f_a}\right)^2}} \quad \ldots\ldots\ldots \quad 31$$

and the quantity of water flowing through this clearance space is

$$Q_{sp} = f_i \xi_i \sqrt{\frac{2\eta g H_n - w_a^2}{1 + \left(\frac{f_i}{f_a}\right)^2}} \quad \ldots\ldots\ldots \quad 32$$

The velocity of flow existing in the outer clearance space is therefore only

$$w_{spa} = \xi_a \sqrt{(2\eta g H_n - w_a^2)\left(1 - \frac{1}{1 + \left(\frac{f_i}{f_a}\right)^2}\right)} \quad \ldots \quad 33$$

and the quantity flowing through the outer clearance space is

$$Q_{sp} = f_a \xi_a \sqrt{(2\eta g H_n - w_a^2)\left(1 - \frac{1}{1 + \left(\frac{f_i}{f_a}\right)^2}\right)}. \quad \ldots \quad 34$$

Hence by using two small clearance spaces the quantity of short-circuited water can be considerably decreased.

The rotation of the water between the impeller and casing also aids in decreasing the short-circuit loss. Assuming frictionless

operation, centrifugal force would create a rotating paraboloid having a head of $\frac{w_a^2}{2g}$ at diameter D_a. On account of the friction of the water against the walls and the individual water particles amongst themselves, the water will not rotate with the full peripheral velocity of the impeller; consequently the rotating paraboloid cannot reach its full head. Assume, on account of friction losses, that the water rotates with a velocity of only ϕu_a and let h_R be the head of the rotating paraboloid at diameter D_a. Then

$$h_R = \phi^2 \frac{w_a^2}{2g} \quad . \quad . \quad . \quad . \quad . \quad . \quad . \quad . \quad 35$$

This pressure h_R is opposed to the pressure H_{sp}. If only one clearance ring is used and the rotating paraboloid is taken account of, there will be a difference of pressure in the clearance space of

$$H_{spa} = \eta H_n - \frac{w_a^2}{2g} - \phi^2 \frac{u_a^2}{2g} \quad . \quad . \quad . \quad . \quad . \quad . \quad 36$$

Hence the velocity of water passing through the clearance space is

$$w_{sp} = \xi_a \sqrt{2g\eta H_n - w_a^2 - \phi^2 u_a^2} \quad . \quad . \quad . \quad . \quad . \quad 37$$

and the quantity of water is

$$Q_{sp} = f_a \xi_a \sqrt{2g\eta H_n - w_a^2 - \phi^2 u_a^2} \quad . \quad . \quad . \quad . \quad . \quad 38$$

Using two clearance rings and considering the rotating paraboloids, the quantity of water flowing through the clearance spaces may be obtained as follows:

Again assume that the rotating paraboloid rotates with a peripheral velocity of ϕu. Then there will be a difference of pressure between a point at diameter D_a and a point at diameter D_i of $\phi^2\left(\frac{u_a^2 - u_i^2}{2g}\right)$.

The difference of pressure H_{spa} will now have only the value

$$H_{spa} = \eta H_n - \frac{w_a^2}{2g} - \left(H_{spi} + \phi^2 \frac{u_a^2 - u_i^2}{2g}\right). \quad . \quad . \quad . \quad 39$$

As before, the condition equation may be written,

$$Q_{sp} = w_{spa} f_a = w_{spi} f_i \quad . \quad . \quad . \quad . \quad . \quad . \quad . \quad (27)$$

Considering equation 39, the velocity w_{spa} is found to be

$$w_{spa} = \sqrt{2g\left(\eta H_n - \frac{w_a^2}{2g} - H_{spi} - \phi^2 \frac{u_a^2 - u_i^2}{2g}\right)} \quad . \quad . \quad 40$$

The quantity of water expressed in terms of diameter D_a is found from equations 27 and 40 to be

$$Q_{spa} = f_a \xi_a \sqrt{\left[2g\eta H_n - w_a^2 - \phi^2 (u_a^2 - u_i^2)\right]\left(1 - \frac{1}{1 + \left(\frac{f_i}{f_a}\right)^2}\right)} \quad . \quad 41$$

and expressed in terms of diameter D_i is found to be

$$Q_{spi} = f_i \xi_i \sqrt{\frac{2g\eta H_n - w_a^2 - \phi^2 (u_a^2 - u_i^2)}{1 + \left(\frac{f_i}{f_a}\right)^2}} \quad . \quad . \quad 42$$

In determining the dimensions of the impeller the quantity of short-circuited water must be taken into account because this water passes through the impeller. It is therefore necessary to design the impeller for a quantity of water Q', the value of which is

$$Q' = Q + Q_{sp} \quad . \quad . \quad . \quad . \quad . \quad . \quad . \quad . \quad 43$$

As can be seen from these derived equations, the short-circuited water depends upon the value of the clearance areas f_a and f_i; the velocity coefficient ξ, which decreases with decreasing clearance; and, if the rotating paraboloid is also considered, upon the coefficient ϕ.

The rotation of H_{sp} and the clearance space losses to the peripheral velocity u_a and the angles β_a and δ_a will be discussed in Article 9.

6. Dimensions of the Suction Pipe.

From the desired quantity of water Q and an assumed suction pipe velocity w_s the clear area of cross section F_s of the suction pipe can be determined as follows:

$$F_s = \frac{Q}{w_s} \quad . \quad . \quad . \quad . \quad . \quad . \quad . \quad . \quad 44$$

and the suction pipe diameter D_s is found from

$$D_s = \sqrt{\frac{Q}{w_s}\frac{4}{\pi}} \quad . \quad . \quad . \quad . \quad . \quad . \quad . \quad . \quad 45$$

The value of the velocity w_s through the suction pipe depends upon the desired quantity of water Q and the desired head H_n. It is best to take the velocity head $\frac{w_s^2}{2g}$ as a certain fraction γ of the total head ηH_n, so that

$$\frac{w_s^2}{2g} = \gamma \eta H_n \quad . \quad . \quad . \quad . \quad . \quad . \quad . \quad . \quad 46$$

or

$$w_s = \sqrt{2\gamma\eta g H_n} \quad . \quad . \quad . \quad . \quad . \quad . \quad . \quad 47$$

The value of the coefficient γ is dependent on the total head H_n and the desired quantity of water. With low-pressure pumps having low heads and large quantities of water γ is taken as 0.08 and sometimes greater, while with high-pressure pumps having large heads and small quantities of water γ equals 0.01 and at times still less.

The coefficient γ is of great importance when it is desired to compare a pump of new design with existing pumps.

Substituting from equation 47 the value of w_s in equation 44,

$$Q = F_s \sqrt{2\gamma\eta g H_n} \quad . \quad . \quad . \quad . \quad . \quad . \quad 48$$

or

$$\frac{Q}{\sqrt{\eta H_n}} = F_s \sqrt{2\gamma g} = K \quad . \quad . \quad . \quad . \quad . \quad . \quad 49$$

The value K will be called the characteristic of centrifugal pumps. A pump already designed can be used for all desired heads and quantities of water for which the expression $\frac{Q}{\sqrt{\eta H_n}}$ remains the same, that is, has the same value of K (see Article 30).

Equation 46 can also be written,

$$w_s^2 = 2\gamma\eta g H_n = C H_n \quad . \quad . \quad . \quad . \quad . \quad . \quad 50$$

This is the equation of a parabola. The suction pipe velocity w_s will therefore increase for equal values of γ and for different desired heads according to a parabola. Fig. 18 shows such a velocity parabola for $\gamma = 0.02$.

The atmospheric pressure A permits theoretically the use of a suction head h_{se} of about 32.8 feet, so that, considering the velocity head $\frac{w_{se}^2}{2g}$ and a friction head $\rho_{se}H_n$,

$$h_{se} + \frac{w_{se}^2}{2g} + \rho_{se}H_n \leqq A.$$

However, the water contains more or less air, and it is therefore advisable to take

$$h_{se} + \frac{w_{se}^2}{2g} + \rho_{se}H_n < 23 \text{ feet}.$$

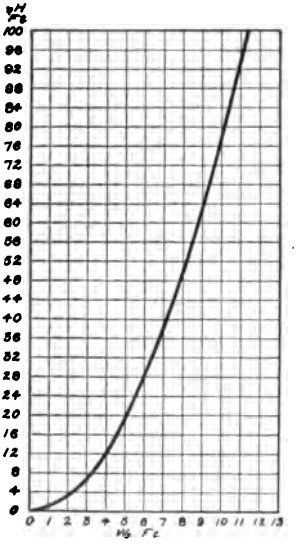

Fig. 18.

7. Determination of the Exit Dimensions for $\delta_e = 90°$.

The second form of the fundamental equation as already derived is

$$u_a w_a \cos\delta_a - u_e w_e \cos\delta_e = \eta g H_n \quad . \quad (15)$$

Let the absolute entrance velocity w_e be taken at right angles to u_e, with which assumption the member $u_e w_e \cos\delta_e = 0$, because $\delta_e = 90°$; so that equation 15 becomes

$$u_a w_a \cos\delta_a = \eta g H_n \quad . \quad . \quad . \quad . \quad . \quad . \quad . \quad 51$$

or

$$\cos\delta_a = \frac{\eta g H_n}{u_a w_a} \quad . \quad . \quad . \quad . \quad . \quad . \quad . \quad . \quad 52$$

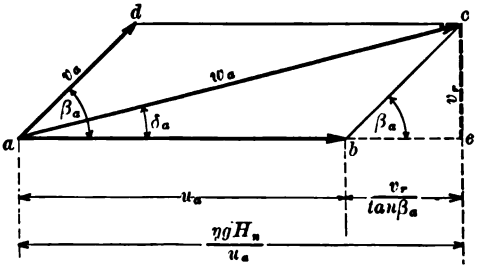

Fig. 19.

From Fig. 19, which represents the exit velocity diagram of a low-speed pump, $\beta_a < 90°$, and

$$\cos\delta_a = \frac{\overline{ae}}{w_a} \quad . \quad . \quad . \quad . \quad . \quad . \quad . \quad . \quad 53$$

Substituting 53 in 52 gives

$$\overline{ae} = \frac{\eta g H_n}{u_a} \quad \ldots\ldots\ldots \quad 54$$

This equation could also be obtained from Fig. 20, which is the velocity diagram of a high-speed pump, where $\beta_a > 90°$. In Fig. 19

$$\overline{be} = \frac{v_r}{\tan \beta_a} \quad \ldots\ldots\ldots \quad 55a$$

or in Fig. 20

$$\overline{be} = -\frac{v_r}{\tan \beta_a} \quad \ldots\ldots\ldots \quad 55b$$

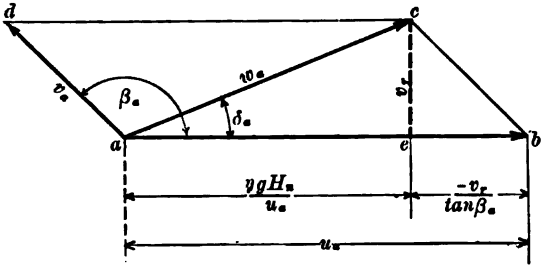

Fig. 20.

The vertical component of the relative exit velocity v_a is v_r. From Fig. 19

$$u_a = \overline{ae} - \overline{be} \quad \ldots\ldots\ldots \quad 56a$$

or from Fig. 20

$$u_a = \overline{ae} + \overline{be} \quad \ldots\ldots\ldots \quad 56b$$

Placing in equations 56a and 56b the value $\overline{ae}$ from equation 54 and the value for $\overline{be}$ from equations 55a and 55b, it follows that

$$u_a = \frac{\eta g H_n}{u_a} - \frac{v_r}{\tan \beta_a} \quad \ldots\ldots\ldots \quad 57$$

Multiplying both sides of the equation by u_a and then adding to both sides of the equation $\left(\frac{v_r}{2 \tan \beta_a}\right)^2$ we have

$$u_a^2 + \left(\frac{v_r}{2 \tan \beta_a}\right)^2 = \eta g H_n - \frac{u_a v_r}{\tan \beta_a} + \left(\frac{v_r}{2 \tan \beta_a}\right)^2,$$

or

$$u_a^2 + \frac{u_a v_r}{\tan \beta_a} + \left(\frac{v_r}{2 \tan \beta_a}\right)^2 = \eta g H_n + \left(\frac{v_r}{2 \tan \beta_a}\right)^2,$$

or

$$u_a + \frac{v_r}{2 \tan \beta_a} = \sqrt{\eta g H_n + \left(\frac{v_r}{2 \tan \beta_a}\right)^2};$$

therefore

$$u_a = -\frac{v_r}{2 \tan \beta_a} + \sqrt{\left(\frac{v_r}{2 \tan \beta_a}\right)^2 + \eta g H_n} \quad . \quad . \quad . \quad . \quad 58$$

Then for $\beta_a = 90°$

$$u_{a\,90°} = \sqrt{\eta g H_n} \quad . \quad . \quad . \quad . \quad . \quad . \quad . \quad 59$$

Attention is called to the fact that in the future all similar values which refer to a velocity diagram having $\beta_a = 90°$ will have the subscript "90°."

With a given head and after assuming the velocity v_r, which can be called the radial exit velocity, the peripheral velocity can be determined from equation 58 for any impeller angle β_a.

A function of the guide vane angle δ_a can be substituted for v_r in equation 57. From Fig. 19 or 20 the following equation may be written:

$$\tan \delta_a = \frac{v_r u_a}{\eta g H_n} \quad . \quad . \quad . \quad . \quad . \quad . \quad . \quad 60$$

or

$$v_r = \tan \delta_a \frac{\eta g H_n}{u_a} \quad . \quad . \quad . \quad . \quad . \quad . \quad 61$$

If the value of u_a from equation 59 is substituted in equation 61 and β_a is taken equal to 90°, equation 61 becomes

$$v_r = \tan \delta_{a\,90°} \sqrt{\eta g H_n} = v_{a\,90°} \quad . \quad . \quad . \quad . \quad . \quad 62$$

The value of v_r from equation 61 placed in equation 57 gives

$$u_a = \sqrt{\eta g H_n \left(1 - \frac{\tan \delta_a}{\tan \beta_a}\right)} \quad . \quad . \quad . \quad . \quad . \quad 63$$

From these equations, after assuming β_a and δ_a, the peripheral velocity u_a can be calculated. The value v_r can then be determined from equation 61.

If the peripheral velocity u_a is fixed by the outer impeller diameter

D_a and the r.p.m., the angle β_a can be calculated by assuming v_r and solving equation 57 for tan β_a, thus:

$$\tan \beta_a = \frac{v_r}{\frac{\eta g H_n}{u_a} - u_a} \quad . \quad . \quad . \quad . \quad . \quad . \quad . \quad 64$$

or by assuming δ_a and solving equation 63 for tan β_a we find

$$\tan \beta_a = \frac{\tan \delta_a}{1 - \frac{u_a^2}{\eta g H_n}} \quad . \quad . \quad . \quad . \quad . \quad . \quad . \quad 65$$

If the peripheral velocity and the outer impeller diameter D_a are given, the revolutions per minute n are found from the equation

$$n = \frac{u_a 60}{D_a \pi} \quad . \quad . \quad . \quad . \quad . \quad . \quad . \quad . \quad 66$$

or by assuming n and D_a the peripheral velocity is

$$u_a = \frac{D_a \pi n}{60} \quad . \quad . \quad . \quad . \quad . \quad . \quad . \quad . \quad 67$$

or by assuming n and u_a the impeller diameter is

$$D_a = \frac{u_a 60}{n \pi} \quad . \quad . \quad . \quad . \quad . \quad . \quad . \quad . \quad 68$$

The value of the relative exit velocity v_a is

$$v_a = \frac{v_r}{\sin \beta_a} \quad . \quad . \quad . \quad . \quad . \quad . \quad . \quad . \quad 69$$

or substituting the angle function of δ_a from equation 61 we get

$$v_a = \frac{\tan \delta_a \eta g H_n}{\sin \beta_a u_a} \quad . \quad . \quad . \quad . \quad . \quad . \quad . \quad 70$$

From Figs. 19 and 20 it can be seen that the value of the absolute exit velocity w_a is

$$w_a = \sqrt{v_r^2 + \left(\frac{\eta g H_n}{u_a}\right)^2} \quad . \quad . \quad . \quad . \quad . \quad . \quad . \quad 71$$

or it may be obtained from equation 52 thus:

$$w_a = \frac{\eta g H_n}{u_a \cos \delta_a} \quad . \quad . \quad . \quad . \quad . \quad . \quad . \quad . \quad 72$$

If the peripheral velocity is not known, w_a is calculated from equations 63 and 72 by assuming β_a and δ_a. As $\frac{1}{\cos^2 \delta_a} = \sec^2 \delta_a = 1 + \tan^2 \delta_a$, equations 63 and 72 give

$$w_a = \sqrt{\frac{\eta g H_n (1 + \tan^2 \delta_a)}{1 - \frac{\tan \delta_a}{\tan \beta_a}}} \quad \ldots \ldots \quad 73$$

The impeller width b_a is determined when the radial exit velocity v_r is assumed, for

$$D_a \pi b_a v_r = Q \quad \ldots \ldots \quad 74$$

or

$$b_a = \frac{Q}{D_a \pi v_r} \quad \ldots \ldots \quad 75$$

If instead of v_r the angle δ_a is used then b_a is found by substituting the value of v_r from equation 61 in equation 75, with the result that

$$b_a = \frac{Q u_a}{D_a \pi \eta g H_n \tan \delta_a} \quad \ldots \ldots \quad 76$$

and then from equation 75 v_r can be found as

$$v_r = \frac{Q}{D_a \pi b_a} \quad \ldots \ldots \quad 77$$

As stated before, these equations for the exit dimensions are valid only when $\delta_e = 90°$, that is, when the absolute entrance velocity w_e is perpendicular to u_e. In the following up to Article 14 δ_e is taken equal to 90°. In Article 14 and subsequent chapters equations are derived for the determination of the exit dimensions for any direction of the absolute entrance velocity, that is, when $\delta_e \lesseqgtr 90°$.

8. Influence of the Impeller and Guide Vane Angles upon the Peripheral Velocity.

In the previous chapter two equations were derived for the peripheral velocity:

I. $$u_a = -\frac{v_r}{2 \tan \beta_a} + \sqrt{\left(\frac{v_r}{2 \tan \beta_a}\right)^2 + \eta g H_n} \quad \ldots \quad (58)$$

II. $$u_a = \sqrt{\eta g H_n \left(1 - \frac{\tan \delta_a}{\tan \beta_a}\right)} \quad \ldots \ldots \quad (63)$$

The first equation can be called the equation of peripheral velocities for similar impeller profiles, for after assuming the radial exit velocity v_r the outer impeller profile is determined for any given diameter D_a. In this equation u_a is dependent upon β_a and v_r. For v_r the angle $\delta_{a\,90°}$ from equation 62 may be substituted, so that u_a is also dependent upon β_a and $\delta_{a\,90°}$. The angle δ_a varies with u_a.

Equation II is the equation of peripheral velocities for impellers of dissimilar profiles. For, with constant angle δ_a and the same impeller diameter D_a the impeller width b_a, and hence the impeller profile, change with varying u_a. In this equation u_a is dependent upon β_a and δ_a.

Equation I is the more useful, because for a certain profile the peripheral velocity can be determined by assuming β_a, while with equation II this cannot be done directly.

Because of its greater usefulness equation I will be more closely examined and the course of the curve for peripheral velocities as derived from this equation will be investigated.

There are three characteristic points for the u_a curve as given by equation 58:

1. When $\beta_a = 0$, u_a will equal 0, that is, the u_a curve passes through the origin of the coördinate system.

2. When $\beta_a = 180°$, for which angle $u_a = \infty$, the curve becomes asymptotic with an angle of slope of 90°.

3. When $\beta_a = 90°$ the curve has a point of inflection, and the angle of the tangent at this point is

$$\tan \phi = \frac{v_r}{2} \quad . \quad . \quad . \quad . \quad . \quad . \quad . \quad . \quad . \quad 78$$

or, substituting the value of v_r from equation 62,

$$\tan \phi = \frac{\tan \delta_{a\,90°} \sqrt{\eta g H_n}}{2} \quad . \quad . \quad . \quad . \quad . \quad . \quad 79$$

The subtangent S at the inflection point is

$$S = \frac{2 \sqrt{\eta g H_n}}{v_r} \quad . \quad . \quad . \quad . \quad . \quad . \quad . \quad . \quad 80$$

or substituting for v_r the angle function of $\delta_{a\,90°}$,

$$S = 2 \operatorname{cotan} \delta_{a\,90°} \quad . \quad . \quad . \quad . \quad . \quad . \quad . \quad . \quad 81$$

Equation 59 shows that the peripheral velocity is independent of v_r or δ_a when $\beta_a = 90°$; hence the ordinate at the point of inflection has the same value for every v_r or $\delta_{a\,90°}$, provided, of course, equal heads are assumed. Three u_a curves and their tangents at the point of inflection are drawn in Fig. 21 for the assumption

$$\sqrt{\eta g H_n} = 10 \text{ feet.}$$

For various assumed values of δ_a calculation gives:

I.	$\delta_{a\,90°} = 5°$	$v_r = 0.876$ foot	$\phi = 23° 40'$.
II.	$\delta_{a\,90°} = 15°$	$v_r = 2.68$ feet	$\phi = 53° 20'$.
III.	$\delta_{a\,90°} = 25°$	$v_r = 4.672$ feet	$\phi = 66° 50'$.

The tangents at the point of inflection clearly show the direction of the u_a curves at that point (Fig. 21).

It can be seen from equations 78 and 79 that the tangent of the angle ϕ is directly proportional to v_r and tan $\delta_{a\,90°}$. Hence the angle ϕ increases or decreases with v_r and tan $\delta_{a\,90°}$ respectively.

While the u_a curves are concave towards the base line from $\beta_a = 0$ to $\beta_a = 90°$ they are convex from $\beta_a = 90°$ to $\beta_a = 180°$. Hence with increasing v_r or $\delta_{a\,90°}$ between $\beta_a = 90°$ and $\beta_a = 0$, the peripheral velocity decreases, and from $\beta_a = 90°$ to $\beta_a = 180°$ it increases.

In high-pressure centrifugal pumps we are forced to make the velocity v_r, and therefore the angle δ_a, small in order to get the impeller width b_a as large as possible. With a small guide vane angle $\delta_a = 5°$ to $10°$, as is usual in high-pressure pumps, it can be seen from the course of the u_a curves that an increase or decrease of the impeller angle β_a has very little influence upon the peripheral velocity, at least within the useful limits.

In low-pressure pumps the guide vane angle δ_a varies widely up to 35°. If a high-speed pump is to be designed, the angle δ_a should be taken as large as possible compared to the angle β_a.

9. Influence of the Impeller and Guide Vane Angles upon the Pressure Difference and Short-circuit Loss of the Clearance Space.

From equation 23, the pressure difference in the clearance space, without considering the rotating paraboloid, is

$$H_{spa} = \eta H_n - \frac{w_a^2}{2g}.$$

Substituting the value for w_a from equation 73, the above equation becomes

$$H_{spa} = \eta H_n \left(1 - \frac{1 + \tan^2 \delta_a}{2\left(1 - \frac{\tan \delta_a}{\tan \beta_a}\right)}\right) \quad . \quad 82$$

The value of the pressure difference is therefore dependent upon β_a and δ_a, increasing with greater values of β_a and δ_a and vice versa. To show this relation clearly, three pressure difference curves are drawn in Fig. 22, assuming as before $\sqrt{\eta g H_n} = 10$ feet. These curves are for $\delta_{a\,90°} = 5°$, 15°, 25°, and are marked H_{sp}.

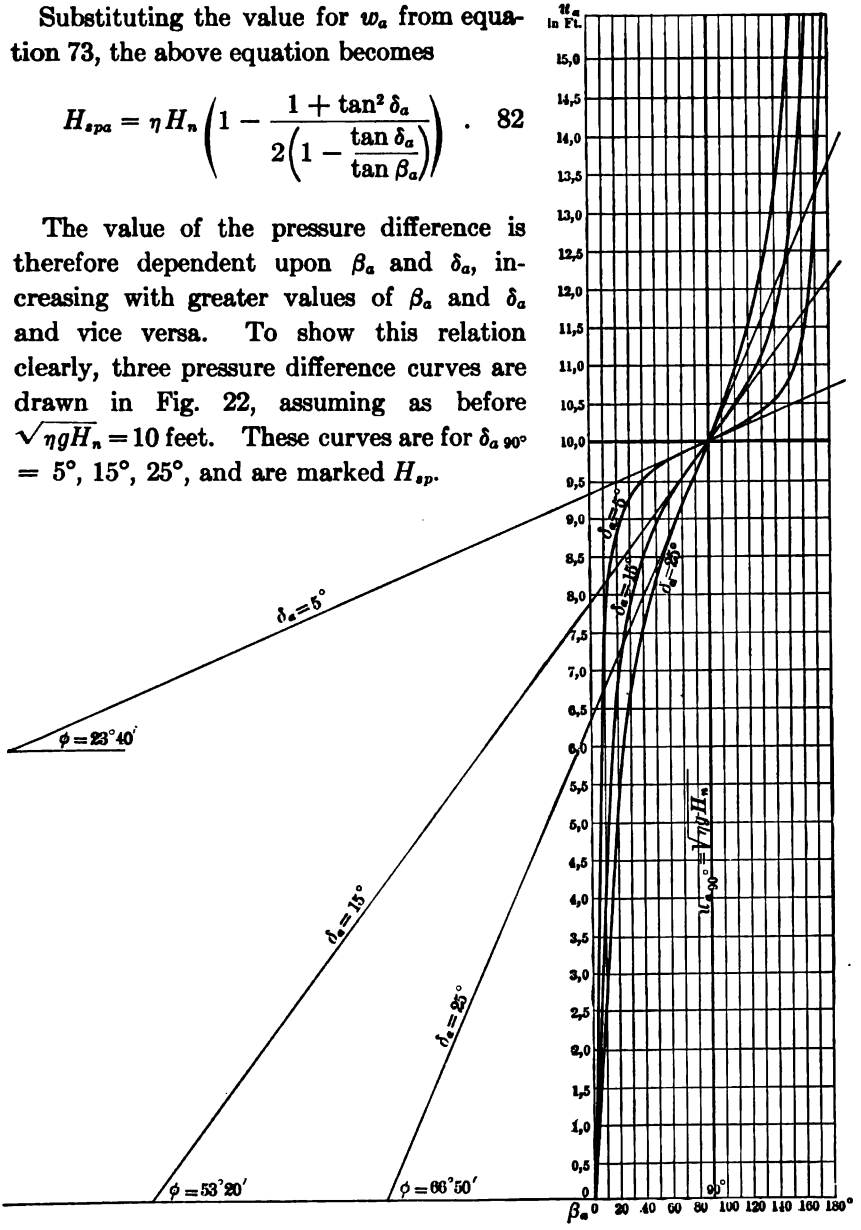

Fig. 21.

It has already been shown (equation 35) that the decrease of pressure difference due to the rotating paraboloid is approximately

$\frac{\phi^2 u_a^2}{2g}$. Assume that the rotating paraboloid revolves with a velocity $\frac{u}{2}$; hence $\phi = \frac{1}{2}$ and

$$\phi^2 \frac{u_a^2}{2g} = \frac{u_a^2}{8g} \quad . \quad . \quad . \quad . \quad . \quad . \quad . \quad . \quad 83$$

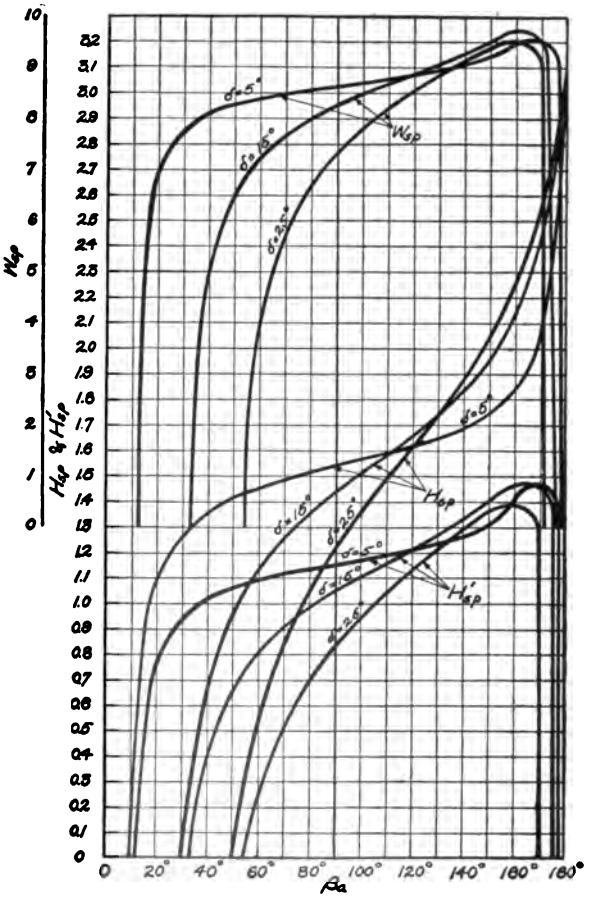

Fig. 22.

Considering these values, a second series of pressure difference curves are drawn in Fig. 22 by subtracting the value of $\frac{u_a^2}{8g}$ from the curves first found. Therefore for $\phi = \frac{1}{2}$ these curves are in accordance with the equation

$$H_{spa}' = \eta H_n \left(1 - \frac{1 + \tan^2 \delta_a}{2\left(1 - \frac{\tan \delta_a}{\tan \beta_a}\right)} - \frac{1 - \frac{\tan \delta_a}{\tan \beta_a}}{8} \right) \quad . \quad . \quad 84$$

Fig. 22 shows also the theoretical velocities with which the water flows through the clearance space, due to the pressure difference. Under the assumption of $\xi_a = 1$ and $\phi = \frac{1}{2}$ the velocity is

$$w_{spa}' = \sqrt{2\,\eta g H_n \left(1 - \frac{1 + \tan^2 \delta_a}{2\left(1 - \frac{\tan \delta_a}{\tan \beta_a}\right)} - \frac{1 - \frac{\tan \delta_a}{\tan \beta_a}}{8} \right)} \quad . \quad 85$$

The pressure in the clearance space will equal 0 when

$$\frac{1 + \tan^2 \delta_a}{2\left(1 - \frac{\tan \delta_a}{\tan \beta_a}\right)} - \frac{1 - \frac{\tan \delta_a}{\tan \beta_a}}{8} = 1.$$

If this expression is greater than 1, the pressure in the clearance space becomes negative, that is, the short-circuited water will flow in the reverse direction or from the suction tube to the impeller exit.

For $\beta_a = 90°$ equation 85 becomes

$$w_{spa\,90°}' = \sqrt{2\,\eta g H_n \left(1 - \frac{1 + \tan^2 \delta_{a\,90°}}{2} - \frac{1}{8} \right)} \quad . \quad . \quad . \quad 86$$

As the velocity coefficient is taken the same for all velocities, the latter are directly proportional to the quantity of short-circuited water. Therefore by choosing a proper scale the velocity curves w_{spa}' represent the quantity of short-circuited water. These considerations give a very clear idea of the influence which the angles β_a and δ_a have upon the quantity of short-circuited water.

With small guide angles, $\delta_a = 5°$ to $10°$, such as are used with high-pressure pumps, the quantity of short-circuited water for high- and low-speed impellers will remain approximately the same between very wide limits; further, the short-circuit losses are not greatly decreased by decreasing the angle β_a.

With a larger guide angle δ_a, such as is used for low-pressure centrifugal pumps, the quantity of short-circuited water varies greatly, depending upon whether the impeller is low or high speed. For instance, if the quantity of short-circuited water is equal to 1.0 for $\delta_a = 25°$ with $\beta_a = 90°$, then it is only 0.39 when $\beta_a = 45°$ and for $\beta_a = 135°$ it is 1.2.

When investigating the influence of the short-circuit loss upon pump efficiency, it is necessary to express the quantity of short-circuited water in per cent of the total quantity desired. The larger the ratio of outer diameter D_a to quantity of water desired, the larger will be the quantity short-circuited when expressed in per cent of the quantity desired. This percentage, for the same values of ηH_n, β_a, and δ_a, is inversely proportional to the quantity of water desired. If, for instance, a pump delivering 100 gallons has a short-circuit loss of 3 per cent thereof, that is, a short-circuited quantity of 3 gallons, then a pump with the same clearance and values of D_a, β_a, and δ_a, and delivering only 50 gallons, has also a short-circuit loss of 3 gallons; still it is no longer 3 per cent, but 3 per cent $\times \frac{100}{50} =$ 6 per cent of the quantity desired.

The ratio $\frac{D_a}{Q}$ is generally smaller with low-pressure than with high-pressure pumps, and therefore the short-circuit loss, referred to the quantity delivered, is greater with high-pressure than with low-pressure pumps.

It is for this reason that the clearance space in high-pressure pumps must be brought to a minimum. This is best accomplished, as already described, by the so-called clearance rim or ring. The rim is often grooved and tongued (Fig. 23). This arrangement,

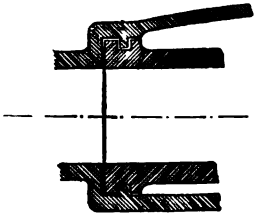

Fig. 23.

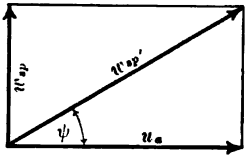

Fig. 24.

however, does not decrease the loss to any great extent, for the direction of the velocity of the short-circuited water is not axial

but combines with the peripheral velocity in producing a resultant velocity w_{sp}' the value of which is (Fig. 24)

$$w_{sp}' = \sqrt{w_{sp}^2 + u_a^2} \quad . \quad . \quad . \quad . \quad . \quad . \quad . \quad . \quad 87$$

The direction of this velocity forms the angle ψ with u_a, so that

$$\tan \psi = \frac{w_{sp}}{u_a} \quad . \quad . \quad . \quad . \quad . \quad . \quad . \quad . \quad . \quad 88$$

A very clever device for decreasing the clearance space is shown in the German patent 142214. Fig. 25 shows this device, which consists of a loose packing ring D carried by the impeller. Segments of a ring R are so placed that their centrifugal force presses the ring D against the casing and thus reduces the clearance space to a minimum. In German patent 117218, the clearance rim is shown adjustable, which in itself is very good, but this construction greatly increases the cost of the pump.

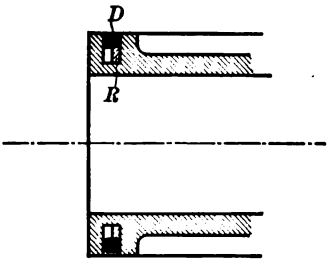

Fig. 25.

Unfortunately, there are no published reports of experiments determining the actual quantity of short-circuited water. Calculations give only very approximate values, because the coefficient of flow is not exactly known and because the clearance is very difficult to measure.

The short-circuited water may be taken as from 4 to 6 per cent of the desired quantity and the impeller calculated for a correspondingly larger quantity.

10. The Angles β_a and δ_a and the Peripheral Velocity of a Centrifugal Pump without Pressure Difference in the Clearance Space.

In the following, for simplicity, the opposing effect of the rotating paraboloid on the pressure difference in the clearance space will not be considered. According to equation 23 the pressure difference will be

$$H_{sp} = \eta H_n - \frac{w_a^2}{2g}.$$

If H_{sp} is taken equal to 0, this equation becomes

$$\eta H_n = \frac{w_a^2}{2g} \quad \ldots\ldots\ldots \quad 89$$

or

$$w_a = \sqrt{2\eta g H_n} \quad \ldots\ldots\ldots \quad 90$$

The velocity head $\frac{w_a^2}{2g}$ represents the entire theoretical pressure head. The action of centrifugal force has been utilized to accelerate the relative entrance velocity v_e to the relative exit velocity v_a. The absolute exit velocity w_a must be transformed entirely into pressure.

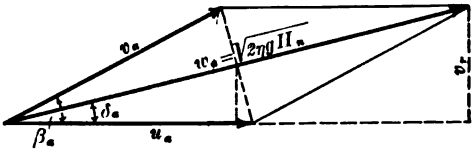

Fig. 26.

From Fig. 26 it can be seen that

$$\sin \delta_a = \frac{v_r}{\sqrt{2\eta g H_n}} \quad \ldots\ldots\ldots \quad 91$$

Substituting the value of v_r from equation 61 in the above gives

$$\sin \delta_a = \frac{\tan \delta_a \eta g H_n}{u_a \sqrt{2\eta g H_n}}.$$

Solving for u_a, we have

$$u_a = \frac{0.5\sqrt{2\eta g H_n}}{\cos \delta_a} \quad \ldots\ldots\ldots \quad 92$$

This equation can also be easily derived from the first fundamental equation. When the absolute entrance velocity w_e is perpendicular to u_e, equation 10 assumes the form

$$u_a^2 - v_a^2 + w_a^2 = 2\eta g H_n \quad \ldots\ldots\ldots \quad 93$$

Then substituting $w_a = \sqrt{2\eta g H_n}$ from equation 90 we have

$$u_a = v_a \quad \ldots\ldots\ldots \quad 94$$

Hence, for the special case of $H_{sp} = 0$, the exit velocity diagram will be a rhombus (Fig. 26). From this figure the former equation can be directly obtained,

$$u_a = \frac{0.5\sqrt{2\eta g H_n}}{\cos \delta_a} = v_a.$$

From the rhombus

$$\beta_a = 2\,\delta_a \quad \ldots\ldots\ldots \quad 95a$$

or

$$\delta_a = \frac{\beta_a}{2} \quad \ldots\ldots\ldots \quad 95b$$

Also

$$\sin \beta_a = \frac{v_r}{u_a} \quad \ldots\ldots\ldots \quad 96a$$

or

$$u_a = \frac{v_r}{\sin \beta_a} = \frac{v_r}{\sin 2\,\delta_a} \quad \ldots\ldots\ldots \quad 96b$$

To derive the peripheral velocity for which $H_{sp} = 0$, calculate from equation 91 the angle δ_a and then from equation 96b the corresponding peripheral velocity u_a.

11. Determination of the Exit Values by Means of κ and λ Curves.

The peripheral velocity u_a from equation 63 is

$$u_a = \sqrt{\eta g H_n}\sqrt{1 - \frac{\tan \delta_a}{\tan \beta_a}}.$$

Let

$$\sqrt{1 - \frac{\tan \delta_a}{\tan \beta_a}} = \kappa \quad \ldots\ldots\ldots \quad 97$$

so that the above equation takes the simple form

$$u_a = \kappa \sqrt{\eta g H_n} \quad \ldots\ldots\ldots \quad 98$$

On Plate I a series of κ curves are shown; the values of κ are calculated for various values of the angles β_a and δ_a. By the aid of these curves various problems can be quickly solved.

For instance, after determining the impeller diameter and prescribing a certain r.p.m. so that the peripheral velocity $u_a = \gtrless \sqrt{\eta g H_n}$,

the coefficient κ may be determined by calculating the necessary peripheral velocity u_a and solving the equation

$$\kappa = \frac{u_a}{\sqrt{\eta g H_n}} \quad . \quad . \quad . \quad . \quad . \quad . \quad . \quad . \quad 99$$

From the κ curves it is possible to read directly which combinations of β_a and δ_a are permissible for the desired peripheral velocity, or by changing the angles β_a and δ_a whether it is possible to obtain the desired r.p.m.

In general, as has already been stated, it is advantageous to assume the radial exit velocity v_r instead of δ_a, or if δ_a is assumed, the value of v_r should immediately be determined; for only after determining v_r and assuming δ_a can the impeller width b_a be determined from equation 75. In order quickly to determine v_r for any given guide vane angle δ_a, or vice versa, the λ curves of Plate I have been drawn. These curves were derived in the following manner:

Equation 62 is

$$v_r = \tan \delta_{a\,90°} \sqrt{\eta g H_n} \quad . \quad . \quad . \quad . \quad . \quad . \quad . \quad (62)$$

Let the velocity head $\frac{v_r^2}{2g}$ be λ times the theoretical head ηH_n, so that

$$v_r = \sqrt{\lambda\, 2\, \eta g H_n} \quad . \quad . \quad . \quad . \quad . \quad . \quad . \quad . \quad 100$$

Substituting this value of v_r in equation 62 we have

$$\tan \delta_{a\,90°} = \sqrt{2\lambda} \quad . \quad . \quad . \quad . \quad . \quad . \quad . \quad . \quad 101$$

or

$$\lambda = 0.5 \tan^2 \delta_{a\,90°} \quad . \quad . \quad . \quad . \quad . \quad . \quad . \quad . \quad 102$$

The λ curve, which according to equation 102 is a parabola, has been calculated for various values of angle δ_a. From this curve plotted for $\beta_a = 90°$, after assuming δ_a, the corresponding value of λ can be read and then v_r determined by solving equation 100. The coefficient λ is independent of the desired head, as shown by equation 102; hence the λ curve may be used for all desired heads.

If v_r is given, λ is calculated from the equation

$$\lambda = \frac{v_r^2}{2\eta g H_n} \quad \ldots\ldots\ldots \quad 103$$

and the angle δ_a corresponding to the coefficient λ can be determined from the curve.

For determining the value of v_r when $\beta_a \gtrless 90°$ the κ curves must also be used. Substituting in equation 61 the value of u_a from equation 98 and the value of $\tan \delta_a$ from 101, the value of v_r is

$$v_r = \frac{\sqrt{\lambda 2\eta g H_n}}{\kappa} \quad \ldots\ldots\ldots \quad 104$$

or solving for λ,

$$\lambda = \frac{v_r^2 \kappa^2}{2\eta g H_n} \quad \ldots\ldots\ldots \quad 105$$

For $\beta_a = 90°$, κ equals 1, and equations 104 and 105 take the form of equations 100 and 103 respectively.

The exit velocity v_r is again calculated by assuming δ_a, or δ_a by assuming v_r, as before explained, but now the coefficient κ must be taken into consideration.

A very simple equation can be derived for the absolute exit velocity w_a, by means of the κ and λ curves as follows:

Substitute the value of v_r from equation 104 and u_a from 98 in equation 71, which becomes

$$w_a = \frac{\sqrt{\eta g H_n}}{\kappa} \sqrt{1 + 2\lambda} \quad \ldots\ldots\ldots \quad 106$$

A very simple construction of the velocity diagram at exit is now possible. In equation 54 substitute the value u_a from equation 98 so that the horizontal component of w_a is

$$\overline{ae} = \frac{\sqrt{\eta g H_n}}{\kappa} \quad \ldots\ldots\ldots \quad 107$$

The three following values, which are easy to calculate, are used in constructing the exit velocity diagram:

1. $$u_a = \sqrt{\eta g H_n} \cdot \kappa.$$

2. $$\overline{ae} = \frac{\sqrt{\eta g H_n}}{\kappa}.$$

3. $$v_r = \frac{\sqrt{\eta g H_n}}{\kappa} \sqrt{2\lambda}.$$

In Fig. 27 $\overline{ab}$ is drawn equal to $u_a = \kappa \sqrt{\eta g H_n}$, and a line parallel to u_a at a distance $v_r = \frac{\sqrt{\eta g H_n}\sqrt{2\lambda}}{\kappa}$. Lay off on $\overline{ab}$ the distance $\overline{ae} = \frac{\sqrt{\eta g H_n}}{\kappa}$ and draw $\overline{ec}$ perpendicular to $\overline{ab}$. Connecting c with a and b and drawing $\overline{ad}$ parallel to $\overline{bc}$, the parallelogram $\overline{abcd}$ gives the desired exit velocity diagram.

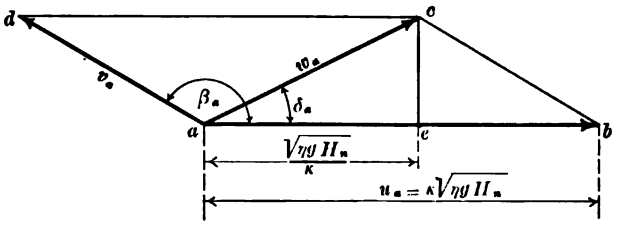

Fig. 27.

When the diagram is derived in this manner, it is well to check the angles β_a and δ_a in order to make sure that no mistake in calculation has occurred. By assuming w_e perpendicular to u_e, that is, $\delta_e = 90°$, and by the aid of the κ and λ curves, every pump can be calculated without the use of a table of trigonometric functions. While great exactness is not obtained by use of the curves, it must be considered that η is more or less arbitrary. The use of these curves will show that they are sufficiently exact.

In order to determine the best dimensions of a pump, it is important to realize that after obtaining κ the curves permit a choice of combinations of β_a and δ_a which is very valuable in obtaining the most advantageous dimensions of a pump.

12. Graphical Determination of the Exit Velocity Diagram.

The following graphical method of determining the exit velocity diagram and thereby u_a can be used for high-pressure pumps because the error inherent in this method is very small for such cases.

Equation 58 is

$$u_a = -\frac{v_r}{2\tan\beta_a} + \sqrt{\left(\frac{v_r}{2\tan\beta_a}\right)^2 + \eta\, g H_n} \quad . \quad . \quad . \quad (58)$$

The member $\left(\frac{v_r}{2\tan\beta_a}\right)^2$ is very small compared to the member $\eta\, g H_n$ and for high-pressure pumps, where β_a is between 45° and 135°, it can be omitted without noticeable error. The above equation then reads

$$u_a = -\frac{v_r}{2\tan\beta_a} + \sqrt{\eta\, g H_n} \quad . \quad . \quad . \quad . \quad . \quad . \quad 108$$

If v_r is assumed, the peripheral velocity u_a can be determined graphically for every angle β_a after calculating $\sqrt{\eta\, g H_n}$.

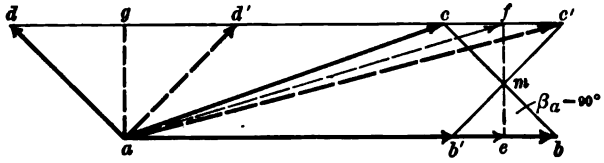

Fig. 28.

The diagram $\overline{aefg}$ (Fig. 28) for $\beta_a = 90°$ is first drawn, and according to equation 59 $u_a = \sqrt{\eta\, g H_n}$. If the peripheral velocity is to be determined for any angle β_a it is only necessary to draw, from the middle point m of $v_r = \overline{ef}$, the angle $\beta_a - 90°$, towards the left downwards if the angle is negative and towards the right downwards if it is positive. The distance $\overline{ab}$ or $\overline{ab'}$ then gives the peripheral velocity corresponding to the angle in question $(+-)$ and the parallelogram $\overline{abcd}$ or $\overline{ab'c'd'}$ is then the velocity diagram corresponding to the angle $(+-)$ in question.

Then

$$\overline{eb} = -\frac{v_r}{2\tan\beta_a} \quad \text{or} \quad \overline{eb'} = \frac{v_r}{2\tan\beta_a},$$

so that

$$u_a = \overline{ae} + \overline{eb} = -\frac{v_r}{2\tan\beta_a} + \sqrt{\eta\, g H_n},$$

or

$$u_a' = \overline{ae} - \overline{eb} = -\frac{v_r}{2\tan\beta_a} + \sqrt{\eta\, g H_n};$$

hence equation 108 is satisfied.

For the special cases in which $\beta_a = 45°$ and $\beta_a = 135°$,

$$u_{a_{\beta_a=45°}} = -\frac{v_r}{2} + \sqrt{\eta g H_n},$$

$$u_{a_{\beta_a=135°}} = +\frac{v_r}{2} + \sqrt{\eta g H_n}.$$

13. Mathematical and Graphical Determination of the Entrance Velocity Diagram when $\delta_e = 90°$.

After assuming the impeller diameter D_e, which extends to the center of gravity of the arc b_e (see Fig. 29), the peripheral velocity u_e can be determined, for the peripheral velocities are directly proportional to the corresponding diameters, or

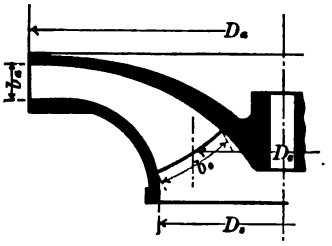

Fig. 29.

$$u_e = u_a \frac{D_e}{D_a} \quad . \quad . \quad . \quad . \quad 109$$

The length of the entrance arc b_e must be chosen so that $D_e \pi b_e = F_s'$, which is equal to the clear cross-sectional area of the suction pipe directly at the entrance to the impeller. The value of the absolute entrance velocity has already been given as

$$w_e = w_s \frac{a_e + s_e}{a_e} \quad . \quad . \quad . \quad . \quad . \quad . \quad . \quad (16)$$

in which a_e denotes the height of channel and s_e the thickness of blade.

Taking into account the short-circuit loss, the impeller must be calculated for a quantity $Q' = Q + Q_{sp}$. The velocity w_s in the suction pipe is increased to a greater velocity w_s' at entrance to the impeller, due to the amount of water short-circuited; hence

$$w_s' = w_s \frac{Q + Q_{sp}}{Q} \quad . \quad . \quad . \quad . \quad . \quad . \quad . \quad 110$$

It is therefore necessary to substitute for w_s in equation 16 the velocity w_s', so that

$$w_e = w_s' \frac{a_e + s_e}{a_e} \quad . \quad . \quad . \quad . \quad . \quad . \quad . \quad 111$$

After assuming the number of impeller blades z_e, the pitch t_e at the inner diameter D_e of the impeller is

$$t_e = \frac{D_e \pi}{z_e} \quad \ldots \ldots \ldots \quad 112$$

The blades at their inner end must form an angle β_e with u_e, so that (see Fig. 12)

$$\sin \beta_e = \frac{a_e + s_e}{t_e} \quad \ldots \ldots \ldots \quad 113$$

If the absolute entrance velocity is to be calculated from equation 111, an assumption of the ratio $\frac{a_e + s_e}{a_e}$ must be made. When $\delta_e = 90°$ the relative entrance velocity v_e is determined from the equation

$$v_e = \sqrt{u_e^2 + w_e^2} \quad \ldots \ldots \ldots \quad 114$$

and the impeller angle β_e from the equation

$$\sin \beta_e = \frac{w_e}{v_e} \quad \ldots \ldots \ldots \quad 115$$

The value of $a_e + s_e$ can now be best determined graphically from a consideration of equation 113.

If an incorrect assumption of the ratio $\frac{a_e + s_e}{a_e}$ was made the calculation must be repeated. This method of calculation necessitating the assumption of $\frac{a_e + s_e}{a_e}$ is very cumbersome. By the aid of equations 111, 113, and 115 a_e might be calculated, but the equation would be of a complicated form.

A very simple graphical method for determining w_e and $a_e + s_e$ will now be shown. This method is due to Adam, who applied it in a similar form for the determination of the exit velocity diagram of a water turbine (Dingl. Polytechn. Journal, 1903).

Equation 111 can be written

$$\frac{w_e}{w_e'} = \frac{a_e + s_e}{a_e} \quad \ldots \ldots \ldots \quad 116$$

The graphical determination of w_e and $a_e + s_e$ can be seen from Fig. 30. A right-angled triangle $\overline{dce}$ was first drawn, whose sides $\overline{dc} = u_e$ and $\overline{ce} = w_e$; the distance $\overline{ef}$ was then added equal to the blade thickness s_e. A line parallel to $\overline{de}$ was drawn through f. The

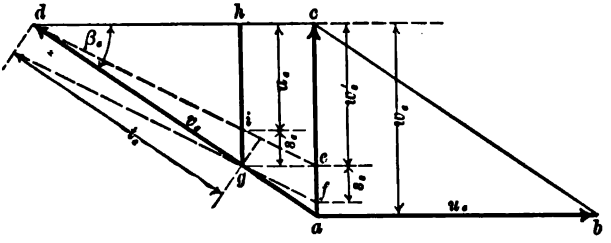

Fig. 30.

arc having t_e as a radius and struck from the point d as a center cuts the parallel line at point g. From g a line is drawn perpendicular to dc, cutting the latter at h and cutting $\overline{de}$ at i. The extension of $\overline{dg}$ meets the extension of $\overline{cf}$ at a. Then $\overline{ih} = a_e$, $\overline{ig} = s_e$, and $\overline{ac} = w_e$. Hence equation 113 is satisfied, because

$$\sin \beta_e = \frac{\overline{hg}}{\overline{dg}} = \frac{a_e + s_e}{t_e}$$

and also equation 116 is satisfied because

$$\frac{w_e}{w_e'} = \frac{a_e + s_e}{a_e}.$$

The parallelogram $\overline{abcd}$ is then the desired entrance velocity diagram.

14. The Entrance and Exit Dimensions when $\delta_e \gtrless 90°$.

In the equations already derived it has been assumed that the absolute entrance velocity w_e is perpendicular to u_e and hence that the angle $\delta_e = 90°$. With this assumption the member $u_e w_e \cos \delta_e = 0$ (equation 15) and therefore it had no effect upon the peripheral velocity. It often occurs, however, for reasons to be discussed later, that the angle δ_e is not 90°; for instance, it is generally smaller than 90° for high-pressure centrifugal pumps. The following discussion will explain the method of calculating exit and entrance dimension when $\delta_e \gtrless 90°$.

Beginning again with the second form of the fundamental equation, we have

$$u_a w_a \cos \delta_a - u_e w_e \cos \delta_e = \eta g H_n \quad . \quad . \quad . \quad . \quad (15)$$

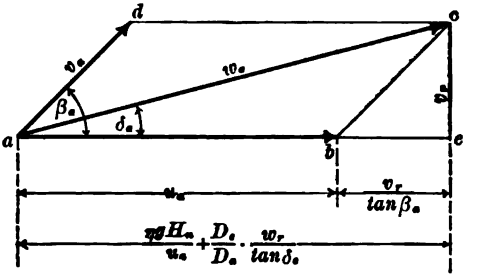

Fig. 31.

From the exit velocity diagram (Fig. 31) it can be seen that

$$\overline{ae} = w_a \cos \delta_a = u_a + \frac{v_r}{\tan \beta_a} \quad . \quad . \quad . \quad . \quad . \quad 117$$

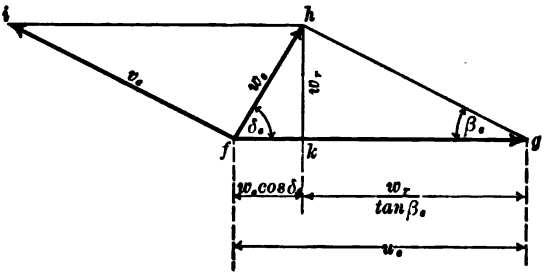

Fig. 32.

From the entrance velocity diagram (Fig. 32)

$$\overline{fk} = w_e \cos \delta_e \quad . \quad . \quad . \quad . \quad . \quad . \quad . \quad . \quad 118$$

The calculation of the entrance area of the impeller is based upon the vertical component of the absolute entrance velocity w_e, which will be called w_r (radial entrance velocity). If w_e and δ_e are given, w_r is calculated from the equation

$$w_r = w_e \sin \delta_e \quad . \quad . \quad . \quad . \quad . \quad . \quad . \quad . \quad 119$$

or if we assume w_r and δ_e, equation 119 may be written

$$w_e = \frac{w_r}{\sin \delta_e} \quad . \quad . \quad . \quad . \quad . \quad . \quad . \quad . \quad 120$$

The distance $\overline{fk}$ may be expressed as

$$\overline{fk} = \frac{w_r}{\tan \delta_e} \quad . \quad . \quad . \quad . \quad . \quad . \quad . \quad . \quad 121$$

so that combining equations 118 and 121 gives

$$w_e \cos \delta_e = \frac{w_r}{\tan \delta_e} \quad . \quad . \quad . \quad . \quad . \quad . \quad . \quad . \quad 122$$

From equation 109

$$u_e = u_a \frac{D_e}{D_a} \quad . \quad . \quad . \quad . \quad . \quad . \quad . \quad . \quad (109)$$

Substituting equations 117, 122, and 109 in equation 15, we obtain, solving for the peripheral velocity u_a,

$$u_a = \frac{D_e}{D_a} \frac{w_r}{2 \tan \delta_e} - \frac{v_r}{2 \tan \beta_a} + \sqrt{\left[\frac{D_e}{D_a} \frac{w_r}{2 \tan \delta_e} - \frac{v_r}{2 \tan \beta_a}\right]^2 + \eta g H_n} \quad 123$$

If F_e is the decreased entrance area due to thickness of blades and F_a the exit area of the impeller, then

$$v_r = \frac{F_e}{F_a} w_r \quad . \quad . \quad . \quad . \quad . \quad . \quad . \quad . \quad 124$$

Substituting this value of v_r in equation 123 the peripheral velocity u_a will be

$$u_a = \frac{w_r}{2}\left(\frac{D_e}{D_a} \frac{1}{\tan \delta_e} - \frac{F_e}{F_a} \frac{1}{\tan \beta_a}\right) + \sqrt{\frac{w_r^2}{4}\left(\frac{D_e}{D_a} \frac{1}{\tan \delta_e} - \frac{F_e}{F_a} \frac{1}{\tan \beta_a}\right)^2 + \eta g H_n} \quad . \quad . \quad 125$$

The determination of the peripheral velocity by means of this equation is rather cumbersome, because the ratios $\frac{D_e}{D_a}$ and $\frac{F_e}{F_a}$ must first be assumed. If the angle δ_e deviates but slightly from 90°, only a very small error is introduced by using the simpler equation 58 or 63. For large deviation of the angle δ_e from 90°, equation 125 and the following must be used for the determination of u_a.

In place of v_r in equation 123, a function of the angle δ_a can be substituted. Substituting the value for $w_e \cos \delta_e$ from equation 122

and the value for u_e from equation 109 in equation 15 we obtain for $w_a \cos \delta_a = \overline{ae}$ the value

$$w_a \cos \delta_a = \frac{\eta g H_n}{u_a} + \frac{D_e}{D_a} \frac{w_r}{\tan \delta_e} \quad . \quad . \quad . \quad . \quad . \quad 126$$

From Fig. 31 it follows that

$$\tan \delta_a = \frac{v_r}{\frac{\eta g H_n}{u_a} + \frac{D_e}{D_a} \frac{w_r}{\tan \delta_e}} \quad . \quad . \quad . \quad . \quad . \quad 127$$

and

$$v_r = \tan \delta_a \left(\frac{\eta g H_n}{u_a} + \frac{D_e}{D_a} \frac{w_r}{\tan \delta_e} \right) \quad . \quad . \quad . \quad . \quad . \quad 128$$

Further,

$$u_a = \frac{\eta g H_n}{u_a} + \frac{D_e}{D_a} \frac{w_r}{\tan \delta_e} - \frac{v_r}{\tan \beta_a} \quad . \quad . \quad . \quad . \quad 129$$

After substituting the value for v_r from equation 128 in equation 129 the peripheral velocity u_a will be

$$u_a = \frac{D_e}{D_a} \frac{w_r}{2 \tan \delta_e} \left(1 - \frac{\tan \delta_a}{\tan \beta_a} \right) + \sqrt{\left[\frac{D_e}{D_a} \frac{w_r}{2 \tan \delta_e} \left(1 - \frac{\tan \delta_a}{\tan \beta_a} \right) \right]^2 + \eta g H_n \left(1 - \frac{\tan \delta_a}{\tan \beta_a} \right)} \quad . \quad 130$$

For the special case of $\beta_a = 90°$ equation 123 or 130 takes the form

$$u_{a\,90°} = \frac{D_e}{D_a} \frac{w_r}{2 \tan \delta_e} + \sqrt{\left(\frac{D_e}{D_a} \frac{w_r}{2 \tan \delta_e} \right)^2 + \eta g H_n} \quad . \quad . \quad 131$$

Substituting in this equation $\delta_e = 90°$ we again obtain the simplified equation $u_{a\,90°} = \sqrt{\eta g H_n}$.

The κ curves (Plate I) may be used in order to determine quickly the expression $1 - \frac{\tan \delta_a}{\tan \beta_a}$ in equation 130. With the aid of the κ curves it is simpler to determine the peripheral velocity from equation 130 than from equation 125.

Fink designed an impeller blade having the relative entrance velocity v_e radial, that is, v_e perpendicular to u_e and $\beta_e = 90°$. With this assumption the peripheral velocity and angle δ_e are found as follows:

For $\beta_e = 90°$

$$\frac{w_r}{\tan \delta_e} = u_e = u_a \frac{D_e}{D_a} \quad \ldots \ldots \ldots \quad 132$$

This value for $\frac{w_r}{\tan \delta_e}$ if substituted in equation 129 will give the peripheral velocity for the assumption $\beta_e = 90°$ as

$$u_{a_{\beta_e = 90°}} = -\frac{v_r}{2 \tan \beta_a \left[1 - \left(\frac{D_e}{D_a}\right)^2\right]} + \sqrt{\left[\frac{v_r}{2 \tan \beta_a \left[1 - \left(\frac{D_e}{D_a}\right)^2\right]}\right]^2 + \frac{\eta g H_n}{1 - \left(\frac{D_e}{D_a}\right)^2}} \quad \ldots \quad 133$$

The angle δ_e is then found from equation 132 to be

$$\tan \delta_{e_{\beta_e = 90°}} = \frac{w_r D_a}{u_a D_e} \quad \ldots \ldots \ldots \quad 134$$

The question now arises, What is gained by making the angle $\delta_e \gtrless 90°$? Assuming $\delta_e = 90°$, the absolute entrance velocity w_e is perpendicular to u_e, and the water will flow through the suction pipe in an axial direction and therefore will traverse the shortest path. If the angle $\delta_e \gtrless 90°$, the water in the suction pipe can no longer flow in an axial direction, but will be set in rotation by the component $w_e \cos \delta_e$ and traverses a spiral path. For this reason not only the suction pipe velocity but also the path described by the water is increased. Both of these occurrences cause greater friction losses. In order to minimize these losses it is advisable to place directing vanes at entrance to the impeller. The object of these vanes is to keep the flow axial in the suction pipe and, further, to give the water at impeller entrance its correct absolute entrance velocity and direction. These directing vanes have therefore an angle of 90° at entrance and approximately the angle δ_e at exit. They decrease the losses in the suction pipe considerably in spite of the fact that friction and shock losses occur, due to the water passing through them. Experiments have proven that the latter losses are smaller than the losses in the suction tube when the directing vanes are omitted.

While on the one hand the losses up to the entrance of the impeller are larger when $\delta_e < 90°$ as compared with $\delta_e = 90°$, on the other hand a smaller loss occurs in the first part of the impeller channels, because by decreasing δ_e the channel height a_e is increased, thereby

decreasing the relative entrance velocity. For with equal values of the peripheral velocity u_e a decreasing angle δ_e will cause the impeller angle β_e to increase. From the expression $a_e + s_e = t_e \sin \beta_e$ it can be immediately seen that if β_e increases $a_e + s_e$ also increases.

Impellers of high-pressure centrifugal pumps for small quantities of water and large heads have very small cross sections at entrance. The friction losses will be very large on account of the high relative velocity of the water. These friction losses can be materially reduced by increasing the entrance cross section of the impeller, because this decreases the relative velocity of the water, for it must be remembered that the friction losses vary approximately with the square of the velocity. With such pumps it is, therefore, advantageous to introduce directing vanes, for although these vanes increase the suction pipe losses they materially decrease the losses in the impeller so that the total effect is very beneficial. A more complete investigation of this subject will be found in Article 25.

In order to obtain a clear conception of the relation of the peripheral velocity, the relative and absolute entrance velocities as well as the magnitude of $a_e + s_e$ to the angle δ_e, an example has been calculated. The derived values corresponding to various values of the angle δ_e are plotted as ordinates in Fig. 33. The example taken is as follows:

$$\sqrt{\eta g H_n} = 32.8 \text{ feet}, \quad D_a = 1.31 \text{ feet}, \quad D_e = 0.66 \text{ foot},$$
$$v_r = 6.56 \text{ feet}, \quad w_r = 9.84 \text{ feet},$$
$$\text{number of impeller blades } z = 8.$$

For these values two examples have been calculated:

$$\text{I.} \quad \beta_a = 90°. \qquad \text{II.} \quad \beta_a = 135°.$$

In Fig. 33 the relation of the peripheral velocity and the relative and absolute entrance velocities as well as the magnitude of $a_e + s_e$ to the angle δ_e is clearly shown. It will be noted that with a large deviation of δ_e from 90° the influence of $u_e w_e \cos \delta_e$ upon the peripheral velocity is quite important, and it would be well in such cases to calculate the peripheral velocity by means of equation 130.

The $a_e + s_e$ curve reaches a maximum for case I ($\beta_a = 90°$) when $\delta_e = 27° 50'$, and for case II ($\beta_a = 135°$) when $\delta_e = 25°$, because for these values $\beta_e = 90°$ and hence (equation 113) $a_e + s_e = t_e$. If the angle δ_e is still further decreased, then $\beta_e > 90°$, that is, the

direction of the blade is reversed and $a_e + s_e$ would again decrease. Such a blade would not of course be used, for then the absolute entrance velocity would become too great.

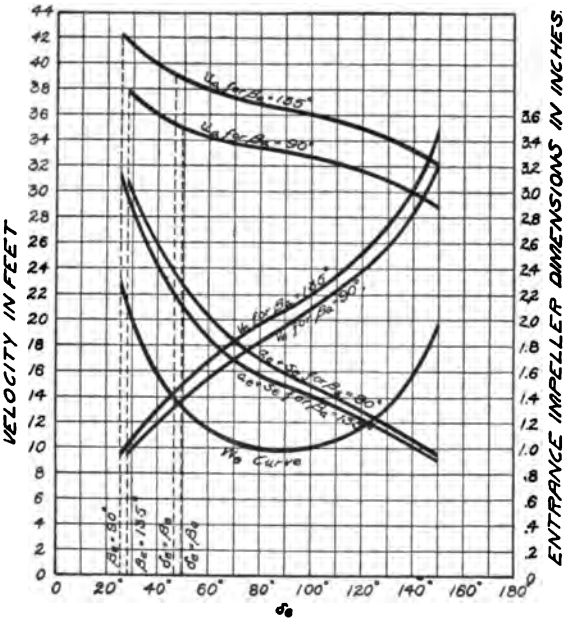

Fig. 33

The best value of the angle δ_e, when it is made less than 90° for the reasons just stated, will now be determined.

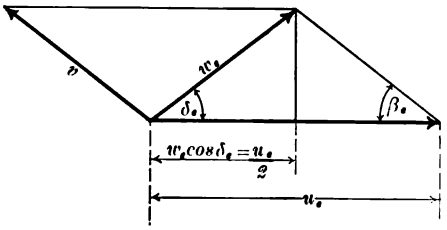

Fig. 34.

The friction losses are approximately proportional to the square of the velocity and will become a minimum at exit from the directing vanes and in the beginning of the impeller channel when the expression $w_e^2 + v_e^2$ is a minimum. This occurs when $v_e = w_e$. When $v_e = w_e$ the angle $\delta_e = \beta_e$. Fig. 34 shows an entrance velocity diagram in which $\delta_e = \beta_e$. Here

$$w_e \cos \delta_e = \frac{u_e}{2} = \frac{u_a D_e}{2 D_a}. \quad . \quad . \quad . \quad . \quad . \quad . \quad . \quad 135$$

Substituting in equation 15 the value of $w_a \cos \delta_a = u_a + \frac{v_r}{\tan \beta_a}$ from equation 117 and for $w_e \cos \delta_e$ its value from equation 135, we find the peripheral velocity for the special case $w_e = v_e$ or $\delta_e = \beta_e$ to be

$$u_{a\beta_e=\delta_e} = -\frac{v_r}{2\tan\beta_a\left[1-\frac{1}{2}\left(\frac{D_e}{D_a}\right)^2\right]} + \sqrt{\left[\frac{v_r}{2\tan\beta_a\left[1-\frac{1}{2}\left(\frac{D_e}{D_a}\right)^2\right]}\right]^2 + \frac{\eta g H_n}{1-\frac{1}{2}\left(\frac{D_e}{D_a}\right)^2}} \quad . \quad 136$$

If $\beta_a = 90°$, the equation takes the form

$$u_{a\,90°\beta_e=\delta_e} = \sqrt{\frac{\eta g H_n}{1-\frac{1}{2}\left(\frac{D_e}{D_a}\right)^2}} \quad . \quad . \quad . \quad . \quad . \quad 137$$

When $\beta_e = \delta_e$, hence $w_e = v_e$, the following values are found for the example quoted above:

For $\beta_a = 90°$,

$u_a = 35.1$ feet, $w_e = v_e = 13.22$ feet, $\beta_e = \delta_e = 48° 20'$.

For $\beta_a = 135°$,

$u_a = 38.97$ feet, $w_e = v_e = 13.97$ feet, $\beta_e = \delta_e = 45° 20'$.

In Fig. 33 these values and also the magnitude of $a_e + s_e$ can be read directly, because the ordinates must pass through the point of intersection of the w_e curve with the corresponding v_e curve.

15. The Entrance and Exit Dimensions for Equal Heads with Varying Quantities.

In the foregoing articles it was assumed that it was necessary to construct a new impeller for each head and quantity of water desired. The assumption will now be made that an impeller with known entrance and exit angles β_e and β_a exists. If this impeller is to deliver various quantities of water at the same head it is necessary to investigate what the entrance and exit velocity diagrams should be for operation without shock. It will be proved that one and the same impeller may be used for varying quantities at constant

head by changing the guide vanes at exit and the directing vanes at entrance provided the latter are used. In practice this is often of great value.

The second form of the fundamental equation from which it is again best to start states that

$$u_a w_a \cos \delta_a - u_e w_e \cos \delta_e = \eta g H_n \quad . \quad . \quad . \quad . \quad (15)$$

It has been found from the exit velocity diagram (see Fig. 32) that

$$w_a \cos \delta_a = u_a + \frac{v_r}{\tan \beta_a} \quad . \quad . \quad . \quad . \quad . \quad (117)$$

The entrance velocity diagram (see Fig. 32) gives

$$kg = \frac{w_r}{\tan \beta_e}; \quad . \quad . \quad . \quad . \quad . \quad . \quad . \quad 138$$

therefore the equation for $w_e \cos \delta_e$ may be written

$$w_e \cos \delta_e = u_e - \frac{w_r}{\tan \beta_e} \quad . \quad . \quad . \quad . \quad . \quad . \quad 139$$

Substituting in equation 15 the values of $w_a \cos \delta_a$ and $w_e \cos \delta_e$ from equations 117 and 139 we obtain

$$u_a\left(u_a + \frac{v_r}{\tan \beta_a}\right) - u_e\left(u_e - \frac{w_r}{\tan \beta_e}\right) = \eta g H_n \quad . \quad . \quad . \quad 140$$

For u_e and v_r substitute their values as given in equations 109 and 124. Then the peripheral velocity can be expressed as

$$u_a = \frac{-w_r\left(\frac{F_e}{F_a \tan \beta_a} + \frac{D_e}{D_a \tan \beta_e}\right)}{2\left[1 - \left(\frac{D_e}{D_a}\right)^2\right]} + \sqrt{w_r^2\left[\frac{\frac{F_e}{F_a \tan \beta_a} + \frac{D_e}{D_a \tan \beta_e}}{2\left[1 - \left(\frac{D_e}{D_a}\right)^2\right]}\right]^2 + \frac{\eta g H_n}{1 - \left(\frac{D_e}{D_a}\right)^2}} \quad . \quad 141$$

The same impeller profile was assumed, therefore the angles β_a and β_e and also the values F_a, F_e, D_a, and D_e are constant. Hence

$$\frac{\frac{F_e}{F_a \tan \beta_a} + \frac{D_e}{D_a \tan \beta_e}}{2\left[1 - \left(\frac{D_e}{D_a}\right)^2\right]} = C_1 \quad . \quad . \quad . \quad . \quad . \quad . \quad 142$$

and

$$\frac{1}{1 - \left(\frac{D_e}{D_a}\right)^2} = C_2 \quad . \quad . \quad . \quad . \quad . \quad . \quad 143$$

and then equation 141 takes the very simple form of

$$u_a = -w_r C_1 + \sqrt{w_r^2 C_1^2 + \eta g H_n C_2} \quad . \quad . \quad . \quad . \quad 144$$

From this equation, after determining C_1 and C_2, the peripheral velocities can be calculated for various velocities w_r, hence for various quantities of water.

The peripheral velocities for the two special cases $\delta_e = 90°$ and $\delta_e = \beta_e$ are derived as follows:

It has been shown that $u_a w_e \cos \delta_a = \eta g H_n$ when $\delta_e = 90°$ and that

$$w_a \cos \delta_a = u_a + \frac{v_r}{\tan \beta_a} \quad . \quad . \quad . \quad . \quad . \quad (117)$$

From equation 124

$$v_r = w_r \frac{F_e}{F_a} \quad . \quad . \quad . \quad . \quad . \quad . \quad . \quad (124)$$

For $\delta_e = 90°$,

$$w_{r_{\delta_e = 90°}} = u_e \tan \beta_e = u_a \frac{D_e}{D_a} \tan \beta_e \quad . \quad . \quad . \quad . \quad 145$$

This value of w_r substituted in equation 124 gives

$$v_r = u_a \frac{D_e}{D_a} \frac{F_e}{F_a} \tan \beta_e \quad . \quad . \quad . \quad . \quad . \quad . \quad 146$$

Placing this value of v_r in equation 117, the value of the peripheral velocity for the case $\delta_e = 90°$ is

$$u_{a_{\delta_e = 90°}} = \sqrt{\frac{\eta g H_n}{1 + \frac{D_e}{D_a} \cdot \frac{F_e}{F_a} \cdot \frac{\tan \beta_e}{\tan \beta_a}}} \quad . \quad . \quad . \quad . \quad 147$$

To determine the quantity of water for the special case $\delta_e = 90°$, solve for u_e in the equation $u_e = u_a \frac{D_e}{D_a}$ and from equation 145 find

the velocity w_r. The quantity of water delivered is then determined from the equation $Q = F_e w_r$.

For $\delta_e = \beta_e$ or $w_e = v_e$

$$w_e \cos \delta_e = \frac{u_a}{2} \cdot \frac{D_e}{D_a} \quad . \quad . \quad . \quad . \quad . \quad . \quad . \quad (135)$$

From Fig. 34, which represents the entrance velocity diagram for the special case $\beta_e = \delta_e$, we have

$$w_r = \frac{u_e}{2} \tan \beta_e = \frac{u_a}{2} \frac{D_e}{D_a} \tan \beta_e \quad . \quad . \quad . \quad . \quad . \quad 148$$

Therefore

$$v_r = \frac{u_a}{2} \frac{D_e}{D_a} \frac{F_e}{F_a} \tan \beta_e.$$

This value of v_r is substituted in equation 117, giving

$$w_a \cos \delta_a = u_a + \frac{u_a}{2} \frac{D_e}{D_a} \frac{F_e}{F_a} \frac{\tan \beta_e}{\tan \beta_a} \quad . \quad . \quad . \quad . \quad 149$$

After substituting equations 135 and 149 in equation 15 the peripheral velocity for the case $\beta_e = \delta_e$ is

$$u_{a\beta_e = \delta_e} = \sqrt{\frac{\eta g H_n}{1 + \frac{1}{2} \frac{D_e}{D_a} \frac{F_e}{F_a} \frac{\tan \beta_e}{\tan \beta_a} - \frac{1}{2} \left(\frac{D_e}{D_a}\right)^2}} \quad . \quad . \quad 150$$

The velocity w_r is determined from equation 148 and the quantity of water delivered from the equation $Q = F_e w_r$. As the entrance and exit cross sections must remain constant, the relative entrance and exit velocities must vary in direct proportion to the quantity of water. The relative entrance velocity is found from the equation

$$v_e = \frac{w_r}{\sin \beta_e} \quad . \quad . \quad . \quad . \quad . \quad . \quad . \quad . \quad 151$$

and the relative exit velocity from the equation

$$v_a = \frac{v_r}{\sin \beta_a} \quad . \quad . \quad . \quad . \quad . \quad . \quad . \quad . \quad 152$$

With a change of w_r and v_r the angles δ_e and δ_a also change, and in the same manner the guide vane cross section at entrance and the directing vane cross section at exit (when directing vanes exist) will also vary.

The angle δ_a can be found after determining u_a (Fig. 31),

$$\tan \delta_a = \frac{v_r}{u_a + \frac{v_r}{\tan \beta_a}} \quad \ldots \ldots \quad 153$$

and the angle δ_e from the equation (Fig. 32)

$$\tan \delta_e = \frac{w_r}{u_e - \frac{w_r}{\tan \beta_e}} \quad \ldots \ldots \quad 154$$

For the absolute exit velocity w_a, Fig. 31 gives

$$w_a = \sqrt{v_r^2 + \left(u_a + \frac{v_r}{\tan \beta_a}\right)^2} \quad \ldots \ldots \quad 155$$

and from Fig. 32 the absolute entrance velocity is

$$w_e = \sqrt{w_r^2 + \left(u_e - \frac{w_r}{\tan \beta_e}\right)^2} \quad \ldots \ldots \quad 156$$

In most cases the determination of these values mathematically is unnecessary and it is advisable to determine them graphically.

The equations just derived do not show the relation between the various values of the velocity diagrams and the quantity of water. In order to make this relation clear several examples have been worked out and the results are shown graphically on Plate II. The velocities are calculated from the derived equations, and velocity heads are plotted as ordinates to the quantities of water. In this work we used the first form of the fundamental equation,

$$\frac{w_a^2}{2g} + \frac{v_e^2}{2g} + \frac{u_a^2}{2g} = \eta H_n + \frac{w_e^2}{2g} + \frac{v_a^2}{2g} + \frac{u_e^2}{2g} \quad \ldots \quad (10)$$

To show the influence of the impeller angle β_a on these values the three following examples have been calculated:

I. $\beta_a = 45°$. II. $\beta_a = 90°$. III. $\beta_a = 135°$.

The same assumptions were made as in the previous example, namely:

$\sqrt{\eta g H_n} = 32.8$ ft.; hence, $\eta H_n = 33.4$ ft.; $D_a = 1.31$ ft.; $D_e = 0.66$ ft.

For $v_r = 6.56$ feet and $w_r = 9.84$ feet let $\delta_e = 90°$.

With the various impeller angles β_a, the constant C_1 will vary according to equation 142. The angle β_e must be determined by finding the peripheral velocity from equation 58 for the special case $\delta_e = 90°$, and then β_e is obtained from the equation $\tan \beta_e = \frac{w_r}{u_e}$.

The constant C_2 is independent of the angle β_a and therefore has the same value in all three examples.

For the various quantities of water the peripheral velocities are determined according to equation 144.

The quantity of water for $\delta_e = 90°$ was taken equal to unity in each example and the various velocities determined for the quantities of water between the limits 0.5 and 1.5. These velocity heads as found from equation 10 for the three examples $\beta_a = 45°$, $\beta_a = 90°$, and $\beta_a = 135°$ are drawn as ordinates to the corresponding quantities of water in Figs. 1, 2, and 3 of Plate II and the points found are connected by curves. In Figs. 4, 5, and 6 the velocities have been drawn as ordinates to the quantities of water.

These curves show clearly the relation between the various values and the quantity of water. For general design the quantities of water between 0.5 and 1.0 are most useful. For quantities of water greater than 1.0 the relative as well as the absolute velocities and therefore the friction losses become too large. The intersection of the w_e and v_e curves of Figs. 4, 5, and 6 gives the special case $w_e = v_e$ and therefore $\delta_e = \beta_e$.

The course of the $\frac{w_a^2}{2g}$ curves in Figs. 1, 2, and 3 is of special interest, for, neglecting the rotating paraboloid, the pressure difference in the clearance space according to equation 23 is $H_{ep} = \eta H_n - \frac{w_a^2}{2g}$. The value of the existing pressure difference in the clearance space can be seen directly from these figures. It is evident that for $\beta_a = 135°$ the pressure difference in the clearance space decreases very rapidly with the quantity of water, while for $\beta_a = 45°$ it remains approximately constant for various quantities of water. For reasons which will be more fully considered later, the angle β_a is almost always larger than 90° in high-pressure centrifugal pumps. When $\beta_a > 90°$, and if the angle $\delta_e < 90°$, the pressure difference in the clearance space and therefore the short-circuit losses will be considerably decreased. This advantage, which in itself is quite valuable, is, in addition, enhanced by the fact that with $\delta_e < 90°$ the

relative entrance velocity and therefore the friction losses in the first part of the blade channel will decrease, due to the enlargement of the entrance cross section.

The value of the angle β_e and the constant C_1 derived for the above examples are:

I.	$\beta_a = 45°$.	$\beta_e = 33° 35'$.	$C_1 = 0.946$.
II.	$\beta_a = 90°$.	$\beta_e = 31°$.	$C_1 = 0.556$.
III.	$\beta_a = 135°$.	$\beta_e = 28° 30'$.	$C_1 = 0.1728$.

16. Construction of the Entrance and Exit Velocity Diagrams and Determination of Suction Pipe Velocity for $\delta_e \gtreqless 90°$.

The determination of the entrance velocity diagram in Article 13 was based upon the suction pipe velocity. After determining the suction pipe velocity w_s' the absolute entrance velocity w_e was graphically determined for the case $\delta_e = 90°$. If the peripheral velocity is calculated by means of equation 125 for $\delta_e \gtreqless 90°$, the vertical component w_r of the absolute entrance velocity w_e must be assumed and then the suction pipe velocity determined. With $\delta_e \gtreqless 90°$ the water will flow through the suction pipe in a spiral path if the directing vanes are omitted. In calculating the cross section of the suction pipe the vertical component of this velocity must be used. It will be designated briefly as suction pipe velocity.

It has been shown that, on account of the addition of short-circuited water, the suction pipe velocity is increased at impeller entrance to the value $w_s' = w_s \frac{Q + Q_{sp}}{Q}$ (equation 110).

The velocity w_s' refers to a quantity of water which includes the short-circuited water, and may be determined from the entrance velocity diagram. The smaller value w_s, which is used to determine the cross section of the suction pipe, can then be determined by decreasing w_s' by the factor $\frac{Q}{Q + Q_{sp}}$. After determining the peripheral velocity, the entrance diagram can be constructed by aid of the protractor as follows:

In Fig. 35, lay off $\overline{ab} = u_e$ and from a draw a line $\overline{ac}$ forming the angle δ_e with $\overline{ab}$; draw $\overline{dc}$ parallel to $\overline{ab}$ with w_r as the perpendicular distance between them. Then $\overline{ac} = w_e$. The parallelogram $\overline{abcd}$ is then the desired entrance velocity diagram.

If a protractor is not at hand the value $\frac{w_r}{\tan \delta_e}$ is determined and laid off along the line $\overline{ab} = u_e$ (Fig. 35) so that $\overline{ae} = \frac{w_r}{\tan \delta_e}$. From e erect a line $\overline{ec} = w_r$ perpendicular to $\overline{ab}$, connect the points a and c and the line $\overline{ac} = w_e$. This latter method of constructing the entrance velocity diagram is preferable because of the exactness in constructing the angle δ_e.

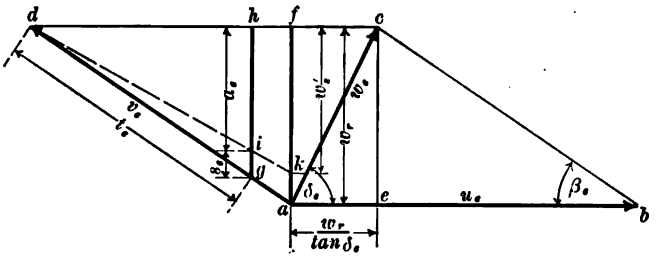

Fig. 35.

Whichever method is used it is best to determine the entrance height $a_e + s_e$ graphically. After assuming the number of blades z_e the pitch t_e is determined, and considering that $\sin \beta_e = \frac{a_e + s_e}{t_e}$ (equation 113), the value of $a_e + s_e$ can be determined graphically as shown in Fig. 35. The suction pipe velocity can be determined analytically from the relation $w_s' = w_r \frac{a_e}{a_e + s_e}$, or more simply by the graphical method, if (after determining $a_e + s_e$ in Fig. 35 where $a_e = \overline{hi}$ and $s_e = \overline{ig}$) the line $\overline{di}$ is drawn and prolonged until it cuts $\overline{af} = w_r$ at k. Then $\overline{fk} = w_s'$ because $\frac{\overline{fk}}{\overline{fa}} = \frac{\overline{hi}}{\overline{hg}}$, hence $\frac{w_s'}{w_r} = \frac{a_e}{a_e + s_e}$.

The suction pipe velocity w_s is then determined according to equation 110, which states that $w_s = w_s' \cdot \frac{Q}{Q + Q_{sp}}$.

In the determination of the peripheral velocity, according to equation 136 for the special case $v_e = w_e$, hence $\beta_e = \delta_e$, the only assumption necessary is that of the ratio $\frac{D_e}{D_a}$; therefore in this case the radial entrance velocity w_r can be taken independently of the radial exit velocity v_r. The suction pipe velocity w_s can now be assumed as before, and after determining the peripheral velocity u_e, the velocity

w_e and the value $a_e + s_e$ can easily be determined graphically as follows:

Draw (Fig. 36) the right-angled triangle $\overline{dfk}$ in which $\overline{df} = \frac{u_e}{2}$ and $\overline{fk} = w_e'$; let $\overline{ke} = s_e$ be the assumed blade thickness. With a pitch t_e as a radius, describe an arc about d which cuts a line drawn through

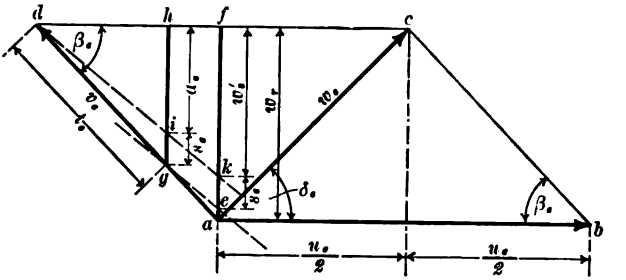

Fig. 36.

e parallel to $\overline{dk}$ at the point g. Prolong $\overline{dg}$ until it cuts the prolongation of $\overline{fk}$ at point a and lay off $\overline{ab} = u_e$ parallel to $\overline{df}$. A line drawn perpendicular to $\overline{ab}$ at a distance from a equal to $\frac{u_e}{2}$ cuts the prolongation of $\overline{df}$ at c, so that the parallelogram $\overline{abcd}$ is the desired entrance diagram. The perpendicular $\overline{gh}$ gives the value $a_e + s_e$ and $\overline{af}$ the value of the radial entrance velocity w_r. In the diagram thus found the conditions fulfilled are

$$\sin \beta_e = \frac{a_e + s_e}{t_e} \quad \text{and} \quad \frac{w_r}{w_e'} = \frac{a_e + s_e}{a_e}.$$

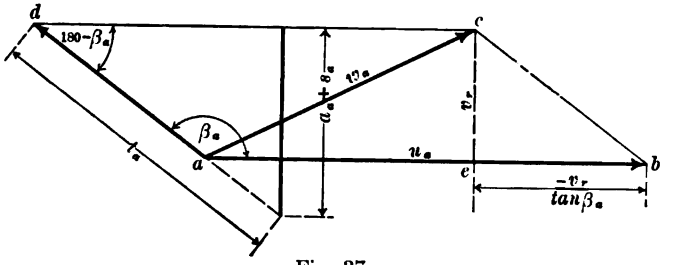

Fig. 37.

The determination of the exit velocity diagram (Fig. 37) is similar to that of the entrance velocity diagram. After calculating the peripheral velocity u_a, lay off the angle β_a with $u_a = \overline{ab}$. At a

distance v_r perpendicular to u_a draw a line parallel to u_a cutting the line forming the angle β_a at point d. The parallelogram $\overline{abcd}$ is the desired exit velocity diagram.

Without a protector the diagram can be constructed graphically by making $\overline{be} = \frac{v_r}{\tan \beta_a}$ and laying it off, if positive, on the prolongation of $u_a = \overline{ab}$ to the right of b, or if negative, to the left of point b (Fig. 37). The perpendicular to $\overline{ab}$ from e meets the line drawn parallel to $\overline{ab}$ from c at a distance v_r, so that the parallelogram $\overline{abcd}$ is again the desired exit velocity diagram.

After assuming the number of blades z_a, t_a is determined, and then considering the equation $\sin \beta_a = \frac{a_a + s_a}{t_a}$ we find graphically $a_a + s_a$.

The exit velocity diagram was determined for a point just before the exit from the impeller, hence the velocity refers to that velocity existing in the contracted exit area F_a due to the thickness of the blades. To be exact, a velocity

$$v_r' = v_r \frac{a_a}{a_a + s_a} \quad \ldots\ldots\ldots \quad 157$$

must be used for the calculation of the actual exit area $F_a' = D_a \pi b_a$. With blades of large pitch it is possible to assume for simplicity without introducing great error that $v_r = v_r'$. With small pitch and correspondingly smaller exit height a_a, it is best to determine the velocity v_r' and then calculate the impeller width b_a from the equation (see equation 75)

$$b_a = \frac{Q + Q_{sp}}{D_a \pi v_r'} \quad \ldots\ldots\ldots \quad 158$$

17. The Involutes for Impeller and Guide Vanes.

(a). *General Consideration of the Use of the Involute.*

The first general fundamental equation (equation 10) shows that the theory of centrifugal pumps depends mainly on the fact that the water in flowing through the impeller and guide vanes is forced to assume a definite velocity by means of the form given to the blade channels. The direction of the water is determined by the entrance and exit velocity diagrams. The equations subsequently derived determined the magnitude of these velocities and with

what angles the impeller and guide vanes must be constructed in order to give the desired head and quantity of water for a certain number of revolutions. In order to fulfill these equations, the first condition is to give the impeller and guide vane channels such a form that the proper velocities and their directions may be correctly obtained.

A great mistake in the construction of centrifugal pumps which can be found to-day in many designs is that the cross sections derived from the calculation of these formulas is not adhered to in the construction of the blades. The result is that the supposed velocity diagrams do not exist and the pump will not give what is desired at the correct number of revolutions. Designers then determine experimentally the number of revolutions necessary to give the desired head and then claim that the equations determined by theory do not give correct results. Chiefly by the aid of experiments the number of revolutions for a certain quantity and head was determined, and one pump after the other was constructed until a series was obtained which in some manner fulfilled the desired conditions. It is to be regretted that such incorrect designs are found to-day in practice and in textbooks. Such designs will now be discussed.

From equations of form similar to those already derived, entrance and exit velocity diagrams are determined. The chief factors in determining the form of the blades are the impeller angles β_e and β_a and the guide angle δ_a. After determining the outer and inner diameters D_a and D_e the design of the impeller blades was very simply accomplished by drawing the angles β_a and β_e at the diameters D_a and D_e and connecting the lines forming these angles by an arc of as large a radius as possible. Recent textbooks even specify what the angle between point of entrance and exit should be in order to obtain a favorable connecting arc.

Blades of this false form are shown dotted in Fig. 38. By comparison with blades of the correct form shown by the heavy full lines of the same figure it will be shown why these false forms are incorrect.

In the design of the blades and blade channels the following conditions must be strictly adhered to in general.

The blade channels must be formed at beginning and end so that the entrance and exit areas, obtained after determining the relative velocities, actually exist in the design. Further, that the direction

of the water velocities, as determined by the angles β_e and β_a, are at right angles to the entrance and exit areas. The following equation must be satisfied:

$$z\, a_e b_e v_e = z\, a_a b_a v_a = Q + Q_{sp} \quad . \quad . \quad . \quad . \quad . \quad 159$$

where $a_e b_e$ and $a_a b_a$ represent the entrance and exit areas of each blade channel and z their number. The channel heights a_e and a_a must be at right angles to both neighboring blades while at the same time avoiding a contraction or enlargement of the stream. Not

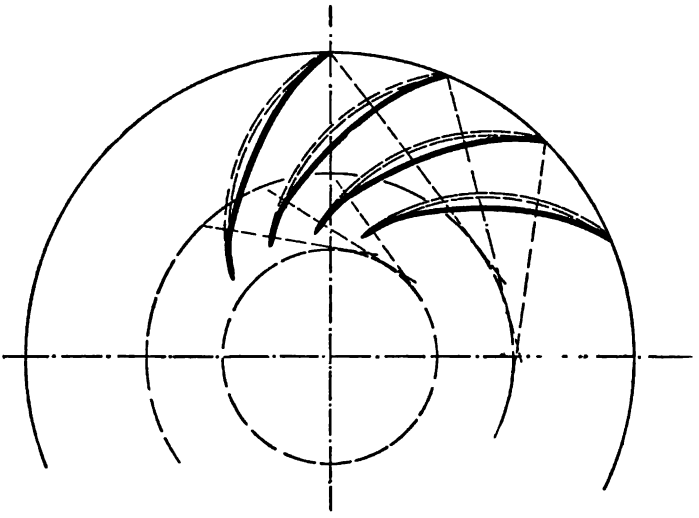

Fig. 38.

until this is so will the direction of the water velocity be at right angles to every point of the entrance and exit areas. The relative velocities assumed in the calculations will then actually be obtained and the assumed velocity diagrams will be correctly formed.

In order to fulfill these conditions the blades at entrance and exit must form equidistant curves at a distance a_e and a_a from one another and form the angles β_e and β_a with the periphery of the circles whose diameters are D_e and D_a. An involute will best fulfill these conditions.

In Fig. 38 the blades represented by heavy solid lines are drawn as involutes at entrance and exit. The cross section of the blade channels at these points corresponds exactly to those given in the calculations. Comparing the heavy and dotted blades, it can clearly be seen that the latter have incorrect entrance cross sections — the

entrance cross section too large, the exit cross section too small. With such cross sections relative velocities other than those given in the diagram will occur, because it is impossible for the calculated diagrams to form. A number of revolutions quite different from the calculated number is necessary to give the desired head and quantity of water.

Exactly the same error is made in the design of the guide vanes as is made in the design of the impeller blades. It is best to have the beginning of the guide vanes form involutes.

It will be shown in the following how to form the involutes at impeller exit and entrance and in the guide vanes.

(*b*). *The Involutes at Impeller Entrance.*

For entrance without shock the blades at entrance must form an angle β_e with u_e. The circle whose diameter is D_e, and to which the entrance diagram refers, should pass through the middle of the entrance height a_e. It will be shown later that diagrams at various points across the entrance height a_e vary. The mean diagram upon which the calculation is based will be taken at the middle of a_e. To avoid a contraction or enlargement of the stream, the blade height a_e must be taken at right angles to the neighboring blades and the blade must form an angle β_e to the periphery at the diameter D_e. The blade at entrance will now be constructed as an involute and its applicability investigated.

If z_e is the number of impeller blades, the diameter d_e of the base circle of the involute is found from the equation

$$d_e = \frac{z_e (a_e + s_e)}{\pi} \quad . \quad . \quad . \quad . \quad . \quad . \quad . \quad 160$$

For simplicity assume that the sides of the impeller, so far as the blades go, remain parallel, that is, the entrance width b_e is equal to the exit width b_a. After assuming D_e and z_e the entrance velocity diagram and the value of $a_e + s_e$ can be found. The method of constructing the entrance involute will now be shown.

The diameter of the base circle is determined according to equation 160. In order to construct two channels, step off the half pitch $\frac{t_e}{2}$ six times on the circle whose diameter is D_e (Fig. 39). Through

the points thus found and alternately designated by 1 and 2 draw tangents to the base circle. On both sides of points 1 lay off along the tangent the distances $\frac{a_e}{2}$ and $\frac{a_e}{2} + s_e$; and on both sides of 2 lay off the distance $\frac{s_e}{2}$. For each blade six points *a*, *b*, *c* and *d*, *e*, *f* are found. The portion *abc* of the involute may be replaced by an arc of a circle

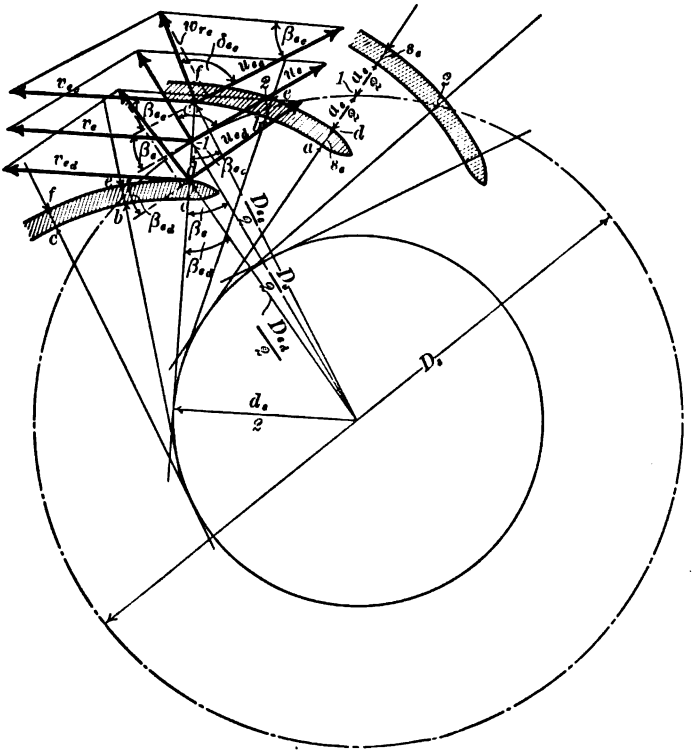

Fig. 39.

whose center lies approximately on the intersection of the two tangents drawn through the two neighboring points 1 on the base circle. In order to be sure of guiding the water correctly it is advisable to prolong the involute beyond *c* about half an inch. The part *def* is made parallel to *abc* when sheet-metal blades are used, but with cast blades it is given a form suitable to the shape of the blade channel.

It can be seen from Fig. 39, and probably needs no further proof,

that the momentary guiding angle of the involute at diameter D_e is equal to the impeller entrance angle β_e. From the figure

$$\sin \beta_e = \frac{d_e}{D_e} \quad . \quad . \quad . \quad . \quad . \quad . \quad . \quad . \quad 161$$

or

$$d_e = D_e \sin \beta_e \quad . \quad . \quad . \quad . \quad . \quad . \quad . \quad . \quad 162$$

If β_e is known, the diameter of the base circle can be found from this equation, and after assuming z_e the value $a_e + s_e$ can be directly determined from equation 160.

The entrance velocity diagrams at various points across the channel height a_e will vary because the diameters and therefore the peripheral velocities do not remain the same. It will be proved that in spite of the change of u_e, β_e, and w_e the relative velocity v_e will have the same value and direction across the entire channel height a_e if the blades are formed by involutes.

The values relating to the points c and d are designated by corresponding indices. The peripheral velocity at point c is

$$u_{e_c} = u_e \frac{D_{e_c}}{D_e} \quad . \quad . \quad . \quad . \quad . \quad . \quad . \quad . \quad 163$$

because the peripheral velocities vary directly with the diameters. As can be seen from the figure,

$$\sin \beta_{e_c} = \frac{d_e}{D_{e_c}} \quad . \quad . \quad . \quad . \quad . \quad . \quad . \quad . \quad 164$$

Dividing equation 164 by 161 we have

$$\frac{\sin \beta_e}{\sin \beta_{e_c}} = \frac{D_{e_c}}{D_e} \quad . \quad . \quad . \quad . \quad . \quad . \quad . \quad . \quad 165$$

from which it is seen that the entrance angles vary inversely with the corresponding diameters.

As the width of impeller remains the same, the vertical component w_r of the absolute entrance velocity w_e varies inversely with the corresponding diameter, so that

$$\frac{w_r}{w_{r_e}} = \frac{D_{e_e}}{D_e} \quad . \quad . \quad . \quad . \quad . \quad . \quad . \quad . \quad 166$$

The entrance velocity diagram is determined by the three values

u_e, β_e, and w_r. For the middle diagram the relative entrance velocity at point 1 can be expressed as

$$v_e = \frac{w_r}{\sin \beta_e},$$

and similarly for the point c, with corresponding indices,

$$v_{e_c} = \frac{w_{r_c}}{\sin \beta_e}.$$

Dividing these two equations and taking into account equations 165 and 166, we have

$$\frac{v_e}{v_{e_c}} = 1; \text{ hence } v_{e_c} = v_e.$$

Similarly for point d we have $v_{e_d} = v_e$.

It is therefore proven that by using an involute for the beginning of a blade the relative entrance velocity v_e remains constant across the entire channel height a_e.

(c). *The Involutes at Impeller Exit.*

The shape of the impeller blade at exit as well as at entrance is preferably made to conform in outline to the involute. Let a_a be the blade channel height, s_a the blade thickness, and z_a the number of blades at impeller exit. The diameter of the base circle for the involute will then be

$$d_a = \frac{(a_a + s_a) z_a}{\pi} \quad \ldots \ldots \quad 167$$

or from Fig. 40,

$$d_a = D_a \sin \beta_a \quad \ldots \ldots \quad 168$$

The value $a_a + s_a$ is calculated from the equation

$$a_a + s_a = \frac{D_a \pi \sin \beta_a}{z_a} \quad \ldots \ldots \quad 169$$

The construction of the involute at the exit is exactly the same as at the entrance. No further proof is needed that the relative exit velocity v_a remains the same across the entire width if the involute is used, or that the general equation

$$\frac{\sin \beta_a}{\sin \beta_a'} = \frac{D_a'}{D_a} = \frac{u_a'}{u_a} = \frac{v_r}{v_r'} \quad \ldots \ldots \quad 170$$

holds.

The velocity diagrams vary across the entire exit height and the various values of u_a, β_a, and v_r are obtained from equation 170. Only the exit velocity diagram calculated for the pump will satisfy the equations derived for the peripheral velocity. All other diagrams across the blade channel height a_a give an incorrect peripheral velocity for the actually existing angles β_a and δ_a, because the resulting calculated peripheral velocities increase as the diameter decreases, which is of course impossible.

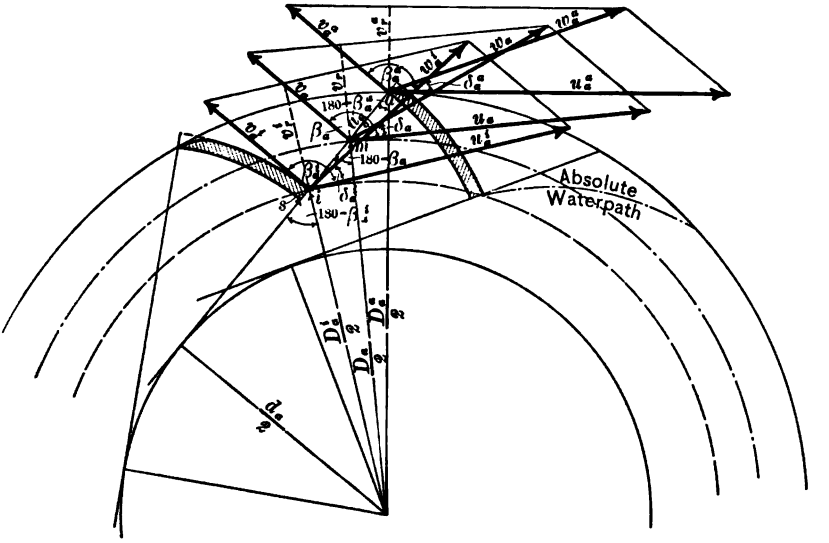

Fig. 40.

From equation 170 and also Fig. 40 it is seen that the angle β_a becomes smaller as the diameter decreases. The angle δ_a will, however, increase towards the center of the impeller in spite of the fact that the angle β_a decreases towards the center, and vice versa towards the outside. The tangent of angle δ_a is found from equation 153,

$$\tan \delta_a = \frac{v_r}{u_a + \frac{v_r}{\tan \beta_a}} \quad . \quad . \quad . \quad . \quad . \quad (153)$$

This equation does not give a good idea of the decrease and increase of δ_a, because the right-hand member contains two variables.

In order to obtain a clear idea of the relation existing between β_a and δ_a with the corresponding diameters we shall solve the exit

velocity diagrams for various diameters, taking a concrete example. For reasons to be discussed later the peripheral velocity is calculated for the diameter D_a at $\frac{a_a}{2}$.

Let $\sqrt{\eta g H_n} = 32.8$ feet and the diameter D_a at $\frac{a_a}{2}$ equal 0.98 foot. For this diameter let the impeller angle $\beta_a = 135°$ and the guide angle $\delta_a = 25°$

From the κ curves (Plate I) for $\beta_a = 135°$ and $\delta_a = 25°$, $\kappa = 1.21$; so that for the assumption $\delta_e = 90°$ $u_a = 32.8 \times 1.21 = 39.69$ feet. From the λ curves for $\delta_a = 25°$ and $\kappa = 1.21$ the radial exit velocity $v_r = 12.63$ feet.

Assuming 12 blades at impeller exit, equation 169 gives $a_a + s_a = 2.22$ inches. Let $s_a = 0.22$ inch; then $a_a = 2.0$ inches. From equation 167 or 168 the diameter of the base circle of the involute is found to be $d_a = 8.48$ inches.

The involutes have been drawn in Fig. 40. The outer diameter $D_a^a = 1.1$ feet is found graphically, as is also the diameter $D_a^i = 0.88$ foot at the beginning of the involute.

The values found for the three points a, m, and i are given in the following table.

	D_a	u_a	β_a	δ_a	v_a	w_a	(u_a)
a	1.1	44.44	141°	20°	17.55	32.96	39.39
m	0.98	39.69	135°	25°	17.55	30.18	39.69
i	0.88	35.16	128°	30°	17.55	28.54	40.67

In the last column of this table the peripheral velocities given are derived from equation 58, and represent the values necessary in order that no shock losses shall occur with the actually existing angles β_a and δ_a. It can be seen that these calculated peripheral velocities vary considerably from the actual existing velocities which are given in the first column.

In order to neutralize this error in the diagrams as much as possible it is necessary in calculating the peripheral velocity for the diagram not to take the outer but to take the mean diameter D_a. If a pump is designed with a diagram based on the outer diameter the peripheral velocity of the impeller will be too small, and in order to

obtain the desired head and quantity of water it will be necessary to increase the number of revolutions beyond those for which it was designed.

Attention is called to the fact that the above is equally true in the design of water turbines. In the design of these wheels for both low and high speeds the error of basing the velocity diagram upon the outer diameter D_a^a is sometimes made. Brake experiments upon such false designs have shown that the turbine developed its greatest power at a number of revolutions quite different from the calculated number. Pfarr of Darmstadt, Germany, in his lectures on hydraulic machinery, called attention to this mistake.

It is usual to have the outer diameter D_a^a a whole number because it is a dimension used in the shops. For this reason the outer diameter must be assumed and the mean diameter calculated after assuming the outer impeller angle β_a. The mean diameter is found mathematically, after assuming the outer diameter D_a^a and the outer impeller angle β_a^a, from the equation (see Fig. 40)

$$\frac{D_a^2}{4} = \frac{D_a^{a2}}{4} + \frac{a_a^2}{4} - \frac{2\,a_a D_a^a \cos(180 - \beta_a^a)}{4}$$

or

$$D_a = \sqrt{D_a^{a2} + a_a^2 + 2\,a_a D_a^a \cos\beta_a^a} \quad . \quad . \quad . \quad . \quad 171$$

The angle β_a is then determined from equation 170. If the mean diameter D_a is given, the outer diameter D_a^a is found from (see Fig. 40)

$$\frac{D_a^{a2}}{4} = \frac{D_a^2 \sin^2\beta_a}{4} + \left(\frac{a_a}{2} - \frac{D_a}{2}\cos\beta_a\right)^2,$$

or

$$D_a^a = \sqrt{D_a^2 + a_a^2 - 2\,a_a D_a \cos\beta_a} \quad . \quad . \quad . \quad . \quad 172$$

The outer and inner diameters, however, can be found more quickly graphically.

If the outer diameter D_a^a and the peripheral velocity u_a^a are given, the latter being derived after assuming the number of revolutions, then the exit involutes can be constructed after assuming β_a^a and z_a. Calculate the diameter of the base circle from equation 168. Graphically or from equation 171 determine the mean diameter D_a and from equation 170 find the angle β_a. For the case $\delta_e = 90°$, κ is determined from the equation $\kappa = \frac{u_a}{\sqrt{\eta g H_n}}$. From the κ curves of Plate I read the angle δ_a corresponding to the derived angle β_a.

By aid of the λ curves find the corresponding radial exit velocity v_r. The impeller width b_a is determined from equation 158. If the width b_a is not suitable for the impeller profile it is necessary to make a more suitable assumption of the angle β_a.

If the mean diameter is given, the outer diameter is determined in a similar manner.

A disadvantage in the use of the involute is that the values of the absolute exit velocity w_a vary across the exit height a_a, as can be seen from the table on page 68. The question arises whether it is not advisable to make the absolute exit velocity across the exit height always the same, that is, to allow it to follow an equidistant curve, hence an involute. Should this be done the relative exit velocity would change across the exit height.

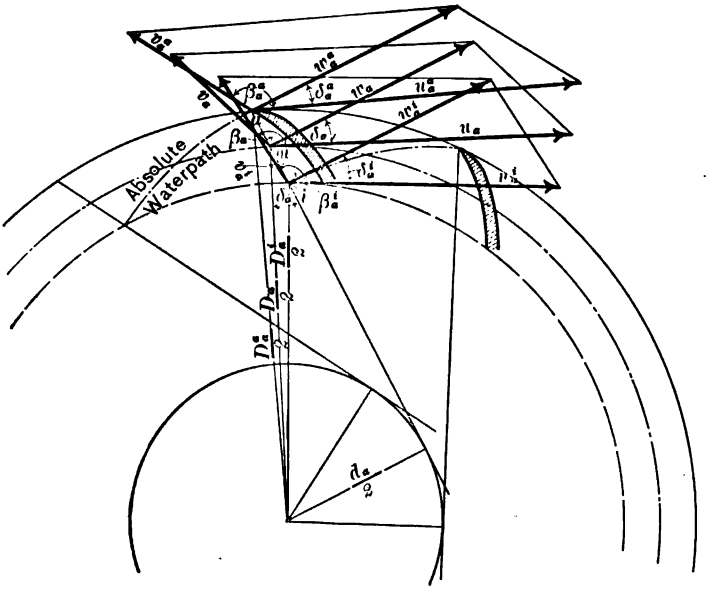

Fig. 41.

For the former example, the absolute path of the water as an involute has been drawn in Fig. 41. After calculating the diagram for the individual points the relative path of the water is determined.

In this case the relative exit velocity varies across the exit width. The water guidance is not as good in the blade channels as when the relative water course is an involute, but it is an advantage to have the absolute exit velocity follow an involute in passing to the

guide vanes, which, as will be shown later, should also be constructed of involute curves. If the relative velocity follows the path of an involute, the absolute water course will not follow an involute but will describe some sort of a similar curve (see Fig. 40). If in this case the water in the guide channels is made to follow the path of an involute, then the absolute exit velocity is forced to change from its first assumed path to that of an involute path, which is accompanied by small losses. In the following table the values of the diagrams at points a, m, and i are given for the assumption that the absolute water path is an involute. As before, the last column shows the peripheral velocities necessary for operation without shock with the existing angles β_a and δ_a according to equation 58.

	D_a	u_a	β_a	δ_a	v_a	v_{ra}	(u_a)
a	1.08	43.30	144°	23°	19.35	30.18	41.33
m	0.98	39.69	135°	25°	17.55	30.18	39.69
i	0.89	35.75	123°	28°	16.40	30.18	36.60

A comparison of these values with those given in the table on page 68 shows that in the last case the difference is not so great between the peripheral velocities calculated from the angles β_a and δ_a and those actually existing. Hence the diagrams agree more closely with the actual conditions if the absolute water path follows an involute than if the relative water path is made to follow an involute.

By very carefully conducted experiments it can be proved that the pump efficiency is slightly increased, for the reasons already given, when the absolute water path is an involute. As the latter method is somewhat complicated, in the following it will be considered for simplicity that the relative water path is an involute, leaving the more refined construction to the conscientious designer.

(*d*). *The Involutes at Guide Vane Entrance.*

The absolute exit velocity w_a which leaves the impeller at an angle δ_a is decreased to a velocity w_a' after exit from the impeller. Its value is

$$w_a' = w_a \frac{a_a}{a_a + s_a} \quad . \quad . \quad . \quad . \quad . \quad . \quad . \quad 173$$

It is assumed that the middle water thread flowing from the point a (see Fig. 42) retains the velocity w_a' until it enters the guide vanes and that the path of the same will be an involute which will have an angle of slope δ_a at the point a where the diameter is D_a.

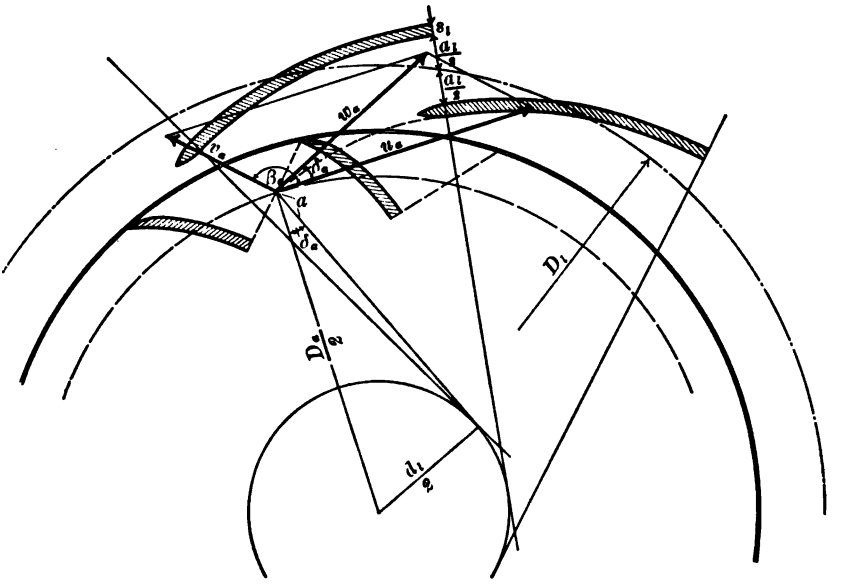

Fig. 42.

The diameter of the base circle of the involute is

$$d_l = D_a \sin \delta_a \quad \ldots \ldots \ldots \quad 174$$

The height of the blade channel is a_l, the blade thickness at entrance s_l, and the number of blades z_l. The value of $a_l + s_l$ is then found from

$$a_l + s_l = \frac{d_l \pi}{z_l} \quad \ldots \ldots \ldots \quad 175$$

If the impeller width at exit is b_a, the height of the channel can be determined from the equation

$$a_l + s_l = \frac{Q}{w_a' b_a z_l} \quad \ldots \ldots \ldots \quad 176$$

and then inversely the base circle of the involute can be determined from equation 175.

After entering the guide channels the velocity w_a' is increased on account of the blade thickness to w_l; hence

$$w_l = w_a' \frac{a_l + s_l}{a_l} \quad . \quad . \quad . \quad . \quad . \quad . \quad . \quad . \quad 177$$

It is advisable to allow a clearance of from one-quarter to three-quarters of an inch between the impeller and guide vanes in order to permit the absolute velocities of the water leaving the impeller at a slightly varying angle δ_a to accommodate themselves to the direction of the involute path in the guide channels. It is to be noted that only the middle water thread leaves the impeller at approximately the correct direction corresponding to the path of the assumed involute.

18. The Guide Vane Casing.

To lead correctly, both as to direction and velocity, the water flowing from the guide channels to the pressure pipe the casing is best made in the form known as spiral. Such a casing finds its best application in designs of low-pressure centrifugal pumps. In multiple-stage high-pressure pumps the guide vanes of the last stage only are surrounded by such a casing, while the other guide vanes have a casing whose form is determined by the requirements of the design of the pump. Spiral casings are made of either rectilinear or circular cross section. The former shape is easier to produce in the foundry, while the latter presents a more pleasing appearance but is more costly.

In the rectilinear form the outer boundary follows the curve of an involute and satisfies the condition that the mean water velocity remains the same throughout the casing. Let A be the height of the casing at the largest cross section, B the width (see Fig. 43), and w_d the mean velocity. With constant width B the height A must decrease linearly at the periphery in order to maintain the constant velocity w_d. The latter condition is satisfied by having the outer boundary curve of the casing an involute. The diameter of the base circle of this involute is

$$d = \frac{A}{\pi} \quad . \quad . \quad . \quad . \quad . \quad . \quad . \quad . \quad . \quad 178$$

The diameter at which the involute starts is designated by d_i.

The angle ϕ at which the water leaves the periphery of the circle is found from the equation

$$\sin \phi = \frac{d}{d_i} \quad . \quad . \quad . \quad . \quad . \quad . \quad . \quad . \quad 179$$

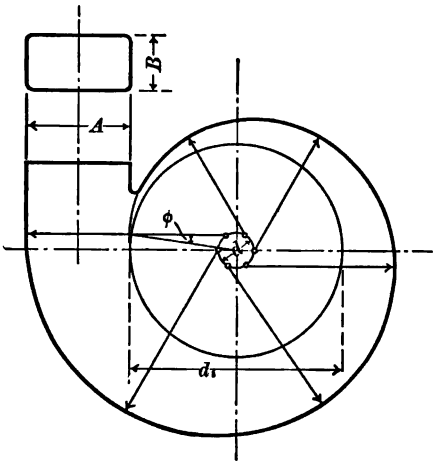

Fig. 43.

To guide the water correctly, in direction and velocity, into the casing, it is necessary to slope the ends of the guide vanes at exit so that the water stream in leaving the diameter d_i will enter the casing at the angle ϕ.

The mean velocity of the water in the casing is taken, if possible, smaller than one-third of the peripheral velocity u_a. At exit from the spiral casing the water is led through a conical pipe to the pressure pipe, in which, as a rule, the water velocity is small. Frequently the exit from the casing is in itself conical.

In a casing of circular cross section the areas of the cross sections must decrease linearly in order to have a constant mean velocity. The construction of the boundary curve of the casing is preferably made by drawing small circles of diameters d_1, d_2, d_3, etc., tangent to the common circle of radius r_i (see Fig. 44). With this assumption an equation can be derived for such a bounding curve.

The quantity of water and the areas of the circles of diameters d_6, d_5, d_4, etc., are proportional to the angles ψ_6, ψ_5, ψ_4, respectively, because the mean water velocity should remain constant. Let Q_1, Q_2, Q_3, etc., be the quantities of water flowing through the cross

sections of the circles whose diameters are d_1, d_2, d_3 respectively. Then

$$\frac{Q_1}{Q_2} = \frac{d_1^2}{d_2^2} = \frac{\psi_1}{\psi_2} \quad \ldots\ldots\ldots \quad 180$$

so that

$$\frac{d_1^2}{\psi_1} = \frac{d_2^2}{\psi_2} = C \quad \ldots\ldots\ldots \quad 181$$

and generally

$$d = \sqrt{C\psi} \quad \ldots\ldots\ldots \quad 182$$

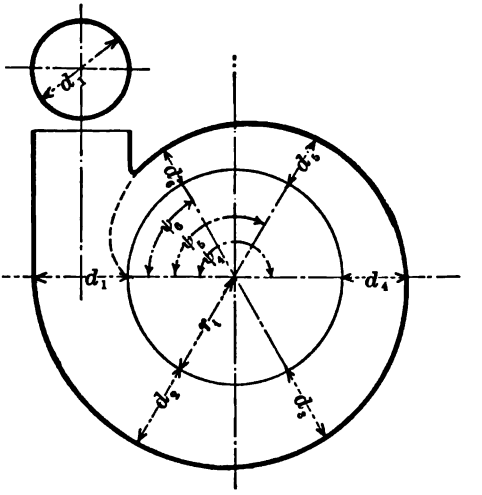

Fig. 44.

The individual circles are to be tangent to a common circle of radius r_i, so that the polar coördinate of the boundary curve at any point of the casing has the value

$$r_a = \sqrt{C\psi} + r_i \quad \ldots\ldots\ldots \quad 183$$

This is the polar equation of a parabolic spiral starting at radius r_i.

Often for cheapness of construction the boundary curve of the casing is made circular, that is, simply placed concentric to the guide vanes (see Fig. 45). With this construction care must be taken to make the cross-sectional area of the casing quite liberal. There exists a place in this casing at which the direction of the flow must be divided. If the cross section is too small at this point great shock losses occur. It is advantageous, with such a casing, to let the water flow from the guide channels as nearly radially as possible.

Placing a circular casing eccentrically about the guide vanes should be strictly avoided. Very large shock and eddy losses occur at the narrowest place because the water is suddenly reversed in direction. The pump efficiency is greatly reduced by such a casing.

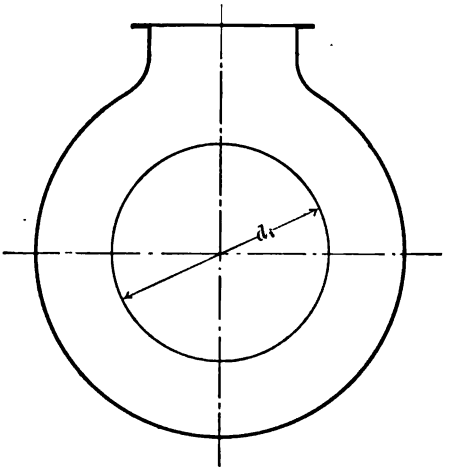

Fig. 45.

19. Axial Thrust.

As has been stated, certain pressures will exist in the spaces between the impeller and its surrounding casing, and if these pressures are not of the same magnitude and are not exerted upon equal areas of the rotating element an axial thrust will be produced. These pressures are caused first by the pressure difference in the clearance space and secondly by the action of centrifugal forces forming a rotating paraboloid.

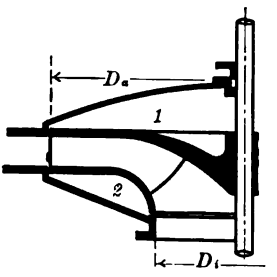

Fig. 46.

An investigation will now be made to determine the pressures in spaces 1 and 2, shown in Fig. 46, how they are formed and how large the resultant axial thrust will be.

Space 1 is not connected with the space at entrance to the impeller, so that, neglecting the rotating paraboloid, the pressure in the clearance space will reach the full value $H_{sp} = \eta H_n - \frac{w_a^2}{2g}$. Neg-

lecting the space occupied by the shaft, the side of the impeller in space 1 will be loaded with a pressure

$$p = \frac{D_a^2 \pi}{4}\left(\eta H_n - \frac{w_a^2}{2g}\right) W,$$

in which W is the weight of a unit volume (cubic feet) of water.

According to the law of communicating tubes, the pressure difference in the clearance space even when considering the influence of the rotating paraboloid will still be $\eta H_n - \frac{w_a^2}{2g}$. If it is again assumed that the rotating paraboloid, on account of friction losses, is rotating at the outer diameter with a velocity ϕu_a, then the load on the impeller will be decreased by an amount equal to the weight of a quantity of water whose volume is that of the rotating paraboloid. The volume of the paraboloid is

$$V = \frac{1}{2} \frac{D_a^2 \pi}{4} \phi^2 \frac{u_a^2}{2g},$$

so that the load P_1 on the impeller in space 1 is equal to

$$P_1 = \frac{D_a^2 \pi}{4}\left(\eta H_n - \frac{w_a^2}{2g} - \frac{\phi^2}{2} \frac{u_a^2}{2g}\right) W \quad . \quad . \quad . \quad . \quad 184$$

In order to make this phenomenon clear imagine a hollow cylindrical vessel entirely filled with water (see Fig. 47). The height of the cylinder is h and the diameter of the base D. The pivot bearing will be loaded, in addition to the weight of the cylinder, with a weight of water equal to $p = h \frac{D^2 \pi}{4} W$. If the vessel is now rotated with a peripheral velocity of u_a, centrifugal force will throw out a quantity of water equal to the volume of the rotating paraboloid thus formed. The volume of this paraboloid is $\frac{1}{2} \frac{\pi D^2}{4} \frac{u_a^2}{2g}$. The pivot bearing will therefore be relieved of the load $\frac{1}{2} \frac{\pi D^2}{4} \frac{u_a^2}{2g} W$. The load on the pivot bearing due to the water remaining in the cylinder will then be

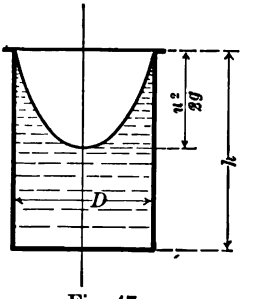

Fig. 47.

$$P = \left(h - \frac{u_a^2}{2g} \frac{1}{2}\right) \frac{D^2 \pi}{4} W.$$

The conditions in space 1 are similar to those of the rotating cylinder.

In space 2 a pressure occurs at the inner clearance ring, taking into consideration equations 29 and 42, the value of which is

$$p_i = \frac{\eta H_n - \frac{w_a^2}{2g} - \phi^2\left(\frac{u_a^2 - u_i^2}{2g}\right)}{1 + \left(\frac{f_i}{f_a}\right)^2} \quad . \quad . \quad . \quad . \quad . \quad 185$$

in which f_a is the outer and f_i the inner clearance space area.

Assuming that the pressure in space 2 is everywhere of the same magnitude p_i, the impeller would be subjected to a load of

$$P_i = W\left[\frac{\eta H_n - \frac{w_a^2}{2g} - \phi^2\left(\frac{u_a^2 - u_i^2}{2g}\right)}{1 + \left(\frac{f_i}{f_a}\right)^2}(D_a^2 - D_i^2)\frac{\pi}{4}\right] \quad . \quad 186$$

By the formation of a rotating paraboloid the pressure p_i increases from D_i to D_a according to a parabola which at diameter D_i has a head $\phi^2\frac{u_i^2}{2g}$ and at diameter D_a a head $\phi^2\frac{u_a^2}{2g}$. The load on the impeller will therefore be increased by the weight of the parabolic end whose volume J is represented by the equation

$$J = \frac{\phi^2}{2}\left(\frac{u_a^2}{2g}\frac{D_a^2\pi}{4} - \frac{u_i^2}{2g}\frac{D_i^2\pi}{4}\right) \quad . \quad . \quad . \quad . \quad . \quad 187$$

so that the load on the impeller in space 2 now becomes

$$P_2 = P_i + JW = \left[\frac{\eta H_n - \frac{w_a^2}{2g} - \phi^2\left(\frac{u_a^2 - u_i^2}{2g}\right)}{1 + \left(\frac{f_i}{f_a}\right)^2}(D_a^2 - D_i^2)\frac{\pi}{4} + \frac{\phi^2}{2}\left(\frac{u_a^2}{2g}\frac{D_a^2\pi}{4} - \frac{u_i^2}{2g}\frac{D_i^2\pi}{4}\right)\right] W. \quad . \quad . \quad . \quad . \quad . \quad 188$$

In the arrangement shown in Fig. 46 the pressure $P_1 > P_2$, so that there is a resultant axial thrust A the value of which is

$$A = P_1 - P_2 \quad . \quad . \quad . \quad . \quad . \quad . \quad . \quad . \quad 189$$

Substituting the values of P_1 and P_2 from equations 184 and 188, the resultant axial thrust is found to be

$$A = \left[\left(\eta H_n - \frac{w_a^2}{2g} - \phi^2 \frac{u_a^2}{2g}\right)\frac{D_a^2\pi}{4} - \frac{\eta H_n - \frac{w_a^2}{2g} - \phi^2\left(\frac{u_a^2 - u_i^2}{2g}\right)}{1 + \left(\frac{f_i}{f_a}\right)^2}\left(D_a^2 - D_i^2\right)\frac{\pi}{4} - \frac{\phi^2}{2}\left(\frac{u_a^2}{2g}\frac{D_a^2\pi}{4} - \frac{u_i^2}{2g}\frac{D_i^2\pi}{4}\right)\right] W \quad . \quad . \quad . \quad . \quad 190$$

In various ways attempts have been made to do away with this troublesome axial thrust, but it has never been wholly accomplished. In the description of the various types of centrifugal pumps this question will receive further attention. It is necessary, especially with high-pressure centrifugal pumps, to supply strong thrust bearings capable of taking thrust in either direction. The spherical bearing has recently been again abandoned because, apparently, the number of revolutions is too high for this type of bearing. An accurately fitted thrust collar bearing has again come into use because this construction is simpler and therefore increases the reliability of the pump.

20. The Multi-stage Centrifugal Pump.

Considering only the question of highest possible efficiency, the design would be limited to a single impeller, that is, a single-stage pump. Pumps which are to deliver large heads are divided into a number of stages; that is, multiple impellers are mounted successively on a shaft, each one of these impellers or stages delivering like fractions of the head. The arrangement of such multi-stage pumps varies considerably, as will be seen later. For the present a three-stage high-pressure pump designed by Jager of Leipzig, Germany, shown in Fig. 48, will be considered.

The head for each stage is limited by efficiency considerations; that is, the clearance and friction losses must not be too great. The allowable peripheral velocity of the impeller limits the head obtainable per stage.

With equal clearance space areas and the use of a clearance ring, the short-circuit loss will increase with increasing head according to the ratio

$$\sqrt{\frac{\eta H_n - \frac{w_a^2}{2g}}{\eta H_n' - \frac{w_a'^2}{2g}}}, \quad \text{where } H_n > H_n'.$$

But it is often necessary, when increasing the heads, to decrease the number of revolutions and to increase the impeller diameter D_a

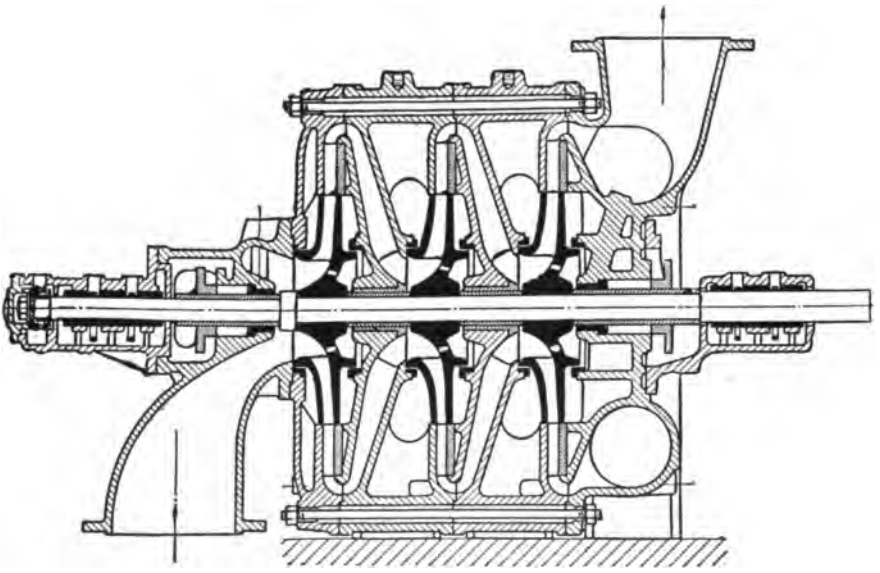

Fig. 48.

and therefore also increase the clearance space area. The short-circuit loss will then be increased, considering the greater clearance space area, by the value

$$\frac{D_a}{D_a'}\sqrt{\frac{\eta H_n - \frac{w_a^2}{2g}}{\eta H_n' - \frac{w_a'^2}{2g}}}.$$

If the head which is too great for a single stage is divided amongst several stages, the pressure in the clearance space will decrease on account of the decreased head, and for the same number of revolutions

the outer impeller diameter will be smaller, thus reducing the clearance space area.

If large heads are used a considerable decrease of hydraulic efficiency occurs, due to the rapid increase of friction losses. Assuming equal quantities of water, the guide and impeller cross sections decrease with the increase of relative velocity. Let a be the height, b the width of a channel, and v the velocity therein. Then, generally, the friction head h necessary to overcome the friction losses along a channel of length l is

$$h = \lambda \frac{(a+b)\, v^2}{2\, ab \cdot 2\, g}\, l.$$

The friction head is therefore proportional to the square of the velocity and to the value $\frac{a+b}{2\, ab}$, which in most cases increases with decreasing guide and impeller cross section.

In order to reduce the friction losses to a minimum, it is necessary to make the velocity v as small as possible and the channel correspondingly as large as possible. This is accomplished by dividing the large head among a number of stages.

Another reason for limiting the head of one stage is that if the water contains sand the high water velocities will cause a rapid deterioration of the blades.

The efficiency of a multi-stage pump is greater than that of a single-stage pump delivering an equal quantity of water with a head equivalent to only one stage of the multi-stage pump. In a multi-stage pump the first stage is the least efficient, due to losses in the suction pipe (see Article 4), whereas in succeeding stages the losses are smaller because instead of a suction pipe a small reversing channel is used which connects the exit of the guide vanes of one stage to the entrance of the impeller of the succeeding stage; in the last stage additional losses in the guide casing occur. In a single-stage pump these losses in the suction pipe and discharge casing occur in one stage, while in a multi-stage pump, if total efficiency is considered, the losses are divided among a number of stages and are less when referred to the total head. The above is also true of the mechanical losses caused by stuffing-box and bearing friction. With one or many stages only one or two stuffing boxes and two bearings are needed, and these mechanical losses remain approximately the same but

may be considered as divided, in a multi-stage pump, among all the stages.

The total head of a stage cannot be given offhand because it depends upon the quantity of water and hence the size of the pump. The larger the quantity of water the larger the head that may be taken per stage. In different designs the head varies between 30 and 200 feet per stage.

The calculation of multi-stage pumps is conducted in exactly the same manner as has been shown for single-stage pumps except that the total head delivered, ηH_n, is divided between the number of stages, and the calculations for the guide vanes and impeller are made for this fractional head.

21. The Centrifugal Pump without Guide Vanes.

Up to this point the assumption has always been made that the water flowing from the impeller with an absolute velocity w_a was carried into guide vanes the object of which was gradually to decrease this velocity and change it into pressure. Not until recently, when high-pressure centrifugal pumps were designed, has the importance of guide vanes been recognized. Formerly centrifugal pumps for small heads were designed without guide vanes. Even to-day there are firms who do not use guide vanes in their designs. Their reasons are that a pump without guide vanes is simpler and safer in operation, that the guide vanes are subject to very great deterioration on account of high water velocities and that they can be easily clogged up on account of the small cross-sectional area. No doubt a pump without guide vanes is simpler and also cheaper to construct, but the safety of operation has little to do with the guide vanes, as no cases are known in which a shutdown was caused by their use. Referring to the wear of the guide vanes, it may be said that with backward-turned impeller blades, that is, $\beta_a > 90°$, the relative entrance velocity v_e and the absolute exit velocity may be taken approximately equal, so that with the same material the wear due to friction of water at high velocities will be no larger in the guide vanes than in the impeller. Clogging of the guide vanes can be avoided by correct design, for it is possible to make the entrance height a_e of the impeller channel smaller than the entrance height a_l of the guide channel, so that foreign substances which can

pass through the impeller will not clog the guide channels. The only advantage of a pump without guide vanes is its simplicity of construction, which permits cleaning and repairing to be easily accomplished. These advantages will probably always be in favor of centrifugal pumps without guide vanes, and the majority of firms undertaking the construction of centrifugal pumps will find it necessary to build cheap pumps without guide vanes as well as pumps having guide vanes. By exact and very careful construction, pumps without guide vanes can be made to give fairly satisfactory efficiencies.

The construction of centrifugal pumps without guide vanes is almost entirely confined to low-pressure pumps; while this construction can never find a place with multi-stage high-pressure pumps.

The calculation of a pump without guide vanes is carried through with the same equations as before except that in determining the peripheral velocity a smaller efficiency must be used. The losses while the water is flowing through the impeller are equally large whether the pump has or has not guide vanes. Considering Fig. 9, the pressure head h_a at point a will be equal in both designs, but the losses during the passage from exit of the impeller to entrance of the casing will be larger when the guide vanes are omitted; in other words, in a pump without guide vanes a smaller per cent of the velocity head $\frac{w_a^2}{2g}$ will be transformed into pressure than in a pump having guide vanes.

In spite of the fact that the friction losses along the guide vanes are absent in a pump without guide vanes, the shock and eddy losses are so great that the total loss, at exit from the impeller to exit of the casing, is much larger, as has been conclusively proved by experiments. The water leaving with a velocity w_a must first find its path, and the decrease of velocity and hence the transformation into pressure will not be so irregular.

The fact that the losses up to the impeller entrance are equally large, whether or not the pump possesses guide vanes, leads to making the pressure head h_a as large as possible in order that the velocity head $\frac{w_a^2}{2g}$ may be as small as possible. By this means the losses after exit from the impeller are not of such great importance. On the

other hand, with increasing pressure head h_a the pressure in the clearance space and therefore the short-circuit losses are increased.

In low-pressure pumps delivering large quantities of water, not only the angle β_a but also the angle δ_a may be increased, and it is possible to secure such peripheral velocities that the opposing pressure head formed by the rotating paraboloid in the clearance space will equal the excess of pressure in the clearance space and thus prevent short-circuit losses. Attention is called to Article 9 and especially to Fig. 22. Experimental work along the line of reducing the short-circuit losses should be very fruitful.

The form of casing surrounding the impeller of a pump without guide vanes is of such importance to the efficiency that only the spiral shape can be considered. The absolute velocity w_a will leave the impeller at a certain angle δ_a, and the spiral casing must be constructed so that the formation angle of the boundary curve of the casing (designated by ϕ, Fig. 43) does not deviate greatly from the angle δ_a, so that the velocity w_a is made to change its direction as little as possible. From the impeller outward, the width of the casing is increased conically in order to decrease the velocity and obtain a transformation into pressure in this part of the casing.

II. CONSUMPTION OF POWER AND EFFICIENCY.

22. General Consideration of Consumption of Power and Efficiency.

To make the centrifugal pump economical it is of the first importance to increase the efficiency as much as possible by proper design. The efficiency of a pump designated by the coefficient ξ is understood to represent the ratio of the work obtained from the pump (output) to the work delivered to the pump (input).

The work obtained, A_w, also called the water work, is expressed in horse power (h.p.) and is found from the quantity of water lifted per minute and the head delivered by means of the equation

$$A_w = \frac{QH_n\gamma}{33000} \quad . \quad . \quad . \quad . \quad . \quad . \quad . \quad 191$$

in which γ is the weight of a cubic foot of the liquid, Q the quantity of liquid in cubic feet per minute, and H_n the desired head in feet.

Let A_e be the work delivered to the pump shaft. The efficiency ξ may then be expressed by the equation

$$\xi = \frac{A_w}{A_e}.$$

The work delivered to the shaft is found from the equation

$$A_e = \frac{QH_n\gamma}{33000\,\xi} \quad . \quad . \quad . \quad . \quad . \quad . \quad . \quad 192$$

The efficiency is dependent upon the value of the hydraulic and mechanical losses. In Article 4 it was partially explained how the hydraulic losses occur and how they are minimized in order to make the hydraulic efficiency as large as possible.

The hydraulic losses are composed of the friction, shock, and eddy current losses. The latter are reduced to a minimum when the velocity diagrams, upon which the calculations are based, are realized at the given number of revolutions. This condition is recognized by the quiet running of the pump.

If the pump rotates at an incorrect number of revolutions, it is

at once known by the rumbling noise inside the casing. By simply touching the pump casing these disturbances may be felt. If the velocity diagrams are actually realized, only a quiet and regular sound of flowing water is heard from the inside of the pump.

For a desired quantity of water, the correct velocity diagram is formed only at a certain head, and it depends upon the skill of the designer whether or not the correct combination of quantity and head is obtained. The careful construction of the blades and vanes in the shop is also of the utmost importance, as will be seen from the following. The finished impeller passes through so many stages of construction that an error in the drawing room at once precludes all possibility of a correct impeller. The entrance and exit cross-sectional areas and angles must be exactly adhered to in the pattern shop and foundry. Above all, the dimensions at entrance of the guide channels must be exactly those found by calculation. In high-pressure centrifugal pumps the entrance heights of the guide channels vary approximately between the limits $\frac{1}{2}$ inch and $1\frac{1}{4}$ inches. If, for example, the calculated value for this height is 0.60 of an inch, and it is actually made 0.56 of an inch, the quantity of water delivered for the rated revolutions will be $56/60 = 0.933$ of the desired quantity of water; hence this difference of only 0.04 of an inch introduces an error of 7 per cent in the quantity of water to be delivered. This example shows with what accuracy we must make the entrance and exit cross sections of the guide vanes and impeller in order to obtain the calculated result.

The correct quantity of water can of course be obtained by increasing the number of revolutions of the driver, but such a procedure unnecessarily increases the pressure head, thereby giving additional work which may not benefit the purchaser.

To decrease the short-circuit losses, the clearance between the clearance rings must be reduced to a minimum.

Conscientious work in the drafting room and careful construction in the shop are the chief requisites in order to obtain good hydraulic efficiencies.

Strictly speaking, only the hydraulic efficiency is used in the calculation of a pump, as can be seen from equation 11 and those following. But to determine the power to drive the pump not only the hydraulic efficiency but also the mechanical and short-circuit losses must be considered.

The work necessary to run the pump light is a certain fraction of the total driving power. Here, as in all other forms of power machinery, this fraction becomes smaller as the size of the machine (total power) increases. It is therefore evident that the over-all efficiency of a centrifugal pump increases as its size (driving power) increases.

The mechanical losses, and therefore the no-load work, can be largely increased by certain circumstances. The friction work of the bearings is quite small with good lubrication, for the weight of the shaft and impeller is not great. If the pump is not direct connected, but has a belt between it and the driver, an additional loss is caused by the belt pull loading the bearings. It is open to question whether in determining the efficiency, the increased friction loss due to the belt should be included as work delivered to the shaft. The stuffing box, through poor design, unequal tightening or too tight an adjustment, is capable of considerably increasing the mechanical losses. Stuffing-box friction is at times a serious matter and many cases might be quoted in which the stuffing box caused complete failure of the pump. It is sometimes necessary, when using high pressures, to relieve the load on the stuffing box by means of some suitable arrangement which allows only a small part of the total pressure to act.

The thrust bearings provided to take care of the axial thrust cause a further friction loss that varies more or less. This bearing varies in design, and can be either a collar, ball, or step bearing.

High-pressure centrifugal pumps when first designed were not constructed with sufficient provision for taking care of axial thrust. On account of the thrust bearing the centrifugal pump was looked upon as unreliable in operation. Safety of operation is of first importance when a pump is used for lifting water in mine work. The effort is now made in all types of high-pressure centrifugal pumps to balance the axial thrust as nearly as possible by suitable design. The pump in which the balance is most complete may be called surest of operation. On account of the high number of revolutions, the thrust bearings cannot stand excessive pressure, no matter how well they are constructed.

While a complete axial balance is never reached by any type at the present time, various designs very nearly attain a complete balance, and therefore the thrust bearing has such small loads that it can no

longer be considered a limiting feature as far as safety of operation is concerned.

The exit losses from the pump casing will be considerable in the case of low-pressure pumps having small heads. In order to carry the water away from the pump, a certain velocity head $\frac{w_d^2}{2g}$ is necessary, which is expressed in equation 8 as a fraction α of the total head H_m. With high heads α has a value 0.005 to 0.01, with low heads and large quantities of water α equals 0.06 to 0.08. In the latter cases special consideration must be given α before choosing the coefficient η.

It is difficult to differentiate the hydraulic from the mechanical losses when given the total efficiency of a centrifugal pump and therefore the curves which follow are only for total efficiency of pumps.

23. Efficiency when the Number of Revolutions is Varied.

In this article it will be shown how the hydraulic and mechanical losses, hence the total loss, change when running a pump at varying speeds. At each number of revolutions the correct diagram (operation without shock) is formed only at a certain head and quantity of water.

For simplicity, assume that the impeller has parallel sides and that the blades from entrance to exit describe an involute with a common base circle as shown in Fig. 49. Let the constant channel height be a, the channel width be b, and the mean length of the channel be l.

First it will be determined how the friction losses change when referred to the existing heads. The hydraulic radius R for the impeller channel is

$$R = \frac{ab}{2(a+b)} \quad \ldots\ldots\ldots \quad 193$$

If v is the velocity in the impeller channel, the friction head due to the flow of water in the channel and causing a loss of pressure head will be

$$h = \lambda \frac{a+b}{2ab} \cdot \frac{v^2}{2g} \cdot l \quad \ldots\ldots\ldots \quad 194$$

The revolutions of the pump are so chosen that the relative velocity v lies between the limits of 30 and 65 feet.

The value for λ was determined experimentally by Weisbach for pipes of circular cross section. Between the velocities 30 and 65 feet λ varies between the limits 0.174 and 0.165. It may be that the value of λ increases for rectangular cross sections such as exist in the impeller and guide channels. For the velocities given within the above limits, however, it is probable that λ does not greatly increase, and therefore no great error is introduced by considering this coefficient as having the same value.

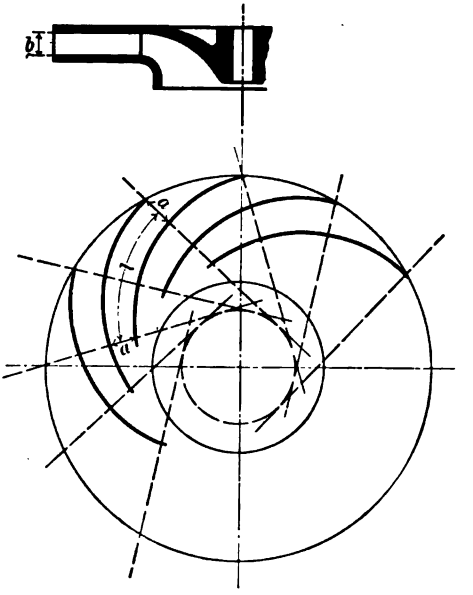

Fig. 49.

The determination of λ for such channels as occur in centrifugal pumps would be of great value.

With the same values of λ the friction heads h for similar channels having various quantities of flow vary as the square of the velocities, that is,

$$\frac{h_1}{h_2} = \frac{v_1^2}{v_2^2} \quad \ldots\ldots\ldots \quad 195$$

The quantity of water, as well as the water velocities in the channel, varies as the square root of the head, so that

$$\frac{v_1}{v_2} = \frac{\sqrt{H_{n_1}}}{\sqrt{H_{n_2}}} \quad \ldots\ldots\ldots \quad 196$$

Substituting this value for $\frac{v_1}{v_2}$ in equation 195, we have

$$\frac{h_1}{h_2} = \frac{H_{n_1}}{H_{n_2}} \quad \ldots \ldots \ldots \quad 197$$

Hence the friction heads vary as the desired heads; that is, in one and the same impeller the friction losses if expressed in per cent of the existing head will be equally large for heads within quite wide limits.

It is plain that this is true for blade channels of other forms as well as that shown in Fig. 49, and also that the same law applies to the friction losses in the guide channels.

Further losses occur in the sudden increase or decrease of the water velocities at entrance to and exit from the impeller and guide vanes due to the thickness of the blades, which produces shocks.

According to experiments by Weisbach and Fliegner with pipes having sudden and gradual enlargements, the friction heads consumed by shock are approximately proportional to the square of the velocities. The same losses occur in impeller and guide channels when the water enters or leaves the channels in the direction of the blades or when the pump operates with correct velocity diagrams. Therefore the shock losses at entrance to or exit from the impeller, if expressed in per cent of the desired head, will be equally large for all heads.

The velocity head $\frac{w_d^2}{2g}$, which is necessary to carry the water away from the pump, is represented in equation 8 as

$$\frac{w_d^2}{2g} = \alpha H_n \quad \ldots \ldots \ldots \quad (8)$$

The velocities w_d at exit from a pump casing will vary, under a change of water quantity, as the square root of the head because the cross section remains the same. Hence the coefficient α will have the same value for all heads.

Collecting the results of all this investigation, it is found that the friction, shock, and exit losses, if expressed in per cent of the existing head, will be independent of the latter. The hydraulic efficiency of a centrifugal pump will remain approximately constant over a wide range of heads provided the pump runs at the correct number

of revolutions for the existing head so that the correct diagrams will be formed.

The variation of mechanical losses will be investigated for similar conditions.

The total work N_a necessary to drive the pump is composed of the work consumed in overcoming the water work N_w, the hydraulic friction work N_h, and the mechanical friction work N_m, so that

$$N_a = N_w + N_h + N_m \quad . \quad . \quad . \quad . \quad . \quad . \quad 198$$

Let

$$N_h = \phi N_w \quad . \quad . \quad . \quad . \quad . \quad . \quad . \quad . \quad . \quad 199$$

and

$$N_m = \psi N_w \quad . \quad . \quad . \quad . \quad . \quad . \quad . \quad . \quad . \quad 200$$

From the preceding investigation it follows that the existing fraction of the water work expressed as hydraulic friction work is independent of the head, hence the coefficient ϕ remains constant.

For the coefficient ψ the conditions are different. If we assume that the bearing thrust load, etc., remain equally large for various heads, then the power necessary to overcome the existing friction work varies as the peripheral velocity or number of revolutions; therefore

$$\frac{N_{m_1}}{N_{m_2}} = \frac{\psi_1 N_{w_1}}{\psi_2 N_{w_2}} = \frac{n_1}{n_2} \quad . \quad . \quad . \quad . \quad . \quad . \quad 201$$

The water work now varies as the square root of the third power of the heads, and the number of revolutions as the square root of the heads; hence

$$\frac{N_{w_1}}{N_{w_2}} = \frac{\sqrt{H_{n_1}^3}}{\sqrt{H_n^3}} \quad . \quad . \quad . \quad . \quad . \quad . \quad . \quad 202a$$

and

$$\frac{n_1}{n_2} = \frac{\sqrt{H_{n_1}}}{\sqrt{H_{n_2}}} \quad . \quad . \quad . \quad . \quad . \quad . \quad . \quad 202b$$

From these equations and equation 201 we have

$$\frac{\psi_1}{\psi_2} = \frac{H_{n_2}}{H_{n_1}} \quad . \quad . \quad . \quad . \quad . \quad . \quad . \quad . \quad . \quad 203$$

Therefore the fraction of the existing water work dissipated as mechanical friction varies inversely with the corresponding heads.

The larger the head and therefore the driving power the smaller the coefficient ψ.

While the value of the friction and shock losses when referred to the head is independent of the same, the mechanical losses will decrease with increasing head. This will now be shown by means of an example.

Given a four-stage high-pressure centrifugal pump delivering 100 cubic feet per minute under a head of $H_n = 400$ feet and requiring a driving power of 100 h.p. The water work N_{w_1} is

$$N_{w_1} = \frac{QH_n\gamma}{33000} = \frac{100 \times 400 \times 62.5}{33000} = 75.8 \text{ h.p.}$$

Let it be assumed that experiments have shown the over-all efficiency to be $\xi = \frac{N_{w_1}}{N_{a_1}} = 0.758$ and that the power required to overcome mechanical friction is $N_{m_1} = 5$ h.p. Let us now see what the efficiency of this same pump will be if it delivers only a head $H_{n_2} = 200$ feet.

With $H_{n_1} = 400$ feet and $N_{a_1} = 100$ h.p. the power required to overcome the hydraulic losses $N_{h_1} = 100 - (75.8 + 5) = 19.2$ h.p. Therefore the coefficient $\phi_1 = \frac{N_{h_1}}{N_{w_1}} = \frac{19.2}{75.8} = 0.253$. Further, as the driving power to overcome mechanical friction $N_{m_1} = 5$ h.p., we have $\psi_1 = \frac{N_{m_1}}{N_{w_1}} = \frac{5}{75.8} = 0.0659$.

The water work N_{w_2} is found according to equation 202a as

$$N_{w_2} = N_{w_1}\sqrt{\frac{H_{n_2}^3}{H_{n_1}^3}} = 75.8\sqrt{\frac{200^3}{400^3}} = 26.8 \text{ h.p.}$$

$$\phi_1 = \phi_2, \quad \psi_2 = \psi_1\frac{H_{n_1}}{H_{n_2}} = 0.0659\frac{400}{200} = 0.1318;$$

hence

$$N_{h_2} = \phi_1 N_{w_2} = 0.253 \times 26.8 = 6.79 \text{ h.p.}$$

and

$$N_{m_2} = \psi_2 N_{w_2} = 0.1318 \times 26.8 = 3.53 \text{ h.p.}$$

Therefore the total driving power is

$$N_{a_2} = N_{w_2} + N_{h_2} + N_{m_2} = 37.12 \text{ h.p.}$$

Hence

$$\xi = \frac{N_{w_2}}{N_{a_2}} = \frac{26.8}{37.12} = 0.722.$$

It is therefore seen that on account of the greater percentage of mechanical losses when referred to water work the over-all efficiency of the pump drops to 72.2 per cent when the pump delivers water under a pressure head of only 200 feet.

24. Decreasing Friction Head in Impeller by Decreasing the Number of Blades.

Hydraulics teaches that the friction head depends upon the area of cross section of flow and the wetted surface. Hence it is advisable to make the cross section of the channels of the guides and impeller as large as possible, and to make the channel heights a as nearly equal to the channel widths b as possible, because of all rectangles having equal areas the square has the minimum periphery.

In order to obtain channels of large cross section as small a number of guide and impeller blades should be chosen as is consistent with a proper guidance of the water. Often wheels are constructed with an unnecessary number of blades, one-half of which could easily be omitted.

Assume again an impeller as shown in Fig. 49. Let the number of blades be in one case z having a channel height a, but let it also be possible to decrease the number of blades to $\frac{z}{2}$ and still have good water guidance so that, for the same impeller angles, the entrance height becomes $2a$ while the channel width b remains the same. Let h_z be the friction head for channel when z blades are used and $\frac{h_z}{2}$ the friction head when $\frac{z}{2}$ blades are used. Then, as v and λ are to remain constant, the following equation may be written (see equation 194):

$$\frac{h_z}{h_{\frac{z}{2}}} = \frac{2(a+b)}{2a+b}.$$

Assuming for instance that for z blades the channel height a is 0.6 inch, and for $\frac{z}{2}$ blades it is 1.2 inches, and that in both cases the

impeller width b is 1.6 inches, then $h_s = 1.57\, h_{\frac{z}{2}}$; that is, the friction head per channel is 1.57 times as large when z channels are used as when $\frac{z}{2}$ channels are used.

The friction head refers to one channel, and as the number of channels was twice as many in the first impeller as in the second the total friction head will be 3.14 times larger in the former than in the latter.

By decreasing the number of blades the friction head caused by blade shock will also be decreased. The resistance head h_s caused by sudden change of cross section is

$$h_s = \frac{\xi (v - v')^2}{2g} \quad \ldots\ldots\ldots \quad 204$$

or, letting $v' = v\frac{a}{a+s}$ (s being the blade thickness),

$$h_s = \xi v^2 \left(1 - \frac{a}{a+s}\right)^2,$$

so that if the coefficient ξ is assumed equally large in each case the following equation holds:

$$\frac{h_{s_1}}{h_{s_2}} = \frac{\left(1 - \frac{a_1}{a_1+s}\right)^2}{\left(1 - \frac{a_2}{a_2+s}\right)^2} \quad \ldots\ldots\ldots \quad 205$$

Referring again to the example used above and taking the blade thickness s for both impellers as 0.16 inch and solving equation 205,

$$h_{s_1} = 3.2\, h_{s_2}$$

This friction head refers to one channel, so that the total resistance head caused by blade shock is 6.4 times as great in an impeller with z blades as in one having $\frac{z}{2}$ blades.

This example shows clearly the gain in efficiency obtainable by decreasing the number of blades. Only as many blades should be used in the impeller and guide vanes as is absolutely necessary for good water guidance.

25. Increase of Hydraulic Efficiency when $\delta_e = \beta_e$ and by Using Directing Vanes at Entrance to Impeller.

The friction loss can be decreased in another way which should be employed when the highest efficiency is sought.

In Article 14 it was shown how the relative entrance velocity could be decreased by decreasing the angle δ_e. Fig. 33 shows plainly the decrease of v_e with the decrease of the angle δ_e; for every δ_e the corresponding velocities have been plotted as ordinates. In order to shorten the path of the water in the suction tube when assuming $\delta_e \gtrless 90°$ directing vanes must be used before entrance to the impeller. These directing vanes serve two purposes: first, they guide the water in the suction pipe in an axial direction; second, they give to the water directly before entrance to the impeller the proper entrance velocity and direction.

When $\delta_e = 90°$ these directing vanes are superfluous, because the water in entering the impeller at right angles will of itself flow axially through the suction tube.

The use of directing vanes will of course somewhat increase the cost of the pump, but it will be shown that for high-pressure centrifugal pumps in which the water velocities are high there is a decided gain in the decrease of friction head.

Any change of the angle δ_e changes also the peripheral velocity, but for simplicity the latter will be considered constant in the following discussion

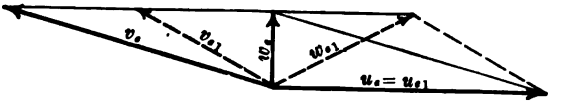

Fig. 50.

Fig. 50 shows in full lines the entrance velocity diagram when $\delta_e = 90°$ and in dotted lines the entrance velocity diagram when $\delta_e = \beta_e$, in which $v_e = w_e$. For $\delta_e = 90°$ let the magnitude of the velocities be u_e, w_e, v_e, and for $\delta_e = \beta_e$ let them be u_{e_1}, w_{e_1}, v_{e_1}. The friction heads for both cases will now be compared.

Let the entrance width b_e be the same in both cases; then the entrance heights designated as a_e and a_{e_1} will be in the inverse ratio to the relative velocities; therefore

$$\frac{a_{e_1}}{a_e} = \frac{v_e}{v_{e_1}} \quad \ldots\ldots\ldots \quad 206$$

According to equation 194 the friction head for $\delta_e = 90°$ is

$$h_e = \lambda \frac{a_e + b_e}{2 a_e b_e} \cdot \frac{v_e^2}{2g} l \quad \ldots\ldots\ldots \quad (194)$$

In the case of $\delta_e = \beta_e$ the water must flow through two channels, first in the directing vanes and then through the impeller. The velocities in both channels are equal because $v_{e_1} = w_{e_1}$. Let h_{e_1} be the friction head lost in each channel; this can be expressed as

$$h_{e_1} = \lambda \frac{a_e + b_e}{2 a_e b_e} \cdot \frac{v_e^2}{2g} l \quad \ldots\ldots\ldots \quad 207$$

Assuming that the channel length l and the coefficient λ are of equal value in equations 194 and 207, the following equation is found by dividing the former by the latter:

$$\frac{h_e}{h_{e_1}} = \frac{a_e + b_e}{a_{e_1} + b_e} \cdot \frac{a_{e_1}}{a_e} \cdot \frac{v_e^2}{v_{e_1}^2} \quad \ldots\ldots\ldots \quad 208$$

The friction head h_{e_1} occurs twice, first in the directing vanes at exit, second in the impeller at entrance. Besides this a small friction head is lost while the water is flowing through the first part of the directing vanes. As the cross sections in the first part of the directing vanes are larger than in the last part the velocity of the water is smaller in the former than in the latter. Therefore we shall assume that this small friction head is equal to $0.5\, h_{e_1}$. The total of all these friction heads is $2.5\, h_{e_1}$. Taking this into account and substituting $a_{e_1} = a_e \frac{v_e}{v_{e_1}}$ of equation 206 in equation 208 the latter takes the form

$$\frac{h_e}{2.5\, h_{e_1}} = \frac{a_e + b_e}{2.5\left(a_e \frac{v_e}{v_{e_1}} + b_e\right)} \cdot \frac{v_e^3}{v_{e_1}^3} \quad \ldots\ldots\ldots \quad 209$$

In example I, Article 31, the following impeller dimensions at entrance and values are given for the entrance velocity diagram when $\beta_e = \delta_e$:

$$w_e = v_e = 27.95 \text{ ft.}, \; a_e = 0.75 \text{ in.}, \; s_e = 0.157 \text{ in.}, \; b_e = 0.858 \text{ in.}$$

When $\delta_e = 90°$ the following values were found:

$$w_e = 12.66 \text{ ft.}, \; v_e = 52.82 \text{ ft.}, \; a_e = 0.394 \text{ in.}, \; s_e = 0.157 \text{ in.}, \; b_e = 0.858 \text{ in.}$$

Substituting these values in equation 209 gives

$$\frac{h_e}{2.5\, h_{e_1}} = 2.1.$$

Therefore the friction losses are 2.1 times as large for the case $\delta_e = 90°$ as for the case $\delta_e = \beta_e$.

On account of the thickness of blades the water velocity increases at entrance to and decreases at exit from the vanes, causing shock losses. When using directing vanes these shock losses occur three times, that is, at entrance to the directing vanes, at exit therefrom, and at entrance to the impeller. When directing vanes are not used the shock losses occur only once, that is, at entrance to the impeller. In spite of this the resistance head due to all these shock losses is considerably smaller when directing vanes are used than when they are omitted.

The resistance head equivalent to this shock loss can be expressed as

$$h_s = k\frac{(v_e - v_e')^2}{2g} \quad \ldots\ldots 210$$

in which

$$v_e' = v_e\frac{a_e}{a_e + s_e},$$

so that

$$h_s = k\frac{v_e^2\left(1 - \frac{a_e}{a_e + s_e}\right)^2}{2g} \quad \ldots\ldots 211$$

and correspondingly for the case $\delta_e = \beta_e$

$$h_{s_1} = k_1\frac{v_{e_1}^2\left(1 - \frac{a_{e_1}}{a_{e_1} + s_e}\right)^2}{2g} \quad \ldots\ldots 212$$

Therefore if $k = k_1$ we have

$$\frac{h_s}{h_{s_1}} = \frac{v_e^2\left(1 - \frac{a_e}{a_e + s_e}\right)^2}{v_{e_1}^2\left(1 - \frac{a_{e_1}}{a_{e_1} + s_e}\right)^2} \quad \ldots\ldots 213$$

Returning again to the example previously quoted and substituting the values there given in equation 213, we get

$$\frac{h_s}{h_{s_1}} = 9.56.$$

When directing vanes are used the same resistance head occurs at exit from the vanes as at entrance to the impeller. Further, at entrance to the directing vanes another, but smaller, resistance head occurs. The latter is smaller because the cross sections of the channels are larger and therefore the velocities correspondingly smaller. Assuming again that this resistance head at entrance is 0.5 of that at exit from the directing vanes, then $\frac{h_e}{2.5\, h_{e_1}} = 3.82$. Therefore, when directing vanes are used and when $\delta_e = \beta_e$ the resistance head caused by all the shock losses is 3.82 times as small as for the case when $\delta_e = 90°$, in which the resistance head is caused by only one shock loss and that at entrance to the impeller.

Without doubt this is sufficient proof that making $\delta_e < 90°$, especially for the case $\delta_e = \beta_e$, causes the friction and shock losses at entrance to the impeller to be considerably decreased notwithstanding the fact that the losses in the directing vanes have been added. Especially in the design of high-pressure centrifugal pumps directing vanes at entrance to the impeller should be used, even though they add to the cost, in order that the highest hydraulic efficiency may be obtained.

The conditions at entrance to the directing vanes are similar to those at impeller entrance, and $w_a^2 + v_a^2$ should be made as small as possible.

26. Comparison of the Friction Heads of Centrifugal Pumps with Impeller Angles $\beta_a = 135°$, $\beta_a = 90°$, and $\beta_a = 45°$; and the Influence of Curvature of Blades upon Efficiency.

The friction losses occurring during the flow of the water through impeller and guide vanes, as mentioned in Article 4, are dependent also upon the shape of the blade and the form of the channel. It was found experimentally that the best efficiencies were obtained when the impeller blades were turned backwards, that is, when $\beta_a > 90°$. The poorest efficiencies were obtained with impeller blades decidedly turned forward, or when $\beta_a < 90°$. Impeller blades with $\beta_a = 90°$ were much poorer in efficiency than impeller blades having $\beta_a > 90°$. Therefore at present in the best designs of centrifugal pumps impeller blades bent backward with $\beta_a > 90°$ are almost exclusively used.

An attempt was made to investigate somewhat more closely the relation of the various types of impeller blades to the efficiency, but of course it was not possible to determine for any one impeller the magnitude of the friction heads caused by the water flowing through the channels, because the coefficients of friction are unknown and can only be found experimentally. Still the relation of the various friction heads can be approximately determined by means of an equation similar to equation 208 by assuming that the coefficients of friction and the lengths of the channels are always equal. The velocities of the water that are dealt with in this case vary between such small limits that this assumption can make no appreciable error.

Figs. 51, 52, and 53 show three impellers with guide vanes. The impellers have the following angles:

$$\text{I. } \beta_a = 135°,$$
$$\text{II. } \beta_a = 90°,$$
$$\text{III. } \beta_a = 45°.$$

Assume as before

$$D_a = 1.31 \text{ feet}, \quad D_e = 0.66 \text{ foot},$$
$$v_r = 6.56 \text{ feet}, \quad w_r = 9.84 \text{ feet},$$
$$\sqrt{\eta g H_n} = 32.8 \text{ feet},$$

and also assume the case $\beta_e = \delta_e$.

For the case $\beta_e = \delta_e$ the peripheral velocities are found from equation 136. The other velocities and channel heights are found partly analytically and partly graphically. The best way to do this will be explained in a later article. In Tables I and II are given the values thus derived for these three impellers and their guide vanes.

Impellers I and II, that is, $\beta_a = 135°$ and $\beta_a = 90°$, have ten blades each. Impeller III with $\beta_a = 45°$ had to have fourteen blades because for a fewer number of blades the involute at entrance could not be made to join the involute at exit. This impeller could not be designed with blades of constant thickness because the blade curvatures would have been too great and would have resulted in a completely useless channel. All three guide vanes have nine blades each.

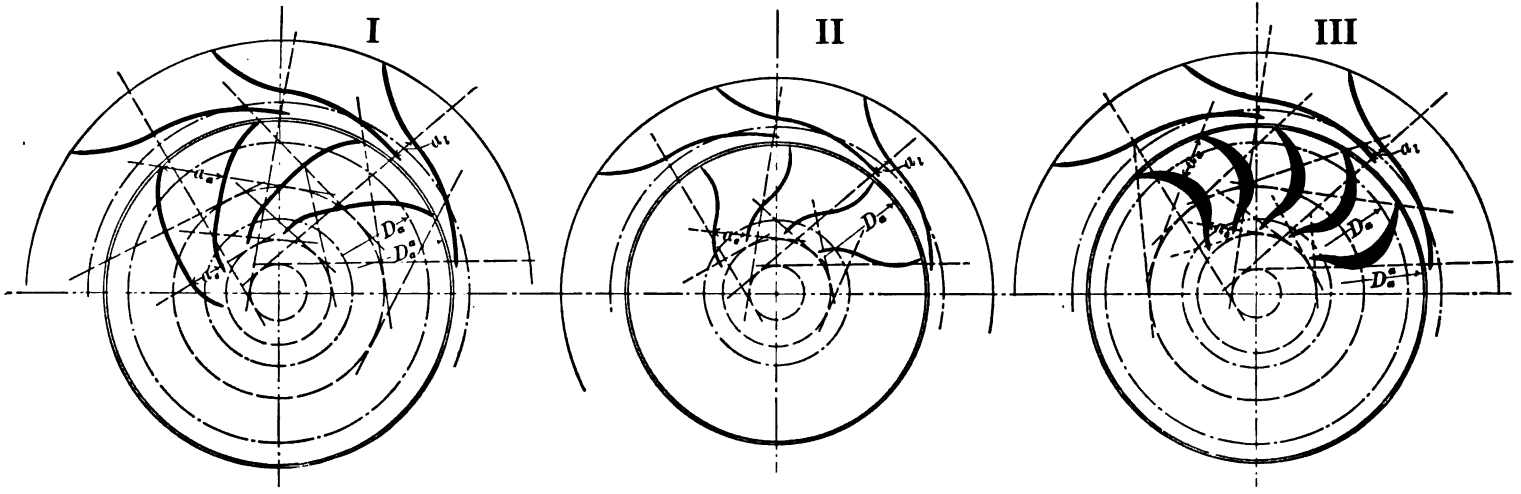

p 100

Fig. 51. $\beta_a = 135°$.

Fig. 52. $\beta_a = 90°$.

Fig. 53. $\beta_a = 45°$.

TABLE I.

Impeller	Entrance				Exit			
	v_e' ft.	v_e ft.	a_e in.	b_e in.	v_a' ft.	v_a ft.	a_a in.	b_a in.
I. $\beta_a = 135°$	13.98	15.35	1.59	1.31	9.38	9.81	3.35	0.98
II. $\beta_a = 90°$	13.22	14.53	1.68	1.31	6.56	6.79	4.88	0.98
III. $\beta_a = 45°$	12.60	14.17	1.22	1.31	9.38	10.01	2.34	0.98

TABLE II.

Guide Vanes	Entrance			
	w_e' ft.	w_l ft.	a_l in.	b_l in.
I. $\beta_a = 135°$	34.32	38.55	0.94	0.98
II. $\beta_a = 90°$	35.79	42.49	0.85	0.98
III. $\beta_a = 45°$	38.55	46.26	0.78	0.98

Let h_{e_I}, $h_{e_{II}}$, $h_{e_{III}}$ represent the resistance heads caused by friction losses and λ_{e_I}, $\lambda_{e_{II}}$, $\lambda_{e_{III}}$ represent the resistance heads caused by shock losses at entrance to the impeller corresponding to impellers I, II, and III respectively. For the resistance heads at exit from the impeller and at entrance to the guide vanes subscripts a and l will be used respectively instead of the subscript e.

Let the resistance heads of impeller I be equal to 1.0 for comparison's sake. The corresponding resistance heads of the other impellers will be compared to this value.

To determine the resistance heads caused by friction losses it is simplest to use an equation similar to equations 208 and 209 which can be written for entrance to the impeller by merely changing the subscripts; hence

$$\frac{h_{e_{II}}}{h_{e_I}} = \frac{(a_{e_{II}} + b_e)}{(a_{e_I} + b_e)} \frac{v_{e_{II}}^3}{v_{e_I}^3} \quad \ldots\ldots\ldots \quad 214$$

This equation cannot be used for impeller III because it has fourteen channels, while the other impellers have only ten channels each. But the equation can be written as follows:

$$\frac{h_{e_{III}}}{h_{e_I}} = \frac{(a_{e_{III}} + b_e)}{(a_{e_I} + b_e)} \frac{a_{e_I}}{a_{e_{III}}} \frac{v_{e_{III}}^2}{v_{e_I}^2} \frac{14}{10} \quad \ldots\ldots\ldots \quad 215$$

TO VIVU
AIMOILAC

If the coefficient k be taken equal throughout, the relation of the resistance heads caused by shock losses at the impeller entrance can be expressed by the equation (see equation 210)

$$\frac{\lambda_{e_{II}}}{\lambda_{e_I}} = \frac{(v_{e_{II}} - v_{e_{II}}')^2}{(v_{e_I} - v_{e_I}')^2} \quad \ldots\ldots 216$$

For impeller III the right-hand side of this equation must again be multiplied by $\frac{14}{10}$, the ratio of the number of blades in each case.

The relations of resistance heads for impeller exit and guide vane entrance can be determined exactly like the above equations by using the correct subscripts.

The short-circuit losses will not be the same for the three impellers, because by changing the absolute exit velocity the excess pressure existing in the clearance space, $\eta H_n - \frac{w_a^2}{2g}$, varies.

In this case also the short-circuit loss q_{sp} is 1.0 for impeller I, and the short-circuit losses of impellers II and III will be compared to this value.

Assuming equal values of the coefficients of friction the following equation may be written:

$$\frac{q_{sp_{II}}}{q_{sp_I}} = \sqrt{\frac{\eta H_n - \frac{w_{a_{II}}^2}{2g}}{\eta H_n - \frac{w_{a_I}^2}{2g}}} \quad \ldots\ldots 217$$

and similarly for the ratio $\frac{q_{sp_{III}}}{q_{sp_I}}$.

In Table III the values of these various relations are given.

TABLE III.

	Impeller Entrance		Impeller Exit		Guide Vane Entrance		Short-circuit Losses
	Friction Losses	Shock Losses	Friction Losses	Shock Losses	Friction Losses	Shock Losses	
I. $\beta_a = 135°$	1.00	1.00	1.00	1.00	1.00	1.00	1.00
II. $\beta_a = 90°$	0.86	0.70	0.34	0.29	1.26	1.21	0.79
III. $\beta_a = 45°$	1.25	2.37	1.61	2.93	1.57	1.42	0.70

According to this table the resistance head caused by friction losses at entrance to the guide vanes is 1.57 times greater for guide vane III than for guide vane I. The resistance heads for impeller III, $\beta_a = 45°$, are at every point considerably greater than those for impeller I, only the short-circuit losses are smaller in case III, and these do not compensate for the other losses, which are considerably greater. The total efficiency of the forward-turned blades will therefore be less than the efficiency of the radial and the backward-turned blades.

The resistance heads at impeller entrance and exit are smallest for impeller II, $\beta_a = 90°$, but at guide vane entrance they are larger than those of impeller I, while the short-circuit losses are smaller. It must be borne in mind, however, that the resistance head at entrance to the guide vanes forms the larger per cent of the total resistance head, because the largest velocities occur at this point; the resistance head at impeller entrance is much smaller and is smaller at impeller exit. It may be correctly assumed that the gain of friction head at impeller entrance and exit will nearly offset the larger loss of friction head at guide vane entrance, so that, considering only those factors just discussed, it would appear that the smaller short-circuit losses of case II cause the radial blades to give a gain in efficiency over those bent backward.

Besides the factors above mentioned, such as friction and shock losses, the form of the blade channels must be considered in determining the hydraulic efficiency of these impellers.

In giving the blade channel its proper form care must be taken in order that the change from relative entrance velocity to relative exit velocity shall occur gradually and, if possible, linearly. The blade curvatures should also have the largest possible radii. These conditions are best fulfilled by a blade channel formed with backward-turned blades, that is, impeller I. In this case it is easy to construct the blades with large radii of curvature and also to construct the impeller channel so that the change from v_e to v_a, hence the change of cross section, shall occur as nearly linearly as possible. The designer can convince himself that this is not easily possible with the radial blades of case II. In case II the first part of the impeller channel cross section diverges more rapidly than the latter portion near the impeller exit and, for this reason, the decrease of velocity when radial blades are used occurs in a manner similar to the curve shown dotted

in Fig. 54. The full line shows the ideal decrease of velocity which can be obtained when backward-bent blades are used. In this case the transformation of velocity into pressure occurs with less shock than when radial blades are used.

Due to a phenomenon which will be briefly alluded to a sharp curvature can also greatly influence the efficiency of flow.

It is generally known that the resistance to flow through a bend increases with decreasing radius of curvature. But the increased friction loss is not alone present because it has been found that another phenomenon takes place when there is flow through sharp curvatures. It is called the phenomenon of *whirling water*.*

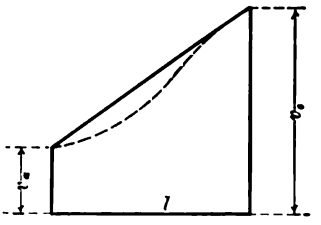

Fig. 54.

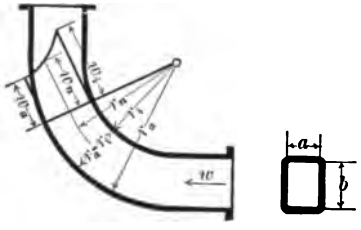

Fig. 55.

Isaachen published the results of some very interesting investigations through curved channels in *Zivil-Ingenieur*, 1894–1896.

In these articles Isaachen proves that in a curved pipe of rectilinear cross section the velocities in radial planes are inversely proportional to the corresponding radii of curvature, so that, if r_a represents the outer and r_i the inner radius of curvature and w_a and w_i the corresponding velocities at these radii (see Fig. 55), the following equation may be written:

$$\frac{w_a}{w_i} = \frac{r_i}{r_a} \quad \ldots\ldots\ldots \quad 218$$

or

$$w_a r_a = w_i r_i = w_n r_n = C \quad \ldots\ldots \quad 219$$

The velocities in radial sections of a curved pipe vary according to an equilateral hyperbola.

To determine the constant C a radius is found where a velocity w_n occurs which has the same value as the mean velocity in the

* Professor Pfarr of Darmstadt, Germany, treats fully of this phenomenon of "whirling water" in his lectures on water turbines, especially when considering the Francis turbine.

straight portion of the channel. This radius has been called by Pfarr the *neutral radius*, and can be determined, according to Isaachen, by the equation

$$r_n = \frac{r_a - r_i}{\text{nat. log}\frac{r_a}{r_i}} \quad \ldots\ldots\ldots \quad 220$$

As r_a and r_i are known, the solution of this equation gives the value of the neutral radius, r_n, and therefore the constant C can be determined by means of equation 219.

The phenomenon that the velocities across a radial section of a curved pipe vary according to a hyperbola also takes place in an impeller channel and can become unpleasantly evident when small radii of curvatures are used.

The water in the channel after passing the blade curvature must still follow a very small approximately straight path up to exit of impeller. Along this path an equalization of the relative velocities cannot occur; that is, the velocities which vary according to a hyperbola across the curved channel section cannot again reach a constant value across the entire height a_a at the impeller exit. The result is that the diagrams found from calculations do not actually occur across the entire exit height and the pump no longer operates without shock.

According to the above a blade should always be constructed with greatest curvature. This is best accomplished by a backward-bent blade. It is often possible to connect the entrance and exit involutes by a straight line so that the radii of curvature of the middle of the blade becomes infinitely large.

The direction of blade curvature must necessarily be reversed in the case of impeller II, which again surely introduces larger losses than occur with blades curved in one direction as shown in impeller I. Besides this, the latter blade can always be designed with larger curvature.

Taking this into consideration, it may be correctly said that the losses due to water flowing through the middle part of an impeller channel, and the losses due to the influence of a greater or less blade curvature, which prevents the water from flowing free of shock across the entire exit height of an impeller and entrance height of a guide vane, will be smaller with backward-turned blades than with radial blades.

In considering the friction, shock, and short-circuit losses the conclusion has been reached that the friction and shock losses are equally large for the backward-bent and radial blades, while the short-circuit losses are larger with the backward-bent blades. This greater short-circuit loss of the backward-bent blades is fully compensated for by the more advantageous form of the blade channel.

Experiments have proved that the best efficiency is realized with the backward-bent blades, and for this reason impeller blades are now almost exclusively designed according to this form.

The losses caused by the sharp blade curvature of impeller III become very noticeable in the total efficiency, and for this reason such blades are entirely out of place in centrifugal pump design.

27. The Efficiency as Determined by Experiment.

In the foregoing it has been shown just what points must be especially considered in the design of centrifugal pumps in order to obtain the highest efficiency. The following experimental data will be con-

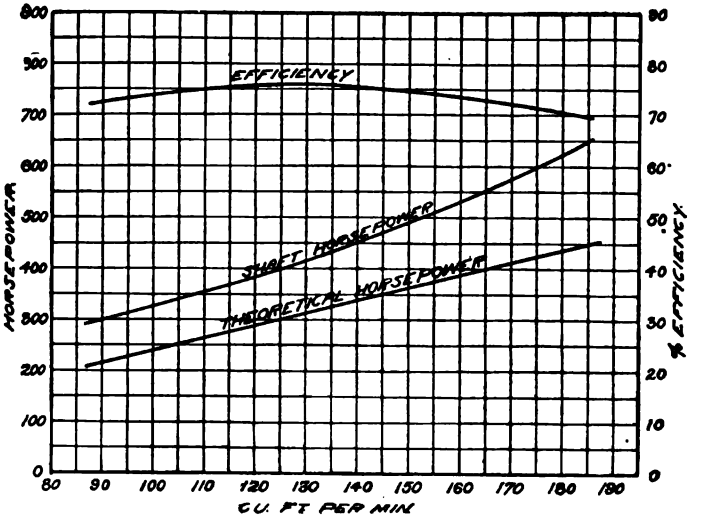

Fig. 56.

sidered and their influence upon the total efficiency will be analyzed. The excellent results obtained by Sulzer Bros. of Winterthur and C. H. Jaeger & Co. of Leipzig have been obtained only by careful

design of the pump in the drafting room and by faultless construction in the shop.

Special consideration is due to the experiments made on Sulzer pumps at the Horcoja Hydraulic Plant in Spain, which will later be more fully described. The results of the experiments are shown in Figs. 56 and 57.*

In both tests the quantity of water was the same, but the manometric head after one year's service was 1276 feet, while after five

Fig. 57.

years' service it was 1575 feet. With 1276 feet head the hydraulic plant operated with three pumps in series, that is, each pump delivered about 425 feet head, while with 1575 feet head an additional pump having 357 feet head was added. Therefore the experimental results refer to three and four pumps respectively, each of which consisted of four stages. The mean number of revolutions in both cases was 870 per minute. As the curves show, the efficiency of the pumps under a mean load of 414 h.p. was 76 per cent, and after five years of service delivering a larger head corresponding to a load of 492 h.p. it was again 76 per cent. According to the report of

* Taken from Herzog, " Electric Railroads and Their Operation," 1905.

the superintendent the pumps were only out of service an average of sixteen hours per month, so that during five years of almost uninterrupted service no decrease of efficiency had taken place. This is a striking proof of the falsity of the frequently made statement that rapid deterioration of impeller and guide vanes on account of high water velocities always occurs in these pumps. Such good and sustained efficiencies were obtained only by very careful construction in which the correct relations of angles, cross sections, number of revolutions to quantity of water and head desired were realized, producing a pump which worked completely without shock.

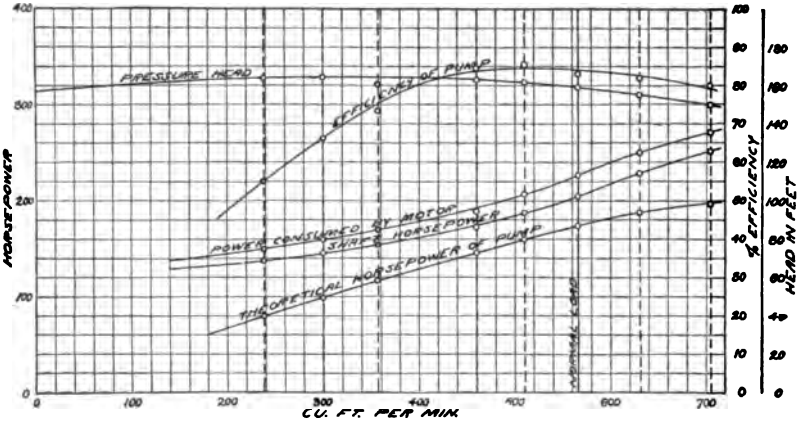

Fig. 58.

The experiments recorded in Fig. 58 are for a two-stage mine-shaft pump having a vertical shaft. These experiments show that in general the larger the capacity of the pump the higher will be the efficiency obtained. This two-stage pump delivers 565 cubic feet of water per minute against a manometric head of 148 feet at 1025 r.p.m. For the guaranteed load the efficiency was 83 per cent, but under other working conditions the curve shows that the efficiency increased to 84 per cent.

Equally good results have been obtained by C. H. Jaeger & Co. with their high-pressure centrifugal pumps. Fig. 59 gives experimental results obtained from a six-stage pump which delivered 71 cubic feet of water per minute against 361 feet manometric head at 1400 r.p.m. The abscissæ represent the quantity of water per minute in 100 parts of the normal quantity desired; the upper curve shows

the head obtained by throttling, and the lower curve, starting from zero, gives the efficiency for the throttled head. An efficiency of 76 to 77 per cent for guaranteed load was also obtained in this case, while with less throttling the efficiency increased to 79 per cent.

For very small quantities of water quite good efficiencies are obtained, as can be seen from the experimental results recorded in Fig. 60. The four-stage pump investigated gave 72 per cent effi-

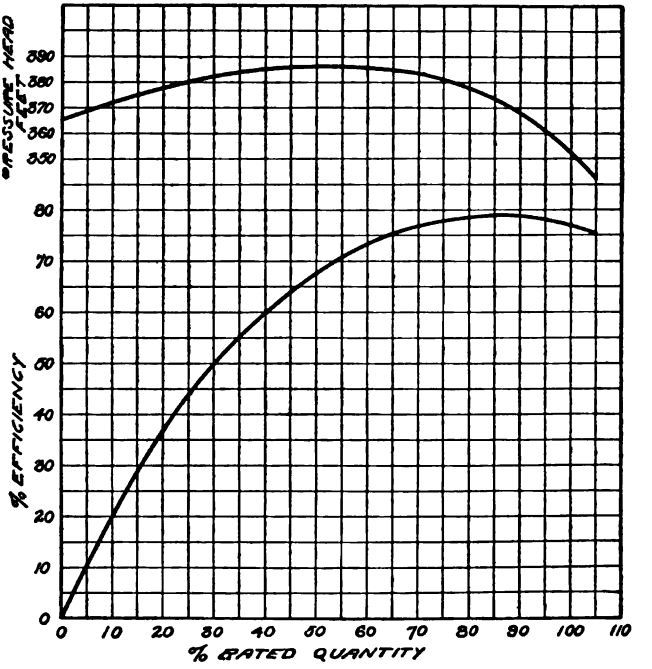

Fig. 59.

ciency at 1430 r.p.m., delivering 15 cubic feet of water per minute against a manometric head of 207 feet. By throttling the quantity of water to 12.7 cubic feet per minute and with a correspondingly larger head the efficiency increased to 73 per cent.

This firm also obtained very high efficiencies for high-pressure centrifugal pumps, but only after years of experience and careful construction.

In the experimental results given by Sulzer and Jaeger the throttled heads were considered in the determination of the efficiency. The

greater head obtained by throttling does not fully benefit the customer, because in most cases only one certain head is of use. The customer will be interested in an efficiency curve which refers to the one head he desires. If this is considered in the above experiments the efficiency curve will decrease rapidly with smaller quantities of water, but for the normal load the efficiency given is correct.

The experimental results given above for high-pressure centrifugal pumps show a total efficiency between the limits of 70 and 80 per cent, varying according to the size and power of the pump. Such high

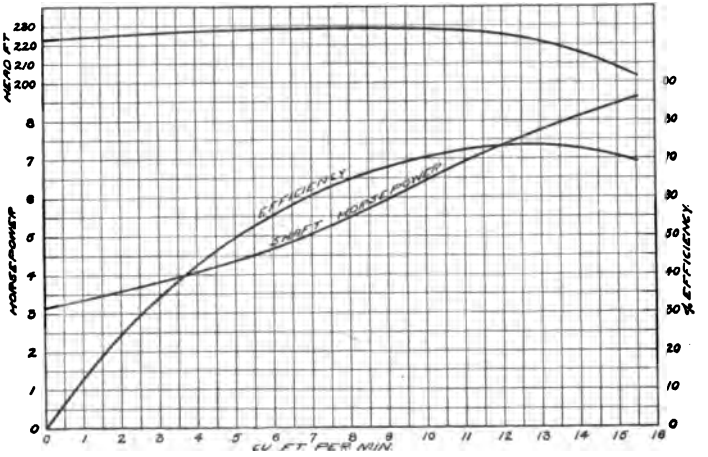

Fig. 60.

values of efficiency, however, can only be reached by proper construction.

As already mentioned, the total loss consists of the hydraulic and mechanical losses. In the hydraulic losses the friction, shock, and exit losses are separated from the short-circuit loss. The former have an influence on the head desired because certain pressure heads are necessary to overcome them, while the short-circuit losses require more work because the pump must also deliver the quantity of water short-circuited.

For the calculation of peripheral velocity, number of revolutions, etc., only those losses are taken which influence the head desired; hence the total working head must be multiplied by the coefficient

$\eta = 1 + \rho + \alpha$ (see equation 11). In determining the dimensions of the impeller channels the quantity of short-circuited water must be considered.

The sum of the short-circuit and mechanical losses is considered to be about 6 per cent of the total loss and then the coefficient η is determined. In order to have a small excess of head at normal load it is well not to take this coefficient too small.

III. THE REGULATION AND CLASSIFICATION OF CENTRIFUGAL PUMPS.

28. Regulating the Quantity of Water by Throttling. Influence of the Quantity of Water upon Head and Losses due to Throttling.

It has been proven that a centrifugal pump will work without shock losses, at a certain number of revolutions, only for one combination of quantity and head and at this point will reach its highest efficiency. If the quantity of water delivered by a pump running at a constant number of revolutions is regulated, which in most cases is brought about by throttling, then operation without shock ceases. This throttling is accomplished by means of a valve in the discharge pipe. Therefore every regulation by means of a throttle valve occurs at the expense of efficiency.

Shock and eddy-current losses ensue at entrance to the impeller, because the quantity of water decreases, causing the absolute entrance velocity at the impeller to assume a direction other than that called for by the slope of the involute angle at the exit from the directing vanes. At impeller exit a correct diagram might occur if it were not for the fact that with decreasing quantities of water the absolute exit velocity, that is, the entrance velocity to the guide vanes, forms a smaller angle δ_a with u_a than is demanded by the entrance involute of the guide vanes.

The magnitude of the losses which occur when the pump is throttled and therefore operating with shock can hardly be determined mathematically. It is the duty of the experimental laboratory to conduct experiments along this line. We shall only attempt to show how the losses mainly occur when throttling and how they may be decreased by suitable design.

Evidently the losses at entrance to and in passing through the guide vanes will be of the greater magnitude. Assume a pump of infinite diameter so that the impeller and guide vanes can be represented as in Fig. 61. The part of the blades which were involutes are now straight lines because the diameter of their base circle is infinite.

The normal diagram upon which the calculation of the pump is based is shown in full lines. The guide vanes form the angle δ_a at entrance.

By throttling the quantity of water the angle δ_a assumes a smaller value. A second diagram, shown dotted in the figure, is that which would occur if the quantity of water were decreased. The absolute velocity w_a' enters the guide vanes at an angle δ_a', and on this account the water stream is no longer parallel to the guide vanes, but will impinge on one side and not touch the other side of the guide vanes. In Fig. 61 an attempt has been made to show this action. On account

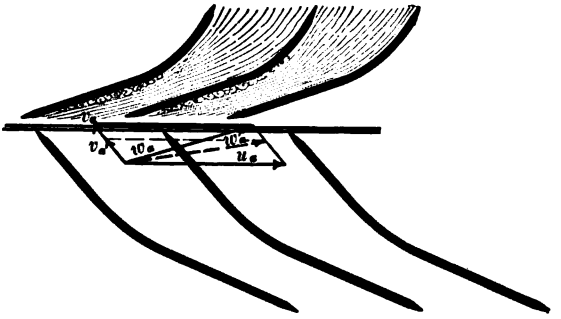

Fig. 61.

of the violent shock against one side of the vanes strong eddy currents occur, which greatly interfere with the regular transformation of the absolute velocity into pressure.

The smaller the quantity of water the larger will be the deviation of the angle δ_a' from the fixed guide vane angle and therefore the shock upon one side of the guide vanes will be more violent, thus increasing the eddy current and therefore the resulting losses.

The losses, due to change of quantity of water, at impeller entrance will be of a smaller value than those at exit. If there are directing vanes the velocity in the space between them and the impeller will have a certain direction. With decreasing quantity of water the angle δ_e also must become smaller in order to have entrance without shock, for otherwise the relative entrance velocity v_e will no longer enter the impeller channels at the impeller angle β_e, that is, in the direction of the impeller blades. If the clearance space between the exit from the directing vanes and the entrance to the impeller is very small the false angle of direction δ_e will prohibit the correct formation

of the entrance velocity diagram; the relative velocity v_e will enter the impeller at a smaller angle β_e' and cause eddy-current losses similar to those at entrance to the guide vanes. If, on the other hand, the clearance space is made sufficiently large the absolute velocity in the clearance space can change its direction. This is due to the influence of the peripheral velocity and the relative velocity v_e which strives to enter the impeller at an angle β_e, so that the angle β_e at impeller entrance can still have the proper value. By having a sufficient clearance it might be possible to obtain a velocity diagram at impeller entrance which is practically free from shock for quantities of water within wide limits.

When a pump is throttled not only is the quantity of water changed but the head also is more or less influenced. In designing the blades of a pump this must be especially considered, for in most cases it is still necessary to obtain the normal head when the pump is throttled. To what degree the various velocities and angles influence the head by decreasing the quantity of water will be investigated in the following. In order to obviate the consideration of shock losses, etc., occurring through throttling assume a pump with guide and directing vanes which may be changed and which are always correct for the existing quantities of water so that the coefficient η may be taken of approximately equal value for various quantities of water.

In the following discussion it is best to start with the first fundamental equation, equation 10, which may be written, if $(1 + \rho + \alpha) = \eta$ (equation 11), as

$$\frac{u_a^2 - u_e^2}{2g} + \frac{v_e^2 - v_a^2}{2g} + \frac{w_a^2}{2g} - \frac{w_e^2}{2g} = \eta H_n \quad . \quad . \quad . \quad 221$$

The individual members upon the left-hand side of the equation will have different influences upon the value of the head as the quantity of water changes.

The first member, $\frac{u_a^2 - u_e^2}{2g}$, will remain constant and independent of the quantity of water because the number of revolutions remains the same.

The second member, $\frac{v_e^2 - v_a^2}{2g}$, can influence the head variously with change of quantity. Accordingly as $v_e \gtrless v_a$ this member will

be positive or negative; for $v_e = v_a$ it is zero and therefore has no influence on the head.

The case $v_e > v_a$ in which the member $\frac{v_e^2 - v_a^2}{2g}$ is positive will first be considered. Referring to Fig. 9, the water when flowing from point e at impeller entrance to point a at impeller exit will have its pressure increased, due to the influence of the value $\frac{v_e^2 - v_a^2}{2g}$, because the velocity v_e decreases to a velocity v_a. If the quantity of water now decreases, the velocities v_e and v_a will also decrease, and the pressure head gained by the change of velocity from point e to a will decrease correspondingly.

Therefore if $v_e > v_a$ the member $\frac{v_e^2 - v_a^2}{2g}$ becomes smaller with diminished quantities of water and hence causes a decrease of head.

If $v_e < v_a$ a certain pressure head is necessary in order to accelerate the velocity v_e to the larger velocity v_a. The difference of these pressure heads must, so to speak, be taken from the pressure ensuing through the action of the centrifugal forces. The smaller the quantity of water the smaller will be the value of the pressure head extracted to overcome the velocity increase from v_e to v_a. Hence if the member $\frac{v_e^2 - v_a^2}{2g}$ is negative it helps to increase the head when the quantity of water is decreased.

For the special case $v_e = v_a$ the value $\frac{v_e^2 - v_a^2}{2g} = 0$ will have no influence upon the head provided the friction head necessary to overcome the losses of the water along the path from e to a is neglected.

The value $\frac{v_e^2 - v_a^2}{2g}$ can be transformed by substituting $v_a = \frac{v_r}{\sin \beta_a}$ and $v_e = \frac{v_r}{\sin \beta_e} \frac{F_a}{F_e}$ so that

$$\frac{v_e^2 - v_a^2}{2g} = \frac{v_r^2}{\sin^2 \beta_e} \left(\frac{F_a}{F_e}\right)^2 - \frac{v_r^2}{\sin^2 \beta_a} \quad . \quad . \quad . \quad . \quad 222$$

The third member of equation 221 is $\frac{w_a^2}{2g}$, the velocity head of the absolute exit velocity. The influence of this member upon the head when the quantity of water is changed can best be seen from Figs. 62, 63, and 64, which represent exit velocity diagrams for $\beta_a > 90°$, $\beta_a < 90°$, and $\beta_a = 90°$. If the angle formed between w_a and v_a

is obtuse for the normal diagram (this being the diagram for normal load, see Fig. 62), the velocity w_a will increase with decreasing quantities of water. On the other hand, if the angle is acute (see

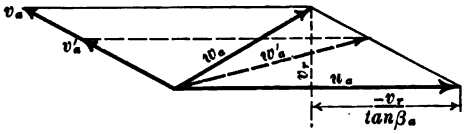

Fig. 62.

Fig. 63), w_a will decrease with decreasing quantity of water. If the angle β_a is not much greater than 90°, the case may arise in which w_a first decreases to a minimum value when w_a is perpendicular to v_a and then again increases. In general it may be said that with $\beta_a > 90°$ the velocity w_a increases with decreasing quantities of water, while with $\beta_a < 90°$ it decreases.

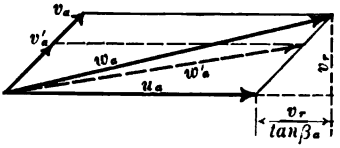

Fig. 63.

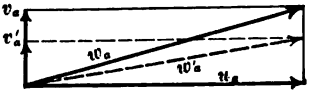

Fig. 64.

For $\beta_a = 90°$ (see Fig. 64) w_a will decrease very little as the quantity of water is decreased.

The effect of the member $\frac{w_a^2}{2g}$ is such, therefore, that for decreasing quantities of water the head will increase if $\beta_a > 90°$ and decrease if $\beta_a < 90°$.

The following equation may be written from the exit velocity diagram:

$$\frac{w_a^2}{2g} = \frac{\left(u_a + \frac{v_r}{\tan \beta_a}\right)^2 + v_r^2}{2g} \quad . \quad . \quad . \quad . \quad . \quad 223$$

The last member on the left-hand side of equation 221 is $-\frac{w_e^2}{2g}$.

If the angle $\delta_e = 90°$ for the normal diagram, then the angle formed by w_e and v_e becomes an acute angle; so that with decreasing quantities of water w_e first decreases to a minimum value when w_e is perpendicular to v_e and then increases. For reasons already

given it is usual to choose the normal entrance velocity diagram, when directing vanes are used, in such a manner that the angle $\beta_e \cong \delta_e$, and therefore the angle between w_e and v_e becomes obtuse (see Fig. 65). In this case the velocity w_e always increases with decreasing quantity of water and the head decreases.

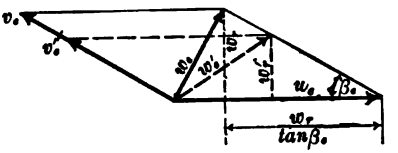

Fig. 65.

From Fig. 65 the following may be written:

$$w_e^2 = w_r^2 + \left(u_e - \frac{w_r}{\tan\beta_e}\right)^2,$$

or, substituting $w_r = v_r \frac{F_a}{F_e}$,

$$w_e^2 = v_r^2\left(\frac{F_a}{F_e}\right)^2 + \left(u_e - \frac{v_r}{\tan\beta_e}\frac{F_a}{F_e}\right)^2 \quad . \quad . \quad . \quad . \quad 224$$

Considering equations 222, 223, and 224, equation 221 assumes the very simple form (similar to that already given in equation 140)

$$\frac{u_a^2 - u_e^2}{g} + v_r \frac{\frac{u_a}{\tan\beta_a} - \frac{u_e}{\tan\beta_e}\frac{F_a}{F_e}}{g} = \eta H_n \quad . \quad . \quad . \quad 225$$

As the number of revolutions remains constant and the investigation is to be carried out upon the same pump, we can write

$$\frac{u_a^2 - u_e^2}{g} = C_1 \quad . \quad . \quad . \quad . \quad . \quad . \quad . \quad 226$$

and

$$\frac{\frac{u_a}{\tan\beta_a} + \frac{u_e}{\tan\beta_e}\frac{F_a}{F_e}}{g} = C_2 \quad . \quad . \quad . \quad . \quad . \quad . \quad 227$$

so that

$$C_1 + v_r C_2 = \eta H_n \quad . \quad . \quad . \quad . \quad . \quad . \quad . \quad 228$$

The total head ηH_n, therefore, will increase with decreasing quantities of water only when the constant C_2 is negative and will decrease when C_2 has a positive value.

In most cases a minimum head, which lies in the region of normal load, is prescribed for a centrifugal pump. The minimum head must still be reached when the pump is throttled and delivering less

water, otherwise the head can be increased only by increasing the number of revolutions, the latter being an impossibility in most installations. If it is desired to obtain the normal head over a wide range by means of throttling, the constant C_2 must be taken negative. This is possible only when the angle $\beta_a > 90°$ and further when the member $\frac{u_a}{\tan \beta_a} > \frac{u_e}{\tan \beta_e} \frac{F_a}{F_e}$. Hence the angles β_a and β_e must be taken as large as possible and the ratio $\frac{F_a}{F_e}$ as much smaller than unity as possible.

In order still to obtain the normal desired head with decreasing quantities of water the backward-bent blade with $\beta_a > 90°$ must be used. In the previous article this blade form has been proved to be the most efficient. Blades bent forward are applicable only to the rare case in which it is desired to obtain decreasing head with decreasing quantity of water.

In the above discussion of the performance of centrifugal pumps while throttling the assumption was made that to secure operation without shock different guide vanes were to be used corresponding to the different quantities of water for one and the same pump, and therefore the coefficient η was assumed approximately constant.

In Fig. 72 theoretical pressure curves are shown as they would be derived for the example calculated in Article 31. These curves are of course straight lines in accordance with equation 228. The ideal curves so derived cannot be obtained in practice because the pump has guide vanes the dimensions of which are so determined that the pump operates at normal load without shock. It is of course impossible to change the guide vanes to suit the diminishing quantities of water. With increase or decrease of the quantity of water shock and eddy-current losses occur at entrance to and exit from the impeller. The value of these losses cannot be determined by calculation but only by experiments. Only from a series of such experiments is it possible to obtain a clear conception as to the value of these losses.

It is not possible for the authors to give the results of such experiments. The experimental results are plotted in numerous curves such as are shown for instance in Figs. 56 to 60. But in order to discuss these curves the exact data as to the design and dimensions of the pumps are necessary. The reason why this information is withheld by manufacturers can be readily understood.

It is only possible to say that the pumps from which the experimental data here given were derived have negative values for the constant C_2. Further, the efficiency curves show that the total efficiency becomes less with decreasing quantities of water. On the one hand this diminution is due to the pumps operating with shock, but on the other hand it is due to the fact that the short-circuit and the mechanical losses are approximately equal for all quantities of water, so that for smaller quantities of water the percentages of loss increase when referred to the total power consumption. For instance, if the consumption of power necessary to overcome these losses at a normal load is 7 per cent of the total power, then it will, taken absolutely, remain approximately the same for half the quantity of water, but referred to the consumption of power now occurring it would amount to about 14 per cent. The decided falling off of the efficiency curve with decreasing quantities of water is due chiefly to this fact.

It should be noted that the equations derived for the relation of pressure head when throttling agree with practice only within small limits of change of water quantity. For very small quantities of water and by complete throttling, the head rises to a greater value than the calculation gives. For complete throttling, this can be explained by the fact that in determining the value $\frac{u_a^2 - u_e^2}{g}$ the velocity u_a no longer refers to the diameter D_a but to the outer impeller diameter D_a^a.

29. Adjustable Guide Vanes.

When the quantity of water passing through an impeller is changed, the guide vane angle, or angle of slope of the involute, will no longer correspond to that angle with which the water leaves the impeller; that is, the direction of the absolute velocity of the water leaving the impeller changes with the quantity of water flowing. Fig. 61 illustrates how losses occur due to this change of quantity of water. An ideal condition would occur if the guide vanes could be adjusted so that the channel cross sections and vane angles would correspond to the quantity of water flowing. This would give operation without shock, which simply means that for any certain quantity of water the correct velocity diagrams will correspond to a certain setting of the guide vanes. This, however, is hardly practical.

There is a form of adjustable guide vane which is generally used for regulating water turbines and which could be used in centrifugal pumps. The guide vanes can be so adjusted that the angle δ_a and the cross section of the guide channels may be increased or decreased. The guide vanes are so arranged that each vane can be simultaneously turned by a suitable mechanism controlled outside of the pump casing. By the use of such adjustable guide vanes it is possible to change the directing angles and entrance heights so that they correspond to a certain quantity of water.

Adjustable guide vanes cannot be used for high-pressure centrifugal pumps because the guide channel heights and cross sections are quite small and also because adjustable guide vanes are difficult to install in a multi-stage design. In low-pressure pumps where large cross sections occur there is no reason why adjustable guide vanes cannot be used. The only reason why such regulation has not been adopted is on account of the greater cost of construction. Commercially it is difficult to have a costly pump competing with cheaper types, even if the former possesses some advantages, and especially when the guaranteed efficiencies at normal load are the same. But with the constantly increasing use of centrifugal pumps there will be many demands for a high efficiency. Should such high efficiency be demanded with varying quantities of water, adjustable guide vanes must come into use in spite of the higher cost. This applies more especially to low-pressure pumps.

Fig. 66 shows a general arrangement of a scheme for adjustable guide vanes. In this case the guide vanes can be turned about the so-called guide vane bolts *a*, which also incidentally stiffen the sides of the pump casing. A small lever *b* rigidly connects each vane to a ring *c*, which is guided by a part of the pump casing and which can be turned by some suitable mechanism. Every position of the ring corresponds to a certain position of all the guide vanes, and assuming careful assembly, any position of the ring will always give uniform entrance heights and entrance angles throughout.

In another arrangement the adjustable guide vanes are connected rigidly to the bolts. The latter are carried through stuffing boxes in the casing. The bolts are connected to small levers which are actuated by a ring supported on the outside of the casing. This ring is also turned by a suitable mechanism. Although this arrangement is more costly than the former it is to be preferred

because the regulating mechanism lies outside of the casing and is therefore more accessible.

The involute shape of the guide vanes is constructed as before for the normal load of the pump (see Fig. 42). When the guide vanes are turned the vanes do not form a true involute; the entrance height and entrance angle become smaller until the latter is approximately zero at the limiting position. In this position the

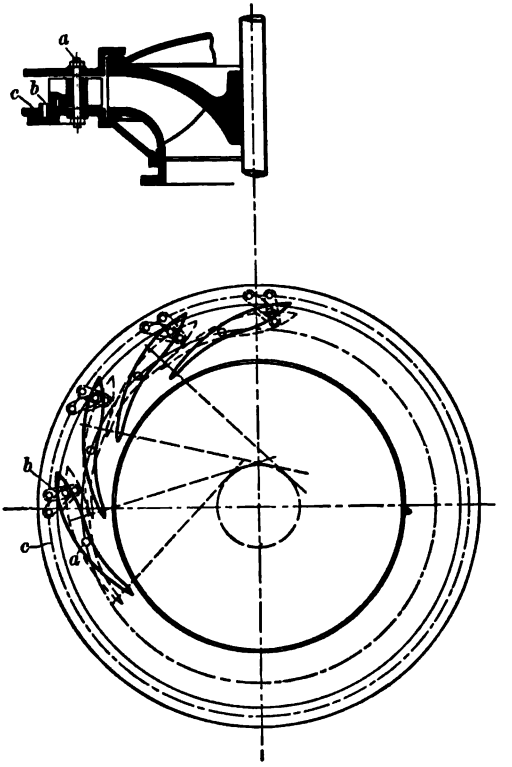

Fig. 66.

involute part of the guide vane lies upon the circumference of a circle. This limiting position of guide vanes is shown dotted in Fig. 66. Attention is also called to Plate VII, in which such adjustable guide vanes are shown.

By the use of adjustable guide vanes it is possible for the water to enter these vanes without shock, even when the quantity of water varies considerably, because it is possible to obtain approximately correct guide vane angles for any quantity of water. There is a small

and negligible error of angle, because with smaller entrance heights the involute should have a different radius of curvature.

When the entrance cross section of the guide vanes is decreased the head necessary to overcome the friction and shock losses increases. With backward-turned blades, now generally used, the absolute velocity increases with decreasing quantities of water; also with decreasing height a_l the value $\frac{a_l + b}{2\,a_l b}$ increases, so that according to equation 194 the friction loss in the guide vanes increases with decreasing quantities of water. With decreasing heights of guide channel the ratio of contraction becomes larger on account of the thickness of the vanes. According to equation 212 the head lost through blade shock will increase with decreasing quantities of water because the water velocities increase.

For constructive reasons the directing vanes at impeller entrance cannot well be made adjustable. As was mentioned in Article 28, the losses due to change of quantity of water will not be very great if the clearance between vanes and impeller is made sufficient.

30. Classification of Centrifugal Pumps.

When manufacturing centrifugal pumps it becomes necessary to decide quickly whether any existing designs of impeller and guide vanes can be used for a certain set of conditions. In this article it will be shown how centrifugal pumps can be classified by certain constants.

Let us assume that a series of pumps has been designed for various heads and quantities of water and that the pumps have been found satisfactory by experiment. It is now necessary to select one of these pumps or to design a new one to meet a certain set of conditions. Before designing a new pump we must decide whether we can utilize old patterns, especially those of the impeller and the guide vanes, without sacrificing the efficiency of the pump.

Of course at first we investigate whether the entire model of some existing pump can be used. This is best accomplished by determining the constant designated in Article 6 as the characteristic K. According to equation 49, $K = \frac{Q}{\sqrt{\eta H_n}}$. For multi-stage pumps H_n is of course the head of one stage, and in calculating such

pumps it is necessary to determine immediately the number of stages. The same pump can be used for all combinations of heads and quantities of water for which $\frac{Q}{\sqrt{\eta H_n}}$ has the same value, hence the same characteristic K. This value K is a common constant for impeller and guide vanes. In order to obtain the value ηH_n the coefficient η must first be assumed. For Q the quantity of water in cubic feet per minute must be obtained.

The number of revolutions per minute of a pump varies as the square root of the total head delivered by that pump, and therefore the same impeller can be used for different heads by simply changing its speed. In order to determine quickly the number of revolutions per minute necessary for any total head it is best to designate each design of pump by the number of revolutions per minute corresponding to some fixed total head. The most convenient value of this fixed total head ηH_n is ten feet and this value will be used in the following problems. That is, any design of pump will be classified under the number of revolutions per minute which is necessary to give a total head ηH_n equal to 10 feet.

The pump must also be classified as to its important dimensions, and it is best to classify it in terms of its outer impeller diameter D_a[a] expressed in feet.

As has been explained in Article 15, the same impeller can be used for different quantities of water, provided the head remains constant, by changing the guide vanes to suit any given quantity. Hence by changing the guide vanes various constants K are obtained for the same impeller. When the quantity of water is changed the peripheral velocity also changes on account of the influence of the angles δ_e and δ_a; hence the number of revolutions per minute changes. It is therefore possible to calculate for each new constant the corresponding number of revolutions per minute referred of course to a total head of $\eta H_n = 10$ feet.

In laying out a new design of pump the constant K and the number of revolutions n are determined for $\eta H_n = 10$. Besides this it is well to determine immediately between what limits the quantities of water may vary for this impeller by simply changing the guide vanes. This leads to the determination of $Q_{\max.}$ and $Q_{\min.}$, and from them the values of $K_{\max.}$ and $K_{\min.}$ can be determined.

The greatest and least quantities of water that can be used with

good efficiency for any one impeller are most simply determined by drawing the entrance velocity diagram. In this diagram we assume what change of angle δ_e is permissible and find the velocity w_r corresponding to the limiting values of δ_e. From this velocity the quantity of water may be readily found. The limiting values of the angle δ_e are dependent upon the impeller angle β_e. In the calculations of a centrifugal pump given later this will be more fully described.

For an existing impeller profile the peripheral velocity u_a is calculated according to equation 141, and when this value of u_a is substituted in the equation $n = \frac{60\,u_a}{D_a \pi}$, the necessary revolutions per minute are found from the equation

$$n = -\frac{60\,w_r}{D_a\pi}\,\frac{\frac{F_e}{F_a \tan\beta_a} + \frac{D_e}{D_a \tan\beta_e}}{2\left[1-\left(\frac{D_e}{D_a}\right)^2\right]} + \sqrt{w_r^2\left[\frac{60}{D_a\pi}\,\frac{\frac{F_e}{F_a \tan\beta_a} + \frac{D_e}{D_a \tan\beta_e}}{2\left[1-\left(\frac{D_e}{D_a}\right)^2\right]}\right]^2 + \left(\frac{60}{D_a\pi}\right)^2 \frac{\eta g H_n}{1-\left(\frac{D_e}{D_a}\right)^2}} \qquad 229$$

Let

$$\frac{60}{D_a\pi}\,\frac{\frac{F_e}{F_a \tan\beta_a} + \frac{D_e}{D_a \tan\beta_e}}{2\left[1-\left(\frac{D_e}{D_a}\right)^2\right]} = A \qquad 230$$

and

$$\frac{60}{D_a\pi}\,\frac{1}{1-\left(\frac{D_e}{D_a}\right)^2} = B; \qquad 231$$

then equation 229 may be written in a simplified form as

$$n = -w_r A + \sqrt{w_r^2 A^2 + B\eta g H_n} \qquad 232$$

To determine the existing radial entrance velocity w_r the entrance area F_e must be known, and then the velocity can be found from the relation $w_r = \frac{Q'}{F_e}$.

In order to determine quickly the number of revolutions for the different quantities of water it is best to determine immediately the constants A and B when laying out a new design of pump and also to state the entrance area F_e so that w_r can be determined. It might also be well to calculate the revolutions per minute for $K_{max.}$ and $K_{min.}$ referred to $\eta H_n = 10$.

Summarizing the above, if we wish to see whether existing patterns or designs can be used for any certain pump problem, a value is assumed for the coefficient η and then the characteristic $K = \frac{Q}{\sqrt{\eta H_n}}$ is determined. We then look in a table to see whether a pump having the same characteristic exists or has been designed and, should this be the case, determine the number of revolutions necessary for this special problem. If this gives a reasonable value for the number of revolutions the existing patterns or design can be used.

Quite often the number of revolutions is prescribed, in which case the number of revolutions for $\eta H_n = 10$ and the characteristic K are determined, and then we can see whether this combination of n and K already exists in some previous model. If this is not the case, we might investigate whether perhaps a part of the patterns or design might be used by looking up in the table of pumps the values of $K_{max.}$ and $K_{min.}$.

IV. THE CALCULATION OF IMPELLER AND GUIDE VANES.

31. Impeller Channel Sections of the Ordinary Type.

(a). *Calculation of Two High-pressure Centrifugal Pumps.*

In the preceding articles it was shown how to determine the entrance and exit velocity diagrams for a centrifugal pump so that it would work without shock, and also how the beginning and end of the blades should be formed from involute curves. In the following it will be shown how the impeller and guide vane channels should be designed. The best way to do this is actually to calculate several pumps and find the cross section of the channels.

First take the simplest case, in which the entrance width b_e is parallel to the axis of the shaft as shown in Fig. 67. If cross sections are taken in planes a–a and b–b at right angles to the shaft axis, the sections will all be the same, and therefore the blades are at right angles to every horizontal cross section. The channel in this case is very simply determined, because the ends of the blades at exit and entrance are involutes and they are connected by a suitable curve, so that the channel has a good form. In doing this it must be borne in mind that the number of blades should be as small as possible.

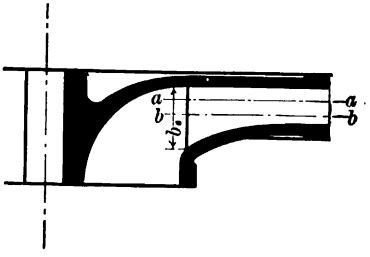

Fig. 67.

Several examples will now be calculated and the construction of the blades considered. The first example will be for an impeller profile as shown in Fig. 67.

Example I. See Plate III. An impeller and guide vanes are to be designed for a multi-stage high-pressure centrifugal pump to meet the following conditions:

$H_m = 65$ feet. $Q = 70$ cubic feet per minute.

The hydraulic efficiency $\frac{1}{\eta}$ will be assumed as 0.75, so that $\eta H_n = 86.67$.

The quantity of water delivered per second is $Q = \frac{70}{60} = 1.167$ cubic feet.

The quantity of short-circuited water will be assumed as 5 per cent of the quantity delivered, so that the quantity of water passing through the impeller and used in the calculation must be

$$Q' \cong 1.225 \text{ cubic feet.}$$

The Impeller. The diameter of the suction pipe is taken as 6 inches ($D_s = 0.5$ foot). The hub of the impeller is $3\frac{1}{8}$ inches in diameter ($d_n = 0.26$ foot). The clear cross-sectional area F_e' at impeller entrance is

$$F_e' = (D_s^2 - d_n^2)\frac{\pi}{4} = 0.143 \text{ square foot,}$$

so that the velocity w_r' through this area is

$$w_r' = \frac{Q'}{F_e'} = 8.57 \text{ feet per second.}$$

Let the outer impeller diameter be 12 inches ($D_a^a = 1$ foot) and the outer impeller angle $\beta_a^a = 155°$.

Let the number of blades $z = 10$.

According to equation 168 the diameter of the base circle for the involute at impeller exit is

$$d_a = D_a^a \sin \beta_a^a = 0.423 \text{ foot,}$$

and according to equation 169 the dimension $a_a + s_a$ is

$$a_a + s_a = \frac{D_a^a \pi \sin \beta_a^a}{z_a} = 0.133 \text{ foot,}$$

The blade thickness is $\frac{5}{32}$ inch ($s_a = 0.013$ foot); therefore the height of the impeller channel $a_a = 0.120$ foot.

The impeller diameter D_a, upon which the calculation of the peripheral velocity is based, can now be determined mathematically by equation 172 as

$$D_a = \sqrt{(D_a^a)^2 + a_a^2 + 2\, a_a D_a^a \cos \beta_a^a} = 0.892 \text{ foot.}$$

This same value can also be found graphically by drawing a tangent

to the base circle and laying off upon this tangent from its point of intersection with the circle of diameter $D_a{}^a$ the distance $\frac{a_a}{2}$, as can be easily understood by referring to Plate III.

The impeller angle at D_a, which is the angle used in subsequent calculations, is found from equation 170,

$$\sin \beta_a = \frac{D_a{}^a \sin \beta_a{}^a}{D_a} = 0.474,$$

or

$$\beta_a = 151^\circ 42'.$$

By assuming an impeller width of $\frac{1}{8}\frac{5}{8}$ inch ($b_a = 0.0495$ foot), the cross-sectional area at exit from the impeller at diameter D_a is

$$F_a' = \pi D_a b_a = 0.139 \text{ square foot.}$$

This exit area is not a clear area, because the blade thickness has not been taken into account. The actual clear area would be

$$F_a = F_a' \frac{a_a}{a_a + s_a} = 0.125 \text{ square foot.}$$

Further, the relative exit velocity v_r through this area is

$$v_r = \frac{Q'}{F_a} = 9.8 \text{ feet per second.}$$

The inner impeller diameter was determined as $7\frac{9}{3}\frac{9}{2}$ inches ($D_e = 0.6068$ foot). This diameter is fixed partly by the diameter of shaft necessary and the thickness of impeller hub and partly by the proper opening necessary to admit water to the impeller. By assuming that $\beta_e = \delta_e$, that is, $w_e = v_e$, the peripheral velocity u_a is found from equation 136, which is as follows:

$$u_{a_{\beta_e=\delta_e}} = -\frac{v_r}{2 \tan \beta_a \left[1 - \frac{1}{2}\left(\frac{D_e}{D_a}\right)^2\right]} + \sqrt{\left[\frac{v_r}{2 \tan \beta_a \left[1 - \frac{1}{2}\left(\frac{D_e}{D_a}\right)^2\right]}\right]^2 + \frac{\eta g H_n}{1 - \frac{1}{2}\left(\frac{D_e}{D_a}\right)^2}} \quad . \quad . \quad (136)$$

from which

$$u_a = 73.12 \text{ feet per second}$$

and

$$u_e = u_a \frac{D_e}{D_a} = 49.55 \text{ feet per second.}$$

The number of revolutions per minute can now be determined as

$$n = \frac{60\, u_a}{D_a \pi} = 1565 \text{ r.p.m.}$$

In order to construct the exit velocity diagram the value $\frac{v_r}{\tan \beta_a}$ is determined and then the diagram can be constructed without plotting the angle β_a. The method is as follows: Fig. 68 is the desired exit

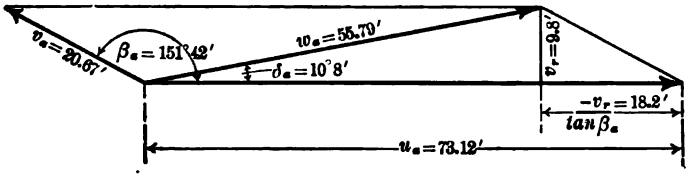

Fig. 68.

velocity diagram. Graphically or mathematically the absolute and relative exit velocities are found, as can easily be seen and understood from the figure. These values are

$$w_a = 55.79 \text{ feet per second,} \quad v_a = 20.67 \text{ feet per second.}$$

The guide vane angle δ_a is best found by means of the equation $\sin \delta_a = \frac{v_r}{w_a}$, from which $\delta_a = 10° 8'$.

The pitch of the blades at diameter D_a when $z = 10$ is

$$t_a = \frac{D_a \pi}{z} = 0.28 \text{ foot or } 3.36 \text{ inches.}$$

The radial entrance velocity at impeller entrance was found to be $w_r' = 8.57$ feet and the peripheral velocity at diameter D_e is $u_e = 49.55$ feet.

The pitch t_e is

$$t_e = \frac{D_e \pi}{z} = 0.19 \text{ foot or } 2.29 \text{ inches.}$$

The entrance velocity diagram and the value of $a_e + \varepsilon_e$ are easily determined graphically from the values just given by the method

explained on page 59. The actual construction of this graphical method is shown in the entrance velocity diagram, Fig. 69, and hardly needs further explanation. It was found that

$w_r = 10.41$ feet per second, $w_e = v_e = 26.86$ feet per second,

$a_e = 0.0607$ foot or 0.728 inch, $s_e = 0.013$ foot or 0.156 inch,

$$\beta_e = \delta_e = 22° 50'.$$

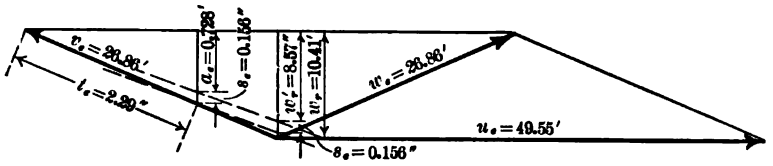

Fig. 69.

To check the graphical determination the value of w_r can be found from the equation $w_r = w_r' \dfrac{a_e + s_e}{a_e} = 10.405$ feet per second.

The diameter of the base circle of the entrance involute can be determined from equation 162 or perhaps more simply from equation 160 as

$$d_e = \frac{(a_e + s_e)\, z}{\pi} = 0.235 \text{ foot or } 2.82 \text{ inches.}$$

The entrance width b_e at the inner impeller diameter D_e is

$$b_e = \frac{Q'}{D_e \pi\, w_r'} = 0.074 \text{ foot or } 0.89 \text{ inch.}$$

After determining all the impeller dimensions given above, the involutes at entrance and exit of the impeller are drawn as described in Article 17. The two involutes are then connected by a suitable curve. This is best accomplished by drawing the entrance involute on tracing paper and moving it in relation to the exit involute until both involutes can be connected by a curve which appears suitable for the form of the blade channel.

In determining the impeller profile care must be taken to adhere exactly to the width $b_a = 0.0495$ foot at diameter D_a and the width $b_e = 0.074$ foot at diameter D_e.

The elbow forming the entrance to the impeller must be so formed that every cross section of this elbow will have the area F_e', so that

there will be no acceleration or retardation of the water flowing through the elbow.

The Guide Vanes. The diameter d_l of the base circle of the involute for the guide vanes is determined from equation 174

$$d_l = D_a \sin \delta_a.$$

It was found that

$$D_a = 0.892 \text{ foot and } \delta_a = 10° 8';$$

so that

$$d_l = 0.157 \text{ foot or } 1.88 \text{ inches.}$$

After assuming the number of vanes $z_l = 8$, the value of $a_l + s_l$ is determined from equation 175,

$$a_l + s_l = \frac{d_l \pi}{z_l} = 0.0616 \text{ foot or } 0.738 \text{ inch.}$$

The blade thickness s_l is assumed as 0.013 foot (0.156 inch); so that the height of the channel $a_l = 0.0486$ foot (0.582 inch).

The value of $a_l + s_l$ can also be found from equation 176, $a_l + s_l = \frac{Q'}{w_a' b_a z_l}$, in which $w_a' = w_a \frac{a_a}{a_a + s_a}$ (equation 173). The quantity of water Q' flowing through the impeller does not flow through the guide vanes, because the value Q' includes the quantity of short-circuited water. If it is assumed that the direction of the water velocity in the clearance space describes an involute, then the velocity w_a' decreases proportionally with the quantity of water, so that the ratio $\frac{\text{quantity of water}}{\text{velocity}}$ stays constant. It is therefore not necessary in the above calculation to take into account the decreased quantity of water due to the absence of the short-circuited water and its correspondingly decreased velocity, and we may use equation 177, which includes the quantity of water Q' and its corresponding velocity w_a'.

The angle of the guide vanes at exit depends upon the shape of the casing surrounding the vanes. If the casing is spiral in form the guide vanes are given an exit angle tangent to the involute of the casing. If the guide vanes are placed concentric to a circular casing, as shown in Fig. 7, it is advisable to make the exit of the vanes radial so that the water will enter the casing radially. If the

water after leaving the guide channels is led through a connecting or reversing channel to another impeller, as is the case with multi-stage high-pressure centrifugal pumps, the exit angle of the guide vanes is made such that the water leaving the guide channel flows in the direction of the connecting channel. The latter is so formed that the absolute entrance velocity to the next impeller receives its proper direction.

It would be advisable to check the calculations of the velocity diagrams by investigating whether the values of the velocities just found fulfill equation 22, which states that

$$\eta H_n = \frac{u_a^2}{2g} - \frac{u_e^2}{2g} + \frac{v_e^2}{2g} - \frac{v_a^2}{2g} + \frac{w_a^2}{2g} - \frac{w_e^2}{2g}.$$

As it was assumed that $\beta_e = \delta_e$, it follows that $v_e = w_e$; therefore

$$\frac{v_e^2}{2g} - \frac{w_e^2}{2g} = 0.$$

Substituting the calculated velocities in equation 22, we find

$$\eta H_n = 86.67 \text{ feet},$$

while the total head upon which all the calculations were based was also 86.67 feet.

A further check upon these calculations, and also an investigation of the change of head when the pump is throttled, can be obtained from equation 225, which states that

$$\eta H_n = \frac{u_a^2 - u_e^2}{g} + \frac{v_r\left[\frac{u_a}{\tan \beta_a} + \frac{u_e}{\tan \beta_e}\frac{F_a}{F_e}\right]}{g} = C_1 + v_r C_2.$$

The values of the constants are

$$C_1 = 89.9, \qquad C_2 = -0.33.$$

For the normal quantity of water delivered $v_r = 9.8$ feet per second; hence

$$\eta H_n = 86.57 \text{ feet},$$

which checks approximately with the initial value.

The constant C_2 has only a small negative value; so that, if the coefficient η remains unchanged, the head increases very slightly as the quantity of water decreases. But considering that the coefficient η increases if the discharge is throttled, then even for a slightly decreased quantity of water the desired head can no longer be reached. Therefore this form of blade is perhaps not useful for a pump which must often deliver less water than that for which it is calculated. It is useful, however, when the discharge or pressure pipe is of considerable length. In this case a certain fraction of the head H_n is necessary to overcome the friction losses in this long pipe, and as this friction head decreases approximately with the square of the velocity in the pipe, it is possible that for smaller quantities of water a smaller H_n will be sufficient. Hence it is possible that for a long discharge pipe, ηH_n can have the same value between certain limits of quantity of water, within which limits η increases and H_n decreases as the quantity of water decreases.

Attention is called to the fact that in cases having a long discharge pipe line it is necessary to design a pump which delivers a decreasing head H_n with decreasing quantity of water. This is preferable to a pump which increases its head greatly when the discharge is throttled, because this increased head increases unnecessarily the power consumption of the pump and the greater head is of no benefit.

After checking the pump calculation in the manner described above the various constants necessary for proper classification of the pump can be determined. A common constant for both the impeller and guide vanes is K, and its value in this case is

$$K = \frac{Q}{\sqrt{\eta H_n}} = \frac{70}{\sqrt{86.67}} = 7.52.$$

As the number of revolutions varies as the square root of the head of any pump, the number of revolutions per minute, n, can be found for this pump when referred to $\eta H_n = 10$. When $\eta H_n = 86.67$ the value of n is 1565; hence when $\eta H_n = 10$ the value of n is 530.

Also taking into account the outer impeller diameter $D_a^a = 1$ foot the pump may be classified as

High-pressure pump, $D_a^a = 1.0$.

$K = 7.52$, $\quad n = 530$.

The impeller and guide vanes of the above pump can therefore be used without change for all cases in which the characteristic K has the value 7.52.

By drawing velocity diagrams it is found that the same impeller can be used for a maximum capacity of 85 cubic feet per minute and a minimum capacity of 55 cubic feet per minute without greatly decreasing the hydraulic efficiency; the only change necessary being the redesign of the guide vanes, which must be made suitable for each quantity. If the coefficient η remains constant we have

$$K_{max.} = 9.12, \qquad K_{min.} = 5.90.$$

To determine the number of revolutions for any value of K the constants A and B are found from equations 230 and 231. In this example they have the following value:

$$A = -2.78, \qquad B = 850.$$

The number of revolutions for any quantity and head of water can now be found from equation 232, which is

$$n = -w_r A + \sqrt{w_r^2 A^2 + \eta g H_n B}.$$

To determine the velocity w_r the entrance area F_e must be given, and then w_r is found from the equation $w_r = \frac{Q'}{F_e}$. To classify the calculated pump exactly we should write

High-pressure pump, $D_a^a = 1.0$.
$K = 7.52, \qquad n = 530.$
$K_{max.} = 9.12, \qquad K_{min.} = 5.90.$
$F_e = 0.118, \quad A = -2.78, \quad B = 850.$

The constant A has quite a small value, so that the number of revolutions changes very little with varying velocities w_r. In the next example this constant has a larger value, and the quantity of water will then have an important influence upon the number of revolutions.

It was found in the blade design for example I that the head would decrease by throttling, that is, by decreasing the quantity of water. The question now arises, If another blade form is taken, how can we

be sure that the pump will deliver at least the normal pressure when it is throttled in order to vary the quantity of water delivered?

In Article 28, this question was briefly discussed. Attention is again called to a point which concerns the choice of the outer and inner diameters of an impeller. In order that ηH_n may increase with decreasing quantity of water the right-hand part of the second member of equation 225 must be negative. The larger this negative value the larger will be the expression $\frac{u_a^2 - u_e^2}{g}$. It is therefore necessary to make the member $-\frac{u_a^2 - u_e^2}{g}$ as large as possible, which is accomplished on the one hand by assuming large values for the angles β_a and δ_a, on the other hand by a suitable assumption of the inner and outer impeller diameters. Placing $u_e = u_a \frac{D_e}{D_a}$ in equation 226, we have

$$C_1 = \frac{u_a^2 - u_e^2}{g} = u_a^2 \left[1 - \left(\frac{D_e}{D_a}\right)^2\right].$$

Hence the smaller the ratio $\frac{D_e}{D_a}$ the larger the constant C_1 and the higher will be the head which the pump can deliver under throttling.

If the inner diameter of the impeller of the above example is decreased the entrance line b_e can no longer be kept parallel to the axis, but must be taken as a curve somewhere in the entrance elbow of the impeller. The determination of the proper blade surface or shape will be discussed in the following article.

Another way of decreasing the ratio $\frac{D_e}{D_a}$ is by increasing the outer diameter D_a^a. In order to show what influence an increase of the outer diameter of an impeller will have on the various calculated values, a second blade form will be calculated for the same example but by assuming the outer impeller diameter $D_a^a = 1.146$ feet (13.75 inches).

EXAMPLE II. See Plate IV. The outer impeller diameter $D_a^a = 1.146$ feet. The impeller profile at entrance shall be the same as in example I, so that

$D_e = 0.50$ ft., $F_e' = 0.143$ sq. ft., $w_r' = 8.57$ ft., $D_e = 0.6068$ ft.

The number of impeller blades will now be $z = 9$. In the first example the number of blades could not be taken less than 10, because

otherwise the entrance and exit involutes could not be connected. With a larger outer diameter the channel heights can be taken greater on account of the correspondingly greater difference of $D_a - D_e$, and therefore the number of blades can be decreased.

We shall again call attention to the fact that the minimum number of impeller blades is determined by the possibility of connecting the entrance and exit involutes. In Article 24 the advantage of obtaining a minimum number of impeller blades was discussed.

With the blade form having the larger impeller diameter the channels will of course become somewhat longer, but the height of channel becomes larger on account of the smaller number of blades. The hydraulic losses for both blade forms will be approximately equal. Because of this the hydraulic efficiency $\frac{1}{\eta} = 0.75$ is assumed as before, so that again $\eta H_n = 86.67$.

The outer impeller angle at diameter $D_a{}^a$ is $\beta_a{}^a = 155°$. Then

$$d_a = 0.484 \text{ foot} \quad \text{and} \quad a_a + s_a = 0.170 \text{ foot.}$$

Therefore the height of channel $a_a = 0.157$ foot and the blade thickness $s_a = 0.013$ foot.

The outer impeller diameter D_a, upon which most of the impeller calculations are based, can be obtained from equation 171 or can be determined graphically. It was found that $D_a = 1.022$ feet and that the blade angle at this diameter is $\beta_a = 151° 42'$.

The impeller width b_a is now assumed. Let $b_a = 0.0394$ foot; from this we find

$$F_a = 0.1168 \text{ square foot and } v_r = 10.5 \text{ feet.}$$

Assuming $\beta_e = \delta_e$, the peripheral velocity is found from equation 136 as

$$u_a = 71.18 \text{ feet per second} \quad \text{and} \quad u_e = 42.2 \text{ feet per second.}$$

The number of revolutions per minute now becomes $n = 1330$. At the inner impeller diameter D_e the pitch $t_e = 0.238$ foot.

According to the construction now well understood, we determine graphically

$$a_e + s_e = 0.101 \text{ ft.}, \quad a_e = 0.088 \text{ ft.}, \quad s_e = 0.013 \text{ ft.}$$
$$\beta_e = \delta_e = 25°, \quad w_r = 9.86 \text{ ft. per sec.}, \quad w_e = v_e = 23.3 \text{ ft. per sec.}$$

The diameter of the base circle for the entrance involute is $d_e = 0.29$ foot.

The entrance area decreased by the blade thickness is $F_e = 0.125$ square foot.

From the exit velocity diagram the relative and absolute exit velocities are found to be

$$v_a = 22.15 \text{ feet per second}, \quad w_a = 52.73 \text{ feet per second}.$$

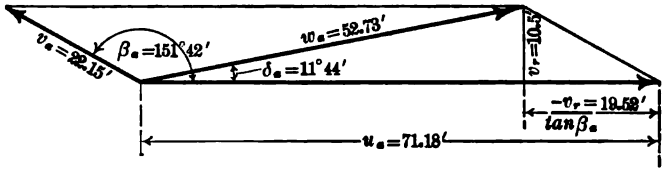

Fig. 70.

Figs. 70 and 71 represent the exit and entrance velocity diagrams in which the values just found are shown.

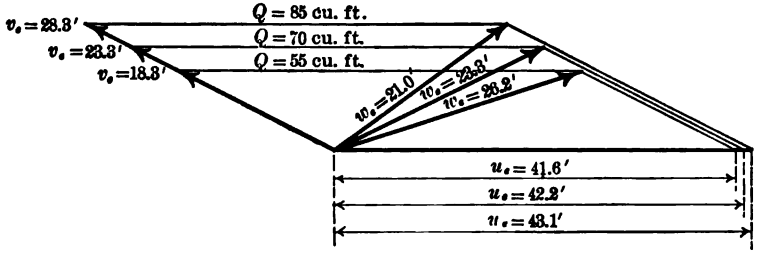

Fig. 71.

For the guide vanes the diameter of the base circle $d_l = 0.208$ foot, and by assuming the number of vanes $z_l = 8$ the height of channel $a_e = 0.0687$ foot and the thickness of vane $s_l = 0.013$ foot.

According to methods already described the involutes can now be drawn and the shape of the guide vane channels determined. (See Plate IV.)

An investigation will again be made to determine the pressure heads which will exist with this form of blade when the quantity of water is diminished. After determining the constants C_1 and C_2 equation 228 can be written

$$\eta H_n = 102 - 1.486 v_r.$$

For the normal quantity of water $v_r = 10.5$ feet per second, from which $\eta H_n = 86.4$ as against 86.67 which was assumed in the calculation.

The theoretical pressure curves for the blade forms I and II are shown in Fig. 72. The abscissæ are quantities of water and the ordinates the total pressure heads ηH_n. It can be seen that the slightly larger impeller used with blade form II considerably aids in increasing the pressure head.

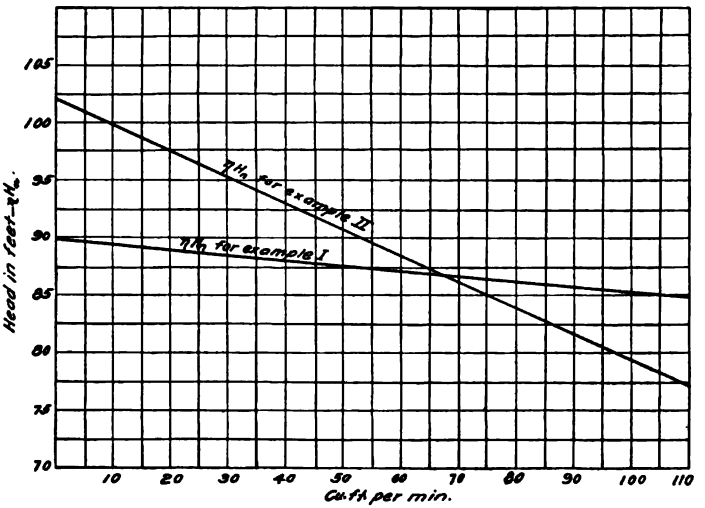

Fig. 72.

Attention might again be drawn to the fact that the theoretical pressure curves shown in Fig. 72 would actually show a different course because the pressures would become larger with decreasing quantities of water. But in spite of this the representation of both pressure curves is of interest in so far as it gives a clear conception of the influence of the various assumptions of the ratio $\frac{D_e}{D_a}$ upon the head.

The characteristic of the pump with blade form II is found as before, $K = 7.52$, but the number of revolutions referred to $\eta H_n = 10$ is in this case $n = 467$, so that the pump may be classified as

High-pressure pump, $D_a^a = 1.146$.

$K = 7.52$, $n = 467$.

As has been previously found,

$$K_{max.} = 9.12, \qquad K_{min.} = 5.90.$$

The constants A and B were found to be

$$A = -10.38, \qquad B = 541.$$

The necessary entrance area for calculating w_r is $F_e = 0.125$ square foot, so that the exact classification of this pump may now be written

$$\text{High-pressure pump, } D_a^a = 1.146.$$
$$K = 7.52, \qquad n = 467.$$
$$K_{max.} = 9.12, \qquad K_{min.} = 5.90.$$
$$F_e = 0.125, \qquad A = -10.38, \qquad B = 541.$$

It is advisable to collect these values derived for various pumps in the form of a table.

For example II the constant A has a larger value than in example I. The number of revolutions corresponding to the maximum and minimum quantities of water (85 cubic feet and 55 cubic feet) can be found as follows:

The angle of the impeller blade at entrance, β_e, must of course remain constant because the same impeller is used. This makes the value of v_e directly proportional to the quantity of water passing through the impeller or discharged by the pump. For the normal quantity (70 cubic feet per minute) $v_e = 23.3$ feet per second; hence for the maximum quantity (85 cubic feet) $v_e = 28.3$ feet per second and for the minimum quantity (55 cubic feet) $v_e = 18.3$ feet per second. As $w_r = v_e \sin \beta_e$, the value of w_r can be found for each value of v_e. For the maximum quantity of water $w_r = 28.3 \sin 25° = 11.98$ feet per second; for the minimum quantity $w_r = 18.3 \sin 25° = 7.74$ feet per second. The number of revolutions for each quantity can now be found from equation 232, so that the following may be written:

For $K_{max.} = 9.12$ corresponding to $w_r = 11.98$ feet, $n = 1358$,
For $K_{min.} = 5.90$ corresponding to $w_r = 7.74$ feet, $n = 1310$,

while the number of revolutions for $K = 7.52$ (for which the guide vanes and impeller of the pump were designed) was $n = 1330$. In Fig. 71 are shown the entrance velocity diagrams for $K_{max.}$ and $K_{min.}$ and their corresponding velocities are dimensioned in the figure.

(*b*). *Calculation and Blade Form of a Low-pressure Centrifugal Pump.*

The blade form of an impeller and guide vanes for a low-pressure centrifugal pump will now be designed. The pump is to comply with the following specification:

$$Q = 636 \text{ cubic feet per minute, } H_n = 26.0 \text{ feet.}$$

The hydraulic efficiency $\frac{1}{\eta}$ is assumed to be 0.80, so that $\eta H_n = 32.5$.

The quantity of water delivered per second is $Q = 10.6$ cubic feet.

The amount of short-circuited water is assumed to be 6 per cent of the quantity delivered, so that the quantity passing through the impeller is

$$Q' = 10.6 + 0.06\ (10.6) = 11.236 \text{ cubic feet per second.}$$

The Impeller. The suction pipe diameter D_s will be assumed as 1.18 feet (14.16 inches). With a hub diameter of $d_n = 0.328$ foot ($3\frac{5}{8}$ inches) the clear cross-sectional area of the suction pipe at entrance to the impeller will be $F_s' = 1.009$ square feet, and therefore the suction pipe velocity at this place will be $w_r' = 11.13$ feet per second.

Let the outer impeller diameter $D_a^a = 2.458$ feet (29.5 inches) and the impeller angle at this diameter be $\beta_a^a = 155°$ and let the number of impeller blades be $z = 12$. The diameter of the base circle for the outer involute is found from equation 168 and is $d_a = 1.038$ feet. By assuming a thickness of blade $s_a = 0.0164$ foot (0.197 inch) the height of the channel is found from equation 169 to be $a_a = 0.256$ foot (3.067 inches).

The outer impeller diameter upon which the calculations are based is found from equation 172 to be $D_a = 2.23$ feet. The pitch at this diameter is $t_a = 0.584$ foot.

The angle of the impeller blade at this diameter is found from equation 170. It is $\beta_a = 152° 17'$.

The friction losses are much smaller in low-pressure centrifugal pumps than in high-pressure pumps because the former have low velocities and larger cross sections of channel. In order to avoid directing vanes at impeller entrance δ_e is taken equal to 90°, so that the absolute entrance velocity w_e is perpendicular to u_e.

By this assumption the calculation of the peripheral velocity is greatly simplified; it can now be found from equation 58 after assuming v_r or from equation 63 by assuming δ_a. To determine quickly the peripheral velocity and the radial exit velocity, the κ and λ curves shown on Plate I can be used. These curves will therefore be used in the present calculation.

The guide vane angle δ_a will be assumed as 25°.

For $\delta_a = 25°$ and $\beta_a = 152° 17'$ the κ curves give $\kappa = 1.37$, hence $u_a = \kappa \sqrt{\eta g H_n} = 44.4$ feet per second.

From this the number of revolutions per minute is found to be $n = 380$.

For $\delta_a = 25°$ the λ curves (see Plate I) give $\lambda = 0.11$; therefore, according to equation 104,

$$v_r = \frac{\sqrt{\lambda 2 \eta g H_n}}{\kappa} = 11.07 \text{ feet per second.}$$

From equation 157

$$v_r' = 10.4 \text{ feet per second,}$$

and the impeller width b_a is found from equation 158 and is

$$b_a = 0.154 \text{ foot.}$$

The clear exit area, after allowing for the blade thicknesses, is

$$F_a = 1.015 \text{ square feet.}$$

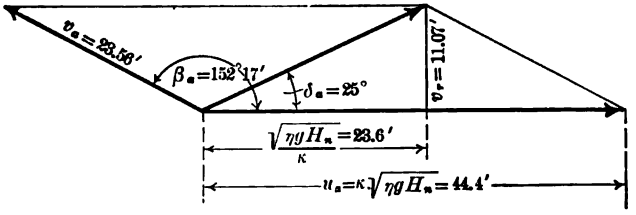

Fig. 73.

In order to construct the exit velocity diagram, determine the value $\frac{\sqrt{\eta g H_n}}{\kappa} = 23.6$, whereupon the exit velocity diagram can be drawn according to the method given on page 40 (see Fig. 73).

Graphically or analytically the relative and absolute exit velocities are found as

$$v_a = 23.56 \text{ feet per second}, \quad w_a = 26.1 \text{ feet per second}.$$

The inner impeller diameter was assumed as $D_e = 1.376$ feet. With $z = 12$ the pitch $t_e = 0.361$ foot.

The peripheral velocity at this diameter is $u_e = 27.4$ feet per second.

The velocity in the suction pipe at impeller entrance was found to be $w_r' = 11.13$ feet per second.

Having the values u_e, w_r', and t_e given, the entrance velocity diagram can be drawn as has already been explained (see Plate V) and the value $a_e + s_e$ can be graphically determined. It has been found that

$$a_e = 0.131 \text{ foot}, \qquad s_e = 0.0164 \text{ foot},$$
$$v_e = 30.15 \text{ feet per second}, \qquad w_e = 12.54 \text{ feet per second}.$$

The diameter of the base circle of the entrance involute is $d_e = 0.565$ foot. The width b_e at impeller entrance is

$$b_e = 0.233 \text{ foot};$$

further, the clear entrance area, taking into account blade thickness, is

$$F_e = 0.895 \text{ square foot}.$$

After all the calculated values for entrance to and exit from the impeller are determined the involutes are drawn and the blade profile is formed. (See Plate V.) In drawing the impeller or blades care must be taken that at the outer diameter D_a the width of the impeller $b_a = 0.154$ foot be adhered to and also at the inner diameter D_e the impeller width $b_e = 0.233$ foot must be kept unchanged. Further, the elbow at entrance to the impeller blades must be so formed that every cross section at right angles to flow must have the value $F_e' = 1.009$ square feet.

The Guide Vanes. The number of vanes will be taken as $z_l = 14$. The diameter of the base circle of the involute is found from equation 174 as

$$d_l = 0.943 \text{ foot},$$

and from equation 175 the height of channel a_l was found to be 0.192 foot, assuming a thickness of vane $s_l = 0.0197$ foot.

Plate V shows the entire form of these vanes.

Consumption of Power. The total efficiency of the pump will be taken as 75 per cent, so that the consumption of power as determined from equation 192 is $N = 41.8$ h.p.

As a check upon these calculations it would be well to see if the calculated velocities fulfill equation 221, and further, in order to have a check as to what the pressure heads will be when the pump is throttled, it is advisable to determine the constants C_1 and C_2 from equation 228.

These constants are found to be

$$C_1 = 38.0, \qquad C_2 = -0.52,$$

so that equation 228 reads

$$\eta H_n = 38.0 - 0.52\, v_r.$$

For the normal quantity of water $v_r = 11.07$, which when substituted in the above formula gives $\eta H_n = 32.3$, which corresponds closely with the value initially assumed. From the value of the constant C_1 it can be seen that the head does not fall below the value of the normal head when the pump is throttled.

Attention is called to the fact that the above pump calculation was made by aid of the κ and λ curves without using a table of trigonometric functions.

In order to classify the pump the characteristic $K = \dfrac{Q}{\sqrt{\eta H_n}}$ is found and also the number of revolutions per minute referred to $\eta H_n = 10$.

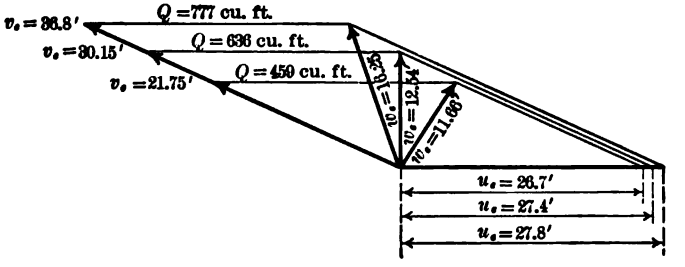

Fig. 74.

The greatest quantity of water which can be delivered by the pump and still retain good efficiency was found by drawing the velocity diagram (see Fig. 74) to be 777 cubic feet per minute and the smallest quantity to be 459 cubic feet per minute. This gives

$K_{max.} = 136.5$ and $K_{min.} = 80.6$. The velocity diagrams for these maximum and minimum values are shown in Fig. 74. From equations 230 and 231 the constants A and B are found to be $A = -2.3$, $B = 116.2$.

The exact classification of the pump may now be written as follows:

Low-pressure pump, $D_a^a = 2.458$.

$K = 111.5$,	$n = 236$.
$K_{max.} = 136.5$,	$K_{min.} = 80.6$.
$F_e = 0.90$, $A = -2.3$,	$B = 116.2$.

32. The Channel Cross Sections and Development of the Blade Ends upon the Surface of a Cone.

(a). *In General.*

In general the weight of a centrifugal pump depends upon the impeller diameter. In order to save weight and also to increase the number of revolutions it is advisable to keep the impeller diameter as small as possible. This is especially true of low-pressure centrifugal pumps, because large impeller diameters mean considerable weight.

In the water turbine industry the desire to get a high number of revolutions and minimum weight of impeller led to the decrease of the impeller diameter. The impeller of a Francis turbine was at first designed with a profile similar to the low-pressure centrifugal pump impeller shown in Fig. 75. The outer diameter was 29.5 inches, but to-day it would be built with an outer diameter equal to the diameter of the suction pipe, or $14\frac{3}{8}$ inches, which naturally increases the number of revolutions and considerably decreases the weight of the impeller.

Even if the conditions are somewhat different in water turbines from those in centrifugal pumps there is no doubt that the low-pressure centrifugal pump will pass through a similar development. In order to fulfill the condition perhaps most desired in a centrifugal pump, that of maintaining at least its normal head when the pump is throttled, the ratio $\frac{D_a}{D_e}$ must always be taken greater than unity, which is not a necessary condition with water turbines.

Let us try to make the inner impeller diameter D_e as small as possible. In doing so we must abandon making the entrance to the impeller parallel to the shaft axis as was done in the three examples of the preceding article.

As has been mentioned, in order to decrease the inner impeller diameter D_e it is necessary to place the impeller entrance inside of the elbow of the impeller profile, so that the entrance line b_e now becomes a curved line which will be called in short *entrance arc.* The center of gravity of this entrance arc lies in the mean inner impeller diameter D_e. This diameter and the length of the entrance arc must be so chosen that the equation $D_e \pi b_e = F_e'$ is fulfilled. In this equation F_e' represents the clear suction pipe cross section about the impeller hub.

After the entrance arc and the mean inner diameter are decided upon, then the outer diameter is, if possible, so assumed that a decrease of pressure does not take place when the discharge is throttled. Special attention must be given to equation 225. In the low-pressure centrifugal pump previously calculated (example III, Plate V) the outer impeller diameter D_a^a was 29.5 inches. In the following a low-pressure pump will be calculated for the same quantity of water and head as in example III. This pump will also fulfill equation 225 but will have an inner impeller diameter of $D_e = 0.866$ foot. The outer impeller diameter will then be reduced to $D_a^a = 1.64$ feet ($19\frac{11}{16}$ inches). The impeller profiles of these two pumps are shown to the same scale in Figs. 75 and 76.

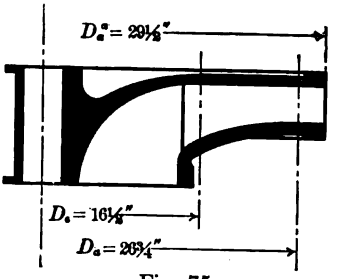

Fig. 75.

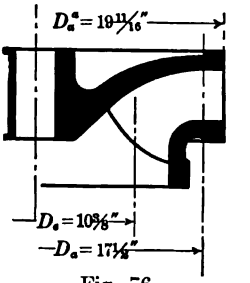

Fig. 76.

In the above case, therefore, it was possible to decrease the impeller diameter from 2.46 feet to 1.64 feet. The pump shown in Fig. 76 will of course have a higher number of revolutions and will be of less weight than the pump shown in Fig. 75. This comparison shows clearly the advantages of high-speed design.

(*b*). *Description of the Channel Cross Sections, with the Calculation and Design of the Blades for Two Low-pressure Centrifugal Pumps.*

It is obvious that any one cross section through the impeller shown in Fig. 76 can no longer determine the shape of the blade. To represent correctly the surface of the blade it must be shown as a development of the ends of the blade upon the surface of a cone. This will be more clearly explained in the following.*

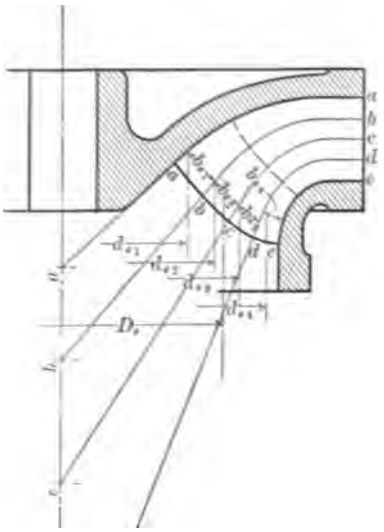

Fig. 77.

Assume that the impeller dimensions at entrance and exit were found and an impeller profile drawn.

Imagine now the impeller subdivided into a number of partial impellers (see Fig. 77) by dividing the exit width b_a equally into a number of parts. The entrance arc is divided into the same number of parts in such a manner that the rotating body formed by each of the subdivided arcs will represent equal parts of the total entrance area. Designating these small arcs consecutively as b_{e_1}, b_{e_2}, b_{e_3}, etc., and letting z be the number of small arcs, then for each subdivision the following condition must be fulfilled:

$$d_{e_1} \pi b_{e_1} = d_{e_2} \pi b_{e_2} = \frac{F_e'}{z} .$$

* We wish to call attention to the fact that the following method of determining the surface of the blade ends by means of cross sections through the channel and blades and by developing the blade ends upon the surface of a cone, was originated in the design of Francis turbines by A. Pfarr of Darmstadt, Germany, while chief engineer with Voith of Heidenheim, in conjunction with C. Hutzelsieder, now chief engineer with Voith. This method was first made public by E. Speidel and W. Wagenbach in *Zeitschrift des Vereins deutscher Ingenieure*, No. 20, Vol. 1899. These two men have only the honor of first bringing the matter to publicity, while a much higher honor is due the originator, A. Pfarr. It is to be regretted that the literature upon this subject always refers to the channel cross sections of E. Speidel and W. Wagenbach, because the priority of this method undoubtedly belongs to A. Pfarr.

The impeller shown in Fig. 77 is divided into four partial impellers. The points a, b, c, d, e on the entrance arc and at impeller exit were determined according to the method just described. The points so found were connected by so-called section lines which are supposed to be as nearly at right angles to the entrance arc as possible, so that the direction of these lines may be considered to represent the direction of the water at entrance to the impeller and also the direction of the water through the impeller. Further, the section lines are so constructed that any curve drawn at right angles to them, as that shown dotted in Fig. 77, will be so divided that the rotation areas of all parts of the curve between any two section lines will be equal. The section lines will then divide the impeller into a number of partial impellers through which equal quantities of water flow.

The peripheral velocities and pitch will vary directly with the diameter at the points a, b, c, d, e, so that for all points along the entrance arc the velocity diagrams and also the heights of channel will be different. To determine the heights of channel, the velocity diagrams must first be determined at the points a to e. It is best to assume that the velocity w_r' exists at entrance to the impeller and is at right angles to the rotation area formed by the entrance arc b_e.

With the following description of the channel cross sections an example will be calculated. For this example the same conditions will be assumed as for example III, that is, the blade form for a low-pressure centrifugal pump is again to be designed for

$$Q = 636 \text{ cubic feet per minute} \quad \text{and} \quad H_n = 26 \text{ feet.}$$

As before, the hydraulic efficiency is assumed as 0.8, so that $\eta H_n = 32.5$. The quantity of water per second passing through the impeller, which includes the short-circuited water, shall again be $Q' = 11.236$ cubic feet.

The suction pipe diameter shall also be the same as before, hence $D_e = 1.18$ feet; so that the clear cross-sectional area of the suction pipe is $F_e' = 1.009$ square feet and the velocity in the pipe will be $w_r' = 11.13$ feet per second. In order at first not to complicate the channel sections too greatly the outer impeller angle will be assumed as $\beta_a = 90°$.

The outer impeller diameter shall now be $D_a^a = 1.64$ feet and the impeller width $b_a = 0.223$ foot.

The peripheral velocity is easily determined because $\beta_a = 90°$, and therefore equation 59 can be used,

$$u_a = \sqrt{\eta g H_n} = 32.4 \text{ feet.}$$

The number of impeller blades is $z = 10$, hence the pitch at the outer diameter is $t_a = 0.515$ foot.

By assuming the blade thickness as $s = 0.0164$ foot the channel height will be $a_a = 0.4986$ foot.

The thickness of the blades decreases the entrance area to

$$F_a = 1.11 \text{ square feet,}$$

and the radial exit velocity through this area is

$$v_r = v_a = 10.14 \text{ feet per second.}$$

The exit velocity diagram can now be drawn (see Plate VI) and the following values determined graphically or analytically:

$$w_a = 33.9 \text{ feet per second} \quad \text{and} \quad \delta_a = 17° 25'.$$

The inner boundary of the impeller profile is now drawn tentatively and an entrance arc drawn which will be as nearly at right angles to the section lines as possible. This entrance arc is taken, if at all possible, as an arc of a circle, because it is easier to determine its center of gravity and therefore its mean inner diameter D_e. Often a parabolic curve is used. The mean diameter of the assumed entrance arc is determined by any of the various methods used in finding the center of gravity of an arc and taking twice the perpendicular distance between this point and the pump axis. Then the area which would be swept through by rotating this assumed entrance arc is found by solving the term $D_e \pi b_e$. If the area thus found is greater or less than the desired area F_e', the entrance arc is either shortened or lengthened until the rotation area equals F_e'. In shortening or lengthening b_e the inner part of the impeller profile is changed.

In Plate VI the entrance arc so found is shown by a heavy dashed and dotted line and b_e was found to be 0.37 foot. The position of the center of gravity of the entrance arc referred to the axis of the pump was found graphically and the impeller diameter D_e determined; it was found to be

$$D_e = 0.866 \text{ foot.}$$

Then

$$D_e \pi b_e = 1.007 \text{ square feet} \cong F_e'.$$

The impeller was divided into four partial impellers. The three points along the entrance arc were determined by the method already described and the section lines were drawn through these points. The diameters for the points a, b, c, d, e on the entrance arc were determined and the corresponding peripheral velocities and pitch were calculated and placed in a table. It is strongly recommended that the values found be immediately placed in such a table on the drawing of the blades so that they are available for a later check.

On Plate VI the entrance velocity diagrams for points a to e are drawn. The values for the absolute entrance velocities w_e and entrance heights a_e are also added to the table. The beginnings of the blades and also their ends, provided $\beta_a > 90°$, are drawn as involutes.

The involutes at the beginning of a blade, that is, at entrance to the impeller, are now drawn upon the surface of a cone whose apex lies at the intersection of the prolonged section lines with the axis of the impeller. From the table on Plate VI it can be seen that the channel heights a_e vary at each of the points on the entrance arc, so that the diameter of the base circle for each point must first be determined from equation 160.

If the involutes are drawn upon the surfaces of the cones the radii of the base circle and the describing circle increase according to the ratio $\frac{fb}{gh}$ (see Fig. 78). To represent the involutes upon the surface of a cone, the cone is developed and upon this developed surface involutes are drawn. Fig. 78 shows the involutes for point b.

For point e the section line runs parallel to the shaft axis, and the beginning of the vanes must be drawn upon the developed surface of the cylinder, upon which the blades are represented as straight lines.

The beginning and end of the involute are now transferred to the section lines by again considering them wrapped about the cone. The points so found are connected by smooth lines. It is best, as before, to sharpen the blades at entrance for a distance of about $\frac{3}{8}$ to $\frac{5}{8}$ inch, and in order to insure proper water guidance the involutes

are lengthened about $\frac{7}{16}$ of an inch. These points also are marked upon the section lines. A curve through the points of the blades then gives the lower limit of the blades in the plan view.

The entrance arc b_e, which represents the line connecting the middle points of the channel heights, is now assumed to lie in a plane parallel to the impeller axis, so that its horizontal projection is represented as a straight line which, if possible, is taken radial. These radial lines, which represent the entrance arc in the plan view, are shown in Plate VI by heavy dashed lines.

The involutes can now be drawn in the plan view by projecting sufficient points from the elevation. The points taken on the section lines have been chosen for this purpose. In Fig. 78 the construction of the involute for the section line *bb* is shown in detail.

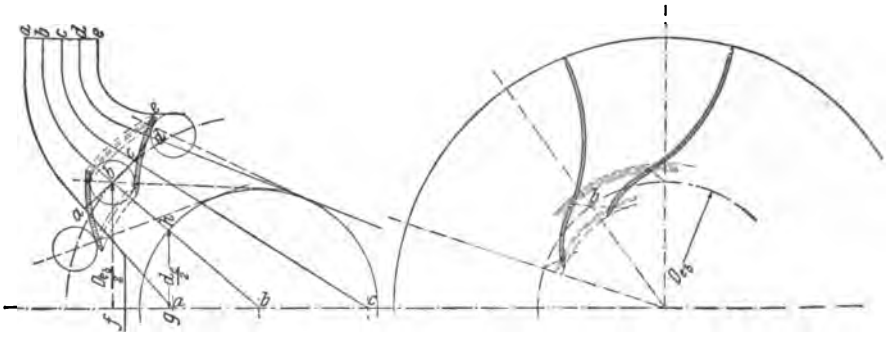

Fig. 78.

For the present example the diameters of the base circles for the involutes for every point upon the entrance arc are found from equation 160 and their values are placed in the table on Plate VI. The diameters of the base circles for the involutes to be drawn upon the surface of a cone are determined graphically. The involutes are drawn according to the method just given and are then transferred to the plan view. The curves which connect the points of the involute for each section line are drawn dashed in the elevation on Plate VI.

The further course of the section lines in the plan view is now assumed according to good judgment and it is best to begin with section line *aa*. This, as well as the other section lines, must turn radial towards its end, because $\beta_e = 90°$ and the connecting curve between the entrance involute and the radial exit line is best drawn

by an arc of a circle of as large a radius as possible. In order to see more clearly the form of the channel three such section lines are drawn in the plan view.

To connect the beginning of the blade with the radial end of the blade for point e, a sloping position of the blade exit height b_a is usually chosen, which was done in the present blade form. This sloping position of b_a, now common with water turbines, has an advantage over a straight position because the blade shock at exit of the water from the impeller does not occur at the same moment across the entire channel width.

The other section lines were drawn in the plan view in the same manner as the section line aa, and care must be taken that they show a smooth course from one to the other. In Plate VI the section lines are drawn in full lines. Viewing two successive blades in the plan view the form of the channel can be recognized to some degree.

For the further determination of the developed surface of the blade so-called axial and horizontal sections are taken. The latter are also called pattern maker's sections, because the pattern maker uses the horizontal sections shown in the plan view for making the block upon which the blade is shaped.

In order to see if the section lines which were partly arbitrarily taken in the plan view have a correct course, and also to obtain accurate points of intersection of the horizontal cross sections with curves upon the surface of the blade, axial sections are used. These sections are straight lines in the plan view. It is best in the present example to take these axial sections as radial lines in the plan view in order that the axial sections may show in the elevation a course similar to the entrance arc.

These axial sections can be located in the elevation by bringing them to intersect the section lines in the plan view and by transferring the points of intersection to the elevation. The points so found in the elevation are connected by smooth lines.

It may happen that the axial sections do not show a regular contour in the elevation, which is accounted for by the fact that the section lines were not correctly assumed in the plan view. The course of the section lines would then have to be changed so that the axial sections in the elevation may have a regular contour, but always keeping in view that the section lines in the plan view must also have a regular contour.

After drawing the axial cross sections the template for the blades can be made from the various sections. To produce this blade surface the horizontal sections or pattern maker's sections are used. These sections are placed in the elevation at certain distances through the impeller at right angles to the axis and then their intersections with the blade surfaces are shown as curves in the plan view. It is advisable to take these sections through the points *a*, *b*, *c*, *d*, *e* at exit because one point of the horizontal section in the plan view is immediately determined. The other sections are spaced about $\frac{3}{8}$ to $\frac{5}{8}$ inch apart, depending upon the size of the impeller. The horizontal sections in the plan view are determined by transferring the intersections of the section lines and the radial lines from the elevation into the plan view. If the radial lines and the section lines have been favorably chosen, the horizontal sections in the plan view will show a smooth and regular contour.

On Plate VI the horizontal sections are shown in the plan and elevation, numbered consecutively 1, 2, 3, etc. The curves in the plan view have a very regular contour. It will be noted that the points of intersection of the horizontal sections with the section line *ee* cannot be determined from the elevation. To determine these points of intersection horizontal sections are drawn through the blade ends upon the development of the cylinder with the same spacing as in the elevation, whereupon the intersecting points on the end of the blade can be transferred to the plan view.

The developed surface of the blades is determined from the horizontal sections shown in the plan view and by representing this blade surface upon a so-called blade form. To make this blade form, boards are taken of a thickness exactly equal to the distance between the horizontal sections. Upon these boards the curves of the horizontal sections are drawn and the boards are cut to these curves. These boards are then nailed together in their proper order and the projecting edges removed by a draw shave, thus giving upon this wooden block a surface equivalent to the developed surface of the blade. In order to determine the exact positions of the boards, one to the other, it is best to give them the form shown on Plate VI. They will all then have a common right angle. If then the boards are placed consecutively with the sides of this right angle exactly in line, then the horizontal sections are exactly in the same position as given on the drawing. In assembling these boards

care must be exercised to note the direction of rotation of the impeller, because it is very easy to make a mistake and produce a blade for an impeller having opposite direction of rotation.

In making this blade form it is best to use the concave side of the blade surface, because a concave shape is easier to make.

The actual sheet-metal blade must have from $\frac{3}{8}$ to $\frac{5}{8}$ inch more metal added for extension into the impeller casting. This extension of the blade is best provided for when the blade sections are determined. The blade profile in the elevation is simply increased by this amount and this new boundary of blade is taken as a section line and transferred to the plan view. The ensuing limits of the actual blade are shown dotted on Plate VI. Another method of construction would be to make the wooden blade form without the additional part necessary on the blade so that it can be cast in, and then to add later this extra allowance upon the form.

Upon this wooden blade form no attention is paid to the sharpening of the blade ends, because this is difficult to take care of, and the developed surface of the blade is produced under the assumption of a constant thickness of blade material.

The curve through the ends of the blades, shown in the elevation by an extra heavy line, is of great importance in the foundry. A core is made of sand and clay whose outline could be swept by this curve turning about the impeller axis. Upon this core the separate blades are set at their proper pitch. The spaces between blades, which form the channels, are filled with sand covered by a coating of clay, thus producing the inner core of the impeller for the foundry.

After the wooden blade form is finished in the pattern shop an iron casting is made from it. By using a paper pattern the blade surface when developed on a plan can be determined. The metal for the blades is cut to this paper pattern. Before this metal is given its proper shape upon the metal form it is sharpened at the proper ends and sufficient dovetails are cut on the other ends so that when the blades are cast in they will be more firmly held by the impeller sides. The blade material is heated red hot and then bent upon the blade form to its proper shape. For very large blades a plaster of Paris casting is taken of the form and from it an upper form cast. The blade is then pressed between these two forms by hydraulic pressure.

For the example given there still remains the determination of the dimensions of the guide vanes.

The diameter of the base circle for the involute is $d_i = 0.49$ foot.

Assuming the number of blades $z_i = 9$ and a thickness of blade $s_i = 0.0164$ foot, the channel height was found to be $a_i = 0.155$ foot.

As low-pressure centrifugal pumps would hardly be constructed with an impeller angle $\beta_a{}^a = 90°$, the determination of the constants and the further investigation of the pump would be of no interest and will therefore be omitted.

EXAMPLE V. See Plate VII. Let us now consider the calculation and blade design of a high-speed pump having $\beta_a > 90°$ for whose regulation adjustable guide vanes are to be provided. The pump shall be designed for the same conditions as in examples III and IV, that is, $Q = 636$ cubic feet per minute, $H_n = 26$ feet, $\eta H_n = 32.5$ feet. The dimensions at entrance shall be the same as in example IV, $D_e = 1.18$ feet, $F_e' = 1.009$ square foot, $w_r = 11.13$ feet per second. The entrance arc shall be the same as before, and the diameter at its center of gravity is

$$D_e = 0.866 \text{ foot.}$$

The impeller angle at the outer diameter shall now be $\beta_a{}^a = 155°$.

The diameter of the base circle for the exit involutes is $d_a = 0.693$ foot.

By assuming the number of blades $z = 10$ and the thickness of the blades $s = 0.0164$ foot, the exit height $a_a = 0.201$ foot.

Graphically and analytically the outer impeller diameter upon which the calculations are based was found to be

$$D_a = 1.46 \text{ feet,}$$

and the impeller angle at this diameter

$$\beta_a = 151° 35'.$$

The impeller width shall again be taken as in example IV as $b_a = 0.223$ foot, and let $\delta_e = 90°$.

The radial exit velocity at diameter $D_a = 1.46$ feet can be found from equations 157 and 158. This takes into account the decreased exit area due to the thickness of the blades. This radial exit velocity is

$$v_r = 11.88 \text{ feet per second.}$$

The clear exit area at diameter D_a is $F_a = 0.946$ square foot.

The peripheral velocity can now be found from equation 58, because v_r and β_a are known.

$$u_a = -\frac{v_r}{2\tan\beta_a} + \sqrt{\left(\frac{v_r}{2\tan\beta_a}\right)^2 + \eta g H_n} = 45.13 \text{ feet per second.}$$

The number of revolutions per minute is $n = 590$.

From equation $u_a = \kappa\sqrt{\eta g H_n}$ we find

$$\kappa = 1.39.$$

From the κ curves (see Plate I) the angle δ_a is found corresponding to $\kappa = 1.39$ and $\beta_a = 151° 35'$. The value found is

$$\delta_a = 27°.$$

In order to draw the exit velocity diagram we determine the value $\frac{\sqrt{\eta g H_n}}{\kappa} = 23.3$ feet. Graphically or analytically

$$w_a = 26.2 \text{ feet per second} \quad \text{and} \quad v_a = 24.9 \text{ feet per second.}$$

The values found for impeller entrance for points a, b, c, d, e are again arranged in a table on Plate VII, and after drawing the entrance velocity diagrams for each of these points the channel heights are determined graphically.

After drawing the section lines the involutes are drawn upon the surface of the cone, and then the various points are transferred upon the assumed section lines. From this the involutes can be drawn in the plan view. The entrance arc could not be taken as radial on the plan view, but had to be taken tangent to a circle whose diameter was $d = 0.148$ foot. If the entrance arc had been taken as a radial line in the plan view it would not have been possible to connect the blade end at point e with the exit involute. It must be remembered that in the elevation the perpendicular distance of the point e at entrance to the horizontal section passing through the point e at exit determines whether a proper connection of these points is possible. Both points can be only a certain distance from one another in the plan view in order to obtain a possible connection between the beginning and end of the blade. There are various ways in which to find just when such a connection is or is not possible. Perhaps the best way would be to take a section

through the plan view as nearly parallel as possible to the section line *ee* and to project into a special elevation the actual view of the beginnings and ends of the blades as they would appear upon a rotating body formed by the section line *ee* in the elevation.

After the involutes for impeller entrance and exit have been drawn in the plan view the section lines are assumed in this view.

In order that the radial sections in the elevation may show a course similar to the entrance arc they are drawn in the plan view not radial but tangent to the circle to which the b_e line was assumed to be tangent. The axial sections are then again transferred to the elevation, and if they do not have a regular contour the section lines in the plan view must be changed accordingly. Considering the previous discussion, the horizontal sections are placed in the elevation and the curves of intersection with the surface of the blade are determined in the plan view. For producing the blade form the concave blade surface is again used. Care must be taken that the sections are chosen through the correct blade surface. In order not to complicate the plan view on Plate VII only the shape of one of the boards of the wooden blade form is there given.

Guide Vanes. The guide vanes are to be made adjustable. As before, the diameter of the base circle of the involute is found for the normal quantity of water. For this quantity $d_l = 0.66$ foot.

Assuming 12 guide vanes and the thickness of vane $s_l = 0.0164$ foot, the entrance height is determined as $a_l = 0.157$ foot.

The entrance involutes are drawn as before. Plate VII shows the further construction of the guide vanes. Special care should be taken that the channel height a_l increases very gradually, which should also be the case for any other position of the vanes. In order to determine the limiting position of the vanes three vanes are cut out of paper, which can then be turned until all three vanes become tangent to a common circle.

In determining the diameter of the bolt or pin about which the guide vane rotates the limiting position of the vane must be taken into account. When the guide vanes are closed the entire pressure head plus suction head is exerted upon the surface of the vanes. If t is the pitch in feet of the vanes in their limiting or end position, and b_a the width of the vanes in feet, then the load in pounds on each vane due to the pressure head of the water will be

$$P = 62.48\, b_a t H_n \text{ pounds.}$$

The bolt or pin will be loaded with a weight P, which must be taken into account when calculating its dimensions.

The characteristic K will have the same value as in examples III and IV, that is, $K = 111.5$.

$K_{max.}$ and $K_{min.}$ will also have the same values as in examples III and IV. In order to determine the constant A the clear entrance area F_e is necessary. The clear entrance area takes into account the thickness of the blades, which decreases the area at entrance a certain per cent. But this ratio of decrease varies along the entrance arc b_e, and it is usual to determine approximately the clear exit area by finding the velocity w_e at the mean diameter d_e.

In this example $w_e = 13.2$ feet per second, from which $F_e = 0.852$ square foot.

The following constants can now be found:

$$A = -4.68, \qquad B = 265.$$

The number of revolutions referred to $\eta H_n = 10$ is $n = 328$.

The pump can now be classified as

$$\text{Low-pressure pump, } D_a = 1.64.$$

$$K = 111.5, \qquad n = 328.$$

$$K_{max.} = 136.5, \qquad K_{min.} = 80.6.$$

$$F_e = 0.852, \quad A = -4.68, \quad B = 265.$$

In order to see the effect on the pressure head of throttling the discharge the constants C_1 and C_2 are determined for equation 225. Solving for these constants we get

$$C_1 = 41.1, \qquad C_2 = -0.731.$$

After substituting the above constants in equation 225 we have

$$\eta H_n = C_1 + v_r C_2 = 41.1 - 0.731\, v_r.$$

For $v_r = 11.88$ the value of ηH_n is 32.42 feet, which checks closely with the assumed value $\eta H_n = 32.5$ feet.

Comparing the value of the constants with those for example III, in which the outer diameter $D_a'' = 2.458$ feet, there will be found a similar relation of the heads under throttling conditions, in spite of the decrease of outer impeller diameter. In the last example the

constant C_1 has even a larger value than in example III, and therefore the outer diameter in the last example could be somewhat reduced. It can therefore be said that the pumps calculated in examples III and V are approximately of equal performance. But the fact must be emphasized that the last pump is much lighter and cheaper to produce on account of its smaller outer diameter. The weights of the completed pumps of examples III and V are to each other as about 5 to 3. Another point worthy of consideration is that the last pump operates at 590 revolutions per minute, while the other pump operates at only 380 revolutions per minute.

The adjustable guide vanes of example V permit a decrease of the quantity of water over very wide limits and still give a high efficiency.

33. Pressure Distribution in a Centrifugal Pump in which Entrance to the Impeller is not Parallel to the Shaft.

In order to decrease the mean inner impeller diameter to a minimum it is necessary to place the line of entrance within the elbow of the impeller. By doing this there will be different peripheral velocities at each point of the entrance line and therefore different entrance velocity diagrams. The constants C_1 and C_2 of equation 225 were determined in example V for a so-called mean diameter which was assumed to be at the center of gravity of the entrance arc. These constants are correct only for a thread of water passing through this center of gravity, while for any other point of the entrance arc there would be different values for the constants C_1 and C_2. Assuming that the impeller and guide vanes are divided into a number of equal partial impellers and guide vanes, there would result a number of partial pumps, and each of these would influence the head differently if their discharge were throttled, as will be explained in the following.

Assume a pump divided into a number of equal partial pumps. Equation 10 must in general be true for each of these partial pumps, only the separate velocities would have different values. The equation reads

$$u_a^2 - u_e^2 + v_e^2 - v_a^2 + w_a^2 - w_e^2 = 2\eta g H_n \quad . \quad . \quad . \quad (10)$$

Let all cross sections of the pump be determined. Let f_e, f_a, f_l be the cross sections of a partial pump in which the velocities v_e, v_a, w_a occur (the blade thickness is assumed infinitely small so that $w_a = w_l$).

The condition equation can now be written, if q represents the quantity of water passing through a partial pump,

$$q = v_e f_e = v_a f_a = w_a f_l \quad \ldots\ldots\ 233$$

hence

$$v_e = \frac{w_a f_l}{f_e} \quad \text{and} \quad v_a = \frac{w_a f_l}{f_a} \quad \ldots\ldots\ 234$$

Further, according to equation 13

$$w_e^2 = u_e^2 + v_e - 2 u_e v_e \cos \beta_e \quad \ldots\ldots\ (13)$$

Substituting these values of v_e, v_a, and w_e in equation 10, and letting $u_e = u_a \frac{D_e}{D_a}$, the absolute exit velocity is found to be

$$w_a = \frac{u_a \frac{D_e}{D_a} \frac{f_l}{f_e} \frac{1}{\cos \beta_e}}{1 - \left(\frac{f_l}{f_a}\right)^2} + \sqrt{u_a^2 \left[\frac{\frac{D_e}{D_a} \frac{f_l}{f_e} \frac{1}{\cos \beta_e}}{1 - \left(\frac{f_l}{f_a}\right)^2}\right]^2 + \frac{2 \eta g H_n - u_a^2 \left[1 - 2\left(\frac{D_e}{D_a}\right)^2\right]}{1 - \left(\frac{f_l}{f_a}\right)^2}} \quad \ldots\ 235$$

In this equation ηH_n is still unknown. Its value depends, according to equation 225, upon the ratio $\frac{D_e}{D_a}$, which has a different value for each partial pump.

Let F_{a_e} be the exit area of a partial pump so that

$$v_r F_{a_e} = w_a f_l$$

or

$$v_r = \frac{w_a f_l}{F_{a_e}} \quad \ldots\ldots\ 236$$

Substituting the above in equation 225 we get

$$\eta g H_n = u_a^2 \left[1 - \left(\frac{D_e}{D_a}\right)^2\right] + \frac{w_a f_l}{F_{a_e}} \left(\frac{u_a}{\tan \beta_a} + \frac{u_a}{\tan \beta_e} \cdot \frac{D_e}{D_a} \frac{F_{a_e}}{F_{e_e}}\right). \quad 237$$

In this equation F_{e_e} is the entrance area of a partial pump. Substituting this value of $\eta g H_n$ in equation 235 we get

$$w_a = -\frac{f_l u_a \frac{1}{F_{a_e} \tan \beta_a}}{1 - \left(\frac{f_l}{f_a}\right)^2} + \sqrt{f_l^2 \left[\frac{\frac{u_a}{F_{a_e} \tan \beta_a}}{1 - \left(\frac{f_l}{f_a}\right)^2}\right]^2 + \frac{u_a^2}{1 - \left(\frac{f_l}{f_a}\right)^2}} \quad . \quad 238$$

The values upon the right-hand side of this equation are equally large for each partial pump, therefore the velocity w_a and the quantity of water delivered are the same for each partial pump. On the other hand, the pressure heads will vary according to equation 237. As the velocity for each partial pump is the same, that is, it is equally large over the entire exit width, there will be unequal pressure heads only while the water is passing through the impeller. But according to the fundamental laws of hydraulics it is hardly possible for varying pressures to occur at exit from the impeller when the velocity v_a is constant. Therefore a pressure equalization must take place in the impeller which will not permit of a further investigation.

It might be well to state that the conditions existing in water turbines are just the reverse of those existing in centrifugal pumps. With the former a certain pressure head is given. For determining the absolute entrance velocity (corresponding to the absolute exit velocity of a pump) equation 235 can be used, from which it can be directly seen that the velocity w_a and therefore the quantity of water varies for each single partial pump. Hence the single partial impellers of water turbines under constant pressure head work with varying quantities of water, while centrifugal pumps deliver equal quantities of water under varying pressure heads.

For the normal quantity of water and head for which δ_e was assumed to be 90° this phenomenon does not occur, because for this special case the values of the velocities at entrance do not influence the pressure head, as can be seen from equation 225 when $\delta_e = 90°$. It then takes the form

$$\eta g H_n = u_a^2 + \frac{v_r u_a}{\tan \beta_a} \quad . \quad . \quad . \quad . \quad . \quad 239$$

V. DESIGN OF IMPORTANT PUMP PARTS.

34. Bearings.

The bearings for centrifugal pumps do not usually give the designer much difficulty, because in designs calling for high speed the rotating parts are generally light and when the design calls for heavy rotating parts the speed is usually low. When the rubbing speeds at the journal can be kept under 70 feet per second and the pressures per square inch of projected bearing area less than 50 pounds per square inch, no difficulty in designing the bearings need be experienced. In steam turbine design rubbing speeds in extreme cases have reached 110 feet per second, while the bearing pressure was 60 pounds per square inch of projected area; and bearing pressures have been used as high as 100 pounds per square inch, while the rubbing speed was 85 feet per second. These extreme cases present great difficulty to the designer because the bearings must be carefully designed and provided with water cooling and lubricated with a liberal supply of oil under pressure so as to keep the bearing temperatures below 200° F. Lasche found that when the temperature of the oil reached 250° F. its lubricating properties suddenly decreased.

Centrifugal pump bearings should always be provided with oil-ring lubrication, and when the friction work between the rotating shaft and its film of oil and between this film of oil and the bearing lining becomes so large that the bearing cannot dissipate this work at a reasonable temperature, forced lubrication should be used.

Let

l = length of bearing in inches,

d = diameter of bearing in inches.

p = bearing pressure in pounds per square inch of projected area $= \frac{\text{bearing load}}{ld}$,

v = rubbing speed in feet per second.

Then the total heat generated per hour by bearing friction, expressed in B.t.u., is

$$Q = \frac{1}{778} ld\,\mu\,pv\,3600 \quad . \quad . \quad . \quad . \quad . \quad . \quad 240$$

in which μ is a coefficient of friction. The value of this coefficient was found by Lasche and Stribeck to depend upon the pressure p and the temperature t of the bearing, provided p remains within the limits of 15 and 200 pounds per square inch and the temperature t between the limits of 80° F. and 212° F. If such is the case the following simple formula holds good:

$$\mu p\,(t - 32) = \text{constant} = 51.2 \quad . \quad . \quad . \quad . \quad 241$$

The heat radiated per hour from a bearing can be expressed in B.t.u. as

$$Q_r = \frac{1}{778} k\,\mu\,dl\,(t - t_o) \quad . \quad . \quad . \quad . \quad . \quad . \quad 242$$

in which t_o is the temperature of the surrounding air and k is a coefficient depending somewhat upon the design of the bearing. If the bearing casting is thin and presents a large radiating surface, k can be taken as high as 150, but if the radiating surface is confined and the air circulation poor k must be taken as low as 50.

When no artificial cooling of the bearing is provided, Q must equal Q_r, and the final temperature of the bearing t can be calculated from equations 240 and 242. If the final temperature is excessive, either the oil or the bearing must be water-cooled. Let Q_o be the heat in B.t.u. per hour imparted to the cooling water either by the oil or by the bearing. Then

$$Q = Q_r + Q_o \quad . \quad . \quad . \quad . \quad . \quad . \quad . \quad . \quad 243$$

The weight of oil necessary per hour is

$$W = \frac{Q_o}{\text{Specific heat of the oil } (t_2 - t_1)} \quad . \quad . \quad 244$$

in which

t_1 = the temperature of the oil entering the bearing in degrees F,
t_2 = the temperature of the oil leaving the bearing in degrees F.

In calculating the weight of water necessary for cooling the bearing or the oil, a very liberal allowance must be made on account of the inefficiency of this method. In most calculations the temperatures are first assumed, and the temperature t_2 of the oil leaving the bearing must of course be taken much lower than the tempera-

ture t of the bearing, so as to be sure that the oil will at least reach the temperature t_2 before it leaves the bearing.

When the bearing is to be cooled by water circulation, the water can either be introduced into a cored space in the lining and pedestal or can be forced through a coil of pipes embedded in the lining. In most cases babbitted linings are used and the cooling water pipes can be arranged within the babbitt. For high-speed work it is

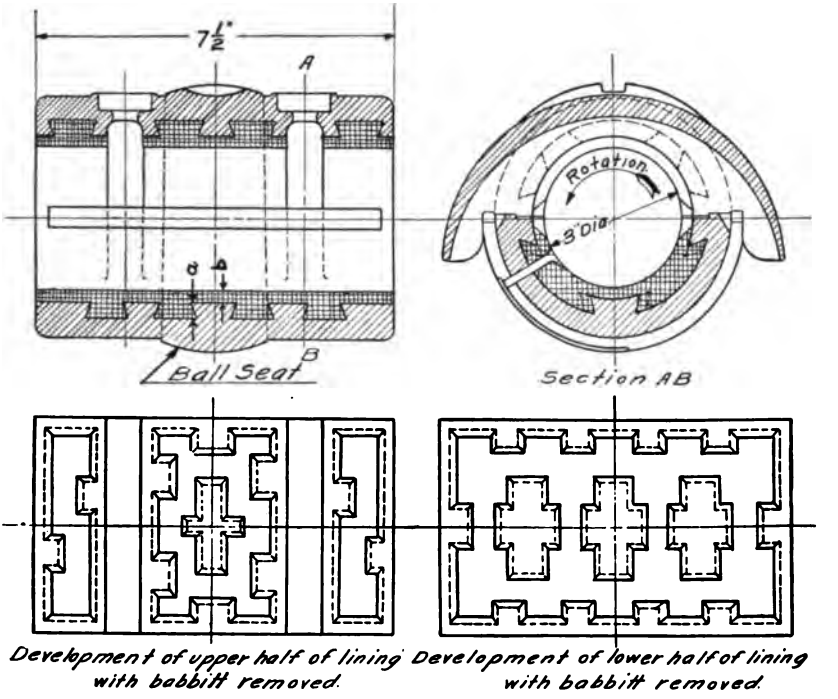

Fig. 79.

best to use ball-seated linings which automatically adjust themselves with the deflection of the shaft or assist the shaft in securing a correct line-up. It is very important, especially in high-speed work, to design the bearing so that the babbitt will not become loose after being in service for some time. The lining shell is usually provided with dovetailed recesses for holding the babbitt, as shown in Fig. 79. These recesses should be made deep enough, a good rule being to have the depth of the recess a somewhat greater than the minimum thickness of the babbitt b. Fig. 79 shows a develop-

ment of the upper and lower halves of the lining without the babbitt, and gives the correct way of arranging the dovetailed recesses, the fundamental idea being that all the recesses of the lining are intimately connected by a "deep way connection."

35. Packings.

The efficiency of centrifugal pumps depends partly upon the proper design of the stuffing boxes and packings. The packing on the suction end of the pump must usually prevent air from leaking into the

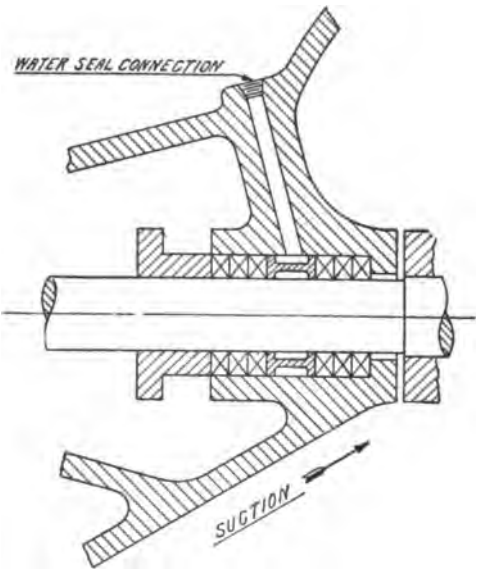

Fig. 80.

pump, and the packing on the high-pressure end must prevent water from leaking out of the pump. The packing in both cases must be tight enough to prevent such leakages and still not create excessive friction losses by binding the shaft.

To prevent air from entering the pump on the suction side a water seal is generally used of a design somewhat similar to that shown in Fig. 80. The packing consists of two distinct lengths with a spacer or lantern between. The object of the latter is to keep the packing away from the opening through which water under pressure is introduced. Any leakage of the inner length of packing permits this water to flow into the pump. The supply of water being ample, no

air can enter the pump and destroy its vacuum. The outer length of packing is used simply to pack against this water under pressure. When cold water is pumped the packing is usually made of hemp, and when hot water is to be handled graphite flax packing is used. Sometimes this soft packing is replaced by leather cupped packing rings, and although these are satisfactory when properly installed, they can and often do give a great deal of trouble.

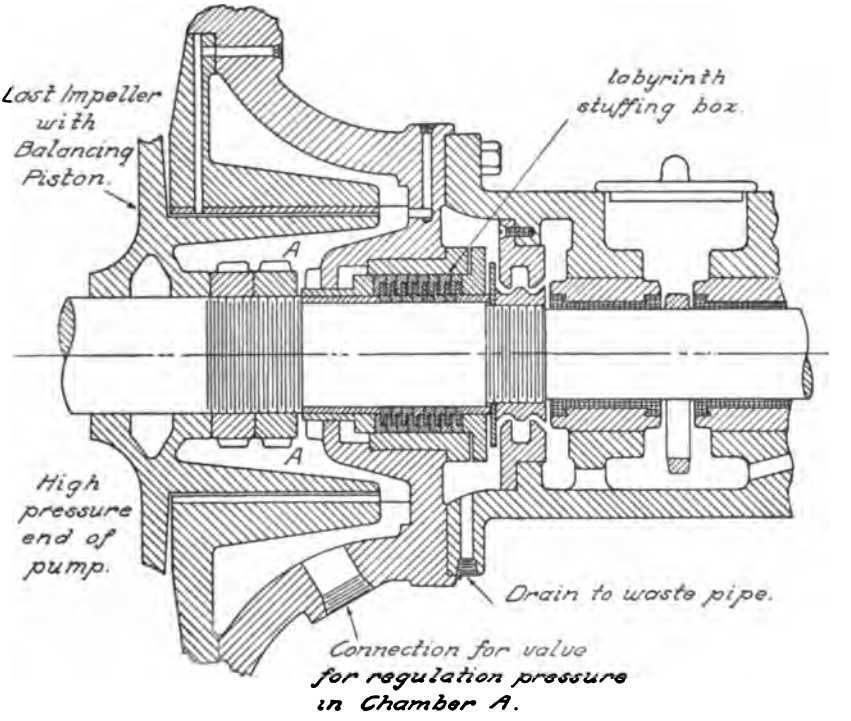
Last Impeller with Balancing Piston.
labyrinth stuffing box.
A
A
High pressure end of pump.
Drain to waste pipe.
Connection for valve for regulation pressure in Chamber A.

Fig. 81.

The stuffing box on the high-pressure end requires still greater care in design. It is always better to have this high-pressure stuffing box rather long, because the packing need not then be set up so tightly. For very high pressures and sometimes even for moderate pressures this packing is also made in two lengths with a spacer or lantern between. All the leakage past the inner section of packing can be drained from the space around the lantern either into the suction end of the pump or into a waste pipe. Fig. 81 shows a stuffing box design which presents a tortuous passage to the escaping water.

Any water which escapes through these close clearances is taken by the drain into the waste pipe.

In multi-stage centrifugal pumps a packing must be used between stages to prevent water leakage. In most cases a long close clearance

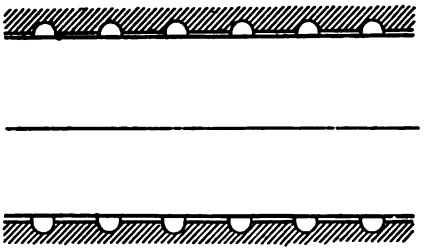

Fig. 82.

fit between the shaft or sleeve and the casing is employed. This design can be seen in the cross-sectional view shown in Fig. 82. Some designers use a labyrinth packing similar to Fig. 83, which has given

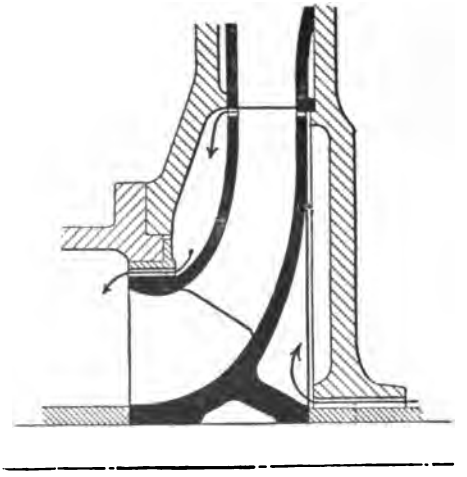

Fig. 83.

excellent results with steam turbines but is useless in centrifugal pumps. The effectiveness of this labyrinth packing is based on the expansion of steam in the enlarged spaces. Incompressible fluids, on the contrary, give only dead water at these points, and the fluid

passes through the close clearance without any disturbance at the enlarged places.

Fig. 84 illustrates another method of preventing leakage between stages. It consists of a close-fitting ring *C* about the shaft or impeller hub and attached loosely to the diaphragm *B* or casing between stages by means of bolts which permit of some radial play. The ring is capable of adjusting itself to any position of the shaft, and is held

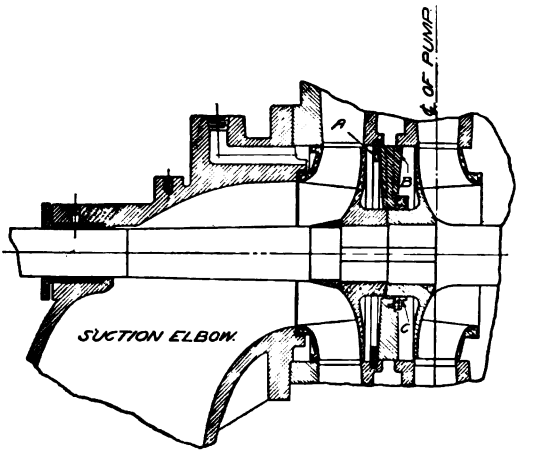

Fig. 84.

against the diaphragm or casing by the difference of water pressure in the two stages. Sometimes provision is made for oil or grease lubrication of this ring, as shown in the figure.

36. Impellers.

Almost all impellers for centrifugal pumps, whether of the single or double inlet type, are cast in one piece; that is, the hub and web are cast integral with the blades and outer side or shroud. In the case of very high speeds, castings cannot be used on account of the high stresses produced in the impeller. The designer must then use a forged steel hub and web with the blades either machined out of the solid forging or the blades made of sheet-steel plates and riveted to the web of the impeller. Sometimes a shroud ring is used and sometimes it is omitted; if used, the blades are riveted or cast to this ring.

In nearly all designs of impellers it is important to investigate

the stresses produced by centrifugal force. At any point within an impeller web both radial and tangential stresses exist. By radial stresses are meant stresses similar to those existing in a straight, thin rod under tension. Tangential stresses are stresses similar to those occurring around the circumference of a thin tube subjected to internal or bursting pressure.

The stresses produced by centrifugal force in a disk the thickness of which does not vary too rapidly, are determined when any two stresses both at the same radius or at different radii are known. The two stresses usually known are the radial stress at the bore of the hub and the radial stress at the periphery of the impeller. The radial stress at the bore of the hub is either nothing if the impeller has no forced fit on the shaft or is equal to the stress produced by the forced fit. If the impeller is loose upon the shaft the radial stress at the bore varies with the speed of the impeller, because as the speed increases the stretch at the bore also increases. The fit is usually made heavy enough so that the impeller will not be loose upon the shaft when running at its maximum speed. In calculating the stresses in an impeller the radial stress at the bore when the impeller is running at its maximum speed should be used. The radial stress at the periphery of an impeller is usually nothing, because no blades or material extend beyond the periphery of the disk.

It is difficult to take into account the stresses produced in an impeller web by the blades attached thereto because the centrifugal force of the blades is distributed along the sides of the impeller web and cannot properly be charged to any particular radius. It is possible to find these stresses exactly, but for practical work it is sufficient to proceed as follows. The maximum stress in the web or disk of the impeller is found as if no blades existed; then the average stresses of the disk with and without blades are found. The maximum stress previously found for the disk without blades is then corrected on the assumption that the maximum stresses in a disk with and without blades vary directly with the average stresses of a disk with and without blades. This assumption, although not correct, errs in the direction of safety, because the actual maximum stress is always slightly lower. A similar process is followed with regard to the stresses in the shroud rings. When the blades are riveted to the impeller disk the calculation of stresses remains the same, and the stresses in the rivets are easily computed.

The radial and tangential stresses produced by centrifugal force in a disk of given shape can be expressed as follows:

$$\frac{d\sigma_r}{dx} = \frac{\sigma_t - \sigma_r}{x} - \left(\frac{t'}{t}\sigma_r + ABx\right), \quad \ldots \quad 245$$

$$\frac{d\sigma_t}{dx} = -\frac{\sigma_t - \sigma_r}{x} - \nu\left(\frac{t'}{t}\sigma_r + ABx\right). \quad \ldots \quad 246$$

in which

σ_r is the radial stress at radius x, in pounds per square inch.

σ_t is the tangential stress at radius x, in pounds per square inch.

t is the thickness of disk at radius x, in inches.

$t' = \frac{dt}{dx}$; that is, if the thickness of disk decreases $\frac{3}{16}$ inch in a radial distance of $\frac{1}{8}$ inch, then

$$t' = -\frac{3}{16} \div \frac{1}{8} = -\frac{3}{2}.$$

$$A = 0.00002842\, N^2 \frac{S}{B},$$

$$B = \frac{E}{1 - \nu^2}.$$

N is the number of revolutions per minute.

S is the specific mass or density of the material of the disk (0.28 pound per cubic inch for steel).

E is the coefficient of elasticity (29 000 000 for steel).

ν is the ratio of lateral contraction to longitudinal elongation (0.3 for steel).

In using these formulas σ_r at the bore is known and σ_t at this point can be found in terms of some unknown constants and σ_r. Then at a short distance f om the bore, t' is found as previously explained. At this new value of x (distance from center of disk) $\frac{d\sigma_r}{dx}$ and $\frac{d\sigma_t}{dx}$, representing the change of the radial and tangential stresses per inch of radius, can be computed. This process is continued with larger or smaller values of dx until the periphery of the impeller is reached. Here σ_r is also known (usually equal to nothing). It is then possible to go back through all the formulas, solve for the unknown constants and find the actual values of σ_r and σ_t at the various radii assumed.

This method is very laborious, especially for disks of large radial dimensions and varying thicknesses, and should be resorted to only in extreme cases. Equations 245 and 246 are more easily handled if the profile of the disk section can be represented by one or more hyperbolas. The hyperbola can be expressed by the equation

$$t = cx^{\alpha} \quad . \quad . \quad . \quad . \quad . \quad . \quad . \quad . \quad 247$$

in which

t is the thickness of the disk at radius x,
c is a constant,
α is a constant either positive or negative; negative when the disk decreases in thickness outward.

The two constants c and α are dependent upon the form of the hyperbola. If this form is given, the values of t at any two radii x and x' are known, from which c and α can be solved by trial and error. When the disk is of uniform thickness $\alpha = 0$.

Equations 245 and 246 become integrable when $t = cx^{\alpha}$. As the disk decreases in thickness outwards α is negative, or $t = cx^{-\alpha}$. Integrating equations 245 and 246 with t expressed as above the following values are obtained:*

$$\sigma_r = \frac{E}{1-\nu^2}[(3+\nu)\,ax^2 + (\psi_1+\nu)\,b_1x^{\psi_1-1} + (\psi_2+\nu)\,b_2x^{\psi_2-1}] \quad . \quad 248$$

$$\sigma_t = \frac{E}{1-\nu^2}[(1+3\,\nu)\,ax^2 + (1+\psi_1\nu)\,b_1x^{\psi_1-1} + (1+\psi_2\nu)\,b_2x^{\psi_2-1}] \quad 249$$

in which

$$a = -\frac{A}{8+(3+\nu)\,\alpha} = \frac{-\,0.00002842\,N^2S\,(1-\nu^2)}{E\,[8+(3+\nu)\,\alpha]} \quad . \quad 250$$

$$\psi_1 = -\frac{\alpha}{2} + \sqrt{\frac{\alpha^2}{4} - \alpha\nu + 1} \quad . \quad . \quad . \quad . \quad . \quad . \quad 251$$

$$\psi_2 = -\frac{\alpha}{2} - \sqrt{\frac{\alpha^2}{4} - \alpha\nu + 1} \quad . \quad . \quad . \quad . \quad . \quad . \quad 252$$

b_1 and b_2 equal constants.

The constants b_1 and b_2 can be found when two given stresses in the section of the disk considered are known. These given stresses

* For the derivation of these formulas see author's translation of Stodola's "Steam Turbines."

may be both radial or both tangential or one of each. In disks with parallel sides and with narrow hubs the entire profile of the disk may be represented by a single hyperbola. In this case, as has been explained, the two given stresses are the radial stresses at the bore and at the periphery. In most cases, however, it will require from two to four hyperbolas to represent the impeller profile accurately. A formula based on equations 248 and 249 has been derived, for the case of four hyperbolas, to solve for the tangential stress at the bore (this being usually the maximum stress in the disk) when the radial stresses at the bore and periphery are given. This formula, however, is very cumbersome, and requires much greater accuracy of

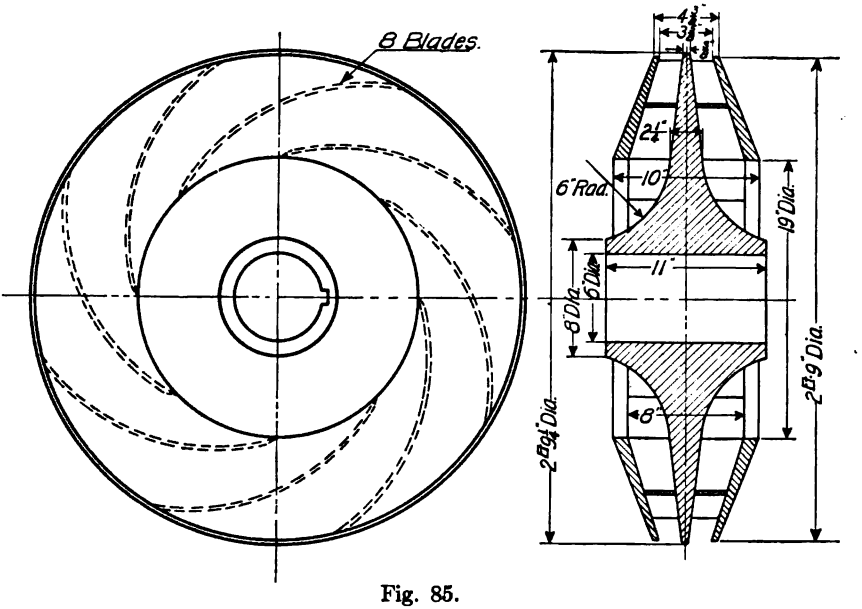

Fig. 85.

computation than that afforded by a slide rule. The process generally followed is therefore one similar to that previously described except that no small distances of x need be taken but only values at the beginning and end of each hyperbolic curve. In order to illustrate this method of calculating stresses in centrifugal pump impellers a typical example will be taken.

Fig. 85 represents a pump impeller designed for very high speeds. The maximum number of revolutions per minute is to be 4200. We shall first determine the distribution of radial and tangential stresses throughout the disk. In order to do this the profile of

the section of the impeller disk is divided into a number of hyperbolic curves. By trial and error we find that four hyperbolas will very closely approximate the impeller disk section. Fig. 86 shows

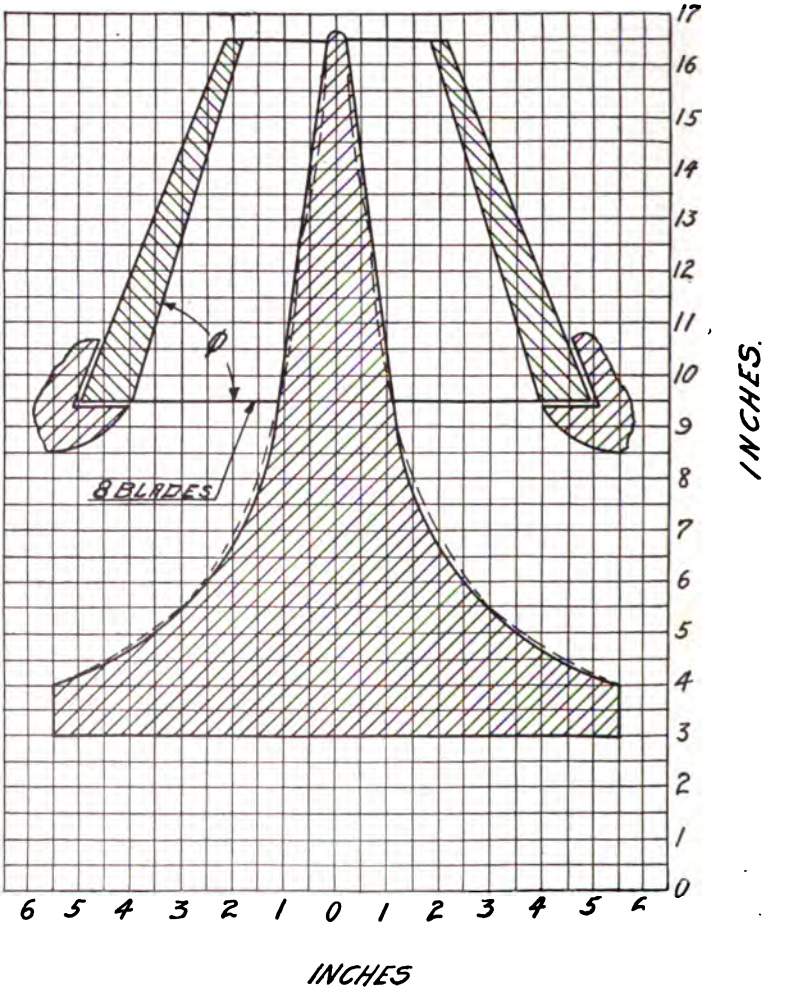

Fig. 86.

how closely the assumed and true sections agree. The latter are in full lines and the former in dotted lines. The first hyperbolic curve is from the bore ($x = 3$ inches) to $x = 4$ inches. This is a straight line and represents a disk of constant thickness. The second hyperbolic curve extends from $x = 4$ inches to $x = 8.7$ inches, the third

curve from $x = 8.7$ inches to $x = 13$ inches, and the fourth curve from $x = 13$ inches to $x = 16.5$ inches.

For the first curve the values of α and c of equation 247 are $\alpha = 0$ and $c = 11$, for the second curve $\alpha = -2$ and $c = 2.6125$, for the third curve $\alpha = -1.6$ and $c = 2.256$, and for the fourth curve $\alpha = -5.5$ and $c = 5.9457$. Taking various values of x, corresponding values of t can be found and all four hyperbolic curves plotted as in Fig. 86. Great care must be exercised in assuming enough curves so that they will agree very closely with the actual profile of the section calculated or else serious discrepancies will occur between the calculated and actual stresses of the impeller, as a very slight change of profile can produce large change of stresses.

By the aid of equations 248 to 252 inclusive, the radial and tangential stresses at any point of the impeller disk can be found. Starting with the radial stress at the bore of the impeller equal to nothing when the impeller is running at 4200 r.p.m., equation 248 equals nothing for $x = 3$ inches. The values of ψ_1 and ψ_2 in the equation are known because $\alpha = 0$ between $x = 3$ and $x = 4$. Inserting all known values in equation 248, it may be written

$$\sigma_{r_3} = 0 = -521.1 + 4142 \times 10^4 b_1 - 2479 \times 10^3 b_2 \quad . \quad 248a$$

and equation 249 may be written

$$\sigma_{t_3} = -300 + 4142 \times 10^4 b_1 + 2479 \times 10^3 b_2 \quad . \quad . \quad 249a$$

The subscript 3 to σ_r and σ_t in the above equations indicates the stresses at the point where $x = 3$ inches.

Solving for b_1 and b_2 from these equations we have

$$b_1 = 1207 \times 10^{-11} \sigma_{t_3} + 9885 \times 10^{-9} \quad . \quad . \quad . \quad 253a$$

$$b_2 = 2016 \times 10^{-10} \sigma_{t_3} - 4460 \times 10^{-8} \quad . \quad . \quad . \quad 254a$$

For $x = 4$ inches, σ_{r_4} and σ_{t_4} can be found by substituting the known values in equations 248 and 249 and the values of b_1 and b_2 just found, the latter remaining constant for all points within the same hyperbolic profile. Hence, substituting these values,

$$\sigma_{r_4} = 0.2185\, \sigma_{t_3} - 453.8 \quad . \quad . \quad . \quad . \quad . \quad 248b$$

and

$$\sigma_{t_4} = 0.7809\, \sigma_{t_3} - 185 \quad . \quad . \quad . \quad . \quad . \quad . \quad 249b$$

As the stresses at the end of the first hyperbolic section ($x = 4$ in.) must be the same as the stresses at the beginning of the second hyperbolic section ($x = 4$ in.) these two equations can be equated equal to each other and the values of the constants b_1 and b_2 of the second hyperbolic section be determined.

Using the values of equation 247 for the second hyperbolic section in equation 248, the latter can be written

$$\sigma_{r_4} = -5294 + 8680 \times 10^5 b_1 - 1065 \times 10^3 b_2 \quad . \quad . \quad 248c$$

and

$$\sigma_{t_4} = -3047.6 + 5315 \times 10^5 b_1 + 2782 \times 10^3 b_2 \quad . \quad 249c$$

Both of these values of radial and tangential stresses must equal corresponding values expressed in equations 248b and 249b, because they refer to stresses at the same point. Equating equation 248b equal to equation 248c and equation 249b equal to equation 249c determines the value of the new constants b_1 and b_2 for the second hyperbolic section. Hence, equating these equations and solving for b_1 and b_2 we get

$$b_1 = 4829 \times 10^{-13} \sigma_{t_3} + 5540 \times 10^{-9} \quad . \quad . \quad . \quad 253b$$

$$b_2 = 1885 \times 10^{-10} \sigma_{t_3} - 2987 \times 10^{-8} \quad . \quad . \quad . \quad 254b$$

For $x = 8.7$ inches, $\sigma_{r_{8.7}}$ and $\sigma_{t_{8.7}}$ can be found by substituting these new values of b_1 and b_2 in equations 248 and 249. Making these substitutions we get

$$\sigma_{r_{8.7}} = 1.4104\, \sigma_{t_3} - 8194 \quad . \quad . \quad . \quad . \quad . \quad 248d$$

$$\sigma_{t_{8.7}} = 1.0486\, \sigma_{t_3} - 4130 \quad . \quad . \quad . \quad . \quad . \quad 249d$$

Proceeding with the third hyperbolic section as with the second,

$$\sigma_{r_{8.7}} = -12\,890 + 1232 \times 10^6 b_1 - 3155 \times 10^2 b_2 \quad . \quad 248e$$

$$\sigma_{t_{8.7}} = -7421 + 8086 \times 10^5 b_1 + 7118 \times 10^2 b_2 \quad . \quad . \quad 249e$$

As these values of the radial and tangential stresses at the beginning of the third hyperbolic section must be equal to the values at the end of the second hyperbolic section (for $x = 8.7$ inches), equation 248d equals equation 248e and equation 249d equals equation 249e. Equating these equations the new values of the constants b_1 and b_2 for the third hyperbolic section can be found. Solving for these values we get

$$b_1 = 1178 \times 10^{-12} \sigma_{t_3} + 3870 \times 10^{-9} \quad . \quad . \quad . \quad 253c$$

$$b_2 = 1342 \times 10^{-10} \sigma_{t_3} + 2255 \times 10^{-7} \quad . \quad . \quad . \quad 254c$$

For $x = 13$ inches, $\sigma_{r_{13}}$ and $\sigma_{t_{13}}$ can be found by substituting these new values of b_1 and b_2 in equations 248 and 249. Solving after making these substitutions we have

$$\sigma_{r_{13}} = 2.3842\,\sigma_{t_3} - 20\,916 \quad . \quad . \quad . \quad . \quad . \quad 248f$$

$$\sigma_{t_{13}} = 1.6306\,\sigma_{t_3} - 11\,297 \quad . \quad . \quad . \quad . \quad . \quad 249f$$

Proceeding as before the values of $\sigma_{r_{13}}$ and $\sigma_{t_{13}}$ for the fourth hyperbolic section may be expressed as

$$\sigma_{r_{13}} = 7713 + 6426 \times 10^{10} b_1 + 1139 \times 10^2 b_2 \quad . \quad . \quad 248g$$

$$\sigma_{t_{13}} = 4440 + 2865 \times 10^{10} b_1 + 6774 \times 10^2 b_2 \quad . \quad . \quad 249g$$

As before, equation 248f equals equation 248g and equation 249f equals equation 249g. Solving these equations for the new values of the constants b_1 and b_2 for the fourth hyperbolic section we have

$$b_1 = 3848 \times 10^{-17}\,\sigma_{t_3} - 4528 \times 10^{-13} \quad . \quad . \quad . \quad 253d$$

$$b_2 = 7800 \times 10^{-10}\,\sigma_{t_3} - 4083 \times 10^{-6} \quad . \quad . \quad . \quad 254d$$

For $x = 16.5$ inches, $\sigma_{r_{16.5}}$ and $\sigma_{t_{16.5}}$ are found by substituting these new values of b_1 and b_2 in equations 248 and 249. Solving we get

$$\sigma_{r_{16.5}} = 7.979\,\sigma_{t_3} - 81\,878 \quad . \quad . \quad . \quad . \quad . \quad 248h$$

$$\sigma_{t_{16.5}} = 3.9584\,\sigma_{t_3} - 36\,996 \quad . \quad . \quad . \quad . \quad . \quad 249h$$

Since $\sigma_{r_{16.5}}$ is the radial stress at the periphery of the impeller and this stress is equal to nothing, the value for σ_{t_3} can be obtained by equating equation 248h equal to nothing. Hence

$$\sigma_{r_{16.5}} = 0 = 7.979\,\sigma_{t_3} - 81\,878,$$

or

$$\sigma_{t_3} = 10\,262 \text{ pounds per square inch} \quad . \quad . \quad . \quad 255$$

Having obtained the value of σ_{t_3}, the constants b_1 and b_2 for all hyperbolic sections can be found from equations 253a, b, c, and d, and 254a, b, c, and d.

For the first hyperbolic section

$$b_1 = 1338 \times 10^{-7} \quad . \quad . \quad . \quad . \quad . \quad . \quad 253e$$

$$b_2 = 2025 \times 10^{-6} \quad . \quad . \quad . \quad . \quad . \quad . \quad 254e$$

For the second hyperbolic section

$$b_1 = 1050 \times 10^{-8} \quad \ldots\ldots\ldots \quad 253f$$

$$b_2 = 1904 \times 10^{-6} \quad \ldots\ldots\ldots \quad 254f$$

For the third hyperbolic section

$$b_1 = 1596 \times 10^{-8} \quad \ldots\ldots\ldots \quad 253g$$

$$b_2 = 1602 \times 10^{-6} \quad \ldots\ldots\ldots \quad 254g$$

For the fourth hyperbolic section

$$b_1 = 5798 \times 10^{-14} \quad \ldots\ldots\ldots \quad 253h$$

$$b_2 = 3927 \times 10^{-6} \quad \ldots\ldots\ldots \quad 254h$$

Having the values of these constants, the stresses at the different radii of the impeller can now be obtained by substituting in equations 248 and 249 the values of b_1 and b_2 just found. Table I was computed in this manner and gives the radial and tangential stresses at various distances from the center of the impeller. These values are plotted in the form of a curve in Fig. 87.

TABLE I.

Distance from Center of Impeller, inches.	Radial Stress σ_r, lbs. per sq. in.	Tangential Stress σ_t, lbs. per sq. in.	Radial Elongation from Center of Impeller, inches.
3.0	0	10 262	0.001062
3.5	1 143	8 820	0.001024
4.0	1 788	7 830	0.001006
5.2	3 645	6 840	0.001031
6.8	5 288	6 579	0.001171
8.7	6 280	6 631	0.001425
10.2	5 929	6 444	0.001641
11.6	5 035	6 050	0.001814
13.0	3 549	5 435	0.001963
14.1	3 106	5 105	0.002030
15.3	1 987	4 534	0.002078
16.5	0	3 626	0.002072

The radial stretch or elongation of the impeller at any distance x from the center can be expressed by the formula

$$\xi = ax^3 + b_1 x^{\psi_1} + b_2 x^{\psi_2} \quad \ldots\ldots\ldots \quad 256$$

in which

$$a = \frac{-(1-\nu^2)\mu\omega^2}{E[8+(3+\nu)\alpha]} = \frac{-0.00002842\,N^2S(1-\nu^2)}{E[8+(3+\nu)\alpha]} \quad . \quad (250)$$

and ψ_1, ψ_2, b_1, b_2 are terms already defined.

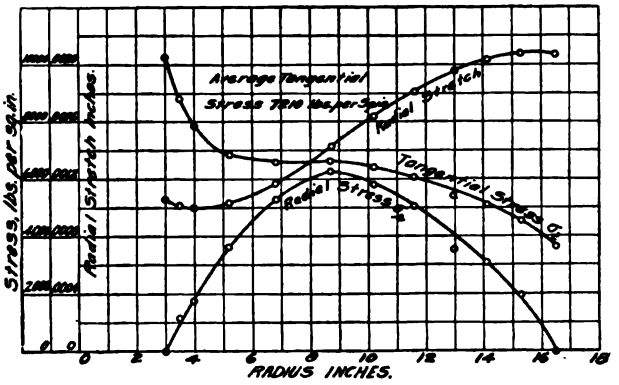

Fig. 87.

In order to obtain the radial stretch at any point of the impeller at distance x from the center, the proper values of b_1 and b_2 as given previously are used with corresponding values of ψ_1 and ψ_2. Solving formula 256 for values of x given in Table I, the radial elongations stated in the table are obtained.

These radial and tangential stresses and also the elongations are for the impeller disk without blades or shroud rings. The blades and shroud rings increase the stresses in the impeller disk, but the exact amount cannot be determined without going through a very elaborate calculation. For practical purposes the average stress can first be found both for the disk without blades and for that with blades. We can then assume that the maximum stress in the impeller without blades is increased by the addition of the blades in the same ratio as the average stress of the impeller without blades is increased by the addition of blades. Finding the average stress of the impeller is also an excellent check of the calculations of the tangential stresses just found.

The average stress in the impeller disk and hub, due to the centrifugal force of its own material, can be expressed as

$$\text{Average } \sigma_t = 0.00002842\,N^2S\,\frac{I}{A} \quad . \quad . \quad . \quad . \quad 257$$

in which

S is the specific density of the material, in pounds per cubic inch,
I is the moment of inertia of the total cross section of the impeller about the axis of the shaft,
A is the area of the total cross section of the impeller,
N is the number of revolutions per minute of the impeller.

For hyperbolic cross sections of the form $t = cx^{\alpha}$ the moment of inertia of cross section is

$$I = \frac{c}{\alpha + 3}(x_2^{\alpha+3} - x_1^{\alpha+3}) \quad . \quad . \quad . \quad . \quad . \quad 258$$

and the area of cross section is

$$A = \frac{c}{\alpha + 1}(x_2^{\alpha+1} - x_1^{\alpha+1}) \quad . \quad . \quad . \quad . \quad . \quad 259$$

where x_2 and x_1 are the terminal radii of the section considered.

Using equations 258 and 259 for the four hyperbolic sections in the problem and substituting the summation of their values in equation 257, the average stress can be found. The summation of the four values of I in this problem is

$$\sum I = \left[\frac{11}{3}(64 - 27) + \frac{176}{1}(8.7 - 4) + \frac{74.1}{1.4}(36.26 - 20.66) + \frac{1.637 \times 10^6}{-2.5}\left(\frac{1}{1106} - \frac{1}{609}\right)\right],$$

or

$$\sum I = 2271 \text{ in.}^{-3} \text{ pounds.}$$

The summation of the four values of A in this problem is

$$\sum A = \left[\frac{11}{1}(4 - 3) + \frac{176}{-1}\left(\frac{1}{8.7} - \frac{1}{4}\right) + \frac{74.1}{-0.6}\left(\frac{1}{4.65} - \frac{1}{3.66}\right) + \frac{1.637 \times 10^6}{-4.5}\left(\frac{1}{301\,500} - \frac{1}{103\,000}\right)\right]$$

or

$$\sum A = 44.28 \text{ square inches.}$$

The average tangential stress at 4200 r.p.m. is

$$\text{Aver. } \sigma_t = 0.00002842\, N^2 S \frac{I}{A} = 140.5 \frac{2271}{44.28} = 7210 \text{ lbs. per sq. in.} \quad 260$$

This average tangential stress agrees well with the values found previously and plotted in Fig. 87. In the latter the tangential stresses vary from 3626 pounds per square inch at the periphery of the disk to 10 262 pounds per square inch at the bore. If a mean line of stress were drawn it would very nearly equal 7210 pounds per square inch.

If the total weight of the blades is W pounds and the radius of their center of gravity is R inches, the average tangential stress in the impeller disk and hub whose total cross-sectional area is A, due to the blades, is

$$\text{Average } \sigma_t = 0.00002842\, N^2 W \frac{R}{2\pi A} \quad . \quad . \quad . \quad 261$$

The weight of the sixteen blades (eight on each side of the disk) is 45 pounds. The radius of their center of gravity is 12.7 inches. Their centrifugal force at 4200 r.p.m. is 286 500 pounds. Hence the additional average stress in the impeller disk due to the weight of the blades is, according to equation 261,

$$\text{Average } \sigma_t = \frac{286\,500}{2\pi \times 44.28} = 1030 \text{ pounds per square inch.} \quad 262$$

The total average stress in the disk is $7210 + 1030 = 8240$ pounds per square inch. Assuming as previously explained that the maximum tangential stress in the impeller is increased in the same ratio as the average stresses, with and without blades, the maximum tangential stress will be

$$\text{Maximum } \sigma_t = 10\,262 \frac{8240}{7210} = 11\,730 \text{ lbs. per sq. in.} \quad . \quad 263$$

The stresses in the shroud rings are calculated similarly to those in the impeller disk. The profile of the shroud ring can be very closely defined by three hyperbolas. The first hyperbola extends from $x = 9.5$ inches to $x = 12.5$ inches, the second hyperbola from $x = 12.5$ inches to $x = 15$ inches, and the third hyperbola from $x = 15$ inches to $x = 16.5$ inches. For the first curve the values of α and c of equation 247 are $\alpha = -1.4$ and $c = 23.69$; for the second curve $\alpha = -2.75$ and $c = 716.7$; for the third curve $\alpha = -5.5$ and $c = 1247 \times 10^5$. These values were again found by trial and error. Proceeding as before, by the aid of equations 248 to 252

inclusive, the radial and tangential stresses at any point of the shroud ring can be found. Keeping the speed at 4200 r.p.m. and beginning with the radial stress equal to nothing at the inner diameter of the shroud ring, the following values can be obtained:

For the first hyperbolic section,

$$\sigma_{r_{9.5}} = 0 = -12\,368 + 8674 \times 10^5 b_1 - 2760 \times 10^2 b_2 \quad 248i$$

$$\sigma_{t_{9.5}} = -7122 + 5915 \times 10^5 b_1 + 5747 \times 10^2 b_2 \quad 249i$$

$$b_1 = 4170 \times 10^{-13} \sigma_{t_{9.5}} + 1371 \times 10^{-8} \quad 253i$$

$$b_2 = 1311 \times 10^{-9} \sigma_{t_{9.5}} - 1720 \times 10^{-6} \quad 254i$$

$$\sigma_{r_{12.5}} = 0.2586\, \sigma_{t_{9.5}} - 5112 \quad 248j$$

$$\sigma_{t_{12.5}} = 0.8069\, \sigma_{t_{9.5}} - 2034 \quad 249j$$

For the second hyperbolic section,

$$\sigma_{r_{12.5}} = 67\,330 + 3853 \times 10^7 b_1 - 1595 \times 10^2 b_2 \quad 248k$$

$$\sigma_{t_{12.5}} = 38\,760 + 2130 \times 10^7 b_1 - 5269 \times 10^2 b_2 \quad 249k$$

$$b_1 = 1118 \times 10^{-14} \sigma_{t_{9.5}} - 1885 \times 10^{-9} \quad 253j$$

$$b_2 = 1079 \times 10^{-9} \sigma_{t_{9.5}} - 1238 \times 10^{-6} \quad 254j$$

$$\sigma_{r_{15}} = 0.5258\, \sigma_{t_{9.5}} - 13\,451 \quad 248l$$

$$\sigma_{t_{15}} = 0.7906\, \sigma_{t_{9.5}} - 5770 \quad 249l$$

For the third hyperbolic section,

$$\sigma_{r_{15}} = 10\,267 + 1305 \times 10^{11} b_1 - 92\,580\, b_2 \quad 248m$$

$$\sigma_{t_{15}} = 5910 + 5795 \times 10^{10} b_1 + 5509 \times 10^2 b_2 \quad 249m$$

$$b_1 = 4698 \times 10^{-18} \sigma_{t_{5.9}} - 1831 \times 10^{-13} \quad 253k$$

$$b_2 = 9416 \times 10^{-10} \sigma_{t_{5.9}} - 1941 \times 10^{-6} \quad 254k$$

$$\sigma_{r_{16.5}} = 0.9064\, \sigma_{t_{9.5}} - 25\,711 \quad 248n$$

$$\sigma_{t_{16.5}} = 0.8894\, \sigma_{t_{9.5}} - 10\,840 \quad 249n$$

Since $\sigma_{r_{16.5}}$ is the radial stress at the periphery of the shroud ring, the stress is equal to nothing; hence

$$\sigma_{r_{16.5}} = 0 = 0.9064\, \sigma_{t_{9.5}} - 25\,711,$$

or

$$\sigma_{t_{9.5}} = 28\,368 \text{ pounds per square inch} \quad 264$$

Having now obtained the value of $\sigma_{t_{4.5}}$, the constants b_1 and b_2 for all three hyperbolic sections can be found from equations 253 i, j, k and 254 i, j, and k.

For the first hyperbolic section

$$b_1 = 2554 \times 10^{-8} \quad . \quad . \quad . \quad . \quad . \quad . \quad . \quad 253l$$

$$b_2 = 3546 \times 10^{-5} \quad . \quad . \quad . \quad . \quad . \quad . \quad . \quad 254l$$

For the second hyperbolic section

$$b_1 = 1568 \times 10^{-9} \quad . \quad . \quad . \quad . \quad . \quad . \quad . \quad 253m$$

$$b_2 = 2934 \times 10^{-5} \quad . \quad . \quad . \quad . \quad . \quad . \quad . \quad 254m$$

For the third hyperbolic section

$$b_1 = 4983 \times 10^{-14} \quad . \quad . \quad . \quad . \quad . \quad . \quad . \quad 253n$$

$$b_2 = 2477 \times 10^{-5} \quad . \quad . \quad . \quad . \quad . \quad . \quad . \quad 254n$$

Having the values of these constants, the stresses at the different radii of the shroud ring can be obtained by substituting in equations 248 and 249 the values of b_1 and b_2 just found. Table II was computed in this manner, and gives the radial and tangential stresses at various distances from the center of the shroud ring. These values

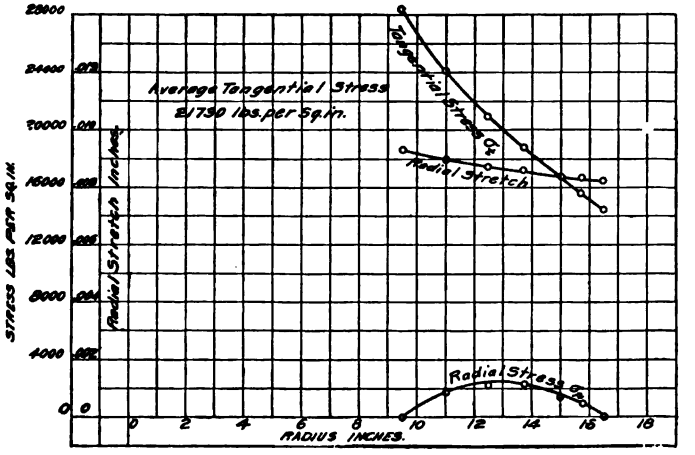

Fig. 88.

are also plotted in the form of a curve in Fig. 88. The radial stretch or elongation of the shroud ring calculated by means of equation 256 is also given in the table and on curve sheet, Fig. 88.

TABLE II.

Distance from Center of Impeller, inches.	Radial Stress σ_r, lbs. per sq. in.	Tangential Stress σ_t, lbs. per sq. in.	Radial Elongation from Center of Impeller, inches.
9.5	0	28 368	0.00930
11.0	1 724	24 083	0.00894
12.5	2 224	20 852	0.00870
13.75	2 229	18 693	0.00855
15.0	1 463	16 656	0.00840
15.75	909	15 537	0.00830
16.5	0	14 391	0.00819

The average stress in the shroud ring due to its own weight can be found by means of equations 257, 258, and 259. The summation of the three values of I of equation 258, for the three hyperbolic sections of the shroud ring is

$$\sum I = \frac{23.69}{1.6}(56.89 - 36.67) + \frac{716.7}{0.25}(1.967 - 1.880) + \frac{12.47 \times 10^5}{-2.5}\left(\frac{1}{1105.9} - \frac{1}{871.4}\right),$$

or

$$\sum I = 668.9 \text{ in.}^{-3} \text{ pounds.}$$

The summation of the three values of A from equation 259 is

$$\sum A = \frac{23.69}{-0.4}\left(\frac{1}{2.745} - \frac{1}{2.460}\right) + \frac{716.7}{-1.75}\left(\frac{1}{114.33} - \frac{1}{83.1}\right) + \frac{12.47 \times 10^5}{-4.5}\left(\frac{1}{3.016 \times 10^5} - \frac{1}{1.961 \times 10^5}\right),$$

or

$$\sum A = 4.33 \text{ square inches.}$$

Substituting these values in equation 257, the average tangential stress in the shroud rings is

$$\text{Average } \sigma_t = 0.00002842\, N^2 S \frac{I}{A} = 140.5 \frac{668.9}{4.33}$$

$$= 21\,730 \text{ pounds per square inch} \quad . \quad . \quad . \quad . \quad 265$$

This average tangential stress checks well with those plotted in Fig. 88, and may therefore be considered a check on the previous calculation.

The stresses in the shroud rings are somewhat high when compared to those in the impeller, and therefore the thickness of the shroud rings should be changed so as to decrease the maximum tangential stress. This can be accomplished by increasing the thickness of the ring at the inner diameter and probably decreasing its thickness at the outer diameter. The radial elongation of the shroud ring should be approximately the same as the radial elongation of the impeller at equal radii. If this is not the case, the part having the smaller elongation will carry the greater share of the blade load. This fact is sometimes taken advantage of when it is desired to have the impeller disk carry the blade load and relieve the shroud rings of this dead load. In the present problem, if the dimensions of the shroud rings are not changed the impeller disk will also be stressed somewhat by having to support part of the shroud rings themselves, the load being transmitted through the blades because one end of the blade is held by the impeller disk, while the other end wants to move with the shroud rings; the latter having the greater radial elongation.

If an impeller is designed without shroud rings, it is important to investigate the bending stresses, or more correctly, the crumpling stresses, in the blades. In Fig. 89 the blade is shown as straight up to a point C. The weight of the triangular piece ABC is $\frac{1}{2}\,abtS$, in which S is the weight of the material per cubic inch. The radius of the center of gravity of this triangle is $r_1 \frac{\cos \phi_1}{\cos \phi_2}$. The centrifugal force of this piece at N r.p.m. is

$$F = 0.00002842\, N^2 \frac{abt}{2} S r_1 \frac{\cos \phi_1}{\cos \phi_2} \quad . \quad . \quad . \quad . \quad 266$$

The force tending to bend the piece ABC about the line AC is $F \cos \phi_2$, and it acts at a distance of $\frac{ab}{3\sqrt{a^2+b^2}}$ from that line, giving a moment

$$M = 0.00002842\, N^2 \frac{abt}{2} S r_1 \cos \phi_1 \frac{ab}{3\sqrt{a^2+b^2}} \quad . \quad 267$$

The section modulus at AC is

$$Z = \frac{t^2}{6}\sqrt{a^2+b^2} \quad . \quad . \quad . \quad . \quad . \quad . \quad 268$$

and hence the bending or crumpling stress produced is

$$\sigma = \frac{M}{Z} = 0.00002842\, N^2 S r_1 \cos \phi_1 \frac{a^2 b^2}{t\,(a^2 + b^2)} \quad . \quad . \quad 269$$

in which

r_1 is the radius at impeller inlet, in inches,
ϕ_1 is the angle between the blade and a tangent to the circle whose radius is r_1,
a is the width of the impeller blade, in inches,
b is the length of blade from impeller tip to point C, in inches,
t is the thickness of blade, in inches.

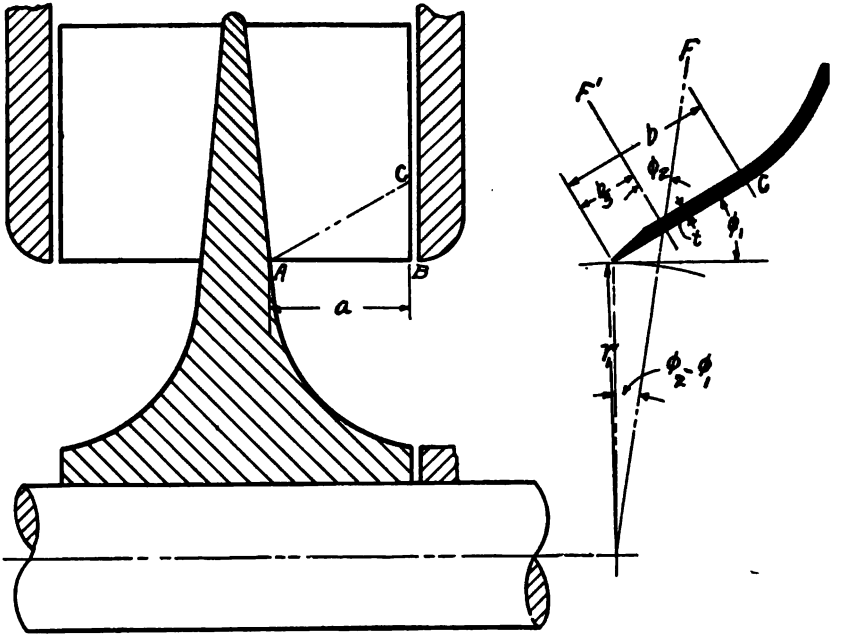

Fig. 89.

37. Diaphragms, Casings, and Heads.

The diaphragms, casings, and heads of centrifugal pumps must often withstand high water pressures, and their strength calculations are important. These castings are usually of a complicated shape, and it is rather difficult to determine the maximum stresses to which these parts are subjected when under hydraulic pressure. The

following method of calculating the stresses will be found useful and experience has shown it to give safe values.

Consider a dished diaphragm, as in Fig. 90, uniformly loaded by a hydraulic pressure and supported around its entire outer circumference. In any cross section AB bending stresses are produced by the loads on each side of this section. As the load on each side of this section is uniformly distributed it can be replaced

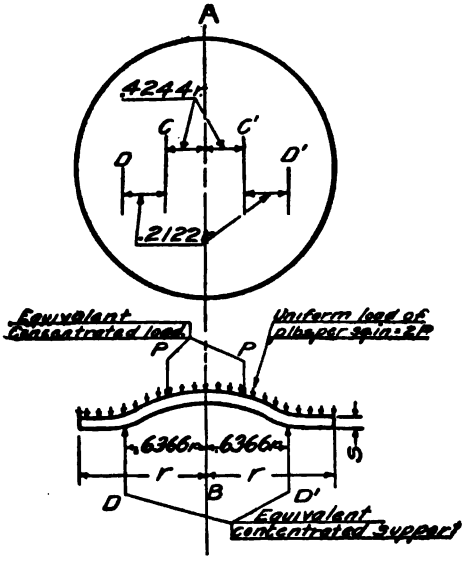

Fig. 90.

by an equivalent concentrated load at the center of gravity of each semicircle (C and C'). The reaction of the support is uniformly distributed around the circumference of the disk, and can be replaced by concentrated reactions at the center of gravity of each semicircumference (D and D'). This new distribution of forces produces the same bending moments about AB as the uniformly distributed forces. If the modulus of section $\frac{I}{C}$ were known for this section, then the mean stresses at the extreme fiber of this cross section could be calculated for any given load by determining the bending moments produced by this load. Actually maximum stresses are produced which are greater than these so-called mean stresses, but

if the cross section is well chosen this method of ascertaining the stresses will be satisfactory because the maximum stresses will not greatly exceed the mean stresses. We shall discuss later the proper choice of cross section, but will first give a graphical method of finding the modulus of section of any cross section.

Let the heavy lines in Fig. 91 represent one half of the cross section of a dished diaphragm, of which AB is the vertical center line. First the original cross section is massed about the center line AB; that is, all horizontal widths of the original cross section are moved over horizontally to the center line, as, for instance, distance CD equals distance C' 6, etc. This new cross section about the center line has the same modulus of section as the original cross section. Next assume arbitrarily the center line of gravity of the cross section. On both sides of this center line of gravity lay off a sufficient number of meridian lines parallel thereto, taking care that there is a meridian line at all points where there is a sudden change of cross section. Assume two arbitrary lines parallel to and equidistant from the center line of gravity outside of the cross section but preferably close thereto. Lay off points 1′ to 10′ so that distance 0′–1′ equals distance 0–1, also distance 0′–2′ equal to distance 0–2, etc. From point 5′ draw a line to point a, which is at the intersection of line 5 with the outline of the massed cross section. Line 5′–a intersects the arbitrary line at b. Connect b to 0 by a straight line. This line b–0 intersects line 5 at c. Similarly connect points 1′ to 10′ to corresponding points of intersection of the meridian lines 1 to 10 with the boundary of the massed cross section. Where these lines intersect the arbitrary line are points to be connected to the origin 0. The intersection of each of these lines to the origin 0 with the original meridian lines will give intersection points on each meridian line similar to that of c. By connecting all these points the cross hatched section as shown in the figure is found. If the center line of gravity was correctly chosen the area of the cross hatched portion above the center line of gravity is equal to that below. If this is not the case a new center line must be taken and the work repeated. The modulus of section can then be obtained from the formula

$$Z = \frac{AK^2}{F} \quad \ldots\ldots\ldots \quad 270$$

in which A is the area of the cross hatched portion on both sides of

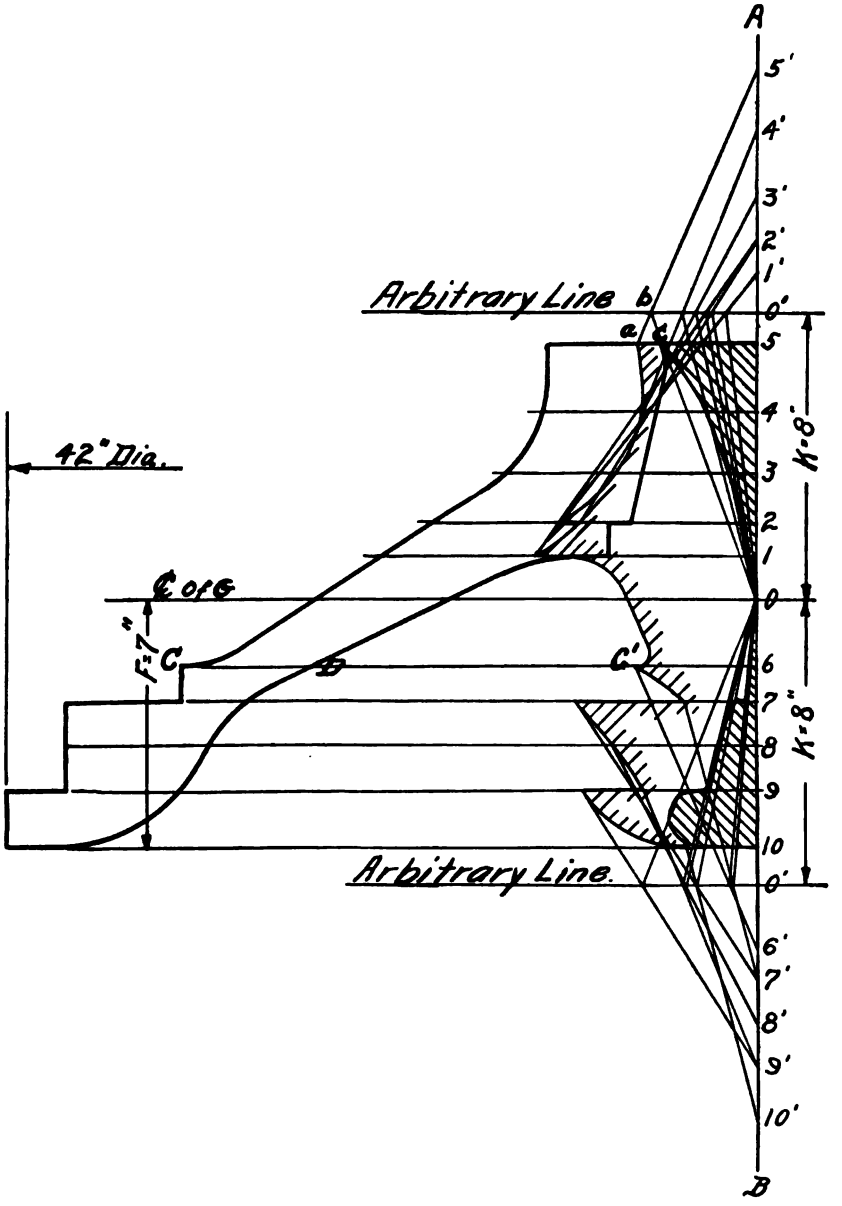
A
5'
4'
3'
2'
1'
Arbitrary Line
b
a
0'
5
4
42" Dia.
3
2
1
℄ of G
0
F=7"
C
C'
6
7
8
9
10
Arbitrary Line.
0'
6'
7'
8'
9'
10'
B
11'-8"
11'-8"

Fig. 91.

the center line of gravity, only one-half of which area is shown in the figure because only one-half of the section of the diaphragm is shown. F is the distance of the extreme fiber from the center line of gravity and K the distance of the arbitrary lines from the origin 0.

Having found the modulus of section, the mean stress at the extreme fiber can be found. If the diaphragm is supported against a rabbet at its outer circumference and is uniformly loaded, the equivalent concentrated loads on each side of the center line would be at the center of gravity of the area of each semicircle or at 0.4244 times the radius of the semicircle. The support around each semicircumference can be replaced by an equivalent reaction at the center of gravity of the semicircumference or at 0.6366 times the radius of the semicircle. The stress at the extreme fiber is equal to the bending moment divided by the modulus of section. If W is the total pressure on the diaphragm in pounds, then one-half W can be considered concentrated at the center of gravity of the area of each semicircumference. The diaphragm can now be replaced by a beam whose cross section is equal to the cross section of the diaphragm supported at two points 0.6366 times the radius of the diaphragm distant from the center of the beam and loaded with two concentrated loads 0.4244 times the radius of the diaphragm from the center of the beam.

The mean stress at the extreme fiber of a beam loaded as stated above with two concentrated loads $\frac{W}{2}$ equally distant from and on both sides of the center of the beam and supported at two points equally distant from and on both sides of the center line of the beam is

$$f = \frac{M}{Z} = \frac{WL}{2Z} \quad \ldots\ldots\ldots \quad 271$$

in which L is the distance from the point of support to the nearest concentrated load, or in this case $L = (0.6366 - 0.4244)\ R = 0.2122\ R$, R being the radius of the diaphragm.

If this mean stress is kept below 3000 pounds per square inch for cast iron, or 9000 pounds for cast steel, the above method will give safe design. But this method must be used with some judgment, for it is easily seen that the cross section can be chosen so slight at

one place and so heavy at another place that the resultant modulus would still give a satisfactory value. The cross hatched area would in the latter case have some very rapid changes of outline, as is perhaps emphasized in the lower half of the cross hatched area in Fig. 91. The upper half presents a better and stronger design. It is therefore necessary not only to keep the mean stresses below the figures given but also to observe the contour of the cross section and eliminate any sudden changes which might produce very high stresses at these points.

The diaphragm illustrated in Fig. 91 is shown in cross section and only one-half of the cross section is drawn, the diaphragm being symmetrical about the axis AB, and therefore the cross hatched area shown in the figure is one-half of the true value when the entire cross section is considered. The cross hatched area is equal to 12.69 square inches, and therefore the area on both sides of the center line AB is 25.38 square inches. The distance from the center of gravity to the extreme fiber of the diaphragm is 7 inches, and the distances from the center of gravity to the arbitrary lines is 8 inches; hence the modulus of section, according to equation 253, is

$$Z = \frac{AK^2}{F} = \frac{25.38 \times 8^2}{7} = 232.$$

The mean stress at the extreme fiber of this diaphragm is found from equation 271. If the load on the diaphragm is 100 pounds per square inch, the total load W on the diaphragm will be $100 \times \frac{(42)^2\pi}{4}$ = 138 545 pounds. The distance L in equation 271 is 0.2122×21 = 4.456 inches; hence equation 271 gives

$$f = \frac{WL}{2Z} = \frac{138\,545 \times 4.456}{2 \times 232} = 1330 \text{ pounds per square inch.}$$

Fig. 92 illustrates the method of finding the modulus of section of a centrifugal pump casing. Only one-half of the cross section is shown, the casing being symmetrical about the vertical reference line. The area of the cross hatched portion is 7.28 square inches, or, when the complete section is taken on both sides of the center

line, the area is 14.56 square inches. Hence the modulus of section is

$$Z = \frac{AK^2}{F} = \frac{14.56 \times 6^2}{5.75} = 91.$$

The test load to which this casing is to be subjected is 240 pounds per square inch; hence the total load is 310 000 pounds. The load is taken on the entire area of the casing up to the bolt circle, which is 3 feet 9½ inches in diameter. The mean stress at the extreme

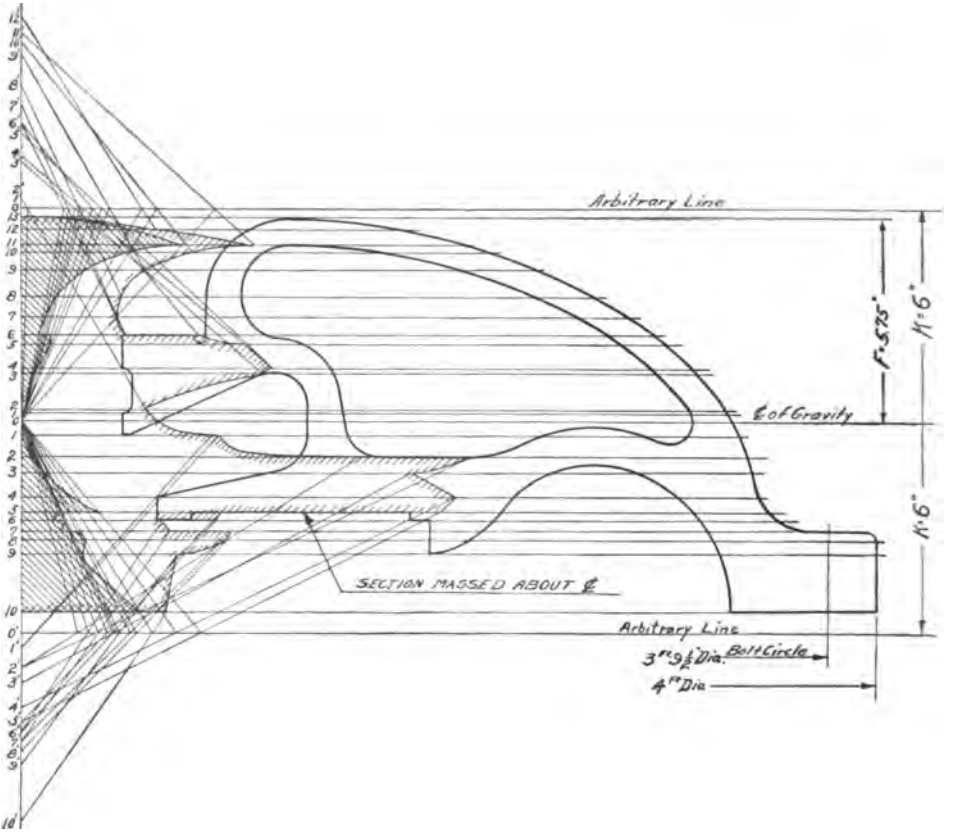

Fig. 92.

fibers of the casing is $f = \frac{WL}{2Z}$. The distance L equals $0.2122\,R$ = 4.82 inches. Hence

$$f = \frac{310\,000 \times 4.82}{2 \times 91} = 8210 \text{ pounds per square inch.}$$

38. Critical Speeds.

The phenomenon of critical speeds is of great importance in the design of high-speed centrifugal pumps. The shaft and the impellers form a rotating element which in practice is not in absolute mass balance. When such a shaft is rotated it experiences more or less violent vibrations. The intensity of these vibrations depends, among other things, on the speed of rotation, the vibrations reaching a very sudden maximum at certain particular speeds, known as critical speeds. It is therefore important to have the revolving element in as good balance as possible, and to avoid running the shaft in the vicinity of its critical speeds.

A revolving element (shaft and impellers) may be out of balance either dynamically or both dynamically and statically. Assume a rotating element mounted on a horizontal shaft, the latter resting upon parallel and level ways. If the center of gravity of the entire rotating element lies exactly in the center line of the shaft the mass will then be in indifferent equilibrium; that is, the shaft will have no inherent tendency to rotate to some particular position. In all practical cases the center of gravity does not lie in the center line of rotation and we have a case similar to that shown in Fig. 93, where m_1 represents an unbalanced mass at a distance r_1 from the axis. The shaft will now be in equilibrium in only two positions. In all other positions it will be subject to a turning moment of $m_1 r_1 \sin\phi$, where ϕ is the angle made by a normal from m_1 to the axis with a vertical plane through the axis. If another mass m_2 is attached to the revolving element at a distance r_2 from the axis, so that $m_1 r_1 = m_2 r_2$, m_1 and m_2 being in the same plane passing through the axis but upon opposite sides, the indifferent equilibrium of the shaft will be restored, or, to use the common phrase, the shaft will be in static balance. Evidently a vertical shaft is always in static balance.

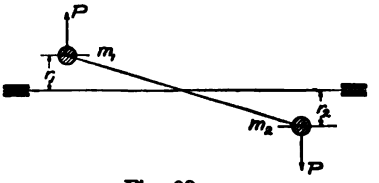

Fig. 93.

A shaft while statically in balance may be subject to severe deflecting forces when set in rotation, as in the case just illustrated. The center of gravity of the two unbalanced masses lies in the axis of rotation; but their centrifugal forces are not balanced but con-

stitute a moment causing opposite forces in the bearings and subjecting the shaft to severe deflecting forces which may be high enough to rupture it. The correct way to neutralize the effect of such unbalanced masses is to balance the rotating element dynamically by adding balance weights in any two planes perpendicular to the axis of the element, preferably the two end planes. Referring to Fig. 94, the effect of the unbalanced mass m_1 is neutralized by adding two masses m_1' and m_1'' at radii r_1' and r_1'' in the two end

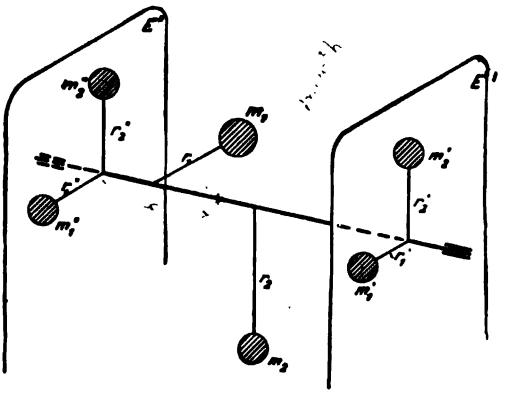

Fig. 94.

planes E' and E'' placed normally to the axis, provided m_1, m_1' and m_1'' are all in the same plane through the axis and provided that

$$m_1'r_1' + m_1''r'' = m_1r_1 \quad . \quad . \quad . \quad . \quad . \quad . \quad 272$$

and

$$m_1'r_1'a_1' = m_1''r_1''a_1'' \quad . \quad . \quad . \quad . \quad . \quad . \quad 273$$

When the shaft is rotating these three masses create centrifugal moments which are in equilibrium; that is, they constitute a system of moments whose arithmetical sum at any point is equal to nothing. Similarly the mass m_2 can be balanced by two masses m_2' and m_2'' at radii r_2' and r_2'', and likewise any other unbalanced masses in the rotating element can be so balanced. If desired, all the balancing masses in the two end planes can be combined into a resultant mass in each plane. Therefore proper mass balance necessitates not only having the center of gravity of the revolving mass coincide with its center of rotation (static balance) but also eliminating the so-called centrifugal moments of the dynamically unbalanced masses (dynamic

balance). Evidently, when a shaft is in dynamic balance it is also in static balance.

In practice, in order to secure static balance, the impellers are mounted individually on an arbor and the latter is placed upon two parallel ways carefully leveled. The heavy side of the impeller will roll downwards, and metal is either removed from this side or weights are added upon the opposite side. After all the impellers are in static balance they are mounted upon the shaft between bearings and slowly brought up to speed until vibration occurs. At this speed the shaft is marked near each end with a pencil, the marking showing the side thrown out, or high side, of the vibrating shaft. It will be found that the high side on one end is 180° from the high side on the other end. It is possible to add weights at both ends of the shaft, or upon the first and last impellers, which will balance the rotating mass dynamically. It can be proved* that when the shaft is rotating at its critical speed the side thrown out, or the high side of the shaft, is 90° behind the actual unbalanced mass considered in the sense of rotation. Therefore balancing weights should be added in this case 90° back of the high side or mark. When the shaft is revolving below the critical speed the high side is less than 90° behind the unbalanced mass, and when revolving above the critical speed the high side is more than 90° behind the unbalanced mass. If the revolving element is subject to the same windage work when rotating in either direction, the shaft can first be marked when running in one direction at any certain speed and then again when running in the opposite direction at the same speed. The actual unbalanced mass lies midway between the two marks, and no notice need be taken whether the shaft was running above or below the critical speed. But when the windage work is not the same for both directions of rotation, as is the case with pump impellers, the above does not hold true, and balancing must be done by rotating the shaft and impellers in one direction, marking the high side at each end of the shaft and estimating how far back of this mark balancing weights should be placed. The method is one of trial and error.

After the shaft has been dynamically balanced with the utmost care, it will in general still have some slight unbalancing, which is entirely harmless if certain definite speeds, called critical speeds, are avoided. At these speeds the shaft is in a state of extreme

* See Stodola, "Steam Turbines," third edition, article 61.

sensitiveness and the slightest disturbance may set it in very violent vibration. These critical speeds can be determined with considerable accuracy from the dimensions of the shaft and the manner in which it is loaded and supported. The lowest critical speed is usually called the first critical speed and the rest are numbered successively. In the present designs of high-speed centrifugal pumps the shaft seldom reaches the third critical speed. It runs either between the second and third critical speeds or between the first and second and frequently below the first; so that in nearly all cases the first critical speed should be determined to make sure that the normal speed is either well below or well above this critical speed, and only in some designs is it necessary to determine the second critical speed.

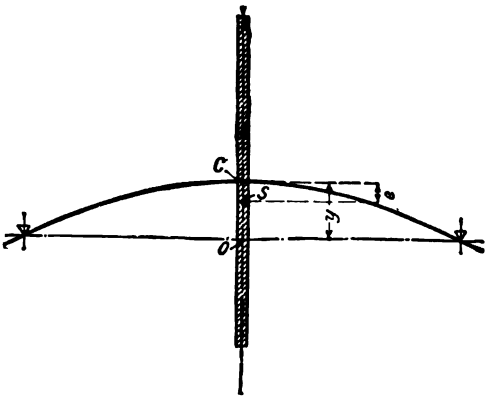

Fig. 95.

Imagine* a disk mounted on a shaft (Fig. 95) so that its center of rotation is at C, and let the disk be slightly out of balance so that its center of gravity is at S. Let the dotted and dashed line from support A to support B represent the center line of the shaft when stationary and bent by the weight of the disk (weight of shaft being neglected). When the shaft is set into comparatively slow rotation the centrifugal force of the unbalanced mass will spring the shaft a distance y and cause it to whip. If m is the mass of the disk, ω its angular velocity, and e the distance of the center of gravity from the center of rotation, then $m(y + e)\omega^2$ is equal to the centrifugal force exerted on the shaft and is balanced by the elastic opposing

* See Stodola's "Steam Turbines" for fuller discussion of the theory of critical speeds.

force of the shaft. The elastic opposing force of a shaft is proportional to the deflection; hence if α is a constant depending upon length of shaft, style of supports, etc., the elastic resisting (opposing) force of the shaft is $P = \alpha y$. Conditions of equilibrium demand that

$$m(y + e)\omega^2 = P = \alpha y \quad . \quad . \quad . \quad . \quad . \quad . \quad . \quad 274$$

Hence the deflection is

$$y = \frac{m\omega^2 e}{\alpha - m\omega^2} \quad . \quad . \quad . \quad . \quad . \quad . \quad . \quad . \quad 275$$

If the angular velocity is increased y also increases and becomes infinitely large when $\alpha - m\omega^2 = 0$, or when

$$\omega = \sqrt{\frac{\alpha}{m}} \quad . \quad . \quad . \quad . \quad . \quad . \quad . \quad . \quad 276$$

This value of ω is called the critical angular velocity. From this it can be seen that the shaft cannot reach the critical speed except

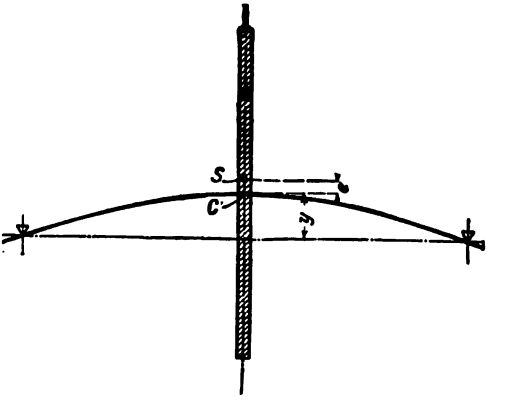

Fig. 96.

when it is constrained by guides or by bearings which act as guides, or when the velocity increases so rapidly that the shaft while passing through its critical speed "has no time" to deflect excessively. Theory and practice agree that after the critical speed has been passed a new condition of stable equilibrium exists and that the center of the shaft C now exchanges its position with the center of gravity S as shown in Fig. 96. The deflection y is now found from the formula

$$m(y - e)\omega^2 = \alpha y \quad . \quad . \quad . \quad . \quad . \quad . \quad . \quad 277$$

or

$$y = \frac{m\omega^2 e}{-\alpha + m\omega^2} = \frac{e}{1 - \frac{\alpha}{m\omega^2}} \quad \ldots\ldots 278$$

The more ω is increased the smaller y becomes, and with infinitely high rotation $y = e$, that is, the disk will rotate about its center of gravity. In practice, careful balancing will make e very small so that the "range" of the critical speed will not be very great; that is noticeable vibrations usually do not begin until the critical speed is nearly reached, and die away soon after the critical speed is passed. Good running can therefore be obtained when the operating speeds are removed from the proximity of the critical speeds.

A method of calculating the critical speed of a rotating shaft with any number of different diameters and with any distribution of masses and for any number of supports has been devised by one of the authors and used successfully for a number of years. The calculations for critical speeds have checked very well with the observed critical speeds. The method will be explained by both graphical and mathematical solutions. The graphical method assists the calculator in quickly detecting errors in the computation and helps greatly in understanding the method. It is therefore strongly recommended.

The general theory of this method is as follows. A shaft with any arrangement of supports (bearings) is loaded with forces W_1, W_2, W_3, . . . at right angles to its axis, which cause deflections y_1, y_2, y_3, . . . at the points where these forces are applied. If all these forces are increased x times their magnitude, the deflections will also be increased x times. This general statement is perfectly obvious. Suppose the shaft is loaded by centrifugal forces instead of static forces, as is the case of a rotating shaft with impellers not in absolute balance. As long as the speed of rotation is low, the deflections due to the centrifugal forces are small, but as these forces increase the deflections also increase in like amount. It is not until the critical number of revolutions is reached that the centrifugal forces become equal to the elastic resisting forces of the shaft and a state of unstable equilibrium exists, for should the deflections from any cause be slightly increased then the centrifugal forces would increase in the same proportion. In other words, at the critical number of revolutions the shaft is in neutral equilibrium for

any deflection. In order to find the critical speed of any shaft it is necessary to determine the elastic curve that the shaft assumes when it is subject to the centrifugal forces of the unbalanced masses at the time the rotating shaft is at or very near to its critical speed. If the elastic curve of the shaft as it approaches the critical speed were known, the critical speed could easily be determined, but as this curve is not known a trial curve must first be assumed and calculations made to check whether this trial curve is or is not the true elastic curve. If the trial curve is not the true curve, the calculations will at least indicate in which direction the trial curve should be changed to approach more nearly the true curve. As the static deflection curve is also an elastic curve of the shaft and is usually determined for purposes of design, it is best to take this curve as the first trial elastic curve, although it must be distinctly understood that the critical speed has nothing to do with the static deflection curve except in cases where the centrifugal forces of all the unbalanced masses have all the same ratio to the static weights of the revolving loads. This is the case of a single load on a shaft when the shaft is considered weightless.

After the static deflection curve is found, the static weights or loads and their corresponding deflections can be used for determining their centrifugal forces $P_1, P_2, P_3, \ldots$ for an assumed number of revolutions per minute. With these centrifugal forces a new elastic curve of the shaft can be determined and their deflections $y_1', y_2', y_3', \ldots$ obtained. Any of these last determined deflections can be made equal to its corresponding deflection on the first trial elastic curve of the shaft by changing the assumed number of revolutions to a higher or lower value simply by multiplying it by the square root of the ratio $\frac{y_1}{y_1'}$. If all the ordinates of the second elastic curve are multiplied by the square root of this ratio, then the new or corrected elastic curve must coincide with the first trial curve if the critical number of revolutions has been correctly assumed. Actually the curves will not agree and we must repeat this method by allowing the new elastic curve to be a second trial curve. Usually from three to five trial curves are needed to determine the critical number of revolutions.

We cannot emphasize too strongly the fact that static deflections have nothing to do with the critical speed because a number of

approximate methods for calculating the critical speed use the static deflections. A good physical conception of what actually occurs when a shaft is rotating aids materially in understanding the phenomenon of critical speed. A loaded shaft held between supports deflects and its axis forms a curve of static deflection. When the shaft is slowly rotated it revolves about this bent axis similarly as would a rotating rope held between two supports with considerable sag. If the rope is turned equally at both ends it will rotate about this curved axis. This represents exactly the rotation of a loaded shaft. If the rotating shaft is in perfect balance it will always continue to rotate in this curved position. Each unbalanced mass on the rotating shaft will, on the other hand, exert a certain centrifugal force upon the shaft, tending to deflect it from its static position. When these centrifugal forces become large enough they will cause the shaft to whip about its curved axis of rotation. We can imagine the shaft reaching such a speed that the centrifugal forces become large enough to balance the elastic resisting forces of the shaft exactly, and this will create a state of neutral equilibrium for any deflection. If the rotating element consists of a shaft of uniform diameter and carrying a single concentrated load, the static deflection curve and the elastic curve of the shaft at the critical speed must be similar because the static weight and the centrifugal force of the unbalanced mass are exactly proportional to one another. In this case the static deflection curve can be used for determining the critical speed. In all other cases the static deflection curve will not give a true indication of the critical speed, although in many cases it gives a very close approximation. The more nearly the static deflection curve is similar to the elastic curve of the shaft at the critical speed the more nearly correct will be the critical speed calculated from the static deflections.

Another formula for critical speed of any shaft based on the equality of the potential and kinetic energies of the shaft can be derived. The potential energy of a shaft carrying loads W_1, W_2, W_3, etc. (centrifugal forces being considered as loads), and having deflections y_1, y_2, y_3, etc., at these loads is

$$\tfrac{1}{2}(W_1y_1 + W_2y_2 + W_3y_3 + \cdots) \quad . \quad . \quad . \quad . \quad 279$$

If these loads while maintaining their deflections y_1, y_2, y_3, etc.,

are rotating with an angular velocity of ω radians per second, their kinetic energy is

$$\frac{\omega^2}{2g}(W_1y_1^2 + W_2y_2^2 + W_3y_3^2 + \cdots) \quad . \quad . \quad . \quad 280$$

At any speed the shaft will finally assume such a shape that

$$\frac{\omega^2}{g}(W_1y_1^2+W_2y_2^2+W_3y_3^2+\cdots)=(W_1y_1+W_2y_2+W_3y_3+\cdots) \quad 281$$

or

$$\omega = \sqrt{g}\sqrt{\frac{W_1y_1 + W_2y_2 + W_3y_3 + \cdots}{W_1y_1^2 + W_2y_2^2 + W_3y_3^2 + \cdots}} \quad . \quad . \quad 282$$

so that when W_1, W_2, W_3, etc., and y_1, y_2, y_3, etc., are known the corresponding ω can be computed. But at the critical speed the shaft is in indifferent equilibrium; that is, at any particular point on the shaft the deflection may be assumed at random. The deflections at all points will of course have to adapt themselves to the assumed deflection, in accordance with the dimensions of the shaft, distribution of load, kind of supports, etc. If the static deflections of the shaft are computed, the largest deflection, or the largest Wy, may be assumed to be exactly correct at the critical speed. The smaller static deflections will be more or less in error, but this error need not be very large because the expression for ω is fairly insensitive to moderate errors in the smaller deflections. Therefore the critical speed may be expressed approximately as

$$N = \frac{30\,\omega}{\pi} = \frac{30}{\pi}\sqrt{g}\sqrt{\frac{W_1y_1 + W_2y_2 + W_3y_3 + \cdots}{W_1y_1^2 + W_2y_2^2 + W_3y_3^2 + \cdots}}$$

$$= 187.7\sqrt{\frac{W_1y_1 + W_2y_2 + W_3y_3 + \cdots}{W_1y_1^2 + W_2y_2^2 + W_3y_3^2 + \cdots}} \quad . \quad . \quad . \quad 283$$

This formula sometimes gives close results, but should not be used except as a trial value. The more nearly the static deflection curve is similar to the elastic curve of the shaft when approaching the critical speed the more nearly correct will this formula be.

From the foregoing it is clear that before the critical speed of a shaft is computed it is desirable to know how to calculate the static deflections of a shaft at various points for any given distribution of loads and supports. The underlying principles for obtaining static

deflections are explained in most textbooks on mechanics, and will be reviewed here very concisely. If $\frac{d^2y}{dx^2}$ denotes the curvature, or change of tangent, at any point on a shaft, M the bending moment at the point, I the moment of inertia of the cross section of the shaft, and E its coefficient of elasticity, then it can be proved that

$$E\frac{d^2y}{dx^2} = \frac{M}{I} \quad \ldots\ldots\ldots \quad 284$$

Integrating this we get

$$E\frac{dy}{dx} = \int \frac{M}{I}dx + C_1 \quad \ldots\ldots\ldots \quad 285$$

and integrating again we get

$$Ey = \int\int \frac{M}{I}dx + C_1x + C_2 \quad \ldots\ldots\ldots \quad 286$$

In the above C_1 is the tangent and C_2 the deflection at the point where $x = 0$, since at that point all integrals must necessarily be equal to nothing. In computing C_1 and C_2 let the deflections for $x = l_1$ and $x = l_2$, be $y = 0$; l_1 and l_2 being the locations of the bearings, which are $l_2 - l_1 = l$ inches apart. Then from equation 286

$$0 = \int\int_0^{l_2} \frac{M}{I}dx + C_1l_2 + C_2 \quad \ldots\ldots\ldots \quad 287$$

and

$$0 = \int\int_0^{l_1} \frac{M}{I}dx + C_1l_1 + C_2 \quad \ldots\ldots\ldots \quad 288$$

Subtracting equation 288 from equation 287,

$$0 = \int\int_{l_1}^{l_2} \frac{M}{I}dx + C_1(l_2 - l_1) \quad \ldots\ldots\ldots \quad 289$$

whence

$$C_1 = -\frac{1}{l}\int\int_{l_1}^{l_2} \frac{M}{I}dx \quad \ldots\ldots\ldots \quad 290$$

and C_2 can be solved from either 287 or 288.

Generally the origin is so chosen that $y = 0$ for $x = 0$. Then $C_2 = 0$ and $C_1 = -\frac{1}{l}\int\int_0^{l} \frac{M}{I}dx$.

When the shaft is of uniform diameter, I is constant and equations 285 and 286 can be integrated by the ordinary rules of calculus. The results of these integrations have been recorded in various handbooks, and the deflections at all points can be readily computed. In shafts used in practice, however, there may be many and large changes of diameter. In such cases the integration of $\frac{M}{I}dx$ must be performed by a step-by-step method; and the method of procedure can be as follows.

A certain number of "shoulders," or changes of diameter, are decided upon, the more insignificant changes of diameter being neglected. The shaft is thus divided up into a number of sections, the points of division being the bearings, the shoulders, and the points of application of the loads. The diameter of each section is therefore constant; and the length of a section is $x_2 - x_1$, where x_2 and x_1 are the distances of the extremities of any section from some origin.

The moment M at any point x can easily be shown to be (considering only concentrated loads)

$$M = M_1 + (M_2 - M_1)\frac{x - x_1}{x_2 - x_1} \quad . \quad . \quad . \quad . \quad 291$$

or

$$M = \frac{1}{x_2 - x_1}\left[M_1x_2 - M_2x_1 + (M_2 - M_1)\,x\right] \quad . \quad . \quad 292$$

where M_2 and M_1 are the bending moments at x_2 and x_1 respectively. Integrating equation 292 it becomes

$$\int \frac{M}{I}dx = \frac{1}{(x_2 - x_1)\,I}\left[(M_1x_2 - M_2x_1)\,x + (M_2 - M_1)\frac{x^2}{2}\right] + C. \quad 293$$

In integrating between any two limits such as $x = x_1$ and $x = x_2$ the integral in equation 293 can be written

$$\int_{x_1}^{x_2}\frac{M}{I}dx = \frac{1}{(x_2 - x_1)\,I}\left[(M_1x_2 - M_2x_1)\,(x_2 - x_1) + (M_2 - M_1)\frac{x_2^2 - x_1^2}{2}\right], \quad 294$$

or

$$\int_{x_1}^{x_2}\frac{M}{I}dx = \frac{1}{2\,I}\left[2\,M_1x_2 - 2\,M_2x_1 + (M_2 - M_1)(x_2 + x_1)\right],$$

or

$$\int_{x_1}^{x_2}\frac{M}{I}dx = \frac{1}{2\,I}\left[2\,M_1x_2 - 2\,M_2x_1 + M_2x_2 + M_2x_1 - M_1x_2 - M_1x_1\right],$$

or

$$\int_{x_1}^{x_2} \frac{M}{I}\,dx = \frac{1}{2I}\left[M_1x_2 + M_2x_2 - M_2x_1 - M_1x_1\right]$$

$$= \frac{1}{2I}\left[(M_1 + M_2)\,x_2 - (M_1 + M_2)\,x_1\right],$$

or

$$\int_{x_1}^{x_2} \frac{M}{I}\,dx = \frac{M_1 + M_2}{2} \cdot \frac{x_2 - x_1}{I} \quad . \quad . \quad . \quad . \quad 295$$

Before the second integral of equation 293 is taken it is advisable to solve for the value of the constant C. In order to do this let $x = x_1$ in equation 293. Then

$$\int_0^{x_1} \frac{M}{I}\,dx = \frac{1}{2(x_2 - x_1)I}\left[2M_1x_1x_2 - 2M_2x_1^2 + M_2x_1^2 - M_1x_1^2\right] + C; \quad 296$$

hence

$$C = \int_0^{x_1} \frac{M}{I}\,dx - \frac{1}{2(x_2 - x_1)I}\left[2\,M_1x_1x_2 - (M_1 + M_2)\,x_1^2\right] \quad . \quad 297$$

Substituting this value of C in equation 293 we get

$$\int \frac{M}{I}\,dx = \frac{1}{2\,(x_2 - x_1)\,I}\left[2\,(M_1x_2 - M_2x_1)\,x + (M_2 - M_1)x^2 - 2\,M_1x_1x_2\right.$$

$$\left. + (M_1 + M_2)\,x_1^2\right] + \int_0^{x_1} \frac{M}{I}\,dx \quad . \quad . \quad . \quad . \quad . \quad . \quad . \quad 298$$

The integration of equation 298 between x_2 and x_1 is

$$\int\int_{x_1}^{x_2} \frac{M}{I}\,dx = \frac{1}{2\,(x_2 - x_1)\,I}\left[2\,(M_1x_2 - M_2x_1)\left(\frac{x_2^2 - x_1^2}{2}\right)\right.$$

$$+ (M_2 - M_1)\,\frac{x_2^3 - x_1^3}{3} - 2\,M_1x_1x_2\,(x_2 - x_1)$$

$$\left. + (M_1 + M_2)\,x_1^2\,(x_2 - x_1)\right] + (x_2 - x_1)\int_0^{x_1} \frac{M}{I}\,dx \quad 299$$

or

$$\int\int_{x_1}^{x_2} \frac{M}{I}\,dx = \frac{1}{6I}\left[3\,(M_1x_2 - M_2x_1)\,(x_2 + x_1)\right.$$

$$\left. + (M_2 - M_1)(x_2^2 + x_2x_1 + x_1^2) - 6\,M_1x_1x_2 + (M_1 + M_2)\,x_1^2\right]$$

$$+ (x_2 - x_1)\int_0^{x_1} \frac{M}{I}\,dx \quad . \quad . \quad . \quad . \quad . \quad . \quad . \quad . \quad . \quad . \quad 300$$

or

$$\int\int_{x_1}^{x_2} \frac{M}{I} dx = \frac{2M_1 + M_2}{6}\left(\frac{(x_2 - x_1)^2}{I}\right) + (x_2 - x_1)\int_0^{x_1} \frac{M}{I} dx \quad . \quad 301$$

The practical use of the above formulæ will be easily understood in the following illustration of the method of obtaining the static deflection curve.

To illustrate the method of calculating critical speeds it would be well to calculate the critical speed of a pump shaft. Fig. 97 represents a pump shaft carrying four impellers W_1, W_2, W_3, and W_4 and supported at each end in a bearing. The distances between center lines of bearings and impellers are also shown. The diameters of the shaft are as follows:

Diameter of shaft between R_1 and S_1 is 2.5 inches.
Diameter of shaft between S_1 and S_2 is 2.75 inches.
Diameter of shaft between S_2 and S_3 is 3.0 inches.
Diameter of shaft between S_3 and S_4 is 3.25 inches.
Diameter of shaft between S_4 and S_5 is 3.5 inches.
Diameter of shaft between S_5 and S_6 is 3.75 inches.
Diameter of shaft between S_6 and S_7 is 2.75 inches.
Diameter of shaft between S_7 and R_2 is 2.5 inches.

The static deflection of the shaft is first determined by treating the shaft as a beam supported at the center lines of the bearings and loaded with concentrated loads at the center line of each impeller. The weight of the shaft will be considered uniformly distributed in this case because the shaft is nearly of uniform diameter. If the diameters of the shaft vary greatly the weight can be considered as a series of concentrated loads applied at the center of each length of uniform diameter, each load being the weight of such a length.

The calculations for static deflection can be conveniently tabulated, and Table I gives the results of the calculations for the pump shaft illustrated in Fig. 97.

Column 1 gives the various points along the shaft at which there is either a change of cross section or a point of application of load.

Column 2 gives the distance (in inches) between successive points, as, for example, the distance from R_1 to S_1 is 7 inches, that from S_1 to S_2 is 20.5 inches, etc.

TABLE I.

1	2	3	4	5	6	7	8	9	10	11	12
Points along Shaft.	Distance between Successive Points. $(x_2 - x_1)$	Distance from the Origin R_1. x.	Bending Moments Due to Weight of Shaft.	Bending Moments Due to Concentrated Loads.	Combined Bending Moments. M.	Moment of Inertia of Cross Section. I.	$\frac{M}{I}$.	$\frac{x_2 - x_1}{I}$.	$\frac{M_1 + M_2}{2}$.	$\int_{x_1}^{x_2} \frac{M}{I} dx = \left(\frac{M_1+M_2}{2}\right)\frac{x_2-x_1}{I}$ between Successive Points.	Total $\int_0^x \frac{M}{I} dx$ from Origin.
	in.	in.	in. lbs.	in. lbs.	in. lbs.	in.^{4}	in.$^{-2}$ lbs.	in.$^{-2}$	in. lbs.	in.$^{-2}$ lbs.	in.$^{-2}$ lbs.
R_1		0	0	0	0		0				0
	7.0					1.918		3.649	−1 550	−5 660	
S_1		7.0			−3 100		−1 615				−5 660
	20.5					2.814	−1 102	7 285	−7 645	−55 620	
S_2		27.5			−12 190		−4 334				−61 280
	4.5					3.976	−3 065	1.132	−13 190	−14 940	
W_1		32.0	−2 270	−11 920	−14 190						−76 220
	7.5					3.976	−3 568	1.887	−14 850	−28 020	
S_3		39.5			−15 510		−3 900				−104.240
	6.5					5.477	−2 832	1.187	−16 085	−19 100	
W_2		46.0	−2 560	−14 100	−16 660						−123 340
	6.5					5.477	−3 041	1.187	−16 440	−19 510	
S_4		52.5			−16 220		−2 960				−142 850
	7.5					7.366	−2 206	1.018	−15 970	−16 270	
W_3		60.0	−2 410	−13 310	−15 720						−159 120
	5.5					7.366	−2 134	0.747	−14 895	−11 120	
S_5		65.5			−14 070		−1 910				−170 240
	8.5					9.401	−1 495	0.904	−12 800	−11 770	
W_4		74.0	−1 810	−9 720	−11 530						−181 980
	4.5					9.401	−1 225	0.479	−10 350	−4 960	
S_6		78.5			−9 170		−975				−186 940
	11.5					2.814	−3 260	4.088	−6 155	−25 180	
S_7		90.0			−3 140		−1 116				−212 120
	6.0					1.918	−1 636	3.128	−1 750	−4 910	
R_2		96.0	0	0	0		0				−217 030

TABLE I.

13	14	15	16	17	18	19	20	21
$(x_2-x_1)\int_0^{x_1}\frac{M}{I}\,dx=a.$	$\frac{(x_2-x_1)^2}{I}=b.$	$\frac{2M_1+M_2}{6}=c.$	$\frac{(x_2-x_1)^2}{I}\left(\frac{2M_1+M_2}{6}\right)=bc.$	$\int\int_{x_1}^{x_2}\frac{M}{I}\,dx_2=a+bc$ between Successive Points.	Total $\int\int_0^x\frac{M}{I}\,dx^2$ from Origin.	$CX.$	$EY.$	$\frac{Y}{\text{(when } E=29\,000\,000).}$
in.$^{-1}$ lbs.	in.$^{-2}$	in. lbs.	in.$^{-1}$ lbs.	in.$^{-1}$ lbs.	in.$^{-1}$ lbs.	in.$^{-1}$ lbs.	in.$^{-1}$ lbs.	in.
					0	0	0	
0	25.55	−516	−13 180	−13 180				
					−13 180	813 130		
−116 000	149.3	−3 065	−457 900	−573 900				
					−587 080	3 194 430		
−275 700	5.09	−6 428	−32 700	−308 400				
					−895 480	3 717 150	2 821 670	0.0973
−572 000	14.15	−7 315	−103 500	−675 500				
					−1 570 980	4 588 360		
−677 800	7.72	−7 947	−61 350	−739 150				
					−2 310 130	45 243 410	3 033 280	0.1043
−802 000	7.72	−8 257	−63 750	−865 750				
					−3 175 880	6 098 450		
−1 071 500	7.54	−8 027	−60 520	−1 132 020				
					−4 307 900	6 971 460	2 663 560	0.0919
−875 400	4.11	−7 585	−31 180	−906 580				
					−5 214 480	7 608 550		
−1 447 000	7.68	−6 612	−50 750	−1 497 750				
					−6 712 230	8 595 910	1 883 680	0.0649
−819 000	2.16	−5 372	−11 600	−830 600				
					−7 542 830	9 118 640		
−2 148 000	47.0	−3 580	−168 300	−2 316 300				
					−9 859 130	10 454 490		
−1 272 700	18.77	−1 047	−19 650	−1 292 350				
					−11 151 480	11 151 480	0	0

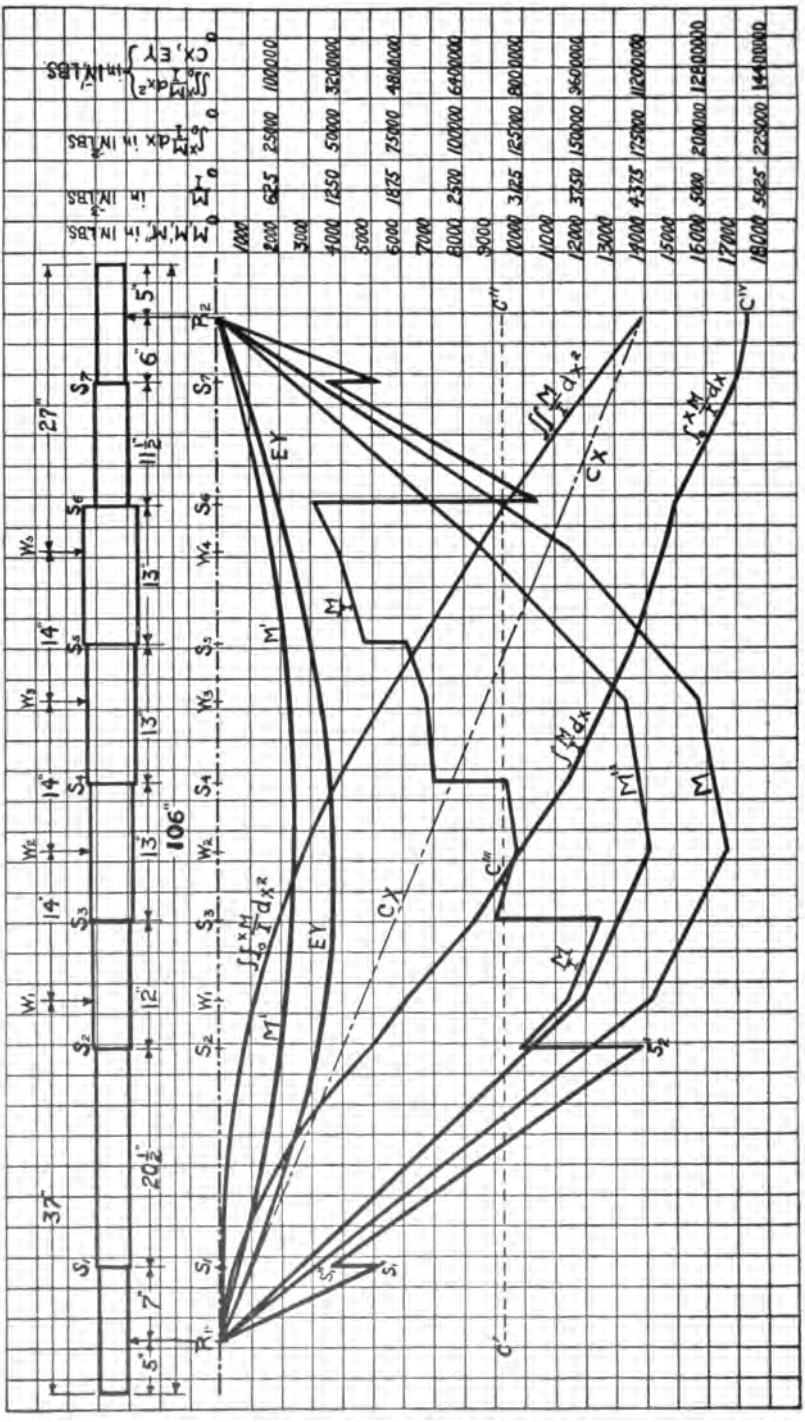

Fig. 97.

Column 3 gives the distance (in inches) from the origin R_1 to the point in question, as, for instance, the distance from R_1 to S_2 is 27.5 inches.

Column 4 gives the bending moments (in inch pounds) due to the weight of the shaft. The weight of the shaft is 214 pounds, and considering this weight uniformly distributed, each reaction at the bearings is 107 pounds. The bending moments under the load points are given in Table II.

TABLE II.

Under Point	Bending Moments in Inch Pounds.
W_1	$-107\times 32+\frac{214}{96}\times 32\times\frac{32}{2}=-2270$
W_2	$-107\times 46+\frac{214}{96}\times 46\times\frac{46}{2}=-2560$
W_3	$-107\times 36+\frac{214}{96}\times 36\times\frac{36}{2}=-2410$
W_4	$-107\times 22+\frac{214}{96}\times 22\times\frac{22}{2}=-1810$

The curve of bending moments due to the weight of shaft is shown as curve M' in Fig. 97 and is a parabola passing through the ordinates as given in Table II.

Column 5 of Table I gives the bending moments (in inch pounds) due to the concentrated loads. The reactions at the supports due to the concentrated loads are determined in Table III.

TABLE III.

Loads, lbs.	Reaction R_1, lbs.	Reaction R_2, lbs.
$W_1 = 217$	$217\times\frac{64}{96}=114.7$	72.3
$W_2 = 212$	$212\times\frac{50}{96}=110.4$	101.6
$W_3 = 200$	$200\times\frac{36}{96}=75.0$	125.0
$W_4 = 186$	$186\times\frac{22}{96}=42.6$	143.4
Total reactions	372.7	442.3

The bending moments due to concentrated loads under the load points are given in Table IV.

TABLE IV.

Under Point	Bending Moment in Inch Pounds.
W_1	$-372.7 \times 32 = -11\,920$
W_2	$-372.7 \times 46 + 217 \times 14 = -14\,100$
W_3	$-442.3 \times 36 + 186 \times 14 = -13\,310$
W_4	$-442.3 \times 22 = -9\,720$

The curve of bending moments due to concentrated loads is shown as curve M'' in Fig. 97.

Column 6 of Table I gives the combined or total bending moments (in inch pounds) under the various points on the shaft. Curve M in Fig. 97 gives the curve of combined bending moments. The addition of the ordinates of the parabolic curve M' and the ordinates of curve M'' will give a very slight curvature to the lines of curve M, but these lines have been taken as straight lines for simplicity, the error being entirely negligible.

Column 7 gives the moments of inertia (in inches^4) of the various cross sections of the shaft. The moment of inertia of the cross section of the shaft from R_1 to S_1 is 1.918, and from S_1 to S_2 it is 2.814, etc.

Column 8 gives the values of $\frac{M}{I}$ (in inch^{-3} pounds) at the various points along the shaft, M being the total bending moment at the point and I its moment of inertia of cross section. Curve $\frac{M}{I}$ in Fig. 97 gives the $\frac{M}{I}$ curve. At points S_1, S_2, S_3, . . ., S_7 the cross section changes suddenly and therefore the $\frac{M}{I}$ curve also changes suddenly, so that at each of these points there are two values for $\frac{M}{I}$.

Columns 9 and 10 give the results of the intermediate steps necessary to calculate the values of the first integral of $\frac{M}{I}\,dx$. From equation 295 we find that

$$\int_{x_2}^{x_1} \frac{M}{I}\,dx = \left(\frac{M_1 + M_2}{2}\right)\frac{x_2 - x_1}{I} \quad . \quad . \quad . \quad . \quad (295)$$

Column 9 gives the values of $\frac{x_2 - x_1}{I}$ and column 10 the values of $\frac{M_1 + M_2}{2}$.

Column 11 gives the values (in inch^{-2} pounds) of $\int_{x_2}^{x_1} \frac{M}{I}\,dx$ between successive points (from x_1 to x_2). These values are found numerically by multiplying the values in column 9 with the corresponding values in column 10. These values can also be found from curve $\frac{M}{I}$ in Fig. 97 as follows. The integral of $\frac{M}{I}\,dx$ between R_1 and S_1 is nothing more than the area between the $\frac{M}{I}$ line from R_1 to S_1 and the horizontal base line R_1S_1, that is, the area of the triangle $R_1S_1'S_1$. The distance S_1S_1' is -1615 and the distance R_1S_1 is 7, so that the area of this triangle is $-\frac{1615 \times 7}{2} = -5660$. The integral of $\frac{M}{I}dx$ between S_1 and S_2 is again nothing more than the area between the $\frac{M}{I}$ line from S_1 to S_2 and the horizontal base line S_1S_2, that is, the area of the trapezoid $S_1S_1''S_2'S_2$. The distance S_1S_1'' is -1102, the distance S_2S_2' is -4325, and the distance S_1S_2 is 20.5; therefore the area of the trapezoid is $\frac{-(1102+4325)}{2} \times 20.5$ $= -55\,620$. We can therefore determine the values in column 11 from the values of the various points on curve $\frac{M}{I}$.

Column 12 represents the $\int_0^x \frac{M}{I}dx$ from the origin (R_1) to the point in question. This is easily determined by adding all the values in column 11 between the origin R_1 and the point in question. Curve $\int \frac{M}{I}\,dx$ in Fig. 97 represents graphically this $\int_0^x \frac{M}{I}\,dx$.

Columns 13, 14, 15, and 16 are intermediate steps necessary to determine mathematically the $\int\int_{x_1}^{x_2} \frac{M}{I}\,dx^2$ between successive points on the shaft. From equation 301 we have

$$\int\int_{x_1}^{x_2} \frac{M}{I}\,dx = x^2 - x_1\int_0^{x_1} \frac{M}{I}\,dx + \frac{(x_2 - x_1)^2}{I}\,\frac{2M_1 + M_2}{6}. \quad (301)$$

Column 13 gives the value $x_2 - x_1\int_0^{x_1} \frac{M}{I}\,dx$ for each point on the shaft. For instance, this value between S_1 and S_2 is found by multiplying the value of $\int \frac{M}{I}dx$ at S_1 (-5660) by the distance between

S_1 and S_2 (20.5), that is, $-5660 \times 20.5 = -116\,000$; or this value between S_2 and W_1 is found by multiplying the value of $\int \frac{M}{I} dx$ at S_2 ($-61\,280$) by the distance from S_2 to W_1 (4.5), that is, $-61\,280 \times 4.5 = -275\,700$. Column 14 gives the values of the member $\frac{(x_2 - x_1)^2}{I}$ of equation 301. That is, the value of this member of the equation from R_1 to S_1 is found by squaring the distance $R_1S_1(7^2)$ and dividing it by the moment of inertia of the cross section of the shaft from R_1 to S_1 (1.918), so that $\frac{7^2}{1.918} = 25.55$. Column 15 gives the values of the last member $\frac{2M_1 + M_2}{6}$ of equation 284. The value of this member between R_1 and S_1 is found by multiplying the moment at R_1 (0) by 2, adding it to the moment at S_1 (-3100) and dividing by 6, or $\frac{0 \times 2 - 3100}{6} = -516$; or the value of this member from S_1 to S_2 is found by multiplying the moment at S_1 (-3100) by 2, adding it to the moment at S_2 ($-12\,190$) and dividing by 6, or $\frac{-3100 \times 2 - 12\,190}{6} = -3065$.

Column 17 is derived from columns 13, 14, 15, and 16, and represents (in inch^{-1} pounds) the $\int\int_x^{x_2} \frac{M}{I} dx$ solved, as shown in equation 301.

Column 18 represents the $\int\int_0^x \frac{M}{I} dx$ from the origin (R_1) to the point in question. This is determined by adding all the values given in column 17 between the origin R_1 and the point in question. Curve $\int\int \frac{M}{I} dx$ in Fig. 97 represents these values. By drawing a straight line from R_1 to the other end of this curve we can determine the value EY at any point by measuring the vertical distance between such a point on the curve and this straight line. These vertical distances can be plotted from the horizontal base line R_1R_2, and the resulting curve EY through these ordinates would give an EY curve, which would represent the deflection (Y) of the shaft multiplied by the constant E (coefficient of elasticity, for steel taken as 29 000 000). Another way of finding this deflection curve by a purely graphical method would be to take the first integral curve $\int \frac{M}{I} dx$ and deter-

mine its constant of integration. This is found by a trial and error method by choosing a horizontal line like $C'C''$ so that the area between the first integral curve $\int \frac{M}{I} dx$ and the constant line $C'C''$ is equal on either side of this constant line, that is, the area $C'R_1C'''$ is equal to $C'''C''C^{IV}$. This area between the line $C'C''$ and curve $\int \frac{M}{I} dx$ can be quickly determined by a planimeter, and line $C'C''$ shifted until the areas on either side of the constant line are equal. The second integral curve EY can then be found by allowing this curve to represent the summation of the areas between curve $\int \frac{M}{I} dx$ and line $C'C''$ up to any point in question. For instance, the ordinate on the EY curve at S_1 is found by making it equal to the area between line $C'C''$ and the $\int \frac{M}{I} dx$ curve from R_1 to S_1, and the ordinate for the EY curve under S_2 is found by making it equal to the area between line $C'C''$ and the $\int \frac{M}{I} dx$ curve from R_1 to S_2, and so on.

When no graphical method is used the ordinates of the EY curve can be determined mathematically from the values in column 18 by taking the last value in that column for point R_2 and dividing it by the distance R_1R_2, that is, $\frac{11\,151\,480}{96} = 116\,160$. This value multiplied by the value of x at any point will give the values of CX in column 19. The value EY, or the ordinates of the g curve, can then be found by adding the value of the second integral in column 18 to the corresponding value of CX in column 19. This is doing mathematically exactly what was done graphically by drawing a straight line from R_1 of curve $\int\int \frac{M}{I} dx$ in Fig. 97 to the other end of this curve and obtaining the value of EY by measuring the vertical distance from any point of this curve to the straight line. By letting $E = 29\,000\,000$ (for steel), Y, or the actual deflection in inches, can be determined for any point. For our problem it is only necessary to determine the deflections under the loads.

After determining the static deflections, a critical speed can be tentatively assumed, but as stated before, it is better to use in most

cases the approximate estimate of critical speed represented by equation 283, which reads

$$N = 187.7\sqrt{\frac{W_1y_1 + W_2y_2 + W_3y_3 + \cdots}{W_1y_1^2 + W_2y_2^2 + W_3y_3^2 + \cdots}} \quad . \quad . \quad (283)$$

In the above equation W_1, W_2, W_3, etc., represent concentrated loads, and therefore the weight of the shaft, which is a distributed load, cannot be taken directly into account. Some allowance can, however, be made by substituting for the actual loads W_1, W_2, W_3, etc., the equivalent loads which would produce the total or combined bending moments in column 6 of Table I. The equivalent concentrated loads and reactions can be found as follows:

$$R_1 = \frac{-14\,190}{32.0} = -\,443.5.$$

$$W_1 = \frac{-\,16\,660 + 4435 \times 46.0}{14.0} = 267.3.$$

$$W_2 = \frac{-\,15\,720 + 443.5 \times 64.0 - 267.3 \times 28.0}{14.0} = 243.2.$$

$$W_3 = \frac{-\,16\,660 + 524.8 \times 50.0 - 226.5 \times 28.0}{14.0} = 231.5.$$

$$W_4 = \frac{-\,15\,720 + 524.8 \times 36.0}{14.0} = 226.5.$$

$$R_2 = \frac{-\,11\,530}{22.0} = -\,524.8.$$

These equivalent concentrated loads and their corresponding deflections substituted in equation 283 give

$$N = 187.7\sqrt{\frac{267.3\times0.0973+243.2\times0.1043+231.5\times0.0919+226.5\times0.0649}{267.3\,(0.0973)^2+243.2\,(0.1043)^2+231.5\,(0.0919)^2+226.5\,(0.0649)^2}}$$

or

$$N = 187.7\sqrt{\frac{87.14}{8.050}} = 618 \quad . \quad . \quad . \quad . \quad . \quad . \quad 302$$

Hence the approximate, or trial, critical speed is 618 revolutions per minute.

The centrifugal forces caused by the equivalent concentrated loads W_1, W_2, W_3, etc., revolving at 618 revolutions per minute

and with an eccentricity equal to their deflections y_1, y_2, y_3, etc., respectively, can be found as in Table V.

TABLE V.

Equivalent Concentrated Loads. lbs.	Deflection y. inches.	Centrifugal Force at 618 r.p.m. C.F. = 10.86 Wy. lbs.	Ratio $\frac{W}{\text{C.F.}}$.
$W_1 = 267.3$	0.0971	282.0	0.944
$W_2 = 243.2$	0.1043	275.5	0.883
$W_3 = 231.5$	0.0914	229.8	1.007
$W_4 = 226.5$	0.0647	159.2	1.423

The centrifugal forces found in Table V can now be used for determining a new elastic curve of the shaft, and a new set of deflections y_1', y_2', y_3', etc., can be obtained. If the critical speed has been correctly chosen and the first trial elastic curve (in this case the static deflection curve) is the true elastic curve which the shaft assumes at the critical speed, we shall find that the deflections y_1', y_2', y_3', etc., will coincide exactly with the deflections y_1, y_2, y_3, etc., of the first trial elastic curve. That this will not be the case in this problem can be seen directly from Table V, because the ratio between the equivalent concentrated loads and their centrifugal forces is not constant. It is therefore necessary to find a new deflection curve, using the centrifugal forces as loads instead of the static weights. Taking these centrifugal forces as loads, the deflection curve is found either mathematically or graphically exactly as described before. Both methods are given without repeating a description of the method.

Table VI gives the results of the mathematical calculations for this new deflection curve and Fig. 98 gives the graphical method.

Table VII gives the deflections taken from Table VI when considering the centrifugal forces given in Table V as loads. In Table VII the first column again gives the original equivalent concentrated loads; column 2 gives the centrifugal forces of these loads at 618 r.p.m. and using the deflections of the first trial curve (static deflection curve); column 3 gives the deflections of the second trial curve,

TABLE VI.

1	2	3	4	5	6	7	8	9	10	11	12
Points along Shaft.	Distance between Successive Points. $(z_2 - z_1)$	Distance from the Origin R_1. z.	Bending Moments Due to Weight of Shaft.	Bending Moments Due to Concentrated Loads.	Combined Bending Moments. M.	Moment of Inertia of Cross Section. I.	$\frac{M}{I}$.	$\frac{z_2 - z_1}{I}$	$\frac{M_1 + M_2}{2}$.	$\int_{z_1}^{z_2} \frac{M}{I} dz = \left(\frac{M_1 + M_2}{2}\right) \frac{z_2 - z_1}{I}$ between Successive Points.	Total $\int_0^z \frac{M}{I} dz$ from Origin.
	in.	in.	in. lbs.	in. lbs.	in. lbs.	in.^{4}	in.$^{-3}$ lbs.	in.$^{-3}$	in. lbs.	in.$^{-2}$ lbs.	in.$^{-2}$ lbs.
R_1		0			0		0				0
	7.0					1.918		3.649	−1 590	−5 800	
S_1		7.0			−3 180		−1 658 −1 132				−5 800
	20.5					2.814		7.285	−7 835	−57 100	
S_2		27.5			−12 490		−4 445 −3 145				−62 900
	4.5					3.976		1.132	−13 515	−15 300	
W_1		32.0			−14 540		−3 660				−78 200
	7.5					3.976		1.887	−15 190	−28 700	
S_3		39.5			−15 840		−3 995 −2 895				−106 900
	6.5					5.477		1.187	−16 400	−19 500	
W_2		46.0			−16 960		−3 100				−126 400
	6.5					5.477		1.187	−16 625	−19 800	
S_4		52.5			−16 296		−2 980 −2 210				−146 200
	7.5					7.366		1.018	−15 895	−16 200	
W_3		60.0			−15 500		−2 105				−162 400
	5.5					7.366		0.747	−14 585	−10 900	
S_5		65.5			−13 670		−1 855 −1 453				−173 300
	8.5					9.401		0.904	−12 250	−11 100	
W_4		74.0			−10 830		−1 150				−184 400
	4.5					9.401		0.479	−9 725	−4 700	
S_6		78.5			−8 620		−916 −3 063				−189 100
	11.5					2.814		4.088	−5 785	−23 700	
S_7		90.0			−2 950		−1 050 −1 540				−212 800
	6.0					1.918		3.128	−1 475	−4 600	
R_2		96.0			0		0				−217 400

TABLE VI.

13	14	15	16	17	18	19	20	21
$(x_2-x_1)\int_0^x \frac{M}{I}dx = a.$	$\frac{(x_2-x_1)^2}{I} = b.$	$\frac{2M_1+M_2}{6} = c.$	$\frac{(x_2-x_1)^2}{I}\left(\frac{2M_1+M_2}{6}\right) = bc.$	$\int\int_{x_1}^{x_2}\frac{M}{I}dx_2 = a+bc.$ between Successive Points.	Total $\int\int_0^x \frac{M}{I}dx^2$ from Origin.	$CX.$	$EV.$	$\frac{Y}{(\text{when } E = 29\,000\,000)}.$
in.$^{-1}$ lbs.	in.$^{-1}$	in. lbs.	in.$^{-1}$ lbs.	in.$^{-1}$ lbs.	in.$^{-1}$ lbs.	in.$^{-1}$ lbs.	in.$^{-1}$ lbs.	in.
					0	0	0	0
0	25.55	−530	−13 500	−13 500				
					−13 500			
−118 900	149.3	−3 142	−469 100	−588 000				
					−601 500			
−283 000	5.09	−6 587	−33 500	−316 500				
					−918 000	3 775 400	2 857 400	0.0985
−586 500	14.15	−7 487	−105 900	−692 400				
					−1 610 400			
−695 000	7.72	−8 107	−62 600	−757 600				
					−2 368 000	5 427 100	3 059 100	0.1055
−822 000	7.72	−8 368	−64 600	−886 600				
					−3 254 600			
−1 097 000	7.54	−8 013	−60 400	−1 157 400				
					−4 412 000	7 078 800	2 666 800	0.0920
−893 400	4.11	−7 445	−30 600	−924 000				
					−5 336 000			
−1 473 000	7.68	−6 362	−48 900	−1 521 900				
					−6 857 900	8 730 500	1 872 600	0.0647
−830 000	2.16	−5 047	−10 900	−840 900				
					−7 698 800			
−2 174 000	47.0	−3 365	−158 200	−2 332 200				
					−10 031 000			
− 1 277 000	18.77	−983	−18 500	−1 295 500				
					−11 326 500	11 326 500	0	0

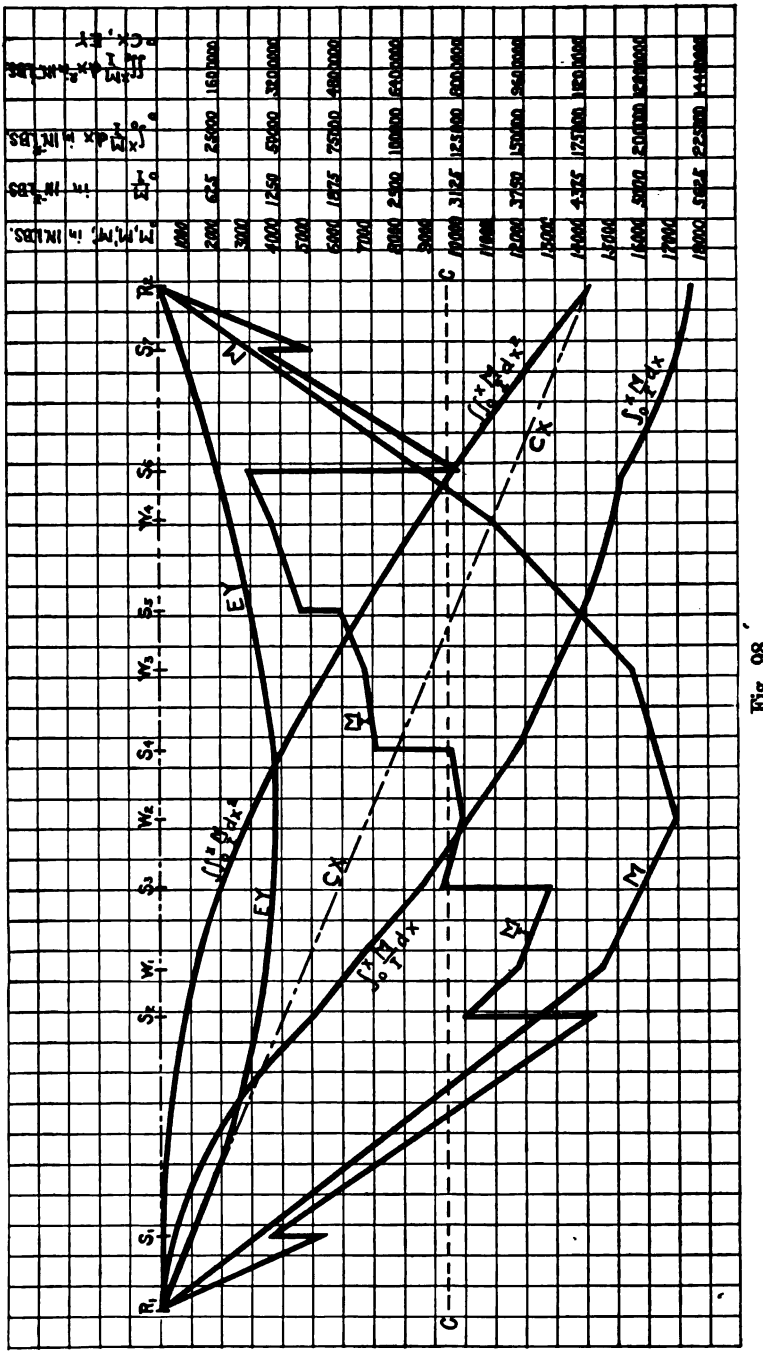

Fig. 98.

which is the deflection curve when using column 2 as loads; column 4 gives the centrifugal forces for the loads in column 1, with the deflections in column 3 at 618 r.p.m. If 618 r.p.m. were the true critical speed, then the ratios shown in column 5 would be unity. In practice, the ratios there given are so near to unity that 618 r.p.m. would be taken as a close enough value to the critical speed, but for illustration we shall proceed another step to show how a still more nearly accurate value can be obtained. If the ratios in column 5 had all been unity, then the sum of the values in column 2 would equal the sum of the values in column 4. Actually, the sum of the values in column 4 is somewhat larger than that of column 2 and therefore 618 r.p.m. must be slightly too great in value. A more nearly correct value would be

$$618\sqrt{\frac{946.5}{954.5}} = 615 \quad . \quad . \quad . \quad . \quad . \quad . \quad 303$$

Using 615 r.p.m. and the deflections of the second trial curve in column 3, Table VII, with the original equivalent concentrated loads a new set of centrifugal forces can be found, as shown in column 6 of Table VII.

TABLE VII.

1	2	3	4	5	6
Equivalent Concentrated Loads. lbs.	Centrifugal Force at 618 r.p.m., using Deflections in Table V. lbs.	Deflections, using Centrifugal Forces in Column 2 as Loads. inches.	Centrifugal Force at 618 r.p.m., using Concentrated Loads of Column 1 and Deflections of Column 3. lbs.	Ratio of Column 2 to Column 4.	Centrifugal Forces at 615 r.p.m., using Loads of Column 1 and Deflections of Column 3. lbs.
$W_1 = 267.3$	282.0	0.0985	285.9	0.986	283.4
$W_2 = 243.2$	275.5	0.1055	278.4	0.990	276.1
$W_3 = 231.5$	229.8	0.0920	231.2	0.995	229.3
$W_4 = 226.5$	159.2	0.0647	159.0	1.001	157.7
	946.5		954.5		

Again finding a new deflection curve, using the centrifugal forces just found in column 6 of Table VII, a third trial elastic curve results. This last curve is found exactly as were the two previous ones and the results of the calculation are given in Table VIII. The corresponding graphical solution is given in Fig. 99.

TABLE VIII.

1	2	3	4	5	6	7	8	9	10	11	12
Points along Shaft.	Distance between Successive Points. $(x_2 - x_1)$.	Distance from the Origin R_1. x.	Bending Moments Due to Weight of Shaft.	Bending Moments Due to Concentrated Loads.	Combined Bending Moments. M.	Moment of Inertia of Cross Section. I.	$\frac{M}{I}$.	$\frac{x_2 - x_1}{I}$.	$\frac{M_1 + M_2}{2}$.	$\int_{x_1}^{x_2} \frac{M}{I} dx = \left(\frac{M_1 + M_2}{2}\right) \frac{x_2 - x_1}{I}$ between Successive Points.	Total $\int_0^x \frac{M}{I} dx$ from Origin.
	in.	in.	in. lbs.	in. lbs.	in. lbs.	in.^{4}	in.$^{-2}$ lbs.	in.$^{-2}$	in. lbs.	in.$^{-2}$ lbs.	in.$^{-2}$ lbs.
R_1		0			0		0				0
	7.0					1.918		3.649	−1 590	−5 800	
S_1		7.0			−3 180		−1 658 −1 130				−5 800
	20.5					2.814		7.285	−7 840	−57 100	
S_2		27.5			−12 500		−4 440 −3 144				−62 900
	4.5					3.976		1.132	−13 530	−15 300	
W_1		32.0			−14 560		−3 663				−78 200
	7.5					3.976		1.887	−15 205	−28 700	
S_3		39.5			−15 850		−4 000 −2 900				−106 900
	6.5					5.477		1.187	−16 405	−19 500	
W_2		46.0			−16 960		−3 100				−126 400
	6.5					5.477		1.187	−16 620	−19 700	
S_4		52.5			−16 280		−2 975 −2 208				−146 100
	7.5					7.366		1.108	−15 890	−16 200	
W_3		60.0			−15 500		−2 105				−162 300
	5.5					7.366		0.747	−14 580	−10 900	
S_5		65.5			−13 660		−1 853 −1 450				−173 200
	8.5					9.401		0.904	−12 235	−11 100	
W_4		74.0			−10 810		−1 148				−184 300
	4.5					9.401		0.479	−9 705	−4 700	
S_6		78.5			−8 600		−915 −3 060				−189 000
	11.5					2.814		4.088	−5 775	−23 600	
S_7		90.0			−2 950		−1 050 −1 540				−212 600
	6.0					1.918		3.128	−1 475	−4 600	
R_2		96.0			0		0				−217 200

TABLE VIII.

13	14	15	16	17	18	19	20	21
$(x_2 - x_1)\int_0^{x_2} \frac{M}{I}\,dx = a.$	$\frac{(x_2 - x_1)^2}{I} = b.$	$\frac{2M_1 + M_2}{6} = c.$	$\frac{(x_2 - x_1)^2}{I}\left(\frac{2M_1 + M_2}{6}\right) = bc.$	$\int\int_{x_1}^{x_2} \frac{M}{I}\,dx^2 = a + bc$ between Successive Points.	Total $\int\int_0^{x_2} \frac{M}{I}\,dx^2$ from Origin.	$CX.$	$EY.$	$\frac{Y}{\text{(when } E = 29\,000\,000)}.$
in.$^{-1}$ lbs.	in.$^{-2}$	in. lbs.	in.$^{-1}$ lbs.	in.$^{-1}$ lbs.	in.$^{-1}$ lbs.	in.$^{-1}$ lbs.	in.$^{-1}$ lbs.	in.
					0	0	0	0
0	25.55	−530	−13 500	−13 500				
					−13 500			
−118 900	149.3	−3 143	−469 300	−588 200				
					−601 700			
−283 000	5.09	−6 593	−33 500	−316 500				
					−918 200	3 773 800	2 855 600	0.0985
−586 500	14.15	−7 495	−106 100	−692 600				
					−1 610 800			
−695 000	7.72	−8 110	−62 600	−757 600				
					−2 368 400	5 424 800	3 056 400	0.1054
−822 000	7.72	−8 366	−64 600	−886 600				
					−3 255 000			
−1 096 000	7.54	−8 010	−60 400	−1 156 400				
					−4 411 400	7 075 800	2 664 400	0.0919
−893 000	4.11	−7 443	−30 600	−923 600				
					−5 335 000			
−1 472 000	7.68	−6 355	−48 800	−1 520 800				
					−6 855 800	8 726 800	1 871 000	0.0646
−829 600	2.16	−5 037	−10 900	−840 500				
					−7 696 300			
−2 173 000	47.1	−3 365	−158 300	−2 331 300				
					−10 027 600			
−1 275 000	18.77	−983	−18 500	−1 293 500				
					−11 321 100	11 321 100	0	0

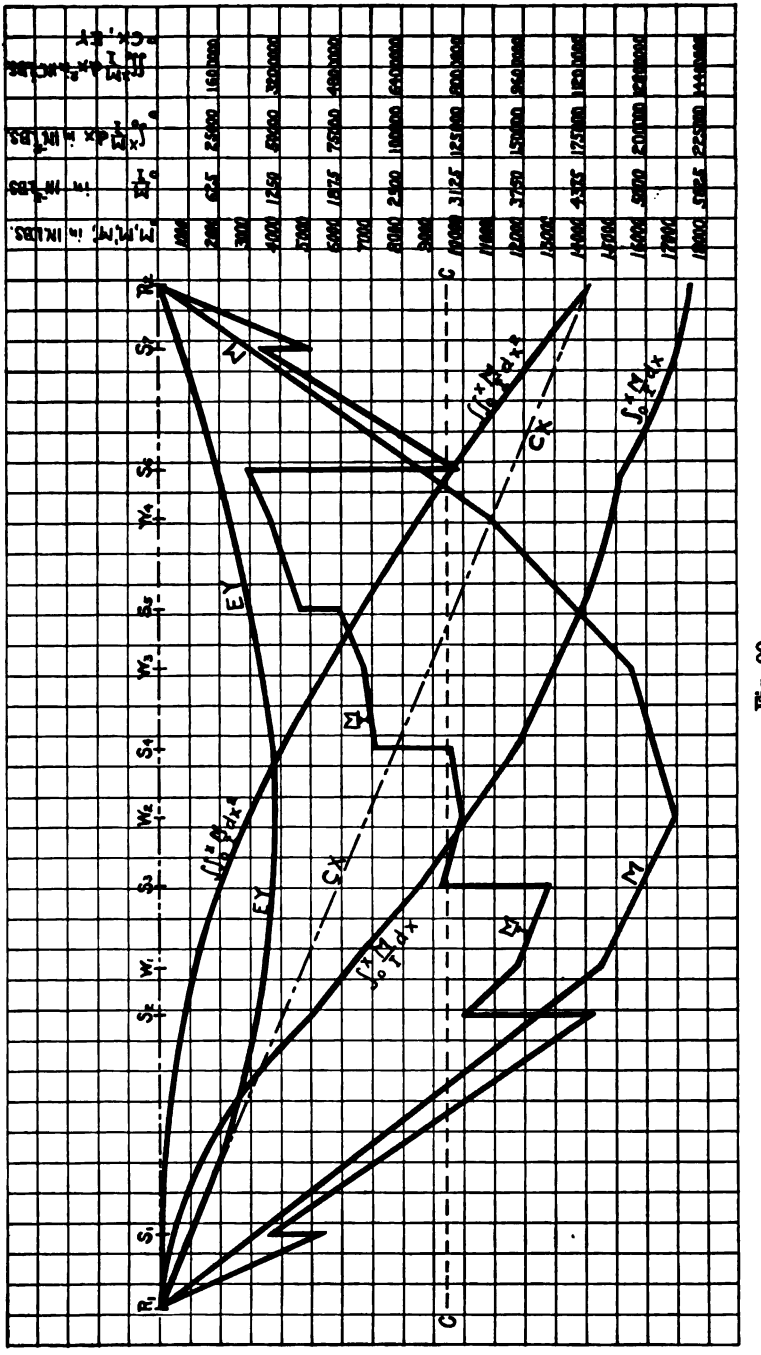

Fig. 99.

TABLE IX.

1	2	3	4	5
Equivalent Concentrated Loads. lbs.	Centrifugal Force at 615 r.p.m. from Column 6, Table VII. lbs.	Deflections, using Centrifugal Forces in Column 2 as Loads. inches.	Centrifugal Forces at 615 r.p.m., using Loads of Column 1 and Deflections of Column 3. lbs.	Ratio of Column 2 to Column 4.
$W_1 = 267.3$	283.4	0.0985	283.4	1.000
$W_2 = 243.2$	276.1	0.1054	275.8	1.001
$W_3 = 231.5$	229.3	0.0919	229.0	1.001
$W_4 = 226.5$	157.7	0.0646	157.4	1.002
	946.5		945.6	

In Table IX the first column again gives the original equivalent concentrated loads; column 2 gives the centrifugal forces of these loads at 615 r.p.m. and using the deflections of the second trial curve as given in Table VII; column 3 gives the deflections of the third trial curve taken from Table VIII and found by using the values in column 2 as loads; column 4 gives the centrifugal forces for the loads in column 1, with the deflections in column 3 at 615 r.p.m. These latter r.p.m. must be nearly equal to the critical speed because the ratio of column 2 to column 4 is practically unity. By adding column 2 and column 4 and again attempting to find a more nearly correct value we would find that

$$615\sqrt{\frac{946.5}{945.6}} = 615 \quad . \quad . \quad . \quad . \quad . \quad . \quad . \quad 304$$

or that 615 r.p.m. is the value of the critical speed.

It will be noticed that the approximate critical speed, according to equation 283, was 618 revolutions per minute, and that the true critical speed is 615 revolutions per minute. In this case the problem was so chosen that the true elastic curve is practically similar to the static deflection curve and therefore equation 283 gave almost the correct result. The method was also carried out to a degree of too great refinement by having too many trial curves, simply to show how each successive step more nearly approaches the correct result.

In cases where the various loads on the shaft (impellers) are forced on, that is, have very tight fits, and especially where the impeller hubs are long and stiff, the shaft becomes less flexible and the critical speed is greater than with impellers that have not as

stiff hubs or have less forced fit on the shaft. It is necessary for the designer to calculate the difference between the moment of inertia of the shaft alone and the equivalent moment of inertia of the shaft with forced-on impellers. This is rather difficult because the original forced fit of the impellers no longer holds when running near the critical speed; the impeller bore of course stretches as the speed of the shaft increases. The obliquity of the impellers when running, due to the deflection of the shaft, also influences the critical speed to some extent.*

* For a more complete discussion see author's translation of Stodola's "Steam Turbines," or the original book, fourth edition.

VI. TYPES OF CENTRIFUGAL PUMPS.

39. Historical Review.

In giving the history of the centrifugal pump it is necessary to include the history of the water turbine, because the former is a natural and logical outcome of the latter. Water wheels were in use in very early times, but the first water turbine which attracted the attention of scientists was a reaction wheel invented and built by Professor Segner,* in 1750. This turbine wheel allowed the water to escape from its periphery in a tangential direction and thus rotate the wheel by the reaction of the discharged water. Although Professor Segner attempted to establish a theory for the flow of water through this turbine, it remained for the great mathematician, Leonhard Euler† to explain the fundamental laws of flow. The latter also suggested a set of guide vanes for Segner's water turbine, which increased its efficiency.

For nearly ninety years after Euler's work, mathematicians and physicists paid no attention to his theories nor made any improvements upon Segner's turbine. In 1827 Fourneyron designed several radial flow turbines which gave such decidedly good results that the interest of scientists was awakened in the theory of these water motors. Poncelet in 1838 presented a paper before the French Academy‡ in which he discussed the shock losses at the ends of the impeller blades. He however limited his discussion by considering the stream of flowing water divided into a number of parallel streams and discussed only the occurrences in one of these streams. He suggested certain coefficients of water contraction to account for the difference between his theory and the results obtained in practice.

* Segner: "Theoria machinae cujusdam hydraulicae et computatio formae atque virum machinae hydraulicae nuper descriptae." Göttingae, 1750.

† Euler: "Recherches sur l'effet d'une machine hydraulique proposée par M. Segner à Göttingue." Histoire de l'Académie Royale, Berlin, 1750; also "Principes généraux du mouvement des fluides," 1755.

‡ Poncelet: "Sur la théorie des effets mécanique de la turbine Fourneyron." Comptes rendus, tome III, 1838.

In 1843 Combes * completed this theory by establishing coefficients of resistance similar to those established by Weisbach. Combes was also the first to refer to Euler's work again. The theory of water turbines was developed exactly as was the so-called practical theory of hydraulics, by limiting the investigation of water flow to two dimensions in a plane, whereas actually the laws for the flow of water should have been expressed in equations containing three dimensions. The coefficients found were unreal, but they corrected the error of neglecting the use of three dimensions. It is surely worth noting that this Poncelet-Combes theory, which was developed into a practical method by Redtenbacher,† contributed very little towards the advancement of turbine design.

New types of turbines were now introduced by engineers who designed them to conform to their practical ideas and from their experimental results without any of them paying much attention to theoretical considerations or established laws.‡ We shall merely mention the axial flow turbines of Henschel (1837) and Jonval, the axial-radial turbines of Francis (1849), the impulse turbines of Zuppinger (1844), Schwammkrug (1849), and Girard (1851), as well as the centrifugal pumps of Appold (1848) and Gwyne (1862). Theorists tried to establish the laws of flow for these new machines as far as the Poncelet method permitted, and succeeded in establishing some general rules of design.

Experiments on the shape of the blades were made in 1876 by R. C. Parsons and published in the Proceedings of the Institute of Civil Engineers, Vol. 47. Unwin, in 1877, derived formulæ from experimental results of Parsons. In 1885, Poillon¶ published a theoretical discussion of nearly all the types of pumps known at that time.

In the meantime the steam turbine began its conquest (about 1887). Zeuner, who had begun in 1856 to investigate the Francis turbine, started to collect all available results of experiments, and

* Combes: "Recherches théoriques et expérimentales sur les roues à réaction ou à tuyaux." Paris, 1843.

† Redtenbacher: "Theorie und Bau der Turbinen und Ventilatoren." Manheim, 1844.

‡ For a fuller description of the origin of water turbines and pumps, see Rühlmann, "Allgemeine Maschinenlehre," Vols. I and IV, 1875.

¶ Poillon: "Traité théorique et practique des pompes et machines à élever les eaux."

in 1899 presented his classical work, "Vorlesungen über Turbinentheorie." This work, like all of Zeuner's writings, was exceptionally good and gave a clear exposition and critical analysis of the fundamental laws of hydraulics. Zeuner made a large number of experiments both with turbine impellers and with steam turbine buckets. This book started a new epoch in the theory of turbines and overshadowed all previous work, and we might say it brought the Poncelet theory to an end.

From the beginning of the twentieth century steam turbines have developed rapidly and have achieved the greatest success of all rotating machines, and no doubt the rapid advance of this type of machine has given the centrifugal pump and the centrifugal compressor a great impetus.

In recent years a great many scientists have contributed to the theory of centrifugal pumps and a large amount of literature has been written. In 1903, Prasil * published an excellent presentation of the laws of flow of liquids through rotating buckets, treating the problem mathematically by means of cylindrical coördinates and using Euler's fundamental equations as a basis. In 1906, Dr. Lorenz † published an excellent treatise on the theory of centrifugal pumps, which started a very voluminous discussion among various writers upon this subject. In recent literature, Wagenbach, Gutermuth, Föttinger, Lewicke, Wagner, Rateau, Proell, Griesmann, Banki, Banninger, and others have contributed directly or indirectly to the better understanding of the theory of centrifugal pumps.

40. Modern Centrifugal Pumps.

All the early types of centrifugal pumps were of the low-pressure type and were used to lift very large quantities of water to small heights, as for example in draining ditches, emptying docks, etc. For this class of work the piston or reciprocating pump would have had excessive dimensions and would have been too expensive and therefore centrifugal pumps were used.

During the last fifteen years the high-pressure centrifugal pump has come into use and centrifugal pump design has gone through a

* Prasil: "Uber Flüssigkeitsbewegungen in Rotationshohlräumen," Schweizerische Bauzeitung, Vol. XLI, 1903.

† Lorenz: "Neue Theorie und Berechnung der Kreiselräder," 1906.

surprising stage of development. It remained for Sulzer Bros. to demonstrate by means of their high-pressure pumps installed at the silver mines in Horcajo, Spain, and at the Geneva waterworks in Switzerland, that it was possible to obtain good efficiency with centrifugal pumps delivering large quantities of water under high heads. The excellent results obtained at these installations led to the general introduction of centrifugal pumps in mines and large waterworks. To-day, centrifugal pumps successfully compete with piston pumps and the centrifugal pump cannot be disregarded in considering new installations of any water capacity whatever.

It is interesting to note that all the larger pump manufacturers are either building or contemplate building centrifugal pumps, chiefly because they realize that centrifugal pumps are superseding the piston type of pump in all services. The reciprocating pump situation to-day resembles that of steam engines some years ago when steam turbines became active competitors of the steam engine.

The chief advantages of centrifugal over reciprocating pumps are lower initial cost, less space requirement, greater adaptability to all possible conditions, less attention while operating, and finally, the great advantage of being capable of direct connection to a prime mover.

Centrifugal pumps are now found in every service imaginable. Recently they have been making great strides in mine work, owing to the small space required, their great reliability, and the light foundation permissible. The centrifugal pump operates without any vibration whatever when direct connected to a motor, and therefore heavy foundations are not necessary, as is the case with reciprocating pumps. This is no mean advantage, because heavy foundations are very difficult to construct in mines.

As the centrifugal pump delivers water continuously and without shock, the chance of breaking pipes is reduced to a minimum. By careful design of the impeller blades it is possible to close a valve at the end of the discharge line without having the pressure rise, thus obviating the danger of breaking the pipe or of shutting down the pump.

That all these advantages have been fully recognized in practice is shown by the speedy introduction of centrifugal pumps.

The reciprocating pump when direct connected to a motor still retains the great advantage of consuming from 5 to 10 per cent less

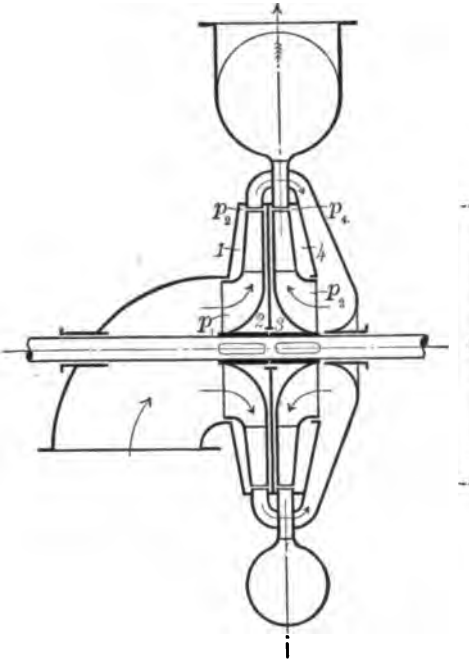

Fig. 100.

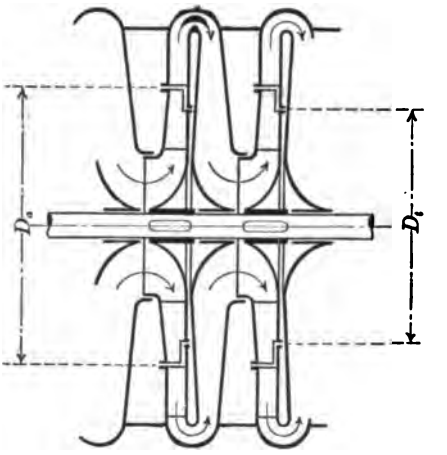

Fig. 101.

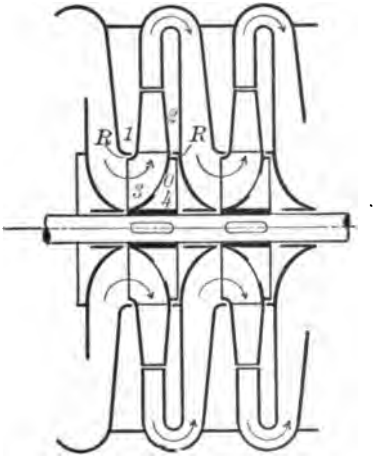

Fig. 102.

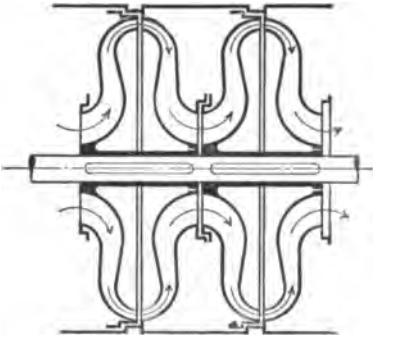

Fig. 103.

power. But if the reciprocating pump is driven by a belt or by gearing, its total efficiency will not be greater than that of a direct-connected centrifugal pump.

Not only is the initial cost of a centrifugal pump less than that of a reciprocating pump, but the motor for the former will also be considerably cheaper than for the latter. Direct-connected centrifugal pumps require high-speed motors, whereas reciprocating pumps require slow-speed motors.

In order that centrifugal pumps may find a still larger field, it is of first importance to obtain the highest efficiency and greatest reliability possible. Too much stress cannot be laid on the fact that centrifugal pumps require very careful design in the drafting room and the best workmanship in the shop, and only then is it

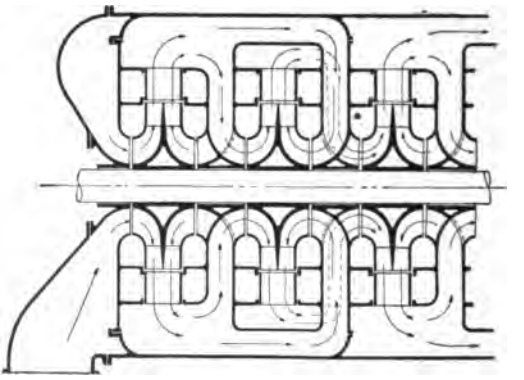

Fig. 104.

possible to obtain satisfactory efficiencies. This is especially true of high-pressure centrifugal pumps. Above all we should avoid using old patterns at the sacrifice of efficiency; each case should be carefully studied and every endeavor made to obtain the highest efficiency. It may truthfully be said that the striking success during recent years of the high-pressure centrifugal pump is chiefly due to the fact that pump manufacturers have insisted upon designs of the highest efficiency and the very best workmanship, irrespective of the increased cost of such designs.

There are various types of high-pressure centrifugal pumps. Five of the best-known types are shown schematically in Figs. 100 to 104. Fig. 100 represents a high-pressure centrifugal pump first designed by Sulzer and known as the Sulzer type. Fig. 101 represents the

Rateau type of high-pressure centrifugal pump. Fig. 102 shows a high-pressure centrifugal pump of the Jaeger type. Fig. 103 represents the Kugel-Gelpke type of high-pressure centrifugal pump. Fig. 104 is a high-pressure centrifugal pump known as the double-inlet or double-suction type.

The distinguishing features in all these types are the method of balancing the axial thrust and the method of guiding the water throughout the pump. The chief difficulty in the design of centrifugal pumps is the problem of eliminating as much of the end thrust as possible, and no design of centrifugal pump can be called reliable which does not practically eliminate axial thrust.

41. Sulzer Pumps.

The Sulzer pump was first made by Sulzer Bros. of Winterthur, Switzerland. This firm deserves the credit of having been the pioneer manufacturer of the modern high-pressure centrifugal pump. Sulzer Bros. were the first to recognize that for pumps delivering high heads guide vanes were necessary in order to obtain satisfactory efficiencies. Fig. 100 represents schematically a Sulzer pump. An equalization of the axial thrust in this type of pump is accomplished by mounting the impellers alternately in a reverse position so that the directions of thrust of any two adjacent impellers are opposite. Let F_1, F_2, F_3, F_4 be the projected areas of the sides of the impellers taken in a plane perpendicular to the shaft axis in the spaces 1, 2, 3, 4 respectively. With a sufficient clearance at the outer diameter of the impeller, pressure p_2 will exist in the spaces 1 and 2 and pressure p_4 in the spaces 3 and 4. As area F_2 is greater than area F_1, the first impeller will have an axial thrust A_1 towards the suction side and its value will be

$$A_1 = (F_2 - F_1)\,(p_2 - p_1),$$

in which p_1 represents the pressure at impeller entrance.

In the second impeller an axial thrust A_2 will exist in the opposite direction, whose value is

$$A_2 = (F_3 - F_4)\,(p_4 - p_3).$$

As these two axial thrusts are in opposite directions they will become neutralized or balanced when $A_1 = A_2$. As areas F_1 and F_2

can be made exactly equal to areas F_4 and F_3, the axial thrust can be eliminated when $(p_2 - p_1) = (p_4 - p_3)$. The difference of these pressures is nothing more than the existing clearance space pressures expressed by equation 23, provided that the rotating paraboloid is not considered. This equation is

$$H_{sp} = \eta H_n - \frac{w_a^2}{2g} \quad . \quad . \quad . \quad . \quad . \quad . \quad (23)$$

By dimensioning each set of guide vanes so that they are all similar, it is possible to keep the velocity head $\frac{w_a^2}{2g}$ equal for every set of guide vanes. If this is the case, the excess pressure in the clearance space is then dependent only upon the value of the existing pressure head ηH_n. In designing the pump the pressure heads of all impellers are taken the same, but through slight errors in construction the calculated values of the pressure heads will not be exactly realized nor will they be exactly equal. The resulting axial thrust caused by this inequality of pressure heads is taken care of by a rigid collar thrust bearing.

The arrangement of the impellers in pairs necessitates carrying the water from the exit of one impeller to the entrance of the next impeller in a novel manner. This arrangement is shown in Fig. 105, which represents a six-stage Sulzer pump in cross section. In this pump the water enters through the suction pipe into the first impeller and then passes through it into the guide channel. From the latter the water is led through a reversing channel, which may be considered a continuation of the guide channel, to the entrance of the next impeller. This reversing channel passes between the succeeding guide channels. This is accomplished by casting the guide apparatus so that alternate passages are provided for the guide and the reversing channels. From the second impeller the water passes through the second set of guide vanes into an S-shaped channel, which leads it to the entrance of the third impeller.

In spite of the complicated water passages the water guidance is very efficient, as there are no very sharp turns used.

Another advantage of arranging the impellers in pairs is that clearance space losses occur only upon one side of the impeller rim. This type has a disadvantage in not being able to use an odd number of impellers, because the impellers must always be arranged in

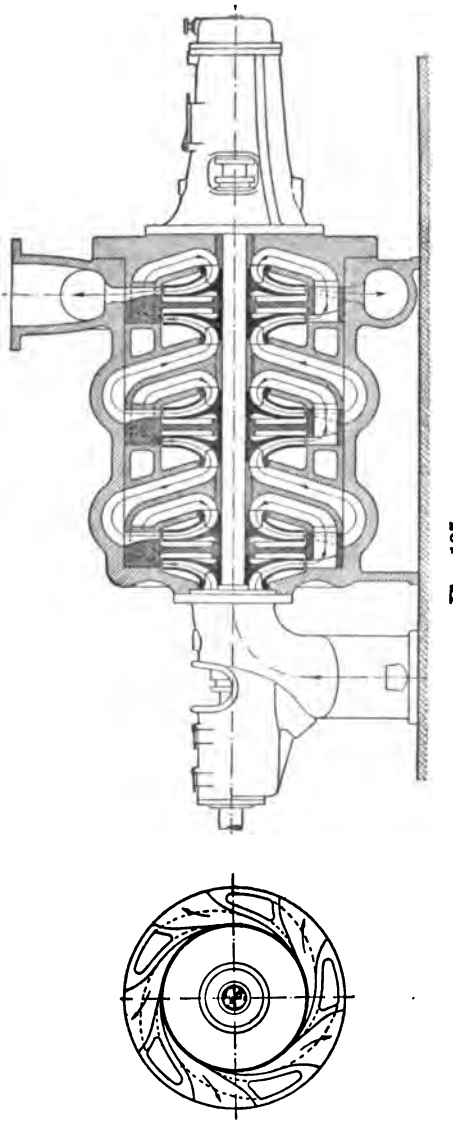

Fig. 105.

pairs in order to balance axial thrust, and therefore this type loses in adaptability for different pressure heads. Another disadvantage is the need of making two patterns for the impellers, one right-handed and the other left-handed. This also demands carrying double the number of impellers in stock for spare or repair parts.

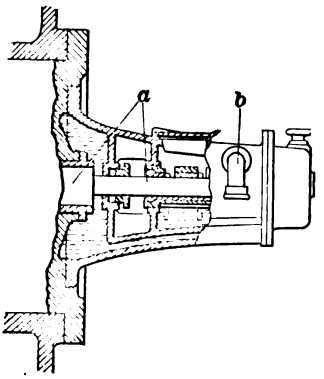

Fig. 106.

The pump shown in Fig. 105 has three pairs of impellers. The water after passing through these six impellers and guide vanes is led to a circular casing, to which is connected a conically diverging delivery pipe. The six impellers with guide apparatus are assembled in a casing cast in one piece. The pump shaft has two bearings. On one end the shaft is carried in a bearing mounted upon the elbow of the suction pipe and provided with ring lubrication. On the other end the bearing is fastened to the head of the casing and this bearing also carries the collar thrust bearing. The stuffing box at the high-pressure end is so arranged (see Fig. 106) that the water

Fig. 107.

leaking through it at *a* enters a hollow space around the shaft lining and flows out of the drainpipe *b*. This arrangement has two advantages: first, the stuffing box is greatly unloaded because it need only hold against a very small unbalanced pressure, which is the differ-

ence between the high pressure in the pump and the pressure necessary to force the water through the drainpipe *b*; and second, the thrust bearing is very efficiently cooled.

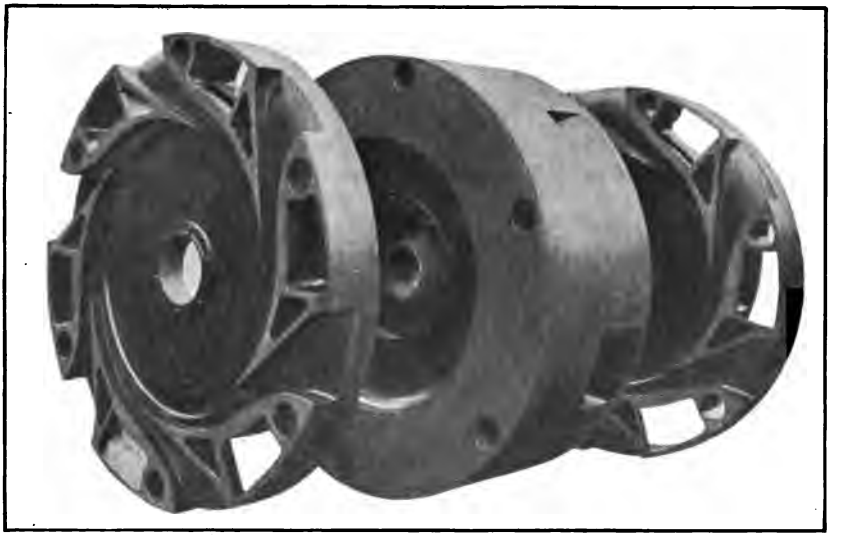

Fig. 108.

Further detailed construction of the Sulzer pump can be seen in Figs. 107 and 108. Fig. 107 shows four impellers arranged in pairs

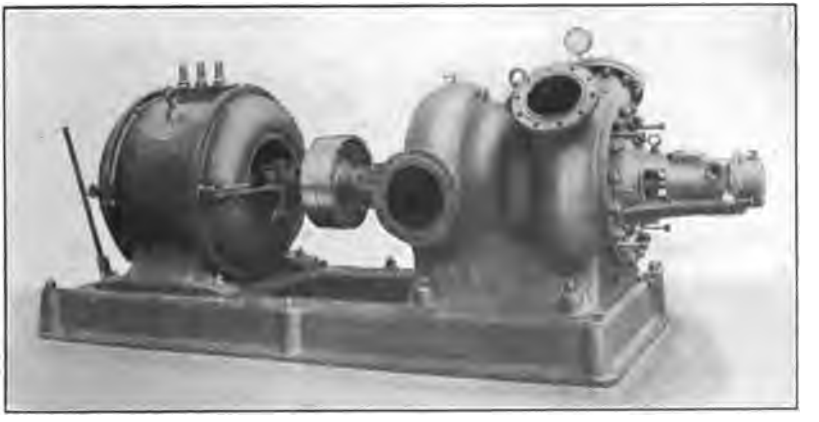

Fig. 109.

upon the shaft, and Fig. 108 the inner parts of the pump, including the guide vanes.

The pump casing is usually made of cast iron, but for high pressures it is made of cast steel. The impeller and guide vanes are made of special composition bronze and the shaft is nickel steel. For special cases certain parts have acid-proof linings. The casing

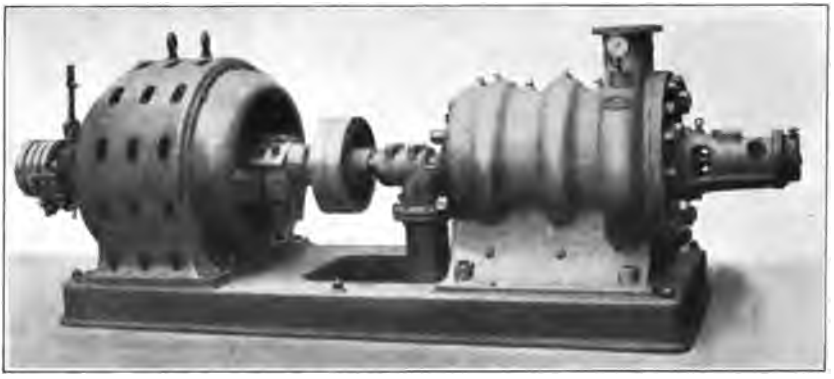

Fig. 110.

is made in one piece and is permanently connected to the foundation. In disassembling this pump the high-pressure head is first removed. This head contains the bearing and is on the free end of

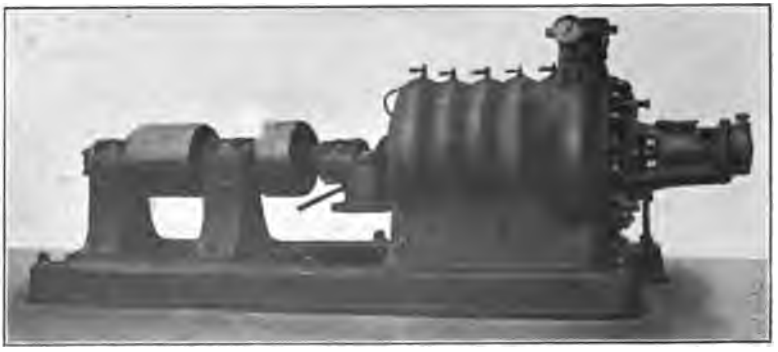

Fig. 111.

the pump. The impellers and diaphragms containing the reversing channels can then be disassembled successively from the shaft. The advantage of this construction is that the suction and discharge pipes need not be disconnected when the pump is opened for inspection.

Figs. 109–112 show other designs of Sulzer pumps. The pump shown in Fig. 109 has no suction pipe elbow, the suction space being a concentric ring, such as is often used when the suction con-

nection must be made at one side. Fig. 110 shows a normal type of Sulzer pump with electric drive and Fig. 111 one with belt drive.

The Sulzer high-pressure centrifugal pump for a mine shaft is mounted vertically and directly connected to a motor. The unit is assembled upon a suitable framework. The general arrangement of such a pump is shown in Fig. 112. The framework is made of structural steel, and wooden shields are placed below and above the unit to protect the pump and motor from falling bodies or from bodies thrown up by explosions. The sheave for the shaft rope used in raising or lowering the pump is fastened to the upper crosspiece of the framework. The sides of the framework are provided with slippers for proper guidance. The motor is generally of the enclosed type and is connected to the pump by a flexible coupling. A ladder placed along the side makes the pump and the motor more accessible. One of the first large installations of centrifugal pumps was for the silver mines of the Compañia Minera y Metalurgia del Horcajo, Spain.* At first only three pumps were installed with equal heads of about 430 feet and operated one above the other in different galleries of the mine. Later a fourth pump of equal head was installed in a still lower gallery. Fig. 113 shows the arrangement of the pumps in the mine. The lowest pump draws the water from a pit and raises it to the next pump. The other pumps receive the water under pressure and therefore work without suction head, so that no air can find a way into the pump. As all the pumps are of the same size they take care of equal quantities of water when running at the same speed.

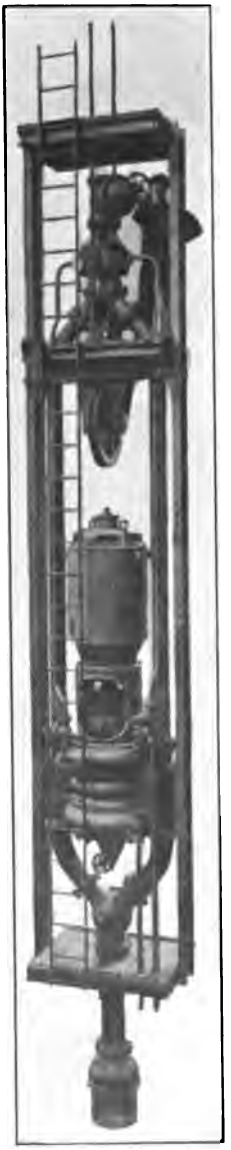

Fig. 112.

* This installation has been discussed in full by Dr. F. Heerwagen in the Zeitschrift des Vereines deutscher Ingenieure, 1901.

While in this case the pumps are placed at various heights, it is best in most cases to install all the pumps in the lowest gallery. This arrangement is shown in Fig. 114, which represents an installation by Sulzer Bros. for the Viktor Mine in Rauxel, Westphalia, Germany. Two four-stage centrifugal pumps were connected in series. At 1040 r.p.m. these pumps deliver 250 cu. ft. of water per min. against a total head of 1720 feet and require 562 h.p. to drive each pump.* Later two six-stage pumps were added of more modern construction, each capable of delivering 230 cu. ft. of water per min. and each connected to a 1100 h.p. motor running at about 1500 r.p.m. These two units, pumping 460 cu. ft. of water per min., occupy practically no more space than the older units supplying only 250 cu. ft. of water per min. The four-stage pumps have impellers 24 inches in diameter, while the six-stage pumps have impellers 20 inches in diameter. One six-stage pump delivers the same head as the two four-stage pumps in series.

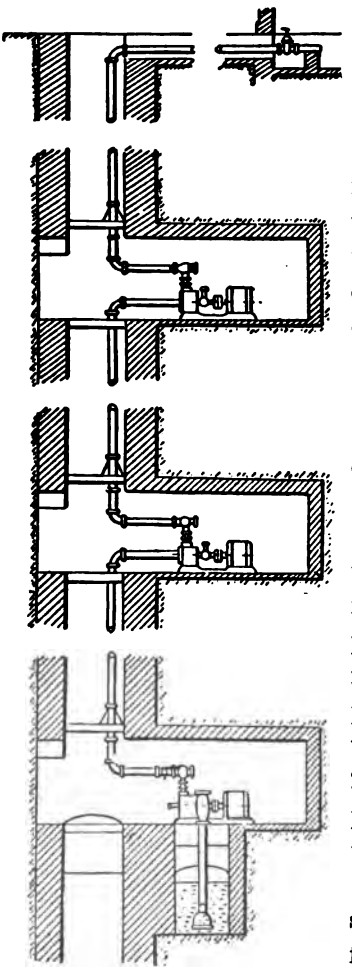

Fig. 113.

The Boiler Inspection Society of Essen, Germany, in 1903 made a very careful test of the two four-stage pumps.† The following results were obtained:

	Under Test Conditions. Per cent.	Under Operating Conditions. Per cent.
Efficiency of the power plant, including the loss of transmission to motors	83.52	82.54
Efficiency of pump installation, motor and pump	71.25	71.25
Efficiency of the pump	76.00	76.00
Efficiency of total installation	59.51	58.79

* Herzog, Elektrische Bahnen und Betriebe, 1905.

† Zeitschrift des Vereines deutscher Ingenieure, 1904.

The arrangement of the pumps and motors is shown in Fig. 115. Pump *A* draws water from the well and discharges it into the intake

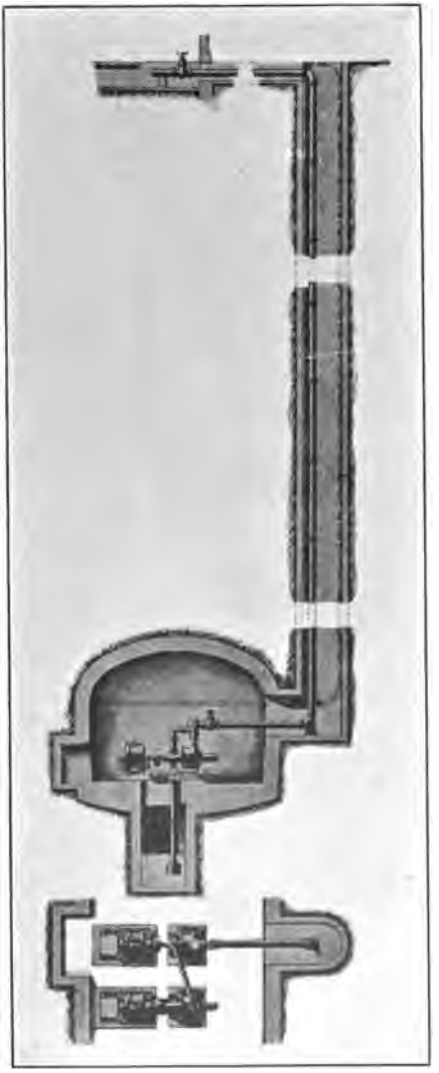

Fig. 114.

pipe of the second pump *B* under a pressure of 882 feet head (382 pounds per square inch). The water leaves the second pump at a head of 1764 feet. This means a pressure of 765 pounds per square

inch in the discharge pipe. The suction line is provided with a safety and a foot valve and the discharge piping contains a throttle and a non-return valve. This prevents the entire water column from exerting a pressure on the pumps should they be stopped. Should no non-return valve be installed then both pump casings must be designed to stand a pressure of 765 pounds per square inch.

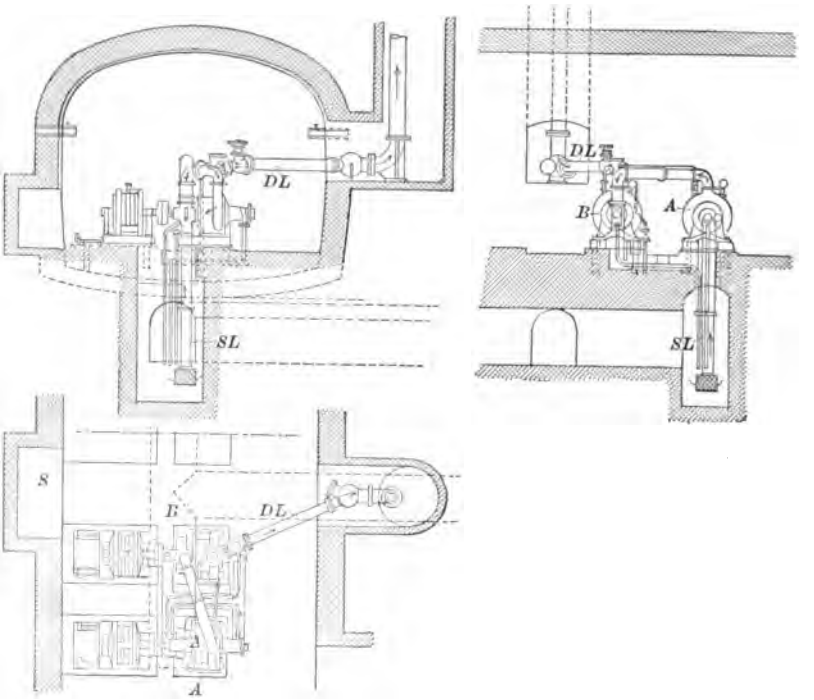

Fig. 115.

The pumps are direct connected to the motors by means of a leather band coupling. The starting and stopping of these pumps are controlled from the power station, so that only an emergency switch and two ammeters need be installed at the pumps. The starting of these pumps is as follows:

The main throttle valve in the discharge piping remains closed. The pumps are filled with water by means of an auxiliary connection to the discharge pipe and all air in the pump casings is allowed to escape. The generator at the power house is then started and its excitation slowly increased. As soon as the pumps show a pressure

of about 407 feet (176 pounds per square inch) greater than the water head in the discharge pipe, the throttle valve is slowly opened. Then this excess of pressure slowly decreases as the quantity of discharge increases. When the throttle valve is closed the load on the generator in the power station is about 30 to 35 per cent of the normal load under operating conditions. As the valve slowly opens the load on the generator increases. The entire time necessary to start this plant from the time current is turned on until water is discharged from the pressure or delivery pipe is said to be only one minute. If the time interval between starting the pumps and opening the throttle valve is too great the water in the pump casings becomes

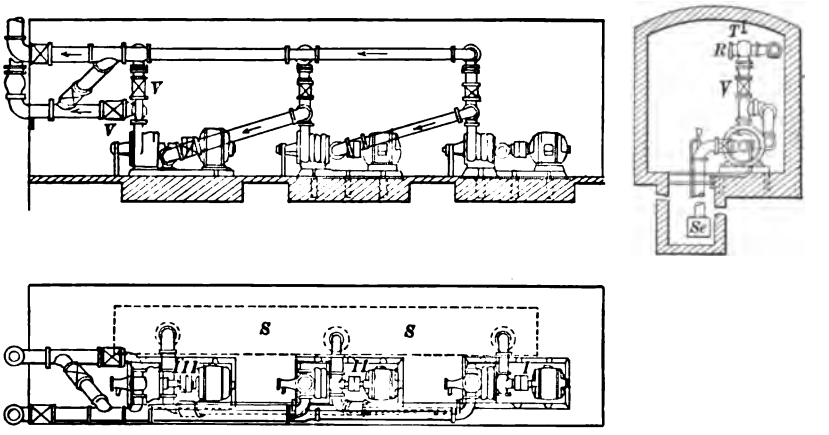

Fig. 116.

heated and it is necessary to shut down the pumps for some minutes and refill them with water. The shutting down of the pumps takes place in reverse order. The throttle valve is first slowly closed and then the generator is unloaded by cutting down the excitation. The attendants control these operations by means of a telephone.

Another very interesting installation of Sulzer Bros. is the pumping station of the Kasimir Mines in Niemce, owned by the Warschauer Gesellschaft für Kohlenbergbau und Hüttenbetrieb. Fig. 116 shows this installation. Three centrifugal pumps are used. Each pump delivers 141.25 cubic feet of water per minute against 538 feet head at 975 r.p.m. The pumps are so arranged that they can operate at

times against high pressure and normal quantity, or at times against low pressure and a large quantity of discharge. When operating against high pressure the pumps are connected in series so that the first pump discharges into the second and the second into the third. By this arrangement the three pumps deliver 141.25 cubic feet of water per minute against a head of 3 times 538 feet, or against a total head of 1614 feet, which lifts the water out of the mine. If the pumps are to deliver a large quantity, the valves are so set that the pumps discharge into a common discharge line and lift the water out of a common well. The three pumps then deliver 3 times 141.25 cubic feet of water per minute, or a total quantity of 423.75 cubic feet of water per minute against a head of 538 feet, which lifts the water to the next higher gallery of the mine. Two discharge pipes are used, one leading to the top of the mine and the other to the next higher gallery.

Centrifugal pumps are of especial value as shaft pumps in mines. The limited space given to mine shafts necessitates a pump occupying minimum space. Electrical power is also a great advantage in this class of work.

Sulzer Bros. installed the first large shaft pump installation in a mine shaft in Silesia, Germany. This installation is of greater interest than ordinary because reciprocating pumps were not capable of taking the water out of the submerged shaft. The service which the pumps had to take care of was briefly as follows.

A shaft 1312 feet deep at the Donnersmarck Mine was to be drained. At a depth of 328 feet springs were encountered which flooded the entire shaft. After the water in the shaft overflowed it was found that there was a constant flow of about 530 cubic feet per minute. An attempt was made to drain this shaft with reciprocating pumps, but only three pumps could be installed in the small cross section of the shaft and these could only deliver 350 cubic feet of water per minute, not considering the time lost on account of the great number of repairs needed. The pumps could not drain the shaft, and finally the mine was abandoned. In order to save this valuable property, Sulzer pumps were ordered as an experiment.

Three shaft pumps were built, each capable of delivering 283 cubic feet of water per minute against 525 feet head when running at 970 r.p.m. The three pumps in parallel could therefore deliver 849 cubic feet per minute. The space occupied by these pumps in

the mine shaft is shown in Fig. 117. When the reciprocating pumps of 350 cubic feet capacity were installed there was not room enough for a cage, while with centrifugal pumps of 849 cubic feet capacity there was room enough for two cages. These centrifugal pumps solved the problem.

The current required by the vertical induction motors was delivered from a power station nearly four miles distant from the mine. The power station contained two gas engines of 2000 h.p. supplied with blast-furnace gas.

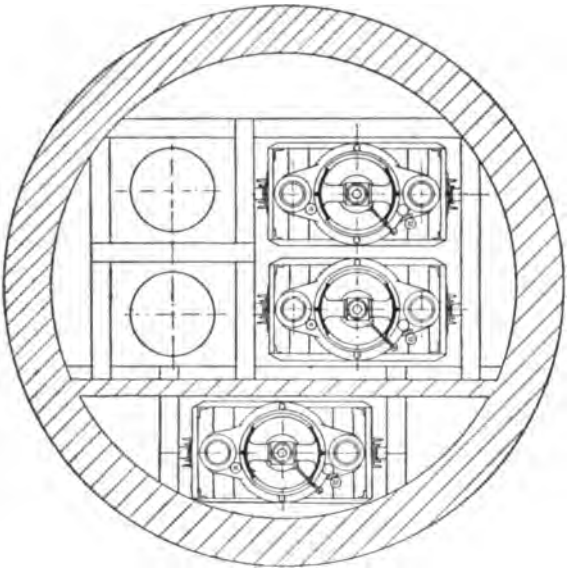

Fig. 117.

After a very short time this shaft was drained and the pumps were permanently installed in the lowest gallery of the mine to keep it drained, which proved that these centrifugal pumps were satisfactory in every particular.

Lately the centrifugal pump has been used in large water-pumping stations. The first large pump of this type was built by Sulzer Bros. for the waterworks of the city of Geneva, Switzerland. Fig. 118 shows this installation of pumps direct connected to motors. The pumps were of two-stage design, with impellers 3.6 feet (43.2 inches) in diameter. At 540 r.p.m. each pump delivered 795 cubic feet

of water per minute against a head of 460 feet, consuming about 1000 h.p.

Sulzer Bros. have installed a very large pumping station for the city of Milan, Italy. At first three pumping stations were installed in which direct-connected induction motors furnished the power for the pumps. All three stations had power supplied from a common power plant. Later a fourth pumping station was installed in which the pumps were belted to gas engines.

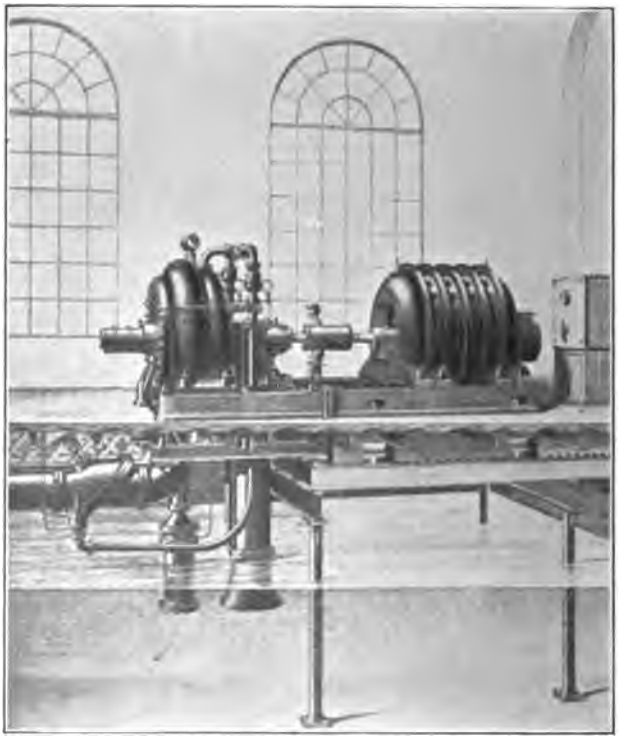

Fig. 118.

The source of water supply in Milan consisted of wells sunk at various places, about forty-five in all. From these wells the water is piped into large receivers, in which a vacuum is held by air pumps. From these vacuum receivers the pumps draw the water. The largest pumping station is in Loreto and is shown in Fig. 119. The pumps draw the water from a common suction pipe out of the vacuum

receiver *SW*. The pipes *S* bring the water to the receiver. All four pumps deliver into a common discharge pipe *D*. The four pumps deliver 509 cubic feet of water against 187 feet head while running at 820 r.p.m. Fig. 120 gives a photographic view of the interior of the pumping station at Loreto.

Although Sulzer Bros. built a large number of pumps of the type shown in Fig. 100, they have now practically abandoned the back-to-back construction and have arranged the impellers as in the Rateau

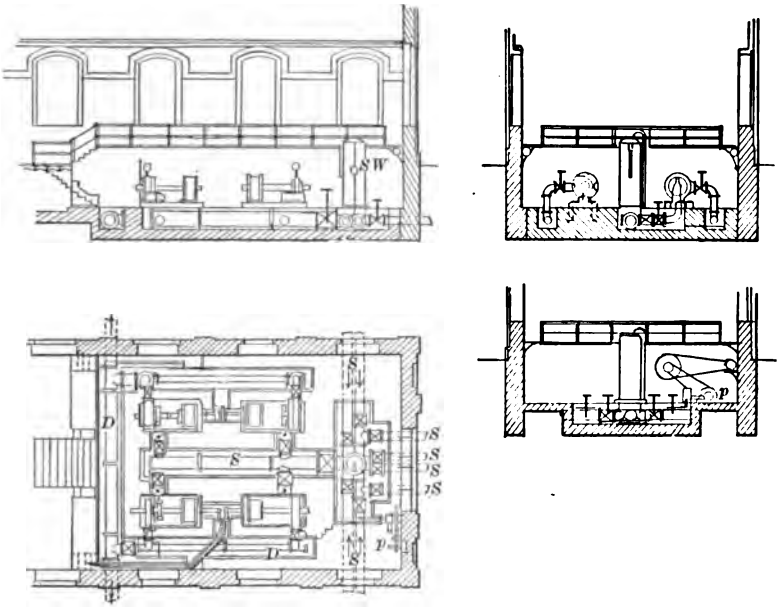

Fig. 119.

and Jaeger types. A pump of their new type was exhibited at the Bavarian Industrial and Trade Exposition in Nuremberg during 1906. The reason for this change evidently lies in the disadvantages mentioned previously. The disadvantages of having to arrange the impellers in pairs, which made such an arrangement less adaptable for different heads and also necessitated the making of right- and left-handed impellers, was a great handicap. The complicated casting necessary for the water guidance was another great disadvantage. Besides all this, experience proved that after a certain time of operation axial thrust developed, which in high-speed pumps could not

be properly cared for. The reason for this increased axial thrust was the wear of the packings between the two impellers of a group. All these disadvantages were sufficient to cause Sulzer Bros. to abandon their old type in spite of the excellent results they had obtained with it.

In Sulzer's latest construction an axial thrust must occur, and this thrust is taken care of by a balancing piston. This piston, Fig. 121, is placed behind the last impeller on the high-pressure end of the pump. The diameter of the piston is so chosen that it can balance

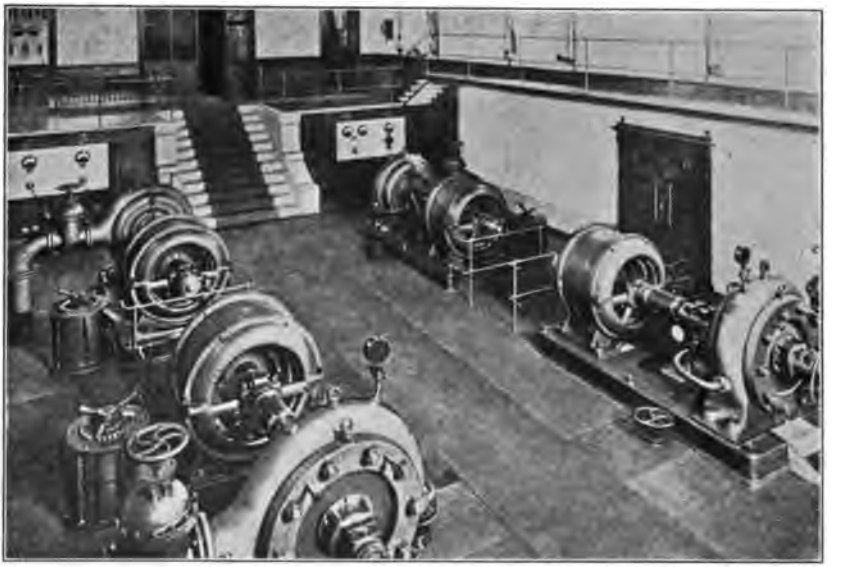

Fig. 120.

the axial thrust developed by the pump. The piston is shown in Fig. 121 as part *P* and is keyed to the shaft. It is held firmly on one side by the impeller *L* and on the other side by a nut *N*. The operation of this balancing piston is as follows.

In the clearance space *a* a high pressure exists, which varies with the final pressure of the pump. The water in space *a* can pass through the annular clearance *d* between the piston and the lining and flow to space *b*, where it is greatly reduced in pressure because of its being throttled by the clearance *d*. From *b* the water flows through the clearance space *c* into a space connected with a drain. Should the pump pressure increase for any reason, the pressure in space *a*

also increases and moves the shaft and piston slightly to the left. This decreases the clearance space *c* until the pressure in *b* has been

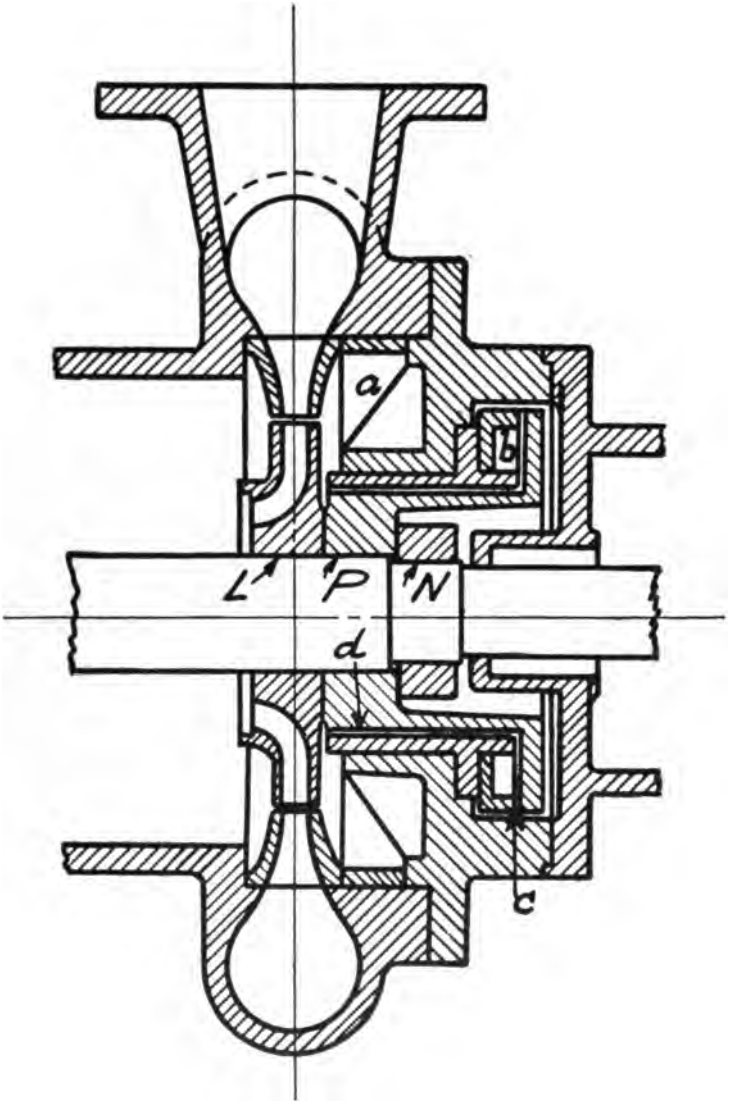

Fig. 121.

sufficiently increased to balance the axial thrust, causing the movement of piston *P*. If the pump pressure decreases, the pressure in *a* also decreases and the shaft and piston move to the right sufficiently

to release some of the pressure in space *b*, thus again balancing axial thrust.

This balancing arrangement is supposed to work automatically and does not necessitate the manipulation of any valves. The movement of the piston and shaft need be but very slight. Placing the balancing piston at the high-pressure end of the pump renders unnecessary a stuffing box packing against high pressure.

42. Rateau Pumps of Sautter Harle & Co.

Fig. 101 shows schematically the arrangement of a Rateau type high-pressure centrifugal pump. This type of pump was first built by Sautter Harle & Co. of Paris. The water guidance in this type

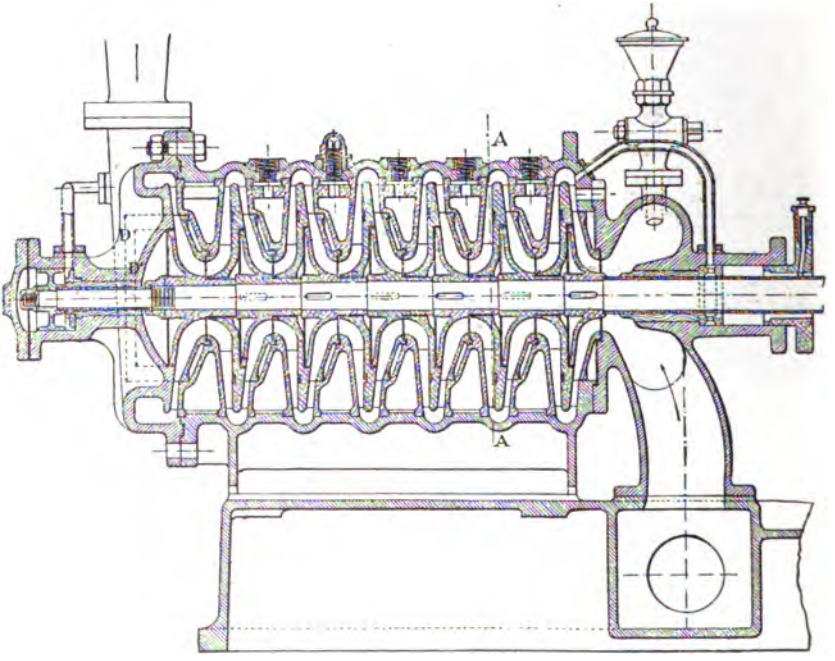

Fig. 122.

is in a wave-like direction. After leaving the impeller the water is carried in a radial direction through the guide vanes and then turned in the reversing channels through approximately 180°. The exit end of the reversing channel contains directing vanes. (See Fig. 122.)

These directing vanes are so formed that one end of the vane lies parallel to the direction of the water in the reversing channel, permitting the water to enter without shock, and the other end of the vane at entrance to the impeller is given the proper direction desired for the absolute entrance velocity. To neutralize the end thrust the two sides of the impeller are shrouded to different diameters. This is clearly shown in Fig. 101. The impeller blades extend to diameter D_a; the left-hand side of the impeller is shrouded to this diameter, while the right-hand side is shrouded only to diameter D_t. A lower pressure exists at diameter D_t than at diameter D_a because

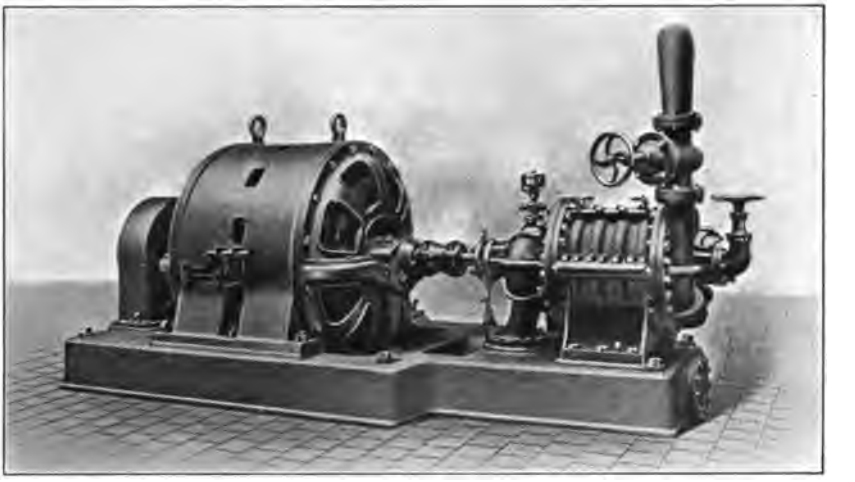

Fig. 123.

the value $\frac{u_a^2 - u_e^2}{2g}$ is smaller at the former than at the latter diameter. This arrangement therefore gives a higher pressure in the clearance space a than in the clearance space b.

It is quite difficult to make a correct choice in the dimensions of the impeller diameters D_a and D_t so that the total pressures on both sides of the impeller will be balanced. This arrangement permits of only a partial balance. Complete balance is finally obtained by means of a balancing piston keyed to the shaft beyond the last impeller on the high-pressure side. This piston rotates in a cylindrical casing with very small clearances. (See Fig. 122.) On one side of the piston full water pressure exists, while the other side can

be connected to any pressure stage or to the suction end of the pump. The axial thrust is neutralized by the difference of the pressures on the opposite sides of the piston. Sautter Harle & Co. found that the surfaces of the piston were worn by the grit carried through with the water. They therefore provided a special lubricating arrangement to prevent the rapid wear of the piston.

By using a part of the impeller blades unshrouded on one side, it can be seen that the flow of water through the impeller is interrupted and that eddy and impact losses must take place.

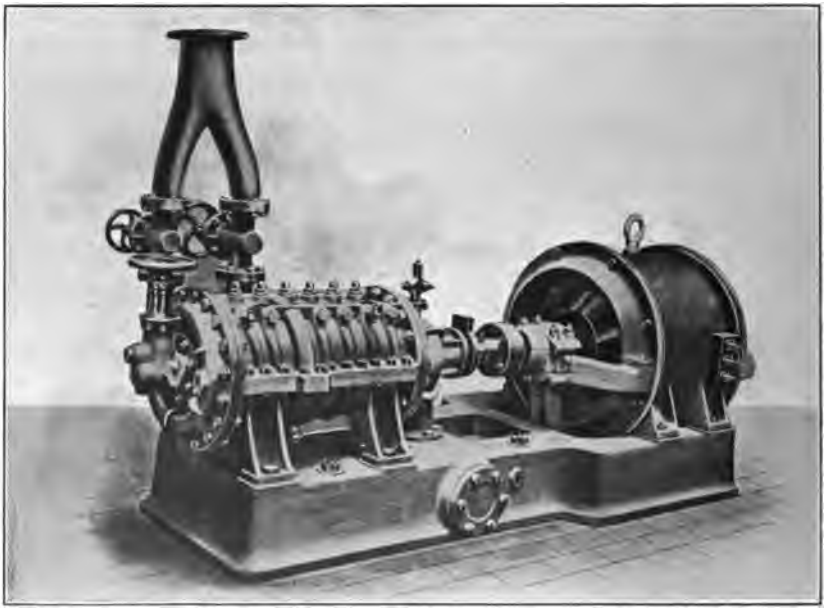

Fig. 124.

The Rateau pump casing is made in two parts and is bolted together in a horizontal plane passing through the center line of the shaft. With this arrangement the inside of the pump is accessible after removing the upper half of the casing. The shaft and impellers can be removed after the suction and high-pressure heads have been disassembled. This construction necessitates making a water joint where three separate parts come together. This occurs in the horizontal dividing plane between the upper and lower casing where the high-pressure and suction heads join the casing. Ex-

perience has shown that at such a place leaks will occur, especially at the high-pressure end.

Fig. 123 shows a motor-driven Rateau pump. This pump delivers 150 cubic feet per minute against a head of 590 feet. It is direct connected to a three-phase, 3000-volt motor running at 1450 r.p.m. The total efficiency of the unit is 57 per cent when running under normal conditions. The shaft efficiency of the pump is 64 per cent. This pump is installed in the mines of the Huanchaca Company in Bolivia, 13 800 feet above the level of the sea. The

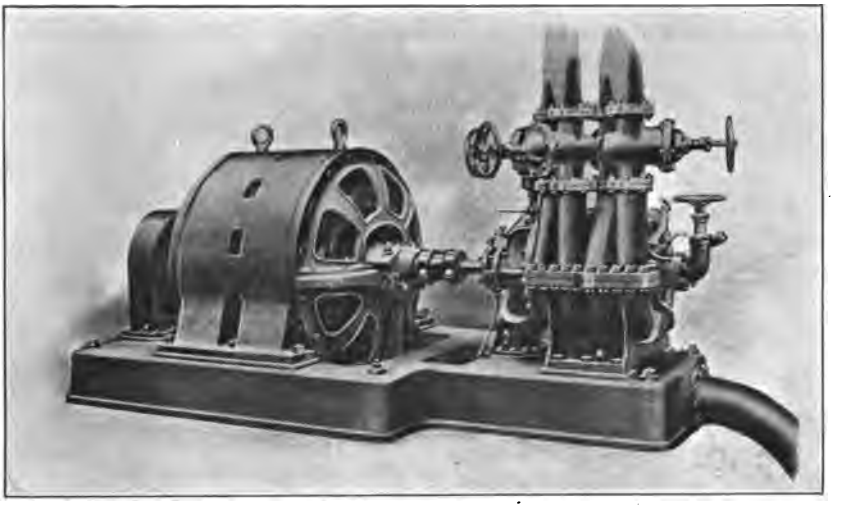

Fig. 125.

barometric pressure at this height is only 17.7 inches of mercury. The pump has a suction head of 8 feet. The conditions under which this pump works make the use of a reciprocating pump prohibitive.

Fig. 124 represents a multi-stage high-pressure pump with two discharge openings. It is installed in the Portes Mines. The pump is direct connected to a three-phase 1000-volt motor running at 1380 r.p.m. The pump is capable of lifting the water to two levels. When working against a head of 270 feet the pump delivers 474 cubic feet of water a minute, and when working against a head of 440 feet it delivers 31 cubic feet a minute.

There is also installed at the Huanchaca Mines a pump capable of delivering 150 cubic feet of water per minute under heads of 100, 200, 300, and 400 feet. This pump is illustrated in Fig. 125. The division of this pump into four pressure heads is very useful in draining the mine and where it is necessary to lift the water from the lower gallery either entirely out of the mine or to any one of the intermediate galleries.

Fig. 126 illustrates a turbine-driven pump installed in a mine in European Turkey. The turbine is a low-pressure unit receiving steam at a pressure of about 10 pounds per square inch. The set

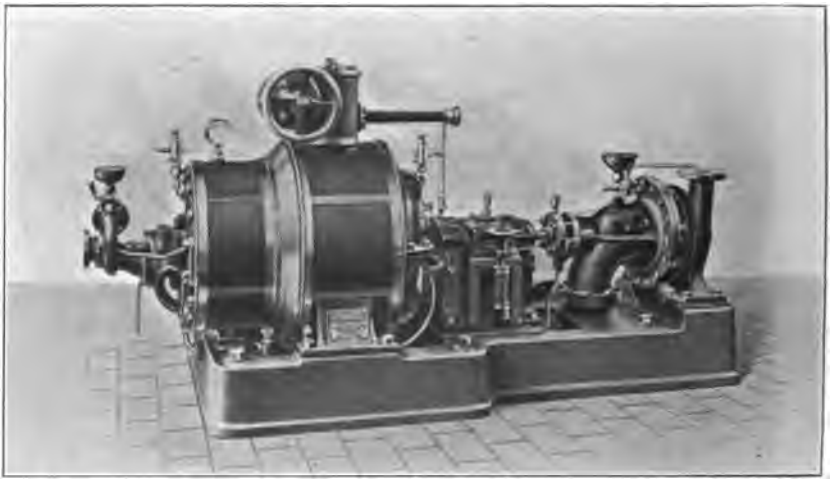

Fig. 126.

runs at 4500 r.p.m. and delivers 65 cubic feet of water per minute against a head of 223 feet. A test of this set was made with 7.7 pounds per square inch steam pressure at the turbine throttle and a vacuum of 25.8 inches of mercury; the number of revolutions was 4460 per minute. The total head delivered by the pump was 228 feet and the quantity of discharge 64.7 cubic feet of water per minute. The total efficiency was about 31 per cent, corresponding to a consumption of 36 pounds of steam per horse-power hour of water pumped.

Fig. 127 shows a turbine-driven pump for the Lens Mines. The unit can deliver 23.5 cubic feet of water per minute against a head of

394 feet, the steam pressure at the turbine being 170 pounds per square inch gauge. Sautter Harle & Co. have been quite successful in getting very good efficiencies even with very small quantities of discharge. They built a pump delivering only 14.5 cubic feet of water per minute against a head of 1312 feet. The pump ran at 2900 revolutions per minute.

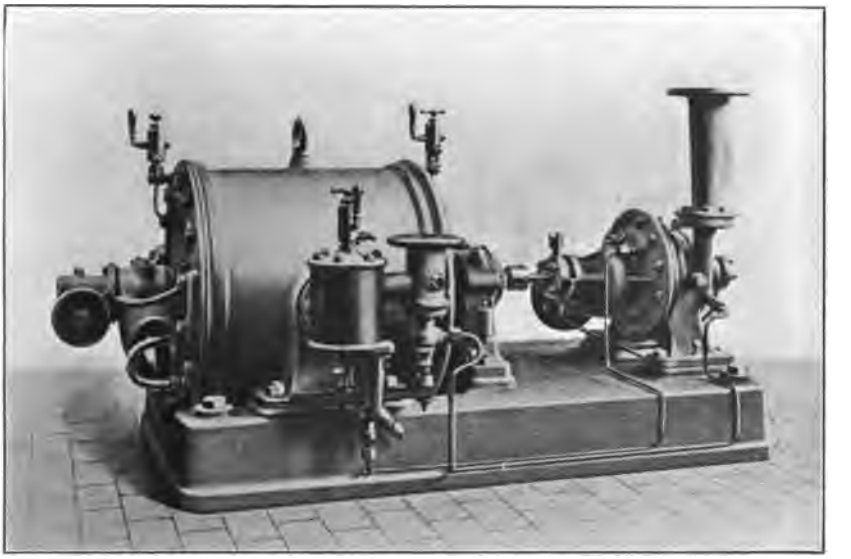

Fig. 127.

Fig. 128 represents an installation of both a high- and low-pressure turbine direct connected to a Rateau centrifugal pump. There is a small pump used for the ejector condenser direct connected to this unit. Fig. 129 gives a plan and elevation view of this installation, in which *A* is the multi-stage pump, *B* the high-pressure steam turbine, *C* the low-pressure steam turbine, *D* the pump for the condenser, and *E* the ejector condenser. Fig. 130 gives a plan and elevation view of the reciprocating pumping unit which was replaced by the turbo pump just described. The latter occupies just one-tenth the space of the former. There is also a decided difference in the foundation requirements in favor of the turbo unit. When the expense of operation and maintenance of the two units are considered the contrast is very marked. Tests of the turbo unit give the following results:

Quantity of water pumped per minute	156.5 cu. ft.
Total head of water	1194 ft.
Revolutions per minute	2200
Steam pressure (absolute)	101 lbs. per sq. in.
Exhaust pressure (absolute)	1.62 lbs. per sq. in.
Consumption of steam per horse power delivered (not including condensation)	22.7
Total efficiency of the unit	0.425

This firm also builds vertical pumps for mine shafts. Fig. 131 illustrates an electrically driven vertical shaft mine pump for the Huanchaca Company of Bolivia. It delivers 151 cubic feet of water per minute against a head of 121 feet. The revolutions per minute

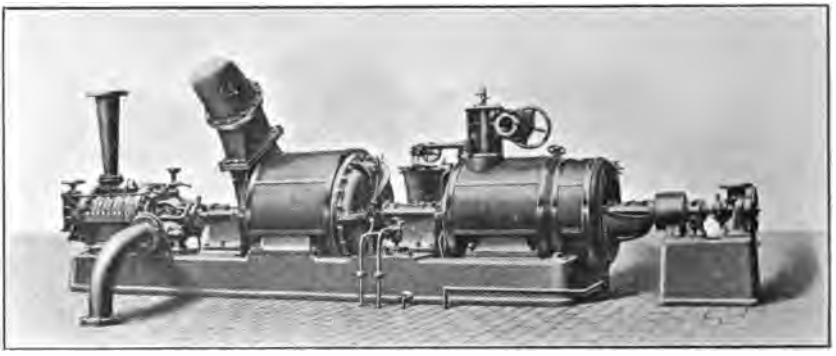

Fig. 128.

are 737 and the efficiency of the complete unit is 65.2 per cent. The motor is a three-phase 500-volt alternator and it consumed 39.7 kilowatts when delivering the quantity of water and head above stated.

Rateau in conjunction with Piccard also designed a multi-stage centrifugal pump driven by a hydraulic turbine. Piccard is known through his engineering work in connection with the hydraulic turbines at Niagara Falls. The hydraulic turbine is mounted on a horizontal shaft carrying the impellers of the multi-stage centrifugal pump. The complete unit is illustrated in Fig. 132. The unit entirely disassembled is shown in Fig. 133. The diameter of the wheel of the water turbine is 12 inches and the turbine develops more than 120 h.p. The pump was built to work against a head of 518 feet at 2300 r.p.m. The tests made in Geneva by Rateau and Piccard gave extremely favorable results. At these tests the highest

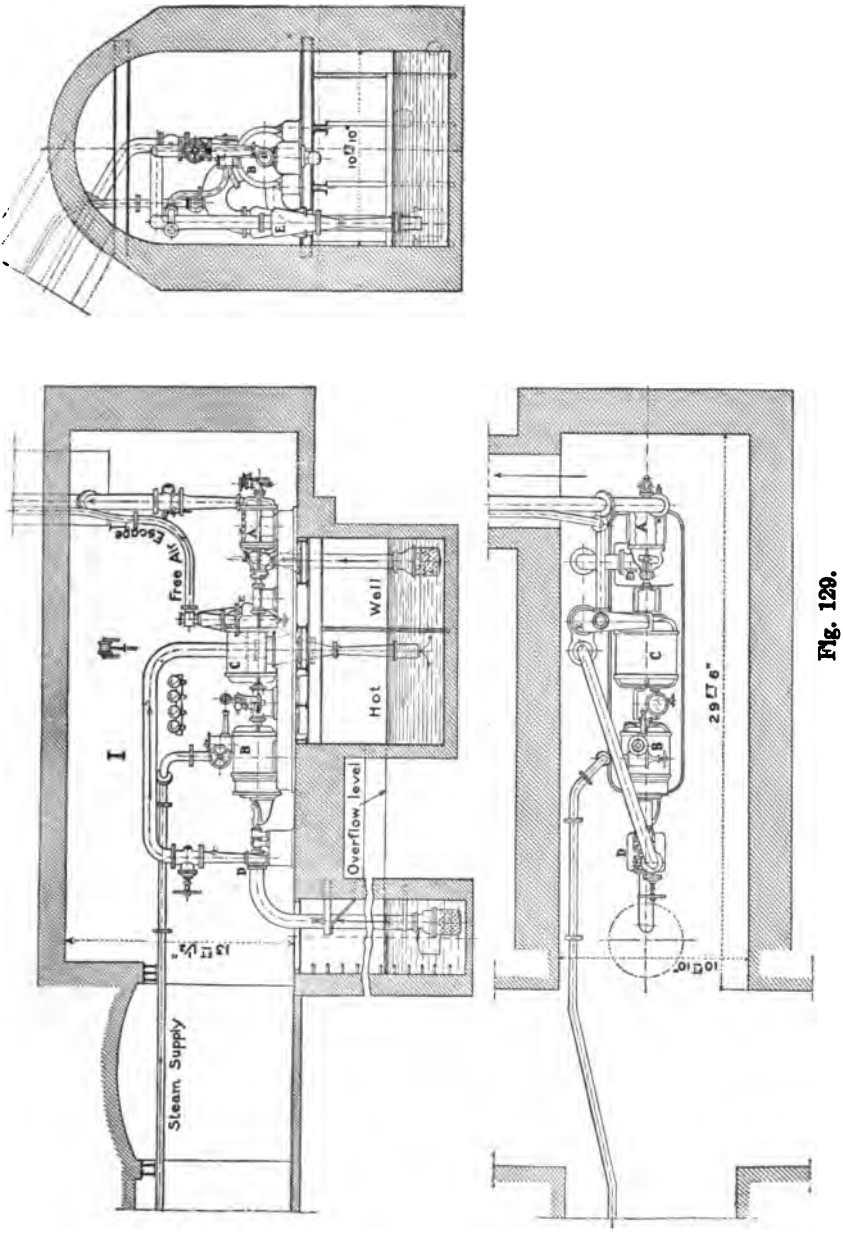

Fig. 129.

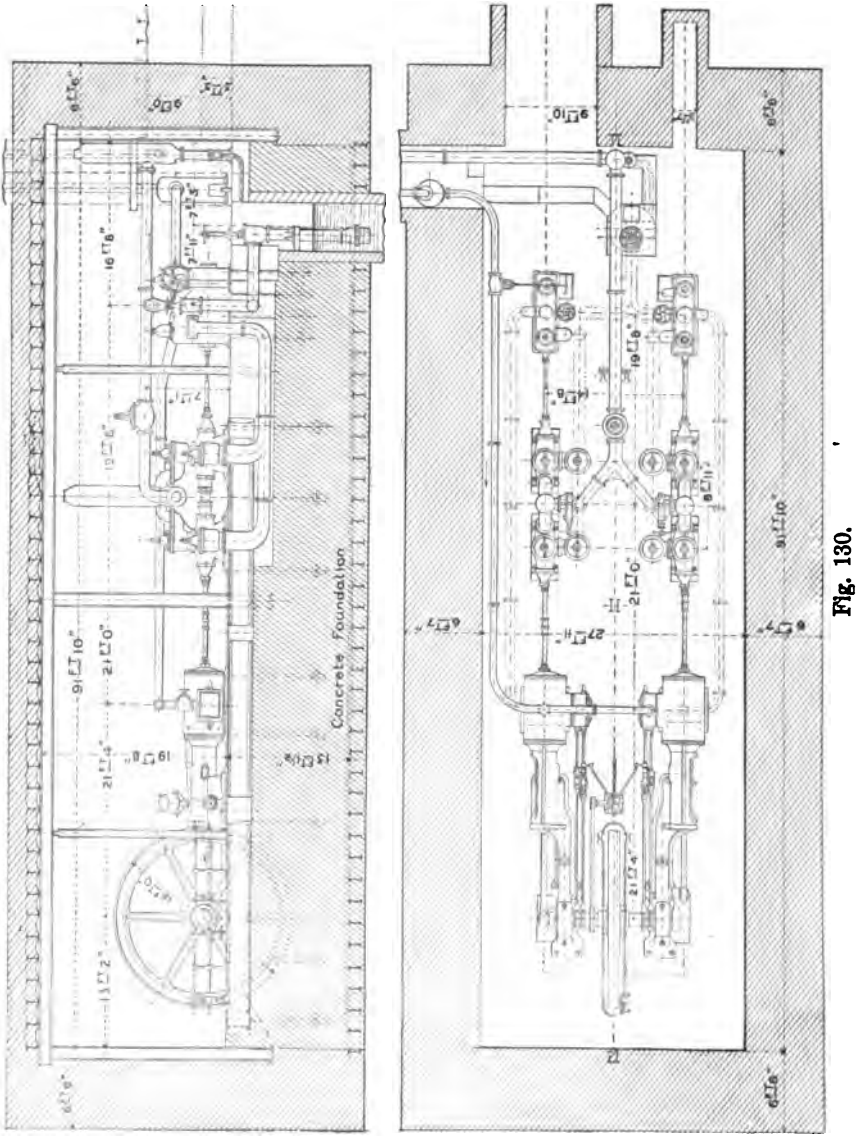

Fig. 130.

head obtainable was 427 feet, which was the height of the highest reservoir in the city. The results of the tests were as follows:

Quantity of water delivered to the hydraulic turbine per minute	173.4 cu. ft.
Head of water for hydraulic turbine	424 ft.
Quantity of water delivered by pump per minute	87.7 cu. ft.
Head delivered by pump	404 ft.
Total efficiency	0.48

Fig. 131.

The efficiency of the centrifugal pump was 68 per cent and that of the turbine 71 per cent, which is very satisfactory for a machine of such small dimensions. This pump was constructed for the Darien Gold Mining Co., and placed at the bottom of their mine. The hydraulic turbine was driven by water carried to it under a very high head, which furnished enough power to lift this same water together with water in the mine up to the surface of the mine.

This kind of hydraulic turbo pump is very useful for lifting water from a small waterfall to hotels or residences situated at higher levels,

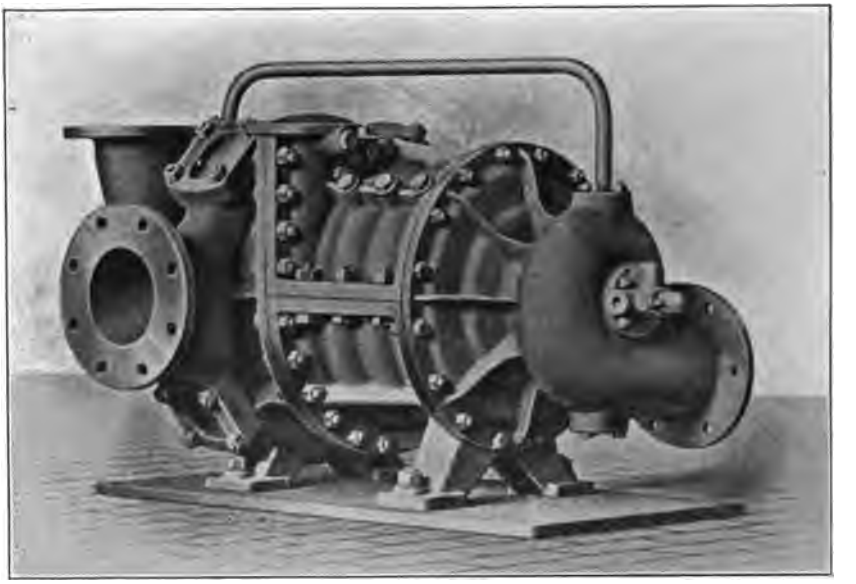

Fig. 132.

or even for supplying water to cities in mountainous regions. In these cases the head available for the hydraulic turbine is less than

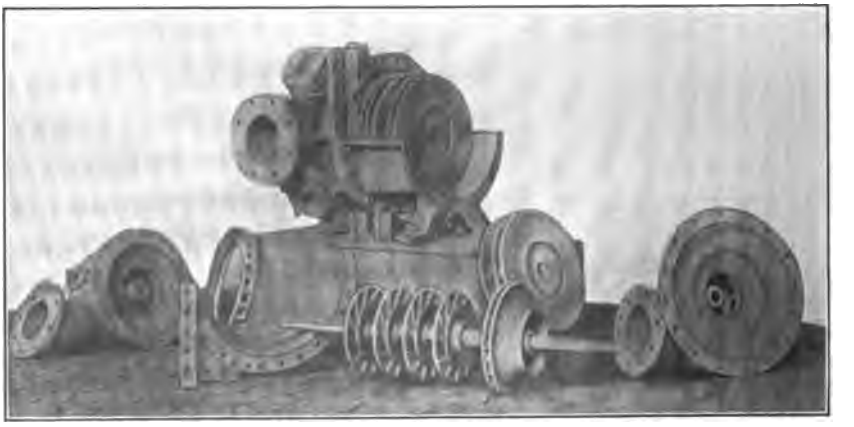

Fig. 133.

the head delivered by the pump, but the quantity delivered to the turbine is much greater than that delivered by the pump.

43. JAEGER PUMPS.

The high-pressure centrifugal pumps of J. H. Jaeger & Co. of Leipzig, Germany, are built as shown schematically in Fig. 102. The Jaeger pump has served as a model for numerous similar designs on account of its simplicity of construction. In this design each impeller is balanced individually. Referring to Fig. 102, each impeller has two packing rings R which form close clearances with corresponding rings fastened to the casing on both sides of the impeller. By making the clearance at the outer rim of the impeller sufficiently large equal pressure will exist in spaces 1 and 2. Spaces 3 and 4 on the inside of the packing rings are connected by a sufficient number of holes through the impeller hub. Neglecting the very slight excess of pressure required to force the water through the holes 0 it may be said that spaces 3 and 4 have the same pressure. An axial movement of the shaft, due to thrust, can be caused only by the velocity head of the water at entrance to the impellers, which acts on every impeller in the same direction. With this arrangement, therefore, it is possible almost wholly to do away with axial thrust, provided a sufficient clearance is allowed at the outer impeller diameter. It is worth mentioning that in this design the impeller sides and the walls of the casing, forming spaces 1 and 2, should be designed with similar outlines so that the rotation paraboloids formed in these spaces are alike, and therefore equal pressures exist in these spaces.

If the outer impeller clearance is very large compared to the inner clearances, the quantity of water short-circuited can be found from equation 26 without taking into account the rotation paraboloid. In this equation D_a equals the diameter of the packing rings. As was explained in Article 5, the short-circuit loss is decreased by using an inner and an outer packing ring. This being the case, the quantity of short-circuited water can be found from equation 32. If the clearance space areas are not equal on both sides of the impeller, there will be unequal pressures in spaces 1 and 2, which can be seen from equation 30. In order to balance the pressure in spaces 1 and 2 in this case, both spaces must be connected by a pipe. But this is difficult to carry out in the present design. An unequal wear of the packing rings in spite of the large outer impeller clearance might cause an unequal pressure distribution in

spaces 1 and 2. This would create an axial thrust. Jaeger has found this to occur and has patented an arrangement which will automatically prevent an axial thrust when there is unequal wear of the packing rings. This arrangement is shown in Fig. 134.

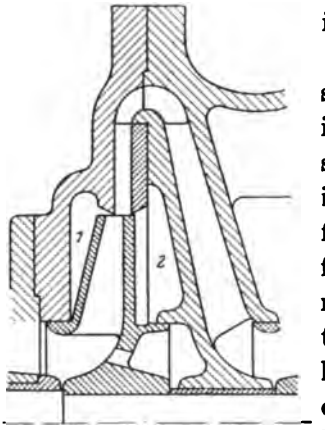

Fig. 134.

The shaft with the impellers has a small axial play, the periphery of the impeller is cylindrical, while the casing surrounding the periphery of the impeller is made conical, as can be seen in the figure. If the impellers or shaft receive for any reason an axial thrust, say from right to left, the impeller will move to the left. The clearance space on the left will be enlarged and its pressure increased above that existing in the right-hand clearance space and the impeller is forced back towards the right. Jaeger also uses a thrust bearing on the suction side of the pump to take up any axial thrust which may exist. This thrust bearing must be of such design as to take up axial thrust but still permit of axial end play. The general features of this bearing are shown schematically in Fig. 135. The shaft at *A* has a number of collars similar to a marine type thrust bearing. These collars rotate within a split cylindrical bushing *B* made of babbitt and secured against rotation by the feather *F*. This bushing is free to adjust itself axially within certain limits between the casing *C* and the pump casing. Ordinarily if no end thrust exists there is a clearance *z* at each end of the bushing, and thrust can be taken up only when the bushing reaches the shoulder *D*. In this way the thrust bearing does not interfere with the automatic arrangement shown in Fig. 134 unless such a large unbalanced thrust occurs as to make it necessary to have the aid of the thrust bearings.

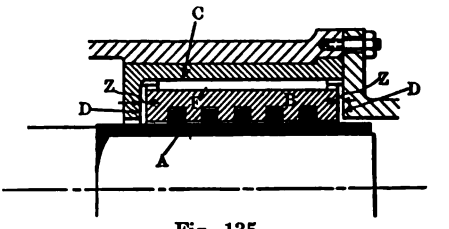

Fig. 135.

It is quite an advantage to balance each impeller separately in a

high-pressure centrifugal pump, for such an arrangement permits the use of impellers having slightly different pressure heads, and

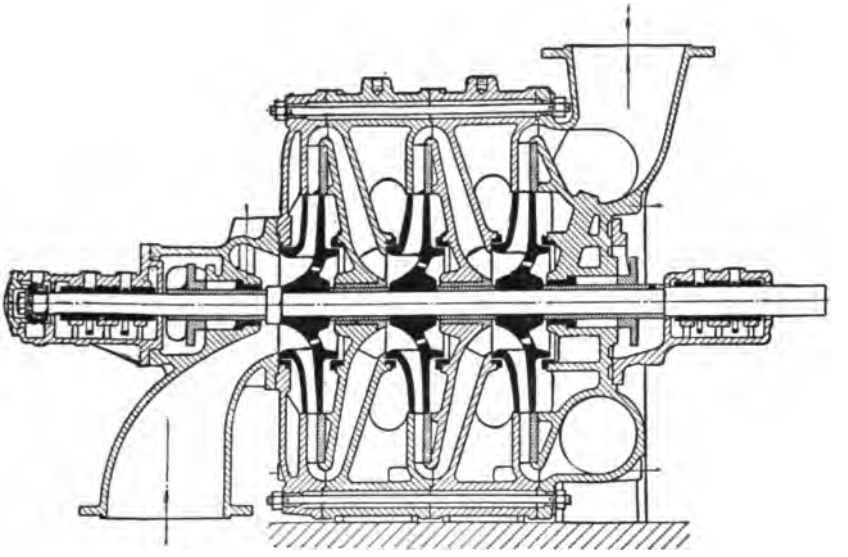

Fig. 136.

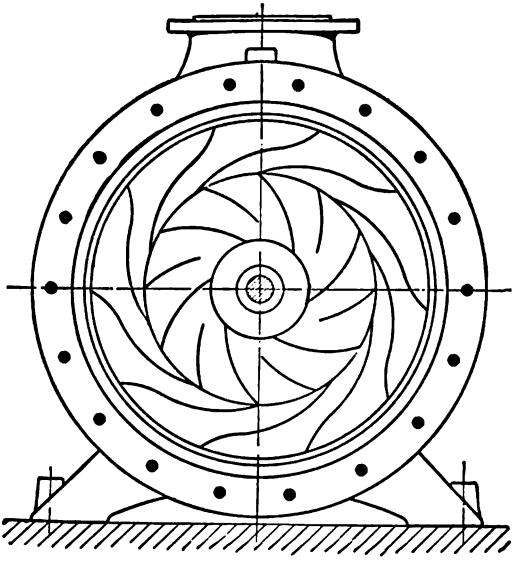

Fig. 137.

still allows the axial thrust to be balanced. For further details of the construction of this type of pump see Figs. 136 and 137.

The water enters through the suction pipe into the first impeller, then passes through the guide vanes lying in the same plane as the impeller. Both the impeller and guide vanes are made of bronze. The guide vanes are supported by the casing and are open on the suction side, which permits machining the guide vanes and thus procuring exact dimensions of the channel. The guide vanes lead the water radially at exit. The water then passes through the

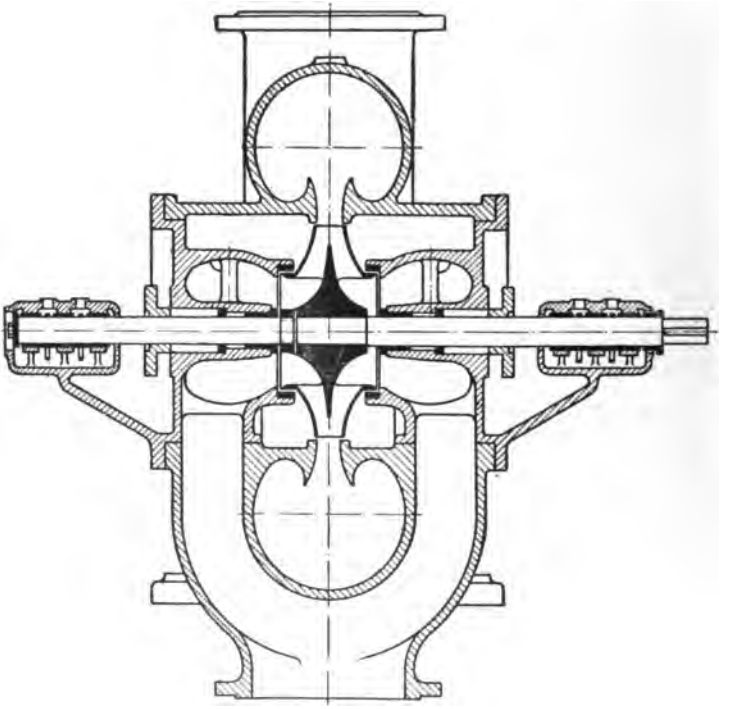

Fig. 138.

S-shaped channel, which carries it to the next impeller. To guide the water correctly, this reversing channel has directing vanes, or ribs. In this manner the water goes from stage to stage until it finally enters a round casing having a conical connection to the pressure pipe.

The casing surrounding the guide vanes consists of a number of like parts corresponding to the number of stages. The separate parts, or sections, are combined into a complete unit by means of through bolts. This subdivision of the casing offers several impor-

tant advantages. If the casing is made in one piece and the inner parts are assembled one after the other, the latter might easily rust tight, which would make disassembly of the pump difficult. By dividing the casing this is avoided and disassembly is much easier. In disassembling this type of pump it is necessary to disconnect either the suction or discharge pipe, depending on which one is located at the free end of the shaft. This can be considered a disadvantage only in the case of large pumps. A more vital object of criticism of this type of pump is the great number of close clearance packings, which require great care in assembly and disassembly. The

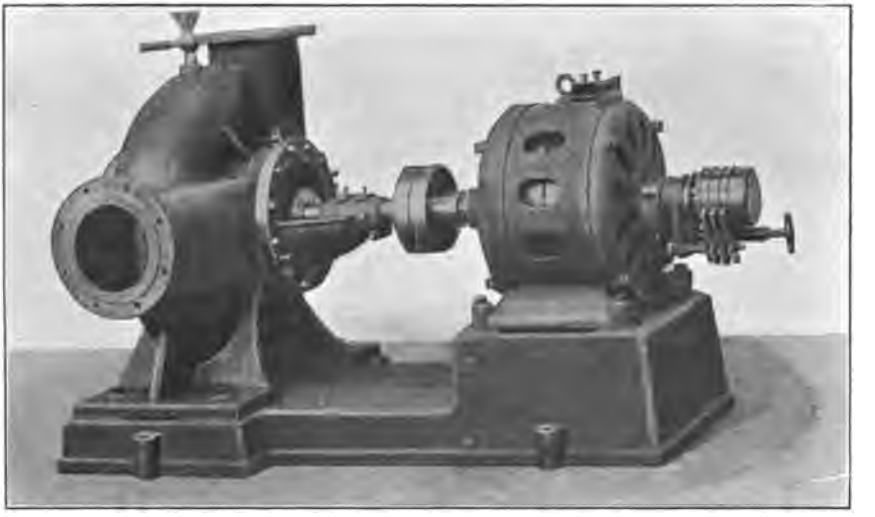

Fig. 139

large number of surfaces to be bolted together require careful drawing up of the bolts, or else the end bearings will be out of line. In manufacturing these pumps the sectional casings must be advantageous both for ease of machining and for interchangeability of parts.

It often happens in shaft pumps that a new stage is to be added to an old pump in order to increase the head. An increase in the number of stages is very easily accomplished in this type of pump when the casing is subdivided. The old pump parts can be used with the exception of the shaft. If the casing is in one piece this part of the old pump could not be used when more stages are to be added.

The shaft is supported on the suction and pressure ends in bearings with ring lubrication. The bearing at the suction end usually contains the thrust collars.

C. H. Jaeger & Co. build three distinct types of centrifugal pumps — the low-pressure pump, the moderate-pressure pump, and the high-pressure or turbine pump. The low-pressure construction

Fig. 140.

has been adopted recently, and takes care of heads up to 80 feet. The pump casing is cylindrical and the pump has no discharge vanes. Fig. 138 shows the general arrangement of a low-pressure pump. The entrance to the impeller is on both sides, which gives a perfectly balanced impeller, provided, of course, that the outer impeller clearance is made sufficiently large. Fig. 139 illustrates a low-pressure centrifugal pump of this type direct connected to a motor.

These pumps have a somewhat unfavorable water guidance at entrance to the impeller, hence they are built only in small sizes. For larger low-pressure pumps the arrangement shown in Fig. 140

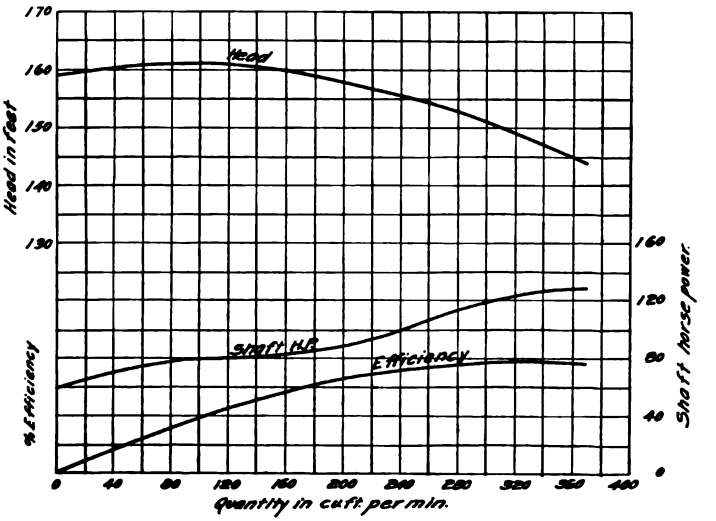

Fig. 141.

is used. Water also enters on both sides of the impeller, but it is led through more gradual bends. This arrangement necessitates,

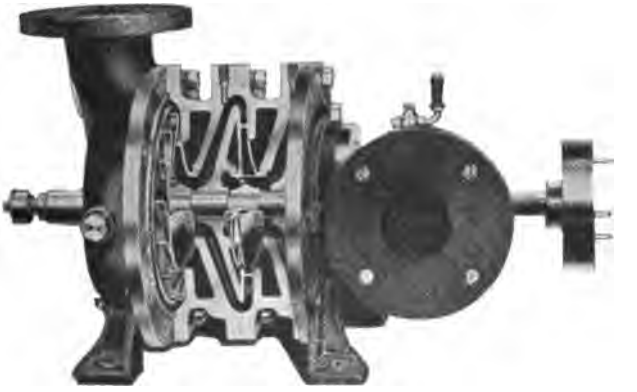

Fig. 142.

of course, two suction pipes. The pump shown in Fig. 140 delivers 1585 to 1765 cubic feet of water per minute against a head of 43 feet when running at 365 r.p.m.

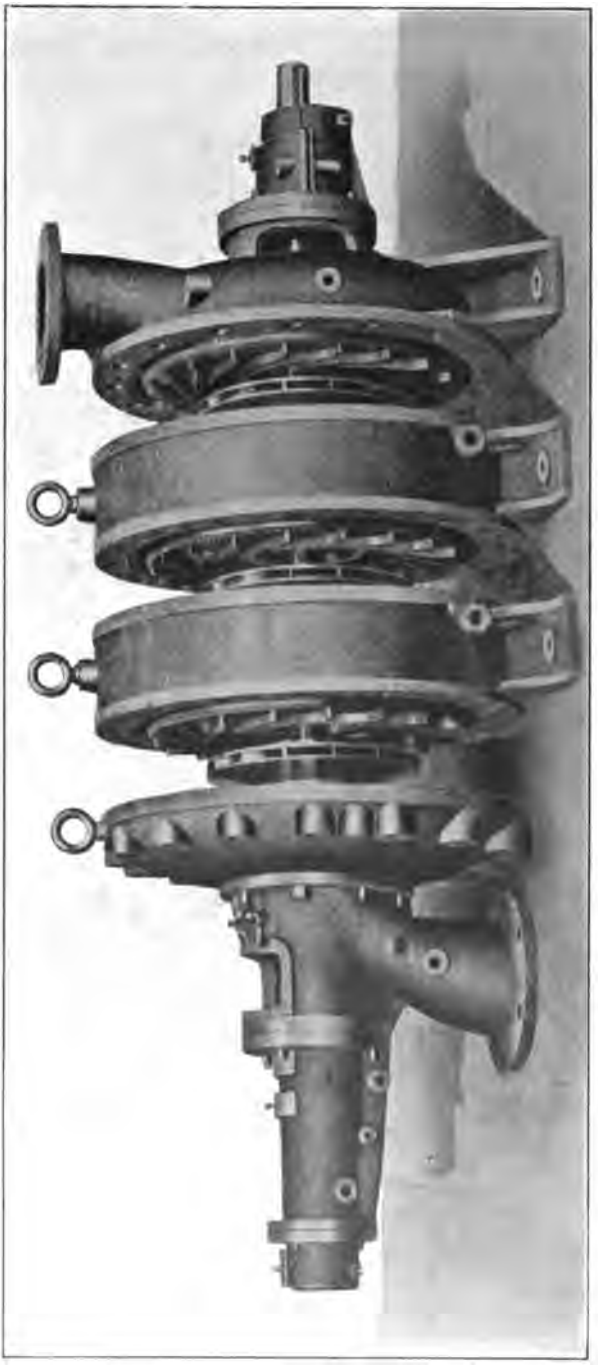

Fig. 143.

For heads between 80 and 150 feet moderate-pressure pumps are used. These pumps are similar to the low-pressure pumps, have no guide vanes, but have the casing volute in shape or are provided

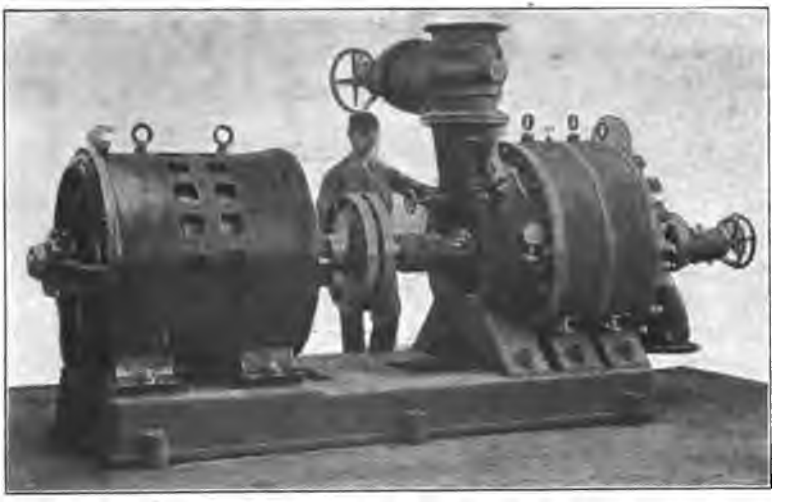

Fig. 144.

with a diverging discharge nozzle. These pumps generally have two suction and two discharge openings, which may be connected by a Y connection. Fig. 141 gives the characteristic curves of a moder-

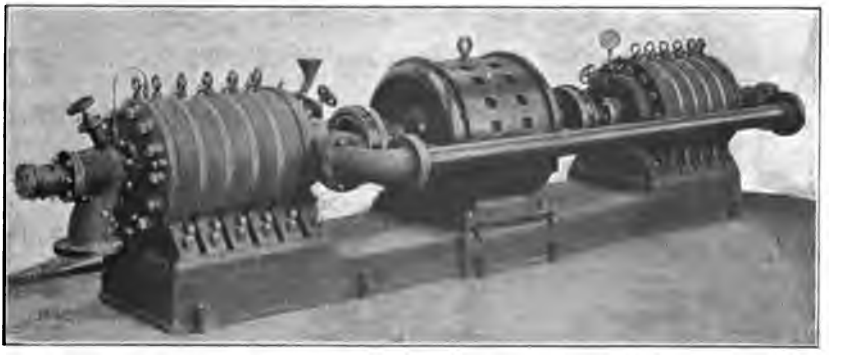

Fig. 145.

ate-pressure pump delivering 336 cubic feet of water per minute against a head of 148 feet when running at 1450 r.p.m.

The high-pressure pumps are nearly all multi-stage and have guide vanes as already described and shown in Figs. 136 and 137.

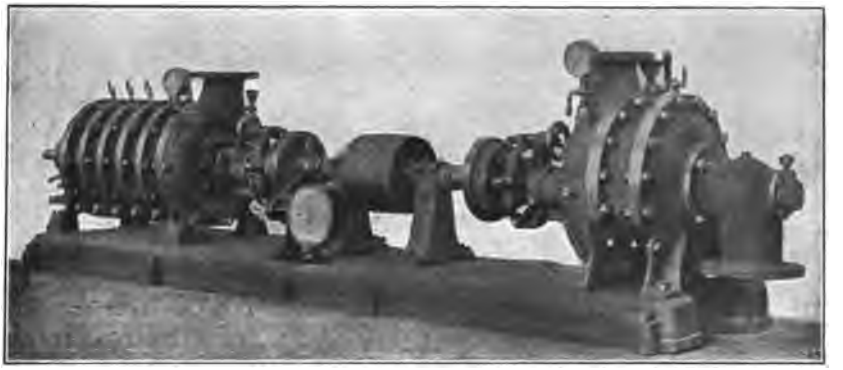

Fig. 146.

Fig. 147.

Fig. 142 shows a model of a three-stage pump in which the packing rings can be clearly seen, and Fig. 143 gives a view of the same pump with the sections separated. In this type of pump it is important that the pump should never be run dry, because the packing would burn out. At the highest point of each pump section a small valve is necessary to permit air to escape when the pump is first filled with water, and a drain valve should be provided so that the pump can be drained for disassembly or to prevent freezing of the water.

Fig. 144 shows a three-stage pump delivering 283 cubic feet of water per minute against 410 feet head. The pump is connected to an induction motor by means of a leather band coupling.

In the twelve-stage pump shown in Fig. 145 the driving motor is placed in the middle, with six stages on each side. These pumps

are not arranged oppositely to balance axial thrust, because there are flexible couplings between the pumps and the motor. A pump with twelve stages would require a shaft of considerable length, and

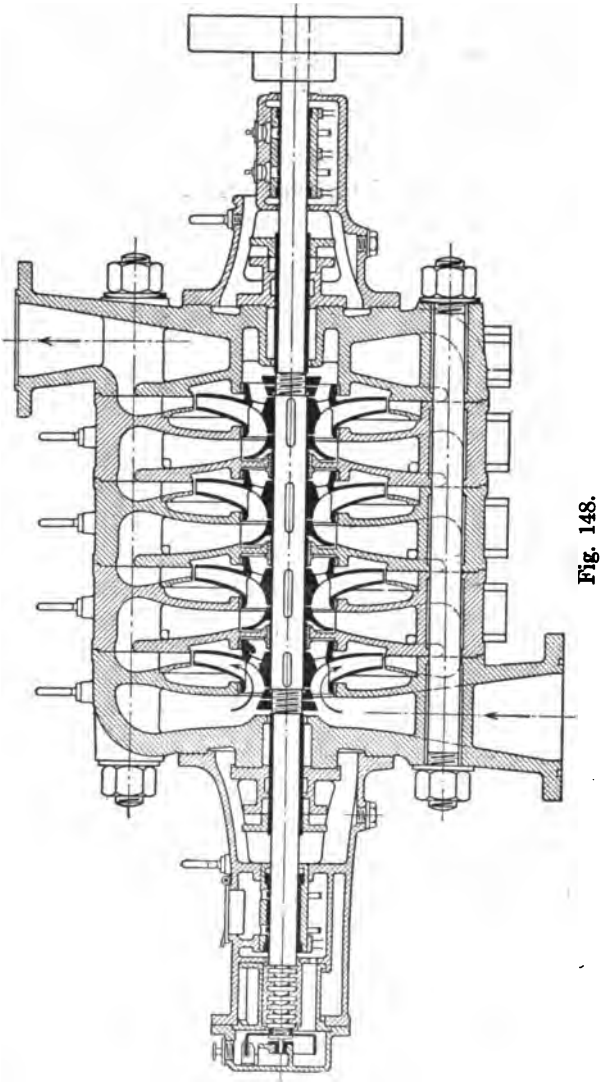

Fig. 148.

if the impellers are not carefully balanced the high number of revolutions will cause vibration of the shaft. Chiefly on account of the latter reason the pump should be divided.

Fig. 146 shows an interesting arrangement of a six-stage and a two-stage pump, which can be connected by means of a clutch to

a common shaft which revolves at 1500 r.p.m. Fig. 147 shows a Jaeger pump for shaft or mine work.

One of the largest installations of C. H. Jaeger & Co. is at the mine "König Ludwig" in Recklinghausen, Germany. The pump consists of eight stages, four stages being placed on each side of the electric motor. Fig. 148 gives a cross section through one of the four-stage pumps of this installation. The pump delivers 247 cubic feet of water per minute against a head of 1903 feet when running at 1470 r.p.m. The maximum capacity of the motor is 1350 h.p. Fig. 149 gives the results of tests on this pump. This pump reaches its maximum efficiency of 76 per cent when deliver-

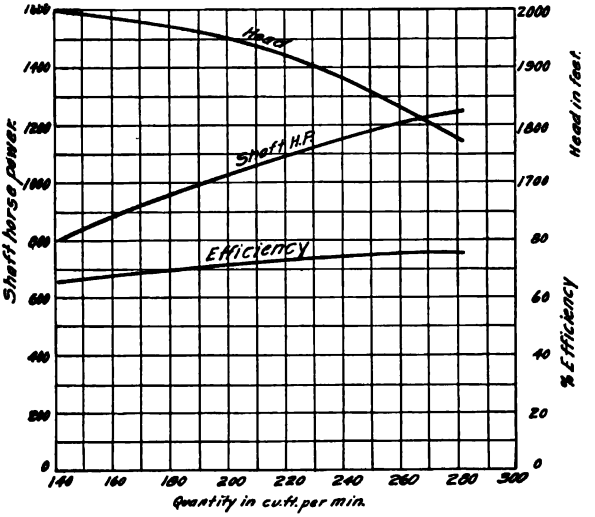

Fig. 149.

ing 268 cubic feet of water per minute against a head of 1843 feet, the pump running at 1475 r.p.m. The power consumption at this load was 1230 h.p. With the throttle on the discharge pipe entirely closed, hence no output, the pressure rose to 2028 feet, taking about 425 h.p. to drive the pump.

An interesting series of curves taken from test results on an eleven-stage pump for the "Westhausen" Mine in Germany is shown in Fig. 150. The normal rating of this pump is 106 cubic feet of water per minute when working against a head of 1375 feet. The motor receives its current from a line supplying a large number of units, and therefore its speed cannot be kept constant. The highest efficiency is 75 per cent, and was obtained when the pump

delivered 98.7 cubic feet of water per minute against a head of 1444 feet when running at 1445 r.p.m. The effective power consumption was 360 h.p. The very flat-pressure curves and the very gradual change of efficiency in the neighborhood of the normal capacity of this pump show how carefully the impeller and guide vanes were designed.

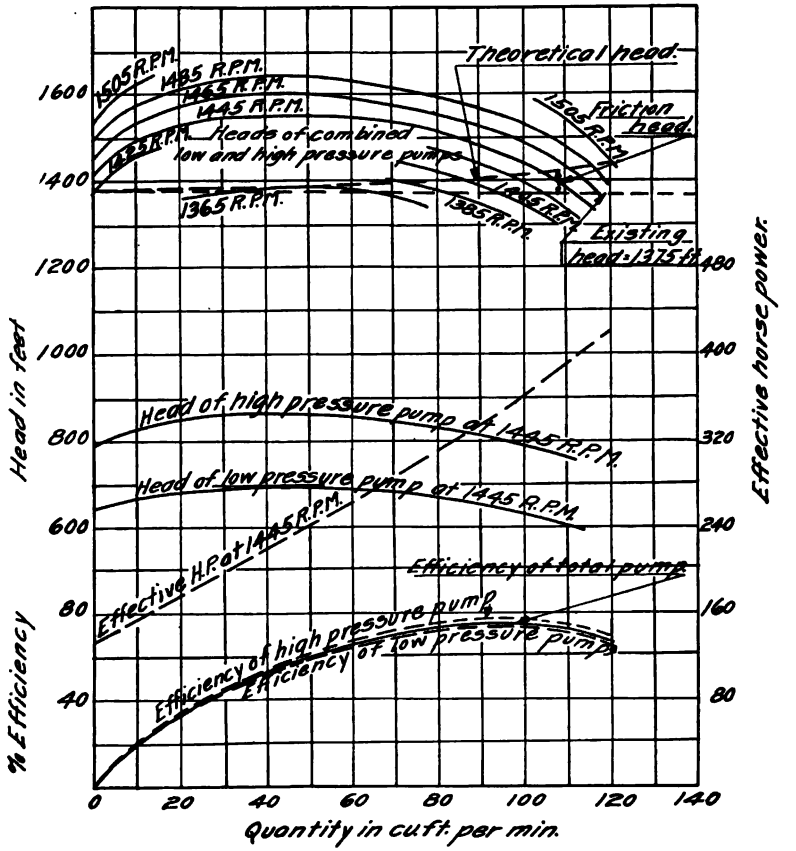

Fig. 150.

Fig. 151 gives a view of a rather novel application of a centrifugal pump for fire-engine service. This pump, driven by a four-cylinder benzine motor, is used for fire service in the town St. Étienne, France. The pump is a three-stage Jaeger pump, capable of delivering 75 cubic feet of water per minute against a head of 236 feet. The benzine motor drives a shaft which can be coupled either to gearing driving the pump or to a chain drive attached to the rear axle.

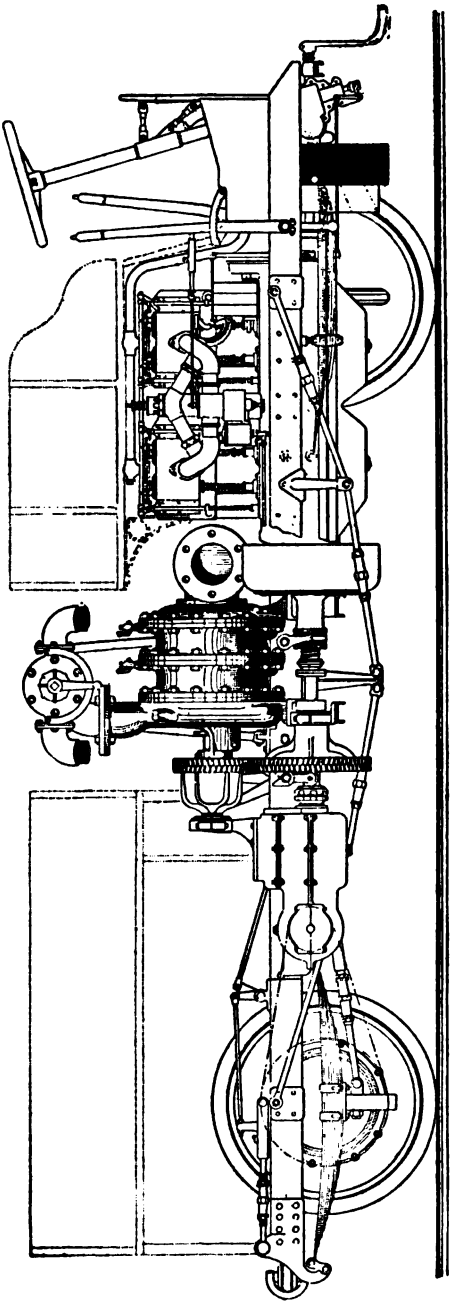

Fig. 151.

44. Kugel-Gelpke Pumps of Escher, Wyss & Co.

The Kugel-Gelpke high-pressure centrifugal pump, first built by Escher, Wyss & Co. of Zurich, Switzerland, differs considerably from the types already described, for in this type both the impeller and guide vanes are S shaped (see Fig. 103). The water enters the impeller channels in an axial direction, and after passing through a double bend of 90° it leaves the impeller channel in an axial direction. The water flows in a similar manner through the guide vanes. A correct design of vanes in the impeller and guide apparatus is supposed to give the water proper guidance.

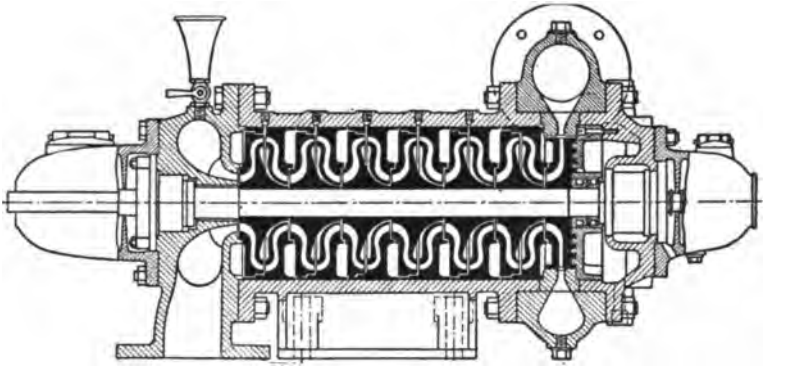

Fig. 152.

This form of water guidance is perhaps very efficient when the pump is working under rated conditions, because the entrance and exit velocity diagrams are correct for these conditions. But if the discharge is throttled, thus decreasing the quantity of water delivered, the water will no longer have the proper velocity to form the correct velocity diagrams, and therefore the efficiency will be greatly diminished by shock losses. In Article 28 attention was called to the necessity of having large clearances between the impeller and discharge vanes. The water being forced through a double bend in the impeller and set in rotation may become quite troublesome, for it is turned through 90° just when the greatest velocities occur.

This type has an advantage over others in its simplicity of construction. The guide vanes and reversing blades are made in one piece. The casing can be made quite small in diameter.

Fig. 152 shows a longitudinal cross section of a seven-stage high-pressure Kugel-Gelpke pump. The guide vanes having the S-shaped channels are assembled in units so that they abut against one another in a cylindrical casing. These guide vanes can be disassembled by slipping them off the shaft at its free end. In the last stage the water leaves the guide vanes in a radial direction, after which it passes radially into the spiral discharge casing.

In the design of Escher, Wyss & Co. water under pressure is admitted into the spaces between the guide vanes and impellers in order to balance the axial thrust. The water pressure is regulated by means of a valve.

The axial thrust can be taken care of only by some special balancing arrangement, just as in the Rateau pump. In the bearing there is also a series of thrust collars to take care of any axial thrust not provided for in the balancing arrangement. This thrust bearing is adjustable and permits an adjustment of the position of the impellers in an axial direction.

45. Worthington Pumps.

Henry R. Worthington of New York, now a part of the International Steam Pump Company, has been building high-pressure centrifugal pumps since 1901, and has sold more centrifugal pumps

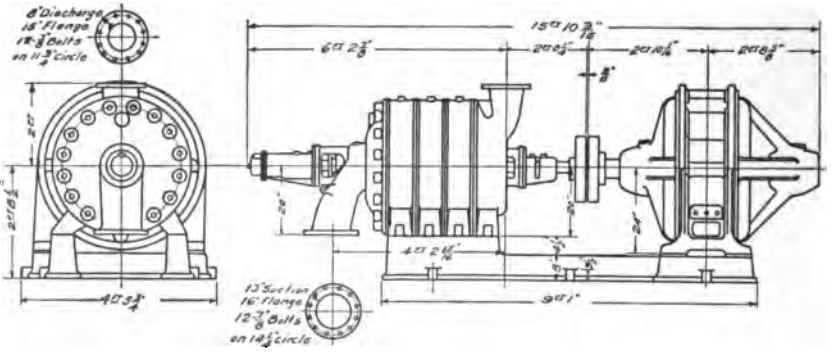

Fig. 153.

than any other manufacturer in the United States. In 1904 this firm secured the rights to build the Jaeger type of pump in all countries except Germany and Austro-Hungary. This type of pump

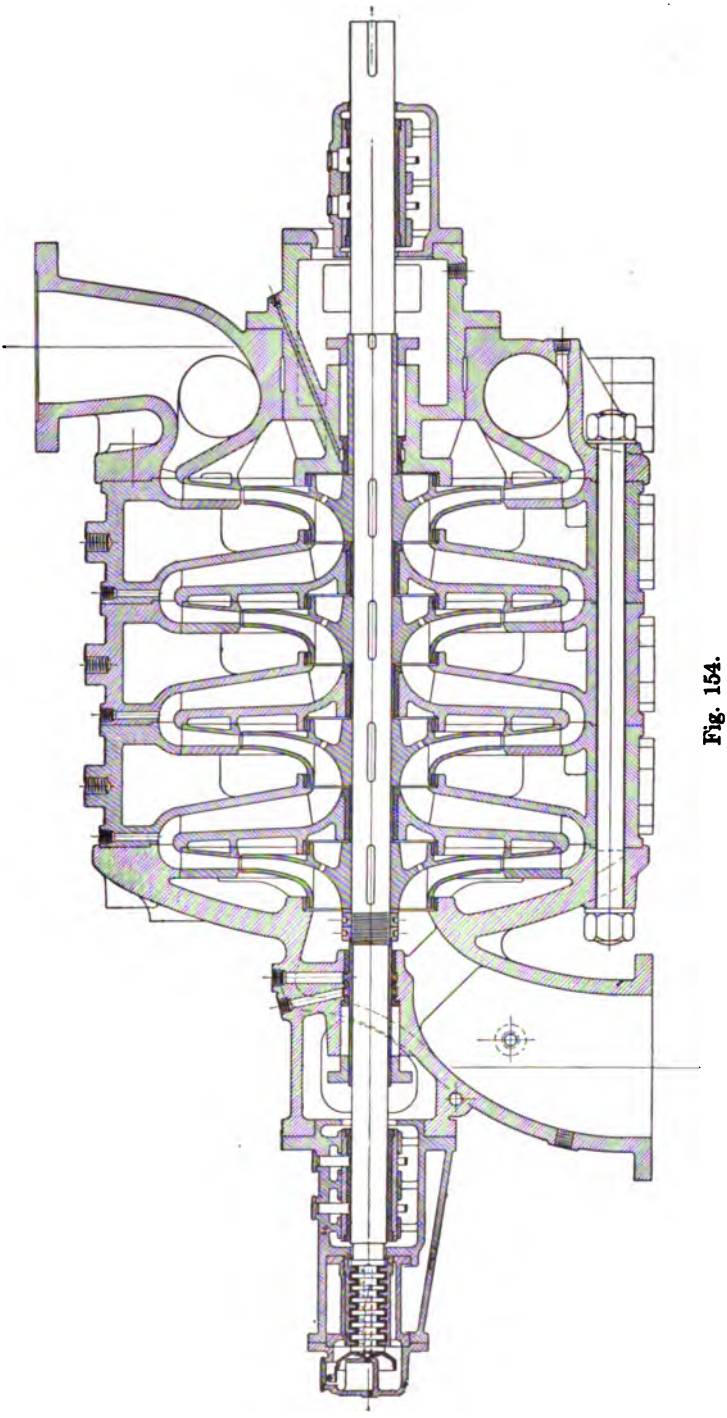

Fig. 154.

has been used extensively and gives good results, but quite recently Worthington developed a new type similar in principle to the double-suction type shown in Fig. 104. This new type is the natural out-

Fig. 155.

come of the desire to build high-pressure pumps of greater speeds, thus increasing the head per stage, decreasing the diameter of the impellers, and reducing the number of stages. The efficiency of this

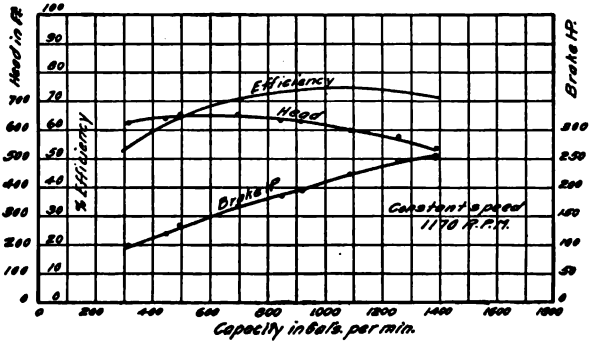

Fig. 156.

new type is greater than that of the old for reasons easily understood from the theoretical discussion given in this book. The axial balance of this type is superior to that of the Jaeger.

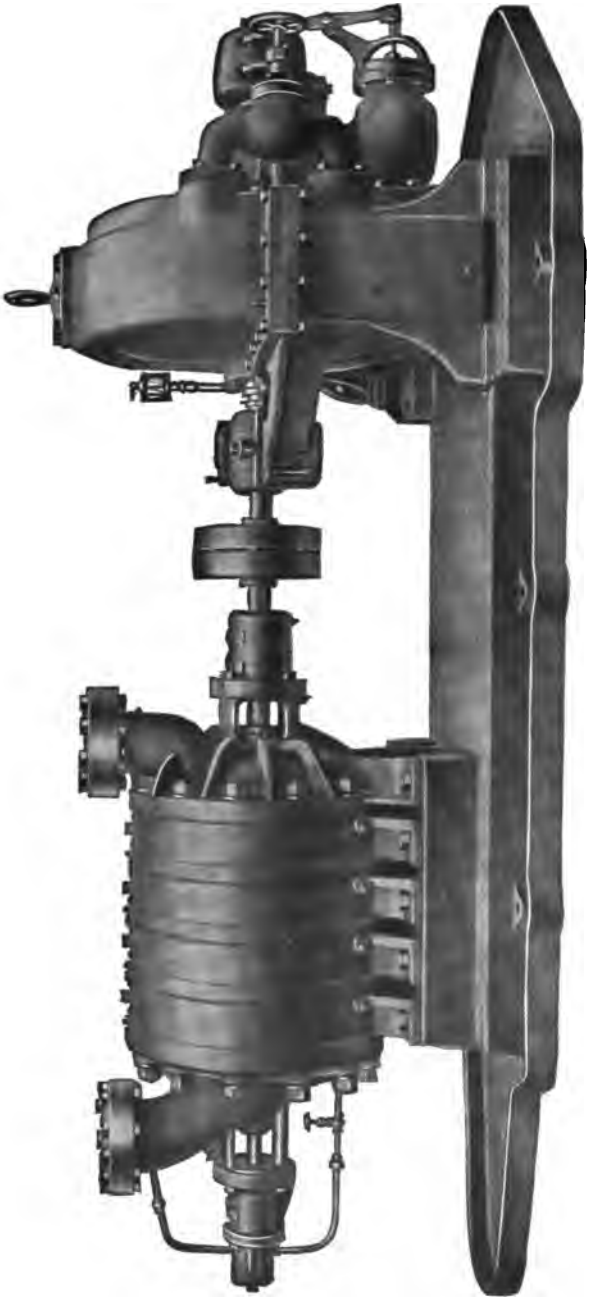

Fig. 157.

Fig. 158.

Centrifugal pumps of the double-suction type are somewhat longer than those of the other types. These pumps are also costlier, because of the more difficult design and greater complexity of the impellers, discharge vanes, diaphragms and casings. In spite of these handicaps the advantages of eliminating axial thrust and of using high-speed drivers force manufacturers to give preference to the double-suction type, especially when very high pressure pumps are contemplated.

Fig. 153 shows an outline view of a four-stage Worthington pump of the Jaeger type capable of delivering 150 cubic feet (1125 gallons) of water per minute against a head of 600 feet. This pump is direct connected to an induction motor running at 1170 revolutions per

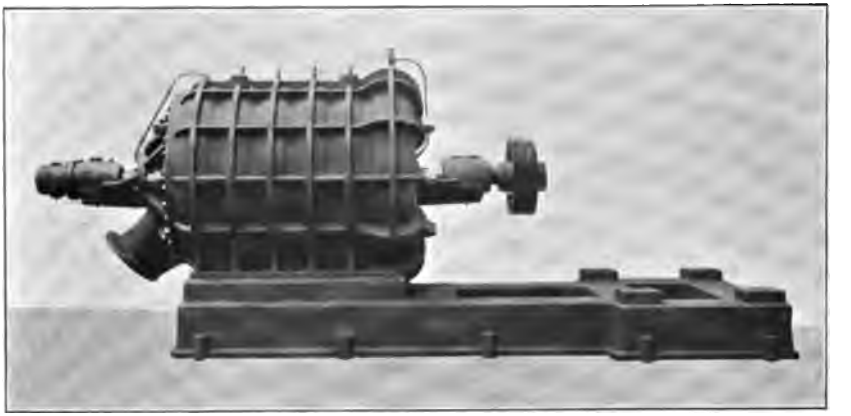

Fig. 159.

minute at full load. A longitudinal cross section through this pump is given in Fig. 154. The diameter of each impeller is 18.5 inches, the diameter of the suction pipe is 10 inches, and that of the discharge 8 inches. The diameter of the shaft varies from 2.5 inches at the suction-end bearing to 3 inches at the bearing on the discharge end. The unbalanced axial thrust is taken care of by a marine type of thrust bearing at the suction end. This thrust bearing is lubricated automatically, the oil being lifted by a rotating disk from an oil reservoir to a chamber feeding into a hole drilled in the center of the shaft throughout the length of the thrust bearing. Each thrust collar receives oil by means of a radial hole from the center of the shaft to the surfaces to be lubricated. When the shaft is revolving, oil is forced through these radial holes by centrifugal

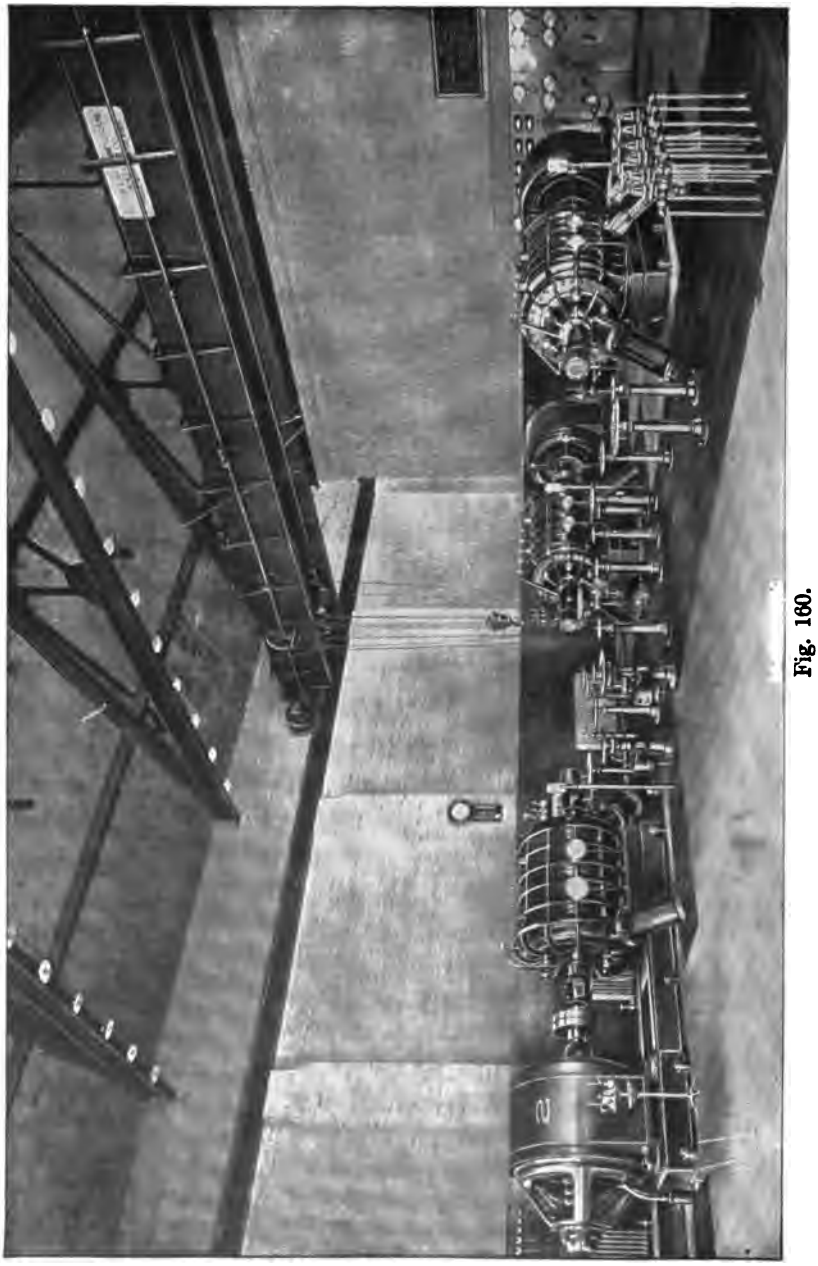

Fig. 160.

force. Both bearings are lubricated by oil rings. The impellers are constructed of bronze and are of the enclosed or shrouded type,

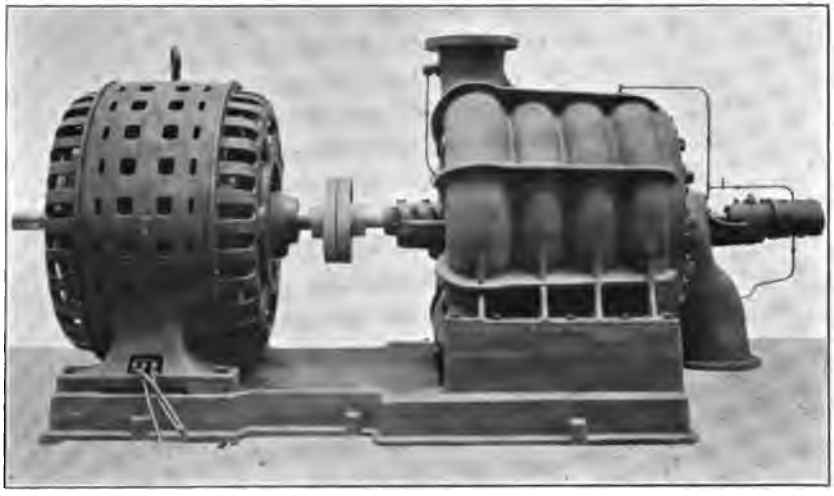

Fig. 161.

having backward-turned blades. They are cast in one piece and machined and polished on the outside. The water channels are

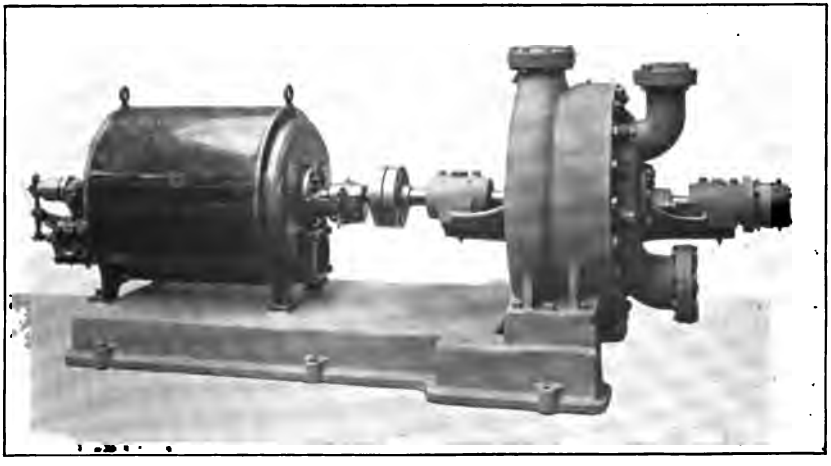

Fig. 162.

chipped and filed to a smooth finish. As in all Jaeger designs, the flanges on both sides of the impeller form a close running-fit with the

clearance rings secured to the pump casing. The discharge vanes are made of bronze, with one side removable (Fig. 155) so that the water passages can be carefully machined and polished in order to reduce the water friction to a minimum. The pump shaft is made

Fig. 163.

of steel, with bronze protecting sleeves. The shaft is a close sliding fit in the impeller hubs, and is provided with a shoulder, against which the impellers and sleeve are secured by means of a nut on the suction end. The stuffing boxes are a part of the bearing brackets, and are between the casing and bearings, to prevent sand

Fig. 164.

and grit from entering the bearings. Water seals are provided for the stuffing boxes, and they are connected by means of suitable piping to the discharge side of the pump. Fig. 156 gives the characteristic curves of this pump as determined by test. When delivering 150 cubic feet (1125 gallons) of water per minute against a head of 600 feet the pump showed an efficiency of 75 per cent.

Fig. 165.

Fig. 157 gives a photographic view of a five-stage Worthington pump of the Jaeger type used for boiler feed. It delivers 67 cubic feet of water (300 gallons) per minute at a pressure of 250 pounds per square inch. The diameter of the discharge pipe is 4 inches. The pump here shown is direct connected to a 100-h.p. Terry steam turbine running at 2100 revolutions per minute. This type of pump for feeding boilers gives an uninterrupted and steady discharge, thus eliminating all shock on the pipe system. No air

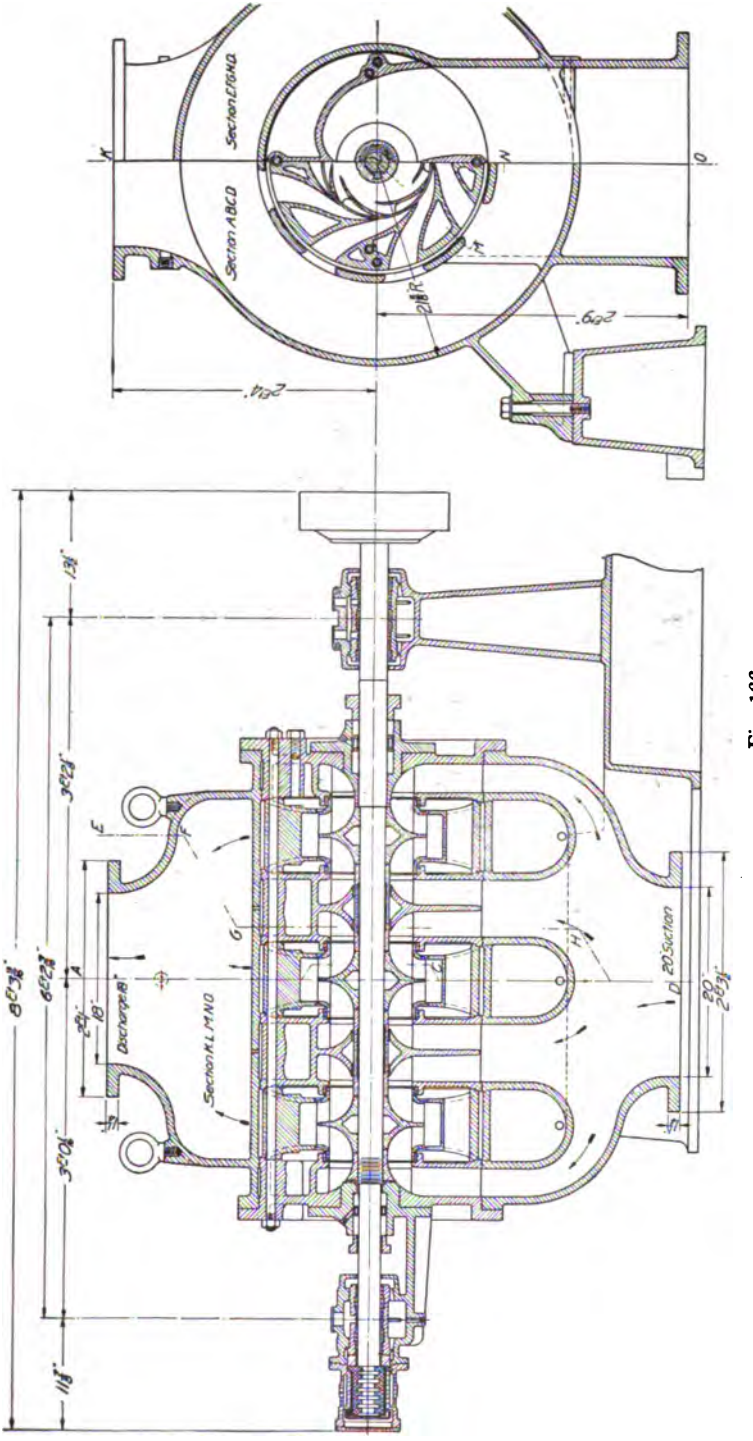
Section EFGHQ
Section ABCD
Section KLMNO
Discharge B
Section PQ

Fig. 166.

chambers or relief valves are necessary, as the pressure will never build up to a dangerous point, even though the discharge valve be entirely closed.

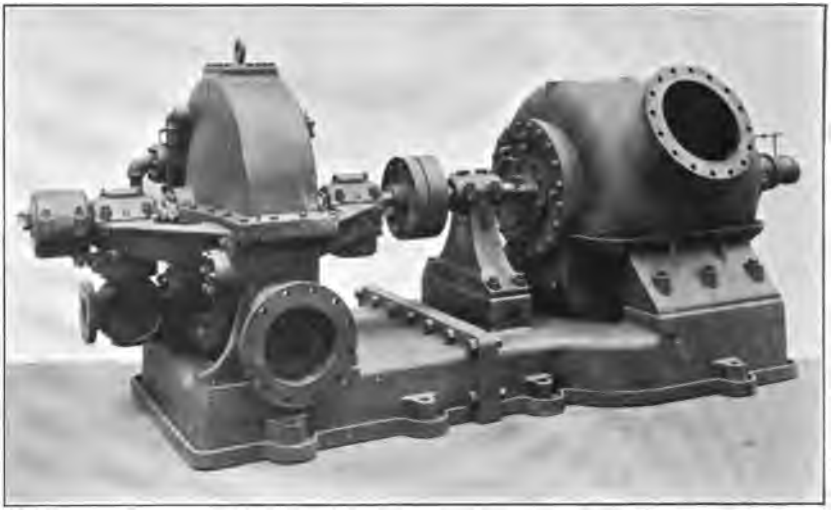

Fig. 167.

When a large number of stages is required Worthington divides them into two pumps arranged on both sides of the motor, so that the unbalanced axial thrust of one pump is opposed to that of the

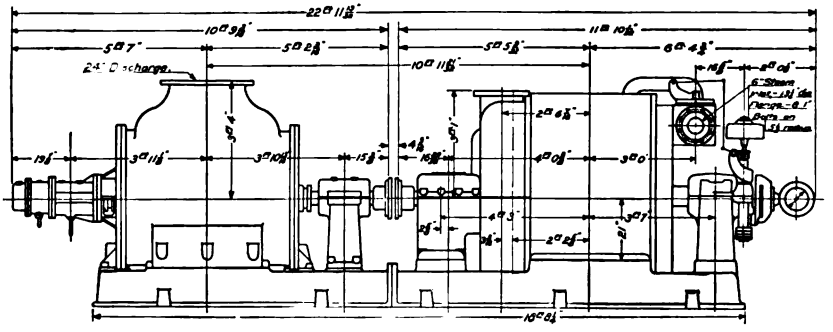

Fig. 168.

other. Fig. 158 shows such an arrangement. The unit consists of ten stages capable of delivering 279 cubic feet of water per minute (3 000 000 gallons per 24 hours) against a head of 750 feet. The driver is a 600-h.p. Westinghouse induction motor. Four of these

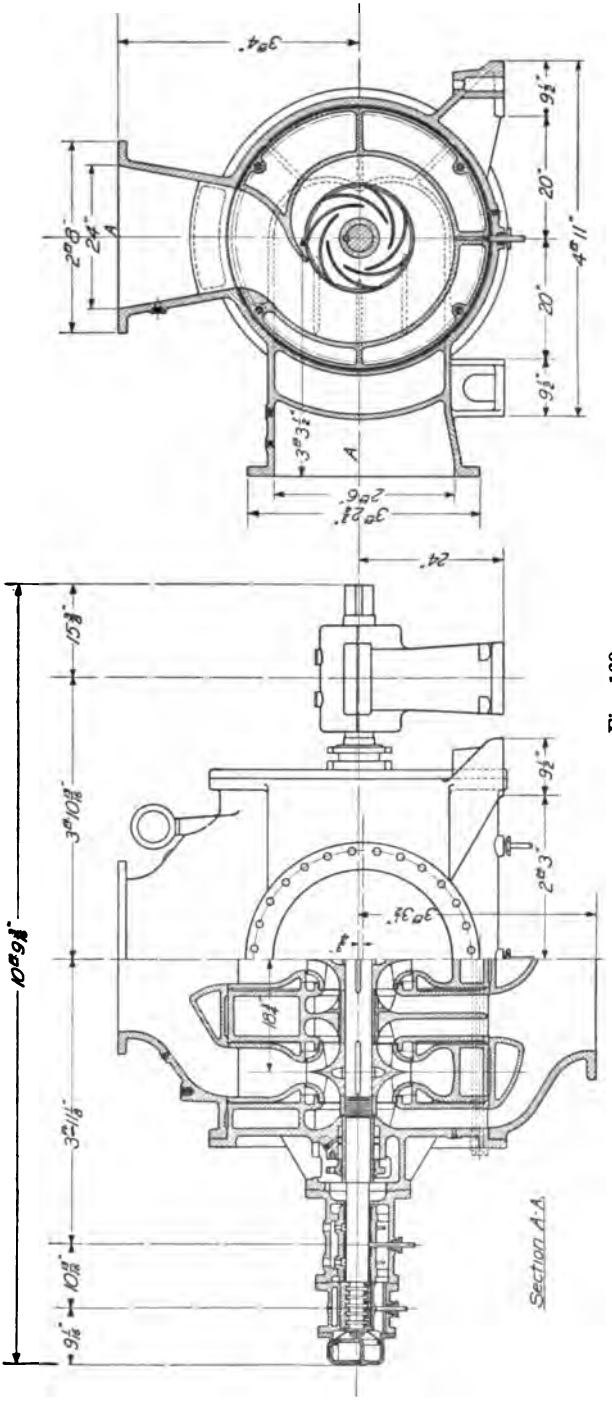

Fig. 169.

units were supplied to the contractors for the Jackson Street Regrade, Seattle, Washington, where nearly two million cubic yards

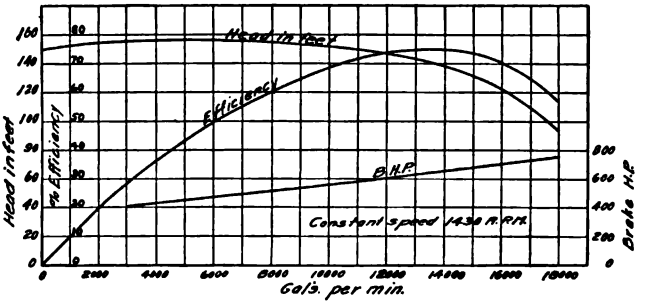

Fig. 170.

of earth were removed with these pumps by a method known as hydraulic mining. This method is less expensive and quicker than

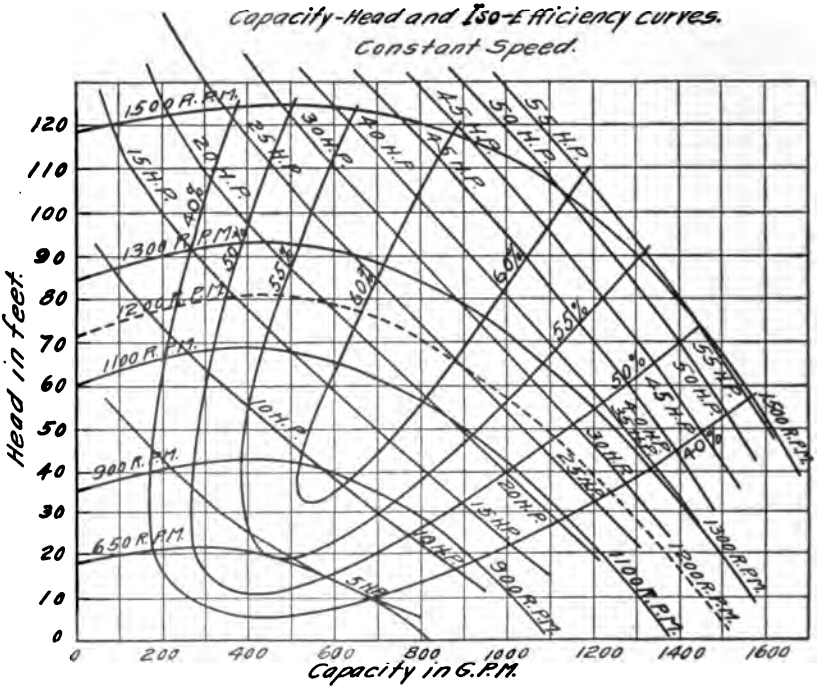

Fig. 171.

the steam shovel whenever it can be employed. The pumps operate in series when a hard stratum is encountered and in parallel for removing the softer material. The same method is employed

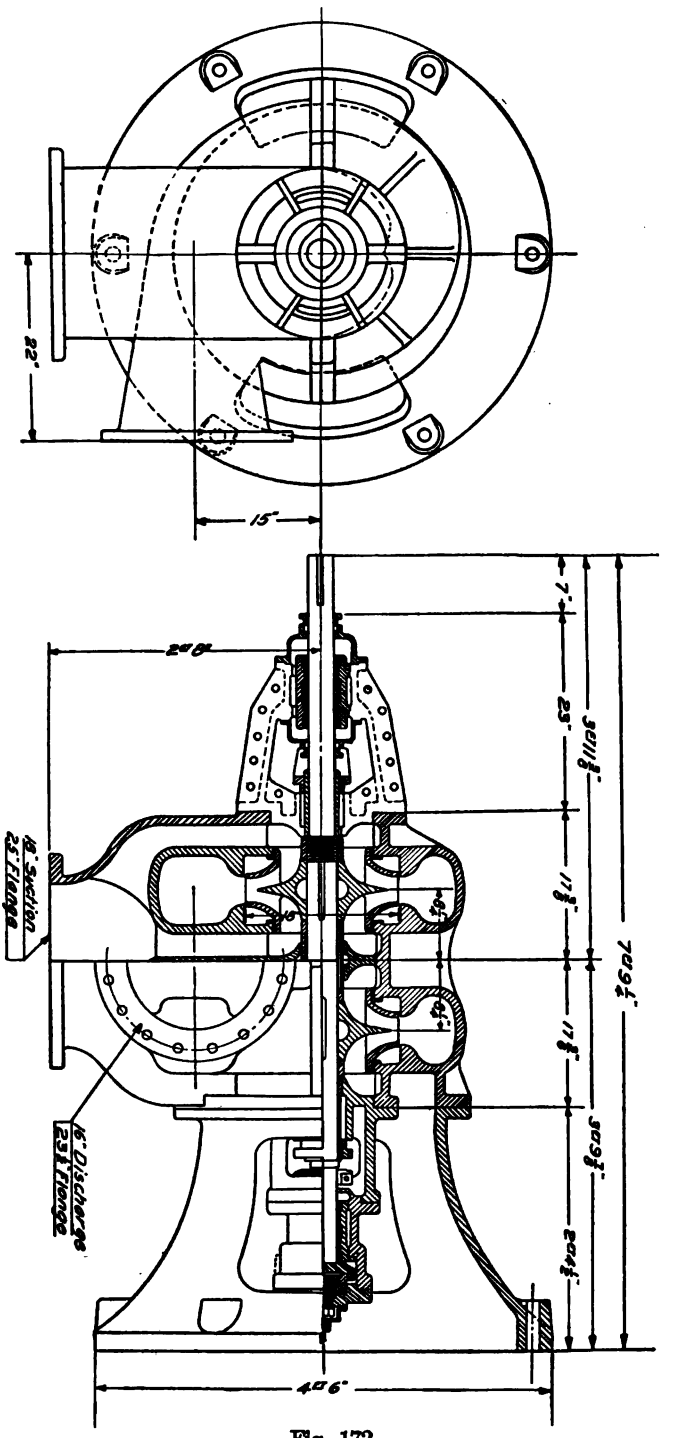
22"
15"
2'0"
12" Suction
25 Flange
16" Discharge
23 Flange
7"
25"
11"
11"
4'0"
4'6"

Fig. 172.

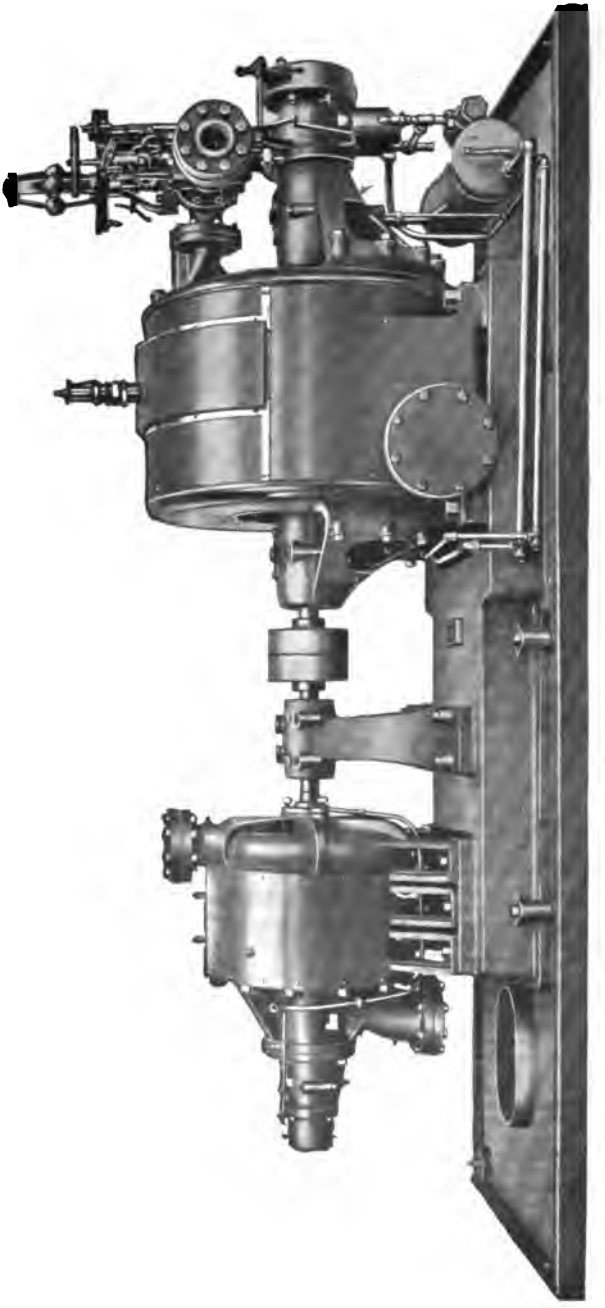

Fig. 173.

in some mines, as for instance the phosphate mines of southern Florida.

It will be noticed that all the Worthington pumps so far described are of the Jaeger type with sectional casings. This firm also builds pumps of the Jaeger type with the casting in one piece, the discharge vanes and impellers being assembled from one end. A good example of this construction is shown in Fig. 159. This figure is a photographic view of a six-stage pump capable of delivering 400 cubic feet (3000 gallons) of water per minute against a head of 700 feet when the pump is running at 725 revolutions per minute.

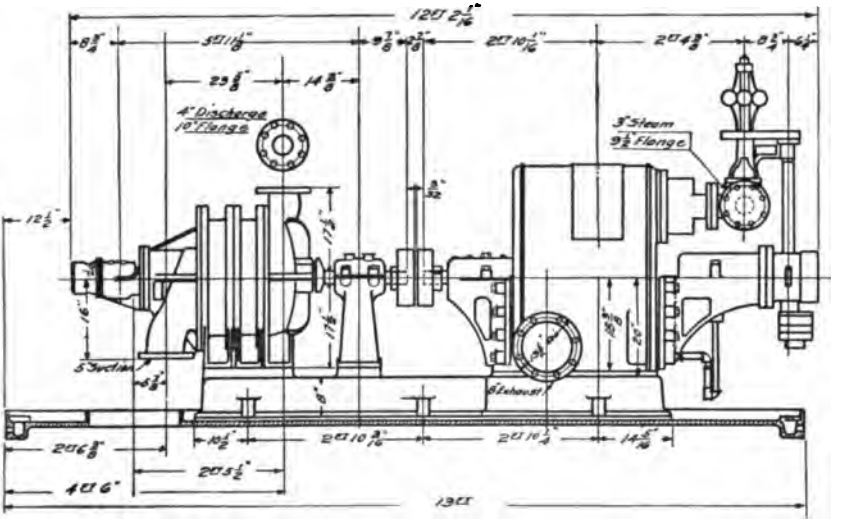

Fig. 174.

This pump is one of eight units installed in Brooklyn, N.Y., for fire protection service. Fig. 160 shows the arrangement of three of these units in the substation, the other five units being installed in the main station. The pumps are direct connected to 800-h.p. Stanley motors.

A similar construction of pump is shown in Fig. 161, which gives a photographic view of a four-stage pump delivering 742 cubic feet (5550 gallons) of water per minute against a head of 442 feet. The diameter of the discharge pipe is 14 inches. The pump is direct connected to a 1000-h.p. Westinghouse motor running at 720 r.p.m.

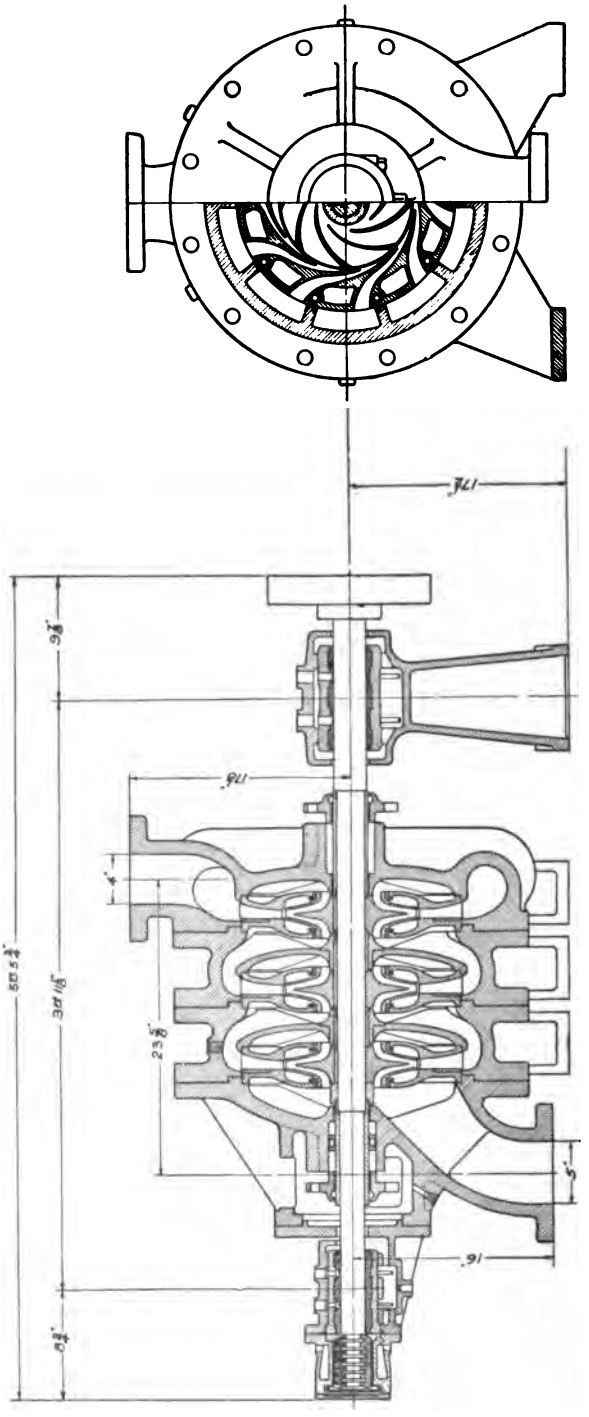

Fig. 175.

Fig. 162 shows a two-stage pump for lifting water out of a hot well. The diameter of the discharge pipe is 5 inches. The pump is capable of delivering 70 cubic feet (520 gallons) of water per minute against a head of 80 feet. This pump is direct connected to a 25-h.p. Kerr steam turbine running at 1200 r.p.m.

This type of pump is also built in vertical units. Fig. 163 is a photographic view of a four-stage pump having a vertical shaft. The pump is installed at the waterworks of the city of Athens, Ga. This unit delivers 240 cubic feet of water per minute (1800 gallons, or 2 000 000 gallons in 24 hours) against a pressure of 150 pounds. The diameter of the discharge pipe is 8 inches.

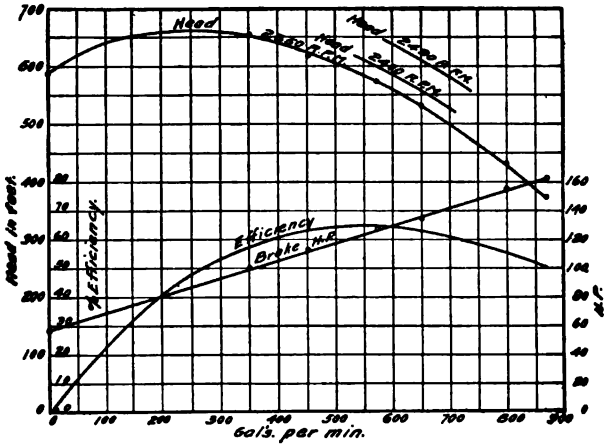

Fig. 176.

The Worthington pumps so far described are high-pressure pumps of the Jaeger type. This firm has also built very good designs of low-pressure pumps of both the horizontal and vertical types. Fig. 164 gives a photographic view of a two-unit low-pressure set. Each unit has an average capacity of 6685 cubic feet (50 000 gallons) of water per minute and is used for emptying dry docks. The pumps work against a head varying from 0 to 35 feet. The diameter of the discharge pipe of each unit is 45 inches, and the suction pipe is carried on both sides of the impeller, forming what is called the double-suction type. These pumps are connected to General Electric motors. Fig. 165 is a photographic view of a vertical low-pressure pump delivering 2925 cubic feet (21 875 gallons) of water per minute

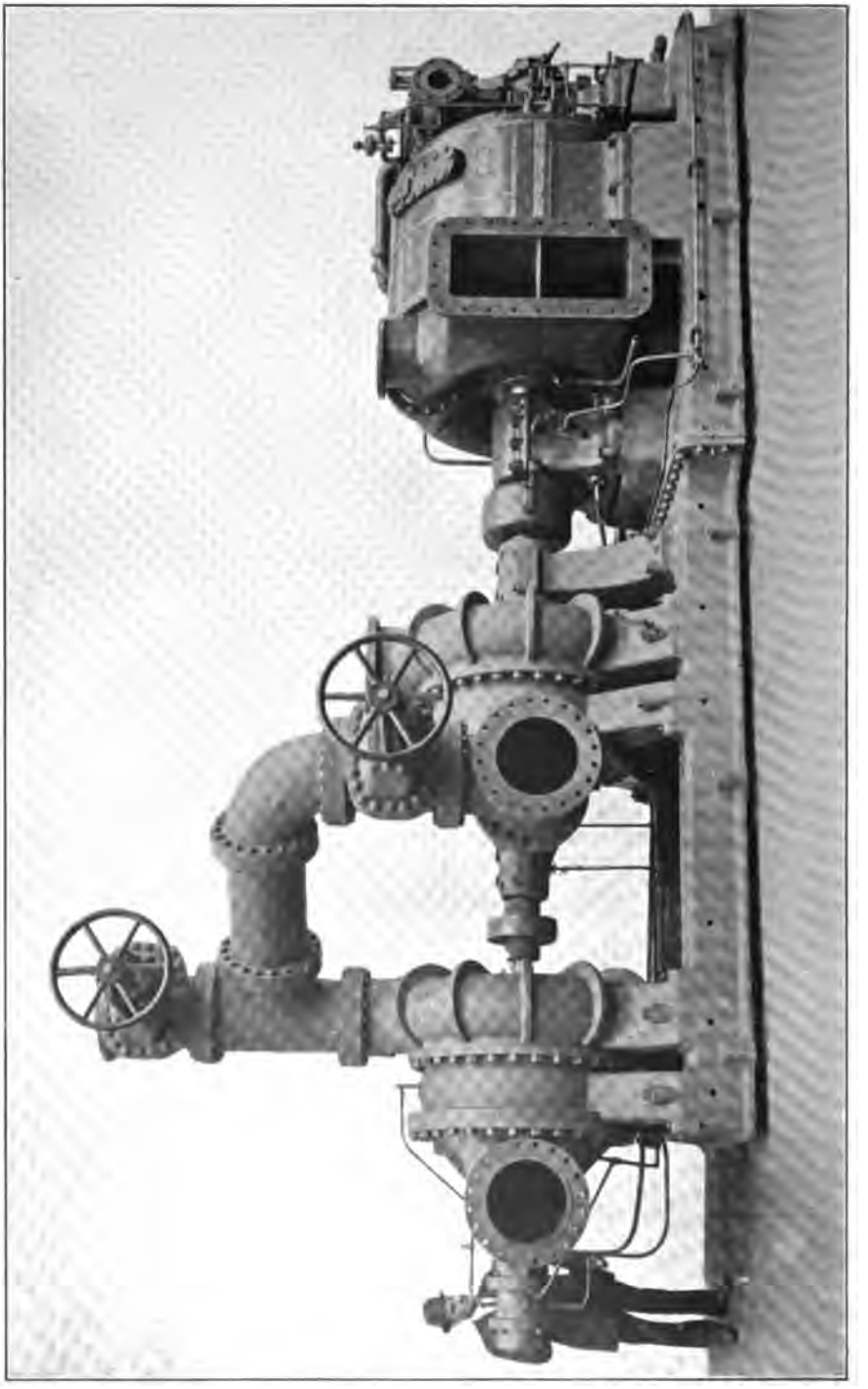

Fig. 177.

against a head of 50 feet, the pump running at 185 r.p.m. The diameter of the discharge pipe is 36 inches.

When large quantities of water are to be pumped at high speeds against low pressures, Worthington places two or more impellers in parallel within the same casing. Fig. 167 shows a tri-rotor pump which delivers 1200 cubic feet (9000 gallons) of water per minute under a head of 40 feet. This pump is driven by a 170-h.p. Terry steam turbine running at a speed of 1500 r.p.m. This unit was for the Southern Pacific Company. Fig. 166 gives a cross-sectional view of this pump, showing the arrangement of the three impellers in parallel. Water enters through the 20-inch suction pipe and passes through the three impellers and is led through discharge vanes into the 18-inch

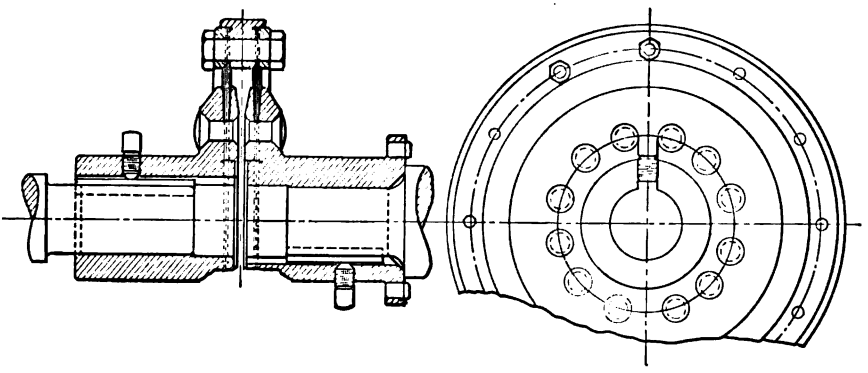

Fig. 178.

discharge pipe. The impellers are of the double-suction type, water being admitted on both sides of the impeller. In order to secure proper alignment of the impellers and discharge vanes a marine type of thrust bearing is used, although this arrangement of impellers does not produce any axial thrust. The rest of the constructive features of the pump are quite evident from the cross-sectional view.

Fig. 168 gives an outline drawing of a tri-rotor pump direct connected to an 800-h.p. Curtis steam turbine built by the General Electric Company. This unit has recently been installed for the Carnegie Steel Company, and is capable of delivering 1870 cubic feet (14 000 gallons) of water per minute against a minimum pressure of 97 feet, a normal pressure of 129 feet, and a maximum pressure of 151 feet. The normal speed of the unit is 1400 r.p.m. Fig. 169 gives a cross-sectional view of the pump, which differs from the

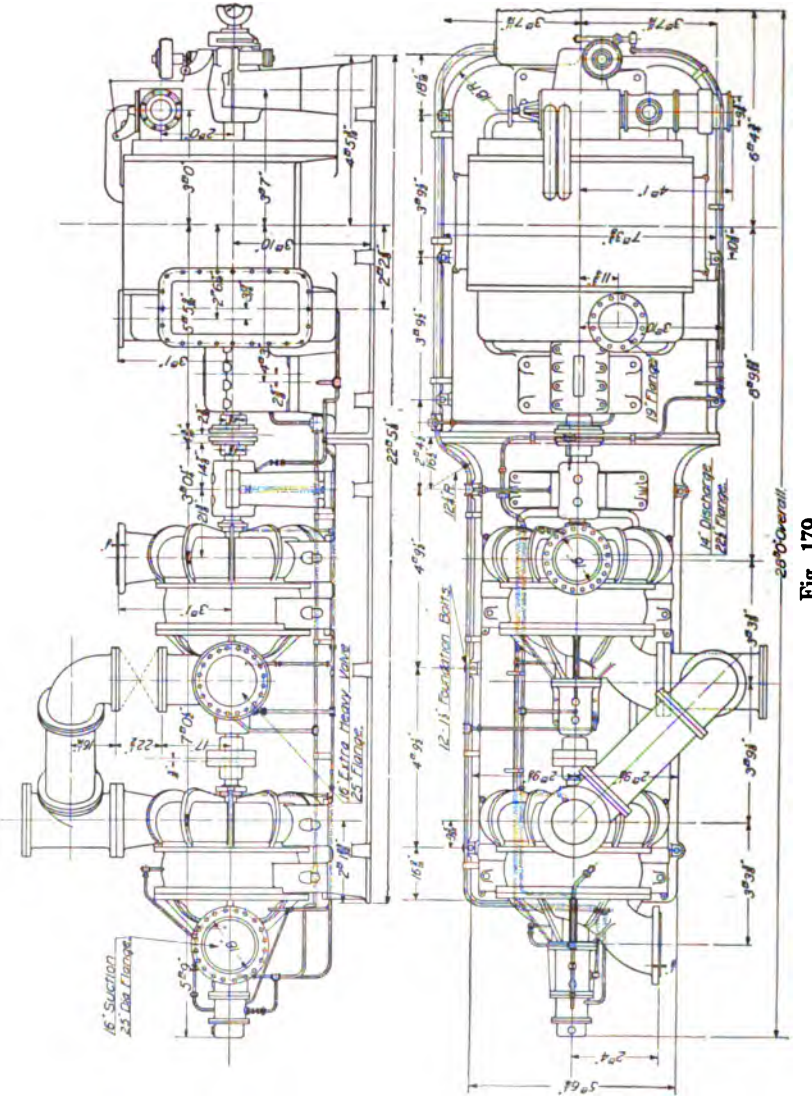
18" Suction
25 Dia. Flange.
16" Extra Heavy Valve
25" Flange.
12 - 1½" Foundation Bolts.
14" Discharge
22½ Flange.
18" Flange.
20'0" Overall.

Fig. 179.

preceding pump in not having any discharge vanes, although the head is quite high. The casing is so constructed as to form a special involute discharge to aid in decreasing the shock losses at exit from the impeller. On account of the dirty and gritty water to be pumped, discharge vanes were not used in this case. Fig. 170 presents the characteristic curves of this pump. At the normal load the efficiency is 75 per cent, which is excellent considering that the pump has no discharge vanes.

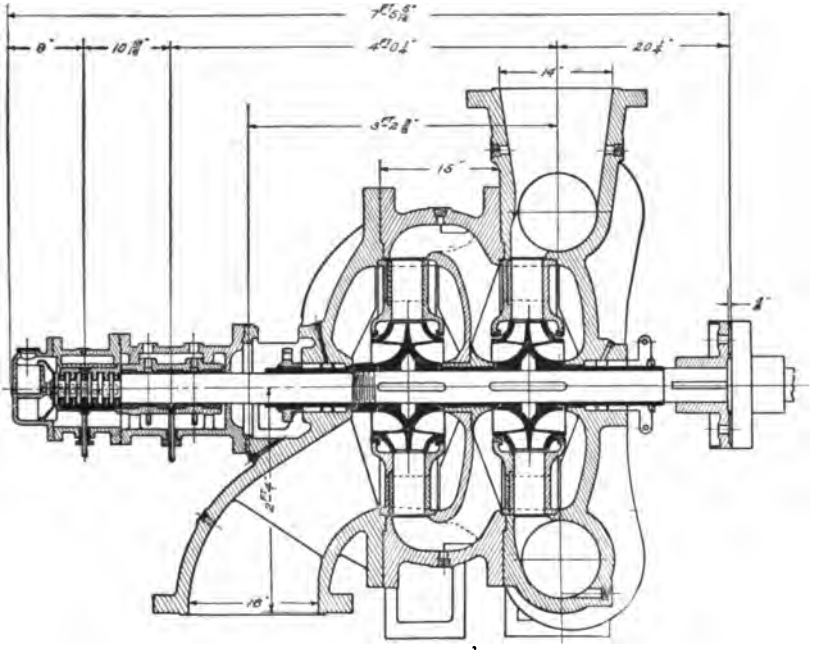

Fig. 180.

Fig. 172 illustrates the construction of a vertical bi-rotor pump having no discharge vanes. The weight of the rotating element is carried on a water step. This pump can deliver 936 cubic feet (7000 gallons) of water per minute against a head of 180 feet at a speed of 1500 r.p.m.

It may be of interest to show the relation between head, capacity, power, and efficiency for various speeds of a low-pressure pump without discharge vanes. Fig. 171 gives a series of curves showing this relationship, taken from actual tests on a Worthington pump having a 5-inch discharge pipe. The iso-efficiency curves are of special

interest, for they show at a glance the region of any per cent of efficiency.

As has been stated, Worthington has recently adopted the double-suction impeller for multi-stage high-pressure, high-speed, and high-efficiency design. A recent installation of this type was for the Commonwealth Edison Company of Chicago. Several units have been installed for boiler feed, and others are being built. A photographic view of one of these units is given in Fig. 173. The pump has three stages and is direct connected to a 150-h.p. Curtis steam turbine built by the General Electric Company. The pump can deliver 60 cubic feet (450 gallons) of water per minute against a

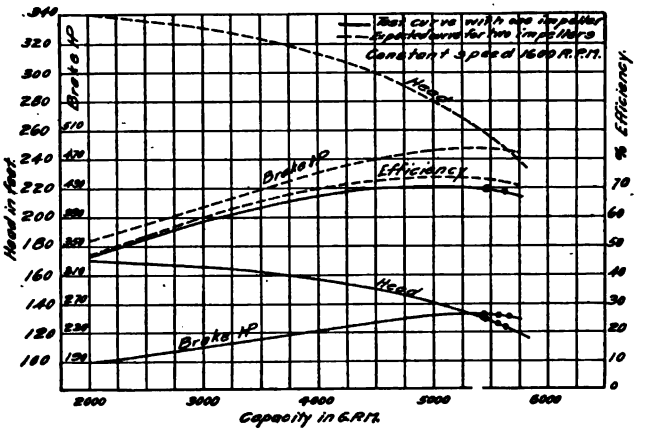

Fig. 181.

pressure of 240 pounds per square inch when operating at a speed of 2400 r.p.m. Fig. 174 gives an outline drawing showing the general dimensions of the unit, and Fig. 175 gives the cross-sectional views of the pump. The water is admitted through the five-inch suction opening to both sides of the first impeller. The discharge vanes are so constructed that the water can pass through cored holes in these vanes and so gain entrance to the opposite suction side. The impellers are of the shrouded type, turned smooth and polished on the outside and carefully chipped and file-finished in the blade channels. The discharge vanes are cast open on one side to permit of accurate machining of the guide channels. A plate is fastened to this open side as shown in the sectional view. The water passes from the

first set of discharge vanes through a reversing channel and is led to both sides of the second impeller, and so on. It should be noted that ribs are provided in the suction pipe and the reversing channels to prevent the water from rotating in these places. Fig. 176 represents the characteristic curves of this pump. At rated normal quantity the head obtained at 2350 r.p.m. was 625 feet (272 pounds per square inch) and the efficiency 63 per cent. The maximum efficiency of 65 per cent was obtained at a capacity of 74 cubic feet

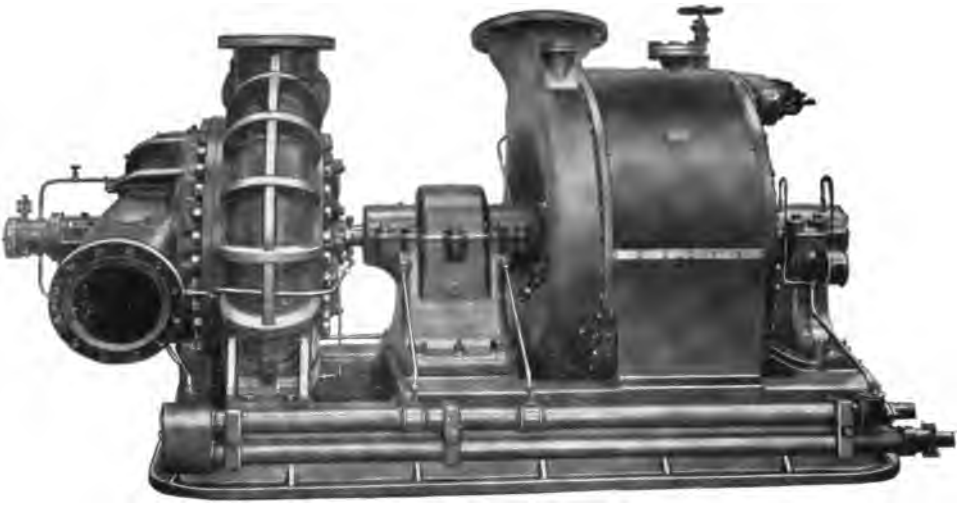

Fig. 182.

(550 gallons) per minute and a head of 585 feet. If the speed is increased the head can be increased as shown. Considering that the capacity is comparatively small and the head very high, the efficiency given by this pump is quite satisfactory.

Fig. 177 is a photographic view of two two-stage pumps of the double-suction type direct connected to a 1000-h.p. Curtis steam turbine built by the General Electric Company. These pumps were made for the Cambria Steel Company. The pumps are so arranged that they operate either in parallel or in series. When operating in parallel they can deliver 1470 cubic feet (11 000 gallons) of water per minute against a head of 250 feet; and when operating in series they can deliver 735 cubic feet (5500 gallons) of water per minute

against a head of 500 feet. The steam turbine runs normally at 1600 r.p.m., but the governor can be adjusted over quite a large range of speeds. The turbine has two bearings, and is connected to the pump shaft by means of a flexible coupling designed by the General Electric Company and shown in Fig. 178. This coupling consists of two disks *A* and *B* made of a number of thin sheet-steel punchings, the outer ends of which are secured to the ring *C*. The inner end of disk *A* is riveted to the turbine shaft coupling *D*, while that of *B* is riveted to the pump shaft coupling *E*. This arrangement permits of lack of alignment between the two shafts, but is perfectly rigid in transmitting the torque. The pumps are similar and have a bearing fastened to the suction end of the casing. A pedestal bearing is provided between the flexible coupling and the pump. The coupling between the two pumps is of rigid construction and is not flexible. The thrust bearing is on the outboard end of the pumps. Fig. 179 gives an outline view of this unit and Fig. 180 a cross section through the outboard pump. The construction of the impellers and discharge vanes is similar to that shown in Fig. 175. As these pumps have not yet been installed, complete tests are not available, but a shop test has been made on one pump with one impeller only. This test will not show as good a result as is expected from the complete unit. Fig. 181 gives in full lines the characteristic curves obtained from the shop test, and the dotted lines represent the expected characteristic curves of a single pump with two impellers. On the whole, these curves are satisfactory, for they represent efficiencies obtained on commercial machines and not on special pumps built for test and then rated at the point of their best efficiency.

It may be of interest, finally, to add a photographic view (Fig. 182) of the Worthington pumps installed on the New York fire boats. These units were the first multi-stage centrifugal pumps driven by steam turbines installed on fire boats. There are two units on board each boat, and each unit is capable of delivering 735 cubic feet (5500 gallons) of water per minute against 125 pounds per square inch pressure, or 600 cubic feet (4500 gallons) of water per minute against 150 pounds per square inch pressure. The normal operating speed is 1800 r.p.m. In cases of emergency the water pressure can be increased by increasing the speed of the turbine. The two units on

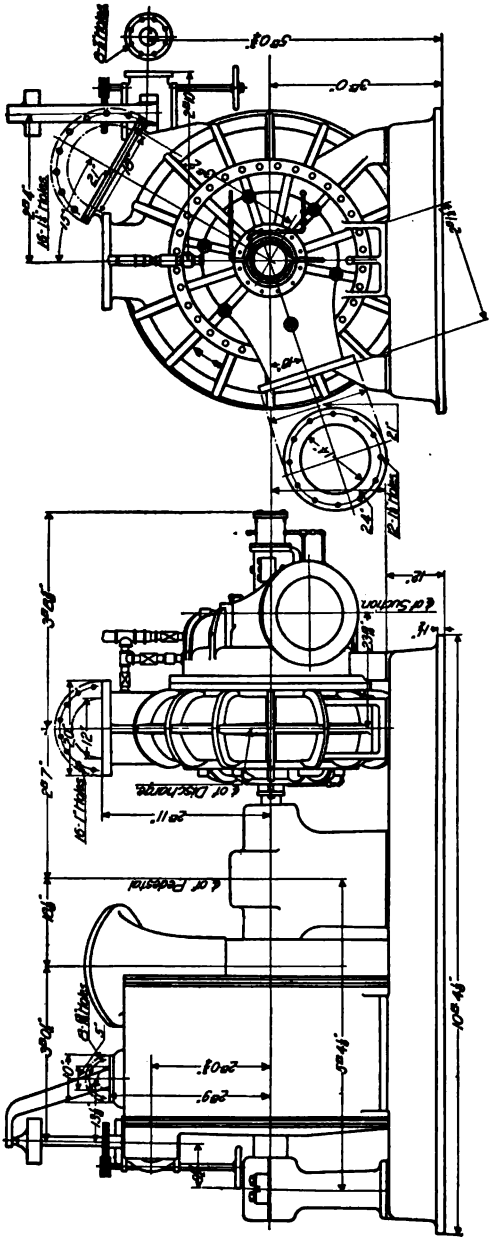

Fig. 183.

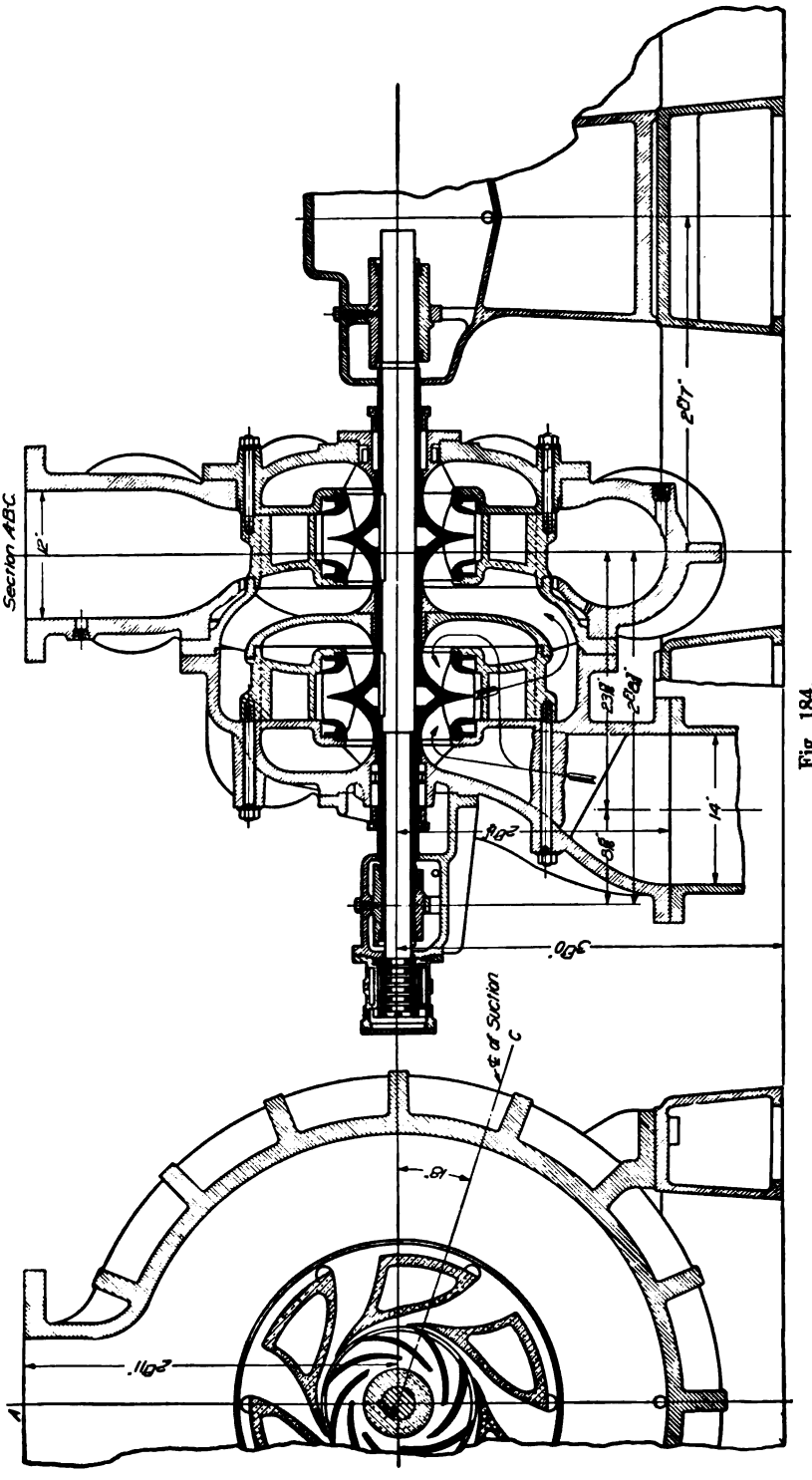

Fig. 184.

each boat are also arranged to work in series and discharge the water at a pressure of 300 pounds per square inch. The turbines are of the Curtis type, having a capacity of 600 h.p., and were supplied by the General Electric Company. Fig. 183 gives an outline view of this set, from which the general dimensions of the unit may be seen, and Fig. 184 gives a cross-sectional view of one of the pumps.

As will be seen, each pump consists of two stages having impellers of the double suction type. Considering the large quantity of water to be handled, the impellers are of quite small diameter. The impellers and discharge veins are made of bronze and the entire shaft is protected by bronze sleeves. The casing is well ribbed and strengthened so as to withstand the high hydraulic pressures. All the bearings of this unit are provided with forced lubrication supplied by an oil pump driven directly from the turbine shaft. In order to secure correct alignment of the shaft, a thrust-bearing of the marine type is provided at the suction end of the pump.

46. Pumps of the Armaturen und Maschinenfabrik A. G.

Figs. 185 and 186 show cross sections of a low-pressure centrifugal pump built by the Armaturen und Maschinenfabrik A. G. of Nuremberg, Germany. These pumps are called "Evolventen" pumps because the water in flowing through the pump traverses four different involute paths. Even in the low-pressure pumps water enters on one side of the pump only, thus differing from the usual construction of low-pressure pumps. The axial balance is obtained in a manner similar to that employed by Jaeger. The clearance rings instead of forming the clearance space upon a cylindrical surface form this space on a radial surface.

Experience showed that water containing much grit would wear the clearance rings unevenly in the old construction, and then an axial thrust would result. In this new construction it is necessary carefully to adjust the impeller axially to prevent rubbing. This is taken care of in the thrust bearing, which permits adjustment while the pump is operating.

The thrust bearing is also provided with an indicator registering the amount of unbalanced axial thrust. While the pump is operating the clearance spaces may be so adjusted that the axial thrust will practically disappear.

The high-pressure centrifugal pumps have a water guidance similar to the Rateau and Jaeger types, but also have several novel

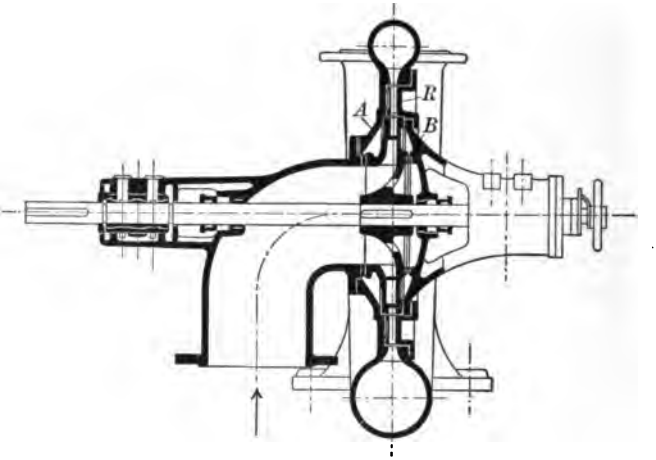

Fig. 185.

features of their own. Fig. 187 shows a five-stage high-pressure pump direct connected to a motor, and Fig. 188 gives a longitudinal

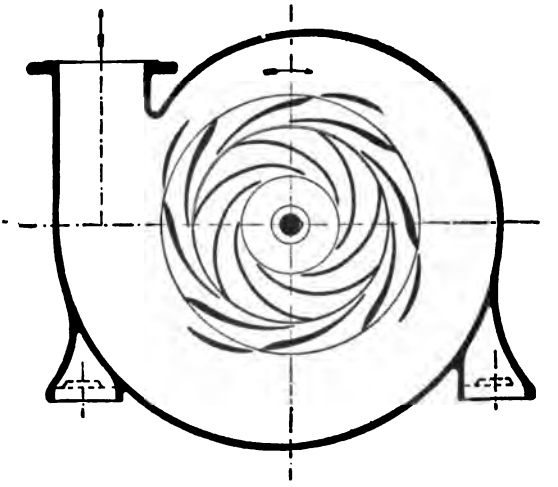

Fig. 186.

cross section of a five-stage pump. The pump is built up in sections of one stage each in order that it may be easily disassembled. Another advantage of this method of construction is that it is possi-

ble to add a number of stages by simply substituting a longer shaft and longer through bolts on the casing.

The impellers are of rather novel design. Fig. 189 shows a cross-sectional view through the blades of an impeller. The entrance and

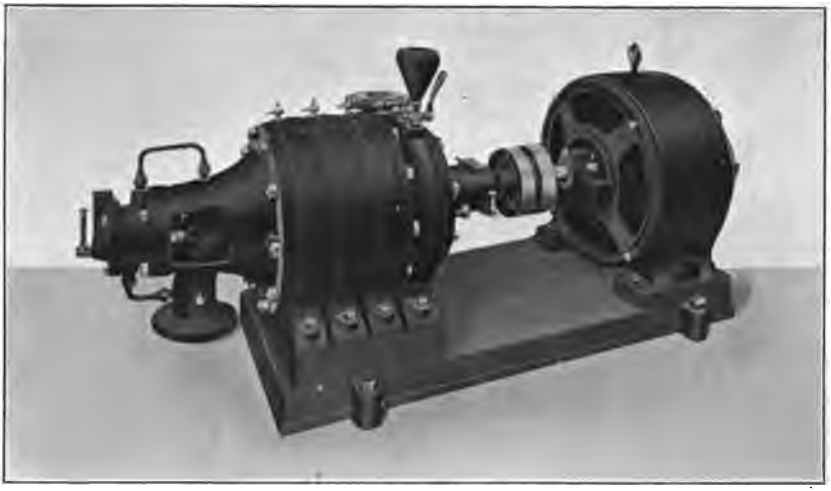

Fig. 187.

exit ends of each blade are involute in form and are connected by a curve of maximum radius. In the usual construction by other pump builders the sides of the impellers are plane surfaces of revolution; that is, if a cross section is taken through the line XY of the im-

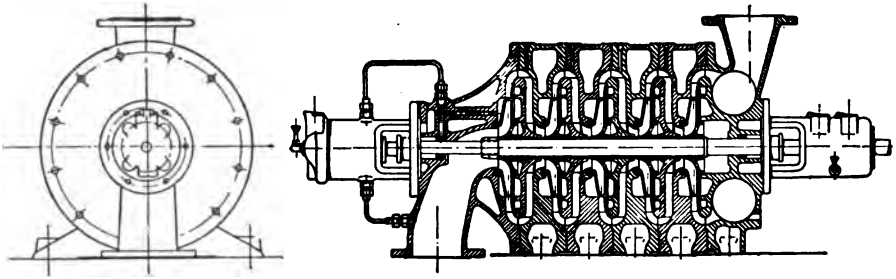

Fig. 188.

peller shown in Fig. 189, it will appear as in Fig. 190, the impeller sides being plane surfaces of revolution, so that at any certain radius the blade height would always be constant. The impeller channel can be represented as in Fig. 192, which is a development of the

channel along the mean path of the water and shows various sections taken at right angles to flow. All these sections taken at

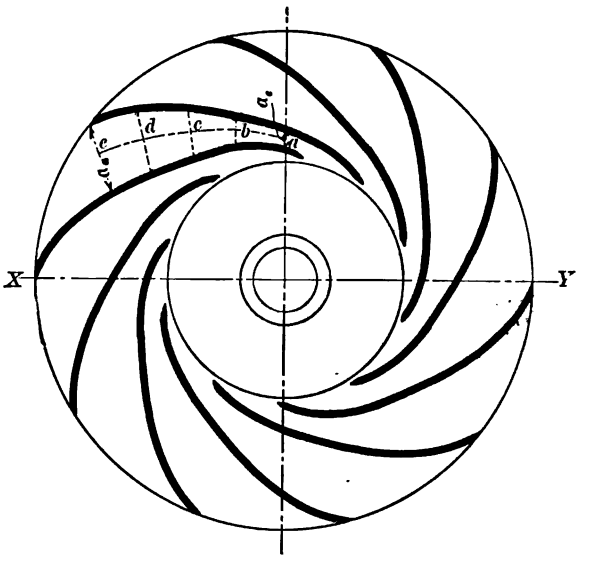

Fig. 189.

a, *b*, *c*, *d*, and *e*, Figs. 189 and 192, at right angles to flow are trapezoids.

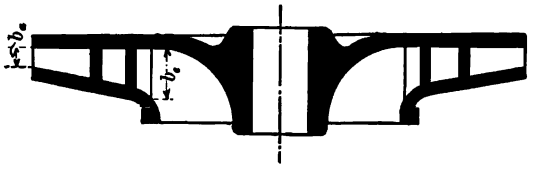

Fig. 190.

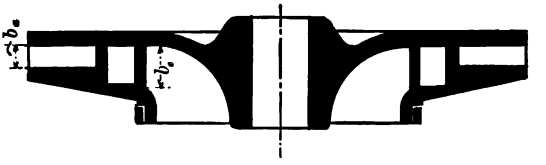

Fig. 191.

The impeller designed by Neumann, chief engineer of the Armaturen und Maschinenfabrik A. G., is so constructed that all cross sections of the impeller channel taken at right angles to flow are

rectilinear, and the variation of cross section from entrance to exit produces a linear change of velocity from entrance to exit of the impeller. Fig. 191 gives a cross-sectional view of such an impeller along the line XY of Fig. 189. The developed channel is shown in

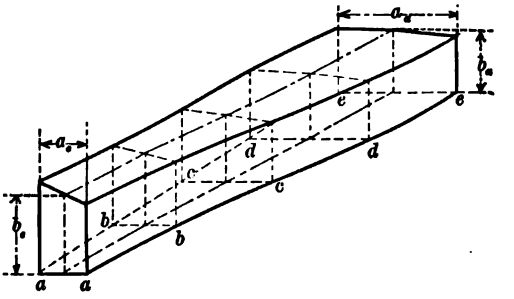

Fig. 192.

Fig. 193, in which the channel cross sections a, b, c, d, and e taken at right angles to flow are rectangles.

Figs. 190 and 191 represent two impellers that were designed to lift 230 cubic feet of water per minute against a head of 164 feet. The relative entrance velocity of each impeller (at point a) was

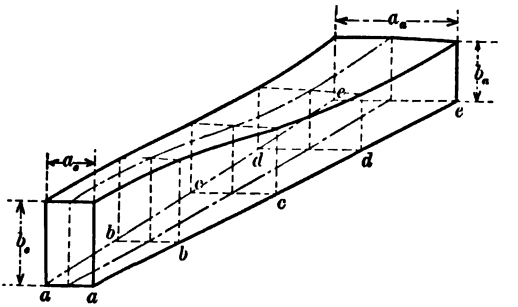

Fig. 193.

calculated to be 52.5 feet per second and the relative exit velocity of each impeller (at point e) was 25.6 feet per second. The decrease of the entrance velocity of 52.5 feet to the exit velocity of 25.6 feet should produce a theoretical pressure head of $\frac{(52.5)^2 - (25.6)^2}{2g} = 32.8$ feet. Fig. 194 shows the decrease of velocity along the impeller

channel from a to e for both designs of impeller. The dotted line represents the decrease of velocity for the impeller, shown in Fig. 190, and the full line the decrease of velocity for the impeller, shown in Fig. 191. In the latter the decrease of velocity is linear and corresponds to the theory presented in Article 4. The dotted curve shows a very rapid decrease of velocity from point a to c. From c to d the decrease of velocity is less. At d the lowest velocity is reached, that of 22.3 feet per second. From d to e the velocity again increases to 25.6 feet per second. Such a decrease and increase of velocity naturally disturbs the proper transformation of velocity head into pressure head, which influences the efficiency of the pump. Shock losses also occur to some extent in an impeller, as shown in Fig. 190.

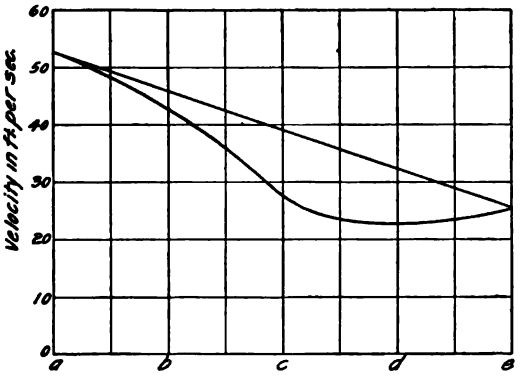

Fig. 194.

Another feature of this type of pump is the method of directing the short-circuited water into the suction pipe. The usual construction is shown in Fig. 195. Fig. 196 shows the design of clearance ring for this type of pump. In Fig. 195 the short-circuited water leaves the clearance space at a high velocity and meets the water of lower velocity entering the impeller perpendicularly. This causes strong eddy currents, which continue up to the entrance of the impeller and hinder a proper entrance of the water to the impeller. The short-circuited water flows from the clearance rings at velocities from 60 to 100 feet per second and over. To obviate this fault, the clearance rings are made as shown in Fig. 196. The water leaving the clearance rings at high velocity meets the main

body of water entering the impeller almost parallel to the direction of flow, thus producing a sort of ejector action. This permits a part of the energy of the short-circuited water to be regained.

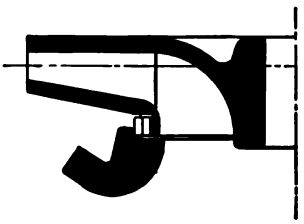

Fig. 195.

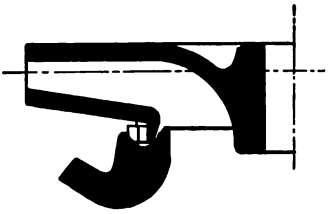

Fig. 196.

In this type of pump axial thrust is taken care of by balancing the pressures upon both sides of the impeller, as in the Jaeger pump. Fig. 197 gives a cross-sectional view of the impeller and casing of a

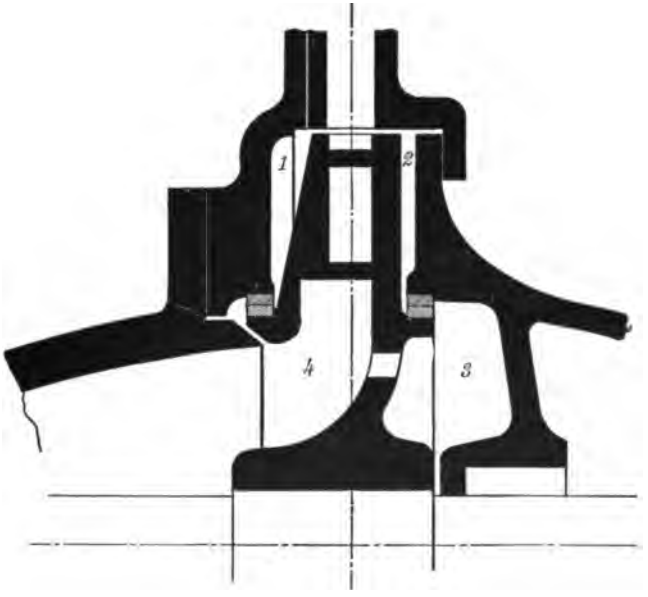

Fig. 197.

multi-stage pump. Clearance spaces 1 and 2 are made of the same size by using clearance rings of the same diameter, and chamber 3 is connected with chamber 4 by holes in the side of the impeller. This

will produce equal pressure in chambers 3 and 4, perfectly eliminating the static pressures. A suitable formation of the clearance

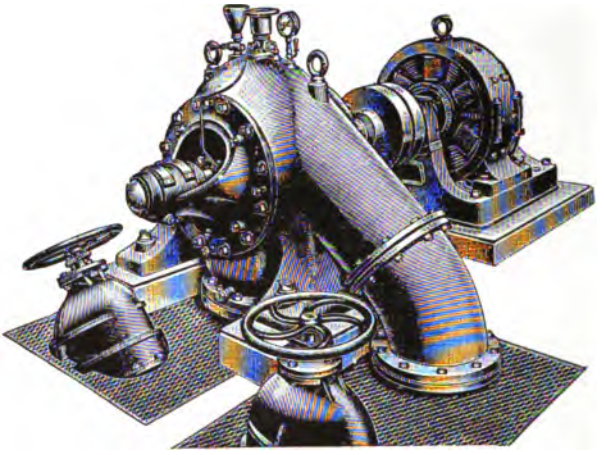

Fig. 198.

at the rings will also produce equal pressures in spaces 1 and 2; since the areas are equal the total pressures will balance each other.

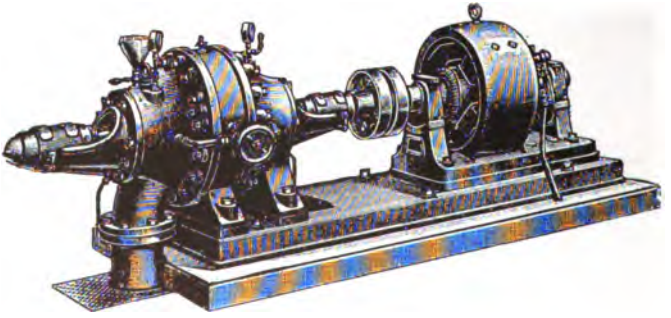

Fig. 199.

The outboard bearing of the pump contains a thrust bearing to take up any small thrust caused by unequal wear of the clearance rings. The thrust bearing is provided with forced lubrication.

The impellers used for high-pressure pumps are made of phosphor bronze. The guide vanes are made of the same material and are open on one side. In multi-stage pumps the casing of the previous stage closes the open side, as can be seen in Fig. 188. In single-stage pumps a cover in the form of a ring is placed over this opening in the side of the guide vanes, as is shown by part *R* in Fig. 185. This construction also permits of cleaning the discharge passages without further disassembly of the pump. The main advantage in making the guide vanes open on one side is that they can be milled to exact dimensions, which is quite important when the water velocity is high. The clearance rings are made of phosphor bronze. The shaft runs in bearings having ring lubrication. The stuffing box is of

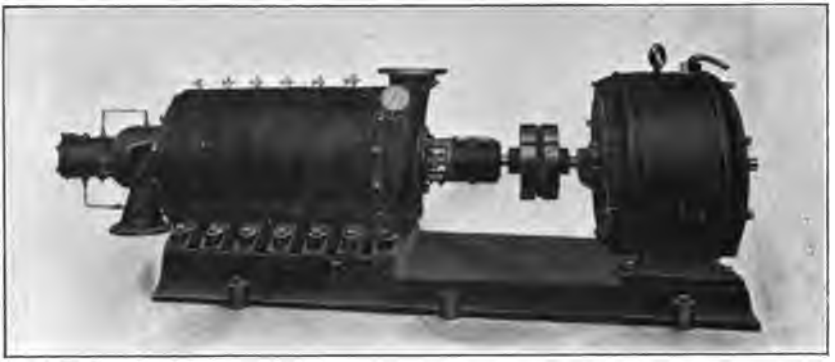

Fig. 200.

the usual design, and the packings are fitted with water seals. The inlet area of the stuffing boxes is larger than the outlet area, so that both the high-pressure and suction sides of the stuffing box pack against pressure and not vacuum.

This firm also designs in special cases one or more spare guide vanes for pumps which must deliver smaller quantities than the rated quantity for any length of time. Such a combination permits the pump to operate at high efficiencies even when delivering one-half the normal quantity of water. If the regulation is by means of a throttle valve, the efficiency usually decreases from 15 to 20 per cent when delivering one-half the normal quantity; and by substituting a new set of guide vanes the efficiency decreases only about 4 per cent. Some pumps are also built with regulation by means of adjustable guide vanes.

Fig. 198 shows a large single-stage high-pressure pump direct connected to a 200-h.p. Siemens-Schackert motor. It delivers 460 cubic feet of water per minute against a head of 165 feet at 1200 r.p.m. Fig. 199 is a two-stage high-pressure pump delivering 90 cubic feet of water per minute against a head of 150 feet; the pump runs at 1100 r.p.m.

Fig. 200 represents a seven-stage pump of this design installed as a fire pump for the Underground Electric Railways Company of

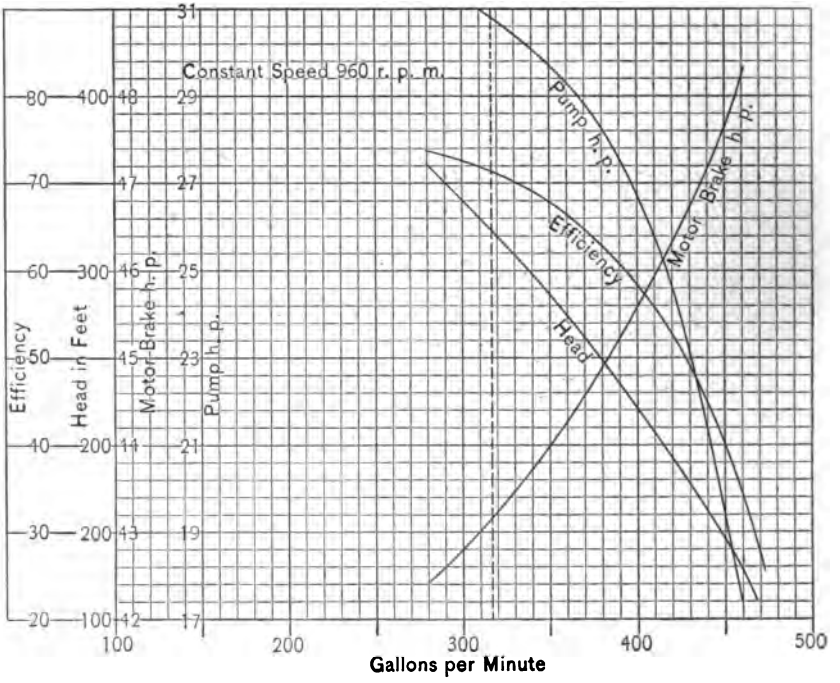

Fig. 201.

London. It is designed to deliver 325 gallons (44 cubic feet) per minute against a head of 140 pounds per square inch (322 feet), and runs at 960 r.p.m. The pump is direct connected to a 50-h.p. induction motor of $33\frac{1}{3}$ cycles, which explains its low speed. Fig. 201 shows the curve sheet for this pump, which has an efficiency of 71.5 per cent at the specified head. The efficiency rises to 74 per cent when the head is increased.

47. I. P. Morris Pumps.

The I. P. Morris Company of Philadelphia, Pa., do not manufacture any standard line of centrifugal pumps, but build both high- and low-pressure pumps specially designed to meet the needs of any customer. Their specialty is low-pressure pumps of large size. One of the largest units installed by this firm is a low-pressure pump for the pumping station of the New Orleans Drainage Commission.

Fig. 202.

The impeller of this pump is 9 feet 4 inches in diameter and the discharge pipe is 6 feet in diameter. It is driven by a 500-h.p. General Electric motor. The shaft of the unit is vertical. The pump is placed in a concrete chamber below the motor, the latter being installed upon the floor of the station. The pump delivers 19 200 cubic feet of water per minute against a head of 10 feet with an efficiency of 74 per cent. The maximum efficiency is 77.5 per cent when the pump is delivering 17 640 cubic feet of water per minute against a head of 11 feet.

Fig. 202 gives a photographic view of a recent design of high-pressure centrifugal pump built for the waterworks of the city of Duluth, Minn. It is a two-stage horizontal shaft pump arranged for

direct connection to a General Electric induction motor. The two impellers are placed back to back so as to reduce the axial thrust. The unbalanced axial thrust is taken care of by a ball bearing attached to the tail bearing. The blade surfaces of the impeller and guide vanes were made smooth in order to minimize the friction losses. The pump is equipped with two ring-oiled babbitted bearings secured to the suction and discharge elbows. The stuffing box on the suction side of the pump is supplied with a bronze spacer ring,

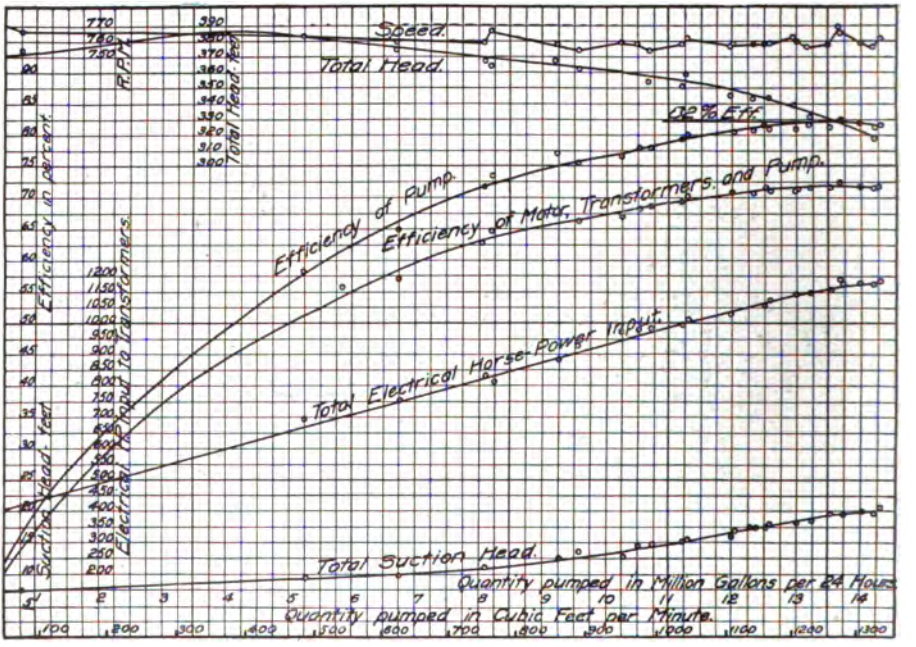

Fig. 203.

into which water is fed. This water seal prevents the air from being drawn through the stuffing box and into the pump through the suction elbow. The performance of this pump is shown in Fig. 203. It will be seen that when the pump delivers water at the rate of 1253 cubic feet per minute (13 500 000 gallons per 24 hours) against a total head of 327 feet and when running at a speed of 755 r.p.m. the pump efficiency is 82 per cent. The combined efficiency of the motor, transformers and pump, when the latter is operating under the conditions above stated, was found to be 72 per cent. The entire

electrical input to the transformers was 1100 h.p. It should be noted that the total head does not vary considerably with change of quantity of water delivered.

The I. P. Morris Company have built several high-speed, high-pressure centrifugal pumps for fire-boat service. The most unique installation of this kind is the one furnished by the General Electric Company for the city of Chicago. The two fire boats are named the *Joseph Medill* and the *Graeme Stewart*. Each boat has two complete units, consisting of a 660-h.p. Curtis turbine direct connected to a 200-k.w., 275-volt direct-current generator and a two-stage centrifugal pump. The pumps were built by the I. P. Morris

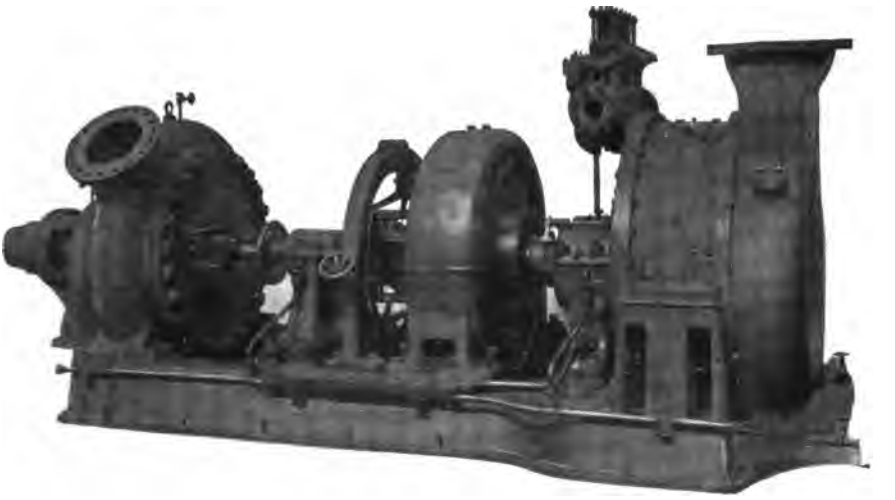

Fig. 204.

Company. The generators serve to provide current for the motors direct connected to the propellers. These motors are of the variable-speed reversing type. In going to a fire the pump impellers run dry and the generators furnish current for propelling the boat. Control of the propelling motors is possible from both the pilot house and the engine room. The captain of the boat usually controls the speed without the aid of the engineer, by means of two rheostats placed in the pilot house. In fact, all steering is accomplished by simply changing the speed of either port or starboard propeller by adding or cutting out resistance in either rheostat.

A photographic view of one of these sets is shown in Fig. 204. The set has three bearings, one between turbine and generator, another between generator and pump, and a third on the outboard end of the pump. The turbine is overhung on the shaft. One

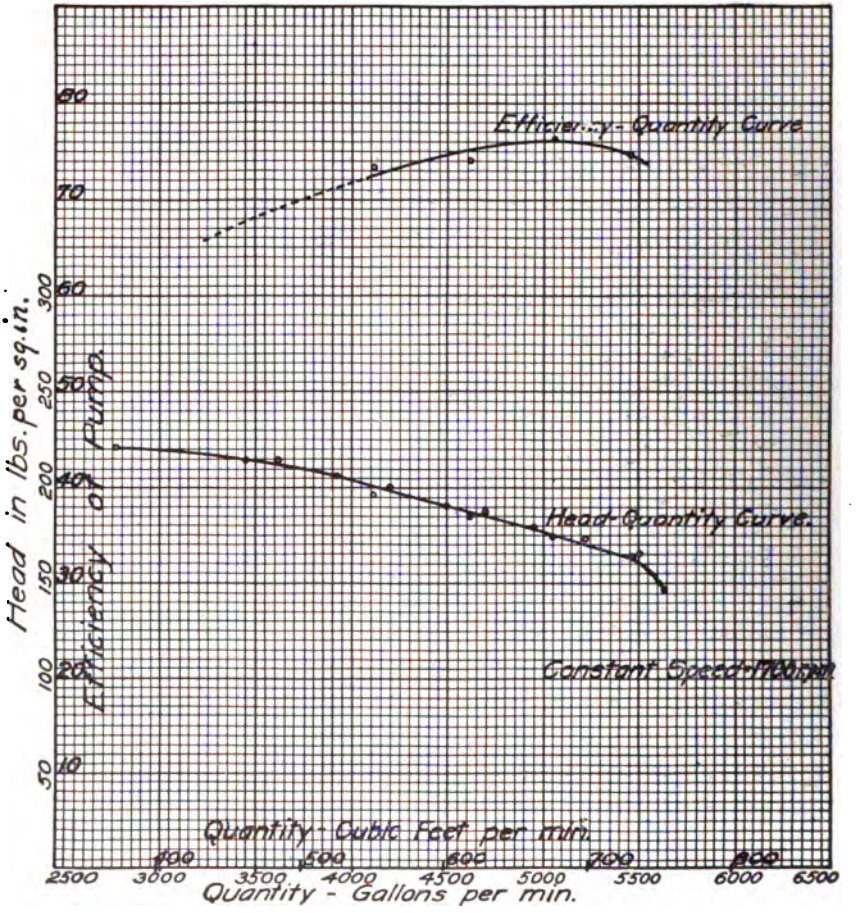

Fig. 205.

shaft extends through turbine and generator and is direct connected to the pump shaft. The entire unit is mounted on a common base. The bearings are supplied with oil under pressure. Each pump has two impellers placed back to back as in the original Sulzer type of pump. The discharge vanes and reversing passages are cast into the casing. The diameter of each impeller is 18 inches. Between

the impellers is a diaphragm holding a packing ring, which can slightly adjust itself centrally as the pump comes up to speed, and which is held in position by water pressure after the pump reaches its normal speed. The two centrifugal pumps on each boat can be operated in series or in parallel. When running in parallel they can deliver 1203 cubic feet of water per minute (9000 gallons per minute) at the nozzles at a pressure of 150 pounds per square inch. When running in series, which is equivalent to acting as a single

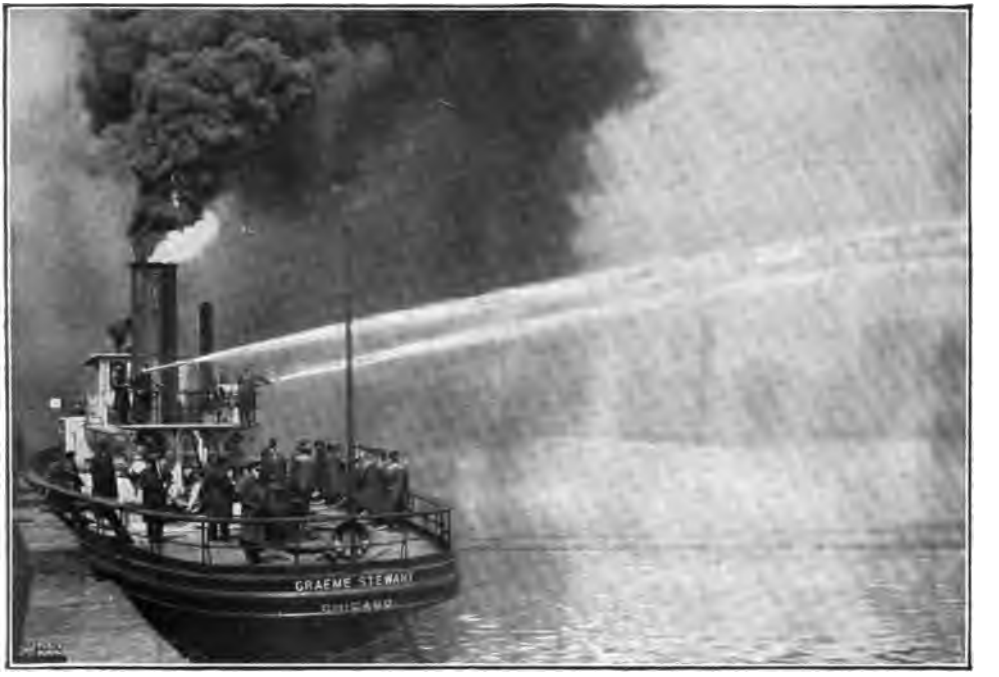

Fig. 206.

four-stage pump, they can discharge 601.6 cubic feet of water per minute (4500 gallons per minute) at 300 pounds per square inch pressure. The water for the pumps is drawn from a 14-inch header which extends across the engine room, and is delivered to bulb-shaped turrets located on the deck amidships. Above the deck turrets is a bridge on which are mounted two 4-inch monitor nozzles with mechanical control. The boats are moored with three mooring spuds, which consist of heavy steel tubing 18 inches in diameter and shod with heavy cast-steel points to take hold of the river bottom. By

means of steam-operated racks and pistons they are raised and lowered through wells in the bottom of the boat.

After the boats were placed in commission they were given capacity tests covering a period of eight hours, during which time at frequent and regular intervals readings were taken. The results obtained are indicated in the following tabulation:

Fig. 207.

Turbine speed (starboard)	1660 r.p.m.
Turbine speed (port)	1634 r.p.m.
Boiler pressure (starboard)	156.8 lbs. per sq. in.
Boiler pressure (port)	156.5 lbs. per sq. in.
Condenser vacuum	27.3 in.
Centrifugal pump pressure (mean)	157.25 lbs. per sq. in.
Number of nozzles	2
Diameter of nozzles	4 in.
Discharge per pump	4808 g.p.m.
Discharge, two pumps	9616 g.p.m.
Total discharge per hour	576 000 gals.
Coal burned, total	26 500 lbs.
Coal burned per hour	3310 lbs.
Coal burned per square foot of grate surface	39.4 lbs.
Steam consumption per horse-power hour	21.5 lbs.

Fig. 205 gives the results of the acceptance test made by the General Electric Company on the centrifugal pump. The pump efficiency was 74.5 per cent at rated load, and reached a maximum of 76 per cent with increased quantity of discharge but lower head. It may be of interest to add Figs. 206 and 207, which represent the *Graeme Stewart* in action.

Another pair of high-pressure centrifugal pumps for fire-boat service was furnished by the I. P. Morris Company to the General Electric Company for the fire boat *McGonagle*. This boat was built for

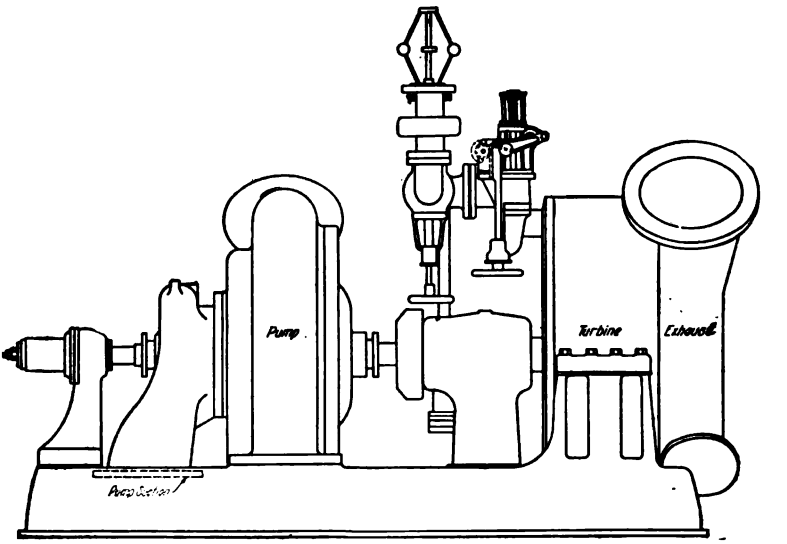

Fig. 208.

the Duluth, Missaba & Northern Railway to protect iron-ore docks at Duluth, Minn. Duplicate sets were installed in a second fire boat built for the same interests. Each of these pumps is driven by an 800-h.p. Curtis steam turbine. Fig. 208 gives an outline assembly of the set, and Fig. 209 a longitudinal sectional view. The unit has only two bearings, with the pump between them and the turbine overhung. The thrust bearing was designed by the General Electric Company. A cross section of the thrust bearing for these pumps is shown in Fig. 210. The thrust bearing is overhung and is mounted on the extended shaft beyond the outboard pedestal. The bearing lining and thrust bearing casing are made in one piece,

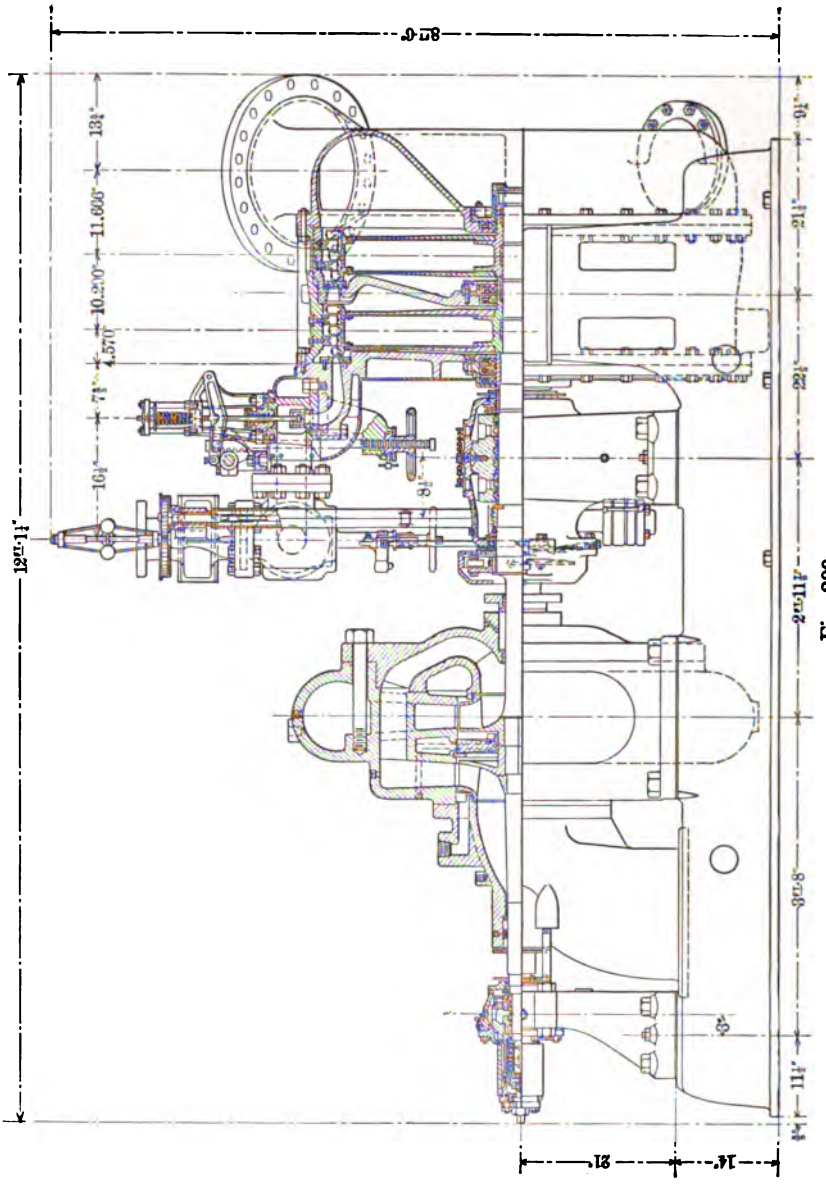

Fig. 209.

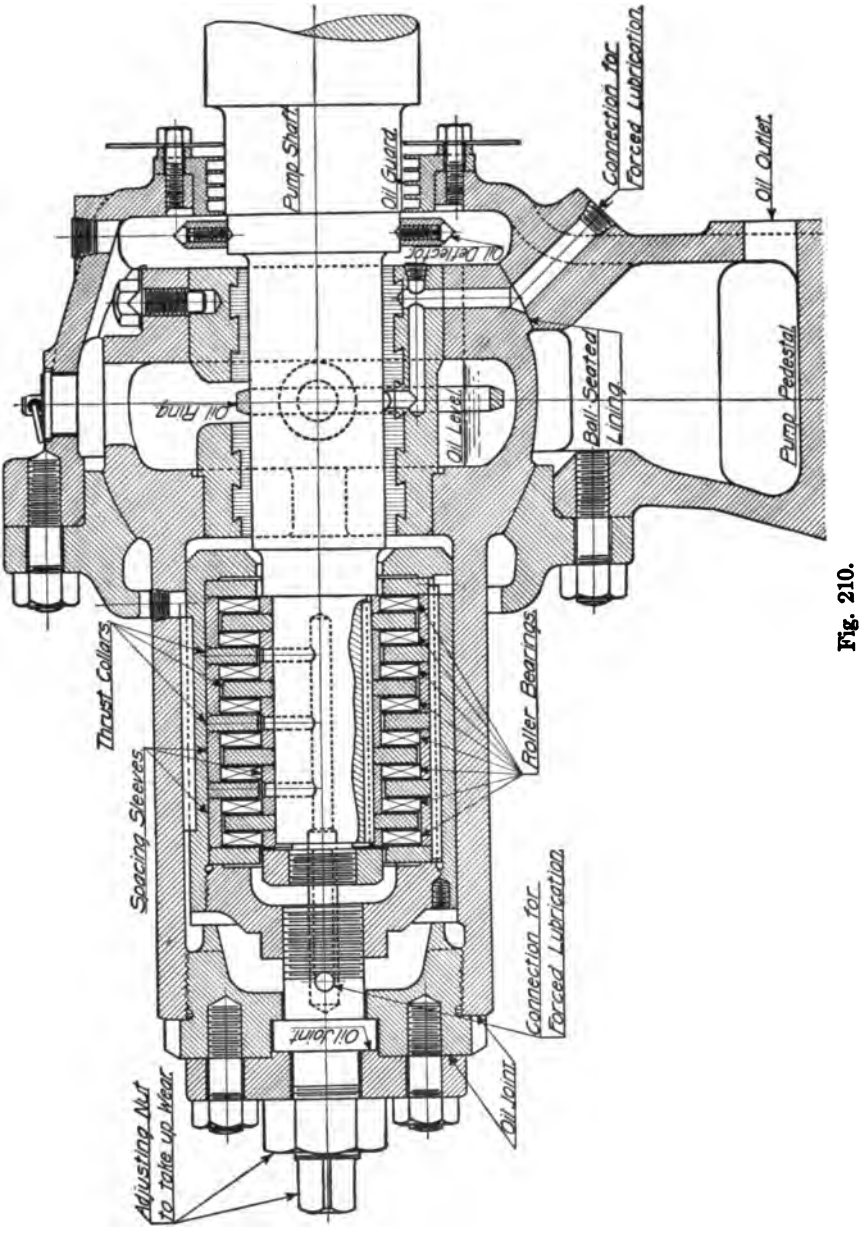
Pump Shaft
Oil Guard
Oil Deflector
Connection for Forced Lubrication
Oil Outlet
Oil Ring
Oil Level
Ball-Seated Lining
Pump Pedestal
Thrust Collars
Spacing Sleeves
Roller Bearings
Oil Joint
Connection for Forced Lubrication
Oil Joint
Adjusting Nut to take up Wear

Fig. 210.

and as the lining is of the spherical seated self-aligning type, the entire thrust bearing adjusts itself to the position of the shaft. The thrust bearing consists of a series of thrust collars keyed alternately to the shaft and bearing casing, with roller bearings between them. The thrust collars on both the shaft and casing are spaced accurately and held in place by spacing sleeves carefully ground to equal lengths.

Fig. 211.

This bearing will take thrust in either direction. The roller bearings are lubricated by oil under pressure supplied through radial holes leading to a hole in the center of the shaft, into which the oil is forced by the oil supply system. This thrust bearing is highly satisfactory and has not given any trouble in service. The turbines are supplied with steam at 180 pounds per square inch pressure, and exhaust into a vacuum of 28 inches. The pumps are two-stage, with impellers arranged back to back and with the discharge vanes and reversing

passages cast into the casing. Each pump is capable of delivering 800 cubic feet of water per minute (6000 gallons per minute) at a pressure of 150 pounds per square inch when running at the normal speed of 1800 r.p.m. The two sets can be operated in series and will then deliver a pressure of 300 pounds per square inch. At the acceptance tests of these pumps the sets operated at their full rated capacity, and the actual steam consumption for both sets was 25 880 pounds per hour. Fig. 211 gives a view of the boat with its three main turret nozzles in operation.

48. Skoda Pumps.

A twelve-stage Rateau pump built by the Skoda Works of Pilsen, Austria, is illustrated in Fig. 212. The outer casing is divided along the longitudinal axis. The inner parts of the casing, which contain the guide and reversing channels, are not divided. In assembling the pumps the impeller and guide vanes are placed alternately upon the shaft. The assembled impellers and guide vanes are then

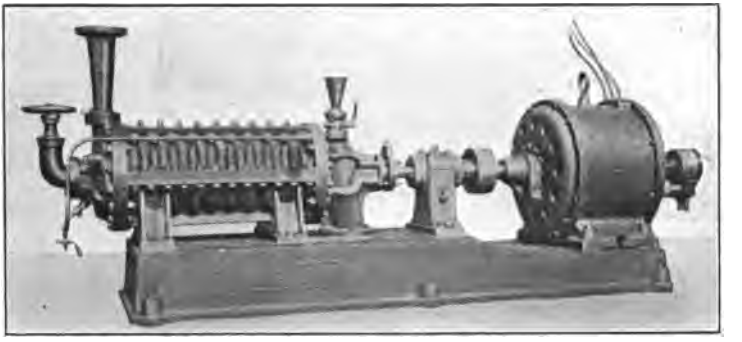

Fig. 212.

lowered into the lower half of the casing. The guide vanes are fastened by means of screws to the casing. The upper half of the casing is then put in place and the suction pipe elbow and high-pressure head are bolted on to the casing. The high-pressure head is made with a spiral-shaped water chamber.

To take up any axial thrust which may occur a collar thrust bearing with oil lubrication is provided. The Skoda Works design has this

thrust either between the pump and motor in a separate pedestal, or one of the motor bearings is constructed to contain the thrust bearing.

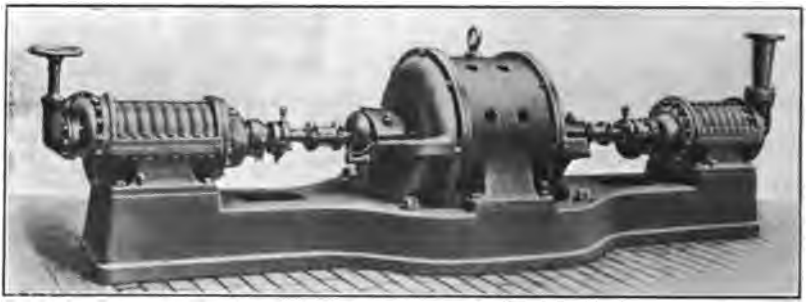

Fig. 213.

The pressure obtained from each stage of a Rateau pump is small. Ordinarily one stage gives a pressure of 65 feet of water. Naturally

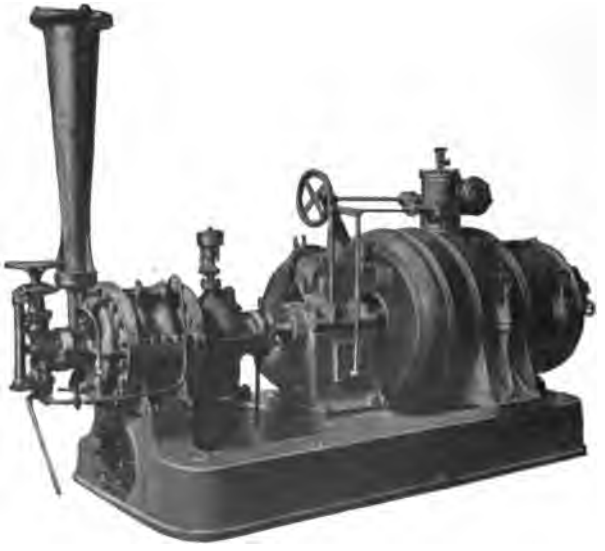

Fig. 214.

the impellers are quite small in diameter. On account of using such small heads per stage, a high-pressure pump requires many impellers and therefore a long shaft, which often necessitates mount-

ing the impellers in groups, each group in a separate casing. The driving motor in such cases is placed between the two pump casings, and the axial thrust is almost wholly balanced by arranging the two groups of impellers so that the thrusts are in opposite directions. Such an arrangement is shown in Fig. 213.

Fig. 214 shows a Rateau pump driven by a steam turbine. The unit was built by the Skoda Works. The pump has four impellers, runs at 3250 revolutions per minute, and delivers 106 cubic feet of water per minute against a head of 682.5 feet. On account of the high speed of the pump each stage gave a head of about 170 feet. It is interesting to note the small space required for this unit; it is 11.5 feet long, 5.75 feet wide, and 5.25 feet high. The conically diverging discharge-pipe permits the use of a smaller casing from which the water leaves at a rather high velocity. This high velocity is gradually reduced in the conical discharge pipe. Fig. 215 shows a mine shaft pump of the Skoda Works design capable of delivering 14 cubic feet of water per minute against 344.5 feet head. Five impellers running at 2900 r.p.m. are used. The pump casing is so designed that a half section can be removed without disassembly of any other part. This permits of an easy inspection.

Fig. 215.

The Skoda Works built a pump for experimental purposes, according to the directions of Rateau, with an impeller of only $3\frac{1}{8}$ inches diameter, which was direct connected to a steam turbine running at 18 000 r.p.m. The pump delivered 25.5 cubic feet of water per minute against 775 feet head. The shaft efficiency of the pump alone was reported to be 60 per cent. With a somewhat reduced quantity of water this small pump delivered heads up to 985 feet.

Fig. 216.

49. Allis-Chalmers Pumps.

The Allis-Chalmers Company of Milwaukee, Wis., have built centrifugal pumps for many years, mostly large pumps of low heads and slow speeds. About five years ago this company began to build multi-stage high-pressure pumps of the Kugel-Gelpke type, according to the designs of Escher-Wyss. They are now contemplating changing from this type of pump probably to the double-suction type illustrated in Fig. 104.

Fig. 216 gives a view of a motor-driven multi-stage pump of the old type. On each side of the motor is a three-stage pump, arranged

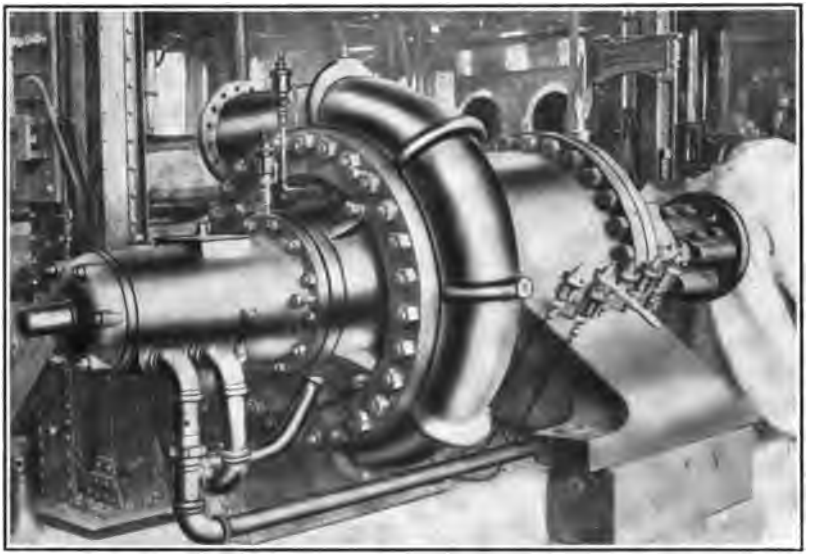

Fig. 217.

so that the unbalanced thrust of one opposes that of the other. Any difference in the end thrust of these two pumps is taken care of by a roller or ball thrust bearing. These two pumps are arranged in series and are therefore the equivalent of a six-stage pump.

One of the best known installations of Allis-Chalmers high-pressure pumps is for the high-pressure fire service for the city of New York. At the present time there are two pumping stations, each containing five units. All the pumps have five stages and are direct connected by means of flexible couplings to induction motors of the

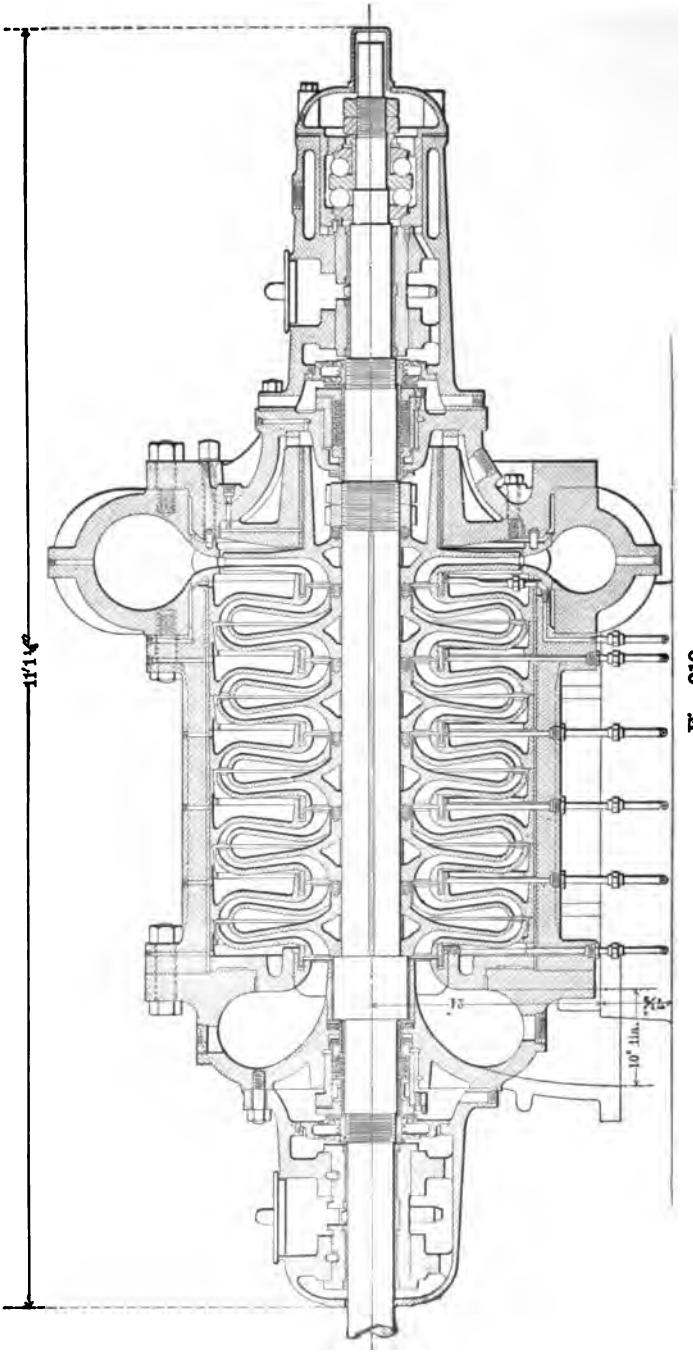

Fig. 218.

Allis-Chalmers type. These motors are of 800 h.p., wound for three-phase, 25-cycle, 6300–6600 volt operation, and designed to run at about 740 r.p.m. Fig. 217 shows a photographic view of one of these pumps and Fig. 218 gives a longitudinal cross section. Each pump is designed to deliver 400 cubic feet of water per minute

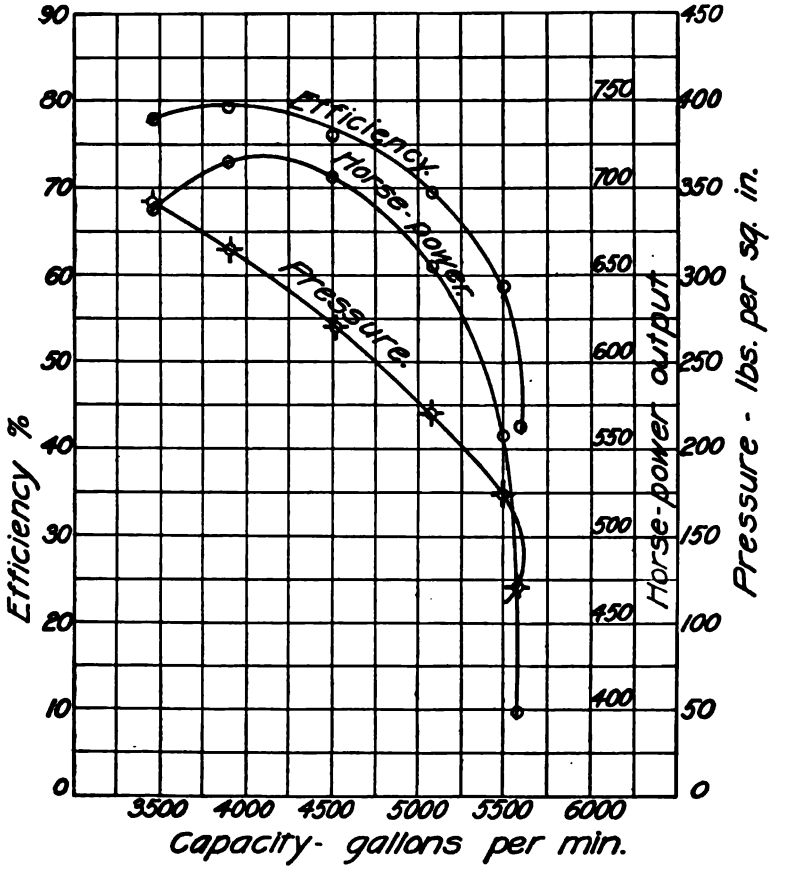

Fig. 219.

against a pressure of 300 pounds per square inch. As can be seen from the figure, axial thrust is partially balanced by means of a balancing piston at the high-pressure end of the pump, which operates in a manner similar to those already described. Any additional end thrust is taken up by ball bearings in the outboard bearing. This ball bearing consists of two rings of 1½ inch diameter steel balls, water cooled and oil lubricated. The balancing piston is

fitted very loosely in order to keep the friction losses small, and as a result a considerable amount of water leaks past it into a chamber at the end of the pump, which is provided with a discharge valve and pipe leading into the suction. Adjusting the valve in this pipe regulates the pressure on the piston. The bearings are of the ring-oiled type. Lubrication is furnished by oil cups to all parts of the impellers and discharge vanes where there are close-running clearances.

Prof. R. C. Carpenter* made exhaustive tests of these pumps, and Fig. 219 gives the characteristic curves of the pump as determined by his tests. The maximum efficiency was 80 per cent, which is very good.

50. Weise and Monski Pumps.

Weise and Monski of Halle, Germany, are favorably known for their reciprocating pumps, and more recently they have taken up the manufacture of centrifugal pumps for both high- and low-pressure service. Their high-pressure pumps are interesting from a constructive standpoint.

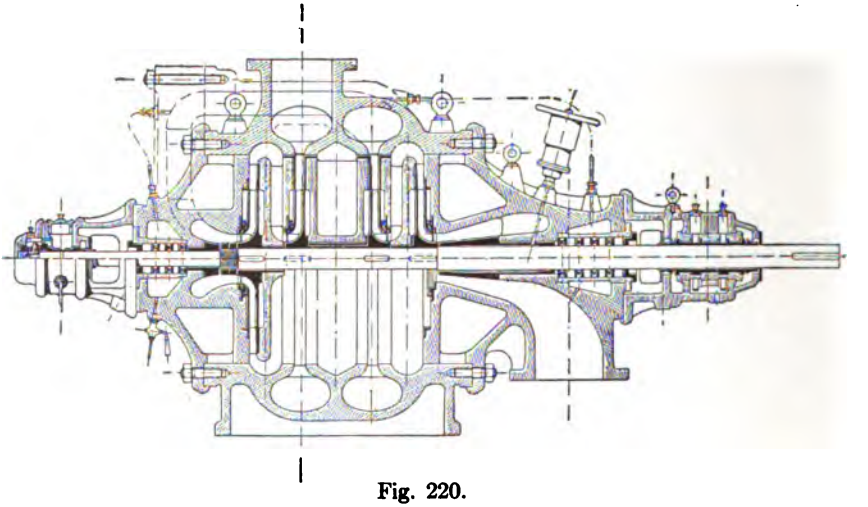

Fig. 220.

Fig. 220 gives schematically a cross section through a multi-stage centrifugal pump built by this firm. The water enters through

* See full report by R. C. Carpenter in Proceedings of the American Society of Mechanical Engineers, 1909.

the suction pipe shown on the right-hand end of the pump. It passes through the first impeller and guide vanes into the reversing channel leading to the second impeller. After passing through this impeller and its guide vanes, it enters a large chamber, shown oval in cross section. This chamber is connected to the suction of the impeller on the extreme left-hand end of the pump. The water now passes through this impeller and guide vanes and its adjacent impeller and guide vanes into the chamber leading directly into the discharge pipe. The water in flowing through the first two impellers flows in an axial direction opposite to the flow through the last two impellers, so that the end thrust developed in the first two impellers is opposite to the thrust developed in the last two impellers. Besides the balancing thus obtained, this scheme has an advantage in not having a high-pressure stuffing box packing; one end has the suction pressure, while the other end packs against the second-stage pressure of the pump. This scheme of balancing is fair, because the thrust of one wheel is always equal and opposite to that of its partner. But when the designer is forced to choose an odd number of stages axial thrust will ensue. These pumps are also provided with a thrust bearing to locate definitely the impellers and to take up any unbalanced thrust. The bearings on both ends of the pump are fastened to the casing and are ring lubricated. The motor is generally placed at the suction end.

The diaphragms between impellers are of cast iron, and these carry the discharge vanes and form the reversing channels. As the casing is not in sections, these diaphragms have bronze sleeves attached; these sleeves form the water joint between diaphragms and casing and prevent the diaphragm from rusting to the casing. The disassembly of the unit is from the left-hand end, and does not necessitate the breaking of the suction or discharge pipe flanges or the moving of the casing from its foundation. The stuffing boxes at both ends of the pump are water cooled, and the suction end is water sealed against air leakage.

Although no high-pressure stuffing box exists, the middle diaphragm must pack against leakage from the high-pressure to about one-half of this pressure. This leakage cannot be readily noticed, but as shown in the figure, the clearance space is small and the length of the packing sleeve is considerable.

Although the general idea of securing axial balance is similar to

the original Sulzer design, it differs fundamentally in that the Weise and Monski design necessitates only one change of direction of the water in the pump, while the Sulzer design has a path for the water which reverses several times. The latter necessitates somewhat complicated castings, especially for the discharge vanes. This firm states that its medium-sized pumps obtain an efficiency of 70 to 75 per cent and large units 80 per cent and above.

Fig. 221 gives a photographic view of a multi-stage pump capable of delivering 210 cubic feet of water per minute against a head of

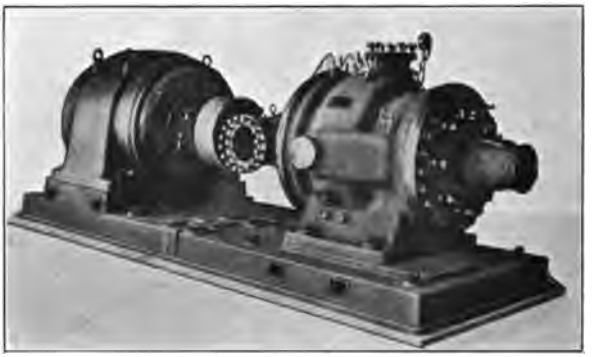

Fig. 221.

1575 feet, or 280 cubic feet of water per minute against a head of 1148 feet.

In 1907 this firm placed in operation a ten-stage double-casing pump capable of delivering 106 cubic feet of water per minute against a head of 2130 feet and occasionally pumping up to 2300 feet. This is reaching a condition of high stresses. Another pump was built capable of delivering 212 cubic feet of water per minute against a head of 1700 feet. The pump required a 1000-h.p. driver.

51. Byron Jackson Pumps.

The Byron Jackson Iron Works of San Francisco, Cal., manufacture high-pressure centrifugal pumps of the Jaeger type. They also build low-pressure pumps for a large variety of work. Fig. 222 gives a cross-sectional view of a two-stage high-pressure pump, which is typical of all their multi-stage designs. As can be seen

from the figure, the impeller blades are backward turned, and the discharge vanes and reversing channels are similar in shape to those of the Jaeger pumps already described. Attached to the last impeller is a revolving piston which serves as a balancing piston for balancing the end thrust. This piston has a slight clearance between it and the casing; this permits part of the water flowing from the periphery of the impeller to leak to the chamber on the other side of the piston. The pressure in this chamber will then be slightly less than the discharge pressure. This pressure exerted over the area of the piston produces a pressure in the direction opposite to that produced by the water in the rest of the pump. The

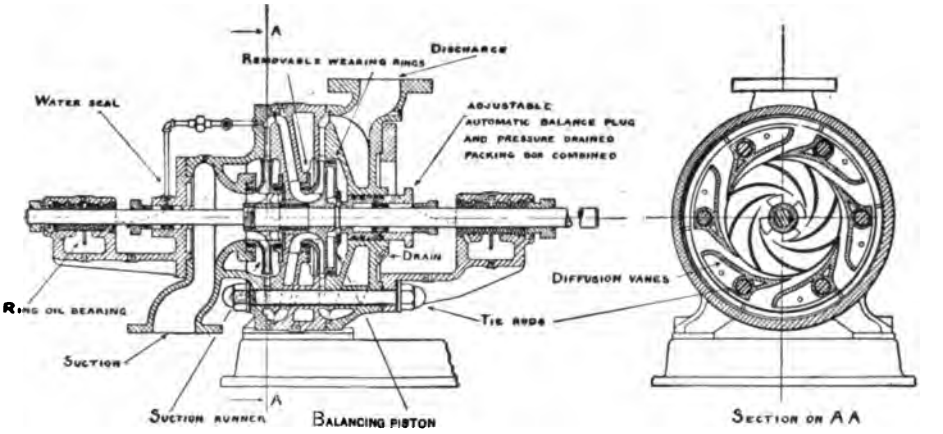

Fig. 222.

area of the piston is so designed that the water pressure upon it can always be greater than the axial thrust. This excess of pressure moves the impellers and shaft slightly to the left, which permits the high-pressure water to escape through the discharge holes into the suction of the last impeller. In this manner axial thrust is balanced automatically. An outside view of this two-stage pump direct connected by means of a flexible coupling to an induction motor is shown in Fig. 223. More stages can be added by simply introducing another section of casing with impeller and using a longer shaft, base, and tie bolts. The bearings are ring lubricated and the packing on the suction end has a water seal. The impellers and discharge vanes are of bronze and the clearance rings on the impellers are renewable.

In pump designs with shaft vertical the axial balance is secured by means of a balancing piston similar to that shown in Fig. 222.

Fig. 223.

Fig. 224 illustrates an arrangement for balancing the axial thrust of vertical pumps. The water is drawn into the impeller *A* through the suction pipe *B* and is delivered into the discharge casing at a

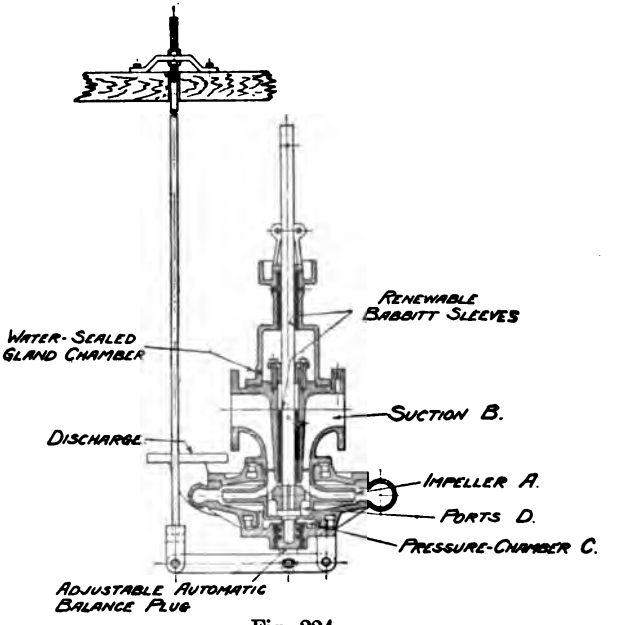

Fig. 224.

pressure equal to the discharge head at which the pump is operated. This discharge pressure will extend to the balancing ring on either side of the impeller, minus a decrease of pressure caused by the

rotating paraboloid of water, as described in Article 19. The balance ring extending from the lower side of the impeller is a running fit in a corresponding flange in the bottom of the pump casing, forming the pressure chamber *C* between the bottom cover of the pump casing and the bottom plate of the impeller *A*. This plate has a central port diverging into ports around the hub of the impeller and extending to the center or vacuum chamber of the impeller. There is an adjustable plug or piston of the same diameter as the central port in the impeller, extending up through the bottom cover of the

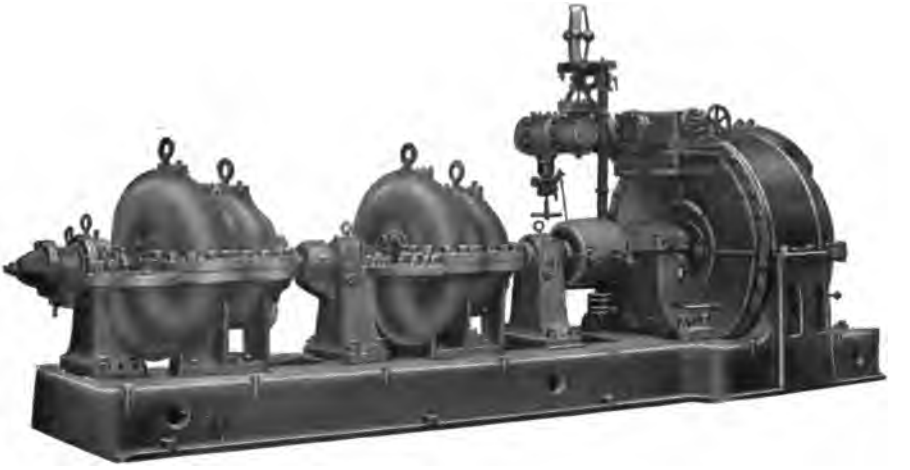

Fig. 225.

casing. This plug is adjustable by means of a lever and usually a rod extending to the surface of the pit or well. In operation a pressure is formed in the chamber *C* under the impeller supplied by the leakage around the balance ring, so that if there were no escape for this pressure there would be an upward thrust equal to the area of this balance ring times the pounds pressure of the head being pumped against. The piston area is so designed that the upward thrust can be larger than the thrust in the opposite direction. If such is the case, the impeller moves slightly away from the plug and the ports *D* are opened, allowing a portion of the water to escape through the ports *D* into the low-pressure chamber of the impeller. In this way balance is secured.

Fig. 225 illustrates one of four units furnished by the Byron Jack-

son Iron Works to the city of San Francisco for its fire boats. As shown in the illustration, each unit consists of two two-stage pumps direct connected to a 600-h.p. 1800-r.p.m. Curtis steam turbine built by the General Electric Company. The pumps are so arranged that they may be run either in parallel or in series; in the former case each unit delivers 668 cubic feet (5000 gallons) of water per minute under a discharge pressure of 150 pounds per square inch, and running in series it delivers 334 cubic feet (2500 gallons) of water per minute under 300 pounds per square inch discharge pressure. These two

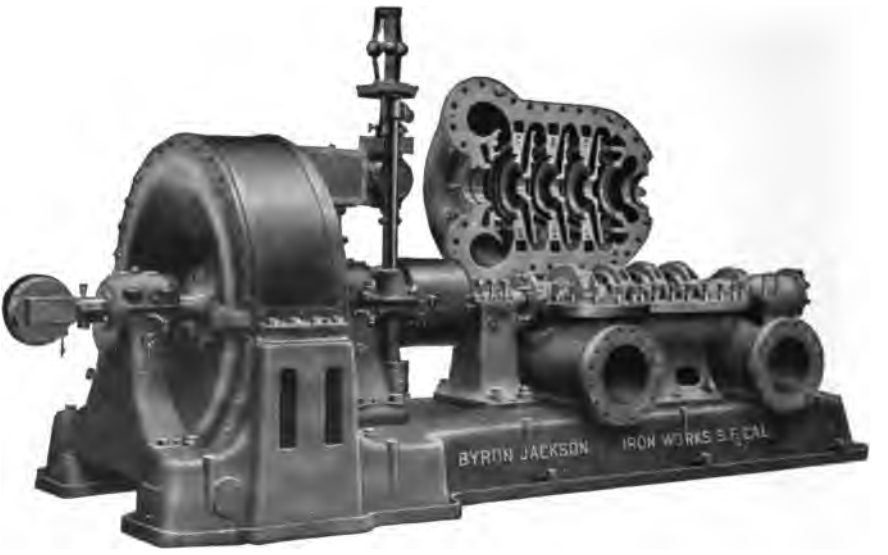

Fig. 226.

fire boats are stationed in San Francisco Bay, and consequently are required to pump salt water, necessitating all parts coming in contact with water, except the casings, being constructed of bronze; the nickel steel shafts are bronze armored. The turbine, operating condensing under steam at 150 pounds per square inch and no superheat, has a water rate of 16.7 pounds per horse-power hour delivered at the pumps when operating under 26 inches vacuum.

Fig. 226 shows a four-stage Byron Jackson pump direct connected to a 750-h.p. Curtis steam turbine built by the General Electric Company. Eight of these units were installed for the city of San

Francisco for fire protection. Each unit is required to deliver 400 cubic feet (3000 gallons) of water per minute under a discharge pressure of 300 pounds per square inch and a suction head of 15 feet. The unit runs at 1800 r.p.m. The illustration shows the top half of the pump casing removed, exposing the impellers and discharge vanes, which, together with the packing boxes and followers, are of bronze. Axial balance is secured as already described. The unit is a four-bearing set, the turbine being connected to the pump by means of a flexible coupling. The turbine operates non-condensing.

52. Pumps of the John McDougall Caledonian Iron Works Company, Limited.

The John McDougall Caledonian Iron Works Company, Limited, of Montreal, Canada, are licensed to manufacture Worthington pumps in Canada. It is therefore not necessary to give any detailed description of their centrifugal pumps, but it is of interest to note some of the novel pump installations made by this firm.

At the municipal waterworks, Port Arthur, Ontario, water turbine driven centrifugal pumps are installed. Fig. 227 gives an illustration of this installation. Two water turbines are installed in a common casing and connected by a coupling. At each free end of the turbines a three-stage centrifugal pump is placed. There is a coupling between each pump and the turbine. It is possible to drive all as one unit, or one pump with both water turbines, or one pump with one turbine. The latter makes practically duplicate units. Each pump is capable of delivering 111 cubic feet of water per minute (1 000 000 British gallons per 24 hours) against 400 feet head. Ordinarily this set operates with one pump driven by both water wheels in order to get rid of the end thrust of the water wheel, the loss due to running under low gate not being of any consequence to the city. The pumps operate at 1100 r.p.m. when pumping against 400 feet head for fire service or to fill the high-level standpipe, and the speed is decreased when less pressure is required.

In the city of Winnipeg, Manitoba, there is an unusual installation of three vertical three-stage pumps for the waterworks system. Fig. 228 illustrates one of these pumps, which has a capacity of 278

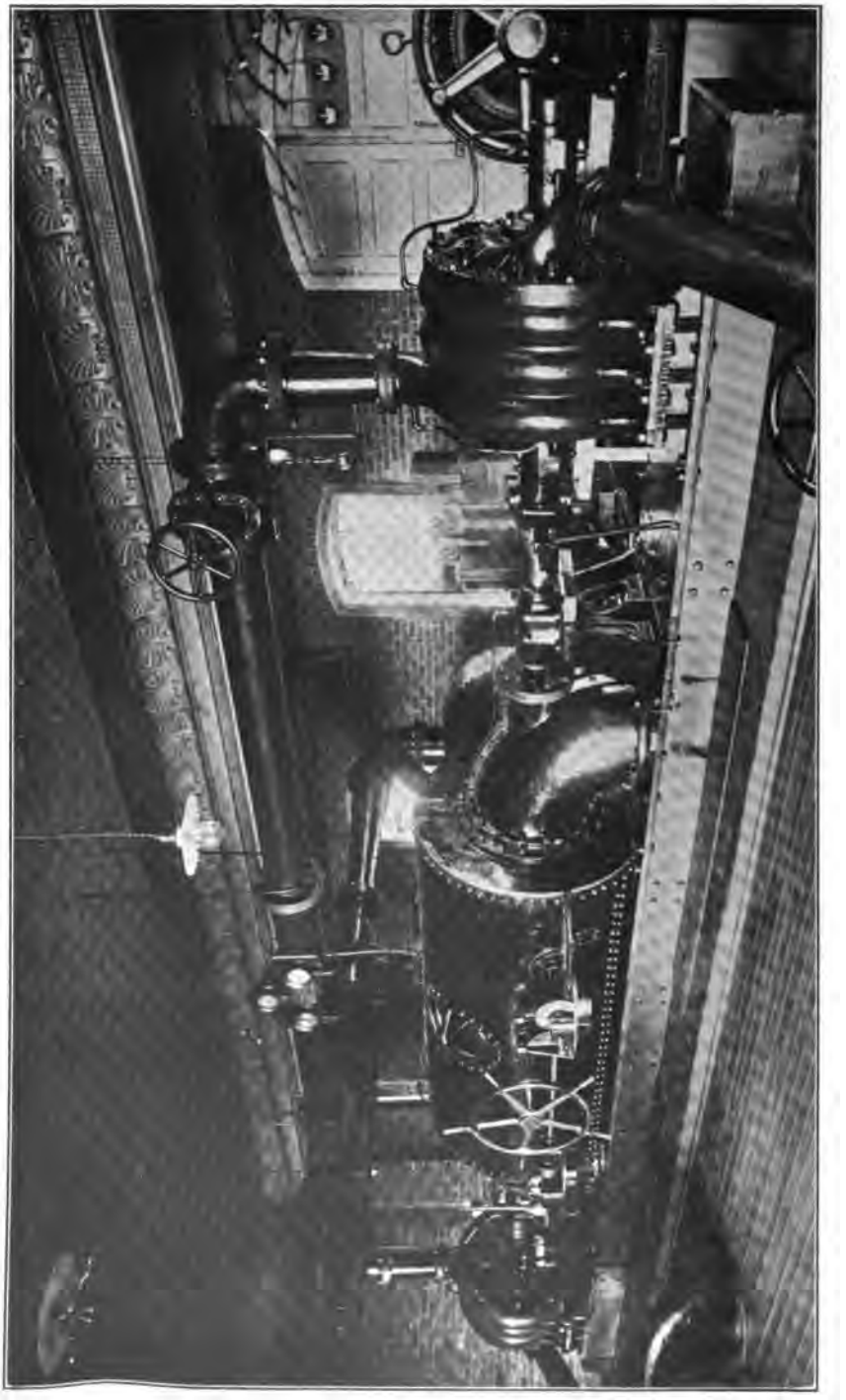

Fig. 227.

cubic feet of water per minute (2 500 000 British gallons per 24 hours)

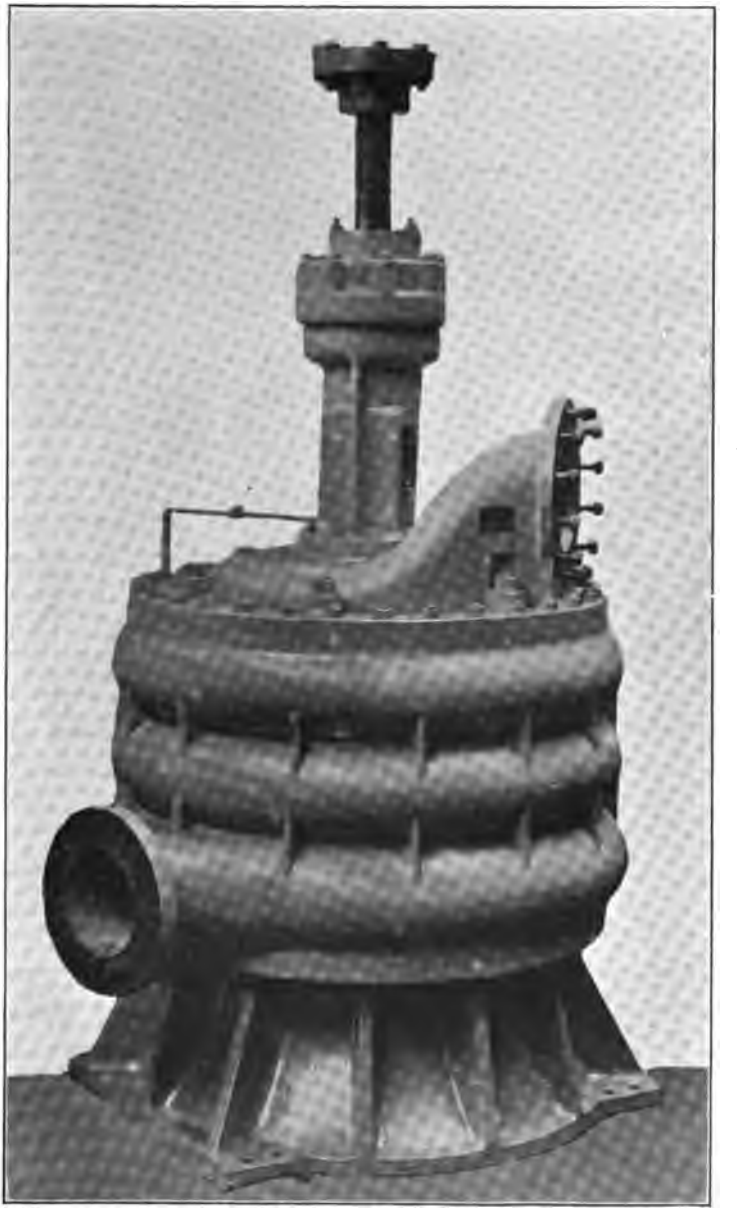

Fig. 228.

against a head varying from 200 to 353 feet. The pumps are motor driven and are installed in a well 90 feet deep, with the motors upon

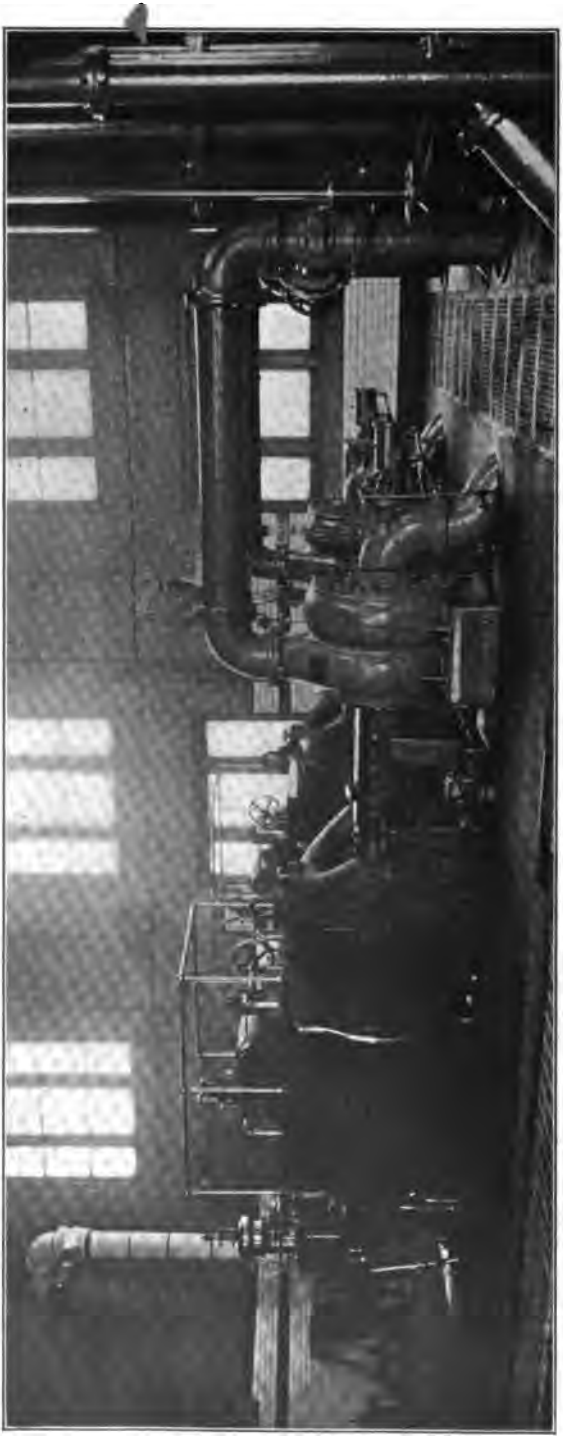

Fig. 229.

the ground level. The shafts pass through air locks, and in order to get at the pumps it is necessary to go into a caisson under a pressure of 35 pounds per square inch.

Each of these vertical pump shafts has three sets of thrust bearings, one for the motor, one for the shaft, and one for the pump, with slip couplings between them. The pumps run at 680 r.p.m. when delivering full pressure, and the speed is reduced by resistance in the motor circuit for lower pressures. The efficiency of the whole unit is low, owing to operating at slow speeds, the use of resistance, and the fact that the couplings and part of the shafting are operating in the water. The city owns its own hydroelectric plant, and mechanical efficiency was not so much an object as the cost of attendance and maintenance.

Fig. 229 illustrates an installation for the high-pressure fire service of the city of Toronto, Canada. This station contains two pumps

Fig. 230.

of two stages each, driven by Westinghouse-Parsons steam turbines. Each pump has a capacity of 556 cubic feet of water per minute (5 000 000 British gallons per 24 hours) against 700 feet head when running at 1700 r.p.m. The pump and turbine each have their

own thrust bearings, the coupling being rigid for alignment but flexible for end motion. As these pumps operate only a few hours each year, efficiency is not important, but reliability and quick starting are the principal objects. A pressure of 300 pounds can be obtained in less than a minute after the alarm is turned in.

Fig. 230 shows a rather novel installation of a three-stage centrifugal pump direct connected to a Belliss triple-expansion engine. The capacity of this unit is 1336 cubic feet of water per minute (12 000 000 British gallons per 24 hours) against 207 feet head when operating at 340 to 350 r.p.m. This unit is installed in the low-level station of the Montreal waterworks. The unit was officially tested by Prof. R. J. Durley of McGill University in November, 1909, and netted the builders a bonus of $10 000. No indicator cards were officially taken, but a representative of the engine builder took cards, and from the indicated horse power shown by these cards the total over-all efficiency was 70 per cent. This included not only pump and engine losses but also the power required to drive the air and feed pumps, which were attached to the main engine, and for which no allowance was made. The following figures give the results of the test:

RESULTS OF TEST MADE ON BELLISS TRIPLE-EXPANSION ENGINE AND WORTHINGTON THREE-STAGE TURBINE PUMP, MONTREAL WATERWORKS LOW-LEVEL PUMPING STATION, 19TH AND 20TH NOVEMBER, 1909.

Pump Performance.

1.	Duration of test	hours	13
2.	Total water pumped during test	Imp. gals.	6 515 000
3.	Average water delivered per hour	Imp. gals.	501 155
4.	Rate of pumping per 24 hours	Imp. gals.	12 027 700
5.	Average pressure gauge reading at pump	feet	196.22
6.	Correction for gauge error	feet	2.30
7.	Average suction gauge reading at pump	feet	7.76
8.	Difference in level of gauges	feet	3.30
9.	Total average corrected head	feet	204.98
10.	Average work done on water per hour	ft. lbs.	1 027 267 520

Steam Consumption.

11.	Average pressure gauge reading at engine	lbs. per sq. in.	146.22
12.	Correction for gauge error	lbs. per sq. in.	1.50
13.	Correction for water in gauge pipe	lbs. per sq. in.	2.00
14.	Average corrected steam pressure by gauge	lbs. per sq. in.	142.72
15.	Barometric pressure	lbs. per sq. in.	14.69
16.	Average absolute steam pressure	lbs. per sq. in.	157.41
17.	Corresponding temperature	deg. F.	362.3
18.	Average actual steam temp. at engine	deg. F.	481.9
19.	Average superheat of steam at engine	deg. F.	119.6
20.	Total steam condensed during test	lbs.	125 644
21.	Average steam condensed per hour	lbs.	9665
22.	Excess superheat over that specified	deg. F.	19.6
23.	Steam consumption per hour corrected to 100° superheat, No. 21 × 1.03	lbs.	9955

Feed Water and Heat Returned to Boilers.

24.	Temperature of water supply	deg. F.	42.0
25.	Average temperature of feed water leaving heater	deg. F.	98.8
26.	Total water supplied to boilers (by meter)	cu. ft.	2795
27.	Correction for error of meter (3%)	cu. ft.	84
28.	Total water supplied to boilers (corrected)	cu. ft.	2879
29.	Average water supplied per hour	cu. ft.	221.46
30.	Density of water at temperature of No. 25	lbs. per cu. ft.	62.03
31.	Average weight supplied to boilers per hour	lbs.	13 737
32.	Heat returned to boilers per hour, No. 31 × (No. 25 − No. 24)	B.t.u.	780 261

Heat Expended and Duty.

33.	Heat required to produce 1 lb. steam of 100° superheat and 157.4 lbs. abs. pressure from water at temperature of No. 24	B.t.u.	1240.8
34.	Weight of this steam per hour equivalent to No. 32	lbs.	629.1
35.	Equivalent consumption per hour, allowing for heat returned to boilers, (No. 23 − No. 24)	lbs.	9326
36.	Duty per 1000 lbs. steam as actually supplied, (No. 10 ÷ No. 21) × 1000	ft. lbs.	106 287 000
37.	Duty per 1000 lbs. steam of specified quality, (No. 10 ÷ No. 23) × 1000	ft. lbs.	103 191 000
38.	Duty as No. 37 but allowing for heat returned to boilers, (No. 10 ÷ No. 35) × 1000	ft. lbs.	110 151 000

Fig. 231 gives the steam consumption per pump horse power per hour as worked up from these tests. The dots represent hourly readings at various superheats. Curve *A* represents the guaranteed steam consumption. The increase of steam consumption due to a change of superheat from 120° F. to 100° F. is from 12.85 pounds to 13.25 pounds, an increase of 3.1 per cent. Therefore 3 per cent was

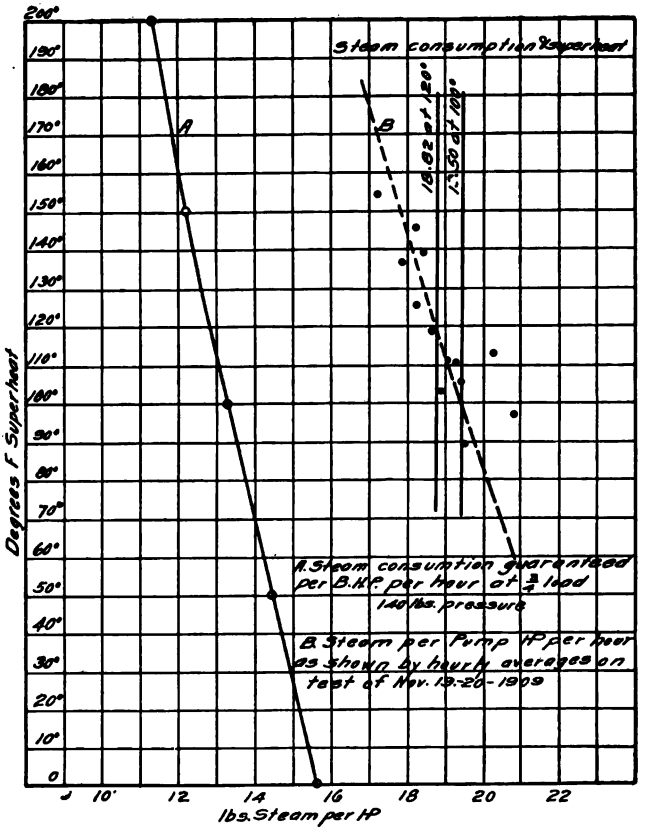

Fig. 231.

used as a correction in the foregoing tables. The duty of the pump and engine, allowing for all heat returned to the boilers, and applying the necessary correction for excess superheat, was 110 151 000 foot pounds per thousand pounds of steam, superheated one hundred degrees.

This plant is novel in its design, on account of the fact that it has always been supposed that it was impossible to make a commer-

cial success with an engine-driven centrifugal pump delivering water against high heads. While the duty obtained does not compare favorably with the best practice in high-duty pumping engines, yet when we consider the fact that the contract price was only one-third of the price asked for vertical triple-expansion pumping engines, the interest on this difference added to the difference in the cost of engine house and foundations would more than compensate for the extra fuel consumption.

53. Alberger Pumps.

The Alberger Pump Company of New York build high-pressure centrifugal pumps of the Jaeger type. They also build a line of low-pressure pumps for motor, engine, or steam turbine drive.

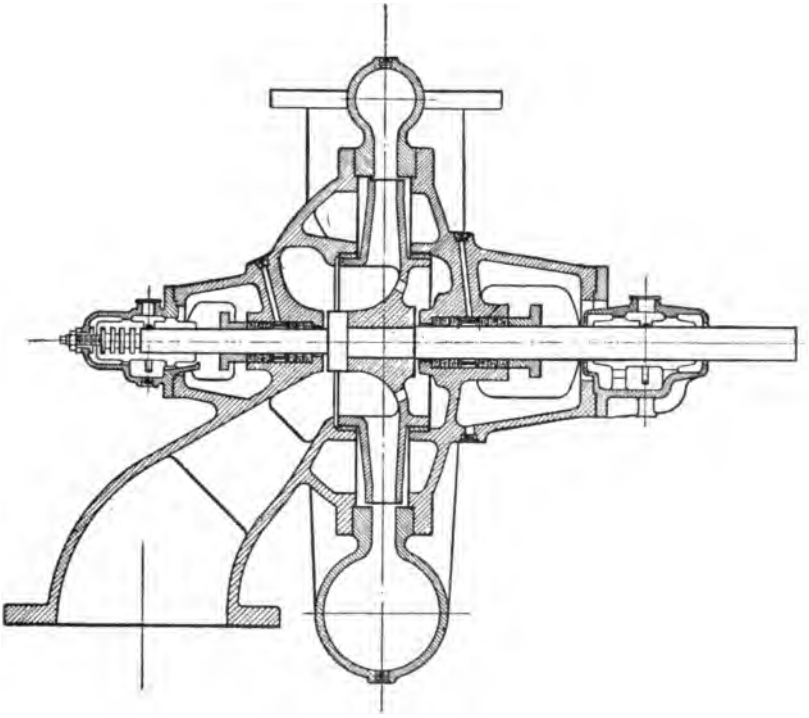

Fig. 232.

Fig. 232 gives a cross-sectional view through a single-stage low-pressure pump for motor drive. The same design, but with larger impeller, is used for direct-connected steam engine drive, and where the speeds are very low a second stage is added. For high-speed

work and low heads, a design similar to that shown in Fig. 233 is used. The dividing line between low- and high-pressure work is about 70 feet head.

For higher heads than 70 feet guide vanes are employed and the design is then similar to that of Jaeger. Fig. 234 gives a cross section through a four-stage high-pressure Alberger pump. The impellers are made of bronze and have backward turned blades. The discharge vanes are also of bronze, and the shaft is protected

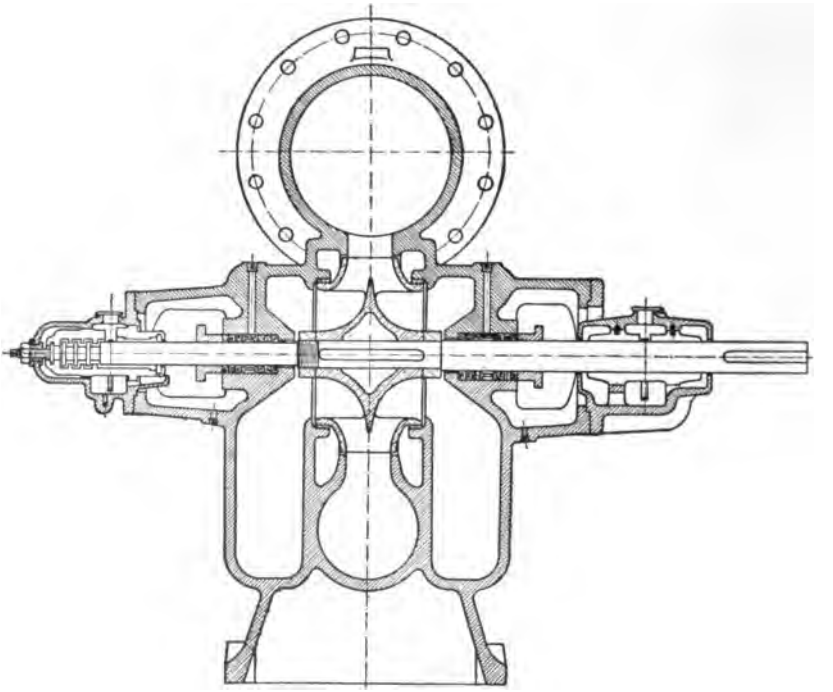

Fig. 233.

by bronze sleeves. The bearing supports are cast integral with the pump casing and the journals are ring lubricated. Close clearance packings are provided between the diaphragms and impellers and between the diaphragms and shaft sleeves, which are renewable. The unbalanced axial thrust is taken care of by a water-cooled marine type thrust bearing. The Alberger pump is built up in sections exactly as described in Article 38. A photographic view of this pump is given in Fig. 235. The pump is shown direct connected to a steam turbine capable of developing 70 h.p. The pump delivers

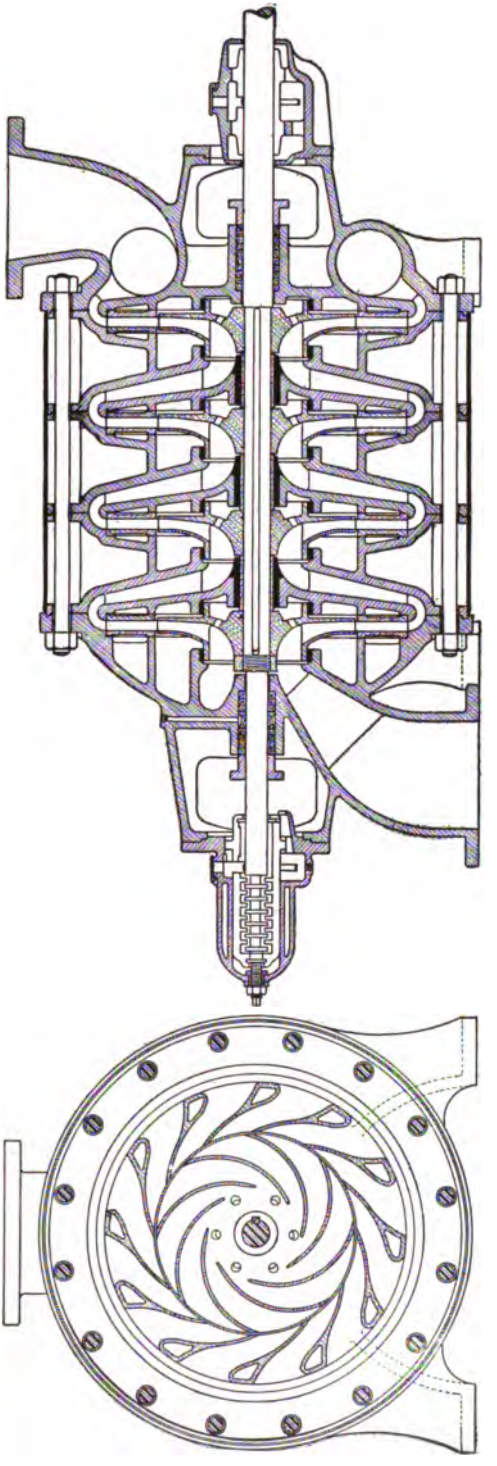

Fig. 234.

47 cubic feet (350 gallons) of water per minute against a pressure of 225 pounds per square inch when running at 2400 revolutions per

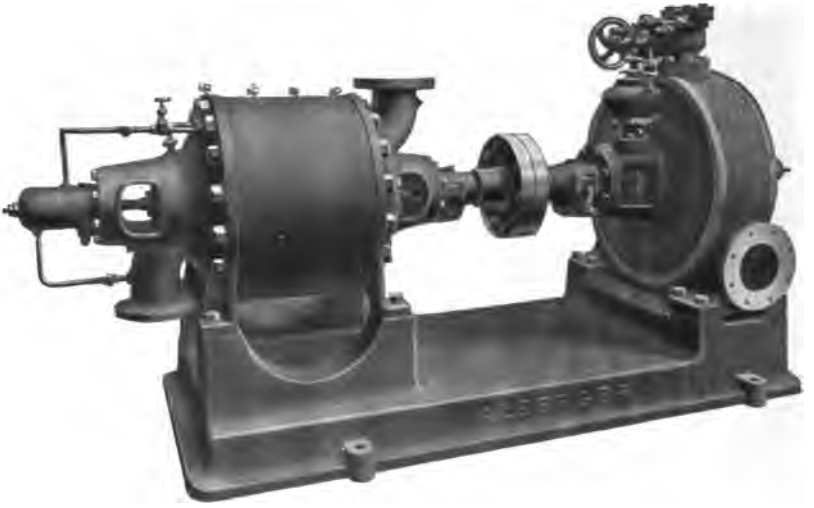

Fig. 235.

minute. This pump is used as a boiler feed pump. This firm has built pumps from 2 inches diameter discharge to 24 inches diameter

Fig. 236.

discharge, having a capacity range from 6.5 to 2400 cubic feet per minute (50 to 18 000 gallons per minute).

Fig. 236 gives a photographic view of a three-stage pump. The Alberger Company furnished a pump of this type for one of the large power houses in Chicago for fire protection. The pump is

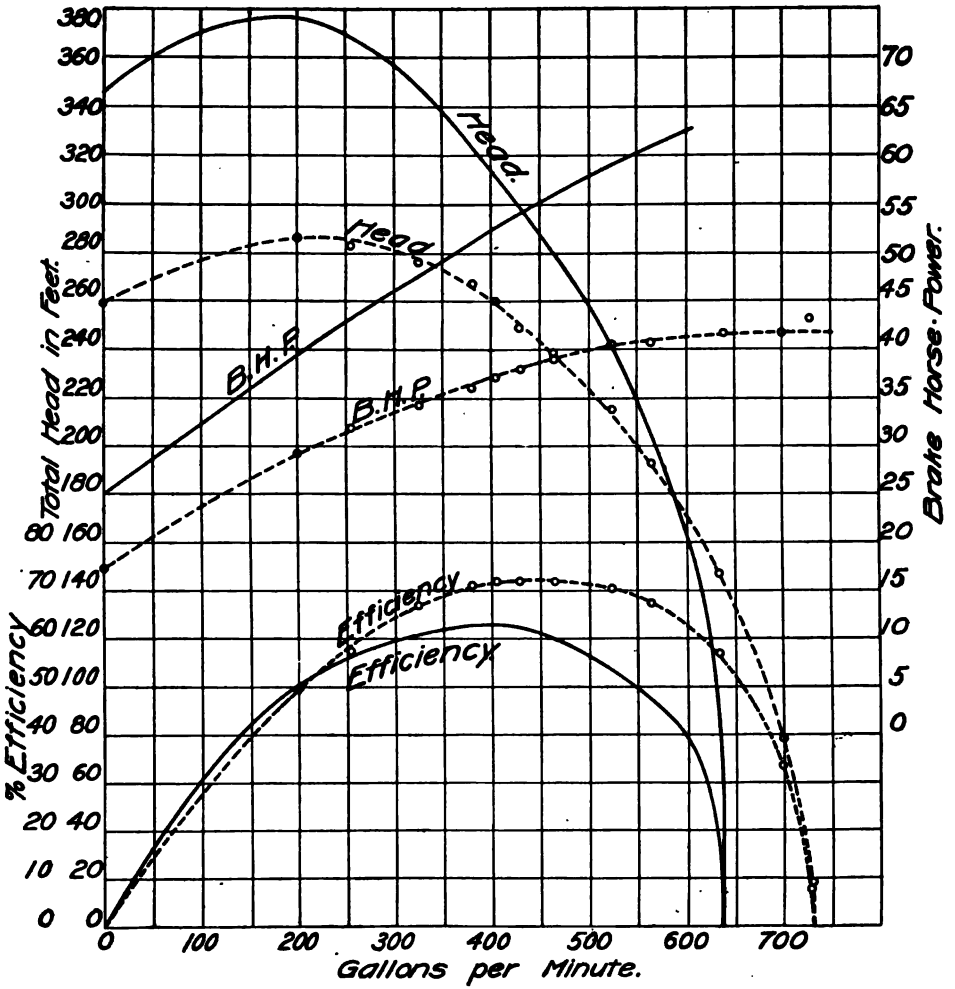

Fig. 237.

direct connected to a 60-h.p. induction motor operating at a synchronous speed of 1800 revolutions per minute. The pump was designed to deliver 53.5 cubic feet (400 gallons) of water per minute against a total head of 300 feet. The diameter of the discharge pipe is 5 inches. Fig. 237 gives in full lines the characteristic curves

of this pump from test data, the speed of the induction motor being 1788 revolutions per minute. It is interesting to note that this pump when running at 1700 revolutions per minute will give a much higher efficiency; the total head of course is considerably decreased. The dotted lines show the characteristic curves for this latter condition.

Fig. 238 represents a two-stage pump designed to comply with the underwriters' conditions for fire protection service. The pump delivers 134 cubic feet (1000 gallons) of water per minute against a

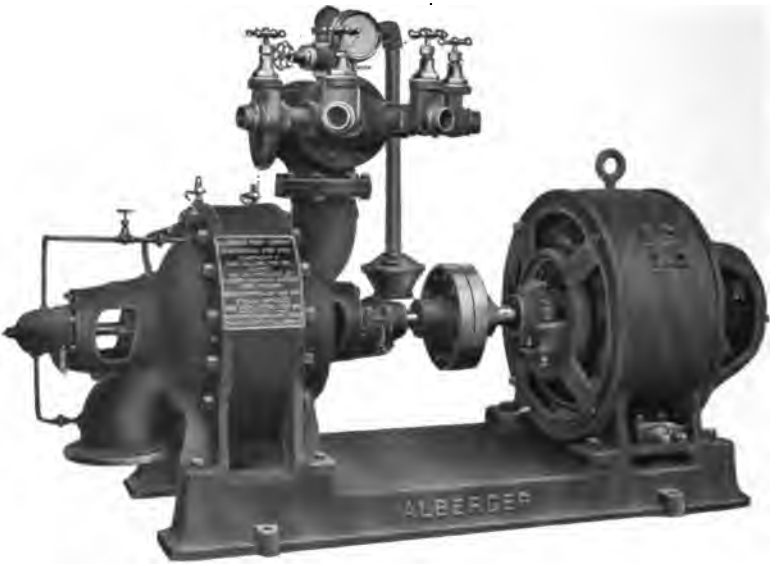

Fig. 238.

pressure of 100 pounds per square inch. This pump is direct connected to a 90-h.p. direct-current motor, and the figure shows the fittings furnished with the pump, as called for by the underwriter specifications. Fig. 239 gives the characteristic curves of this pump taken from actual tests and shows an efficiency of over 69 per cent. The normal speed is 1400 revolutions per minute.

Another set of characteristic curves for a two-stage pump is given in Fig. 240. The pump when delivering 40 cubic feet (300 gallons) of water per minute against a head of 120 feet, and running at 1720 revolutions per minute, gave an efficiency of 70 per cent.

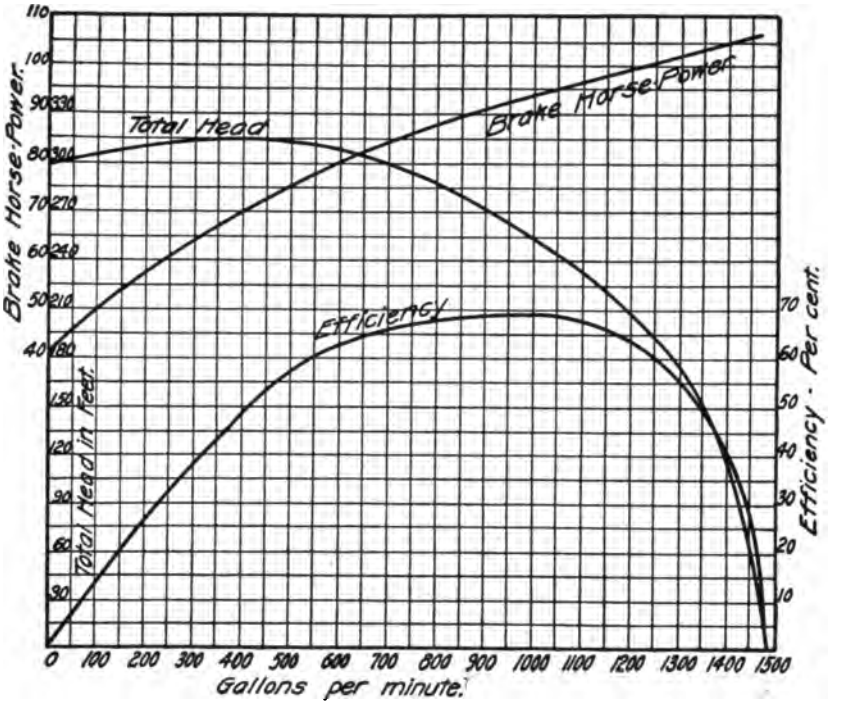

Fig. 239.

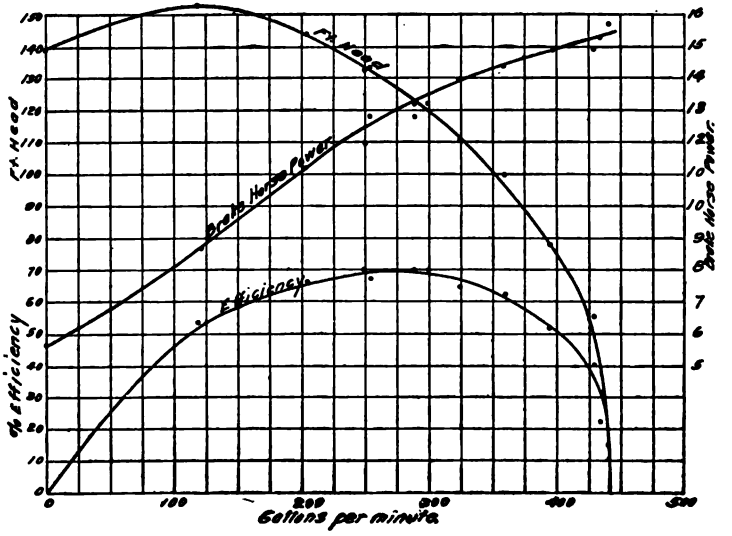

Fig. 240.

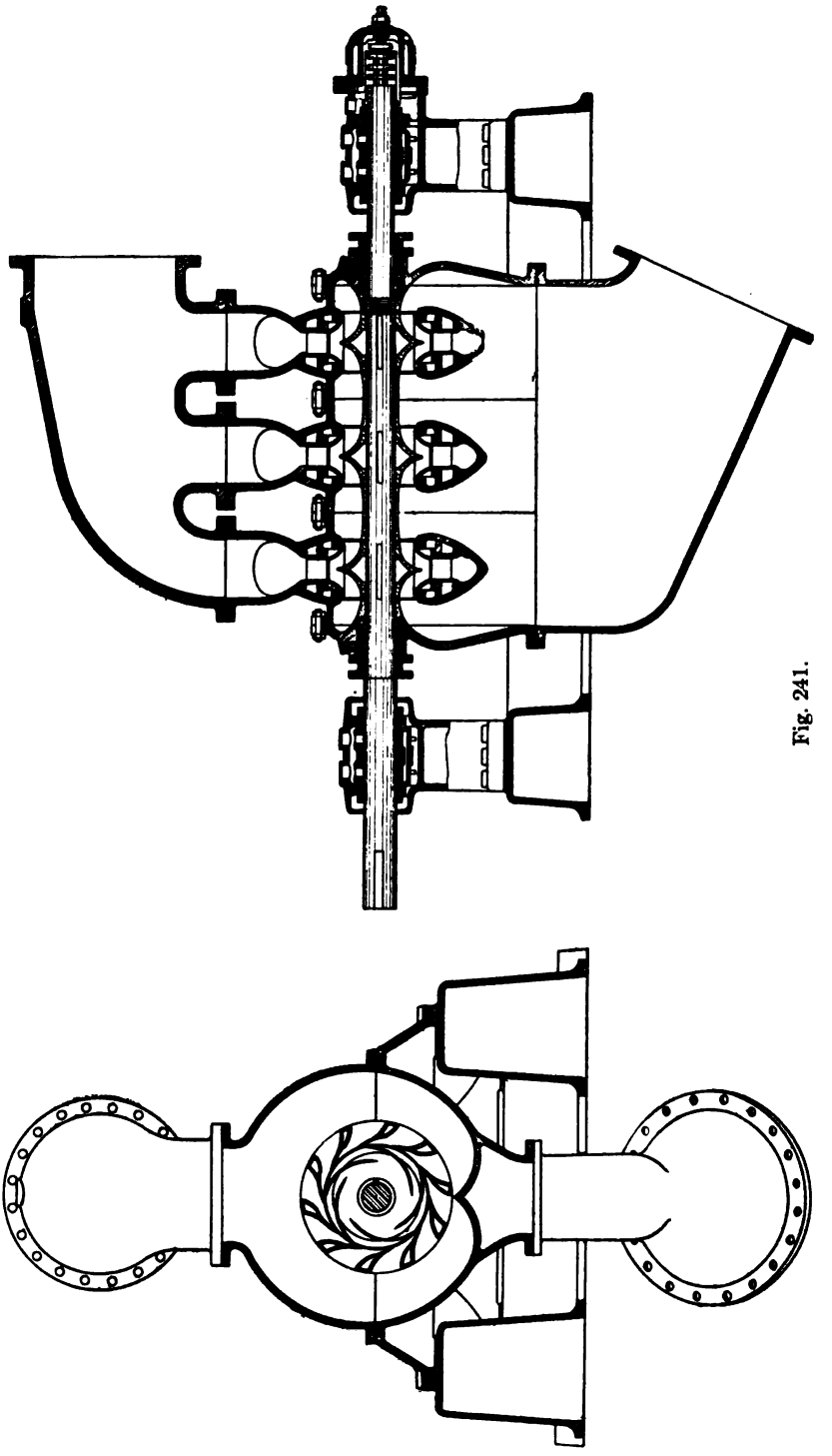

Fig. 241.

A rather novel design of a large pump is shown in the cross-sectional view, Fig. 241. The three impellers work in parallel, all taking water from a suction pipe of 28 inches diameter and discharging into a pipe of 24 inches diameter. The novel features of this design are that the pump is built up of sectional units and can be built in either one, two, three, or four sections, depending upon the quantity of water to be handled and the speed available and also upon the design of the casing, which is not only in sections but split horizontally and with removable suction and discharge pipe fittings.

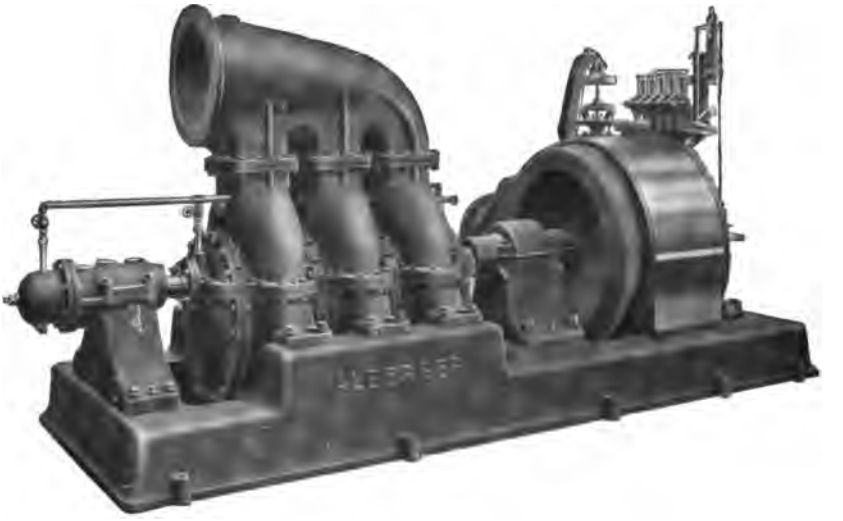

Fig. 242.

Fig. 243 gives an outline view of this pump direct connected to a 400-h.p. Curtis steam turbine made by the General Electric Company, and Fig. 242 shows a photographic view of this unit. Two of these units have recently been installed for the Standard Oil Company for general water supply at their refinery, Point Richmond, Cal. Each pump is capable of delivering 1860 cubic feet of water per minute (20 000 000 gallons per 24 hours) against a head of 80 feet. The speed of the unit is 1250 revolutions per minute. The Alberger Company have applied for patents on this general construction.

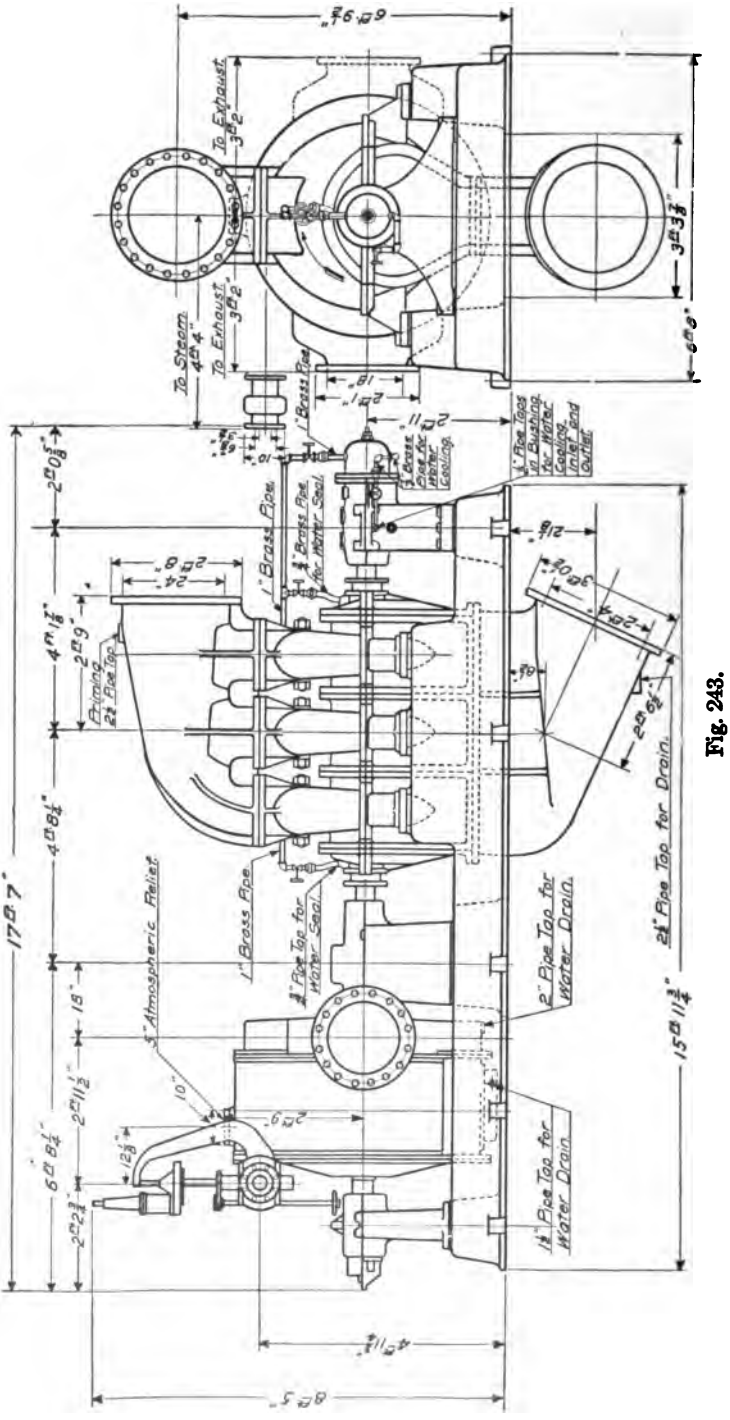
To Exhaust
To Exhaust
To Steam
1" Brass Pipe
1" Brass Pipe
1" Brass Pipe
1" Brass Pipe
1" Pipe Tees in Bushing for Water Cooling, Inlet and Outlet
1" Brass Pipe for Water Cooling
1" Brass Pipe for Water Seal
Piping 2" Pipe Top
1" Brass Pipe
1" Pipe Top for Water Seal
2" Pipe Top for Water Drain
2" Pipe Top for Drain
1" Pipe Top for Water Drain
5" Atmospheric Relief

Fig. 243.

54. Mather & Platt Pumps.

Mather & Platt, Ltd., of Manchester, England, are among the oldest manufacturers of centrifugal pumps, having built such pumps since 1876. The first pump built was the Mather-Reynolds centrifugal pump, according to the patents taken out by Professor Reynolds in 1875. At the present time they manufacture pumps for all classes of service.

A view of a standard type of high-pressure pump manufactured by this firm is shown with all parts disassembled in Fig. 244. The

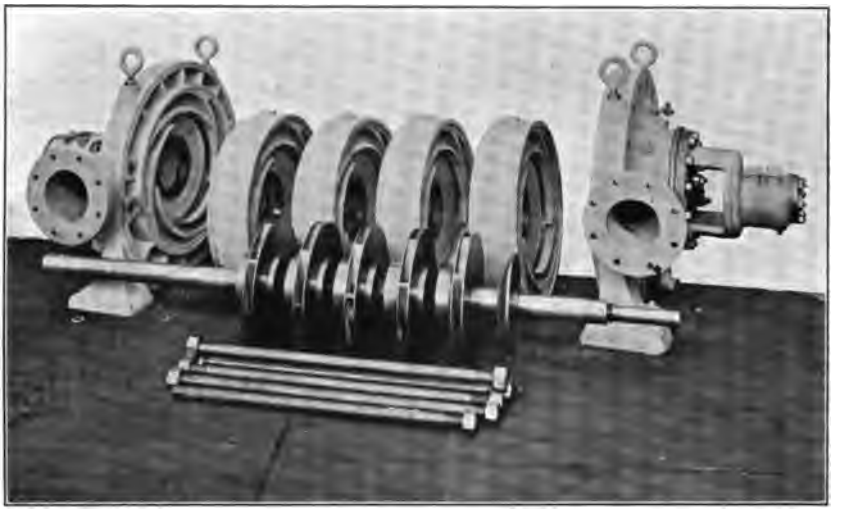

Fig. 244.

pump illustrated is a five-stage pump; the impellers are of the single-inlet type; the casing is divided into sections, the suction end of the pump being on the left-hand side of the photograph and the discharge on the right-hand side. The discharge vanes are cast to sections of the casing, which are rabbeted together when assembled and held in position by through bolts passing through the suction and discharge head flanges.

Fig. 245 is a photographic view of a three-stage high-pressure pump electrically driven and capable of furnishing 1680 cubic feet (10 500 British gallons) of water per minute against a head of 404 feet when running at 470 revolutions per minute. Three of these units are installed at the Montreal Water and Power Com-

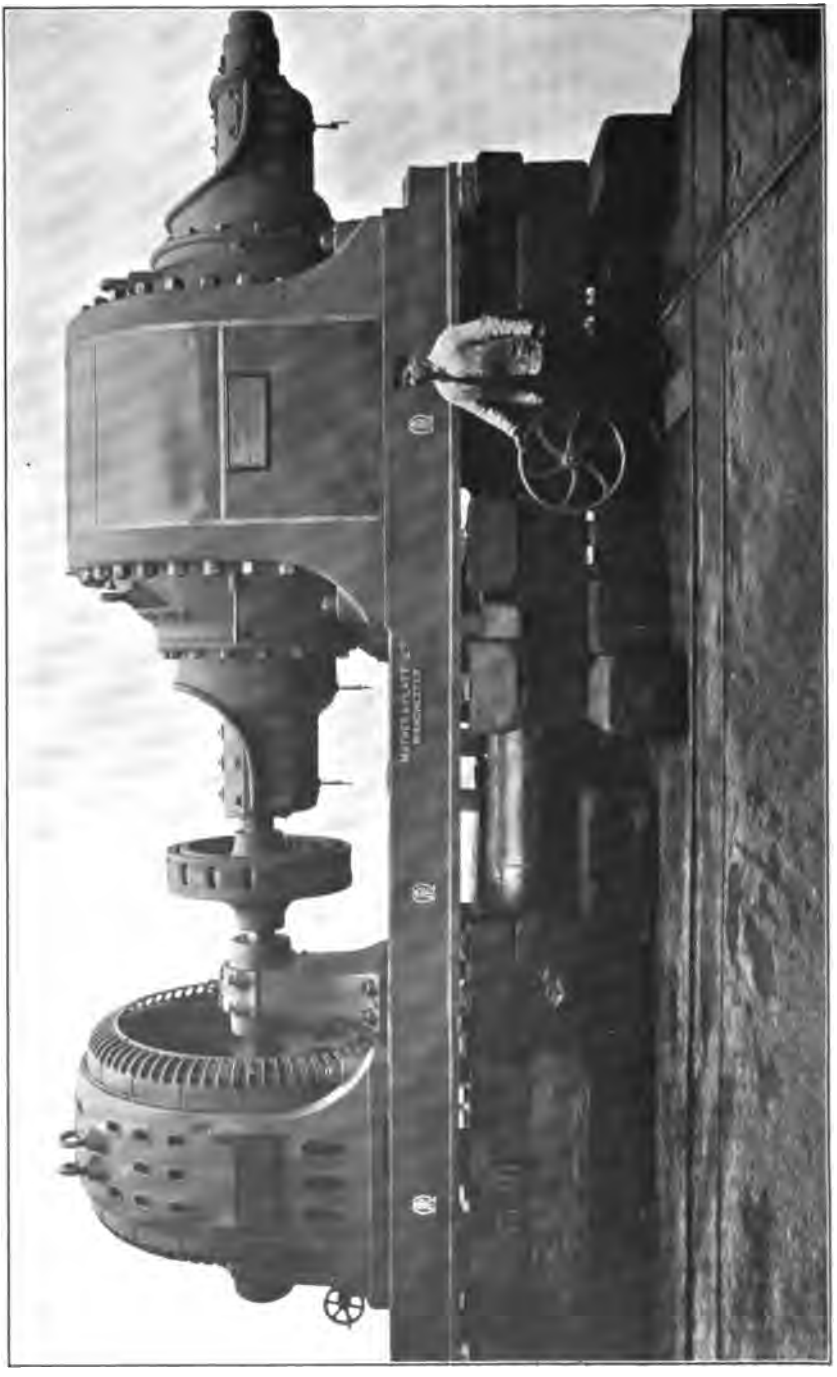

Fig. 245.

pany's plant. The general design of the pump is shown clearly in the cross-sectional view, Fig. 246. The bearings are ring lubricated. The unbalanced axial thrust is almost wholly taken care of by the balancing piston *P* on the discharge end of the pump. Chamber *A* is filled with water from the high-pressure discharge side of the pump, and chamber *C* is connected through a balancing valve and pipe to the suction end of the pump. If the unbalanced axial thrust is towards the left, the clearance between chamber *B* and chamber *A* is increased, and that between *B* and *C* decreased because the piston *P* moves to the left. This raises the pressure in *B* until balance is secured. Should the axial thrust be in the opposite direction, the pressure in *B* decreases. This means of balancing is nearly automatic, and depends somewhat upon the setting of the balance valve *D*. Should there be any unbalanced axial thrust not taken care of by this balancing arrangement, it will load the ball thrust bearing provided for that purpose upon the extreme discharge end of the shaft. The rest of the detail construction of this pump is clearly shown in the drawing.

A rather interesting high-pressure pump of special design for colliery sinking or draining purposes is shown in Fig. 247. This pump is electrically driven by an alternating-current motor of 2000 volts and 350 brake h.p. The pump delivers 96 cubic feet (600 British gallons) of water per minute against a head of 1230 feet. The speed of the unit is 1450 r.p.m. Even for the high duty for which this pump is made the over-all dimensions are small, due to the high speed of rotation. The pump is arranged for suspending vertically in the shaft during sinking operations, and when the ultimate depth of the shaft is reached the pump can be laid horizontally and used as an ordinary, stationary mine pump. Fig. 248 is a photographic view of this pump suspended vertically, and the feet for horizontal installation can be plainly seen.

Referring to the pump section in Fig. 247, it will be noticed that the impellers are arranged in two groups back to back, that is, with the suction side of four impellers facing the opposite direction from the suction end of the other four. This insures an almost perfect axial balance, but in order to deal with any slight unbalancing there may be due to wear or the weight of the impellers when the pump is suspended vertically, the special balancing device shown on the suction end of the pump is provided. The two special views of this

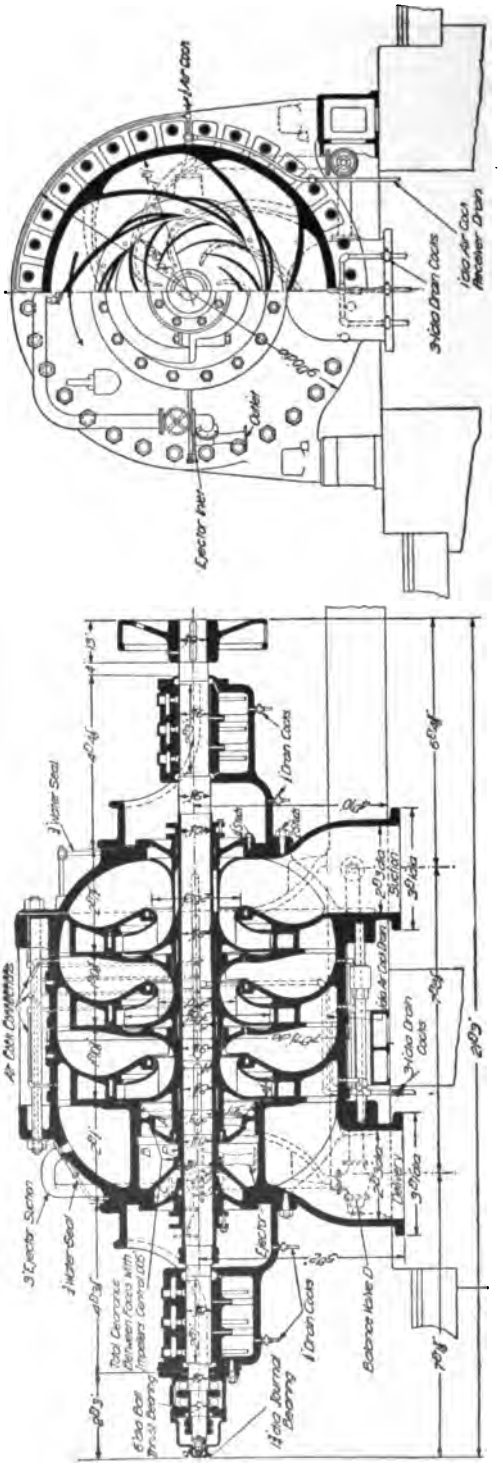
Ejector Inlet
Outlet
Water Seal
Drain Cocks
Balance Valve
Ejector

Fig. 246.

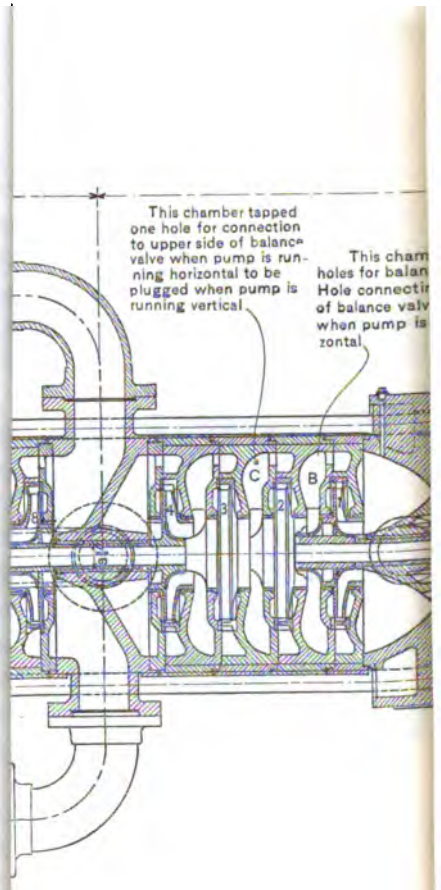
This chamber tapped one hole for connection to upper side of balance valve when pump is running horizontal to be plugged when pump is running vertical
This cham
holes for balan
Hole connecti
of balance valv
when pump is
zontal
C
B
A
1
2
3

balancing device show the connection to the upper and lower sides of the balancing valve. The principle of operation of this valve is similar to that of the balancing piston described before. The upper side of the valve is connected by means of a $\frac{3}{8}$-inch pipe to the space *C* between the second and third impellers when the pump is running horizontally and to the space *B* between the first and second impellers when the pump is running vertically. The lower side of the balancing valve is connected to space *B* between impellers 1 and 2 in both cases. When the pump is operating vertically the higher pressure in space *C* helps to support the weight of the rotating parts.

The main portions of the casing of the pump, containing the discharge vanes, are constructed of close-grained cast iron. The discharge vanes are provided with renewable hard bronze tips so constructed that the whole of the throat of the discharge passage is of hard metal, resisting wear and easily renewable; a further advantage of the bronze tip lies in its acid-resisting properties. The impellers are all constructed of bronze and are accurately machined all over, carefully balanced and secured to the mild-steel shaft by means of an accurately fitted feather key. It will be

Fig. 248.

noticed that there is a central bronze sleeve upon the shaft rotating in the central internal bearing of the pump; at the outer ends of the shaft other bronze sleeves and nuts hold all of the impellers firmly in position. The central bearing is water lubricated, but is provided with a small amount of grease lubrication at starting.

The casings of the pump, though of cast iron, are provided with wrought-steel hoops shrunk on to enable the pump to withstand the great head. Each section of casing is rabbeted into the adjacent one, and the whole is made to form one complete unit by long substantial steel bolts passing from the delivery to the suction end casings. The pump shaft is connected to the driving shaft of the motor by means of a flexible coupling of special design, which allows for any possible inequalities in lining up and for any damage the pump shaft might suffer in the shaft of the mine.

The motor is of an entirely enclosed type with short-circuited rotor, thus giving a very simple construction. The stator is water cooled by tapping the discharge pipe with a $\frac{3}{8}$-inch copper connection and valve, which allows water to enter under pressure into the water jacket of the stator. The latter is provided with a $\frac{3}{4}$-inch outlet. To effect starting, a special multi-point automatic transformer starter is provided, and the unit is started up with the delivery valve on the pump closed, so that the power taken under starting conditions is not more than about 30 per cent of the power taken at full load.

Mather & Platt, Ltd., also build high-pressure centrifugal pumps of the double-inlet type. A cross-sectional view of such a pump, driven by a Zoelly steam turbine, is shown in Fig. 249. A number of these units are installed at the Montreal Water and Power Company's plant in Canada. Each pump delivers 1680 cubic feet (10 500 British gallons) of water per minute against a head of 410 feet when running at 1500 r.p.m. The normal load on the turbine is 1800 h.p. The pump has two impellers working in parallel, that is, both impellers receive water from the suction pipe and deliver it to a common discharge pipe. The water enters the suction pipe under a head of 10 feet and flows into the middle of the pump casing. From here it divides into four streams entering on both sides of each impeller. In this arrangement no axial thrust can be produced. Fig. 250 gives a cross section through the pump, in which the cored openings through the discharge vanes are shown. These openings permit the passage of the water from the middle of

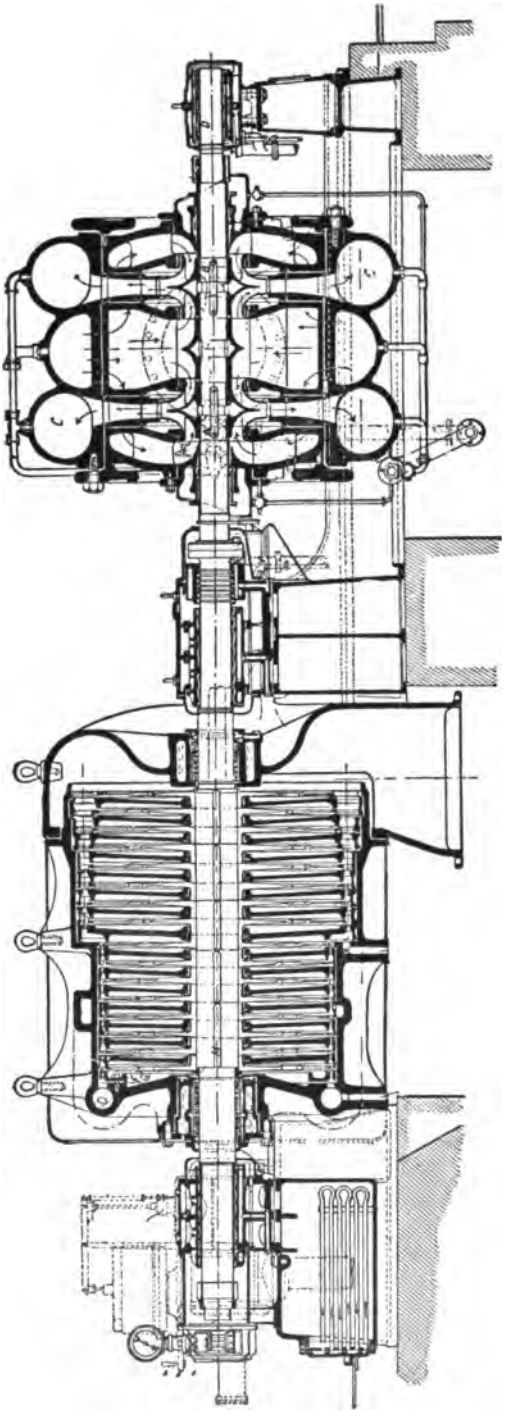

Fig. 249.

the pump casing to the opposite suction side of each impeller. The water on leaving the guide vanes enters the two circular chambers C, the latter being united at the discharge pipe. The end of the pump shaft is supported in a long bearing, and both the turbine bearing and pump bearing are provided with forced lubrication. The steam turbine has sixteen stages, which are divided into two groups of eight wheels each. The second group is of larger diameter than the first. All the newer turbines of this type are now built in this manner. The turbine is supplied with superheated steam at 165 pounds per

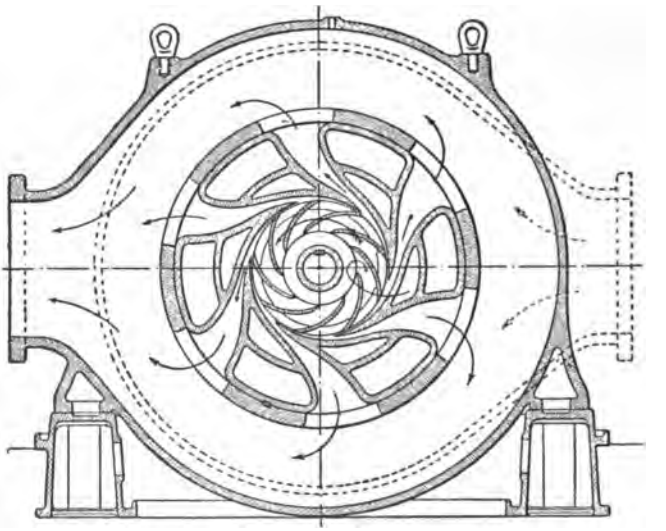

Fig. 250.

square inch pressure. The length of the entire unit is about 21 feet. The governor of this unit is of a somewhat unique construction. It is known as the Chorlton-Whitehead governor. Fig. 251 gives sectional views through this governor. The entire governor casing is filled with oil. The governor spindle passes through a long sleeve and operates the throttle valve directly. Pins A are fastened to the casing and form centers for the double bell crank DC. The vertical arms C, C' are attached to the weights E, E', and the horizontal arms D, D' transmit motion to the governor spindle. The weights are held in position by the springs F, F', the latter tied together by means of through bolts, preventing the springs from moving outward.

The compression in the springs balances the centrifugal forces of the weight in all positions, so that the governor is isochronous. The

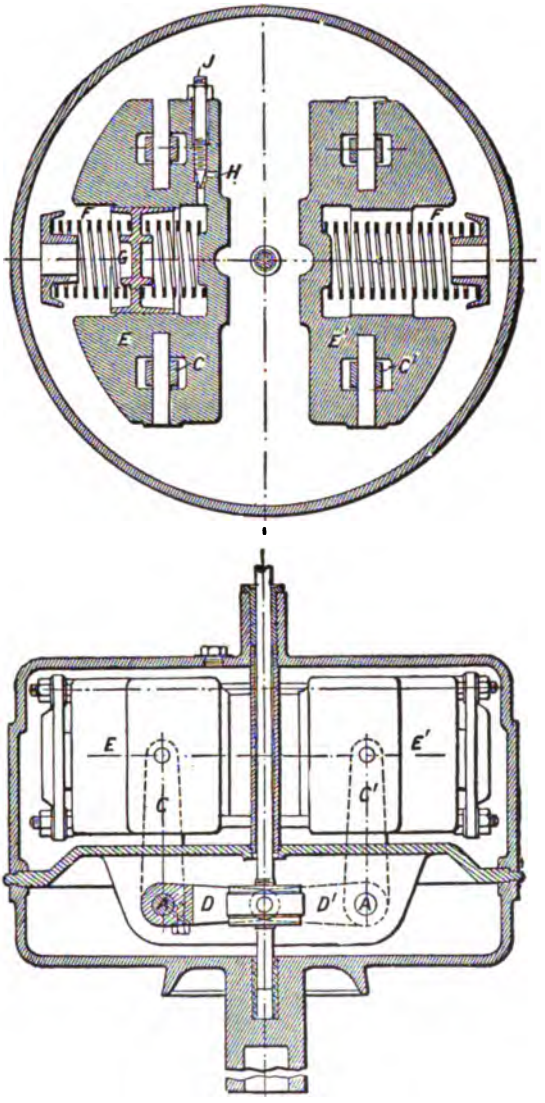

Fig. 251.

stability for regulation is obtained by means of a piston *G* which produces a dashpot effect either by forcing the oil out through the small opening *H* or by drawing it in through this opening. The oil

flow through H is controlled by means of a needle valve J. The pistons simply destroy, more or less, a part of the forces produced by the springs F.

Fig. 252 is a photographic view of an electrically driven pump specially designed for boiler feed purposes. The two units of the pump are arranged to work in series. The ultimate pressure required is 200 pounds per square inch at the boilers plus friction in piping and economizers. The pump delivers 22.5 cubic feet of water per minute when running at 1100 r.p.m. Fig. 253 gives a cross-sectional view of one section of this pump. It consists of six stages with single-inlet impellers. It will be noticed that there is no external bearing at the discharge end; this means that a troublesome gland under high pressure is dispensed with, and further, that the shaft

Fig. 252.

is much stiffer, due to its shorter length. The arrangement for securing axial balance is extremely simple and is of the latest type developed by this firm. It is placed on the extreme high-pressure end of the pump. The valve V is screwed on the end of the shaft and forms a close clearance space between chambers A and B and between chambers A and C, the total clearance between the valve and faces being 0.003 inch. Chamber A is supplied with water at the pressure of some intermediate stage, and chamber C is connected to the suction end of the pump. The varying pressure in chamber B, caused by a slight movement of the valve V with the shaft, creates the necessary balancing pressure. At the suction end of the pump there is an external bearing of the self-oiling type. At the point where the shaft passes through the suction chamber a stuffing box and gland are provided and are fitted with a water supply to prevent air leakage into the pump. Fig. 254

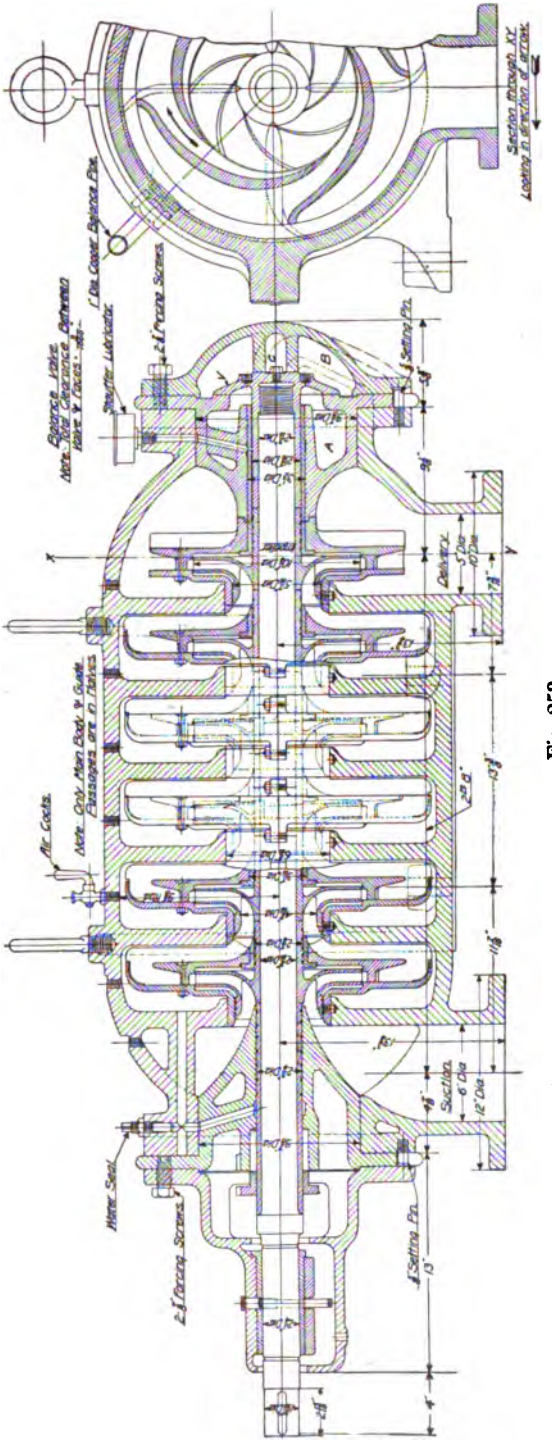
Section through XY
Looking in direction of arrows
Gauge Valve
Set Clearance Between
Valve & Faces
Steadies Vertical
4 Union Screws
Water Seal
4 Gland Screws
Air Cocks
Note Only Main Body & Guide
Passages are in Halves
Suction
6" Dia
12" Dia
Delivery
5" Dia
10" Dia
4 Setting Pin
13"

Fig. 253.

gives a view of the pump opened up and shows the ease of disassembly.

Fig. 255 gives a cross-sectional view of an electrically driven pump, especially designed for working in a deep well and adapted to being entirely submerged in water. During normal working hours, when the pump is in operation, the water is lower and well below the level of the pump; it is not necessary, therefore, for the unit to be at work during the week-ends, and during the stoppage the water rises above

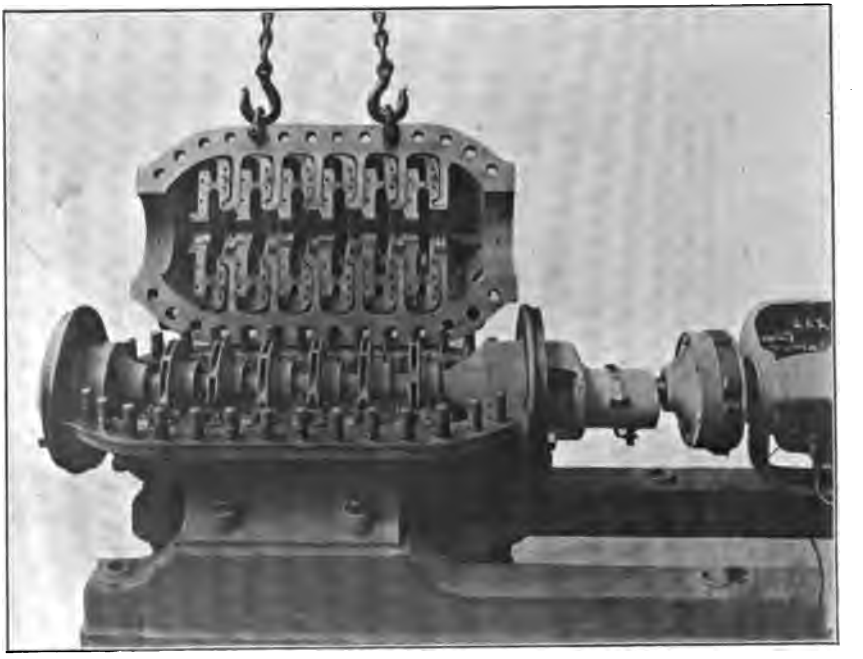

Fig. 254.

the pump and motor to a height of 100 feet. The motor is protected from damage by the air-tight dome or bell which surrounds it, but to make quite certain that no harm can come to it while under water, compressed air is supplied to the dome from the surface, a pressure of air being maintained in the dome greater than the pressure due to the level of the water above the unit. The unbalanced axial thrust is taken care of by a ball thrust bearing. The pump delivers 160 cubic feet (1000 British gallons) of water per minute against a head of 265 feet at 970 r.p.m.

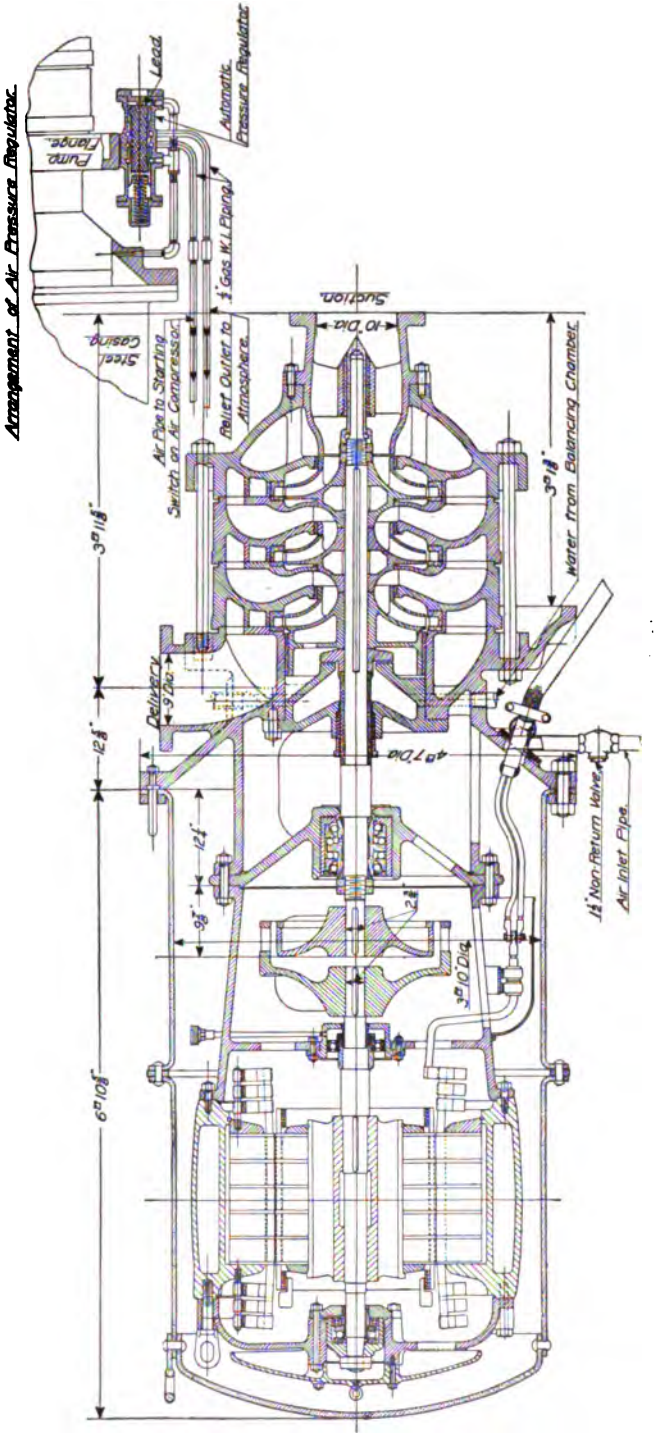
Arrangement of Air Pressure Regulator.
Lead.
Pump Flange.
Automatic Pressure Regulator
1" Gas W.I. Piping
Relief Outlet to Atmosphere.
Air Pipe to Starting Switch on Air Compressor.
Steel Casing
Suction
10" Dia.
Water from Balancing Chamber.
3'-11"
12'-8"
6'-10"
Delivery 9" Dia.
12"
9'-8"
2'-8"
4'-0" Dia
3'-10" Dia
1½" Non-Return Valve
Air Inlet Pipe.

Fig. 255.

A very novel unit is shown in Fig. 256 and in section in Fig. 257. It is a combination of a high-pressure centrifugal pump and a single-stage steam turbine, particularly designed for fire purposes. The impeller of the pump and the wheel of the turbine are mounted on

Fig. 256.

the same shaft, the latter being supported in substantial self-oiling bearings, thus insuring the utmost rigidity. The pump can deliver 104 cubic feet (650 British gallons) of water per minute against 250 feet head. The unit runs at 3000 r.p.m. As there are only two rotating wheels, the greatest possible simplicity is obtained and the unit can run continuously without fear of breakdown. Owing to the

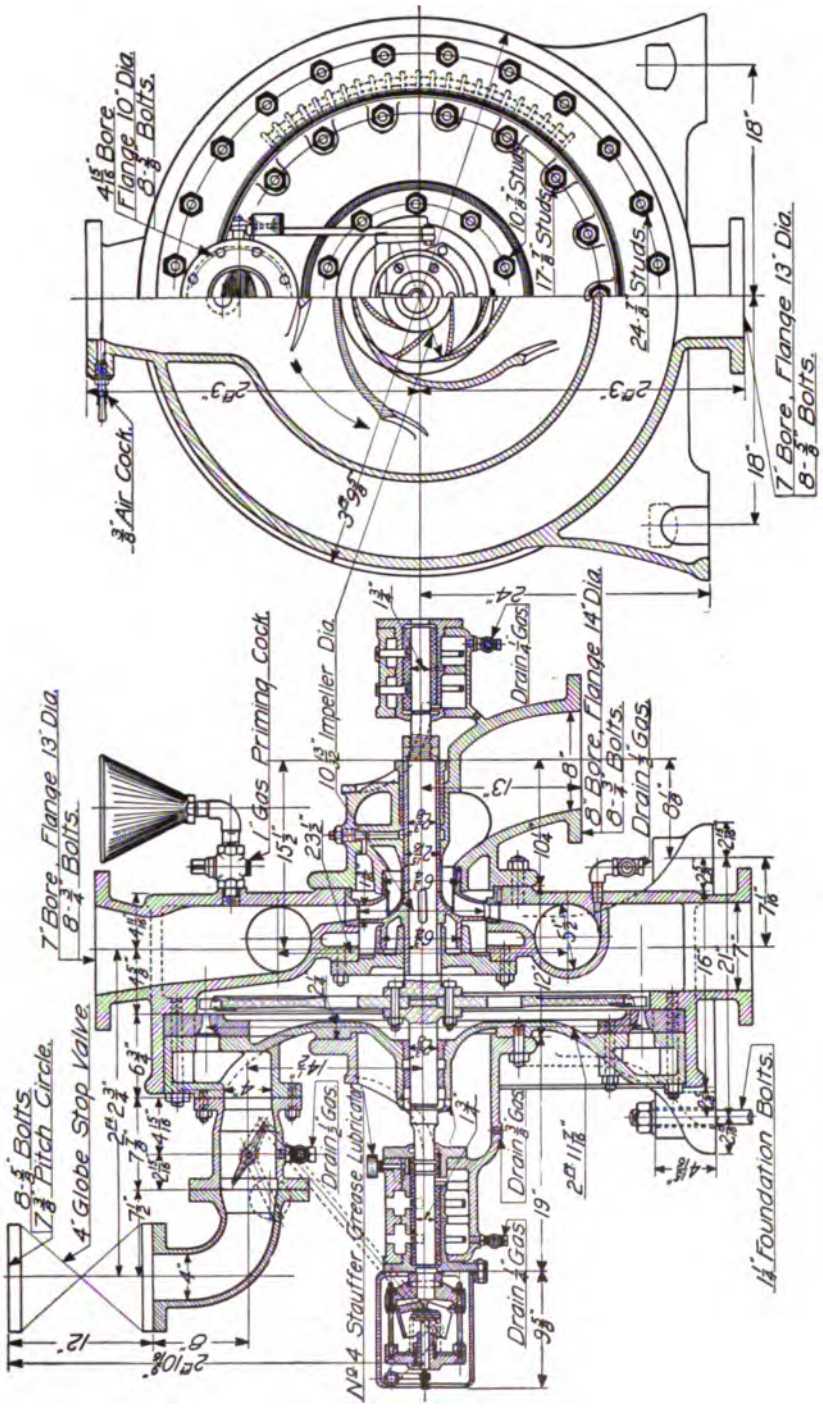
4 15/16" Bore, Flange 10" Dia. 8-3/4" Bolts.
10-3/4" Studs.
17-3/4" Studs.
24-3/4" Studs.
18"
18"
7" Bore, Flange 13" Dia. 8-3/4" Bolts.
3/8" Air Cock.
2" 3".
2" 3".
3" 9".
13"
2"
Drain 1/4" Gas
8" Bore, Flange 14" Dia.
8-3/4" Bolts.
Drain 1/4" Gas.
6 1/8"
10 13/16" Impeller Dia.
1" Gas Priming Cock.
15 1/2"
23 1/2"
7" Bore, Flange 13" Dia. 8-3/4" Bolts.
8-3/4" Bolts. 7 3/8" Pitch Circle.
4" Globe Stop Valve.
2" 2 3/4"
6 3/4"
7 3/8"
4 1/8"
2 15/16"
7 1/2"
4"
12"
6"
2" 10 3/8"
Drain 1/4" Gas
No 4 Stauffer Grease Lubricator
Drain 1/4" Gas
Drain 1/4" Gas
Drain 1/4" Gas
2" 11 7/8"
19"
9 3/8"
1 1/4" Foundation Bolts.
7 1/8"
16"
21"
2 3/8"
3 5/8"
5 1/2"
10 1/4"
6 1/8"
13"
12"
24"
14"
13"
29"
29"
32"
4 1/8"
4 1/8"

Fig. 257.

high speed of rotation the quantity and head are very great in pro-

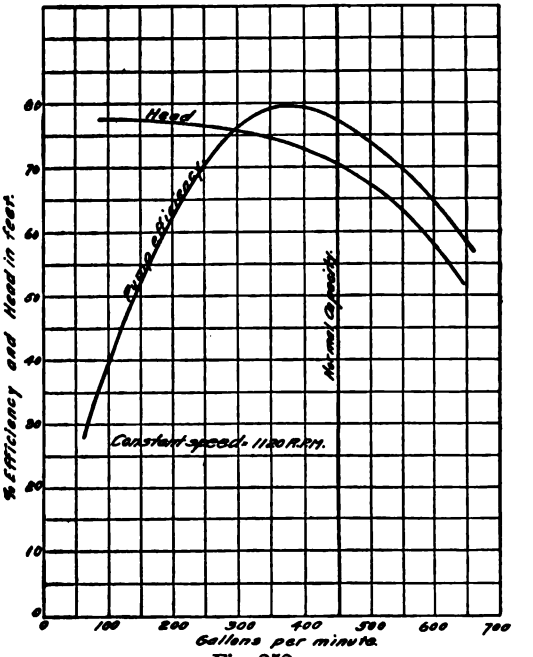

Fig. 258.

portion to the size of the pump. The steam consumption with only

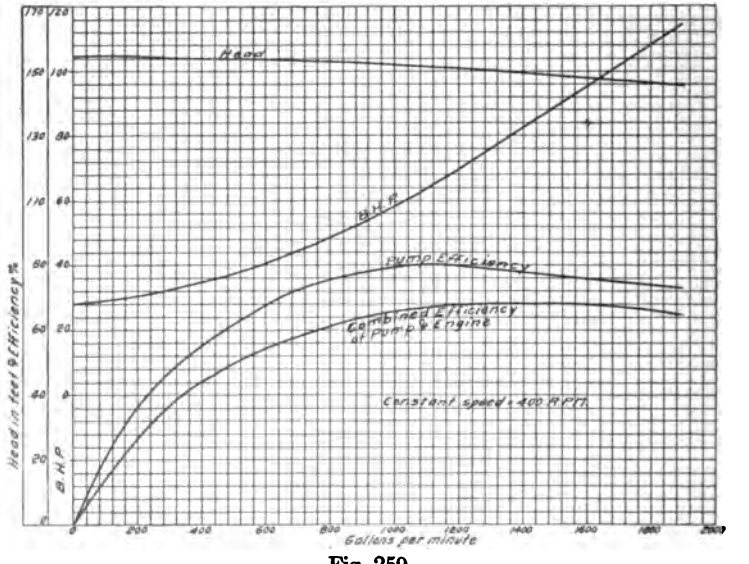

Fig. 259.

one row of buckets in the turbine is naturally somewhat high, but

as the pump is only required for fire purposes, the economy is not a vital consideration.

Several characteristic curves of Mather & Platt pumps are of interest. Fig. 258 gives the results of tests on a small high-pressure single-stage pump designed to deliver 72 cubic feet (450 British gallons) of water per minute against a head of 70 feet. The normal revolutions per minute are 1120. The maximum pump efficiency of 80 per cent was obtained at 390 gallons per minute with a head

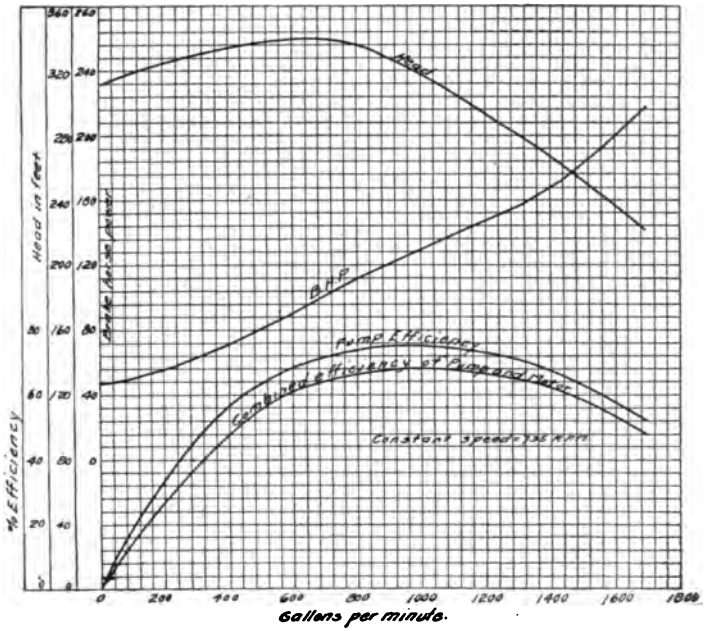

Fig. 260.

of 73 feet when running at normal speed. When delivering 450 gallons per minute the head obtained at 1120 r.p.m. was 71 feet and the efficiency of the pump was 77.5 per cent.

Fig. 259 gives the characteristic curves of a four-stage pump driven by a Belliss & Morcom engine running at 400 r.p.m. The normal load of the pump is 1400 gallons per minute against a head of 150 feet. Special notice should be taken of the constant head obtained over the entire range of output. Although the maximum pump efficiency does not occur at the rated load, the combined efficiency

of pump and engine has its maximum of 64 per cent at the rated load. The pump efficiency at this load is 78 per cent, although it

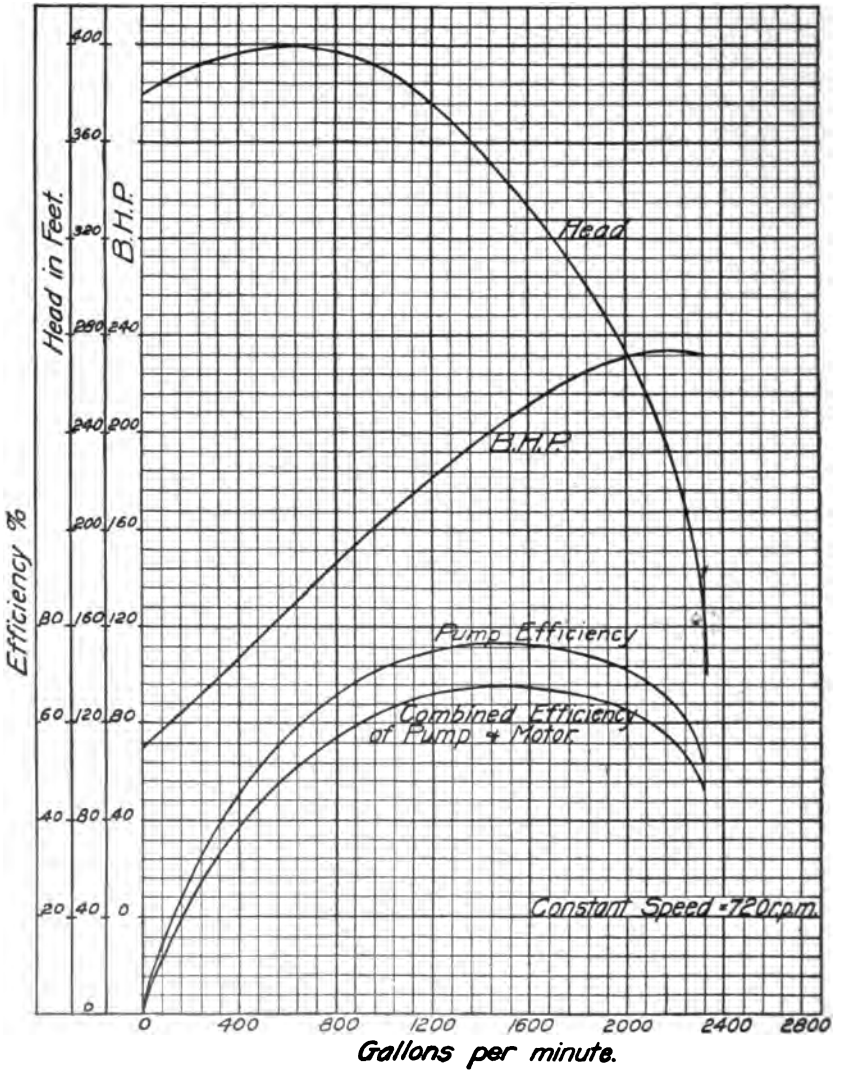

Fig. 261.

reaches a maximum of 80 per cent when discharging 1100 gallons per minute.

Fig. 260 gives the characteristic curves obtained from a test of a four-stage high-pressure pump designed to deliver 1000 gallons per

minute against 320 feet total head when running at 735 r.p.m. The variation of head with quantity is quite different from that in the tests previously given. The maximum pump efficiency was 75 per cent and the combined efficiency of pump and electric motor was 68 per cent.

Fig. 261 gives the results of tests upon a five-stage motor-driven pump running at 720 r.p.m., the normal duty being 1600 gallons per minute against 330 feet head. The characteristic curves show that the motor can never be overloaded excessively, because with increasing quantity the delivered head decreases so rapidly that the power required decreases when the pump is delivering a larger quantity than 2250 gallons per minute. The brake horse power of the motor required at normal load is 220, whereas the maximum load that can be placed on the motor is below 240 h.p. The pump efficiency is 76 per cent and the combined efficiency of pump and motor 68 per cent.

55. De Laval Pumps.

The De Laval centrifugal pump is manufactured by the De Laval Steam Turbine Company, Trenton, N. J. This concern is affiliated with the Aktiebolaget De Lavale Angturbin of Sweden, the Société De Laval of France, the English De Laval Steam Turbine Company, and the Maschinenbau-Anstalt Humboldt of Germany, all working under the De Laval patents and exchanging technical information, designs, drawings, etc. The De Laval Company claims to be the first to manufacture the modern high-speed small-diameter type of pump in this country, the complete line, practically as it is to-day, having been placed on the market in 1901, and to have been the first to use the horizontally split casing consisting of only two castings.

In their multistage designs the De Laval Company use impellers similar to those shown schematically in Fig. 100. The De Laval pumps are characterized by a number of distinctive features, the most important of which is the absence of discharge vanes. They use a so-called whirlpool chamber and volute, which serve as the diffuser. It is not necessary to enter here into a discussion of the advantages and disadvantages of using discharge vanes, as these have been fully covered in another chapter of the book, but it may

be interesting to know that the necessity of discharge vanes becomes less apparent the higher the speed of the pump, which corresponds to an impeller of small diameter. In order to obtain the excellent efficiencies secured with De Laval pumps the contour and shape of the whirlpool chamber and volute must be made quite smooth and accurate; and to accomplish this all pump casings, both of the single-stage and multistage types, are cast in dry sand molds, which insure such accurate contours and smooth surfaces, and also make possible the casting of these parts in one piece, obviating recourse to removable or sectional diaphragms inserted in the casing.

Split casings are used throughout, so arranged that all moving, wearing, and internal parts can be removed after lifting the casing cover and removing the bearing caps, and without disturbing the suction or discharge connections, the pumps thus differing from the side-plate single-stage pumps, and from multistage pumps, in which the internal diaphragms or partitions are solid disks threaded on the shaft between the impellers.

All the main members of the pump subject to wear are protected by small replaceable parts, such as shaft sleeves, the labyrinth packing rings attached to the casing and to the impeller, the bushings protecting the diaphragms of multistage pumps, and the bearings. These parts are manufactured to limit gauges on an interchangeable system to facilitate rapid and accurate replacement.

Bronze is used for the impellers and for all working parts coming in contact with the liquid, except where other metals are required by reason of the character of the liquid handled. Bronze is used on account of its ability to resist corrosive action of water and to retain its shape and polish for an indefinite period.

The speeds of De Laval pumps are much higher than those commonly used; for instance, pumps are regularly built to operate direct connected to De Laval single-stage impulse turbines, at speeds of 4000 r.p.m. and above, and as an extreme case, impellers have been constructed to generate 700 feet head at 20 000 r.p.m. By dint of careful designing and superior finish, checked by repeated tests, these results have been accompanied by high efficiencies.

In ordinary service relatively high heads are generated per stage, single-stage pumps, for instance, being built for feeding boilers

against pressures of 175 pounds per square inch. The attainment of such high heads per stage with good efficiency is made possible

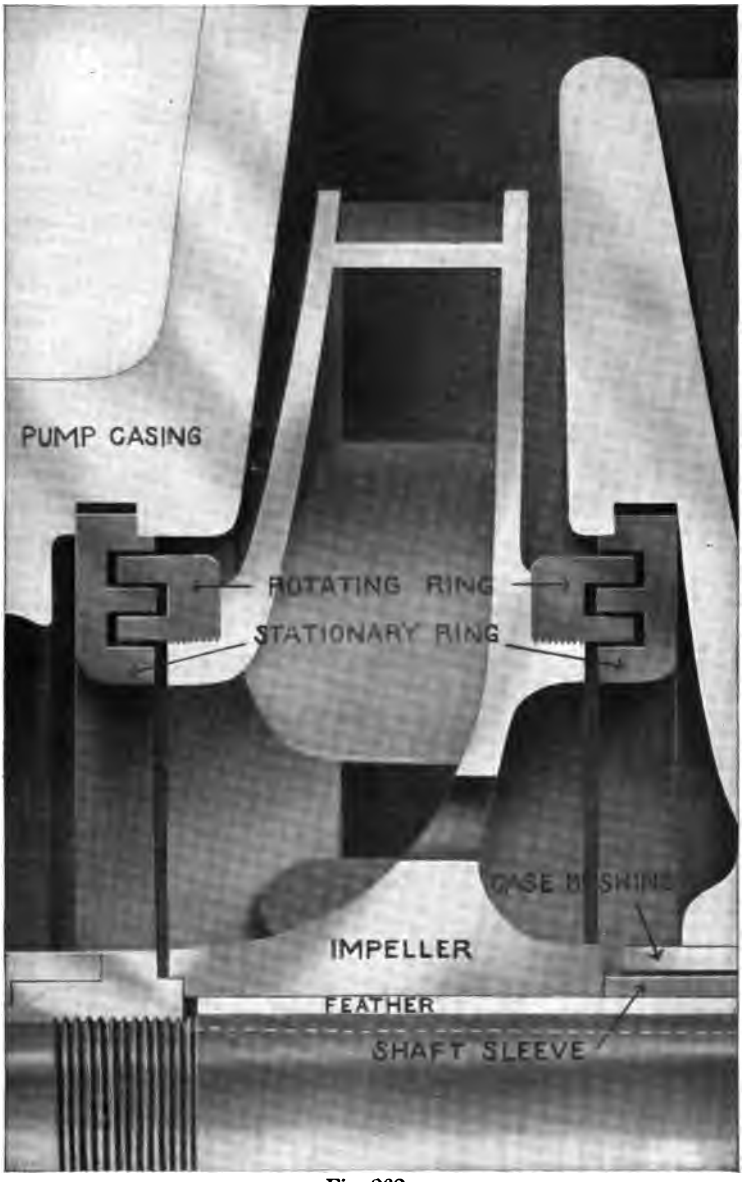

Fig. 262.

by the use of labyrinth packing rings attached to the casing and to the impeller, which prevent the leakage of water back from the dis-

charge chamber into the suction chamber. The labyrinth rings give a longer leakage path within limited space and introduce several abrupt turns in the course of the water, thus increasing the resistance to leakage. As a consequence the volume of leakage and the loss of power therefrom are reduced. Fig. 262 shows clearly the design of these labyrinth rings. The rotating parts are screwed upon both sides of the impeller, and the stationary parts are fastened to the pump casing, both being renewable.

A careful examination of the characteristic curves of De Laval pumps shows that the pumps are designed to be self-regulating,

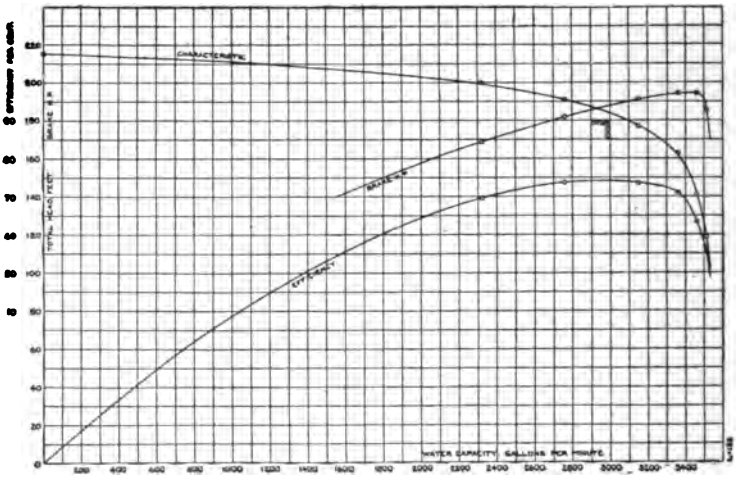

Fig. 263a.

a feature that has been described and attention called to it in the theoretical discussion in this book. The pump impeller is so designed that if the output is increased beyond the rated quantity or point of maximum efficiency at a given speed, the power taken by the pump will drop off rather than increase. This is important, since any pump may be overloaded, as for instance by failure of the discharge piping, but in such case the power-limiting characteristic prevents overloading of the motor, and makes it feasible to install a motor of just sufficient size to care for the power required under normal operating conditions. Were a larger motor installed in order to take care of a rising power characteristic, it would, under rated conditions, normally run underloaded and hence at lower efficiency.

Closely related to this feature of the drooping power characteristic is the importance of being able to design pumps accurately to fit specified conditions. The meaning of this will be seen by referring to the characteristic curves representing the performance of De Laval pumps as shown in Figs. 263a and 263b, where there will be noted in each case a small crosshatched corner. This indicates the delivery and head which the pump was specified to show at a stated speed. The actual performance curve as plotted from test readings shows how near this point was approximated by the designer of the pump. In Fig. 263b it will be seen that there are two such

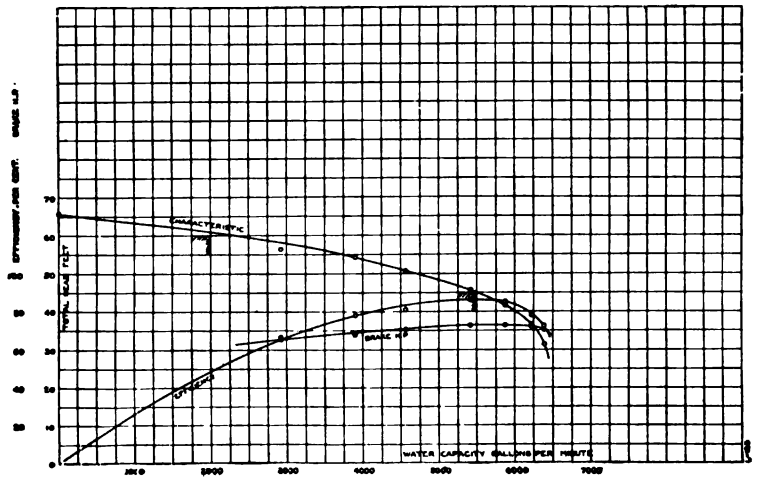

Fig. 263b.

specified points; that is, the pump was guaranteed to deliver 2000 gallons per minute against a head of 60 feet and 5500 gallons per minute against a head of 45 feet. The De Laval Company state that it is their practice to design each impeller separately; that is, no impellers or impeller patterns are carried in stock. Before shipment every pump is thoroughly tested throughout the range of its capacity and a record is carefully kept of its performance. From all these tests are found suitable coefficients which can be used in future designs.

Fig. 263a represents the characteristics of a two-stage pump designed to deliver 3000 gallons per minute against 180 feet head and to be driven by a 200-horsepower induction motor at 880 r.p.m.

Fig. 263b shows the characteristics of a single-stage pump designed to deliver 5500 gallons per minute against 45 feet head, or 2000

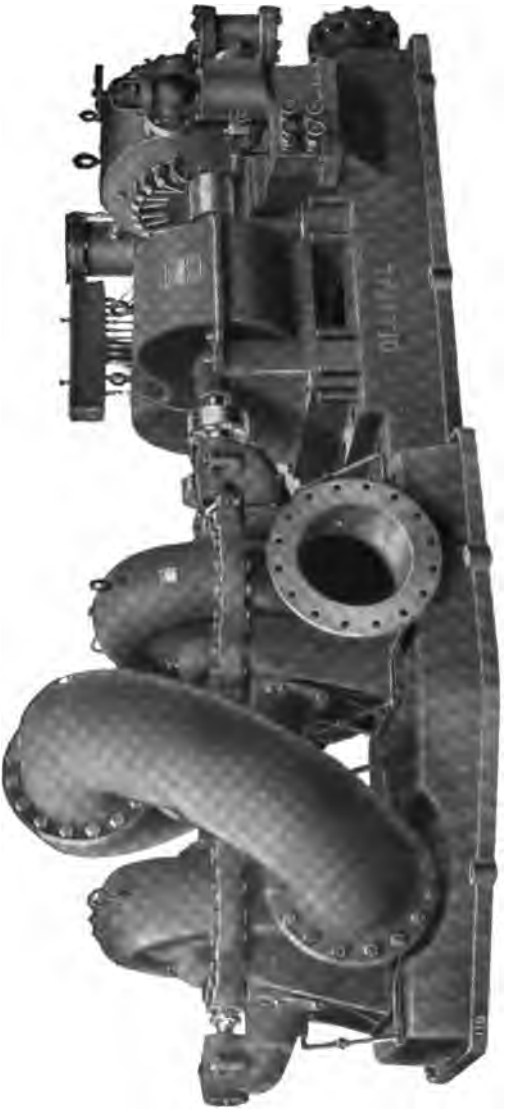

Fig. 264.

gallons per minute against 60 feet head, when driven at 860 r.p.m. by a 75-horsepower induction motor. This pump was to serve as a circulating pump for a barometric condenser; the higher head being

required to start the barometric condenser without assistance from the air pump.

Attention is called to another peculiarity of the head capacity curves of these pumps. It will be noticed that they slope continuously from the shut-off point to the maximum delivery, that is, there is no rise of pressure with initial increase in delivery. It is

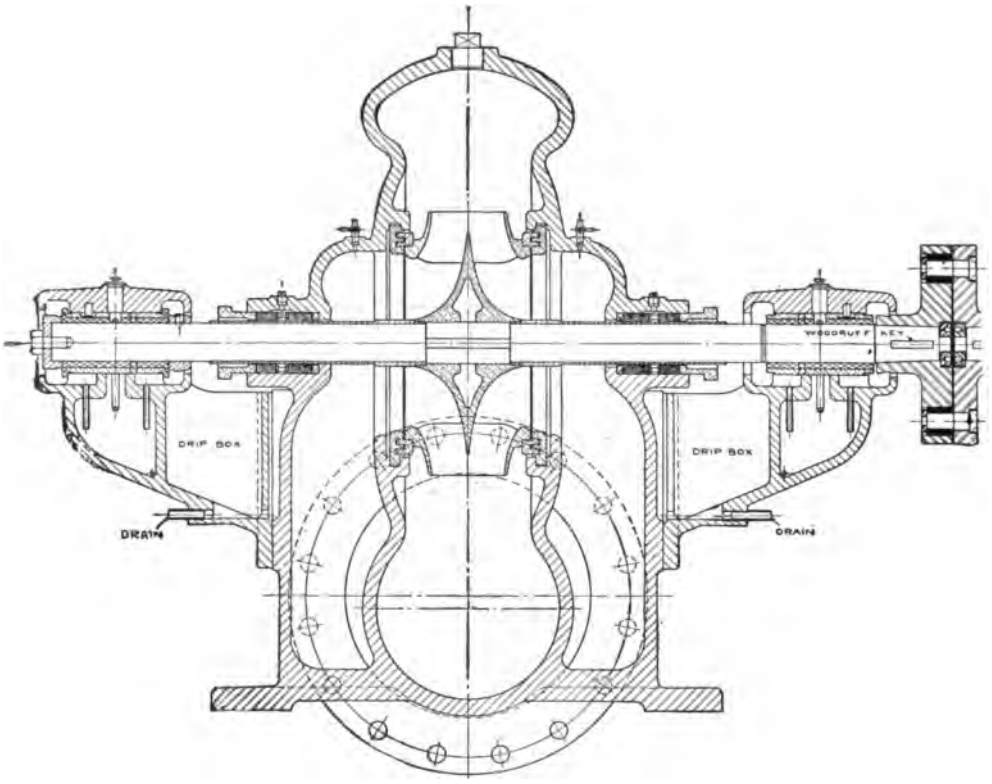

Fig. 265a.

claimed that such initial rise of pressure renders a pump unsuitable under certain conditions. For instance, if the head generated at no delivery is 215 feet, and the head generated at the delivery corresponding to the highest efficiency is 235 feet, the pump could not start delivering against a static pressure of 235 feet, such as that of a standpipe, without increasing the speed or opening a by-pass. After bringing the delivery up to the desired amount, the speed could then be reduced, the flow throttled, or

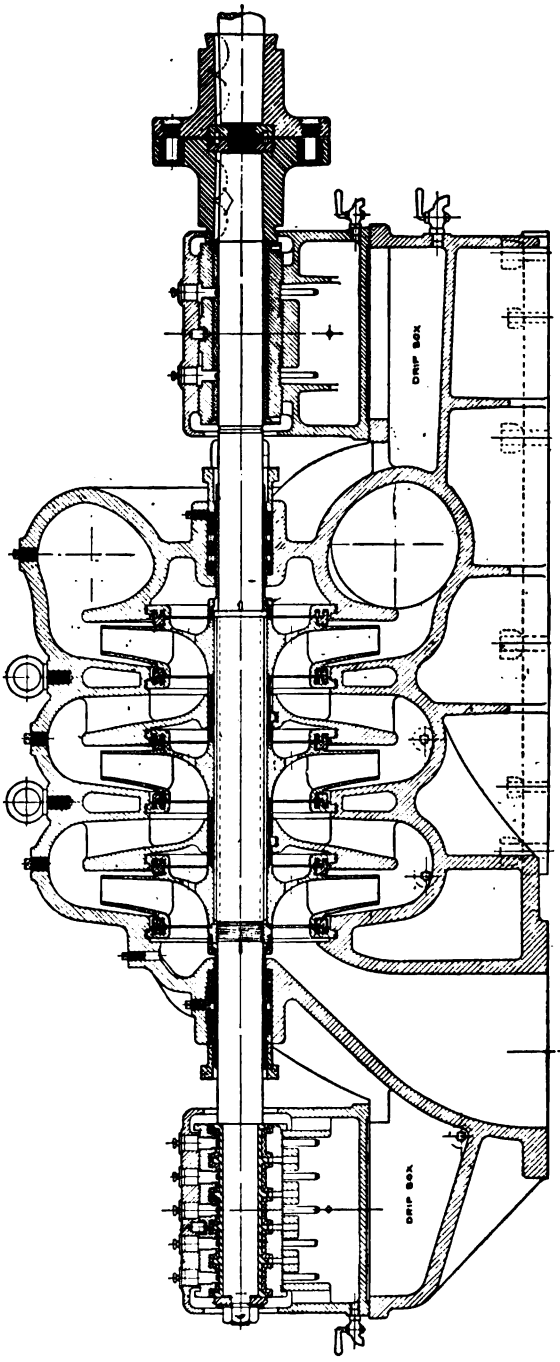

Fig. 265b.

the by-pass closed, but the pump would be left in a state of unstable equilibrium and, if it should lose the flow, would not be able to regain it automatically.

Fig. 264 illustrates two single-stage pumps driven by a De Laval combined high- and low-pressure geared turbine. Fig. 265a gives a cross-sectional view through a typical single-stage double-suction

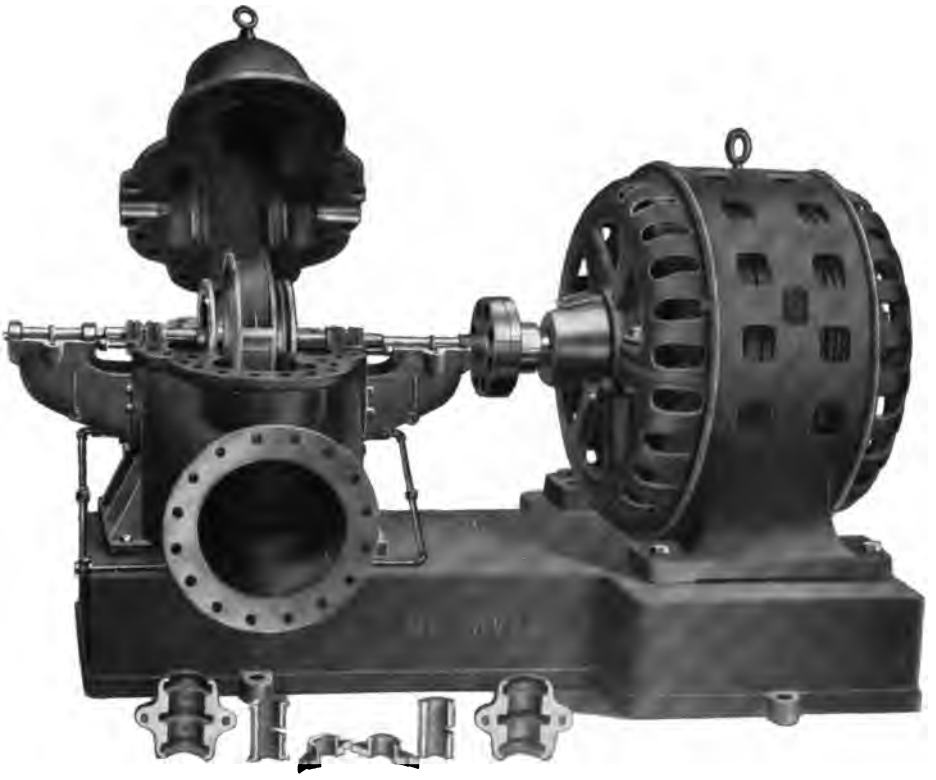

Fig. 266.

centrifugal pump, showing the labyrinth packing rings between impeller and casing, the bronze sleeve-protecting shaft, the split packing bushing, and the flexible coupling.

Fig. 265b shows a section of a De Laval three-stage pump. The pump casing is split horizontally and the top half of the casing can be removed without disturbing the suction or discharge connections. The construction of the labyrinth packing rings and the bronze

protecting bushing on the diaphragms and casing, and the marine type of thrust bearing, can be clearly seen.

Fig. 266 shows a photographic view of a single-stage motor-driven pump with the pump case cover lifted and bearing caps removed. The shaft, impeller, and labyrinth packing rings can be removed bodily without disturbing the suction or discharge piping.

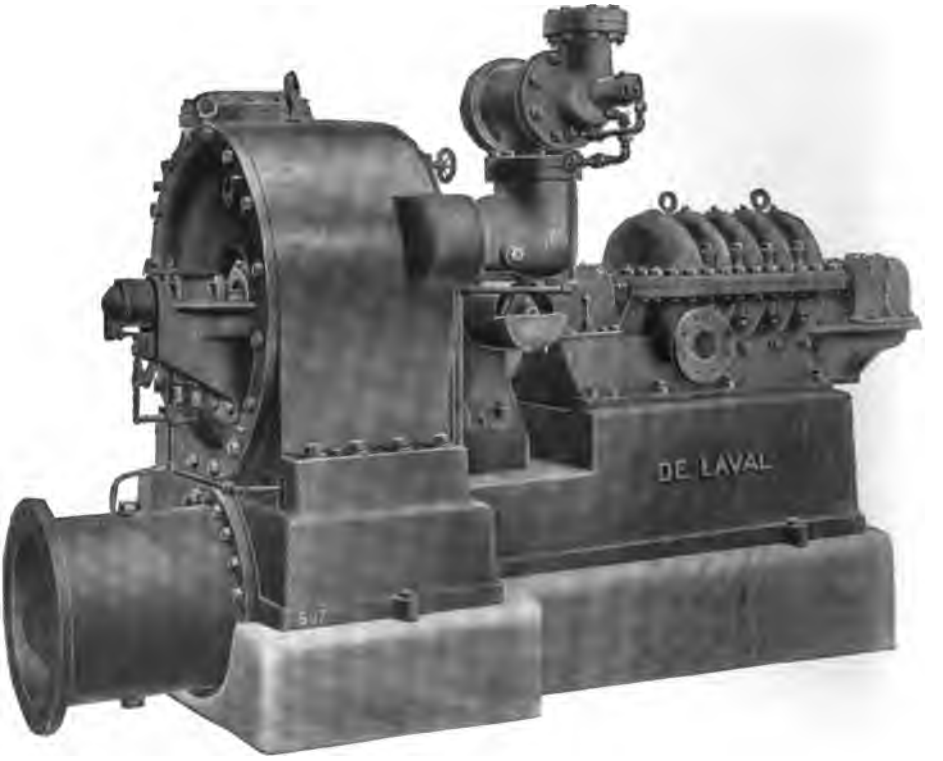

Fig. 267.

Fig. 267 gives a photographic view of a direct-connected five-stage turbine-driven pump, capable of delivering 66.8 cubic feet of water per minute (500 gallons per minute) against a pressure of 600 pounds per square inch when running at 2900 r.p.m. This set is used for furnishing hydraulic pressure service in steel mills.

56. R. D. Wood Pumps.

R. D. Wood & Co. of Philadelphia build chiefly large single-stage pumps for comparatively low pressures, but have also built some high-pressure multi-stage pumps. The low-pressure pumps are usually of the double-inlet type, with a volute casing, although some of the smaller pumps have a suction pipe at one side of the casing, with a single-inlet impeller. Fig. 268 shows a large single-stage

Fig. 268.

pump having a capacity of 10 000 cubic feet (75 000 gallons) of water per minute. The head is 80 feet and the diameter of the discharge pipe is 54 inches. This pump is for direct connection to a steam engine. Fig. 269 shows a single-stage pump for handling sewage at Santos, Brazil. The pump discharges against a head of 60 feet. It is direct connected to a motor by means of a flexible coupling. The pump bearings are supported upon the casing and are ring lubricated. Axial thrust is taken up by ball bearings at the extreme suction end of the shaft. Fig. 270 gives a cross-sectional

view of a similar pump but of nearly double the capacity; in this view the pump construction can be more clearly seen. The impeller in this case is of the Jaeger design. The clearance between impeller and casing is made cylindrical and of the same diameter on both sides of the impeller, in order to assist in equalizing axial thrust. Packings are provided at both ends of the shaft and are supplied with a water seal to prevent air leakage into the suction pipe. No discharge vanes are employed in these types of pumps.

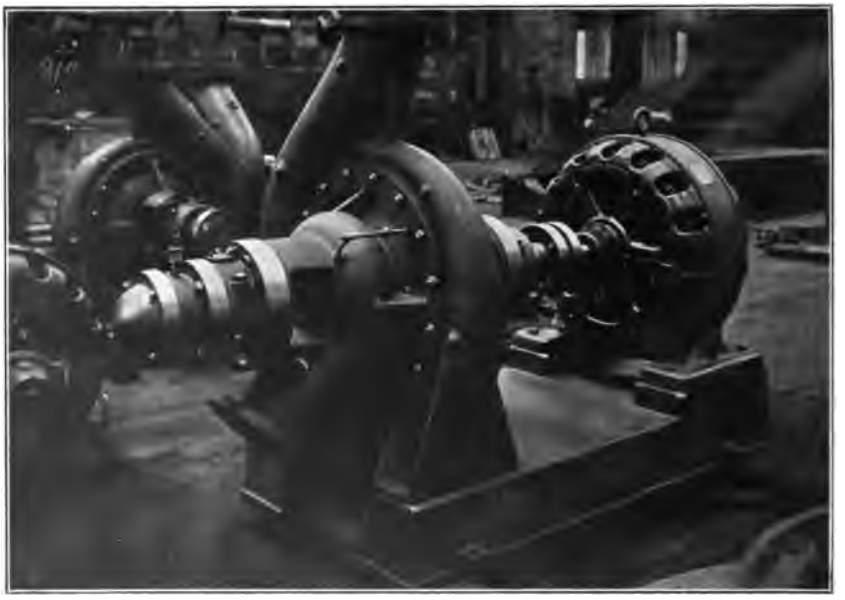

Fig. 269.

Fig. 271 gives a cross-sectional view through a two-stage pump. The Sulzer type is here employed. The two impellers are placed upon the shaft, back to back, and are definitely located by an adjusting nut at the entrance end of each impeller. The two impellers are separated by a diaphragm supported in the casing by a rabbet and held securely by studs. The diaphragm forms a close clearance with the hub of the impellers. Close clearances are also formed between the impellers and the casing upon cylindrical surfaces. The casing has the usual cored passages of Sulzer construction. The bearings are supported upon the pump casing and are ring lubri-

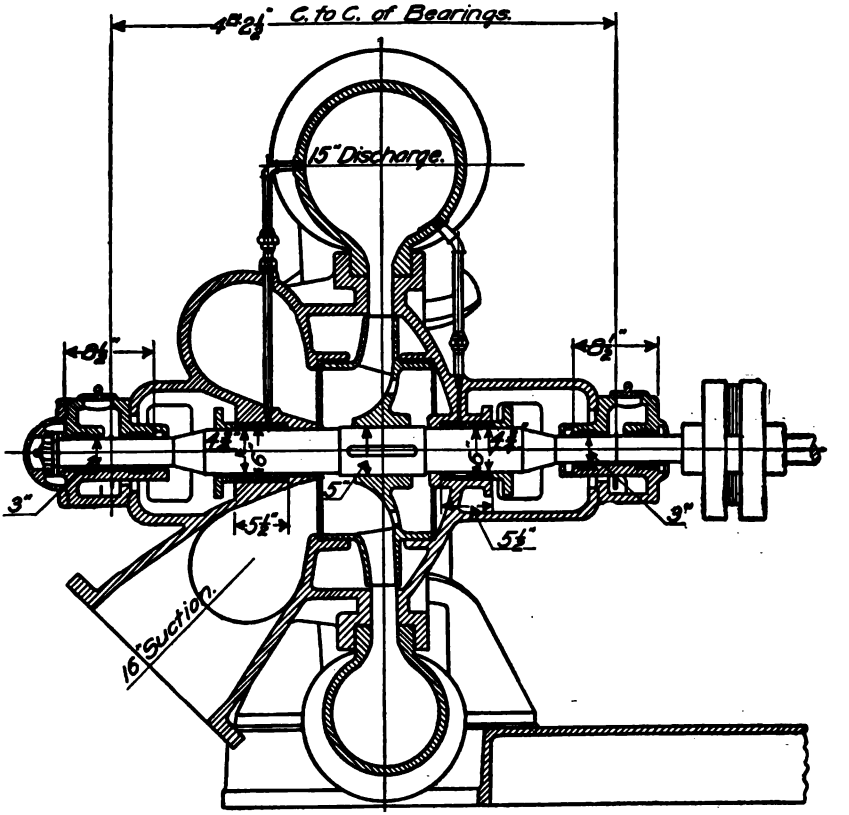

Fig. 270.

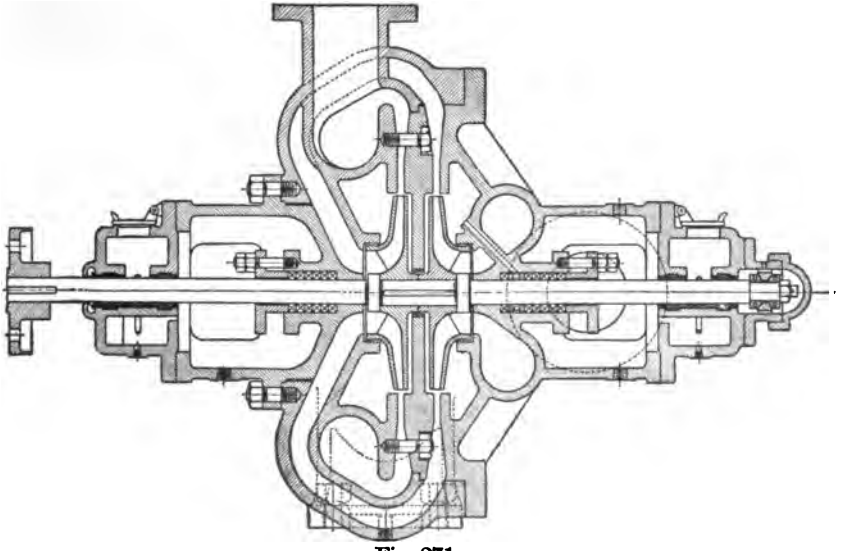

Fig. 271.

cated. Axial thrust is taken care of by ball thrust bearings placed on the suction end of the shaft.

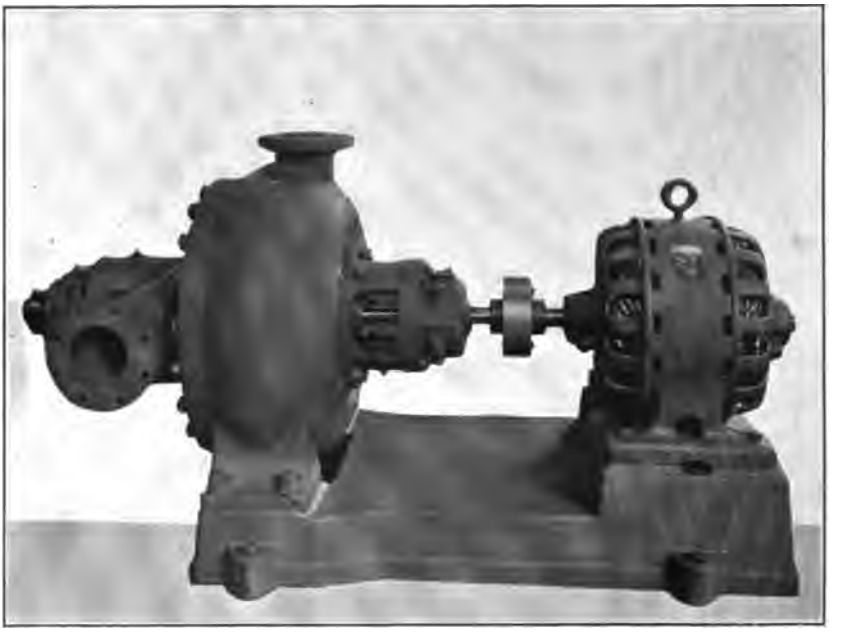

Fig. 272.

Fig. 272 illustrates a two-stage pump installed for town water supply in Juarez, Mexico. This pump is motor driven and works against a head of 200 feet. Its construction is exactly as shown in the cross-section of Fig. 271.

57. Brodnitz & Seydel Pumps.

The centrifugal pumps built by Brodnitz & Seydel of Berlin, Germany, are noted for their range of adaptability and design. This firm builds different types for clean, sandy, and slimy water, and has been building centrifugal pumps as a specialty since 1860. Curiously, this firm has not made use of guide vanes even in their high-pressure centrifugal pump design.

Fig. 273 shows a type of high-pressure centrifugal pump similar in principle to the Sulzer pump. The high-pressure centrifugal pumps of Brodnitz & Seydel are naturally a much older type than the Sulzer design.

In the pump illustrated in Fig. 273 the water enters at impeller *B* and flows through it directly into a spiral casing *C*. It is then

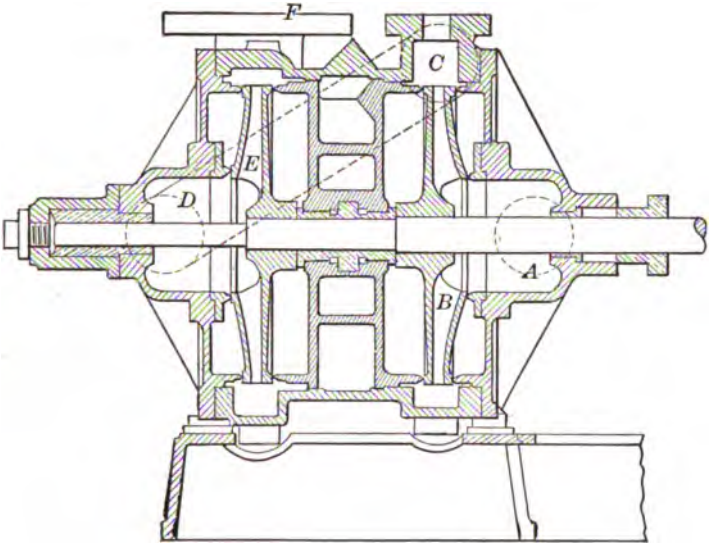

Fig. 273.

carried from *C* to *D* by means of a connecting pipe located outside of the casing. From *D* the water enters the next impeller, *E*. In

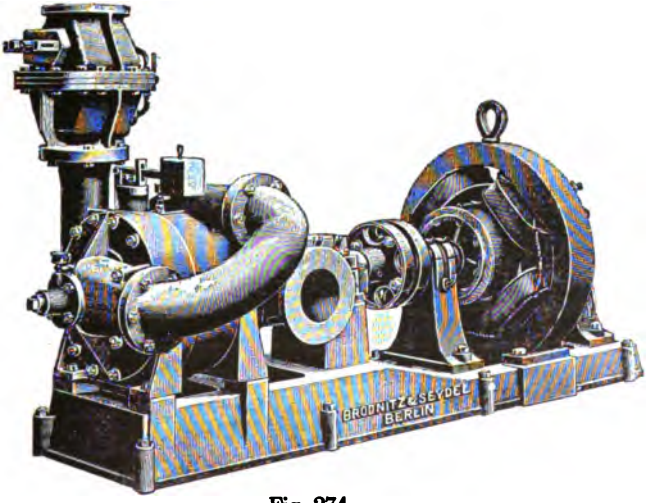

Fig. 274.

Fig. 274 the outside view of this pump is shown. The connecting pipe can be clearly seen. The water, after passing through the

second impeller, again enters a spiral casing. The discharge end of this pump is in the form of a conically diverging pipe.

On the pressure side of this pump the shaft is held in an enclosed bearing lubricated by a suitable grease, while on the suction side the shaft passes through a ring-oiled bearing which is mounted in a pedestal supported upon the bedplate.

As in the Sulzer pump, a complete balance of the axial thrust, by arranging the impellers back to back, can be secured only when both stages deliver the same heads and when the outer rim clearance is sufficiently large compared to the inner clearance. To take care of the axial thrust completely a thrust bearing is necessary.

For larger heads two or three pumps placed on both sides of the driver are used. In this arrangement only four stages can be used, so

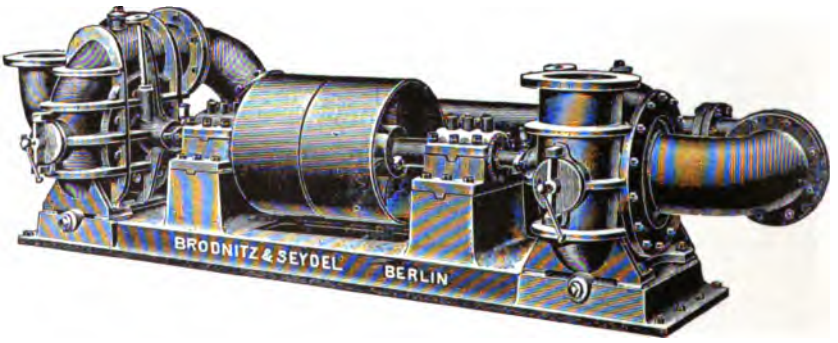

Fig. 275.

that these pumps are not suitable for high heads. We shall not discuss the question whether this pump without guide vanes can compete commercially with other pumps having well-designed guide vanes and therefore higher efficiencies.

Fig. 275 shows a centrifugal pump designed for water containing a large amount of sand or slimy masses. The pump is quite similar to the pump just described, except that there is one stage on each side of the driving pulley. The impellers and clearance rings are made of cast steel in order to withstand excessive wear. For cleaning the mud drum and the side chambers of the impellers a supply of clean water is provided. This pump was made for the canton of St. Gallen in Switzerland and is used for removing the dredged gravel and clay. It works very satisfactorily in spite of these adverse conditions.

Brodnitz & Seydel have been successful also in the construction of low-pressure centrifugal pumps. They were the first in Germany to build centrifugal pumps for dock and drainage service. An

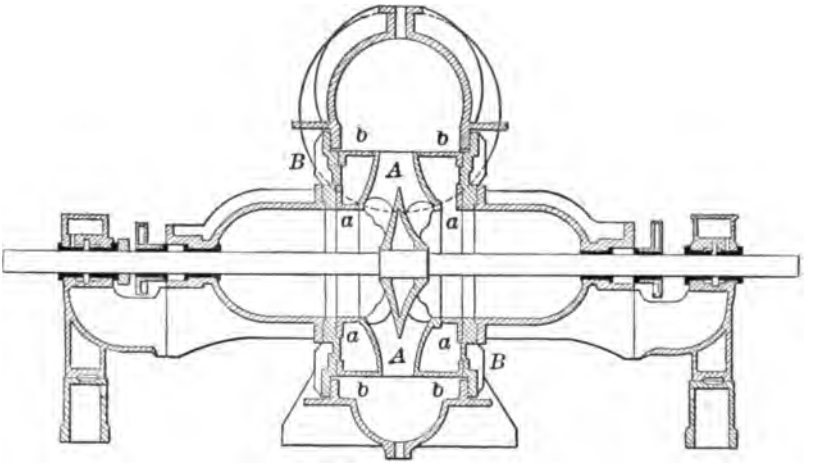

Fig. 276.

entire series of these pumps is in operation at the Royal Docks at Kiel, Wilhelmshaven, and Danzig. The general arrangement of such low-pressure pumps delivering large quantities of water at small pressure heads is shown in Figs. 276 and 277. The water is led to the double-sided impeller by two symmetrically arranged elbows. The inner and outer clearance spaces are formed by specially inserted packing rings *a* and *b*. It is of interest to note that in order to obtain a good formation of the rotation paraboloid, used for decreasing the excess pressure in the clearance space, the spaces between the two packing rings are made of sufficient size and of exactly the same shape. This firm also manufactures

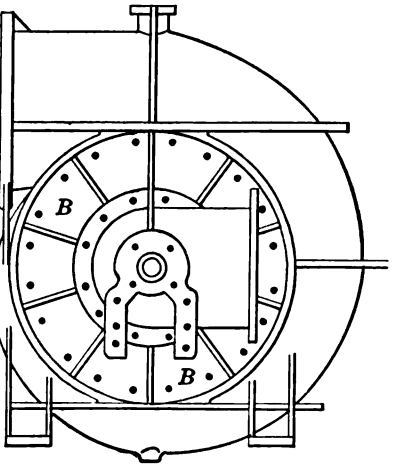

Fig. 277.

as a specialty the so-called Liliputian centrifugal pumps. Fig. 278 shows a two-stage pump of this type direct connected to a motor.

Fig. 278.

The illustration gives an idea of how small this set is. Its uses are not very varied, the pump serving chiefly for operating small water fountains.

58. Berliner Maschinenbau Pumps.

The Berliner Maschinenbau A. G. of Berlin, Germany, succeeded the firm of L. Schwartzkopff, who built centrifugal pumps similar to the Kugel-Gelpke type. Recently the Berliner Maschinenbau

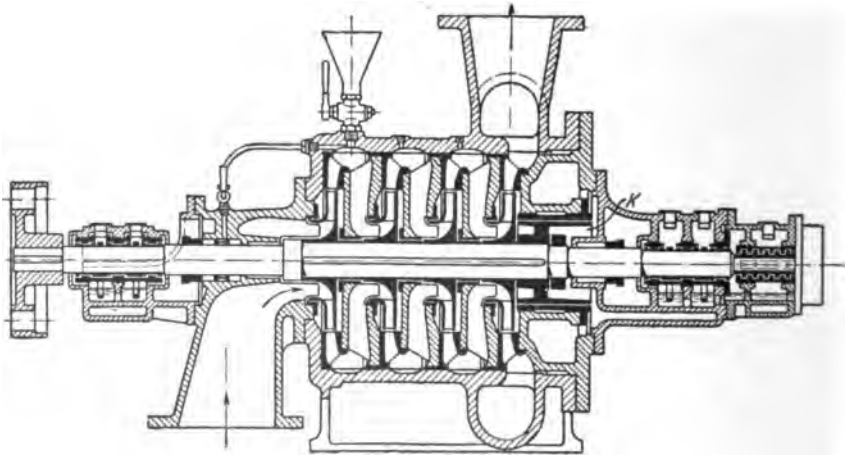

Fig. 279.

have changed the type to that shown in Fig. 279. The unbalanced axial thrust of all the impellers is taken care of by an automatic balancing piston *K*. The arrangement of this balancing piston is

shown more in detail in Fig. 280. The pressure prevailing in the space *b* is smaller than the total pressure developed by the pump, as a pressure throttling takes place through the clearance space *c*. If the axial thrust developed in the impellers increases, the piston *d* moves towards the left and increases the clearance at *c*. This decreases the throttling effect at *c* and permits the pressure in *b* to increase. Consequently the pressure on the piston increases automatically, corresponding to the increase of the axial thrust developed in the impellers. When this axial thrust decreases, the piston moves towards the right and the regulating surfaces at *c* approach each other, thereby increasing throttling and decreasing the pressure in *b*. Thus the pressure on the balancing piston automatically increases and decreases with a change of axial thrust. Besides this balancing arrangement the pump is provided with a collar thrust bearing, mounted upon the extreme high-pressure end of the shaft, and takes care of any unbalanced thrust not taken care of by the balancing piston. Some axial play is necessary in this thrust bearing or else it will not permit the slight axial movement necessary when the balancing piston operates. The thrust bearing is oil lubricated from the same reservoir as the adjacent bearing.

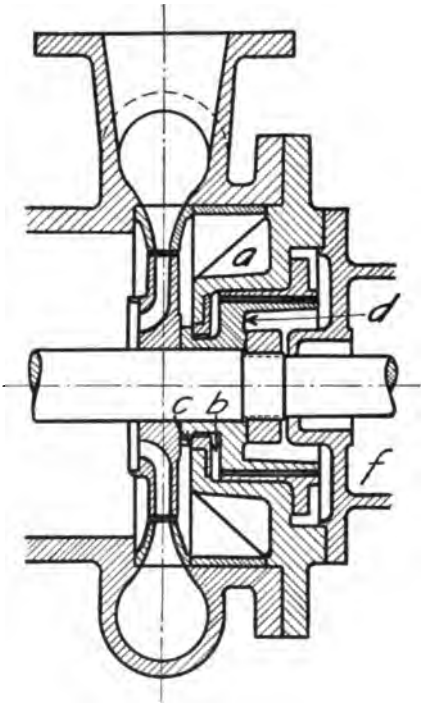

Fig. 280.

The casing is made in one piece, the heads and diaphragms being assembled inside of this casing. It is worth noting that the guide vanes are made very short, and that the reversing channels contain longitudinal ribs throughout their entire length, preventing the water from whirling and giving it proper guidance at entrance to the next impeller. Fig. 281 gives a photographic view of a high-pressure pump installed in the Roland Mine, Germany. The pump

Fig. 281.

lifts 106 cubic feet of water per minute against a head of 1510 feet. Eleven impellers are used and therefore the number of revolutions

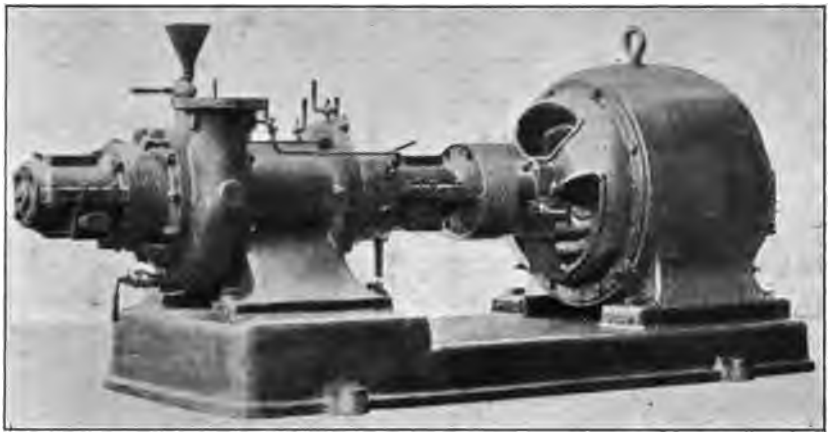

Fig. 282.

per minute is low. The pump parts are assembled within a one-piece casing, and the pumps are placed on both sides of the motor,

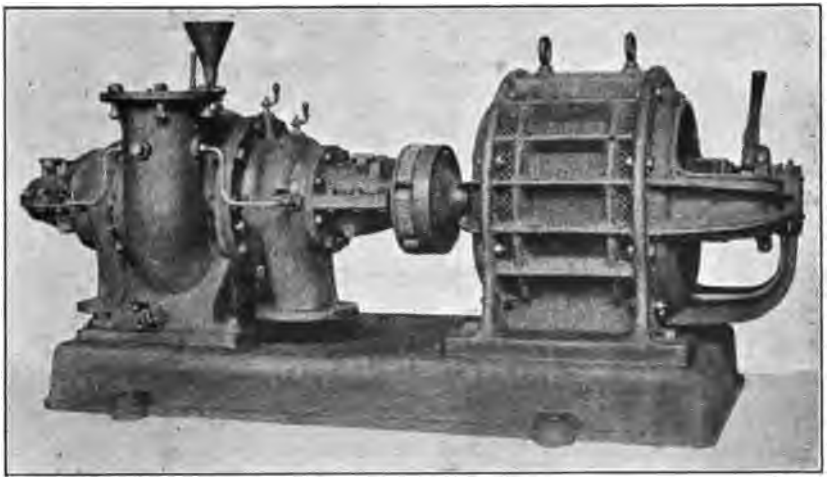

Fig. 283.

with five impellers in one pump and six impellers in the other pump.

Figs. 282–284 show pumps of the Kugel-Gelpke type built by this company prior to changing their design. These pumps are

direct connected to motors of their own manufacture. Fig. 282 shows a five-stage high-pressure pump. The rigid construction of the outer bearing is worth noticing. The pump shown in Fig. 283 has the suction entrance on both sides, which partially balances the axial thrust. Fig. 284 shows a small high-pressure pump with vertical shaft. The motor is mounted at quite a distance from the pump because the latter often operates submerged.

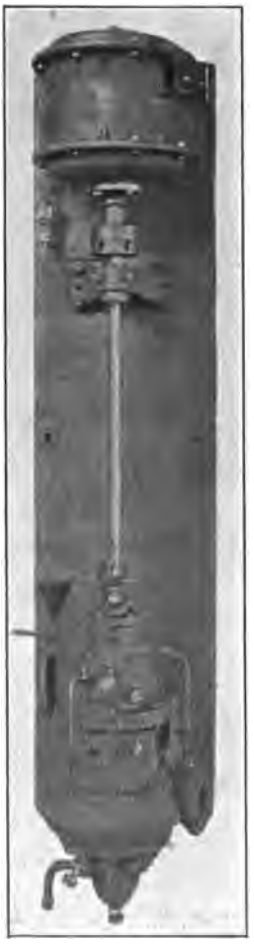

Fig. 284.

59. Willans & Robinson Pumps.

Willans & Robinson of Rugby, England, build centrifugal pumps to the designs of Mr. Jens Orten-Boving. The general design of their multi-stage pumps is shown in Fig. 285. Water enters through the suction pipe on the left and passes through the impellers successively. From the exit of any impeller the water enters guide vanes and is then guided by reversing channels to the entrance of the next impeller. Axial balance is automatically secured by the balancing piston on the high-pressure end of the pump. The operation of this piston can be easily understood from the figure. A proof that this balancing arrangement is efficient lies in the fact that no thrust bearings are furnished with these pumps. The impellers and guide vanes are made of bronze, and all the water passages are either machined or finished by hand. The shaft is made of nickel steel, and where it passes through the stuffing boxes it is covered by renewable bronze bushings. The bearings are cast in one piece with the end covers and are of the ring-lubricated type. The main casing is a single piece lined with bronze. The guide vane diaphragms fit cylindrically into the casing. The stuffing boxes on both the high- and low-pressure ends pack against low

pressure only, and the one on the suction end carries a water seal.

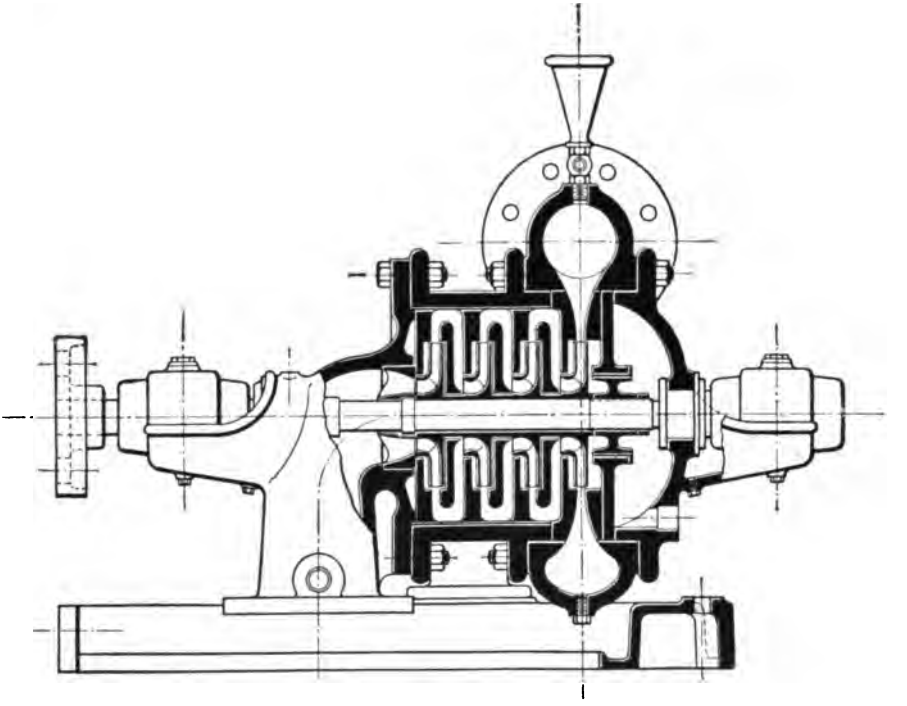

Fig. 285.

This firm builds a standard line of both high- and low-pressure pumps. Fig. 286 illustrates a high-pressure pump direct connected to a direct-current motor.

60. Dayton Pumps.

The Dayton Hydraulic Machinery Company of Dayton, Ohio, build high-pressure centrifugal pumps with a suction pipe at each end of the machine and the discharge pipe located in the middle of the pump casing. Fig. 287 gives a longitudinal cross section of a two-stage high-pressure pump. Water is admitted at both ends and passes through the two end impellers and discharge vanes into reversing channels, which lead the water to both sides of the middle impeller. The water on leaving this impeller passes through a set of discharge vanes to the discharge pipe. In this arrangement axial

thrust is eliminated; but a two-stage machine virtually consists of four impellers, because the water passes from either end of the pump towards the middle. Such an arrangement requires a somewhat longer pump. The only axial thrust possible in this arrangement would occur if any impeller should deliver a slightly higher head than

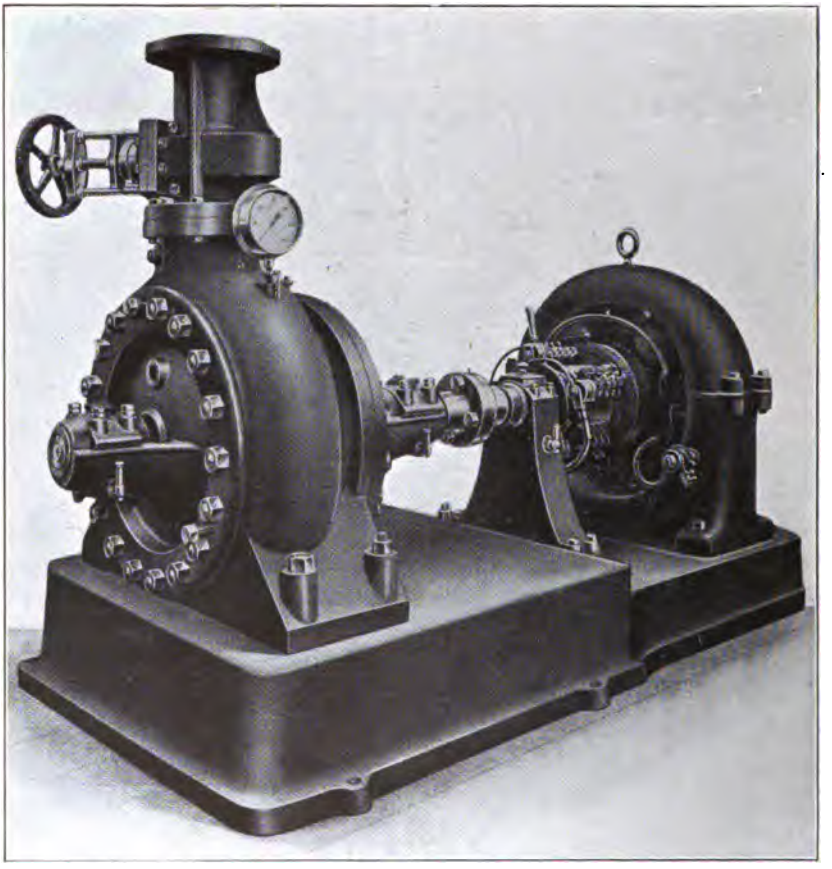

Fig. 286.

the corresponding impeller in the other half of the pump. This somewhat larger head may be produced by small errors of construction and cannot be in any way serious. Another decided advantage of this arrangement of impellers is that no high-pressure stuffing box is necessary. The only stuffing boxes necessary are on the two suction ends, and these are made air-tight by introducing a water seal.

Fig. 288 gives a photographic view of a three-stage pump. This pump is capable of delivering 33.4 cubic feet (250 gallons) of water per

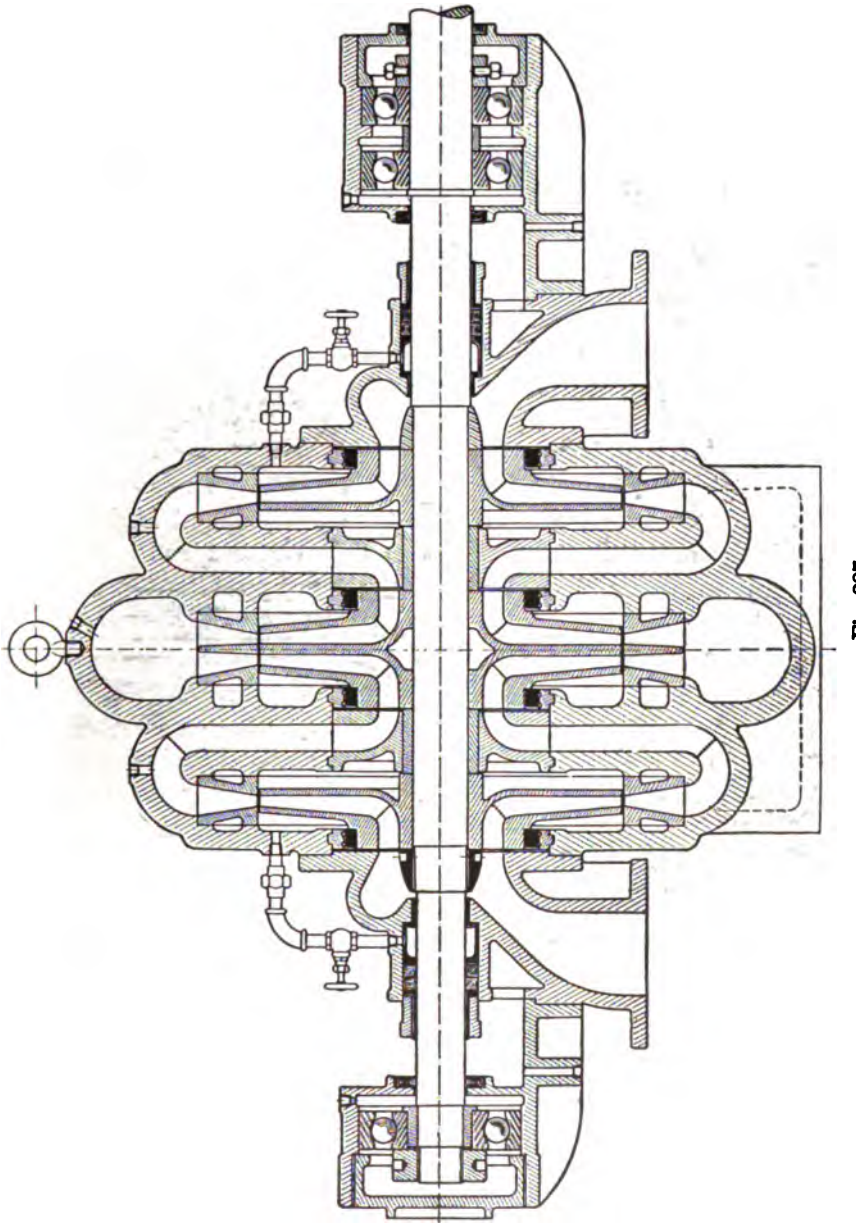

Fig. 287.

minute against a head of 500 feet when running at 1740 revolutions per minute.

Fig. 289 represents a fire underwriters' pump. This pump can deliver 133.7 cubic feet (1000 gallons) of water per minute against 110 pounds per square inch pressure. The pump is direct connected

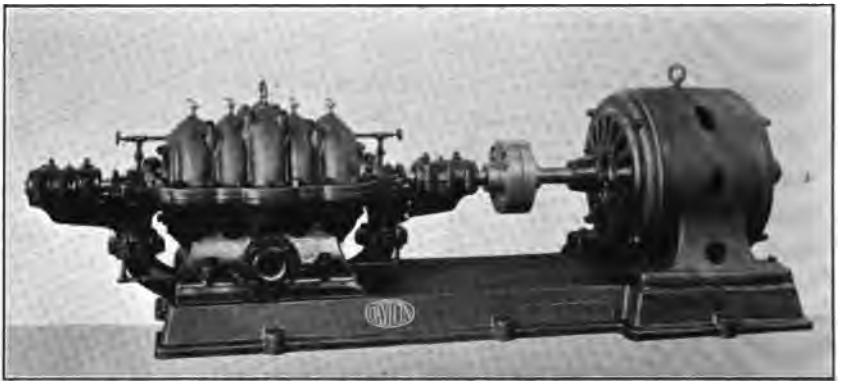

Fig. 288.

to a 100-h.p. Westinghouse type "S" motor running at 1400 revolutions per minute. The motor is entirely enclosed and is ventilated by means of a blower driven from the pump shaft.

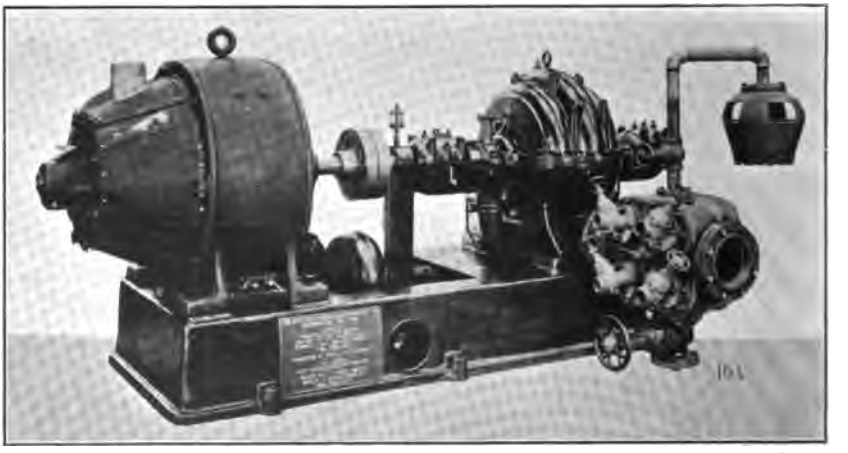

Fig. 289.

It will be noted that in these illustrations the pump casing is divided into two parts along a horizontal plane, the two parts being doweled together, and that all the pipe connections, both for the suction and discharge, are in the lower half casing. This permits of quick accessi-

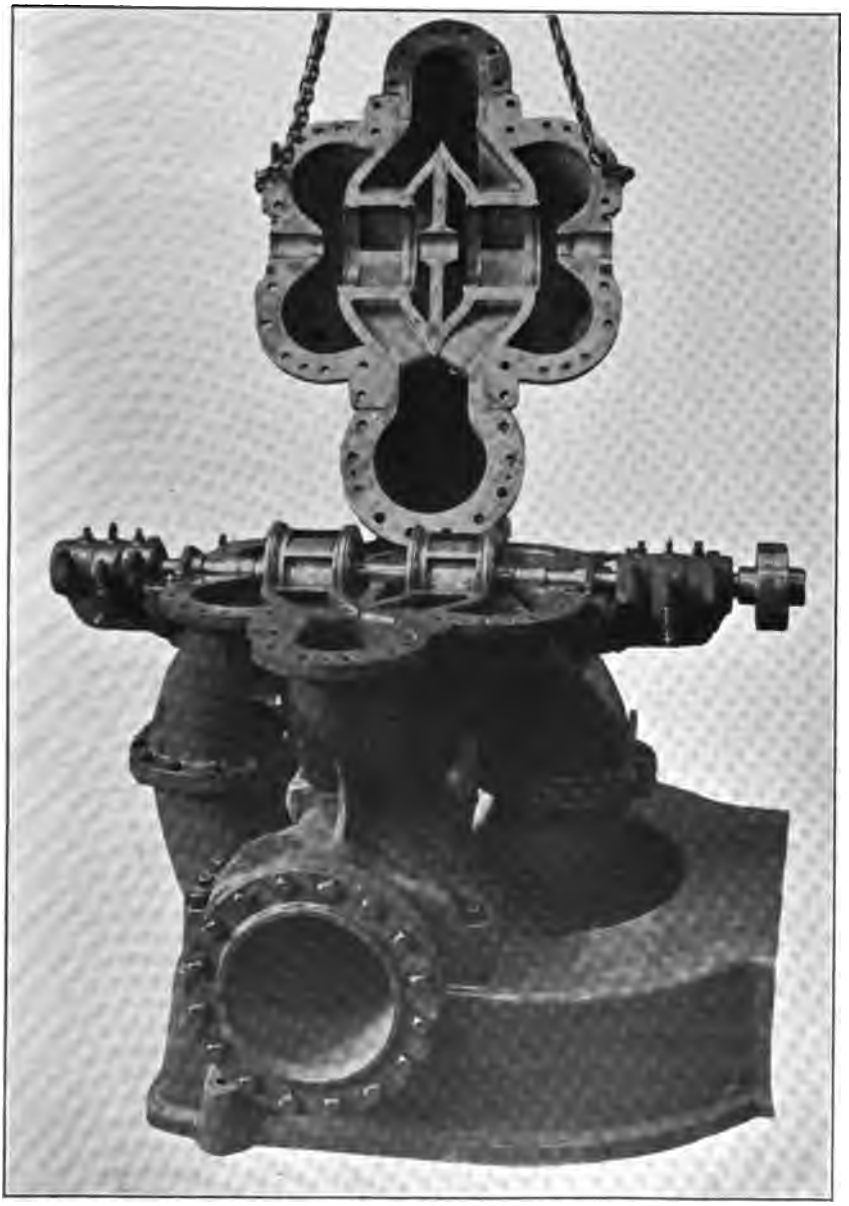

Fig. 290.

bility because the upper half casing can be easily and quickly removed. The packings between stages are kept in place and rigidly held by long screws passing through the casing, as can be seen in Figs. 288 and 289. The impellers, guide vanes, reversing channels, and clearance rings are not made in halves, and are all lifted out of the lower half casing together with the shaft. The shaft is supported either in ball bearings or in babbitt-lined bearings. The latter are

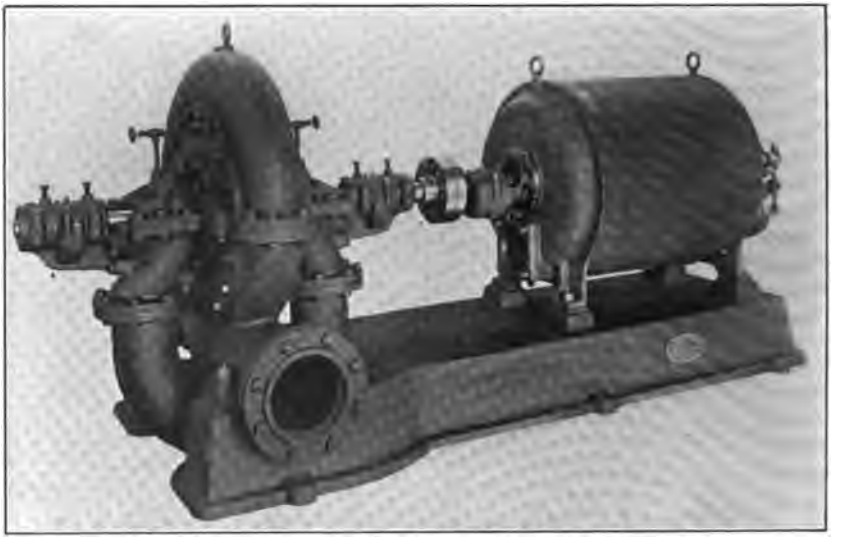

Fig. 291.

ring lubricated. The only parts of the pump subject to any appreciable wear are the clearance rings between impeller and casing, and these can be very easily renewed.

Fig. 290 shows to good advantage the accessibility of these pumps. The illustration shows a biplex volute pump. This type consists of a single-stage pump having two impellers working in parallel. The pump can deliver 802 cubic feet (6000 gallons) of water per minute against a head of 35 feet when running at 1800 revolutions per minute. The diameter of the discharge pipe is 15 inches.

This firm also builds high-speed pumps without discharge vanes, known as volute pumps. Fig. 291 shows a high-speed volute pump having a discharge pipe 8 inches in diameter. The pump can deliver 200 cubic feet (1500 gallons) of water per minute against a

head of 80 feet. It is direct connected to a Kerr steam turbine running at 3000 revolutions per minute.

Fig. 292 gives the characteristic curves of a single-stage volute pump, that is, a pump without discharge vanes. The pump is rated at 53.5 cubic feet (400 gallons) of water per minute with a head of 140 feet. The best efficiency is obtained at 1520 revolutions per minute and when the pump is delivering 47.7 cubic feet of

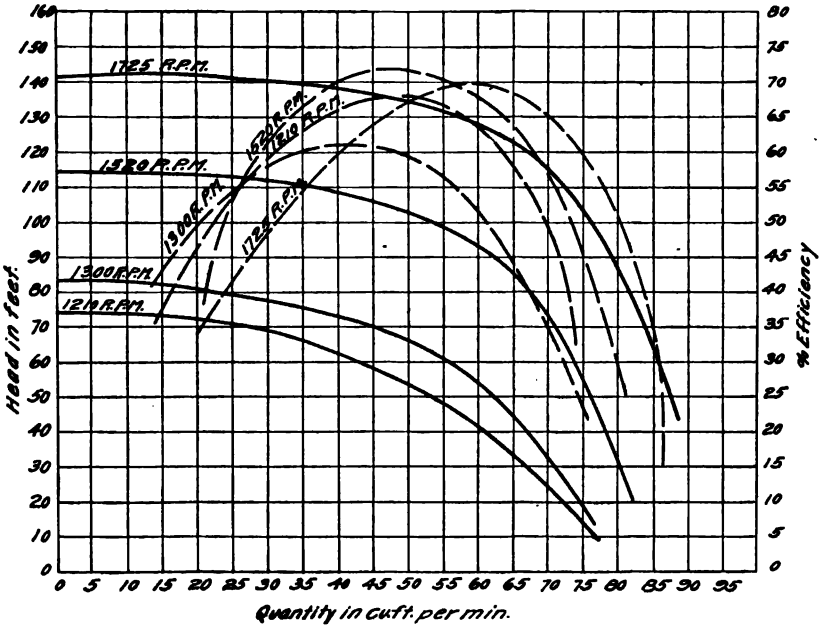

Fig. 292.

water per minute against a head of 103 feet. The efficiency at normal load, when running at 1520 revolutions per minute, is 71 per cent, which is very good for a pump without discharge vanes.

61. Borsig Pumps.

Figs. 293 to 296 show centrifugal pumps manufactured by A. Borsig of Berlin, Germany. Fig. 293 represents the normal type of a multi-stage high-pressure pump direct connected to a motor. The casing surrounding the guide vanes has a smooth cylindrical form. Upon removing the front head, the guide vanes and impellers

can be removed singly, or by removing the coupling the entire interior of the pump can be removed assembled. The impellers are fastened to the shaft by means of keys and lock nuts, which permit also of easy disassembly. Axial thrust is taken care of by extending the entrance side of several impellers so as to form a rotating disk or plate beyond the impeller blades. This extended side of the impeller serves as a side plate for the discharge vanes. The ends of the discharge vanes form a close clearance with this rotating disk. As the other side of the impeller extends only to the beginning of the discharge vanes, there will be a difference of pressure of the water escaping into the clearance space on either side of the impeller, the extended side being in a region of higher pressure. It

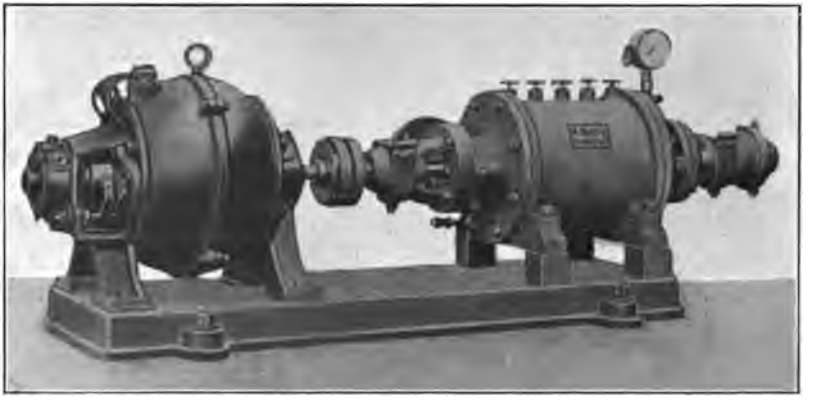

Fig. 293.

is not possible entirely to take care of axial thrust by this arrangement because the pressure in the clearance space cannot be definitely determined. Borsig therefore uses a thrust bearing to prevent axial movement of the shaft.

With very large heads the axial thrust is balanced by arranging the impellers in opposing groups, which of course necessitates the use of rigid couplings. Fig. 294 shows such an arrangement. To aid assembly these groups of impellers are placed on a common bedplate with the driving motor. This bedplate is extended in both directions beyond the pump casings, and is provided with slides so that the casing can be drawn away from the inner parts of the pump by means of jackscrews. In Fig. 294 the casing at one end of the

pump has been drawn away. The pressure pipe contains a non-return valve, and the suction elbow is provided with a safety valve, so that even if the non-return valve becomes inoperative the suction piping is protected against high pressure.

Fig. 294.

A. Borsig builds low-pressure centrifugal pumps for quantities of water from 70 to 1000 cubic feet per minute and for heads up to 100 feet. Fig. 295 shows the standard form of their low-pressure pumps, which consists of a single impeller with water entrance on both sides of the impeller. The middle piece of the spiral casing has very broad feet resting upon the bedplate. Attached on either side of this casing are the suction heads in the form of elbows pointing downward. These elbows have cast to them brackets supporting the bearings. The two suction elbows are bolted to a common suction pipe. The discharge pipe is a part of the spiral casing and is conical in form. The spiral form of the casing with its diverging discharge pipe reduces gradually the velocity of the water after it leaves the impeller and no discharge vanes are used. The packing on both ends has a water seal, as these packings must prevent air leakage into the pump casing. The bearings are ring lubricated and lined with babbitt. Whenever these pumps are driven by means of belts and pulleys a third bearing is provided which is mounted upon the bedplate as shown in the illustration. The entire design is extremely rugged.

Fig. 296 shows a smaller low-pressure pump direct connected to an electric motor. In the smaller low-pressure designs the casing is

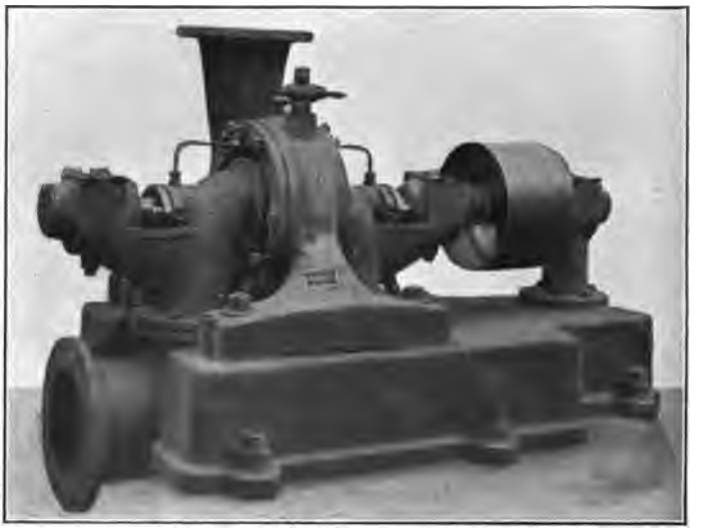

Fig. 295.

made cylindrical instead of spiral and no conical discharge pipe is used, but in this design, as well as in the previous, special attention

Fig. 296.

was paid to proper water guidance. The cross sections at entrance to and exit from the impellers are of ample dimensions, and every sharp turn is avoided as far as possible.

62. Buffalo Pumps.

The Buffalo Steam Pump Company of Buffalo, N. Y., manufacture centrifugal pumps similar in principle to the original Sulzer type. Their pump construction can be seen in Fig. 297, which shows a four-stage pump. Water enters through the suction pipe on the left and passes through the impellers from left to right. As in the Sulzer design, the impellers are arranged in pairs so as to balance end thrust. Any remaining end thrust is taken care of by a thrust bearing. The casing is made in one piece, and the impellers, discharge vanes, diaphragms, and reversing channels are all assembled

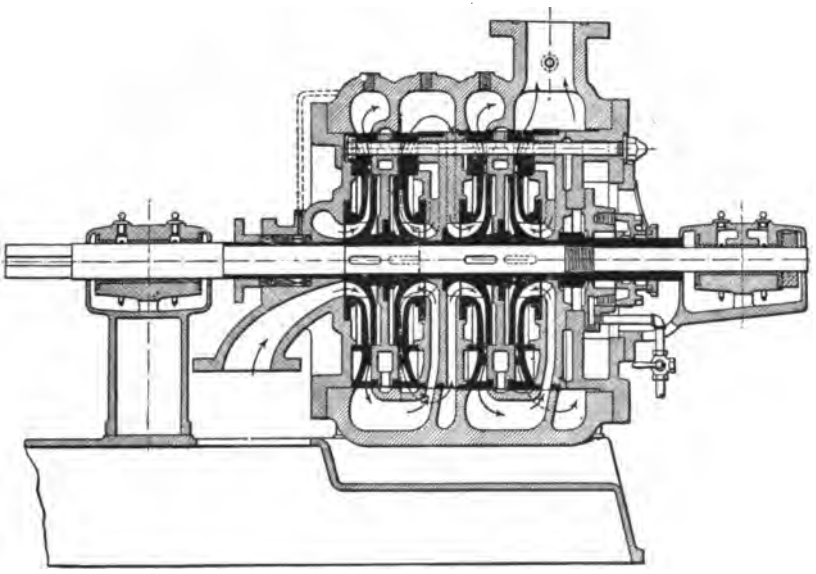

Fig. 297.

from the discharge end of the pump. The bearing on the suction end is mounted upon a pedestal, while that on the high-pressure end is supported upon the high-pressure head. Beyond this bearing the thrust is carried. Fig. 298 gives a cross section through the thrust bearing, which is self-lubricating and water cooled. The oil chamber in the outboard bearing is connected to the oil chamber of the thrust bearing. A rotating disk on the end of the shaft lifts the oil to the top, where it is wiped off by a close clearance pin into an upper oil reservoir which feeds oil into the hole in the center of the shaft. Centrifugal force then throws the oil against the rubbing surfaces of

the thrust bearing. The oil finally overflows through an oil drain back into the oil chamber of the bearing.

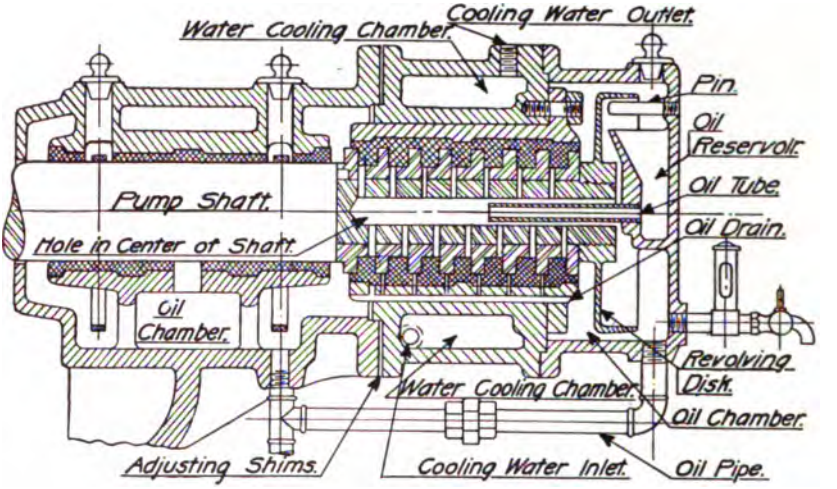

Fig. 298.

Fig. 299 gives the characteristic curves of a two-stage pump capable of delivering 133.7 cubic feet (1000 gallons) of water per minute

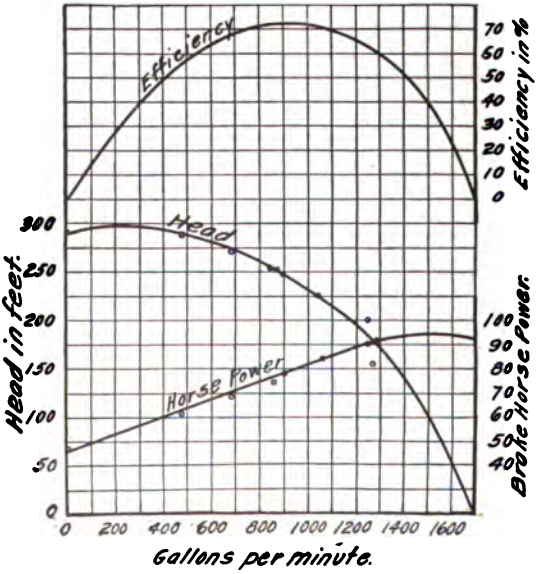

Fig. 299.

against a head of 230 feet. The pump runs at 1140 r.p.m. The efficiency at this point is the maximum, about 72 per cent.

63. Gebauer Pumps.

Fr. Gebauer of Berlin, Germany, builds both high-pressure and low-pressure centrifugal pumps. The low-pressure centrifugal pumps are of rather novel design in that the base plate for both the pump

Fig. 300.

and its driver is used as a part of the pump's suction pipe. This arrangement makes these pumps rather cheap and simple. The water can be admitted at either end or at both ends of the base. Fig. 300

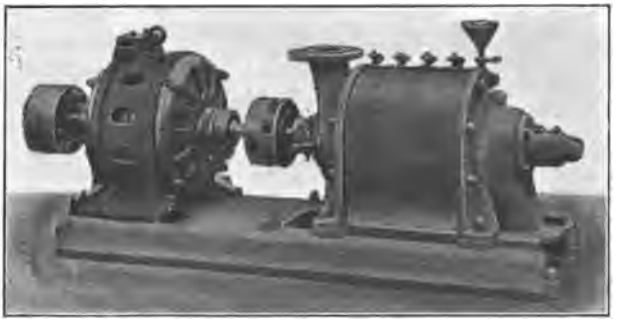

Fig. 301.

shows a pump of this design capable of delivering 353 cubic feet of water per minute against a head of 33 feet. This pump is one of the smaller units, and similar designs are built up to a capacity of 5300 cubic feet per minute.

The pump is of the double-suction type having one impeller. Water is admitted through the end elbows, which are bolted directly to the base. The casing is of spiral form and contains no discharge vanes.

Fig. 302.

Fig. 301 represents the normal type of a high-pressure centrifugal pump made by this firm. The casing is in cylindrical sections, one section for each stage of the pump. These sections are rabbeted one into the other and all held together by means of through bolts. If for any reason another stage is to be added all the old pump parts can be used except the shaft and the through bolts, which would have to be made longer. This construction of casing is similar to the Jaeger design. This pump has of course discharge vanes of the usual form. The suction pipe extends downward through the bedplate and has the outboard bearing and thrust attached to it. The motor is direct connected to the pump by means of a flexible coupling.

Fig. 302 shows a mine shaft pump of Gebauer design. The suction pipe joins the pump casing at two points 180° apart and the discharge pipe is also attached to the casing at two points 180° apart. The motor and step bearing are mounted directly above the pump, and the entire structure is carried in a frame made of channel irons.

64. Allen Pumps.

W. H. Allen, Son & Company of Bedford, England, manufacture centrifugal pumps for a large range of service. Their multi-stage pumps have a water guidance similar to the Jaeger type and the pump is built up in sections similar to most Jaeger types. There is, however, a somewhat novel difference in that no holes are provided through the impeller sides for securing axial balance. Fig. 303 gives a longitudinal cross section through a four-stage pump. It will be noted that the impeller hub is so arranged that it forms a part of the water passage at entrance to the succeeding impeller. A possible

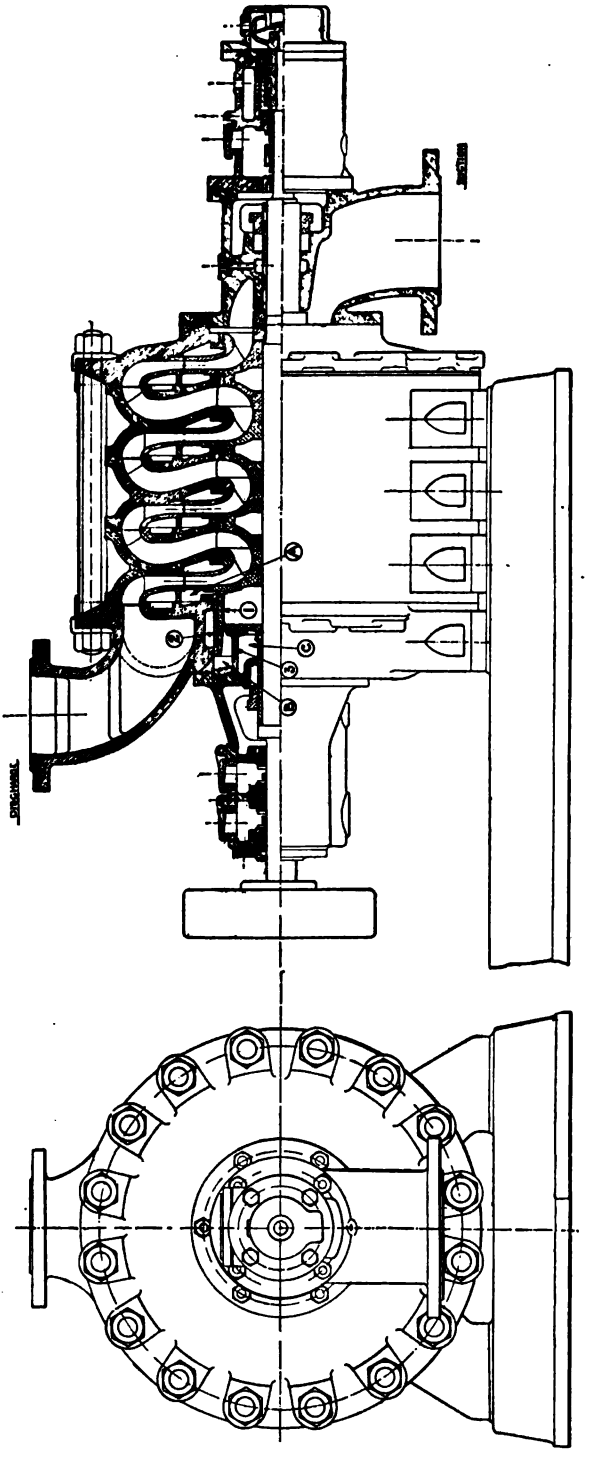

Fig. 303.

objection to this design might be that the water on leaving the reversing channel enters a rotating elbow before it reaches the entrance of the next impeller. This rotating elbow must produce some rotation of the water, depending partly upon the smoothness of the elbow and partly upon the velocity of the water. Even if the entrance angle of the impeller is designed to allow for this rotation, there must be considerable disturbance at the end of the reversing channel, which contains ribs to prevent the water from rotating. It is extremely difficult correctly to design the entrance edge of an impeller blade when the water is rotating, because the velocity of rotation is not uniform across the entrance width.

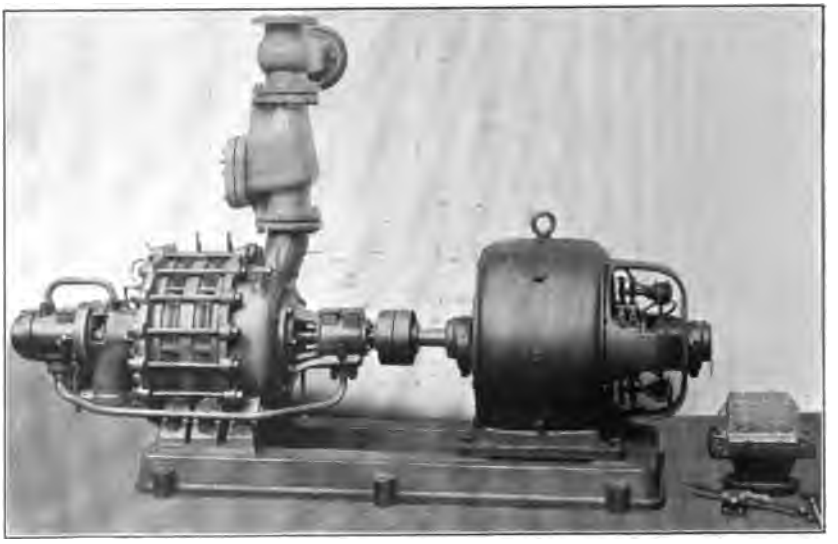

Fig. 304.

Axial balance is secured by a balancing piston on the high-pressure end of the pump. The piston marked (1) in the figure rotates with a running clearance between it and the bushing (2) fastened to the pump casing. The cylinder marked (3) is also attached to the pump casing and is provided with a facing against which the radial facing on the balancing piston runs. The collar thrust bearing on the suction end of the pump permits of a very slight axial movement, which also gives a small varying clearance between the radial facings of the piston (1) and cylinder (3). The short-circuited water from the periphery of the last impeller flows from the annular chamber

A to chamber *B*. The clearance between the piston (1) and the cylinder (3) regulates the pressure of the water in chamber *B*. When this pressure is large enough to overbalance the axial thrust, the

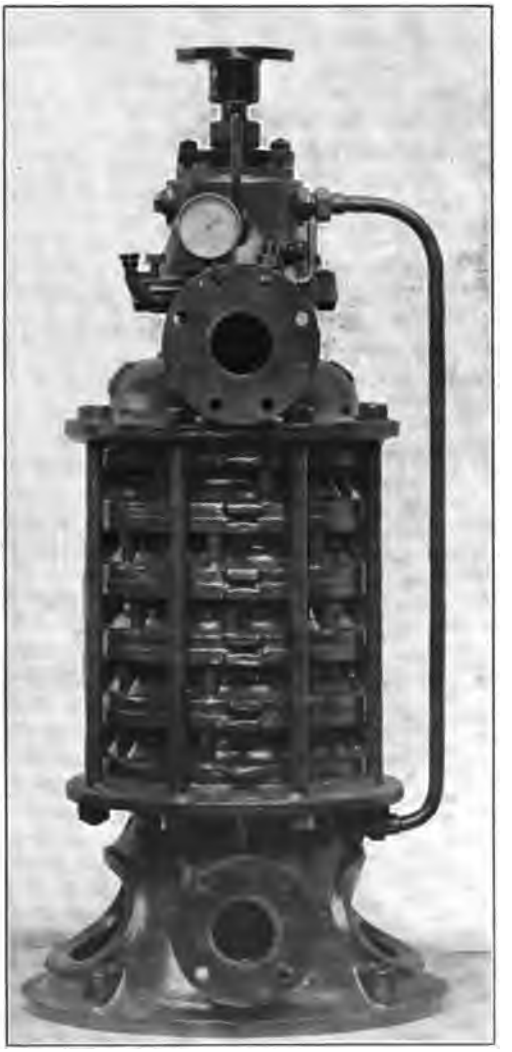

Fig. 305.

clearance between piston and cylinder increases because the shaft has a slight axial play, which again diminishes the pressure in chamber *B*. When the axial thrust is greater than the pressure exerted on

Fig. 306.

the piston, the clearance is decreased and the pressure in chamber *B* is increased, thus again securing balance.

Fig. 304 is a photographic view of a three-stage pump having the suction and discharge pipes 5 inches in diameter. This pump is designed to deliver 40 cubic feet (250 British gallons) of water per minute against a total head of 209 feet. When running at a speed of 1000 to 1050 r.p.m. the pump requires approximately 26.5 brake h.p. The casing of this pump is of cast iron and the impellers and guide vanes are of bronze, the shaft being of nickel steel.

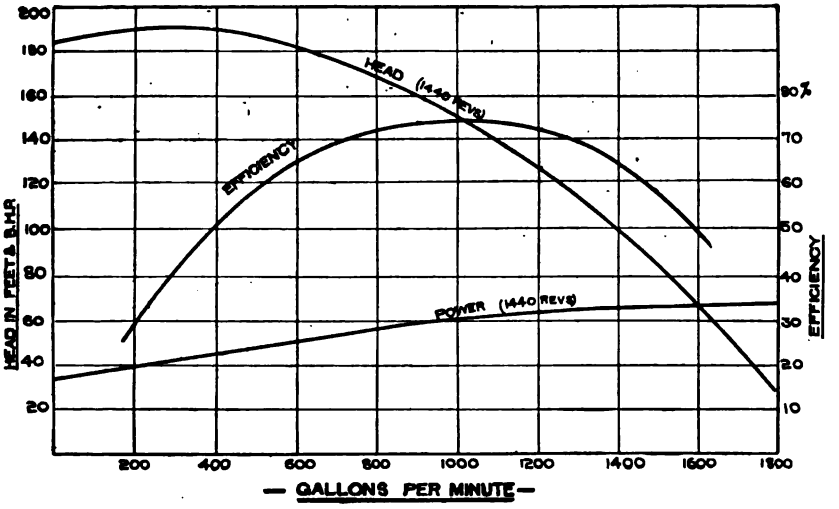

Fig. 307.

Fig. 305 illustrates a multi-stage pump with vertical shaft used as a boiler feed pump. This pump delivers 16 cubic feet (100 British gallons) of water per minute against 210 pounds per square inch boiler pressure. The pump runs at 2000 r.p.m. and has an efficiency of 61 per cent.

Fig. 306 shows a photograph of a seven-stage pump designed to deliver 84 cubic feet (525 British gallons) of water per minute against a total head of 1443 feet when running at 1600 r.p.m. The suction and discharge pipes are 7 inches in diameter. Under normal load and speed the pump requires approximately 382 brake h.p. This pump is not built up in sections, but the casing proper is in one piece. The seven impellers are keyed on a nickel-steel shaft. The

impellers and guide vanes are made of bronze, machined and polished all over. The guide vanes are bolted to the sides of the reversing channels and all are held in place by a common casing. The portion of the impeller which runs in the reversing chamber is encircled by a gun-metal liner or clearance ring. The walls of the reversing channels are fitted with gun-metal bushings where they fit into the casing, in order to prevent corrosion. The shaft runs in ring-lubricated bearings and is kept in its correct position by a collar thrust bearing. The suction gland is water sealed, and the

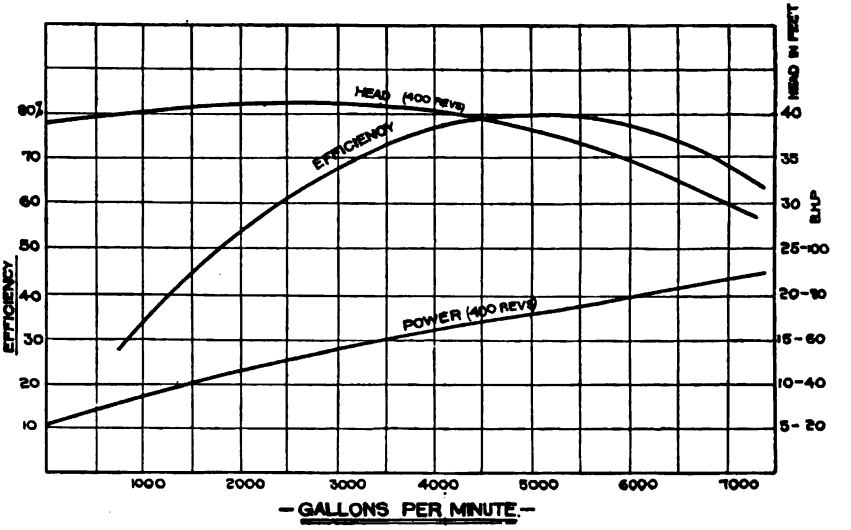

Fig. 308.

gland on the pressure side has to withstand atmospheric pressure only.

W. H. Allen, Sons and Co. build centrifugal pumps to suit both the type of driver and the required working conditions. This is best illustrated by the two characteristic curves shown in Figs. 307 and 308.

Fig. 307 represents the performance of a pump for which the working conditions require a small variation in power with great variations of head and quantity, the driver in this case being a three-phase motor. Fig. 308 gives the characteristic curves of a pump for which the working conditions are constant head with great variations of quantity, the driver being a steam engine.

65. Novel and Miscellaneous Designs.

A novel type of centrifugal pump has been designed by Professor Novak, for which he claims quite high efficiencies. Fig. 309 gives two cross sections of a single-stage high-pressure Novak pump built for R. Meyer, Mülheim, Germany. The pump consists of a single impeller $13\frac{3}{4}$ inches in diameter, surrounded by a set of floating

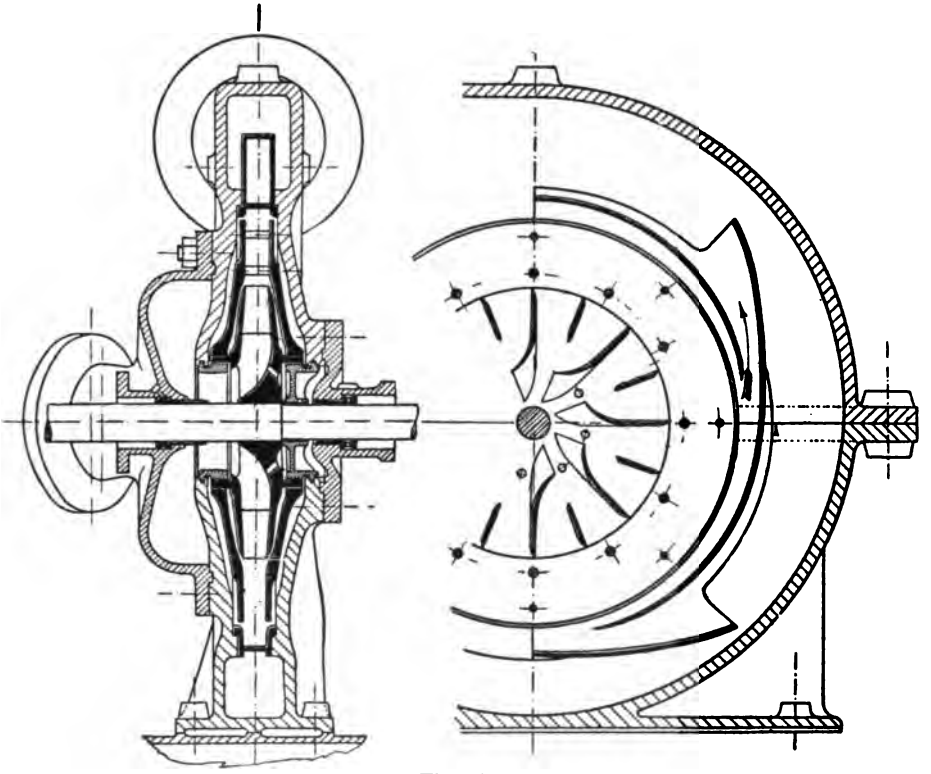

Fig. 309.

guide vanes, which are free to rotate about the impeller and which are centered upon its hub. Surrounding this floating set of guide vanes is a casing containing stationary guide vanes. The water enters the impeller as in the usual designs, but upon leaving it strikes the floating guide vanes. As the entrance angle of these vanes is not correct when they are stationary, the water impinges upon them and sets them rotating until the entrance angle is nearly correct for proper entrance of the water. The water then leaves

the rotating guide vanes at a lower speed and higher pressure. The guide vanes in the casing are intended to transform the remaining velocity into pressure. The general idea is excellent because the main object is to obviate shock and entrance losses to the guide vanes while the water velocity is high. The floating guide vanes can be said to adjust their entrance angle automatically by increasing or decreasing the speed of rotation to suit any certain quantity of discharge. Tests have been made with the floating guide vanes held stationary and left free and the two results compared to prove the superiority of the latter arrangement. Such comparison is of course not convincing, because the floating guide vanes held stationary are not of the proper design for stationary use. The pump

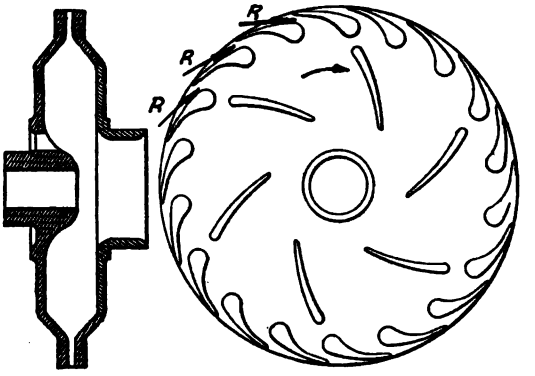

Fig. 310.

should be compared to one of standard design having the same diameter of impeller and designed for the same quantity and speed.

It is quite doubtful if this design can become commercial. A certain power is expended in keeping the vanes rotating, and the transformation from velocity into pressure in these vanes is not very efficient.

Messrs. Thomas Parker, Limited, of Wolverhampton, England, build the Rees Roturbo pump, the impeller of which is illustrated in Fig. 310. The six inner vanes are merely ribs to prevent the whirling of the water. The central reservoir of the impeller is full of water and is kept under centrifugal pressure when the pump rotates. The main idea of the inventor is the small discharge nozzles at the periphery of the impeller, which produce a nozzle effect and

cause a reaction of the water jet in the direction *R-R*. The centrifugal pressure in the central reservoir of the impeller is converted into velocity energy as the water passes through the nozzles at the periphery, and this velocity is reconverted into pressure by stationary guide vanes in the pump casing. The reaction of the water jet produces a turning moment on the impeller in the same direction as the driving moment. At a certain quantity of discharge this reaction increases faster than the driving effect, so that the driving motor cannot be overloaded. This is useful in cases where

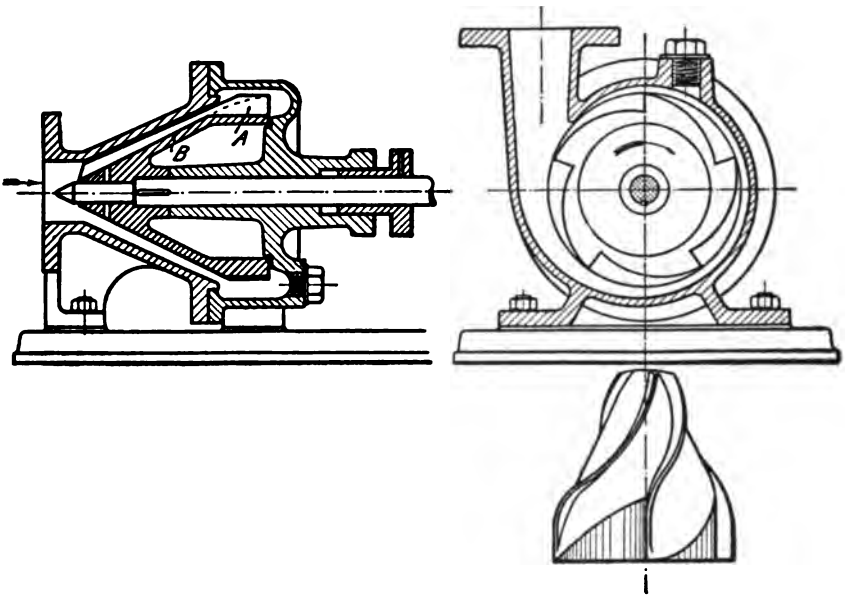

Fig. 311.

the head, and therefore the quantity, varies greatly, as in a pump for dry-dock service. For this class of service these pumps may be as economical as other types, and are therefore found installed at many English seaports.

Messrs. James Simpson & Co., Limited, Newark, England, build pumps without discharge vanes, but design the helical casing with extreme care so that the velocity transformation into pressure energy takes place under very favorable conditions. This design is an attempt to return to the original centrifugal pump without guide vanes, but to determine the shape of the casing by applying the experience obtained in the use of guide vanes. With absolute exact-

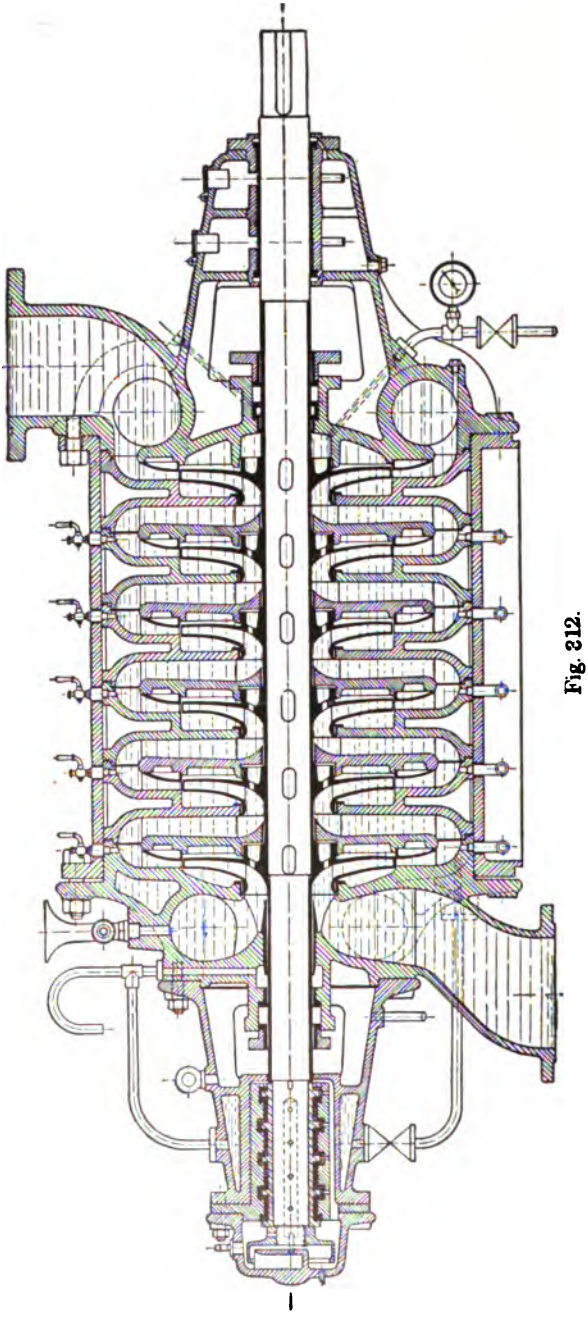

Fig. 212.

ness of form and perfect smoothness of casing very good efficiency has been obtained with pumps operating at high speeds. This firm has patented a design on this principle for multi-stage work.

Quiri & Cie. of Schiltigheim, Germany, build a screw pump which is also a centrifugal pump. The impeller *A* (Fig. 311) has a conical addition *B* which carries blades of a screw form, the object of which is to lead the water gradually from an axial to a radial flow. The water flowing radially strikes the apex of the cone and is guided to the screw, where it is set in rotation and lifted by centrifugal force. The axial velocity gradually decreases as the radial velocity increases, until finally the water enters the actual impeller *A*. These pumps are usually built in pairs with the motor between them. Axial thrust is then eliminated.

Klein, Schanzlin & Becker of Frankenthal, Germany, build multi-stage centrifugal pumps having a water guidance similar to the Jaeger type. Fig. 312 gives a sectional view of a six-stage pump and shows the novel feature of a cylindrical casing made in halves, containing the guide vanes and reversing channels, but so constructed that the water pressure is not exerted upon it. The casing merely serves to center the various units of guide vanes and reversing channels, and can be made very light. The axial thrust is taken up in a thrust bearing, which serves both as a journal and thrust bearing. This bearing is automatically oiled by the small oil-lifting device shown on the extreme end of the bearing. The bearing itself is water cooled.

VII. TESTING OF CENTRIFUGAL PUMPS.

66. Methods of Testing Pumps.

The testing of centrifugal pumps is quite simple, and the method usually employed depends partially upon the quantity of water discharged and the head against which the pump operates. Several important points, however, must be taken into account when testing a pump and determining its availability to the service in question. If the pump is to be installed with a long suction line, the test must be conducted under similar conditions or proper allowances must be made. The same thing holds true of the discharge end of the pump. If the friction head is large, the pump will operate quite differently from a pump without friction head. All measurements of pressure should be made in a straight portion of the water piping sufficiently far removed from elbows, turns, or valves. Quite erroneous results may be obtained by taking readings at points where the water is disturbed.

In measuring the head or suction pressure, a mercury column or a carefully calibrated pressure gauge is used. A Pitot tube placed in the center of the pipe and pointing against the stream is connected to the mercury column, or pressure gauge. The readings will then give the pressure head plus the velocity head at that point.

In determining the total head against which the pump operates the datum line should be taken at the center line of the pump. If the discharge pressures are taken above the center line, the distance from the center line to the measuring point should be added to the observed head, and if the suction head is measured below the center line, its distance from the center line should be added to the observed suction head.

There are four methods generally used for obtaining the quantity of water passing through a pump:

1. The Venturi water meter.
2. The Weir tank.
3. The nozzle.
4. The Pitot tube.

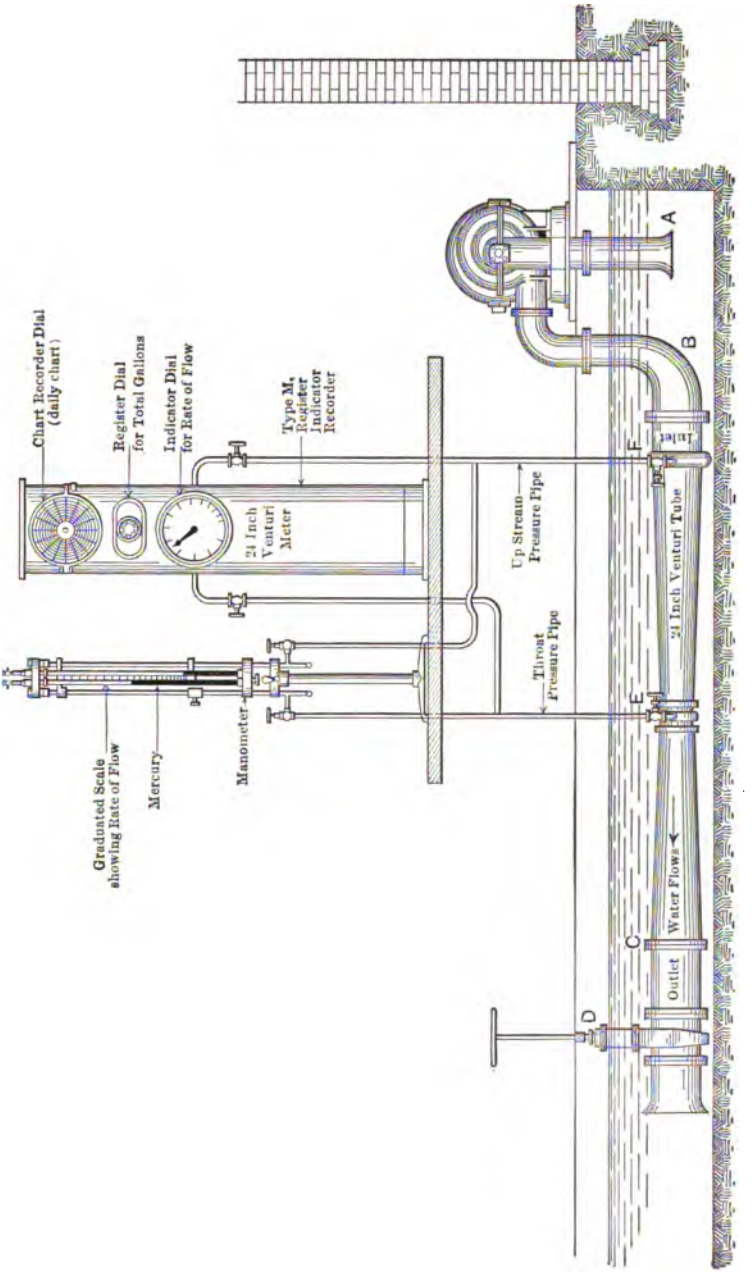
Chart Recorder Dial (daily chart)
Register Dial for Total Gallons
Indicator Dial for Rate of Flow
Type M, Register Indicator Recorder
24 Inch Venturi Meter
Graduated Scale showing Rate of Flow
Mercury
Manometer
Up Stream Pressure Pipe
Throat Pressure Pipe
24 Inch Venturi Tube
Water Flows
Outlet
A
B
C
D
E
F

Fig. 313.

1. *Venturi Water Meter.* The Venturi water meter, when carefully handled, gives very accurate results. Fig. 313 shows an excellent arrangement for testing a centrifugal pump by means of a Venturi meter. Valve *D* is used for regulating the required head against which the pump is to work. The Venturi meter indicates the quantity of water passing through it, on a mercury "U" gauge, the two limbs of which are connected to the Venturi meter at *E* and *F*. The difference of pressure recorded in the two limbs

Fig. 314.

of the gauge is in proportion to the square of the discharge from the pump. If the scale is graduated in proportion to the square roots of the pressures so as to read in gallons or cubic feet per minute the quantity of water discharged can be read without the necessity of any calculation whatever. The figure also shows a recording, registering, and indicating device connected in parallel with the mercury column.

In making the connections to the Venturi meter and discharge pipe it is advisable to connect to four points around the pipe, 90°

apart, so as to get average readings. The accuracy of the Venturi meters is guaranteed by the makers of the instruments to be within two per cent.

2. *Weir Tank.* For measuring quantity of discharge, especially for very large units, the Weir tank can be used. Fig. 314 illustrates a Weir tank with the water discharging through the calibrated orifice. Care must be taken that the tank is divided into two or more chambers so that the disturbances of inflow do not affect the water at discharge. The Weir tank is often used as a check upon the readings taken by one of the other methods, especially that of the Pitot tube or nozzle, because when using the Weir tank it does not require much greater labor to take the nozzle or Pitot tube measurements.

To measure the head on the crest of a Weir a hook gauge is generally used. This instrument is quite common and needs no explanation. The scale on the gauge and its vernier can be made to read directly in cubic feet or gallons.

3. *The Nozzle.* Fig. 315 shows a form of nozzle which can be employed for measuring quantity of discharge. Any nozzle used should be carefully calibrated and a curve of discharge drawn, giving the quantity of discharge from the nozzle for various pressures at the point where the pressure gauge is attached. The nozzle shown in Fig. 315 has the following dimensions:

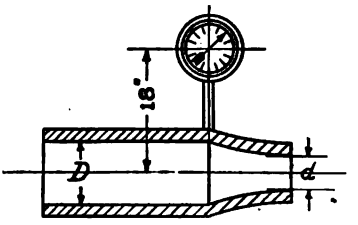

Fig. 315.

$$D = 14.422 \text{ inches diameter.}$$
$$d = 4.5 \text{ inches diameter}$$

The distance from the center of the nozzle to the pressure gauge is 18 inches. Fig. 316 gives the discharge curve of this nozzle. The quantity of water discharged in gallons per minute can be expressed by the formula

$$Q = 1963\, d^2 c \sqrt{\frac{h}{1 - c^2\left(\frac{d}{D}\right)^4}} \quad . \quad . \quad . \quad . \quad 305$$

in which c is a coefficient of discharge equal to 0.99 for this nozzle, h the pressure head in the nozzle in feet, d the diameter of the

throat of the nozzle in inches, and D the diameter of the nozzle at which the pressure is measured.

If the pressure is measured in pounds per square inch by a pressure gauge, then

$$h = 2.304\,P + m \quad . \quad . \quad . \quad . \quad . \quad . \quad . \quad . \quad 306$$

in which P is the pressure in pounds per square inch and m the distance from the center of the nozzle to the pressure gauge in feet.

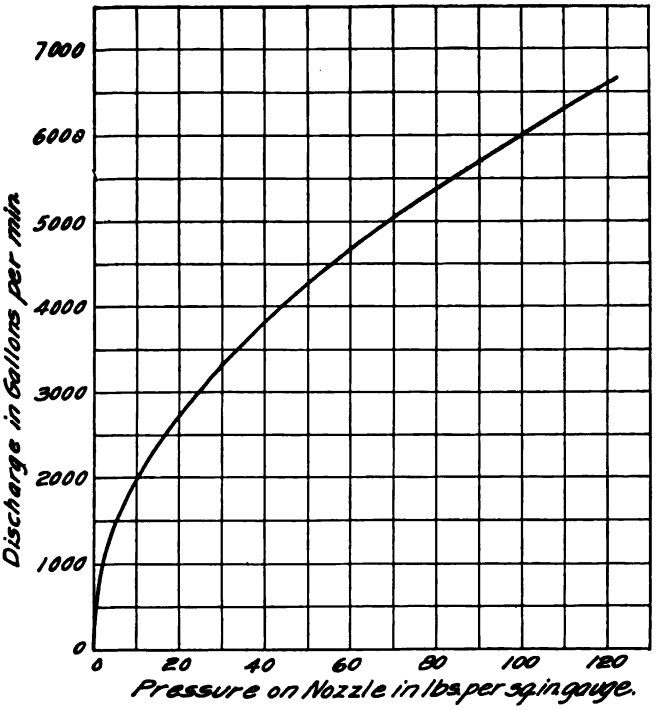

Fig. 316.

This formula takes into consideration the velocity of approach and the water column between the nozzle and gauge.

4. *The Pitot Tube.* Fig. 317 illustrates an arrangement for measuring the quantity of discharge by means of a Pitot tube. The tube measures the velocity head at the orifice of the discharge nozzle, and the quantity of discharge can be found from the formula

$$Q = cA\sqrt{2gh} \quad . \quad . \quad . \quad . \quad . \quad . \quad . \quad 307$$

in which Q is the quantity of discharge in cubic feet per second, c a constant of the nozzle, usually varying between 0.95 and 0.98, A the area of the nozzle in square feet, and h the velocity head in feet.

The Pitot tube readings can only be accurate with a very carefully calibrated nozzle and a careful determination of the coefficient c.

In all these methods of test care must be exercised that the discharge of the pump does not influence the water entering the suction

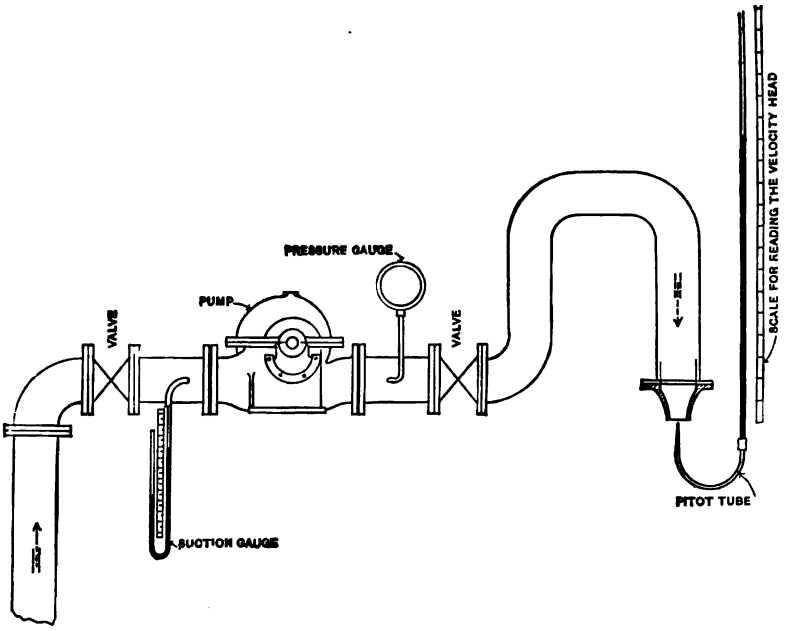

Fig. 317.

pipe. The authors know of tests having been made in which the water flowed through a closed circuit, which usually gave the pump a higher efficiency than it deserved. It is always preferable to have the discharge water flow into a tank open to the atmosphere and its high velocity of discharge entirely destroyed before the water again enters the suction end of the pump.

To obtain the efficiency of a pump it is necessary to measure not only the quantity of discharge and the total head but also the horse-power input to the pump. This is usually obtained by first measuring the power input to the driver or motor and determining

the latter's efficiency. The pump efficiency can then be easily obtained.

When using a steam turbine or engine it is often difficult and expensive to determine the brake horse-power input to the pump. For this reason the guarantees are frequently made in terms of work delivered to the water and amount of steam used by the driver. It is usually expressed in the number of million foot pounds delivered to the water per 1000 pounds of steam at some specified set of conditions, and this is called the "duty" of the unit. A better way of expressing the "duty" of a pumping unit is in the number of foot pounds delivered per B.t.u.'s of energy in the steam used.

INDEX.

A.

PAGE

Absolute path of water through impeller 67, 70
Adam 43
Adjustable guide vanes 119, 156
Alberger pumps 343
Allen, W. H., Pumps 406
Allis-Chalmers pumps 325
Angles β_a and δ_a, determination of 35
Appold 224
Armaturen and Maschinenfabrik A. G. pumps 301
Axial centrifugal pumps 4, 76
Axial thrust 19, 76, 87
see also Balancing piston.
indicator 301

B.

Babbitted bearings 163
Backward turned impeller blades, efficiency of 98
Balancing piston, Allen, W. H. 408
Allis-Chalmers 327
Berliner Maschinenbau 389
Byron Jackson 331
Kugel-Gelpke 272
Mather and Platt 355
Sulzer 244
Willans and Robinson 392
Balancing, static and dynamic 191
Ball-seated linings 163
Ball thrust bearing 327
Banki 225
Banninger 225
Bearing pressures 161
Bearings, ball seated 163
Bearings, cooled by radiation 162
Bearings, design of 161
lubrication of 161
method of babbitting 163
rubbing speed of 161
spherical seated 320
temperatures of 161
thrust, *see* Thrust bearing.
water cooling of 162

PAGE
Berliner Maschinenbau pumps 388
Bi-rotor centrifugal pumps 295
Blade design, impeller 60
Blades, number of impeller 93
Borsig pumps 399
Brodnitz and Seydel pumps 384
Buffalo pumps 403
Built-up impellers, design of 167
Byron Jackson pumps 330

C.

Calculation of a low-pressure centrifugal pump 140, 146
impeller and guide vanes 126
two high-pressure centrifugal pumps 126
Casings and heads, strength of 184
circular 75
losses in 17
pump 1
round 5
spiral 5, 73
the guide vane 73
Center of gravity, determination of 186
Centrifugal action in centrifugal pumps 1, 9
force of water 9
stresses produced by 168
pumps, axial 4, 76
calculation of low-pressure 140, 146
high-pressure 126
characteristic of 23
classification of 4, 112, 122
double inlet type 229
suction type 229
duty of 424
efficiency of 85
enclosed 4
experimental efficiency of 106
friction losses in 12
for fire boat service 301, 313, 317, 334
engine service 270, 367
stations 289, 310, 325, 334, 339
hydraulic mining 286
friction head of 9
high-pressure 4, 6
historical review of 223
horizontal 4
hydraulic efficiency of 11
hydraulic losses in 85
low-pressure 4, 7
mechanical losses in 85
modern 225

PAGE
Centrifugal pumps, multi-rotor 293, 295, 350
-stage 6, 79
open 4
pressure distribution in 7, 158
head of 9
regulation of 112
screw 417
shock losses in 12
single-stage 6
submerged 5
testing of 418
types 223
Alberger 343
Allen, W. H. 406
Allis-Chalmers 325
Armaturen and Maschinenfabrik A. G 301
Berliner Maschinenbau 388
Borsig 399
Brodnitz and Seydel 384
Buffalo 403
Byron Jackson 330
Dayton 393
De Laval 371
Escher, Wyss & Co. 271
Gebauer 405
Jaeger 79, 106, 108, 229, 257
Klein, Schanzlin and Becker 417
Kugel-Gelpke 229, 271
Mather and Platt 353
McDougall, John, Caledonian Iron Works Co. 335
Morris, I. P., Co. 311
Novak 413
Quiri and Co. 417
Rateau 229, 246
Rees Roturbo 414
Sautter, Harle and Co. 246
Simpson 415
Skoda 321
Sulzer 4, 7, 106, 226, 228, 229
Weise and Monski 328
Willans and Robinson 392
Wood, R. D., and Co. 381
Worthington 272
shaft pumps, *see* Shaft pumps.
velocity head of 9
vertical 4
without guide vanes 5, 82
with guide vanes 5
Channel cross sections 144
Characteristics of centrifugal pumps 23
Chicago fire-boat pumps 313

PAGE
Chorlton-Whitehead governor 361
Circular pump casings 75
Classification of centrifugal pumps 4, 112, 122
Clearance rings, impeller 166
space losses 17
pressure difference in 17
Coefficients of nozzles 421
Combes 224
Condition equation 7
Consumption of power and efficiency 85
Critical speeds 191
approximate formula for 199
graphical determination of 196
mathematical determination of 196
Curves κ and λ 37

D.

Dayton pumps 393
Deflection of pump shafts, determination of 199
De Laval pumps 371
Design of important pump parts 161
Determination of exit values by means of κ and λ curves 37
Diaphragm packings, design of 166
packing rings 167
Diaphragms, strength of 184
Dimensions of suction pipe 22
Directing vanes, use of 95
Discharge losses 11
Double suction pump 229
Duluth fire-boat pumps 317
Duty of centrifugal pumps 424
Dynamic balancing 191

E.

Efficiency and consumption of power 85
hydraulic 11
when $\delta_e = \beta_e$ 95
of backward turned impeller blades 98
centrifugal pumps, experimental 106
without guide vanes 82
forward turned impeller blades 98
multi-stage centrifugal pumps 81
radial impeller blades 98
with varying number of revolutions 88
Elbows, flow of water through 104
Enclosed centrifugal pumps 4
Entrance and exit dimensions for equal heads with varying quantities 51
velocity diagrams when $\delta_e \gtreqless 90°$ 44
Entrance pipe 1
velocity diagrams 3, 12

PAGE
Entrance velocity diagrams for $\delta_e \gtrless 90°$ 57
when $\delta_e = 90°$ 42
Escher, Wyss and Co. pumps 271
Euler, Leonhard 223
Evolventen pumps 301
Exit and entrance dimensions for equal heads with varying quantities 51
velocity diagrams 3, 12
for $\delta_e \gtrless 90°$ 44, 57
$\delta_e = 90°$ 24
graphical determination of 40
Experiments upon the efficiency of centrifugal pumps 106

F.

Fire boat, centrifugal pumps for, Byron Jackson 334
Morris, I. P. 313, 317
Worthington 301
engine, centrifugal pumps for 270, 367
stations, centrifugal pumps for 289, 310, 325, 334, 339
Fliegner 90
Flow of water through a centrifugal pump 1
pipes and elbows 104
Forced feed lubrication of bearings 161
Forward turned impeller blades, efficiency of 98
Föttinger 225
Fourneyron 223
Francis 224
Friction and shock losses 12
head 9
losses 10, 12
in impeller 13
suction pipe 12
Fundamental equation 7, 10, 12

G.

Gebauer pumps 405
General Electric Company, thrust bearing 317, 319
Girard 224
Governor, Chorlton-Whitehead 361
Graphical determination of center of gravity 186
critical speeds 196
deflection of shafts 199
exit velocity diagram 40
modulus of section 186
Griesmann 225
Guide vanes 1
adjustable 119, 156
angles, influence upon peripheral velocity 28
angles, influence upon short-circuit losses 30
calculation of 126
casing 73

PAGE
Guide vanes, involutes 60
at entrance 71
losses in 15
pumps with 5
without 5, 82
Gutermuth 225
Gwyne 224

H.

Heerwagen, Dr. F 235
Henschel 224
High-pressure centrifugal pumps 4, 6
calculation of 126
packing 165
speed impellers, design of 167
Historical review of centrifugal pumps 223
Horizontal centrifugal pumps 4
Hot water packing 165
Hutzelsieder, C 146
Hydraulic efficiency 11
when $\delta_e = \beta_e$ 95
losses in centrifugal pumps 85
mining, centrifugal pumps for 286
turbines 252, 336

I.

Impeller 1
angles, influence upon peripheral speed 28
short-circuit losses 30
blade design 60
development 144
efficiency of backward turned 98
forward turned 98
radial 98
strength of 167
built up 167
calculation of 126
channel section 126, 144
clearance rings 166
design of 167
involutes 60
losses 13
number of blades of 93
radial stresses in 168
shroud rings 167
strength of 167
stresses in high-speed 168
stretch of, due to centrifugal force 176
tangential stresses in 168
with riveted blades 167

PAGE
Influence of guide vane angles upon peripheral velocity 28
impeller angles upon peripheral velocity 28
Involutes at guide vane entrance 71
impeller entrance 63
exit 66
their use 60
Isaachen 104
Iso-efficiency curves of pumps 295

J.

Jaeger pumps 79, 106, 108, 229, 257
Jonval 224

K.

Klein, Schanzlin and Becher pumps 417
Kugel-Gelpke pumps 229, 271

L.

Labyrinth packings, De Laval 373
water packing 165
Lasche's experiments on bearing temperatures 161
Leather cupped packings 165
Lewicke 225
Linings, ball seated 163
Lorenz 225
Losses, clearance space 17
discharge 11
friction 10, 12
hydraulic 85
in casing 17
delivery pipe 11
entrance or suction pipe 12
guide vanes 15
impellers 13
mechanical 85
shock 10, 12
short-circuit 19, 33, 86
Low-pressure centrifugal pumps 4, 7
calculation of 140, 146
Lubrication of bearings 161

M.

Mather and Platt pumps 353
McDougall, John, Caledonian Iron Works Co. pumps 335
Mechanical losses in centrifugal pumps 85
Method of babbitting bearings 163
Methods of testing pumps 418
Miscellaneous and novel designs 413
Modern centrifugal pumps 225

PAGE
Modulus of section, determination of 186
Morris, I. P., pumps 311
Multi-rotor centrifugal pumps 293, 295, 350
Multi-stage centrifugal pumps 6, 79
efficiency of 81

N.

Neumann, Fritz 304
New York fire-boat pumps 301
Novak pumps 413
Novel and miscellaneous designs 413
Nozzle coefficients of flow 421
measurements by 418, 421
Number, correct, of impeller blades 93
of revolutions, efficiency with varying 88

O.

Oil for bearings 161
Open centrifugal pumps 4
Orten-Boving, Jens 392

P.

Packings, design of 164
diaphragm 166
high-pressure 165
hot water 165
labyrinth 165
leather cupped 165
water seal of 164
Packing rings for diaphragms 167
Paraboloid, rotating 21, 31, 77
Parsons, R. C. 224
Peripheral velocity, determination of 35
influence of impeller and guide vane angles upon 28
Pitot tube, measurements by 418, 422
Pfarr, Prof. A. 69, 104, 146
Piccard 252
Pipes, flow of water through 104
Poillon 224
Poncelet 223
Portable centrifugal pumps 270, 367
Prasil 225
Pressure difference in clearance space 17
Pressure distribution in centrifugal pumps 7, 158
head of centrifugal pumps 9
on bearings 161
Proell 225
Pump parts, design of important 161
types, *see* Centrifugal pump types.

Q.

PAGE

Quiri and Co. pumps 417

R.

Radial impeller blades, efficiency of 98
stresses in impellers 168
Radiation, bearings cooled by 162
Rateau 225, 252
pumps 229, 246
Redtenbacher 224
Rees Roturbo pumps 414
Regulation by throttling 112
Roller bearing thrust 319
Rotating paraboloid 21, 31, 77
Round pump casing 5
Rubbing speed of bearings 161
Rühlmann 224

S.

San Francisco fire-boat pumps 334
Sautter, Harle and Co. pumps 246
Schwammkrug 224
Screw pumps, Quiri 417
Segner 223
Self-aligning thrust bearing 319
Shaft pumps 4
Berliner Maschinenbau 392
Gebauer 406
Jaeger 268
Mather and Platt 357, 365
Rateau 252
Skoda 323
Sulzer 235
Shafts, calculation of critical speeds of 191
deflection of 199
Shock and friction losses 9, 10, 12
Short-circuit losses 33, 86
influence of guide vanes upon 30
impeller angles upon 30
Short-circuit water 19
Shroud rings, stretch of, due to centrifugal force 181
Simpson pumps 415
Single-stage pumps 6
Skoda pumps 321
Speeds, critical 191
Spherical seated bearings 320
Speidel, E. 146
Spiral pump casing 5, 73
Static balancing 191
Stodola 170, 193, 194, 222

PAGE
Strength of diaphragms ... 184
impellers ... 167
impeller blades ... 184
pump casings and heads ... 184
Stresses, calculation of, in pump diaphragms, casings and heads ... 184
in high-speed impellers ... 168
produced by centrifugal force ... 168
Stretch in impellers due to centrifugal force ... 176
shroud rings due to centrifugal force ... 181
Striebeck, experiments on lubrication of bearings by ... 162
Stuffing boxes, design of ... 164
Submerged pumps ... 5
Suction head, maximum practical ... 24
theoretical ... 24
packing ... 164
pipe ... 1
dimensions of ... 22
friction in ... 12
velocity for $\delta_e \leqq 90°$ ... 57
Sulzer pumps ... 4, 7, 106, 226, 228, 229

T.

Tangential stresses in impeller ... 168
Temperature of bearings ... 161
Testing of centrifugal pumps ... 418
Theoretical head of pump ... 11
Throttling, regulation by ... 112
Thrust, axial ... 19, 76, 87
see Balancing Piston.
bearings ... 79
Allis-Chalmers ... 327
Armaturen and Maschinenfabrik A. G. ... 301
Buffalo ... 404
General Electric Co. ... 317
marine type ... 258
roller ... 319
self-aligning ... 319
Skoda ... 321
Weise and Monski ... 329
Worthington ... 277
Tri-rotor centrifugal pumps ... 293, 350
Turbines, hydraulic ... 252, 336
Types of centrifugal pumps ... 223
see Centrifugal pump types.

U.

Unwin ... 224
Use of directing vanes ... 95

V.

PAGE
Velocity diagram, entrance 3, 12
for $\delta_e \lesseqgtr 90°$ 44, 57
when $\delta_e = 90°$ 42
exit 3, 12
for $\delta_e \gtreqless 90°$ 44, 57
$\delta_e = 90°$ 24
graphical determination of 40
distribution in centrifugal pumps 7
head of centrifugal pumps 9
Venturi water meter 418, 420
Vertical centrifugal pumps 4

W.

Wagenbach, W. 146, 225
Wagner 225
Water-cooled bearings 162
meter, Venturi 418, 420
packings, design of 164
path, absolute, in impeller 67, 70
seal for packings 164
turbines for driving pumps 252, 336
Weir tank measurements 418, 421
Weisbach 90, 224
Weise and Monski pumps 328
Whirling water phenomenon 104
Willans and Robinson pumps 392
Wood, R. D., pumps 381
Worthington pumps 272

Z.

Zeuner 224
Zuppinger 224

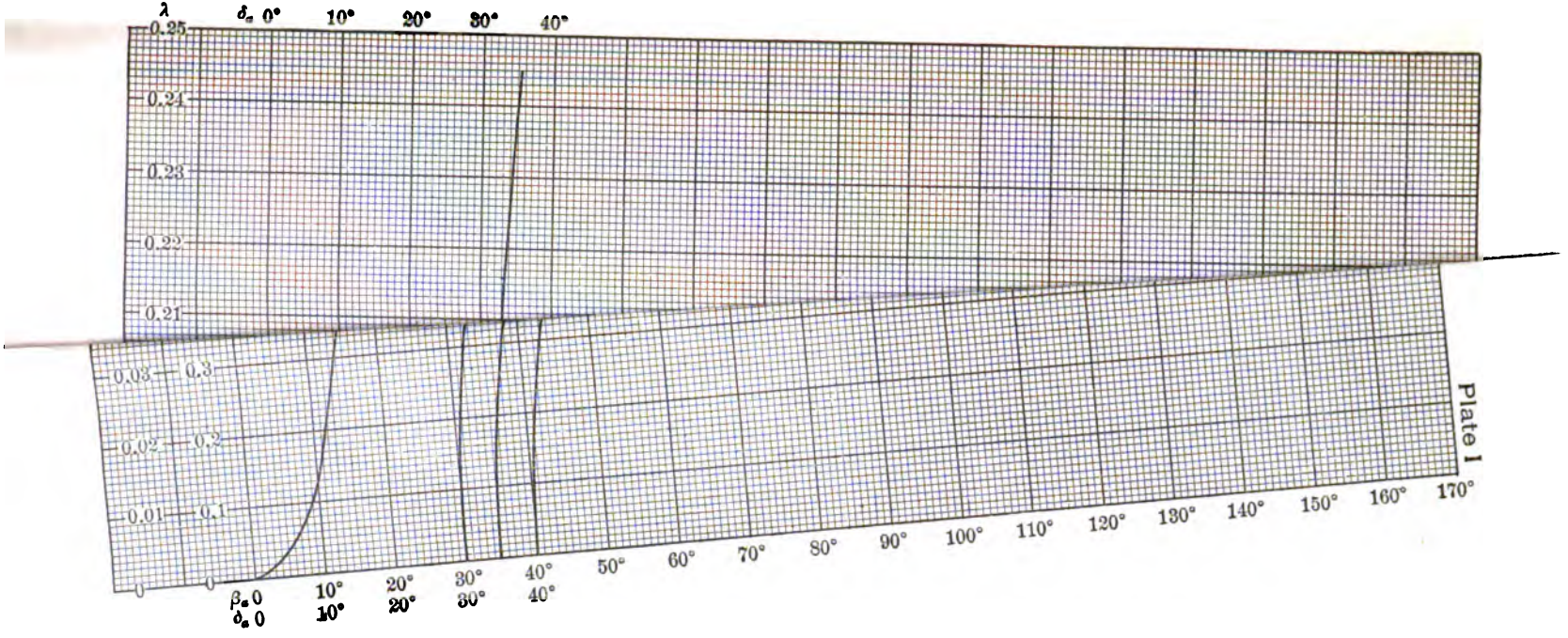
λ
δ= 0°
10°
20°
30°
40°
0.25
0.24
0.23
0.22
0.21
0.03
0.02
0.01
0
0.3
0.2
0.1
0
β= 0
δ= 0
10°
10°
20°
20°
30°
30°
40°
40°
50°
60°
70°
80°
90°
100°
110°
120°
130°
140°
150°
160°
170°

Plate I

Fig. 3

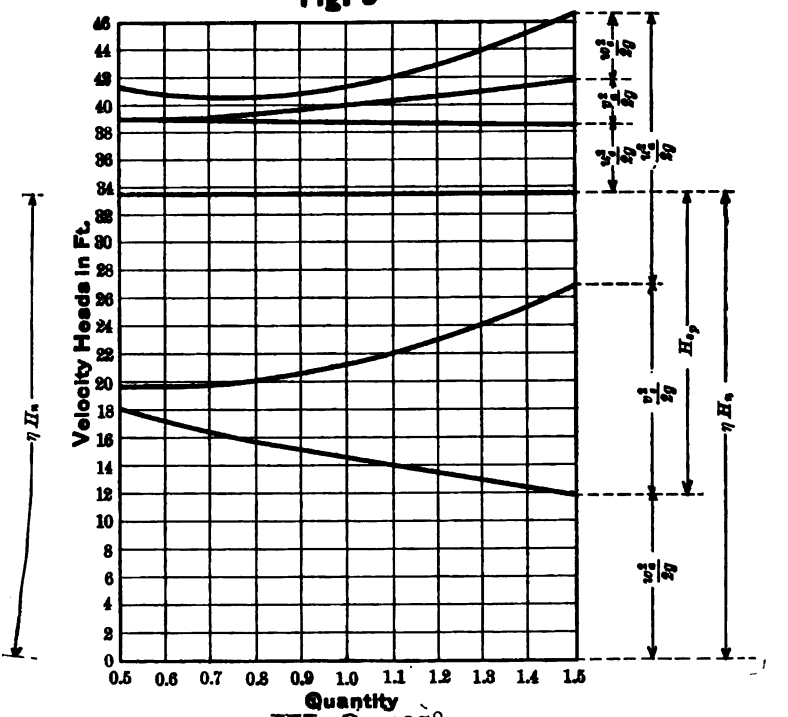

III, $\beta_a = 135°$

Fig. 6

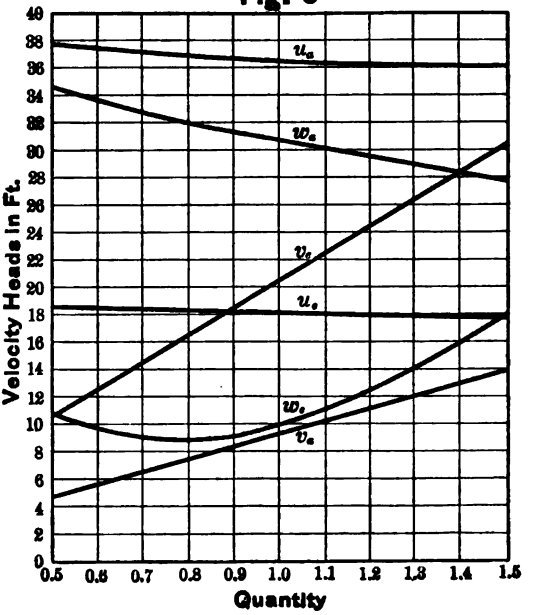

High Pressure Centrif

$D_s^* = 1.0$ $K = 7.52$

$K_{max.} = 9.12$ $K_{min.} =$

$F_s = 0.118$ $A = -2.78$

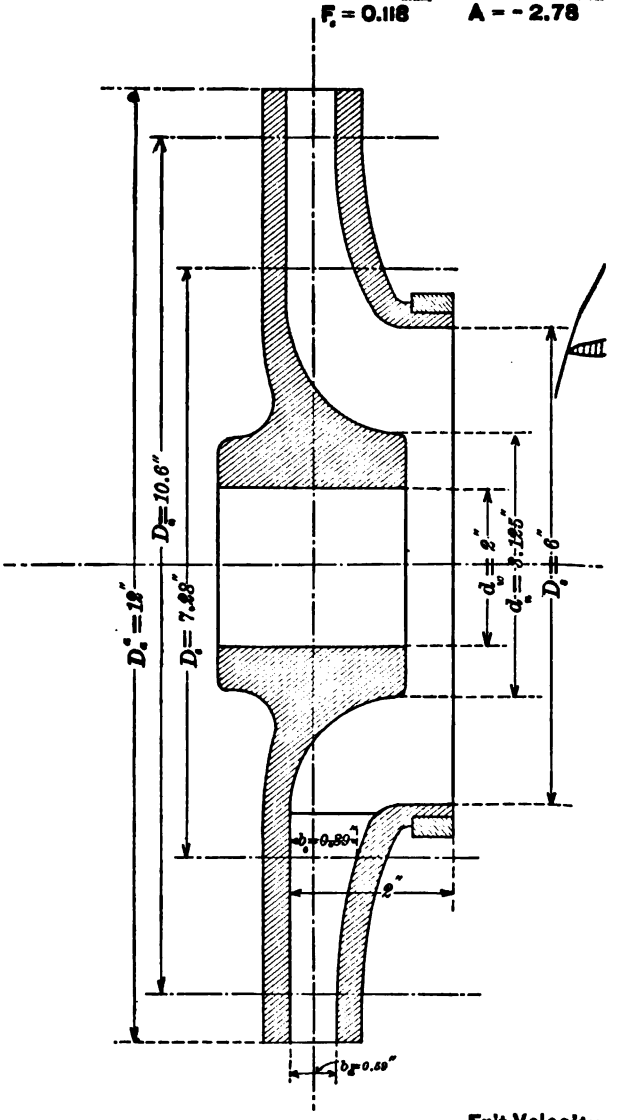

Exit Velocity

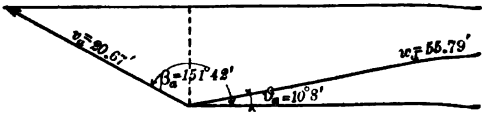

ugPump.

130

5.9

B50.

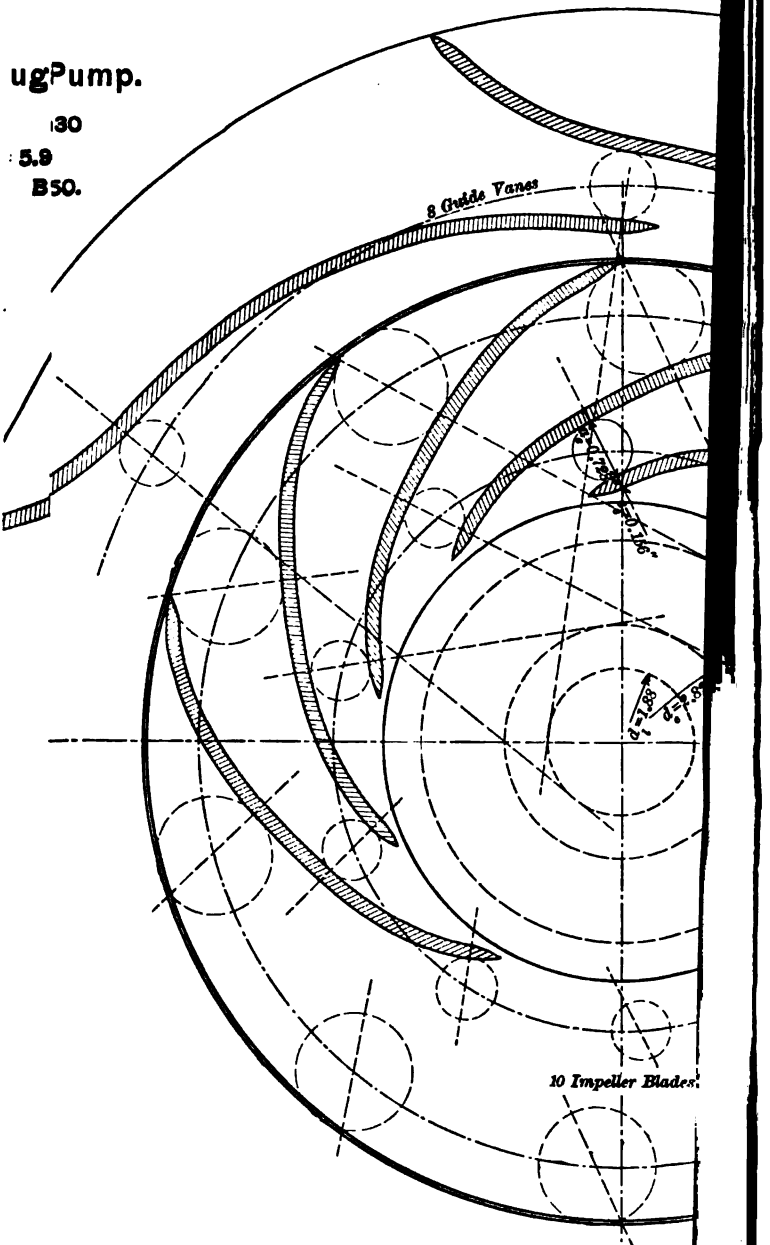

Velocity Diagrams for $\eta H_s = 86.67$ ft.

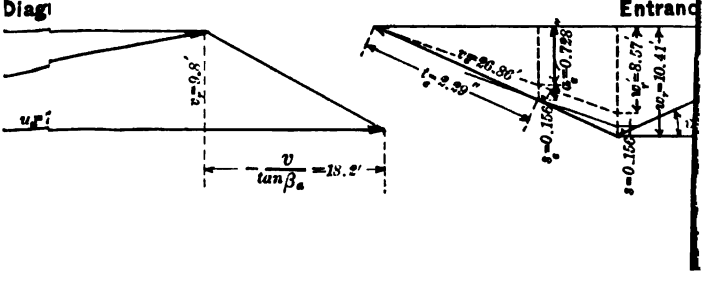

Plate IV

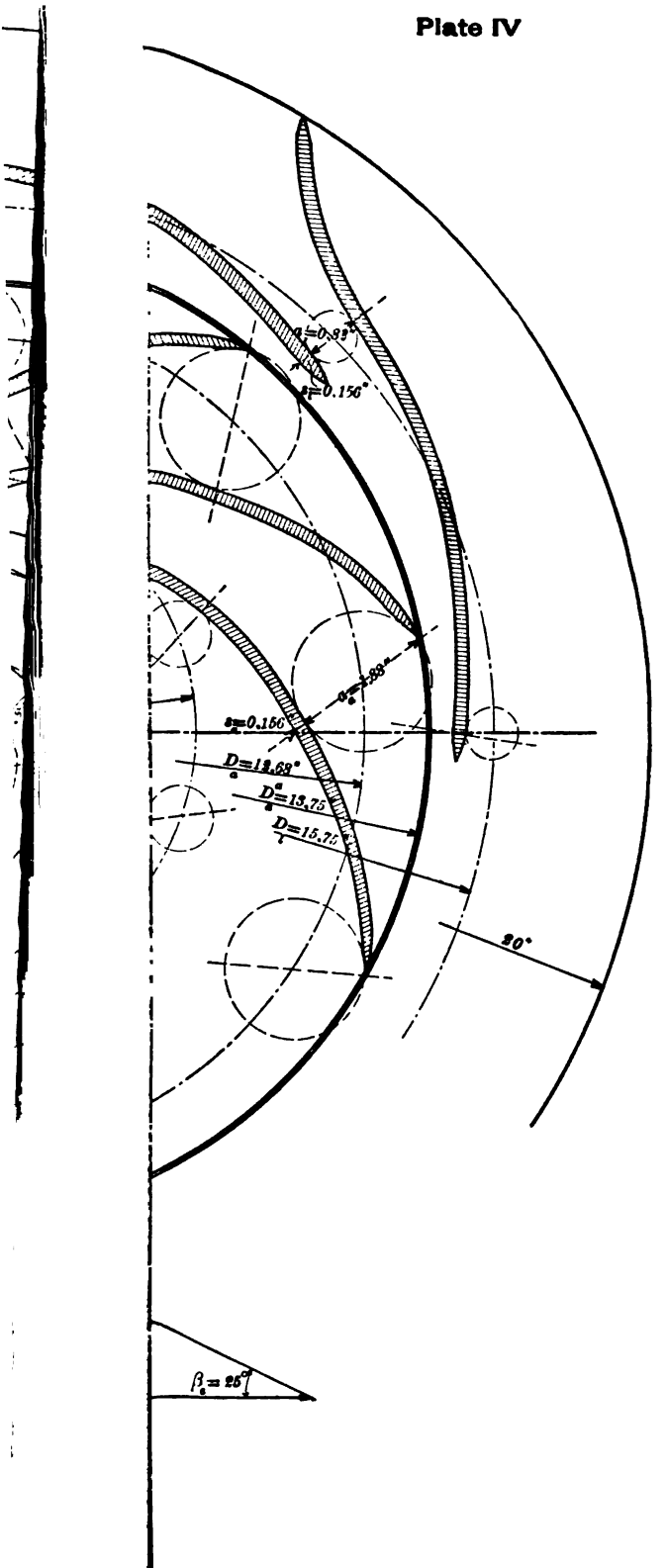

Pressure Centrif

D_e = 1.64 K = 111.5

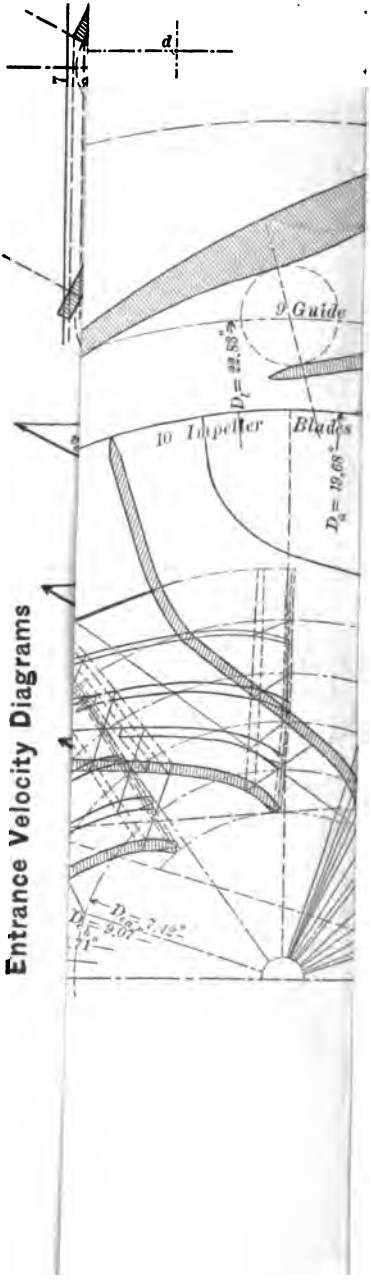

Centrifugal Pump.

K=111.5 n=328

$K_{min.}$=80.6

=4.68 B=265

Plate VII

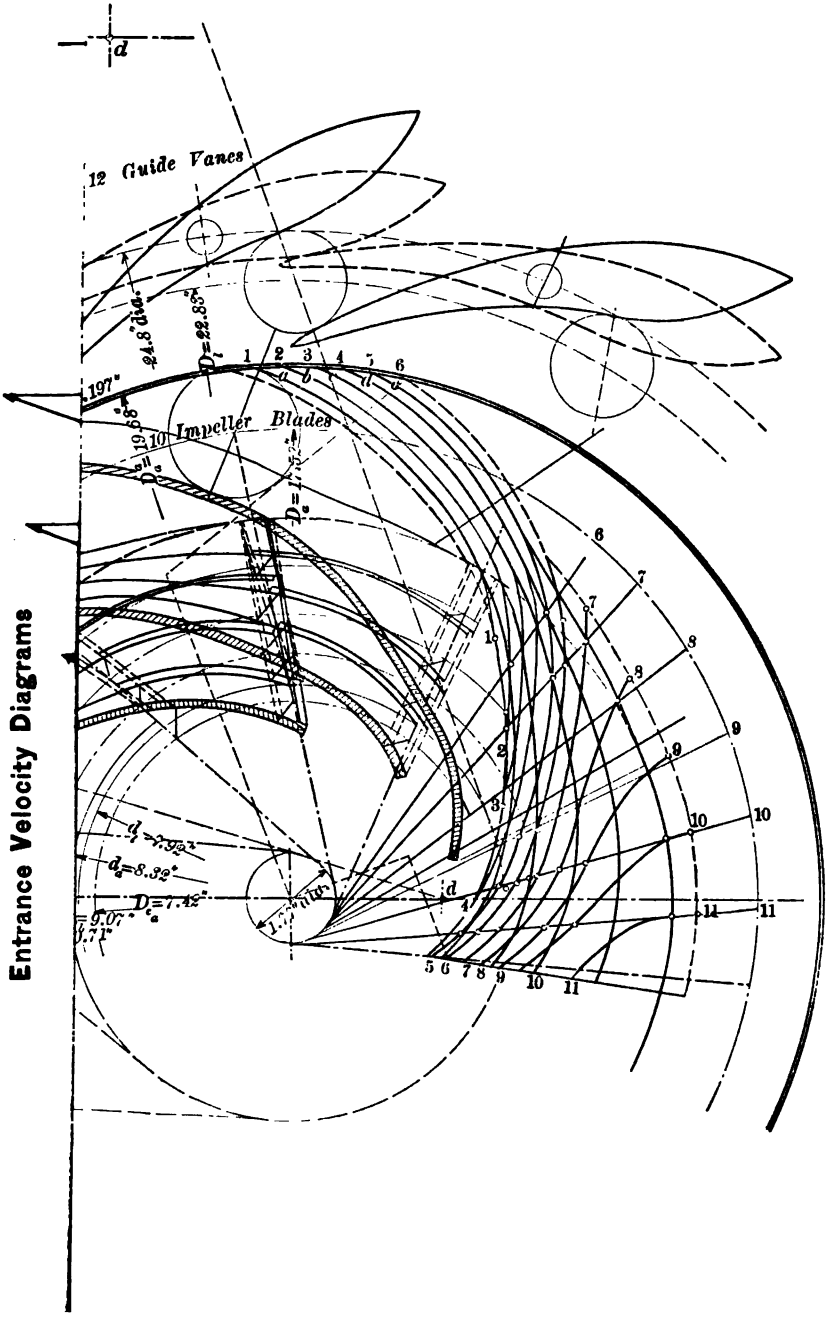

UNIVERSITY OF CALIFORNIA LIBRARY
BERKELEY

Return to desk from which borrowed.
This book is DUE on the last date stamped below.

JAN 16 1948
O Keefe 2/16

11Jun'51 P

MAY 9 1 1955 LU

10Mar'50AB

1Dec'56GR

18Aug'50

REC'D LD

DEC 13 1956

12Jul51VW

25Jul51LU

27Feb'57PW

18Jun'53LM 0

REC'D LD

12 1953 LU

FEB 13 1957

LD 21-100m-9,'47(A5702s16)476

YC 67038

LIBRARY USE
RETURN TO DESK FROM WHICH BORROWED

LOAN DEPT.

THIS BOOK IS DUE BEFORE CLOSING TIME
ON LAST DATE STAMPED BELOW

LIBRARY USE
NOV 1 3 19

REC'D LD
NOV 13'63 -4 PM

LD 62A-20m-9,'63
(E709s10)9412A

General Library
University of California
Berkeley